

1-1-2011

Differences between adult and pediatric neck muscle stress due muscle recruitment patterns

Renee Dawson
Wayne State University,

Follow this and additional works at: http://digitalcommons.wayne.edu/oa_dissertations

Recommended Citation

Dawson, Renee, "Differences between adult and pediatric neck muscle stress due muscle recruitment patterns" (2011). *Wayne State University Dissertations*. Paper 536.

This Open Access Dissertation is brought to you for free and open access by DigitalCommons@WayneState. It has been accepted for inclusion in Wayne State University Dissertations by an authorized administrator of DigitalCommons@WayneState.

**COMPARISON OF ADULT AND PEDIATRIC NECK MUSCLE
STRENGTH AND RESPONSE**

by

RENEE M. DAWSON

DISSERTATION

Submitted to the Graduate School

of Wayne State University,

Detroit, Michigan

in partial fulfillment of the requirements

for the degree of

DOCTOR OF PHILOSOPHY

2012

MAJOR: BIOMEDICAL ENGINEERING

Approved by:

Advisor

Date

© COPYRIGHT BY

RENEE M. DAWSON

2012

All Rights Reserved

ACKNOWLEDGMENTS

Completing this degree is the fulfillment of a lifelong dream, but like so many accomplishments in life, I couldn't have done it alone. I would first like to give my thanks and appreciation to my advisor, Dr. John M. Cavanaugh whose support and mentorship helped make this degree a reality. Thank-you for believing in me and this project, when life, distance and children, at times, made the task seem insurmountable.

Thank-you to Dr. Cynthia Bir and Dr. Michele Grimm for generously agreeing to sit on my committee; your insights, advice and constant support throughout this process has been invaluable. To Dr. Chris VanEe, thank-you for agreeing to step in at the last moment. To Dr. Bill Altenhoff, your advice at the beginning of this project was very much appreciated.

To Dr. Mark Haacke and Mr. Zahid Latif at the MRI Institute for Biomedical Research for allowing me the use the research MRI. To Zahid in particular for the countless hours you spent developing the imaging protocol with me, and the easy way you had with the children.

Don Sherman and Matt Mason your help in the construction and assembly of the swing fixture was uniquely appreciated when, at seven months pregnant, I was no longer able to climb ladders safely. To Nate Dau and Craig Foster thank-you for your help in setting up and troubleshooting TDAS, you saved me many hours

of frustration. To Dr. Nadia Azar, I learned a lot about EMG from you; thank-you for being a great friend and teacher.

To Stewart Dawson, thank-you for your time and expertise without which I would not have been able to build the floor of the swing fixture. To Stephanie Séguin, thank-you for your help with the processing of the video data, it promised to be a long, difficult task – you lightened my load.

To my best friend Kelly Trask, thank-you for helping me reason through some difficult problems and for helping me get through the tough times by pushing me to keep working.

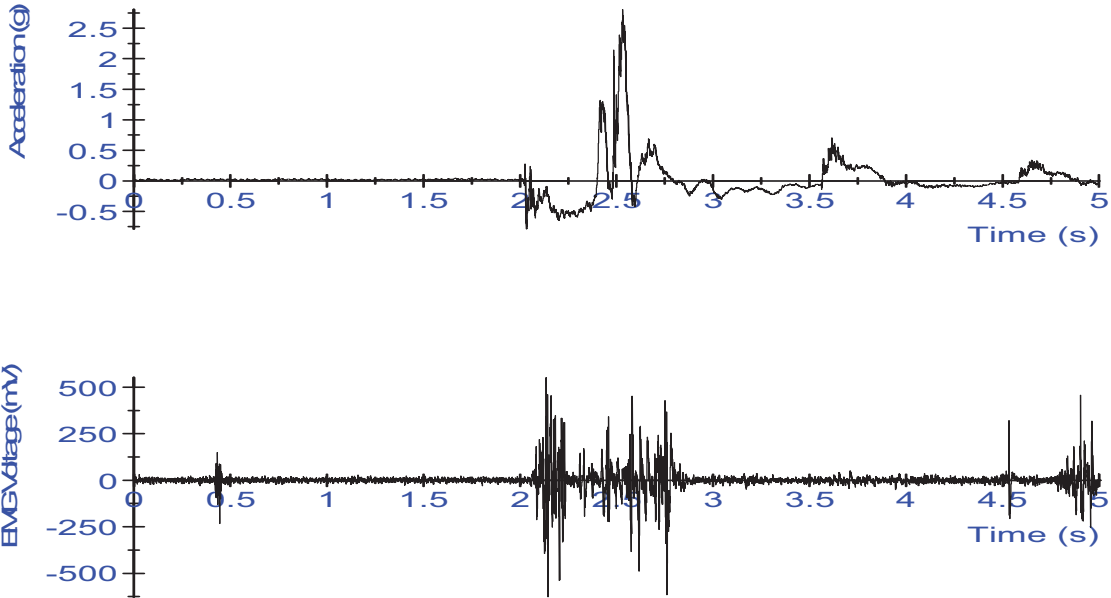
To my family, no words can express how much your tireless support and unconditional love has meant to me. To my parents Flora and Yvon Boudreau, you've driven many kilometers through some questionable weather to ensure that I reached the end of this degree. I can't thank-you enough. Mum, you have been an inspiration to me. To my husband, Ian Dawson, the journey has been longer than we expected or planned, but your constant love and support has been the wind in my sails that has kept me going. And finally to my lovely girls, Katharine and Sarah thank-you for being the most patient pre-schoolers Mummy could wish for, I love you both very much. Your passenger safety was my motivation.

TABLE OF CONTENTS

ACKNOWLEDGMENTS	ii
LIST OF TABLES	ix
LIST OF FIGURES	xii
CHAPTER 1 BACKGROUND AND SIGNIFICANCE	1
1.1 EPIDEMIOLOGY	1
1.2 RESPONSE AND SCALING	3
1.3 SPECIFIC AIMS	14
CHAPTER 2: ANATOMY AND PHYSIOLOGY OF THE CERVICAL MUSCLES	18
2.1 INTRODUCTION	18
2.2 ANATOMY	18
2.2.1 Bony Structure of the Neck.....	18
2.2.2 Musculature of the Neck.....	19
2.3 MUSCLE PHYSIOLOGY AND NEURAL CONTROL	23
2.4 SUMMARY	29
CHAPTER 3: SUBJECT SELECTION AND ANTHROPOMETRICS	30
3.1 INTRODUCTION	30
3.1.1 Subject Selection.....	30
3.1.2 Subject Contra-Indications	31
3.2 METHODS	32
3.2.1. Anthropometric Measurements	32
3.2.2 Calculation Neck Circumference from MRI.....	32
3.3 RESULTS	34

3.4 DISCUSSION.....	36
3.4.1 Anthropometrics	36
3.4.2 Measurements Of Neck Circumference.....	38
3.5 CONCLUSIONS.....	40
CHAPTER 4: MUSCLE CROSS-SECTIONAL AREA AND MOMENT ARMS BASED ON MAGNETIC RESONANCE IMAGING MEASUREMENTS	
4.1 INTRODUCTION	41
4.2 METHODS	44
4.2.1 Test Procedure	44
4.2.2 Data Analysis	46
4.2.2.1 Muscle Length.....	50
4.2.2.2 Muscle Cross-Sectional Area.....	53
4.2.2.3 Moment Arms.....	54
4.2.3 Calculating Cross-Sectional Area	55
4.2.4 Statistical Analysis.....	56
4.3 RESULTS	57
4.4 DISCUSSION	64
CHAPTER 5: DETERMINATION OF NECK MUSCLE FORCE AND STRESS AT C-4 VERTEBRAE DURING A MAXIMAL VOLUNTARY CONTRACTION	
5.1 INTRODUCTION	75
5.2 METHODOLOGY.....	77
5.2.1 Force and EMG Data Collection:.....	77
5.2.1.1 Instrumentation	77

5.2.1.2 Electrode Placement.....	78
5.2.1.3 Maximal Voluntary Contraction Data Collection Set-up	81
5.2.2 Data Processing	83
5.2.2.1. Data Filtering.....	83
5.2.2.2 Normalizing EMG data.....	84
5.2.3 Force Calculations.....	85
5.2.4 Statistical Analysis.....	96
5.3 RESULTS	96
5.3.1 Force and EMG	96
5.4 DISCUSSION.....	104
5.5 CONCLUSIONS.....	114
CHAPTER 6: THE NECK MUSCLE RESPONSES OF 50 TH PERCENTILE ADULT MALES AND 10 YEAR OLD BOYS IN LOW SPEED FRONTAL IMPACTS	
6.1 INTRODUCTION	115
6.2 METHODS	120
6.2.1 Instrumentation.....	120
6.2.2 Test Fixture	123
6.2.3 Data Analysis	128
6.2.4 Dynamic Force Calculations.....	132
6.3 RESULTS	138
6.3.1 Dynamic Moment.....	140
6.3.2 Electromyography Results.....	151

6.4 DISCUSSION.....	167
6.5 CONCLUSIONS.....	174
CHAPTER 7 LATENCY OF NECK MUSCLE RESPONSE AND HEAD	
DISPLACEMENT DURING DYNAMIC LOADING	175
7.1 INTRODUCTION	175
7.2 METHODOLOGY.....	178
7.2.1 Test Set-up.....	178
7.2.2.1 Latency of Muscle Response	179
	
.....	180
7.2.2.2 Head Displacement.....	181
7.2.3 Statistical Analysis.....	186
7.3 RESULTS	186
7.3.1 Latency.....	186
7.3.2 Head Displacement	195
7.4 DISCUSSION.....	200

7.4.1 Latency.....	200
7.4.2 Head Displacement	208
CHAPTER 8: SUMMARY AND CONCLUSIONS	211
APPENDIX A MR Images Used In Calculation of Muscle Moment Arms and Cross-Sectional Areas.....	220
APPENDIX B Tables and Figures for Chapter 5 Determination of Muscle Force and Stress at C-4 Vertebrae During a Maximal Voluntary Contraction.....	240
APPENDIX C Tables and Figures for Chapter 6 Determination of Muscle Force and Stress at C-4 Vertebrae During a Maximal Voluntary Contraction.....	364
APPENDIX D Swing Fixture Design Data.....	440
APPENDIX E Approvals form Human Investigations Committee.....	446
REFERENCES.....	448
ABSTRACT.....	464
AUTOBIOGRAPHICAL STATEMENT.....	467

LIST OF TABLES

Table 3-1	Anthropometric measurements of children and adults used as subjects in this study.	35
Table 3-2	Measured and calculated neck circumference values for 10-year-old boys.	36
Table 3-3	Comparison of study height and weight results to published reports in the literature for 10-year old boys and 50 th percentile adult males...	38
Table 3-4	Comparison of study neck circumference results to neck circumference values reported in the literature.....	40
Table 4-1	Muscle origin and insertion locations.....	49
Table 4-2	Muscle length, moment arm and the physiologic cross-sectional area of the SCM for the 10 year old boys and 50 th percentile male subjects.....	58
Table 4-3	Anatomical Cross-Sectional Area of the sternocleidomastoid, trapezius, splenius capitis and scalene at C4 for both adult and 10 year old male subjects.....	64
Table 4-4	x- and y-components of the SCM and trapezius moment arms for the 10 year old male and adult male sample groups.....	66
Table 4-5	Cross-sectional area (cm ²) of the sternocleidomastoid, trapezius, splenius capitis and scalene muscles as reported in the literature for a adult males compared to results measured in this study.....	72
Table 5-1	Direction of Maximal Voluntary Contraction for SCM, trapezius, splenius capitis and scalene muscles.....	86
Table 5-2	Cross-sectional area of the posterior and postero-lateral muscles for both 10-year old male and 50 th percentile adult male subject groups.....	89
Table 5-3	Mean applied forces, mean applied moments and moment arms for both 10-year-old male and 50 th percentile adult male subject groups.....	99
Table 5-4	Maximum and EMG activation values (μ V) and normalized %MVC values for extension and flexion and peak EMG activation values (μ V) in lateral bending.....	101

Table 5-5	Calculated force values in flexion and extension for the SCM, trapezius,/splenius capitis, and middle scalene muscles for (a) 10 year old boys and (b) 50 th percentile adult males.....	103
Table 5-6	Calculate stress (N/cm ²) values in flexion and extension for the SCM, trapezius,/splenius capitis, and middle scalene muscles for (a) 10 year old boys and (b) 50 th percentile adult males.....	104
Table 5-7	Published muscle force values calculated using an EMG-assisted optimization model compared with the results of this study (Dawson, 2011).....	107
Table 5-8	Predicted applied moment values for 10-year old boys using the Wolanin et al. [1982] scaling model.....	111
Table 5-9	Results of neuromuscular efficiency for the 10-year old male and 50 th percentile males based on the Grosset et al. [2008] relationship...	114
Table 6-1	Coordinates of the intervertebral (IV)disc centroid and the Center of Gravity (CG) measured from the MR-images of Chapter 4.....	132
Table 6-2	Acceleration of the the cg of the head calculated for the 10-year old male subjects using the 3-2-2-2 acceleration data.....	146
Table 6-3	Acceleration of the the cg of the head calculated for the 50 th percentile adult male subjects using the 3-2-2-2 acceleration data.....	147
Table 6-4	Mean peak moments in extension and flexion for tensed and untensed muscle impacts for 10-year old boys.....	150
Table 6-5	Mean peak moments in extension and flexion for tensed and untensed muscle impacts for 50 th percentile adult males.....	151
Table 6-6	EMG values and %MVC values for the 10 year old male subjects in both the dynamic tensed and untensed conditions.....	154
Table 6-7	EMG values and %MVC values for the 50 th percentile adult male subjects in both the dynamic tensed and untensed conditions.....	161
Table 6-8	Results of the dynamic neuromuscular efficiency for the 10-year old male and 50 th percentile males based on the Grosset et al. [2008] relationship.....	174
Table 7-1	Measurements of the head marker from the calibration shot of the high speed video camera.....	184

Table 7-2	Latency of tensed and untensed muscles under dynamic test conditions for 10 year old boys from time of swing release.....	190
Table 7-3	Latency of muscle activation in response to peak swing acceleration in the tensed and untensed muscle conditions for the 10-year old male subject group.....	191
Table 7-4	Latency of tensed and untensed muscle dynamic test conditions for 50 th percentile adult males from time of swing release.....	194
Table 7-5	Latency comparison of tensed and untensed muscle conditions for 50 th percentile adult males.....	195
Table 7-6	Number of tests discarded from head displacement analysis due to fallen marker, lighting issues or swing release delay (S17).....	196
Table 7-7	Maximum head excursion for 10-year old boys in the dynamic tensed and untensed conditions. Table shows actual displacement values as well as displacement values normalized to seated erect height.....	197
Table 7-8	Maximum head excursion for 50 th percentile adult male subjects in the dynamic tensed and untensed conditions.....	199
Table 7-9	Published values of muscle response latency relative to both onset of sled acceleration and peak sled acceleration.....	203

LIST OF FIGURES

Figure 1-1(a)	Neck Response Corridor in Frontal Flexion [Mertz and Patrick, 1971].....	5
Figure 1-1(b)	Neck response Corridor in Extension [Mertz and Patrick, 1971]...5	
Figure 1-1(c)	Lateral Flexion Corridor [Patrick & Chou, 1976].....	5
Figure 1-2	Neck Muscle Cross-Sectional Area Regression and Scaling Law [Miller, 2003].....	8
Figure 1-3	Standard Flexor Stress Regression Model [Miller, 2003].....	9
Figure 1-4	Head excursion comparison between child cadaver (bold black trace) and crash test dummy (light black lines) with respect to the trajectory of the child restraint shield. [Cassan FB., et al., 1993].....	12
Figure 1.5	Study Flow chart showing the various data collected and their analytical objective.....	16
Figure 2-1	MR-image of the bony structure of the cervical spine. MR-image was part of the imaging protocol contained in this study.....	19
Figure 2-2	Cross-sectional area of the neck at C4 showing the musculature of the neck.....	20
Figure 2-3	Illustrations from <i>Gray's Anatomy</i> [1918] showing (a) the sternocleidomastoid, (b) the trapezius, (c) the splenius capitis and (d) scalene muscles.....	22
Figure 2-4	Structure of a Muscle (www.sirinet.net/~jgjohnso/amuscle.html).....	23
Figure 2-5	Hierarchy of motor control [VANDER, 1990].....	26
Figure 2-6	Cross-section of the ear and vestibular organs contributing to the vestibular-collic reflexive pathway. Images from http://www.thefullwiki.org/Vestibular_system#Vestibulo-ocular_reflex .28VOR.29	28

Figure 3-1	Axial cross-section of the neck at C4 – the red ellipse approximates the circumference of the neck. The pink and blue lines show the short axis (SA) and long axis (LA) used to calculate neck circumference.....33
Figure 4-1	Anatomical Planes of the human body [www.spineuniverse.com].....45
Figure 4-2	Line of action for the sternocleidomastoid (SCM), trapezius (TRAP), splenius capitis (SPL) and scalene muscles(SCAL) for (a) 10 year old male subject (left) and (b) 50 th percentile male subject.....52
Figure 4-3	Single image slice showing the Anatomical Cross-Sectional Area (ACSA) muscle boundaries for (a) a 10-year old male subject and (b) a 50 th percentile adult male subject.....54
Figure 4-4	Transverse muscle moment arms – sternocleidomastoid (SCM); scalene (SCAL); splenius capitis (SPL) and trapezius (TRAP) at C4 plane for (a) 10 year old boy and (b) 50 th percentile male....55
Figure 4-5	Moment arm comparison between 10 year old boys (light data set) and 50 th percentile adult males (dark data set).....59
Figure 4-6	Muscle moment arms measured in the transverse C4 plane compared with the age of the subject for the sternocleidomastoid (SCM $r=0.789$, ■); the trapezius (TRAP $r=0.713$, ●); splenius capitis (SPL $r=0.495$, ◆); and the anterior scalene (SCAL $r=0.415$, ▲).....60
Figure 4-7	Muscle moment arms measured in the transverse C4 plane compared with the height of the subject for the sternocleidomastoid (SCM $r=0.855$, ■); the trapezius (TRAP $r=0.841$, ●); splenius capitis (SPL $r=0.670$, ◆); and the anterior scalene (SCAL $r=0.447$, ▲).....61
Figure 4-8	Cross-sectional area the sternocleidomastoid compared with age ($r=0.741$), results showed a significant correlation ($p<0.02$).....62
Figure 4-9	Cross-sectional area of the sternocleidomastoid compared with subject weight ($r =0.723$), results showed a significant correlation ($p<0.02$).....62
Figure 4-10	Cross-sectional area of the sternocleidomastoid compared with subject height ($r =0.725$), results showed a significant correlation ($p<0.02$).....63

Figure 4-11	Transverse slice at C4-vertebra (a) 10-year old boy; (b) 50 th percentile adult male. Arrow indicates the larynx in both subjects.....	67
Figure 5-1	Placement of EMG electrodes over the sternocleidomastoid, splenius capitis and scalene muscles.....	81
Figure 5-2	Static test fixture. The position of the load cell was adjustable to align with the center of gravity of the subject's head.....	82
Figure 5-3	EMG recording of the right SCM in flexion (a) raw data; (b) filtered/rectified data.....	85
Figure 5-4	Axial MR-image at C4/5 for (a) 50 th percentile adult male and (b) 10-year-old boy. The boundaries show the muscle or muscle groups recorded by a pair of electrodes – SCM, SCAL, POST and P-L. Moment arms were taken from the centroid of the muscle group to the centroid of the neck.....	88
Figure 5-5	Free Body Diagram of (a) the Head/Neck to C4; (b) section at C4/C5 showing the forces and moment arms contributing to $M_{c4,y}$	91
Figure 5-6	Comparison of average applied moments in 3 bending directions between 50 th percentile adult males and 10-year old boys.....	100
Figure 6-1	Schematic of data collection systems.....	122
Figure 6-2	Drawings completed mouthpiece assembly.....	123
Figure 6-3	Schematic of the dynamic test fixture swing.....	125
Figure 6-4	Photographs showing (a) the swing fixture and its component parts (b) the shock absorbers and (c) the chair and turntable assembly.....	127
Figure 6-5	MR-images of adult subject S08 showing the anatomical landmarks used to determine the moment arms to the occipital condyle (OC).....	131
Figure 6-6	Free Body Diagram of (a) the Head/Neck to C4; (b) section at C4/C5 showing the forces and moment arms contributing to M_y	133

- Figure 6-7** Acceleration trace for (a) adult testing (b) 10-year old male tests and (c) the average acceleration for each subject group – 10-year olds (black), adult males (red).....140
- Figure 6-8(a)** Acceleration data from 3-2-2-2 for accelerometers in the x and z-directions for a 10-year old boy during a tensed muscle impact. HDX, Y, Z denote the bar on which the accelerometer was attached, and x, y, z-dir denotes the direction of acceleration measured.....142
- Figure 6-8(b)** Acceleration data from 3-2-2-2 for accelerometers in the y-direction, and the calculated acceleration at the CG of the head in the x and z-directions and the angular acceleration about the y-axis for a 10-year old boy during a tensed muscle impact.....143
- Figure 6-9(a)** Acceleration data from 3-2-2-2 for accelerometers in the x and z-directions for a 50th percentile male during a tensed muscle impact. HDX,Y,Z denote the bar on which the accelerometer was attached, and x,y,z-dir denotes the direction of acceleration measured.....144
- Figure 6-9(b)** Acceleration data from 3-2-2-2 for accelerometers in the y-direction, and the calculated acceleration at the CG of the head in the x and z-directions and the angular acceleration about the y-axis for a 50th percentile male during a tensed muscle impact..145
- Figure 6-10(a)** Total moment at C4 for (a) Tensed Muscle Impact and (b) Untensed muscle impact for a 10-year old male subject.....149
- Figure 6-10(b)** Total moment at C4 for (a) Tensed Muscle Impact and (b) Untensed muscle impact for a 50th percentile adult male subject.....149

- Figure 6-11** The EMG activation trace of both the SCM and posterior muscle group for the (a) tensed muscle impact, and (b) untensed muscle impact for a 10-year old male relative to the swing's acceleration and the moment at C4. On average, the SCM's peak EMG occurs prior to the swing's peak acceleration while the posterior muscles' peak EMG occurs after the swing's peak acceleration, regardless of the muscle condition.....155
- Figure 6-12(a)** Raw EMG data for the right hand side muscles for a 10-year old male subject in a tensed muscle impact. The units for the y-axis are in mV.....157
- Figure 6-12(b)** Filtered rectified EMG data for the right hand side muscles for a 10-year old male subject in an tensed muscle impact. The units for the y-axis are in μV158
- Figure 6-12(c)** Raw EMG data for the right hand side muscles for a 10-year old male subject in an untensed muscle impact. The units of the y-axis are in mV.....159
- Figure 6-12(d)** Rectified, filtered EMG data for the right hand side muscles for a 10-year old male subject in an untensed muscle impact. The units for the y-axis are in μV . The difference in the time scale between the raw and filtered data is due to synchronization with acceleration data.....160
- Figure 6-13(a)** Raw EMG data for the right hand side muscles for a 50th percentile adult male subject in a tensed muscle impact. The units of the y-axis are in mV.....162
- Figure 6-13(b)** Rectified, filtered EMG data for the right hand side muscles for a 50th percentile adult male subject in an untensed muscle impact. The units for the y-axis are in μV . The difference in the time scale between the raw and filtered data is due to synchronization with acceleration data.....163
- Figure 6-13(c)** Raw EMG data for the right hand side muscles for a 50th percentile adult male subject in an untensed muscle impact. The units of the y-axis are in mV.....164
- Figure 6-13(d)** Rectified, filtered EMG data for the right hand side muscles for a 50th percentile male subject in an untensed muscle impact. The units for the y-axis are in μV . The difference in the time scale between the raw and filtered data is due to synchronization with acceleration data.....165

- Figure 6-14** The EMG activation trace of both the SCM and posterior muscle group for the (a) tensed muscle impact, and (b) untensed muscle impact for a 50th percentile adult male relative to the swing's acceleration and the moment at C4. On average, the SCM's peak EMG occurs prior to the swing's peak acceleration while the posterior muscles' peak EMG occurs after the swing's peak acceleration, regardless of the muscle condition.....167
- Figure 7-1** Swing pulse and EMG activation trace for SCM showing the two instances where latency was calculated – (1) response to swing release and (2) response to peak swing acceleration.....181
- Figure 7-2** Positive direction of the coordinate system of video image used for measuring head displacement. The measurement shows the calibration of distance measurements.....183
- Figure 7-3** Timing of shock absorber contact – (a) Frame 233 (t=464ms) shows a gap between the shock absorber and the swing frame. (b) Frame 235 (t=468ms), no gap remains. This was considered to be initial swing contact with the shock absorber.....185
- Figure 7-4** Acceleration pulse and EMG traces for the right-side muscles in (a) tensed and (b) untensed muscle dynamic tests for 10-year old male subject. Arrows indicate the time of EMG onset for (1) swing release and (2) peak acceleration. Latency values are shown in tables 7-2 and 7-3 respectively.....189
- Figure 7-5** Acceleration pulse and EMG traces for the right-side muscles in (a) tensed and (b) untensed muscle dynamic tests for 50th percentile adult male subject. Arrows indicate the time of EMG onset for (1) swing release and (2) peak acceleration. Latency values are shown in tables 7-4 and 7-5 respectively.....193
- Figure 7-6(a)** Trajectory of the cg of the head for 10 year old male subjects during tensed muscle, dynamic impact.....198
- Figure 7-6(b)** Trajectory of the cg of the head for 10-year-old male subjects during untensed muscle, dynamic impact.....198
- Figure 7-7(a)** Trajectory of the cg of the head for 50th percentile adult male subjects during tensed muscle dynamic impact.....200
- Figure 7-7(b)** Trajectory of the cg of the head for 50th percentile adult male subjects during untensed muscle dynamic impact.....200

CHAPTER 1 BACKGROUND AND SIGNIFICANCE

1.1 EPIDEMIOLOGY

Motor vehicle accidents remain among the leading causes of injuries and death in children ages 0-18 years of age despite the advances in motor vehicle safety and child safety restraints [Cirak, 2004; Kokoska ER, 2001; Brown RL., 2001].

Although the occurrence of spinal injuries in children is low, accounting for only 1-2% of all reported injuries [Cirak, 2004; Zukerbraun, 2004; Kokoska ER, 2001; Brown RL., 2001], retrospective studies conducted at Level 1 trauma centers in Canada and the United States show that children sustaining spinal injuries have a higher mortality rate (17%) than adults [Kokoska ER, 2001; Brown RL., 2001], a high rate of traumatic brain injuries [Cirak, 2004; Zukerbraun, 2004; Kokoska ER, 2001; Brown RL., 2001], a higher rate of permanent cord injury [Zukerbraun, 2004] and longer hospitalization time than adults [Givens, 1996]. The average age of the patients in these studies was 10 years old.

In all reported pediatric patients sustaining spinal injuries, the injuries were predominantly to the cervical spine. Cirak et al. [2004] found that thoracic injuries accounted for only 1-10% of all reported pediatric spinal injuries, depending on the study. Cervical spine injuries in children are categorized as either muscular sprains or vertebral and spinal cord injuries. Of the 1-2% of reported spinal injuries, 68% are muscular sprains and of this group, 82.3% are located in the cervical spine [Cirak, 2004].

Anatomical immaturities in pediatric patients together with their relatively large head cause the fulcrum, or point of rotation, of the head/neck to be higher in children than in adults [McCall, 2006; Cirak, 2004; Zukerbraun, 2004; Lustin 2003]. Studies have shown that children ages 0-8 years most frequently sustain injuries between the occiput and C4, whereas adults with cervical spine injuries typically have injuries below C4 [McCall, 2006; Cirak, 2004; Zukerbraun, 2004; Lustin 2003; Kokoska ER, 2001; Brown RL., 2001]. Although most studies have shown that children older than 8-years old exhibit adult-like injury patterns, the spinal anatomy continues to change late in adolescence. Unlike adult patients with spinal injuries, differences in the pediatric anatomy make the diagnosis of spinal injuries in pediatric patients difficult. Prior to the prevalence of MRI and CT in hospitals, pediatric patients frequently presented with spinal cord injuries without any radiologic abnormalities (SCIWORA). Retrospective studies found 46% of pediatric patients had no radiologic abnormalities [McCall, 2006; Cirak, 2004; Kokoska ER, 2001; Brown RL., 2001].

Traumatic head injuries are present in 94% of the spinal injuries cases reported [Cirak, 2004; Zukerbraun, 2004; Kokoska ER, 2001; Brown RL., 2001]. In many cases, brain injury was considered to be the cause of death. Given the severity of closed head injuries in children injured in a motor vehicle accident, Brown et al., have proposed that the occurrence of neck injuries may be overlooked and under reported [2001].

A study by Givens et al. looked at the socio-economic effect of spinal injuries in children and found an increase in the length of hospital stays and

recovery time in children [1996]. While the occurrence of reported neck injuries in children is low, the implications are significant.

1.2 RESPONSE AND SCALING

The most comprehensive response data for the mid-size male neck in flexion and extension was developed by Mertz and Patrick [1969, 1971]. Other work contributing to the biofidelic response of the dummy neck was conducted by Ewing et al. [1968] and Tarrière et al. [1969]. The Mertz and Patrick study defined the range of motion of the head relative to the torso, the static strength of the neck in flexion and extension, and the dynamic strength and response of the neck in flexion and extension (figs 1a and 1b). In 1976, Patrick and Chou undertook a similar set of experiments to determine the human neck's response in 90° lateral bending. However, the 90° corridor (Figure 1c), like the flexion and extension corridors, is based on data obtained from dynamic tests of a sample of four mid-sized males (per 1960 census data) volunteers.

These corridors represent the response of the neck by describing the moment of the head relative to its angle of displacement from the neutral position. Based on shape of the curve and knowledge of a generic stress-strain curve, it can be inferred that the corridors describe the behavior of the head and neck as follows:

- (1) The initial slope of these corridors represents elastic deformation of the muscles and ligaments of the neck within the physiologic range. In this region no injury or pain was reported.

- (2) Eccentric muscle contraction occurs in the plateau region, a region of constant moment resistance, representing a region of plastic deformation [Miller, 2003].
- (3) The threshold of pain occurs beyond the plateau region where muscle fibers and ligaments begin to stretch beyond their physiologic limits. Further up this slope above the plateau region ligamentous injury begins to occur. The studies were conducted with both relaxed and tensed muscle tone to obtain a full understanding of the neck response. The area under the curve is determined by the muscle tone of the neck at the time of impact. The upper limit of the curve in the non-injurious region represents a maximally contracted muscle, or the maximum muscle response.

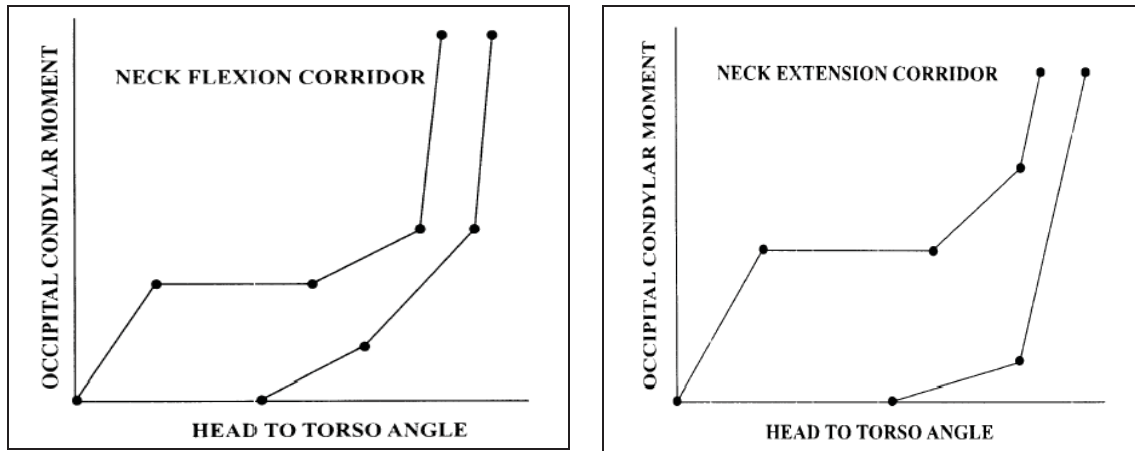


Figure 1-1(a): Neck Response Corridor in Frontal Flexion [Mertz and Patrick, 1971]

Figure 1-1(b): Neck response Corridor in Extension [Mertz and Patrick, 1971]

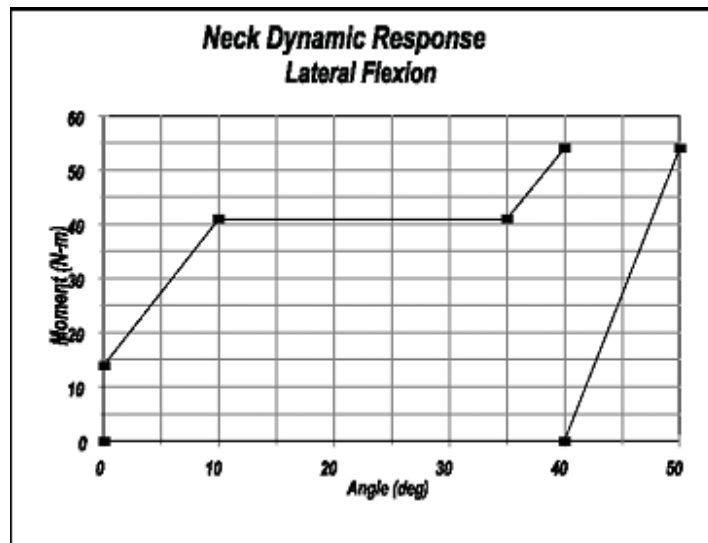


Figure 1-1(c): Lateral Flexion Corridor [Patrick & Chou, 1976]

The 50th percentile ATD mechanical neck incorporates, as closely as possible, the flexion and extension response data of Figures 1a and 1b so as to perform biofidelically in frontal impact events [Culver, 1972; Wismans, 1983]. The mechanical neck's response in lateral bending was a secondary consideration in

the Hybrid III design and therefore, not incorporated. Later, a Side Impact Dummy was developed to evaluate the performance of an occupant in a lateral impact event; however, the mechanical neck used in the design was that of the Hybrid III frontal ATD. Newer ATD's such as THOR [NHTSA, 2001] and World SID [Cesari et al, 2001] include the lateral bending corridor proposed by Patrick and Chou [1976] (Figure 1c) in the design criteria for the mechanical neck.

When the safety regulations increased their scope to include the evaluation of restraints for children and small females, there was a need for small female and child ATD's. Pediatric cadaveric data was not available from which to develop the 3-year-old ATD, therefore, the child ATD was developed from the data of the mid-size male using a scaling technique developed by Wolanin and Mertz [1982]. The scaling model assumes 1) equivalent stress, meaning that force per unit of cross-sectional area is constant between adults and children; 2) equivalent geometry and 3) equivalent moment arms. Mathematically this is expressed as

$$M_C = M_A * \frac{A_C * D_C * \sigma_C}{A_A * D_A * \sigma_A}$$

Where:

M_A = Moment of the adult head about the neck

M_C = Moment of the child head about the neck

A_A = cross sectional area of the adult neck

A_C = cross sectional area of the child neck

D_A = the moment arm of the adult neck

D_C = the moment arm of the adult neck

σ_A = physiologic stress of the adult muscle

σ_C = physiologic stress of the child muscle

In the absence of pediatric physiologic data the ratio of σ_C/σ_A was assumed to be one. Using the linear relationship of the neck anthropometry developed by Snyder et al. [1972] the equation was reduced to

$$M_C = M_A \times \lambda_{NC}^3$$

Where

$\lambda_{NC}^3 =$ is the scalar of $(A_C \times D_C)/(A_A \times D_A)$

This scaling model was also used to develop the small female ATD, the 12 month old Child Restraint Air Bag Interaction (CRABI) dummy, the 6-year old Hybrid III dummy and most recently the 10-year-old Hybrid III dummy.

In 2003 Miller et al. evaluated the validity of the scaling relationship described above by comparing the anthropometry and muscle strength of adults and children in a two part study. In part one of the study MR-images of the neck were used to determine if a relationship existed between the age of the subject and the diameter, circumference, moment arm and cross-sectional area of the neck. Using a linear regression analysis of the neck circumference data and the moment arm data showed that the linear relationship assumed by Wolanin et al. [1982] in designing the child crash dummy does exist, as shown below in figure 1-2.

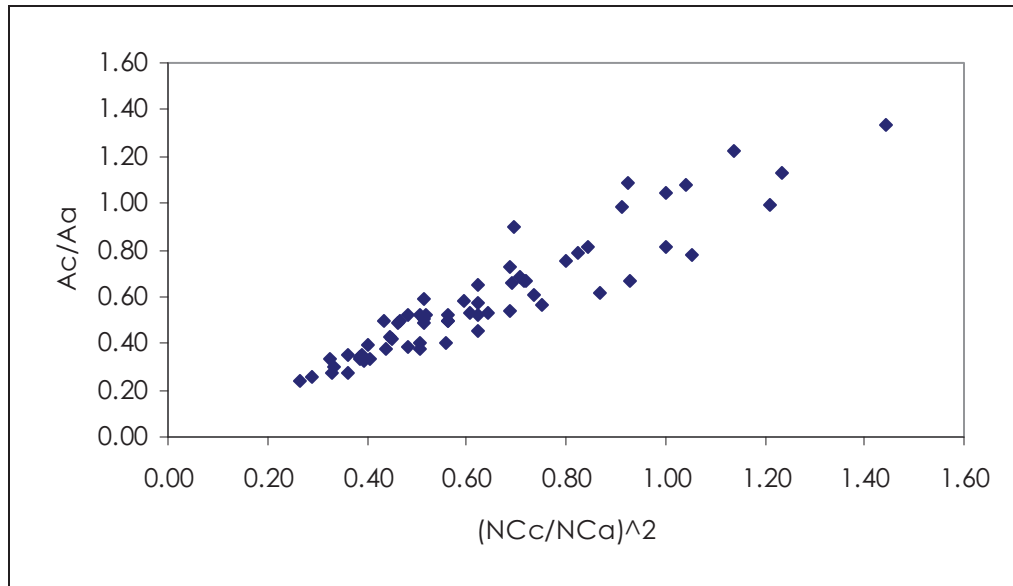


Figure 1-2: Neck Muscle Cross-Sectional Area Regression and Scaling Law [Miller, 2003]

In the second part of the study, an exercise machine measured the eccentric muscle force generated in the biceps brachii of the arm. Although arm muscles were used rather than neck muscles, the eccentric contraction of these muscles simulated the plateau region of the neck response curves developed by Mertz and Patrick [1974]. The muscle stress was calculated using the measure muscle force recorded from the exercise machine and the physiologic cross-sectional area of the biceps brachii, as determined from the MRI protocol. A regression analysis of the muscle stress of the biceps brachii to the age of the subject showed a positive slope of increasing muscle stress with age rather than the traditionally hypothesized equal stress.

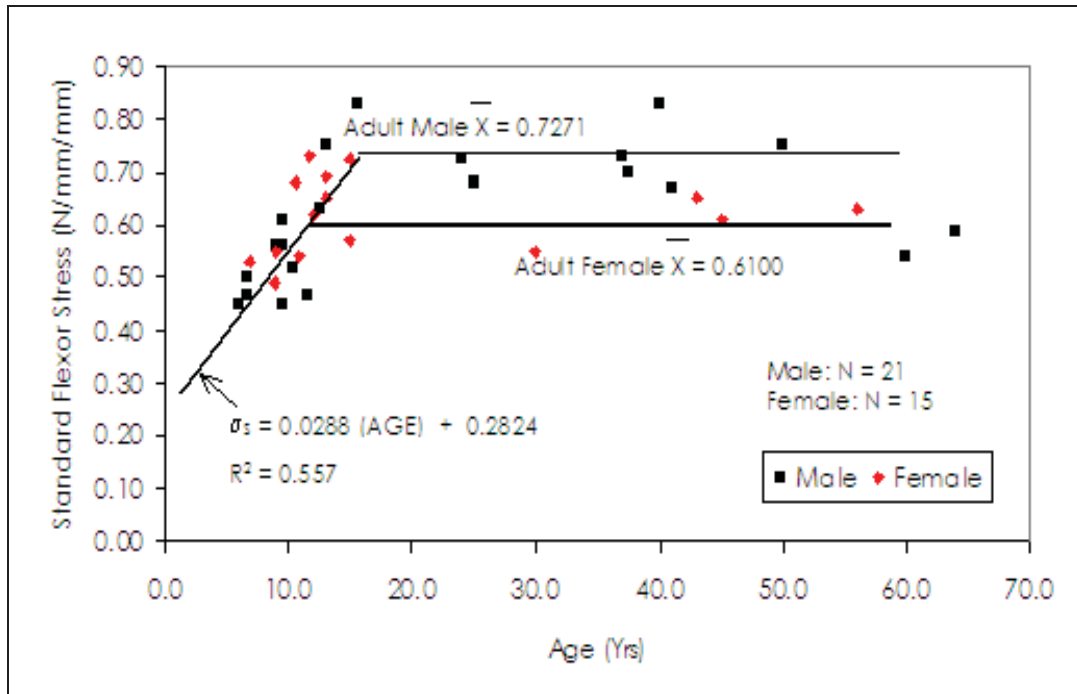


Figure 1-3: Standard Flexor Stress Regression Model [Miller, 2003]

The results of the Miller study are comparable to results obtained in other studies in which muscle specific tension, or stress, defined as force over physiologic cross-sectional area (F/PCSA), was compared to that measured in adults. In their 1994 study Kanehisa et al., calculated the strength to CSA ratio of the quadriceps femoris in adults and children of both genders. Strength was measured at multiple speeds on an isokinetic dynamometer. Anatomical cross-sectional area was measured mid-thigh using an ultrasonic device. The results showed that adults had significantly higher strength to CSA ratio than children ($P < 0.05$). The results also showed that the differences in this ratio increased with increasing contraction velocity. Although the cause of this increase was not specifically addressed, it was suggested that the lesser stress value may be attributed to a child's inability to fully recruit their motor units as the speed of

contraction increased. Halin et al. [2003], studied the ability of children to recruit motor units by calculating the muscle stress in arm muscles of adult males and young boys in a fatigue study. The results showed that the stress in adult males was significantly higher than in young boys ($P < 0.001$). The study also showed that young boys fatigued at a faster rate than adult males, suggesting that young boys are less able to recruit their type I (slow twitch) muscle fibers. In other studies Kanehisa et al. [1994, 1995] reported a significant difference in stress of the ankle plantar between subjects ages 10-12 years old and subjects ages 16-18 years old ($P < 0.001$) even when the cross-sectional area was normalized to limb length. Sunnegardh et al. [1988] also reported an increase in stress from ages 7-13 years of age. In a longitudinal study of children ages 10-14 years of age, De Ste. Croix et al. [2002] reported an increase in the muscle stress of the leg flexors and extensors with age but noted that cross-sectional area was not the only predictor of muscle strength, citing muscle mass and stature as confounding factors. Not all studies agree with these findings; notable studies by Deighan et al. [2002a, b] found no difference in the muscle stress of elbow flexors and extensors with age. Differences in the location of the measurements may account for their results.

Few studies have been conducted to evaluate the changes of muscle stress with age in the neck muscles. Mayoux-Benhamou et al. [1989] measured the muscle stress in the dorsal neck muscles, but did not consider potential differences in this measurement with respect to aging. In a 2001 study, Vasavada et al. measured the neck moments at multiple levels of the neck and in

multiple directions for both male and female subjects. Male subjects produced higher neck moments than female subjects, however, these differences between the two genders could not be accounted for using only the Wolanin scaling model. A similar result was obtained in a cervical strength study by Garces et al. [2002]. The discrepancy between what is predicted by the model and what is actually measured suggests that the Wolanin model is incomplete in its current form.

In a series of studies by Kumar et al. [2000, 2001, 2003, 2004, 2005], the electromyographical (EMG) response of specific neck muscles, sternocleidomastoid, splenius capitis and trapezius, was reported in various loading directions in both quasi-static and dynamic loading conditions. These studies showed that the muscles had different activation levels and that the activation levels changed as the direction of the impact changed. Muscle activation levels are defined as the levels of electrical potentials of an activated muscle cell [Vander, 1990]. Their studies attempted to quantify the force in each individual muscle during these impact events but fell short of resolving the total neck force into components. Stress was not evaluated in their study, nor were children.

To date, little child neck response data exists. Heidleberg University in Germany [Cassan et al., 1993] ran tests that compared the response of the 3-year old child dummy to that of a child cadaver matched for size, age and weight. The dummy and cadaver were similarly restrained and tested in a series of frontal impacts ranging from 31-50km/h. The results showed that under the same

test conditions, the cadaver had greater head excursion than the dummy, indicating that the dummy neck is stiffer, as shown Figure 4.

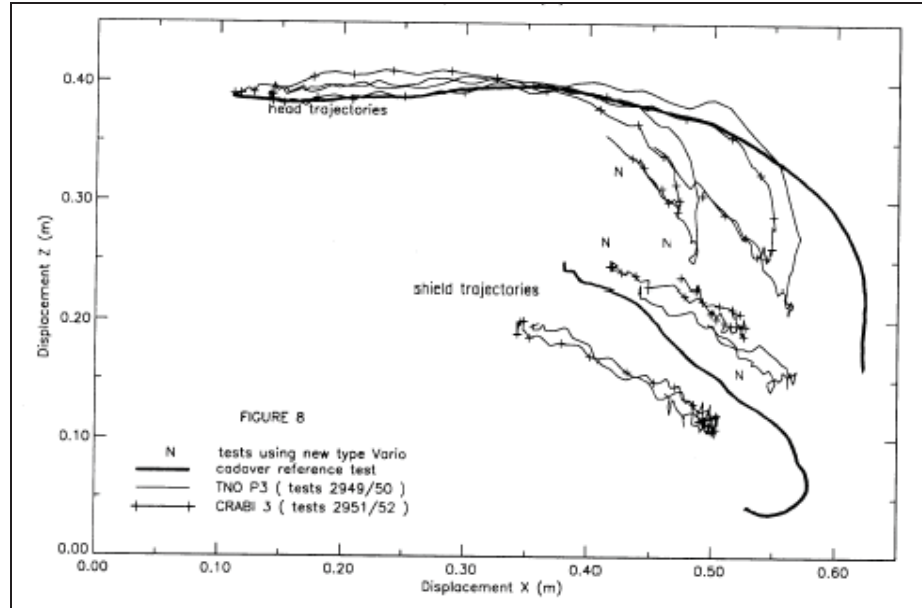


Figure 1-4: Head excursion comparison between child cadavers (bold black trace) and crash test dummy (light black lines) with respect to the trajectory of the child restraint shield. The cadaver excursions are greater in both the x and z-directions [Cassan FB., et al., 1993]

Wismans and Maltha [1979] also compared the performance of child crash test dummies to the responses of child cadavers matched for age, size and weight. They found that “the most significant difference between the dummy and cadaver response was the motion of the head and upper torso.” [Wismans, 1979] The cadaver had a head excursion of 37cm as compared to the dummy’s head excursion of 29cm. In their test, the cadaver struck the arm rest of the child seat “which was not the case with the dummy due to its greater stiffness” [Wismans, 1979]. Based on their studies comparing child cadavers to child dummies, Kallieris et al. also concluded that due to their stiffness, dummies can be used for

“rough” evaluations of child restraints but that studies with child cadavers were necessary to determine tolerance limits and protection criteria [1976]. In accident reconstruction studies Newman et al. [1993] found that in addition to the stiffer ATD neck, the dummy was under-predicting neck tension and extension loads.

In the year 2001 there were an estimated 42,116 people killed in motor vehicle crashes [reported by NASS-GES, NHTSA docket# 02-12151]. Of this group, approximately 3% were children between the ages of 0 and 8 years old. In 2000, 2,938,000 people were injured in motor vehicle accidents. Of this group, children accounted for approximately 5%. Although the percentage of child fatalities is small, frontal and side crashes remain the number one cause of death and a significant cause of injury for children in the 0-8 year old age group.

As the regulations governing automotive safety improve, there is an opportunity to upgrade and improve the surrogates (ATDs) that are used to determine safety system compliance. It is critical that child neck strength be studied and understood so that surrogates can be properly designed to reduce child head and neck injuries.

1.3 SPECIFIC AIMS

This is a basic science study in which the physiologic differences between the neck response of adults and children were quantified. The objective of this research was to compare the neuromuscular response in the neck between adults and children, and to determine if differences affect the ability of the neck muscles to generate force and limit head movement during an impact event. The specific aims of the study include:

1. Calculation of the physiologic cross-section area (PCSA) of the sternocleidomastoid, the splenius capitis, the trapezius and the scalene muscles in 50th percentile adults males and 10-year old boys using Magnetic Resonance Imaging (MRI).
2. Determination of Electromyographic (EMG) activation values for the sternocleidomastoid, the posterior neck muscles, the postero-lateral neck muscles and the scalene muscle; and to calculate the reaction force for the sternocleidomastoid, the splenius capitis, the trapezius and the scalene muscles for adult males and 10-year boys under quasi-static loading conditions.
3. Determination of Electromyographic (EMG) activation values – the value in μV , of the electrical potential of the active muscle (see Chapter 2) - for the sternocleidomastoid, the posterior neck muscles, the postero-lateral

neck muscles and the scalene muscle; head acceleration and head excursion for adult males and 10-year boys in a low speed frontal impact.

4. Determination of physiologic muscle stress in quasi-static and low-speed dynamic loading conditions for adult males and 10-year boys. Based on the calculated muscle stress, determine whether equal stress, as assumed in the Mertz and Wolanin scaling relationship [1982] is a valid assumption.

The specific aims and hypotheses of this study were evaluated through a series of studies. A flow chart showing what was expected of each subject and how the collected data was used is shown below in figure 1-5.

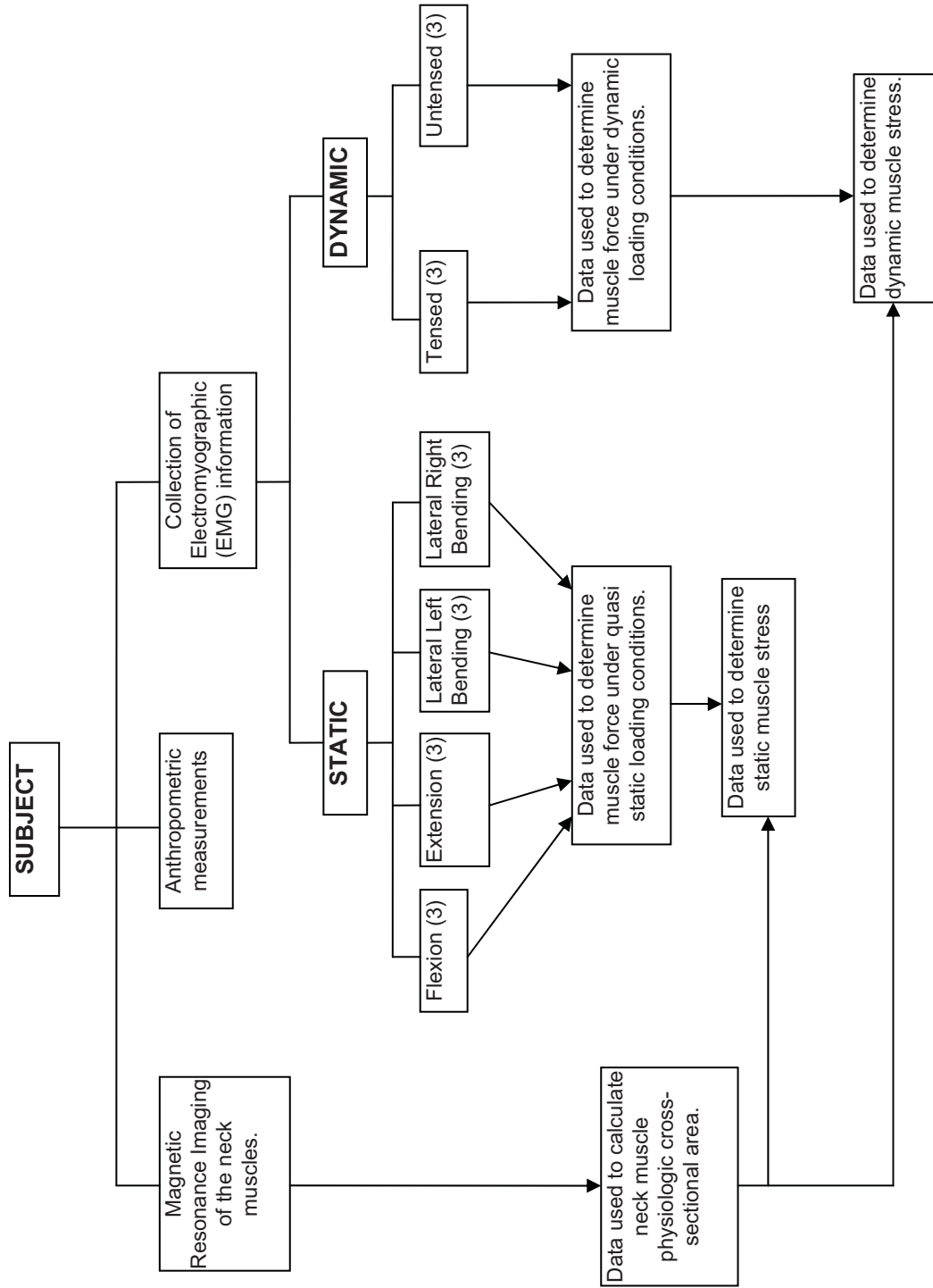


Figure 1-5: Study Flow chart showing the various data collected and their analytical objective.

It is hypothesized that due to a child's inability to fully recruit his/her muscles that,

1. The neck muscles stress under static loading (MVC) will be greater in adults than in children. That is that the ratio of muscle stress between adults and children will not equal to 1.0 as previously assumed.
2. The ratio of child to adult muscle stress will be less during the untensed dynamic condition than during the tensed dynamic condition and both these ratios will be less than during the static loading condition. It is expected that, regardless of the loading condition, that all ratios will be less than 1.0 as previously assumed.
3. The relative head excursion of the child will be greater than that of the adult, even during the tensed impact condition. This will be further proof of recruitment deficiencies in children given that both the adult and the child subjects were tensing their muscles prior to impact eliminating any issues associated with latency of the signal from the brain.
4. The latency between the onset of muscles activation and swing acceleration will be greater in children than adults during the dynamic events due to the differences in their ability to recruit their muscles

CHAPTER 2: ANATOMY AND PHYSIOLOGY OF THE CERVICAL MUSCLES

2.1 INTRODUCTION

The neck determines “the global movement of the head relative to the rest of the body” [Lee, 2006]. It acts as a conduit for the blood vessels to and from the brain and encloses the spinal cord. Injuries to the neck, particularly the spinal cord in the cervical region have significant life altering and potentially life ending consequences. The muscles of the cervical spine provide a means of protecting the cervical spine by stabilizing and maintaining posture of the head. This stability is effected through reflexive neuromuscular response strategies.

2.2 ANATOMY

2.2.1 Bony Structure of the Neck

The neck consists of a bony structure of seven cervical vertebrae. C1, called the atlas is a “ring-like, kidney shaped bone” [Moore and Daley, 1999] that carries the skull. C2, called the axis has a bony protuberance, the odontoid process, which projects upwards from its body and mates to the dens foramen which is held in place by the transverse ligament. These vertebrae, together with the 7th cervical vertebra, are irregular in their shape relative to the other vertebrae of the cervical spine. C7 called the vertebral prominens, has a long spinous process. The 3rd – 6th cervical vertebrae are typical vertebrae in size and shape.

The vertebrae are separated by intervertebral discs provide flexibility. The spinal column also articulates about a series of zygapophysial joints located at

each vertebral arch. The cervical spine is held together by a series of ligaments. The vertebral column encloses and protects the spinal cord. Figure 2-1 shows a mid-sagittal view of the cervical spine.

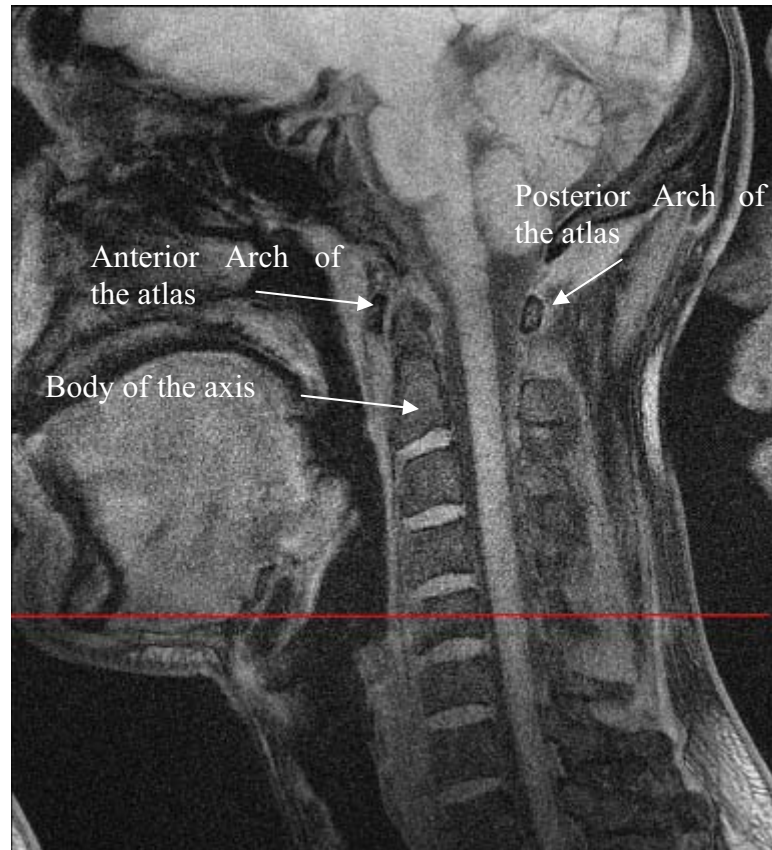


Figure 2-1: MR-image of the bony structure of the cervical spine. MR-image was part of the imaging protocol contained in this study.

2.2.2 Musculature of the Neck

The muscles of the neck are divided into superficial and deep structures. These muscles provide stability to the head and neck and allow for the flexion, extension and rotation of the neck and head. Figure 2-3 shows both an MR-image taken from the imaging protocol in this study and a drawing of the same cross-section.

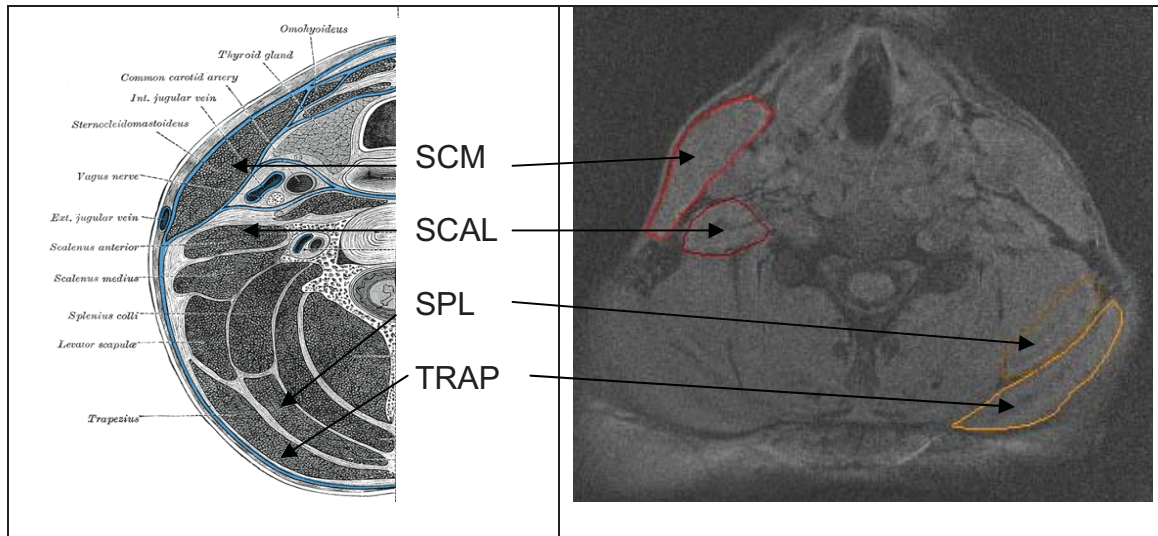


Figure 2-2: Cross-sectional area of the neck at C4 showing the musculature of the neck.

In this study, the forces and moments of the sternocleidomastoid, the trapezius, the splenius capitis and the scalene muscles were determined under static and dynamic loading conditions and in both flexion and extension. These muscles were used because they are superficial neck muscles that can easily be identified and instrumented. The responses of these muscles were considered to be similar to the deeper muscles with similar orientation and function. These deeper muscles include, in the posterior muscle group the splenius cervicis, semispinalis capitis, semispinalis cervicis and multifidus. In the postero-lateral muscle group, the deep muscles include, the longissimus, and in the anterior/antero-lateral muscle group, deep muscles include, the longus colli and longus cervicis.

The sternocleidomastoid (SCM) is a large superficial muscle on the anterior aspect of the neck. It attaches superiorly to the lateral surface of the mastoid process of the temporal bone and to the superior nuchal line. Inferiorly, it

has two heads; the sternal head attaches to the manubrium of the sternum and the clavicular head attaches to the superior surface of the clavicle [Moore and Daley, 1999]. Working bilaterally, the primary function of the SCM is to flex the neck [Moore and Daley, 1999]. The trapezius muscle is “a large, flat, triangular muscle that covers that covers the posterolateral aspect of the neck and thorax” [Moore and Daley, 1999]. The primary function of the cervical fibers of the trapezius is to elevate the scapula. At its origin of the trapezius attaches to the medial third of the superior nuchal line -a bony ridge that extends on each side of the skull from the occipital protuberance to the mastoid process of the temporal bone [Merriam-Webster, 2002] -the external occipital protuberance, the ligamentum nuchea and the spinous processes of C7-T12. [Moore and Daley, 1999] The trapezius inserts on clavicle, the acromion process and the spine of scapula. The splenius capitis, a deep cervical muscle, lies under the trapezius. Acting bi-laterally, the splenius capitis extends the head and neck. The splenius capitis also flexes and rotates the head [Moore and Daley]. The splenius capitis has its origin on the ligamentum nuchea and the spinous processes of T1-T6. It inserts on the lateral aspect of the mastoid process and superior nuchal ligament. The scalene muscles, anterior, posterior and middle, are also deep cervical muscles. Their primary function is to flex the neck laterally. The anterior scalene also rotates the neck. The muscles originate on the posterior tubercles of the transverse processes of C4-C6 (posterior and middle scalene) and the transverse processes of the C4-C6 vertebrae (anterior scalene). The scalene

muscles insert on the 1st and 2nd ribs [Moore and Daley, 1999]. Figure 2-3 (a)-(d) shows all the muscles described above.

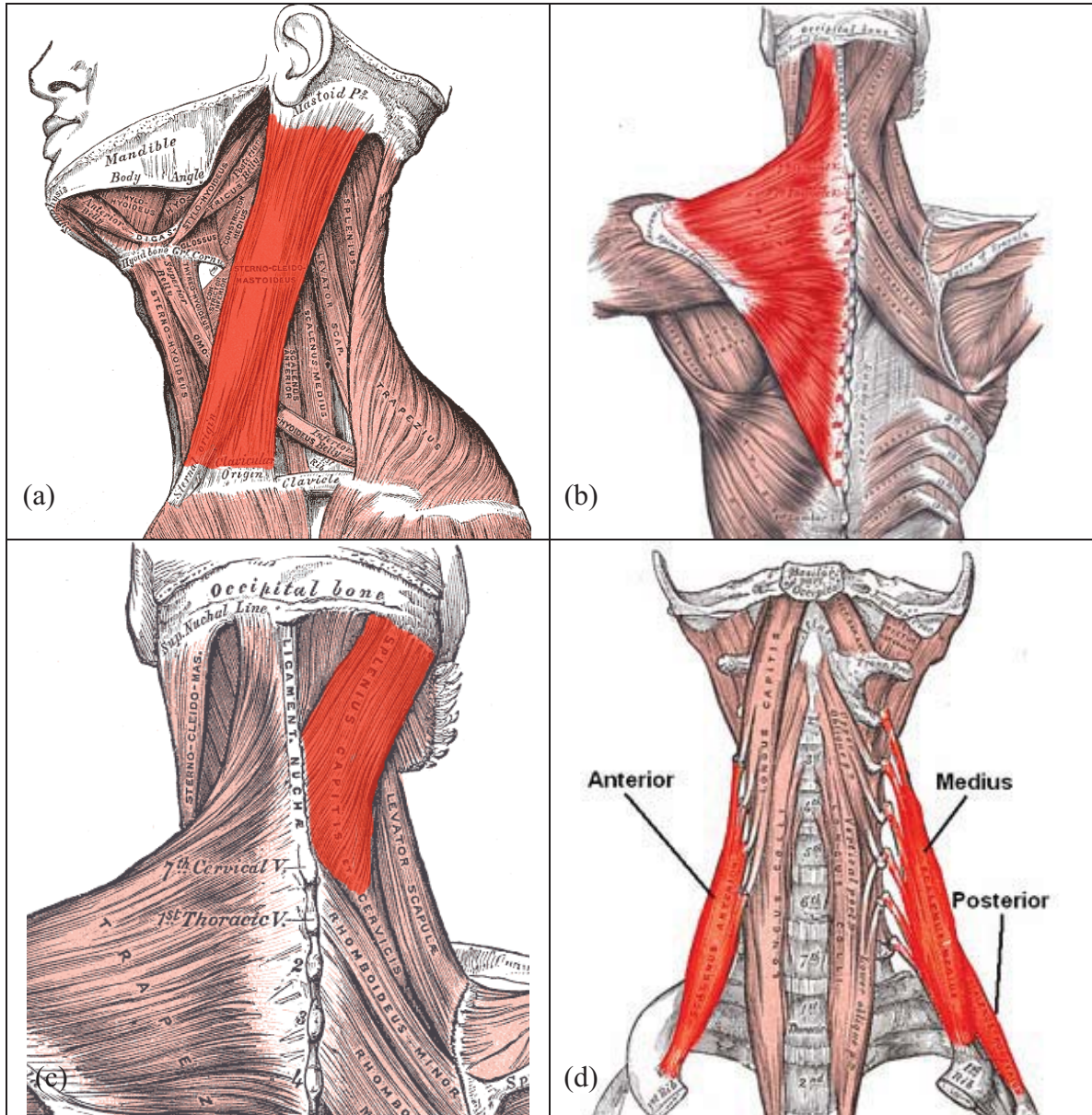


Figure 2-3: Illustrations from *Gray's Anatomy* [1918] showing (a) the sternocleidomastoid, (b) the trapezius, (c) the splenius capitis and (d) scalene muscles

Although the splenius capitis and scalene muscles are considered to be deep cervical muscles, they wrap from the lateral aspect of the neck to the posterior

aspect of the neck through the posterior triangle of the neck. The posterior triangle of the neck is a triangle bounded by the sternocleidomastoid, the trapezius and the clavicle. In the posterior triangle of the neck, they are the most superficial muscles.

2.3 MUSCLE PHYSIOLOGY AND NEURAL CONTROL

The mammalian skeletal muscle is organized in a series of progressively larger bundles of fiber-like units held together by connective tissue. The largest bundle, the muscle itself, is a collection of muscle fascicles which is in turn a bundle of muscle fibers (Figure 2-4).

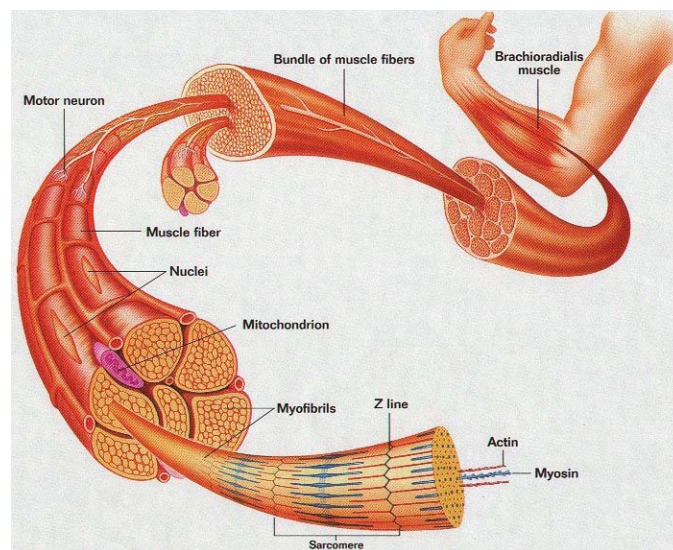


Figure 2-4 Structure of a Muscle (www.sirinet.net/~jgjohnso/amuscle.html)

A single muscle fiber is a multinucleated cell that developed from the fusion of myoblasts, mononucleated cells, during fetal development. It consists of

a bundle of myofibrils. The thick and thin filaments of the myofibril make-up the sarcomere; this is the contractile unit of the muscle. Single fiber contraction is achieved when the thick and thin filaments of the myofibrils slide relative one another, described by the “sliding filament” theory. Full muscle contraction occurs when parallel sarcomeres in parallel fibers contract in unison.

Muscle contraction is the result of cross-bridge cycling, the act of the myosin globular head repeatedly binding to and releasing from the actin molecule. The cycle is a multi-step process initiated by the infusion of Ca^{2+} into the cell. The release of Ca^{2+} into the cell is controlled by the electrical depolarization of the muscle plasma membrane, known as an action potential, or in the case of a muscle, a motor unit action potential (MUAP). Depolarization of the muscle plasma is initiated by stimulation of the motor end plate of the muscle by the motor neuron using control strategies originating in both the central nervous system (CNS) and the peripheral nervous system (PNS) depending on the motion or response required from the muscle. Together the motor neuron and muscle fibers it stimulates make up the neuromuscular unit. Motor neurons originate in either the brainstem or the spinal cord. The axons of the motor neuron are the largest diameter neuron, and myelinated for high velocity signal transmission [Vander, 1990].

The action potential in the muscle-plasma membrane releases the neurotransmitter acetylcholine to the muscle fiber resulting in a muscle action potential. It is the muscle action potential that causes the release of Ca^{2+} into the muscle fiber. This influx of Ca^{2+} facilitates the cross-bridge cycling mentioned

above. The cross-bridge cycling causes the muscle fiber to contract or **twitch**. Muscle contraction is the result of the superposition of all muscle twitches. Electromyography (EMG) records the superposition of the electrical potentials of the muscle action potentials generated during muscle contraction [Normann, 1988]. Measures of muscle activation provide information on not only the normal functioning of the muscle or motor unit, but also information on damaged or diseased muscles, and on the neural control of muscle.

The tension developed in a muscle is governed by (1) the tension developed in each muscle which is regulated by the influx of Ca^{2+} , as described above and (2) the number of muscle fibers recruited during the contraction [Vander, 1990]. Both the depolarization of the membrane and the recruitment of muscle fibers are regulated by neuromuscular recruitment strategies that vary depending on whether the movement is a voluntary action or an involuntary action. Although let it be noted that no movement is completely voluntary or completely involuntary. While a particular motion may be made consciously, muscles of postural support or the inhibition or an antagonist action are involuntarily activated as well [Vander, 1990]. All movement is controlled by a hierarchy organization of brain centers through a series of feedback and feed forward loops as shown below in figure 2-5.

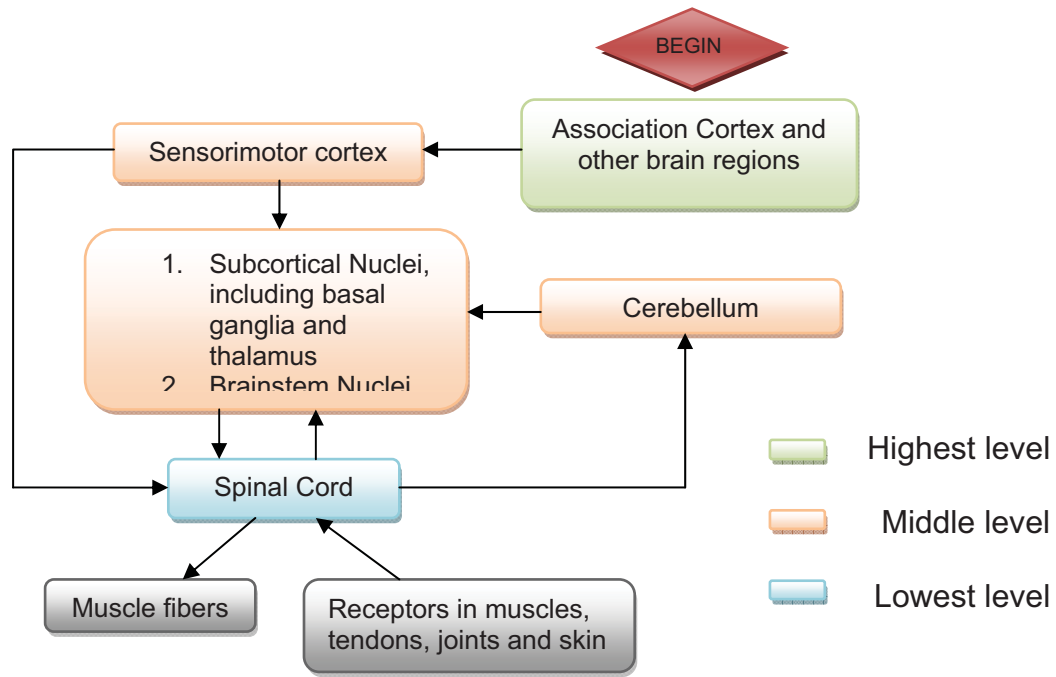


Figure 2-5: Hierarchy of motor control [Vander, 1990]

It is the neurons in the middle level of the motor control hierarchy that determine the “motor program” [Vander, 1990] required to execute specific movements. In most cases, voluntary motion requires coordination from all levels of the hierarchy, although newer studies are beginning to show that repetitive motion such as walking are controlled by a central pattern generator, neural networks capable of effecting motion independent of central input [Hooper, 2000]. Reflex actions also use the hierarchy, but instead of motion being initiated in the highest level, input from the muscles to the spinal cord produces a muscle response [Vander, 1990]

The reflex response in skeletal muscles is initiated in response to muscle lengthening or in response to pain. The pain reflex pathway is not discussed in this paper. Muscle lengthening is monitored by stretch receptors - specialized

structures called muscle spindles which consist of muscle fibers embedded with the nerve endings of afferent nerve fibers [Vander, 1990]. Stretch receptors act in response to two kinds of stimuli – (1) the magnitude of the stretch, or (2) both the magnitude and the speed with which the muscle-spindle has been stretched. The response is generated through the spinal cord rather than higher centers of motor control, causing one of several muscle contraction outputs – (1) contraction of the stretched muscle and/or synergistic muscles; and (2) contraction of the stretched muscle and/or inhibition of antagonist muscles.

In the neck there are additional reflexive pathways with the specific purpose of stabilizing the head and maintaining posture. [Morningstar, 2005]. These pathways are (1) the vestibular collic, (2) the cervicospinal and (3) the vestibular ocular. These pathways are able to operate independently or in combination [Squire, 2003]. The ocular and vestibular pathways, acting independently, use sensory input of the eye and vestibular organs to relay information to the higher centers of the brain, including the colliculus, information about the position of the head. The eyes provide visual input to determine the position of the head relative to a stable base – when standing, this base is generally the feet. [Morningstar, 2005] Information ascends from the optic nerve. The vestibular system is a significant component in maintaining posture of the head and is particularly pertinent to the reflexive muscle response in impact conditions. The organs of the vestibular system, shown below in figure 2-6, the utricle, saccule and semicircular canals are designed to detect specific types of motion [Morningstar, 2005]

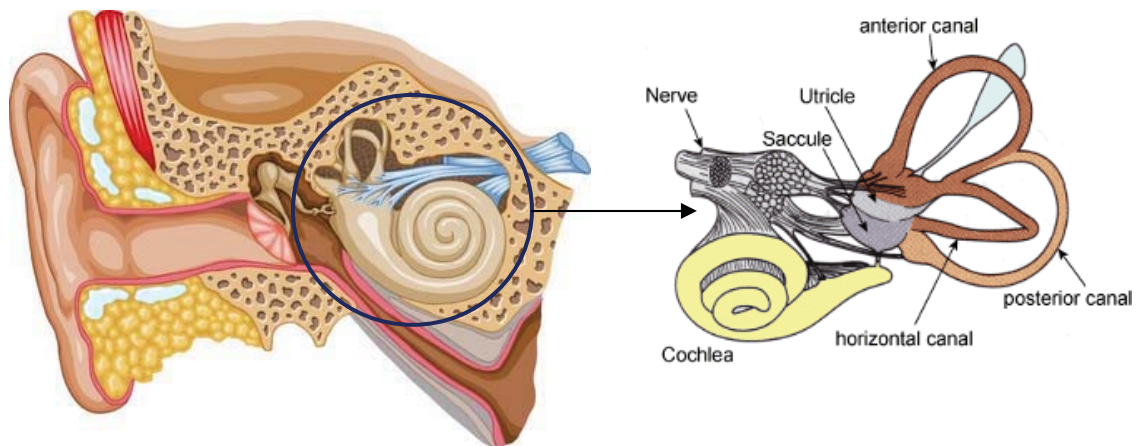


Figure 2-6: Cross-section of the ear and vestibular organs contributing to the vestibular-ocolic reflexive pathway. Images from http://www.thefullwiki.org/Vestibular_system#Vestibulo-ocular_reflex_.28VOR.29

The utricle and saccule detect linear acceleration relative to a baseline acceleration of 1g. The canals detect angular acceleration. The sensory information is carried through the vestibular nerve. The vestibular colic has a very short latency response period, approximately 24.5ms. This was demonstrated in a study by Ito et al. [1997] in which the latency of muscle response in a 1g head drop of normal patients was compared to that of labyrinthine deficient (LD) patients. Normal patients showed increased EMG within 24.5ms of head drop while LD patients showed no muscle response until 67.4ms after head drop. The LD patients had a latency response consistent with a cervicospinal reflexive response [Hain, 2009]. The cervicospinal reflexive pathway is similar to the stretch reflex of the limbs. Due to the large number of flexor/extensor and postural muscles in the neck, there is a high density of muscle spindles in the neck which oppose the lengthening of the cervical muscles [Squire, 1997, Morningstar, 2005]. In addition to the muscle spindles, there is variety of

mechanoreceptors in the neck that serve to provide information about the posture of not only the head/neck but the trunk as well. These include receptors in the facet joints and capsules and the spinal ligaments. The reflexive response of the cervicospinal reflexive pathway is coordinated in the brainstem, and as mentioned previously, has a relatively long latency of muscle response (approximately 67.4ms) when compared to other reflexive pathways in the cervical region.

Although these reflexive pathways have been described individually, reflexive response for stabilizing the head is generally due to a combination of two or more of these pathways, in particular, the interaction of the visual and vestibular systems – the vestibular-ocular response pathway which serves to compensate for motion head through various eye movements [Morningstar, 2005]. Similarly, the cervico-ocular is an interaction between the cervicospinal and visual reflexive pathways where eye movement changes in relation to trunk movement [Morningstar, 2005].

2.4 SUMMARY

The objectives of this study include the study and analysis of the EMG and neuromuscular responses of the muscles in the neck. Comparisons will be made between these responses in adults and children to further understand the development of the neuromuscular system and how immaturities affect a child's ability to stabilize the head relative to the body in impact situations.

CHAPTER 3: SUBJECT SELECTION AND ANTHROPOMETRICS

3.1 INTRODUCTION

3.1.1 Subject Selection

The objective of this study was to compare the neck responses of the 50th percentile adult male to that of the 50th percentile 10-year-old male. Subjects in this study were screened to meet the height and weight criteria of a 50th percentile. Adult male subjects were considered to be 50th percentile if they weighed 170lbs+/-10lbs and were 68-70 inches in height. Boys, ages 9-11 years old, weighing 77.5lbs +/- 2lbs and 50-52 inches in height were recruited for this study.

The range of weight and height stipulated for this study is consistent with the published specifications for the 50th percentile adult male Hybrid III and the 10-year old Hybrid III Anthropometric Test Devices (ATD's). The height and weight range for the 10-year-old boy also corresponds to the Centers for Disease Control growth charts, published May 2000. Relative to the population in the United States, data published by Ogden et al., [2003] and the National Center for Health Statistics [2008] show that for similar heights, the average weight of both the 50th percentile adult male and 50th percentile 10-year old male has increased by approximately 10lbs in the last 30 years. The Hybrid III dummies do not reflect this increased weight. Subjects in this study were chosen to match ATD specifications.

3.1.2 Subject Contra-Indications

Subject selection was limited to healthy adult males and boys age 9-11 years old who have no prior history of neck injury or chronic neck pain. Subjects who were considered to be overweight or obese were excluded from the study. In addition, those participants with a neuromuscular disorder, those who were extremely inactive with under-developed muscles and those who were highly active with overdeveloped muscles were excluded for the study. Participants were also screened for contraindications to magnetic resonance imaging including, but not limited to:

- orthopedic implants
- intracranial vascular clips
- implanted electronic devices such as neural stimulators and pace-makers,
- heart valves
- claustrophobia

This research plan was approved by the Wayne State University Human Investigations Committee (HIC) on February 1, 2005. Re-approval was obtained in December 2006. The approval number for the study is 121204M1F. The paediatric HIC was approved April 3, 2007; HIC approval number 026307MP4F.

3.2 METHODS

3.2.1. Anthropometric Measurements

Subject anthropometrics were measured at the beginning of the study.

Measurements included in the study were:

- **Weight** – measured using a bathroom scale
- **Standing height** – measured with the subject standing with his back to a wall, feet together, heels against the wall. Standing height was measured from the crown of the head to the floor with a tape measure.
- **Neck Circumference** – measured using a cloth tape measure, except where neck circumference data was missing, then neck circumference was calculated from MR-images at C4.
- **Seated Erect Height** – measured on the dynamic test fixture, from the crown of the head to the top of the fixture's seat cushion.

3.2.2 Calculation Neck Circumference from MRI

Using the MR-images obtained during this study, neck circumference was calculated at C4 for all subjects. Calculated results were compared to measurements taken with the cloth tape measure as described above.

The cross-sectional area of the neck can be approximated as an ellipse (figure 3-1), where circumference is calculated according to the following formula,

$$C_{\text{ellipse}} = \pi \sqrt{2 * \left[\left(\frac{1}{2} LA \right)^2 + \left(\frac{1}{2} SA \right)^2 \right]}$$

Where,

The **short axis (SA)** follows the axis of the saggital plane, from the skin of the pharynx, through the centerline of the trachea and spinal column to the skin on the posterior aspect of the neck (figure 3-1).

The **long axis (LA)** follows the coronal plane from right to left, intersecting the midpoint of the short axis at 90° (figure 3-1). The lengths of both the long and short axis were measured using SPIN-2008, an MRI analysis program developed at Wayne State University.

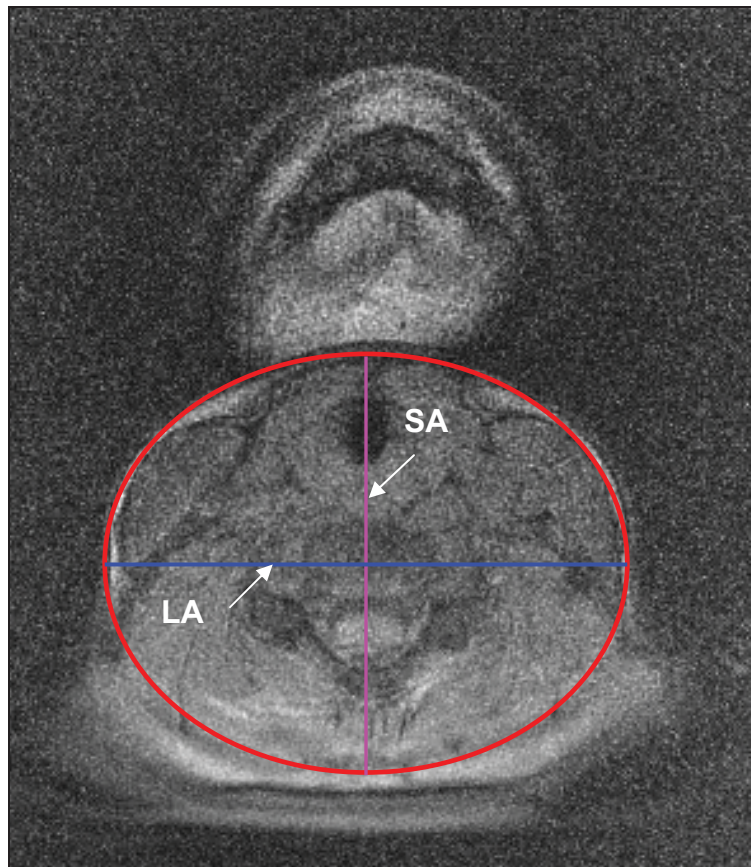


Figure 3-1: Axial cross-section of the neck at C4 – the red ellipse approximates the circumference of the neck. The pink and blue lines show the short axis (SA) and long axis (LA) used to calculate neck circumference.

3.3 RESULTS

Twenty-three subjects were initially enrolled in the study. One child was removed from the study since it was unknown prior to the study that he suffered from Attention Deficit Hyperactivity Disorder and was unable to perform the tasks required. Two adults were removed from the study due to scheduling conflicts. The anthropometrics for the remaining subjects are shown below in Table 3-1. Missing values for seated height and height were estimated from the seated height/height (SH/H) ratio as detailed by Fredriks et al. [2005]. The Fredriks et al. collect sitting height and height data from subjects ages 0-21. The results of their study show that the ratio of SH/H is approximately 52% for subjects after the age of 3 years.

Average 10-year boys

Subject	Age	Neck Circumference (in)	Height (in)	Weight (lbs)	Seated Erect Height (in)
K01	10.0	11.5	53.0	68.6	26.4
K03	10.0	12.9	55.8	95.0	27.8
K04	10.0	11.8	55.3	67.0	27.4
K05	11.0	12.8	61.0	92.0	29.6
K06	11.0	11.4	62.0	96.0	30.4
K07	10.0	12.4	59.0	81.0	30.4
K08	10.0	12.0	56.3	76.0	28.0
K09	9.5	12.4	53.0	83.0	26.6
K10	10.0	12.0	58.3	78.0	28.4
K11	10.0	11.0	50.8	53.0	26.0
average	10.2	12.0	56.4	79.0	28.1
SD		0.6	3.6	13.6	1.6

Average Adult Males

Subject	Age	Neck Circumference (in)	Height (in)	Weight (lbs)	Seated Erect Height (in)
S08	29.0	15.0	70.0	170.0	34.8
S09	37.0	14.7	69.0	137.0	34.3
S10	28.0	17.2	68.0	165.0	34.6
S11	24.0	14.2	68.0	145.0	35.2
S13	29.0	15.6	70.0	185.0	34.4
S14	26.0	14.4	69.5	174.0	33.6
S15	40.0	14.6	68.5	145.0	32.4
S16	47.0	15.4	67.5	172.0	33.5
S17	54.0	16.4	69.8	162.0	35.2
S20	42.0	15.2	70.0	175.0	34.8
average	35.6	15.3	69.0	163.0	34.3
SD		0.9	1.0	15.7	0.9

Table 3-1: Anthropometric measurements of children and adults used as subjects in this study. Neck circumference values shown in red are those calculated from MR-images. Seated height values shown in red were estimated from the seated height to height (SH/H) ratio by Fredriks et al. [2005]

Neck circumference was calculated from the MR-images at C4 for all the 10-year old boys. Results of the calculations and the percent difference between the measured and calculated values are shown below in Table 3-2. The average calculated neck circumference was 29.35+/-1.58cm. All calculated values were less than 10% different (average 3.92% difference) from the measured values.

Average 10-year boys

Subject	Neck Circumference (cm)	Neck Circumference Calc. (cm)	% difference (M-C)/M*100%
K01	28.8	28.8	0.0
K03	32.2	32.2	0.0
K04	29.5	29.0	1.7
K05	32.0	29.9	6.6
K06	28.5	28.5	0.0
K07	31.0	31.7	2.3
K08	30.0	29.0	3.3
K09	31.0	28.6	7.7
K10	30.0	29.0	3.3
K11	27.5	26.8	2.5
average	30.1	29.4	3.9
SD	1.5	1.6	

Table 3-2: Measured and calculated neck circumference values for 10-year-old boys. Red values are those values of neck circumference that were calculated.

3.4 DISCUSSION

3.4.1 Anthropometrics

The average height and weight for both subject groups met the range set for this study. The average weight of the 50th percentile adult males was at the low end of the range, 163lbs +/- 15.66lbs. The average height of adult subjects in this study was 69.03" +/- 0.96". The 10 year old male subjects in this study had

an average weight of 78.96lbs +/- 13.6lbs and average height of 56.81"+/-3.65". The average height of the adult subject group was close to the 68" height of the 50th percentile adult male ATD [Humanetics, 2011]. The average weight of the adult subject group is 8lbs less than the Hybrid III ATD's 171.3lbs +/- 2.6lbs. The average height and weight of the 10-year old boys in this study, corresponded well with the height and weight of the 50th percentile male as shown in the Centers for Disease Control's growth chart, published in 2000. Average height and weight also corresponds well with the design dimensions of the Hybrid III dummy – height: 77.61" and weight: 51.05lbs [FTSS]. The seated height for both subject groups in this study also corresponded well with their respective ATD's. The adult males in this study had an average seated height of 34.23"; the 50th percentile Hybrid III has a seat height of 34.8+/-0.2". Similarly, the 10-year-old males in this study had a seated height of 28.13" as compared to the 10-year old ATD's seat height of 28.5".

With respect to the average American population, the height of the subjects in both sample groups corresponds to reports published by Vital and Health Statistics [2003] and by the Centers for Disease Control [2009]. With respect to weight, the average weight of both sample groups falls below the average in both these reports. Both these reports show the alarming trend of 10lb increased in average body weight over the last 30 years. Table 3-3 shows the guidelines for average height and weight values for a 50th percentile 10-year old boy as given by the CDC growth chart, the population averages reported by the

Vital and Health Statistics for 10 year old boys and 50th percentile males and the design dimensions of the corresponding ATD's.

Average 10 Year Old Boys

Study/Reference	Height (in)	Weight (lbs)	Seated Height (in)
CDC Growth Chart [2002]	54.4	71	
CDC NHANES data [2003-2006]	55.7	82.2	
Vital Health and Statistics			
1999-2002	55.7	84.9+/-1.8	
1976-1980	55.6	79.7+/-1.6	
Arbogast [2009]	55.52	71.06	28.74
10-year Old Hybrid III	51.05	77.61	28.5
Dawson study - 10 year-old boys	56.8+/-3.7	79.0+/-13.6	28.1+/-4.2

Average Adult Males (20+ years old)

Study/Reference	Height (in)	Weight (lbs)	Seated Height (in)
CDC NHANES data [2003-2006]	69.7	188.8	
Vital Health and Statistics			
1999-2002	69.4+/-0.1	191.0+/-1	
1976-1980	69.1+/-0.1	173.8+/-0.4	
Arbogast [2009]	70	177.8	36.73
50th percentile male Hybrid III	68	171.3+/-2.6	34.8+/-0.2
Dawson study - 50th percentile adult mal	69.0+/-1.0	163.0+/-15.7	34.2+/-2.7

Table 3-3: Comparison of study height and weight results to published reports in the literature for 10-year old boys and 50th percentile adult males.

3.4.2 Measurements Of Neck Circumference

Measurements of neck circumference are in recent reports, being used as predictors of obesity in both adults and children. Obesity was not a focus of this study; however, measurements of neck circumference from this study are

comparable to baseline reported by these studies. Studies by Mazicioglu et al. [2010] and Hatipoglu et al. [2009] report a neck circumference of 28.10 +/-2.1cm and 29.0cm respectively, for healthy, average weight pre-pubertal boys, ages 6+. The average neck circumference reported in this study for 10-year-old boys was 30.05 +/-1.53cm (measured) or 29.35 +/-1.58cm (calculated). The neck circumference data for this study is higher than the average data reported by Arbogast et al. [2009] for their study comparing the kinematics of children to adults in low speed frontal impacts. Arbogast et al. report a neck circumference of 28.6cm for their 10-year-old sample group. The neck circumference for the adult males in their study was reported as 39.95cm. In this study, the measured neck circumference of the 50th percentile adult male subject group was 38.33 +/-2.34cm. In obesity studies, similar to those reported on above for children, the neck circumference of adults of healthy normal weight was reported as 40.5cm [Preis et al., 2010] and 39.3+/-2.4cm [Ben-Noun et al., 2006]. Table 3.4 shows neck circumference values reported in the literature for healthy normal 10-year olds and adults, as compared to the results of this study.

Average 10 Year Old Boys

Study/Reference	Neck Circumference (cm)
Mazicioglu et al. [2010]	28.10+/-2.1
Nafiu et al. [2010] (boys age 7.7+/-1.5years)	28.1+/-1.9
Hatipoglu et al. [2009]	29
Arbogast et al. [2009]	28.6
Miller [2003] (children M/F ages 6-10)	26.8+/-1.75
Dawson study Data (measured)	30.1+/-1.5
Dawson study Data (calculated)	29.4+/-1.6

Average Adult Males (20+ years old)

Study/Reference	Neck Circumference (cm)
Preis et al. [2010]	40.5
Arbogast [2009]	39.59
Ben-Noun [2006]	39.2+/-2.4
Miller [2003]	38.4
Dawson study Data (measured)	38.3+/-2.3

Table 3-4: Comparison of study neck circumference results to neck circumference values reported in the literature.

3.5 CONCLUSIONS

The anthropometric measurements taken as part of this study correspond well to both the results reported in the literature for the healthy, normal weight subject, as well as to the design dimensions of the Hybrid III ATDs.

CHAPTER 4: MUSCLE CROSS-SECTIONAL AREA AND MOMENT ARMS BASED ON MAGNETIC RESONANCE IMAGING MEASUREMENTS

4.1 INTRODUCTION

Magnetic resonance imaging and other imaging techniques have been used as a non-invasive, reliable, in-vivo means of measuring muscle volume [Smeulders, 2010]; muscle moment arms [Arnold, 2000]; and muscle cross-sectional area (CSA) [Oksanen, 2007; DeLoose, 2009; Stemper, 2010]. A 1991 study by Engstrom et.al comparing muscle cross-sectional area values calculated using MRI and CT to cadaveric results, found that the estimate of the CSA of cadaveric thigh muscles using MRI was within +/- 7.5% of the dissected measurements while CT scans tended to produce results which overestimated muscle CSA by 10-20%. Similarly Arnold et al. [2000], found that in combination with a biomechanical models, MRI moment arm measurements were within 10% of experimental values.

Studies have used various imaging techniques to measure the cross-sectional area and length of the muscles of the upper and lower extremities. Alway et al. [1990] used computerized tomography (CT) to determine the CSA of the elbow flexors in their study which compared the peak torque per muscle cross-sectional area of trained bodybuilders to recreational weightlifters. Although the study found that trained male bodybuilders had a greater CSA to lean body mass ratio than the other subject groups in the study, the results showed that there was no significant difference between subject groups in the peak torque to muscle cross-sectional area ratio. In a similar study, Ichinose et

al., [1998], used ultrasonography, instead of CT, to measure the morphology of the triceps brachii, specifically, muscle thickness and angle of pinnation. The aim of their study was to determine if the differences in force generation capacity between male and female athletes could be attributed to differences in muscle morphology. The study concluded that differences in force generation were more likely due to differences in muscle CSA rather than muscle thickness and angle of pinnation. Engstrom, [1991] and Funkanaga, [1992] both used MRI to determine muscle morphology. The Engstrom et al. study compared to morphological measurements using MR-images and CT scans to cadaveric data. Funkanaga [1992] used MRI to estimate the PCSA of the human thigh.

In spite of the accuracy and reliability of measurements of muscle morphology made using imaging techniques, few studies have been done to determine the morphology of the muscles in the neck. In 1998 Kamibayashi et al. determined neck muscle morphology of 14 neck muscles by dissecting the cervical spine of 10 adult male cadavers. Their study measured muscle mass, sarcomere and fascicle length and angle of pinnation. From this data the physiologic cross-sectional area (PCSA) of the 14 neck muscles was calculated. VanEe et al. conducted a similar study in 2000, combining cadaveric dissection with Magnetic Resonance Imaging to evaluate the PCSA of 24 neck muscles. Similar to the Kamibayashi study, 6 male cadaver cervical spines were dissected. The origins and insertions of each muscle were noted; sarcomere and fiber length were measured. MRI was used to determine muscle volume. According to the VanEe study, muscle volume measured by cadaveric dissection when

compared to live subjects, is often underestimated due to pre-mortem atrophy and post mortem dehydration. The PCSA of the 24 muscles in the VanEe study was calculated from the MRI-based muscle volume measurements and the muscle mass ratios determined from cadaveric dissection. Miller et al., [2003] conducted a study at Wayne State University involving adult males and children, in which the cross-sectional area of the extensor muscles of the neck was measured at C5. The Miller study also included imaging the upper extremity.

MRI studies to measure muscle cross-sectional area are now being conducted in an effort to understand sources of chronic pain. The 2007 study by Oksanen et al., compared the neck muscle cross-sectional area (CSA) of male and female adolescents (average age 17 years old) with and without chronic headaches. Results showed that the CSA of certain muscles was greater in chronic headache sufferers than in non-sufferers. In cases of males with migraines headaches, the CSA of the right sternocleidomastoid, the sternocleidomastoid combined with the scalenes muscles, the left semispinalis capitis and left semispinalis capitis combined with the splenius capitis was greater ($p < 0.05$) than in males who did not suffer from migraine headaches. The cause of these morphological changes is still under investigation. The 2009 study of fighter pilots by DeLoose et al., also studied the changes in neck morphology with respect to chronic pain. Thirty-five fighter pilots, 10 of whom suffered from chronic bi-lateral neck pain, voluntarily enrolled in the study. MRI-based results showed that the relative CSA was significantly greater in the semispinalis cervicis

($p < 0.001$) and multifidus ($p < 0.008$) of pilots with chronic neck pain compared to pilots without pain.

The purpose of this study was to determine the length; axial muscle moment arm at C4; the anatomical cross-sectional area of the sternocleidomastoid, the trapezius, the splenius capitis and the scalene muscles; and the physiologic cross-sectional area of the sternocleidomastoid using magnetic resonance imaging in 10 year old male and 50th percentile adult male subjects.

4.2 METHODS

4.2.1 Test Procedure

The 1.5 Tesla Siemens Sonata Magnetic Resonance Imager at Harper University Hospital (Detroit, MI) was used to image the neck muscles of each subject in the study. Four imaging sequences in addition to the initial localizing sequence were used to image the neck of each subject from the top of the head to the second thoracic vertebra. In order to maximize the contrast between the muscles and the surrounding tissues, all sequences were T1 weighted, fat-saturated images. A voxel size of 0.5mm x 0.5mm x 5mm was used in all sequences. The voxel size denotes the size of each image pixel (0.5mm x 0.5mm) and the thickness of the image slice (5mm). Three of the four sequences were 56-slice sequences in the axial plane (the plane parallel to ground – see figure 4-1), the first sequence sliced the neck in the true anatomical axial plane. The second and third axial sequences were sliced perpendicularly to the line-of-action of the sternocleidomastoid (SCM) and the scalene muscles, respectively.

The fourth sequence, a 32-slice sequence, imaged the neck in the sagittal anatomic plane (see figure 4-1).

Subjects were placed supine in the magnet with their legs and back parallel to the ground. Support for the lower back was provided by placing pillows under the subject's knees. The subject's neck was similarly supported in a comfortable position using padding. A Circularly Polarized (CP) head/neck and spine coil combination was placed over the subject's neck which served to augment the imaging signal in the neck region. Subjects were given earplugs to help reduce the noise made by the imager. Music was played during imaging to help subjects relax. Imaging time was approximately 15 minutes.

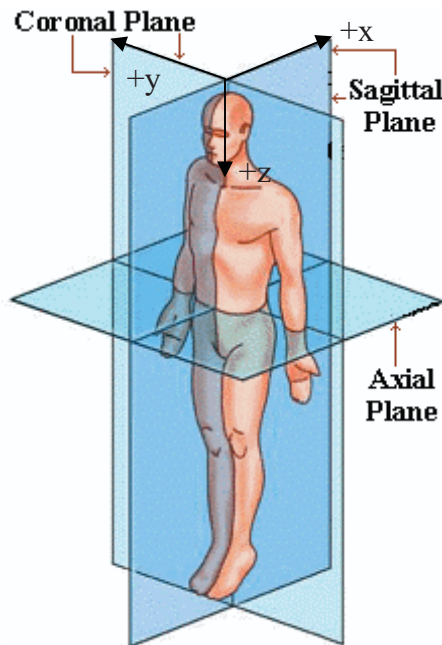


Figure 4-1: Anatomical Planes of the human body [www.spineuniverse.com]

The coordinate system used in this MRI study was as follows: the z-axis is perpendicular to the axial plane, positive downward. The x-axis is parallel to the sagittal plane, positive in the anterior to posterior direction, and the y-axis is parallel to the coronal plane, positive from left to right.

4.2.2 Data Analysis

SPIN'08, a software developed at The MRI Institute for Biomedical Research, Detroit, MI, was used to measure muscle length from its origin to the mid-point of the C4 vertebral body. SPIN'08 was also used to determine the moment arms of the SCM, trapezius, splenius capitis, the scalene (anterior, middle, and posterior) muscles at the mid-point of the C4 vertebral body in the axial plane. The mean moment arm of the trapezius/semispinalis capitis and splenius capitis/levator scapula were also determined for the same axial location. ImageJ, available from the National Institutes of Health, was used to calculate the centroid of each of the muscle cross-sectional areas and the centroid of the intervertebral disc at C4 [Moroney et al., 1988, Choi et al., 2000, Stemper et al., 2010]. The forces and moments were evaluated at C4 since there is some evidence to suggest that a large number of neck injuries occur in this area. Torg et al. [1991] reported that 74% of teardrop neck fractures in football occur at C5 and 16% occur at C4. A retrospective study of cervical injuries entered into a traumatic injury database at a Level 1 trauma center in Ontario, Canada, showed that injuries to C5 accounted for 22% of all traumatic injuries to the cervical spine. Spinal cord injuries accounted for 27% of the reported traumatic injuries,

and of the reported spinal cord injuries, 27% were reported at C4-5 [Prasad, VSSV et al., 1999].

The images used for the CSA and moment arm measurements in this study were taken at the mid-point of the C4 vertebrae. The location referred to C4/5 in the published literature is at the intervertebral disc between the C4 and C5 vertebral bodies. The difference between this location and the midpoint of the C4 vertebral body is approximately 7.5mm – or 1.5 image slices, but this varies with subject size. The difference between the CSA measurements at these two locations, however is negligible. The location of the mid-point of the C4 vertebrae was chosen in this study because the images were consistently clear across all subjects, and showed good muscle delineation.

The images slices used for measuring muscle cross-sectional areas and moment arms were determined using first the saggital image at the centerline of the body (this is the image at the plane of symmetry that runs from the top of the head down to the toes dividing the left side from the right). Using this image, starting at C1 (the first cervical vertebra) the vertebrae were counted down to C4. At the center of this vertebra a line was drawn through the vertebral body. This line was parallel to the top and bottom of the vertebral body, and not parallel to the top and bottom of the image. This was the location of the axial images used to measure the muscle CSA.

The chosen axial image was compared to other images either drawn or MR-images published in anatomy text books, anatomy atlases and other published journal articles to ensure that the location corresponded with the C4 vertebra.

Papers by Moroney et al. (1988) and Siegmund et al. (2000) provided particularly good images for comparison purposes.

SPIN'08 does not directly measure length or area. However, by using pixel coordinates and pixel size, values for muscle length, moment arm and muscle cross-sectional area were indirectly calculated. The header information of each test sequence provides information on the pixel size, slice thickness and grid size. As mentioned in section **4.2.1 – Test Procedures**, the pixel size was set to $x=0.5\text{mm}$ by $y=0.5\text{mm}$. In this study the grid was set to 512 rows by 384 columns for each image in each sequence. Using this grid, the (x,y) coordinates (in the axial plane) and (x,z) coordinates (in the sagittal plane) denoting the endpoints of each muscle's length and moment arm were determined. The coordinate system was used in this study is shown in Figure 4-1. This method of determining length is the one programmed into Image J. SPIN'08 was used as the primary tool in spite of this since the imported images require no format conversion prior to analysis, and the contrast/brightness of the image is more easily adjusted, which enable better muscle boundary differentiation in some images.

Muscle length was measured from the origin to insertion, with the exception of the trapezius. Only the length of the superior region (the cervical region) of the trapezius was measured in this study. Chapter 2 – Anatomy and Physiology of the Cervical Spine provides a detailed description of the anatomy and function of each of the above mentioned muscles. Table 4-1 provides the origin and insertion locations used to calculate muscle length.

Muscle Name	Muscle Origin	Muscle Insertion
Sternocleidomastoid	- manubrium sterni, medial portion of the clavicle	- mastoid process of the temporal bone - superior nuchal line
Trapezius	- external occipital protuberance - nuchal ligament	- posterior border of lateral 1/3 of clavical, acromium process
Splenius Capitis	- spinous process of C7-T6 - nuchal ligament	- mastoid process of the temporal bone, and occipital bone
Anterior, Middle and Posterior Scalenes	- cervical vertebrae C2-C7	- first and second rib

Table 4-1: Muscle origin and insertion locations

For this study, moment arms were defined as the distance from the centroid of the intervertebral disc to the centroid of the muscle's cross-sectional area in the C4 plane (figure 4-3). The centroid of an area is determined by integrating with respect to the area of the region of interest (ROI). In two-dimensions, these integrals are as follows:

$$C_x = \int \frac{xdA}{A} \quad 4-1$$

$$C_y = \int \frac{ydA}{A} \quad 4-2$$

where C_x and C_y are the x- and y-coordinates of the centroid, and A is the area of the region of interest.

In this study, the centroids were calculated using ImageJ. The boundary of the cross-sectional area of the muscle at C4 was traced using the polygon selections function of the software. The centroid was calculated by the program's **Measurement** function. Both the muscle centroid and the intervertebral (IV) disc centroid at C4 were calculated using the same method.

Muscle length and moment arms were calculated by first finding the length of the line in pixels,

Muscle length:

$$\text{Length}_x (\Delta x_L) = X_{insertion} - X_{origin} \quad 4-3$$

$$\text{Length}_z (\Delta z_L) = Z_{insertion} - Z_{origin} \quad 4-4$$

$$\text{Muscle length} = \sqrt{(\Delta x_L)^2 + (\Delta z_L)^2} \quad 4-5$$

where (Δx_L) = the x-component of length

and (Δz_L) = the z-component of length

Moment Arm:

$$\text{Length}_x (\Delta x_{MA}) = X_{centroid} - X_{IV \text{ disc centroid}} \quad 4-6$$

$$\text{Length}_y (\Delta y_{MA}) = Y_{centroid} - Y_{IV \text{ disc centroid}} \quad 4-7$$

$$\text{Moment Arm} = \sqrt{(\Delta x_{MA})^2 + (\Delta y_{MA})^2} \quad 4-8$$

where (Δx_{MA}) = the x-component of length

and (Δy_{MA}) = the y-component of length (see fig. 4-4)

Length/moment arm in millimetres was determined by multiplying length values in pixels by the pixel dimension of 0.5mm.

4.2.2.1 Muscle Length

Muscle length was measured in two-dimensions along the line of action of the muscle to the C4 plane. Muscle curvature was taken into account only as the

muscle followed the kyphotic curvature of the neck. The medial/lateral curvature of the muscle around the neck was not taken into account in the measurement of muscle length. The pixel coordinates of the muscle origin and the coordinates of the muscle insertion were recorded for each muscle in the study. Figure 4-2 shows line of action for the trapezius, splenius capitis, scalenes and sternocleidomastoid muscles for (a) a 10 year old male subject and (b) 50th percentile adult male subject. The calculated muscle lengths are shown in Table 4-2.

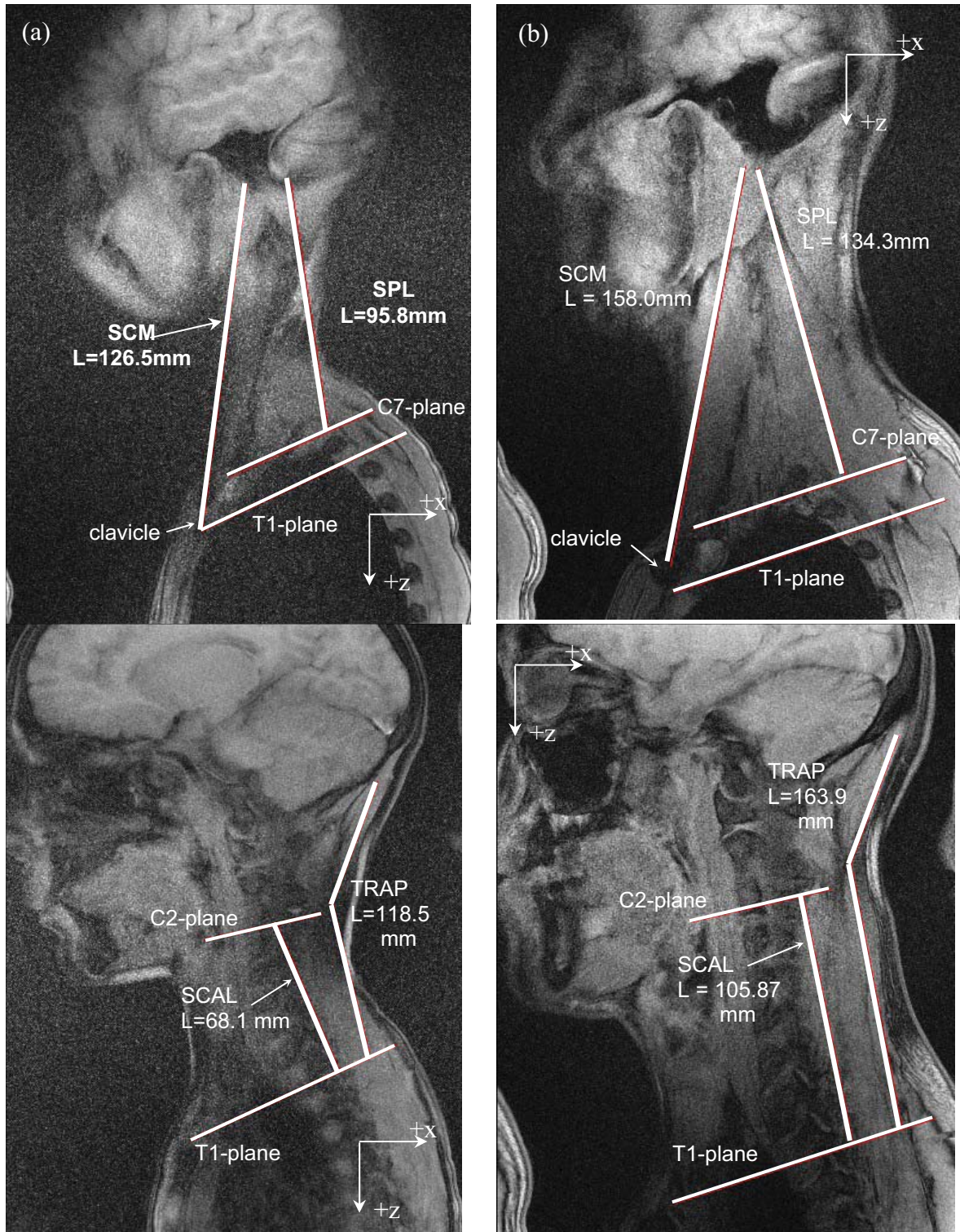


Figure 4-2: Line of action for the sternocleidomastoid (SCM), trapezius (TRAP), splenius capitis (SPL) and scalene muscles (SCAL) for (a) 10 year old male subject (left) and (b) 50th percentile male subject (right)

4.2.2.2 Muscle Cross-Sectional Area

The anatomical cross-sectional area of the SCM, trapezius, splenius capitis and scalene muscles in the C4 axial plane and physiologic cross-sectional area of the SCM were determined using SPIN '08. Muscle CSAs were measured at the mid-point of the C4 vertebral body. The slice used was compared to published images [Moroney, 1988; VanEe, 2000; Deloose, 2009] to ensure that it corresponded to the correct spinal level. Cross-sectional area was determined by determining the number of pixels inside the boundary of a particular region of interest (ROI). In this case the ROI was the boundary of the muscle. The number of pixels inside the ROI was multiplied by the area of the pixel (0.5mm x 0.5mm). This provided area in mm². The cross-sectional area of the neck was determined in the same manner, where the region of interest was the entire circumference of the neck.

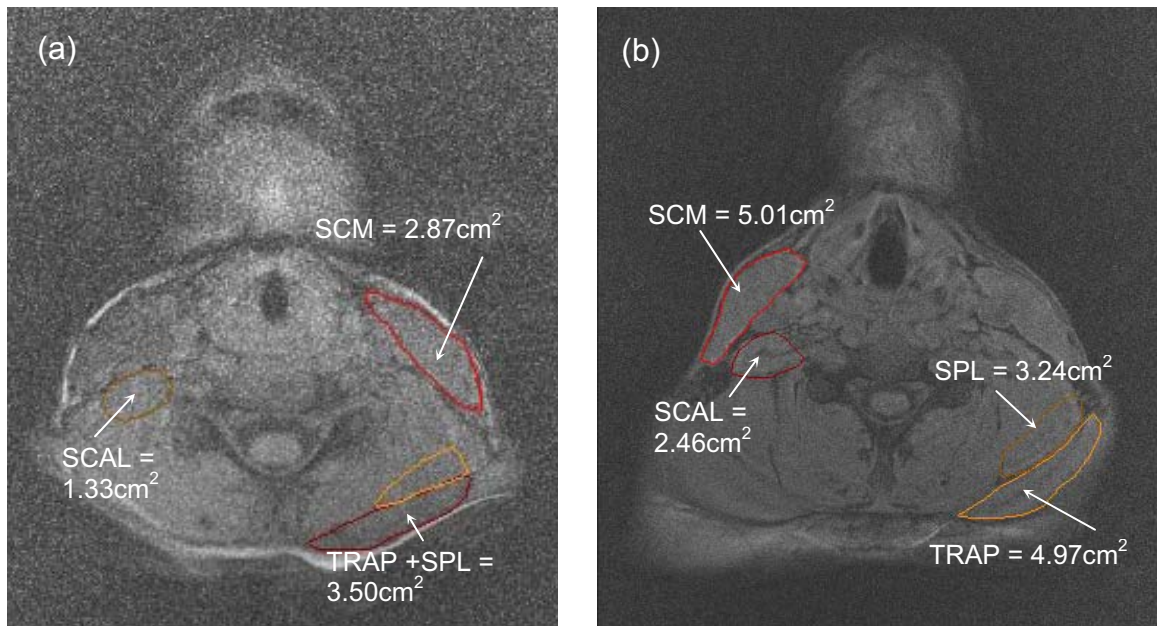


Figure 4-3: Single image slice showing the Anatomical Cross-Sectional Area (ACSA) muscle boundaries for (a) a 10-year old male subject and (b) a 50th percentile adult male subject.

4.2.2.3 Moment Arms

The muscle moment arms were measured at the mid-point of the C4 vertebra. The moment arm was measured from the centroid of the muscle to the centroid of the C4 vertebral body. The centroids were determined using the centroid function in Image J, available through the National Institutes of Health since SPIN'08 does not calculate centroid values. A similar approach was used by Moroney et al., [1988], and Stemper et al. [2010]. Their measurement was from the muscle centroid to the centroid of the intervertebral disc. The ROI's were first determined using SPIN'08. The images with the marked ROI's were saved as jpg. files. In Image J, using the "polygon selections" function, the ROI's on the jpg. files were retraced to match those done using SPIN'08. Using the "measurement" function, centroid values for each ROI was calculated. The jpg. image maintains the same pixel size and grid size as in SPIN'08, which means that the coordinate locations are the same between SPIN'08 and Image J.

As with the muscle cross-sectional area, a boundary was drawn around the circumference of the neck at C4, the measurement function in ImageJ calculated the center of the circumference boundary.

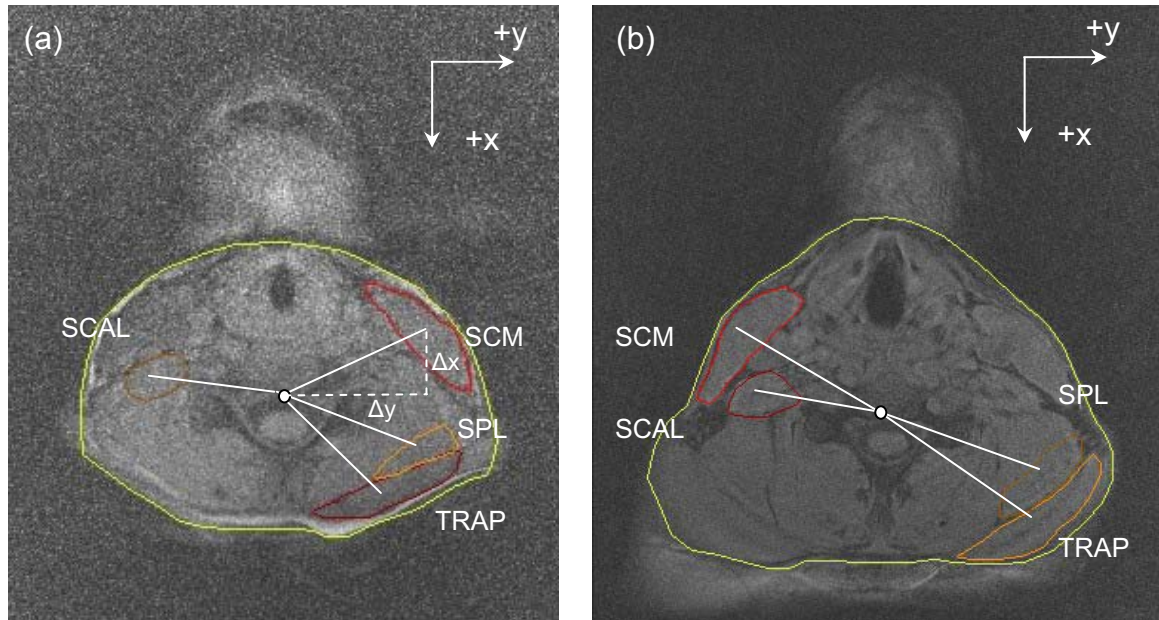


Figure 4-4: Transverse muscle moment arms – sternocleidomastoid (SCM); scalene (SCAL); splenius capitis (SPL) and trapezius (TRAP) at C4 plane for (a) 10 year old boy and (b) 50th percentile male. Δx and Δy , the x- and y-components of the moment arms are shown for the SCM in figure (a).

4.2.3 Calculating Cross-Sectional Area

Physiologic cross-sectional area (PCSA) is determined according to the formula shown below:

$$\text{PCSA} = \frac{\text{Muscle Volume} \cdot \cos(\text{Angle of pinnation})}{\text{fascicle length}} \quad 4-8$$

Where muscle volume was determined by the summation of the Anatomical Cross-Sectional Area (ACSA) at each slice multiplied by the distance between the slices for the length of the muscle. The muscle length as measured from the MR-image is the distance between the upper-most and lower-most portion of the muscle that are visible. In the Funkanaga et al. [1992] description, fascicle length was determined from previously published studies of cadaveric muscle

dissections. In their studies Kamibayashi et al. [1998] and VanEe et al. [2000] calculated muscle PCSA from muscle volumes calculated from MR-images and muscle-tendon length and fascicle length by dissection. Muscle-tendon length is the total length of the muscle from its origin to its insertion, including the muscle tendon, whereas the fascicle length is the length of the muscle fiber alone. In their study, VanEe et al., reported that muscle fibers extended 72.6 +/-9.4% of the origin to insertion length. Morphological data, including fascicle length and angle of pinnation is not available for children; therefore, PCSA in this study was calculated using muscle length rather than fascicle length.

The angle of pinnation is defined as the angle that the muscle fascicles make with the line of action of the muscle. The Kamibayashi et al. [1998] study also reported, in a sample of 10 cadaveric specimens, that the average angle of pinnation for each of the muscles in the neck ranges from subject to subject between 0-20°. For this study, it was assumed that the angle of pinnation is 0° since it cannot be determined through non-invasive techniques. The cosine of the angle range (0-20°) ranges from 0.94-1.0, resulting in a 6% difference from the low end to the high end of the pinnation angle range. Therefore, PSCA was calculated as muscle volume divided by muscle length without incorporating the pinnation angle in the calculations.

4.2.4 Statistical Analysis

Student's t-tests were used to determine the significant difference between the mean of the cross-sectional areas of the adult and child sample

groups for each muscle. Linear regression analysis was used to determine the correlation between age and moment arm, moment arm and stature, age and cross-sectional area, and cross-sectional area and stature and weight.

4.3 RESULTS

Muscle length, moment arms in the axial plane, and SCM physiologic cross-sectional area were calculated for all subjects in the study. The measured values are shown below in Table 4-2.

10 Year Old Boys

Subject	Muscle Length (from insertion to C4) - (mm)				Moment Arm Length at C4 (mm)				PSCA (cm ²)
	SCM	TRAP	SPL CAP	SCAL	SCM	TRAP	SPL CAP	SCAL	SCM
K01	126.50	118.02	95.80	68.06	39.64	43.27	43.00	31.91	1.90
K03	115.34	119.28	96.98	75.79	39.64	52.36	49.75	38.92	2.32
K04	152.57	122.58	110.37	111.96	35.38	41.93	35.22	32.31	1.85
K05	149.65	106.30	104.46	81.25	40.50	47.06	42.44	34.05	1.79
K06	142.01	130.19	106.29	80.82	40.19	48.54	33.31	37.41	2.35
K07	149.58	129.46	103.94	59.63	43.36	47.28	39.12	33.60	2.12
K08	125.53	113.69	86.83	64.83	35.93	47.50	41.23	33.46	1.91
K09	125.79	115.10	92.18	71.89	38.86	45.97	38.56	32.90	2.68
K10	128.08	122.12	94.64	78.94	37.68	44.93	36.95	33.94	2.45
K11	108.90	88.03	79.77	69.72	35.79	40.75	36.55	32.56	1.95
Average	132.39	116.48	97.13	76.29	38.70	45.96	39.61	34.11	2.13
Std. Dev.	15.20	12.29	9.42	14.39	2.52	3.41	4.73	2.28	0.30

50th Percentile Adult Males

Subject	Muscle Length (from insertion to C4) - (mm)				Moment Arm Length at C4 (mm)				PSCA (cm ²)
	SCM	TRAP	SPL CAP	SCAL	SCM	TRAP	SPL CAP	SCAL	SCM
S08	158.04	163.09	161.49	105.87	52.31	65.03	58.18	42.72	2.79
S09	168.76	114.81	131.84	104.81	48.65	58.29	51.32	35.60	4.96
S10	143.69	156.28	120.30	97.40	55.91	60.34	46.92	28.73	5.07
S11	170.25	174.19	131.62	107.86	47.09	56.23	48.78	41.24	4.95
S13	182.48	168.70	128.30	106.85	50.45	50.76	51.72	37.42	3.96
S14	174.90	146.89	115.81	94.30	45.14	60.43	51.68	33.56	2.95
S15	169.21	140.96	122.84	125.42	47.36	60.98	51.18	38.36	3.20
S16	173.77	163.50	124.30	97.81	49.32	57.96	49.35	36.73	3.06
S17	166.50	165.15	134.37	103.56	51.22	63.29	51.23	35.65	4.04
S20	179.45	172.96	144.68	117.50	46.94	66.46	58.54	33.66	3.65
Average	168.71	156.65	131.56	106.14	49.44	59.98	51.89	36.36	3.86
Std. Dev.	11.14	18.17	13.29	9.42	3.15	5.09	3.54	3.36	0.88

Table 4-2: Muscle length, moment arm and the physiologic cross-sectional area of the SCM for the 10 year old boys and 50th percentile male subjects. PCSA values shown for subjects K04, S10 and S16 are estimates based on anatomical cross-sectional area (ACSA). For subjects where calculation of PCSA was not possible due to image quality, the PCSA was estimated from the anatomical cross-sectional area (shown in red).

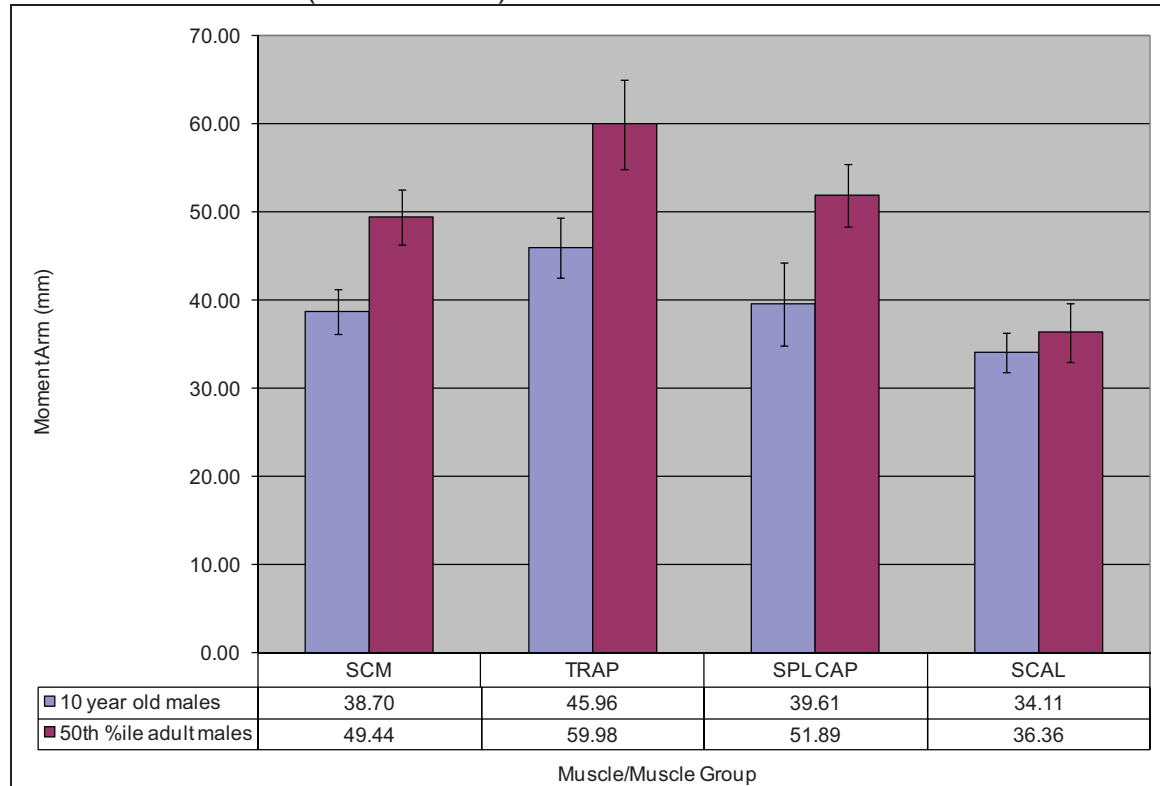


Figure 4-5: Moment arm comparison between 10 year old boys (light data set) and 50th percentile adult males (dark data set). The moment arm of the SCM, trapezius and splenius capitis was significantly greater in adults than in the 10-year old male subject group ($p < 0.02$). The difference between the moment arm of the scalene muscles of adults and 10-year old boys was not significant.

There was a significant ($p = 0.05$) positive correlation between age and moment arm, for the SCM, trapezius and splenius capitis. The scalene muscles, at C4 showed no correlation between age and moment arm length (figure 4-6). Similarly, there was a positive correlation between moment arm and the stature of the subject for the SCM ($r=0.889$), the trapezius ($r=0.866$) and the splenius

capitis ($r=0.792$). All correlations were significant ($p<0.05$) (figure 4-7). The correlation between stature and the length of the scalene moment arm was not significant ($r=0.364$).

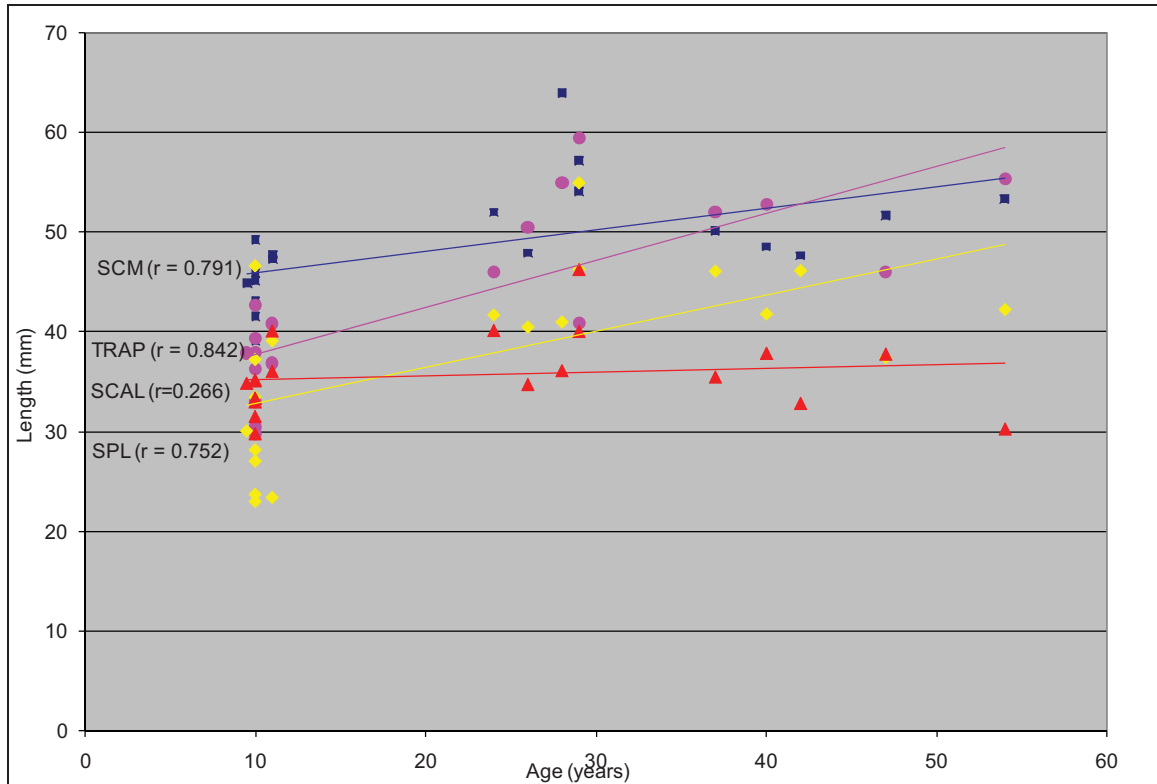


Figure 4-6: Muscle moment arms measured in the transverse C4 plane compared with the age of the subject for the sternocleidomastoid (SCM $r=0.789$, ■); the trapezius (TRAP $r=0.713$, ●); splenius capitis (SPL $r=0.495$, ◆); and the anterior scalene (SCAL $r=0.415$, ▲).

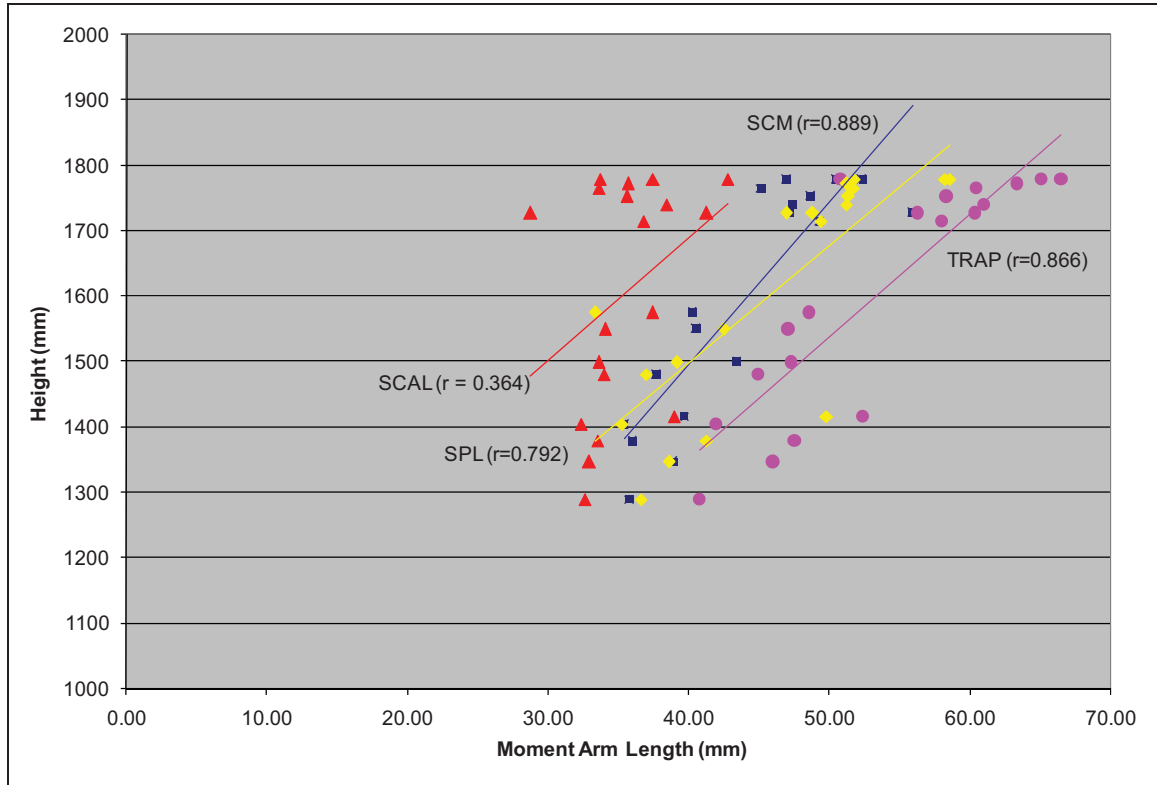


Figure 4-7: Muscle moment arms measured in the transverse C4 plane compared with the height of the subject for the sternocleidomastoid (SCM $r=0.855$, ■); the trapezius (TRAP $r=0.841$, ●); splenius capitis (SPL $r=0.670$, ◆); and the anterior scalene (SCAL $r=0.447$, ▲).

The relationship between and physiologic cross-sectional area of the SCM and age shows a positive, significant ($p < 0.02$) correlation ($r = 0.739$), (figure 4-8). The results also show a positive, significant ($p < 0.02$) correlation between the physiologic cross-sectional area of the SCM and both height ($r=0.725$) and weight ($r=0.723$), shown in figures 4-9, and 4-10 respectively.

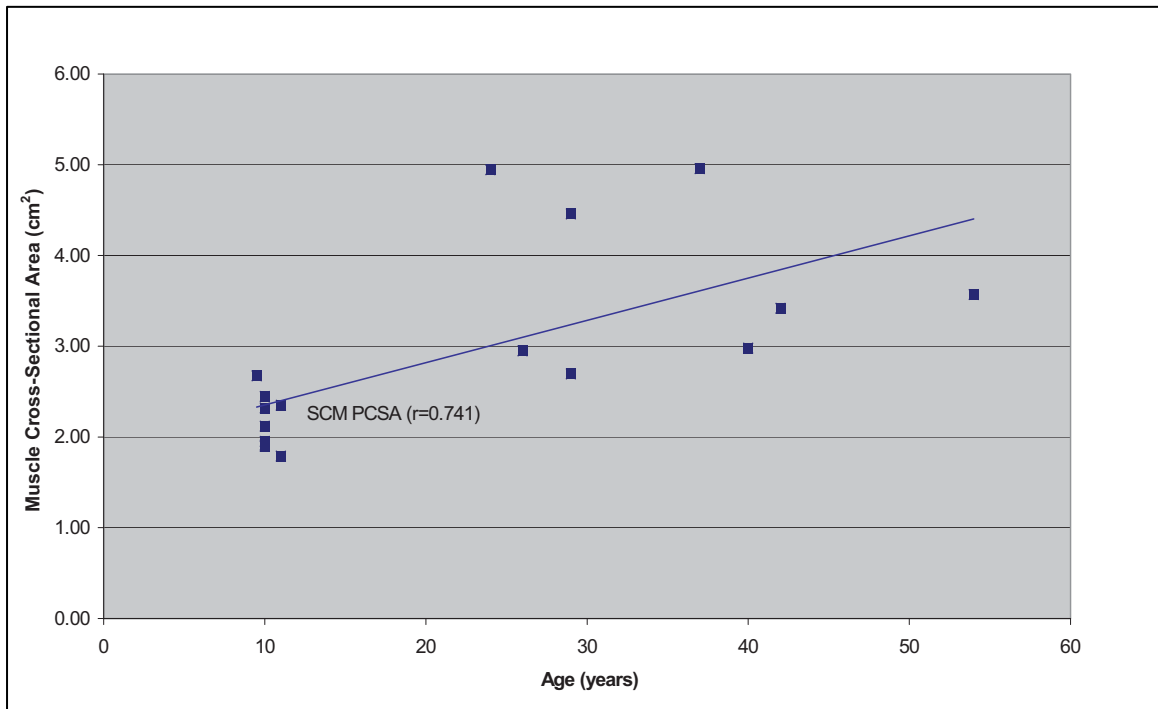


Figure 4-8: Cross-sectional area the sternocleidomastoid compared with age ($r=0.741$) results showed a significant correlation ($p<0.02$).

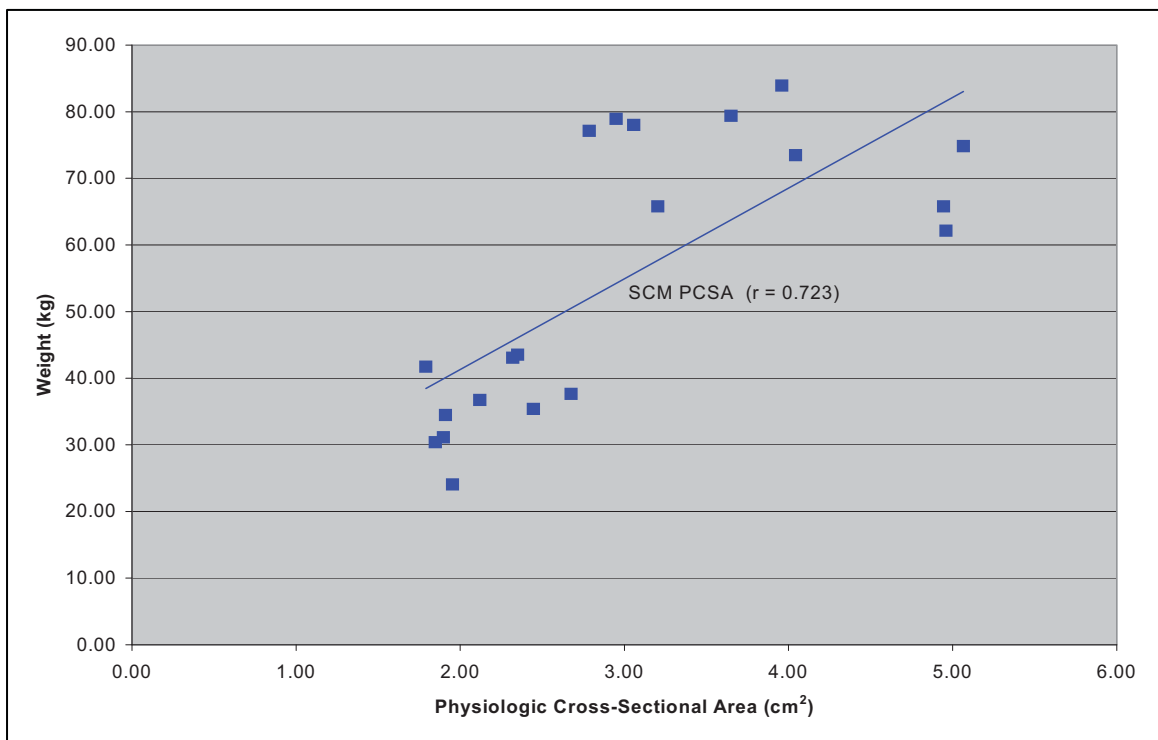
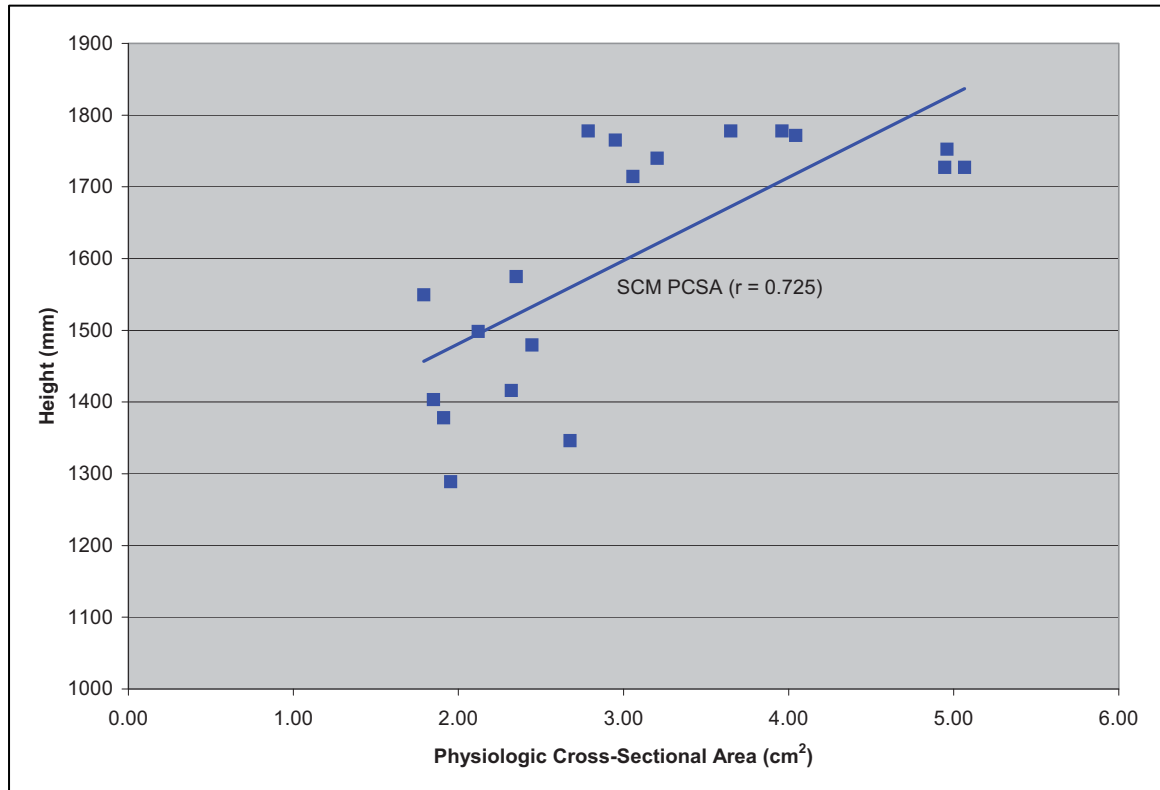


Figure 4-9: Cross-sectional area of the sternocleidomastoid compared with



subject weight ($r = 0.723$), results showed a significant correlation ($p < 0.02$).

Figure 4-10: Cross-sectional area of the sternocleidomastoid compared with subject height ($r = 0.725$), results showed a significant correlation ($p < 0.02$).

The mean of the SCM physiologic cross-sectional area for the 50th percentile adult male sample group was $3.86 \pm 0.88 \text{ cm}^2$, and for the 10 year old male sample group was $2.13 \pm 0.30 \text{ cm}^2$. When compared, the adult physiologic cross-sectional area was significantly greater ($p < 0.02$) than that of the 10 year old males. Table 4-3 gives the estimated anatomical cross-sectional areas of the SCM, trapezius, splenius capitis, anterior scalene and the neck cross-sectional area at C4.

Average 10-year boys

Subject	Anatomic CSA at C4 (cm ²)				
	SCM	TRAP+SPL	SCAL	POST	P-L
K01	2.84	3.44	0.96	6.15	3.10
K03	3.28	4.59	1.20	8.58	3.88
K04	2.87	2.30	1.14	5.68	2.66
K05	3.65	3.62	0.97	6.30	2.92
K06	3.76	3.41	0.78	8.08	3.61
K07	3.76	1.58	0.71	7.45	3.37
K08	2.82	1.76	0.80	9.31	3.61
K09	3.55	3.51	0.79	8.15	2.41
K10	3.27	2.46	1.03	7.35	2.93
K11	3.46	2.20	0.78	6.88	2.44
average	3.33	2.89	0.92	7.39	3.09
SD	0.37	0.97	0.17	1.16	0.51

Average Adult Males

Subject	Anatomic CSA at C4 (cm ²)					
	SCM	TRAP	SPL	SCAL	POST	P-L
S08	4.71	4.96	3.08	1.12	13.02	8.42
S09	4.87	2.71	2.50	1.32	11.54	5.38
S10	6.90	5.09	2.57	1.19	13.13	7.28
S11	5.96	2.48	3.00	1.59	10.30	4.35
S13	5.51	2.53	2.43	1.17	13.38	4.72
S14	5.40	3.06	2.60	1.45	11.94	5.79
S15	4.86	2.70	2.22	1.04	12.69	4.23
S16	4.17	2.06	2.52	0.96	9.83	4.45
S17	5.08	3.19	2.47	1.28	14.47	5.47
S20	5.13	2.80	1.99	1.42	13.95	5.54
average	5.26	3.16	2.54	1.25	12.42	5.56
SD	0.76	1.03	0.32	0.20	1.51	1.35

Table 4-3: Anatomical Cross-Sectional Area of the sternocleidomastoid, trapezius, splenius capitis and scalene at C4 for both adult and 10 year old male subjects. Neck cross-sectional values, based on MR-images, was calculated at C4.

4.4 DISCUSSION

The results of this MRI study, showing a correlation between age and moment arm length are consistent with previous studies [Wolanin, 1982; Miller, 2003]. For the SCM, although the difference in total moment arm length between 10 year-old boys and adult males is significant ($p < 0.05$), the mean of the x-component of the adult male's moment arm is similar to that of the 10 year-old boy (Table 4-4). This may be due to development of the larynx during puberty and its prominence in post-pubertal males [Wysocki, 2008; Kahane, 1982]. During puberty the size of the larynx changes in both size and proportion [Wysocki, 2008]. The thyroid cartilage increases in size and also changes shape, creating the Adam's apple [Bluestone, 2003]. While larynx is not prominent in all adult male subjects, the MR-images shown below in Figure 4-11 shows the SCM of the adult subject to be more posterior-lateral than in the pre-pubescent 10-year old male. No studies were found which compared the relative position of the muscles pre- and post-puberty. However, in this study the images seem to indicate that position of the flexor muscles, in particular the SCM is affected by changes to the larynx. Based on the basic moment equation, one of the possible results of this change in muscle position should be the increase in the ability for the flexor muscles to generate force in response to an applied moment in flexion/extension.

$$M = d \times F$$

4-9

Where d = moment arm; F = force and M = applied moment.

Average 10-year old boys

	SCM Coordinates				SCM		
	Centroid		IV Disc Centroid		Length (mm)		Moment Arm Length (mm)
	y	x	y	x	y	x	
K01	267.48	235.91	190.366	254.302	38.56	9.20	39.64
K03	270.80	238.38	193.963	257.877	38.42	9.75	39.64
K04	266.31	273.45	196.555	285.29	34.88	5.92	35.38
K05	109.11	251.72	185.463	278.764	38.17	13.52	40.50
K06	113.03	237.80	186.806	269.704	36.89	15.95	40.19
K07	113.99	216.58	199.04	233.474	42.53	8.45	43.36
K08	261.94	238.29	198.478	271.987	31.73	16.85	35.93
K09	108.31	241.84	181.596	267.718	36.64	12.94	38.86
K10	122.89	259.09	197.804	267.299	37.46	4.11	37.68
K11	117.65	257.33	187.581	272.59	34.96	7.63	35.79
					37.02	10.43	38.70
					2.85	4.24	2.52

Average Adult Males

	SCM Coordinates				SCM		
	Centroid		IV Disc Centroid		Length (mm)		Moment Arm Length (mm)
	y	x	y	x	y	x	
S08	105.31	241.34	200.621	284.497	47.66	21.58	52.31
S09	102.69	215.24	199.029	228.877	48.17	6.82	48.65
S10	96.00	249.00	194.724	301.506	49.36	26.25	55.91
S11	99.29	241.65	191.571	260.469	46.14	9.41	47.09
S13	103.73	250.40	201.6	274.932	48.93	12.27	50.45
S14	160.09	166.29	248.956	182.162	44.43	7.94	45.14
S15	167.11	170.42	261.825	171.394	47.36	0.49	47.36
S16	281.81	231.09	183.405	237.849	49.20	3.38	49.32
S17	81.90	225.05	184.143	231.508	51.12	3.23	51.22
S20	102.63	226.62	195.912	216.11	46.64	5.25	46.94
					47.90	9.66	49.44
					1.90	8.30	3.15

Table 4-4: x- and y-components of the SCM and trapezius moment arms for the 10 year old male and adult male sample groups. The x-component of the SCM was measured to be the same between adult males and 10 year old males, likely due to the prominence of the pharynx. Both the x- and y-components of the trapezius moment arm are larger in the adult males ($p=0.02$).

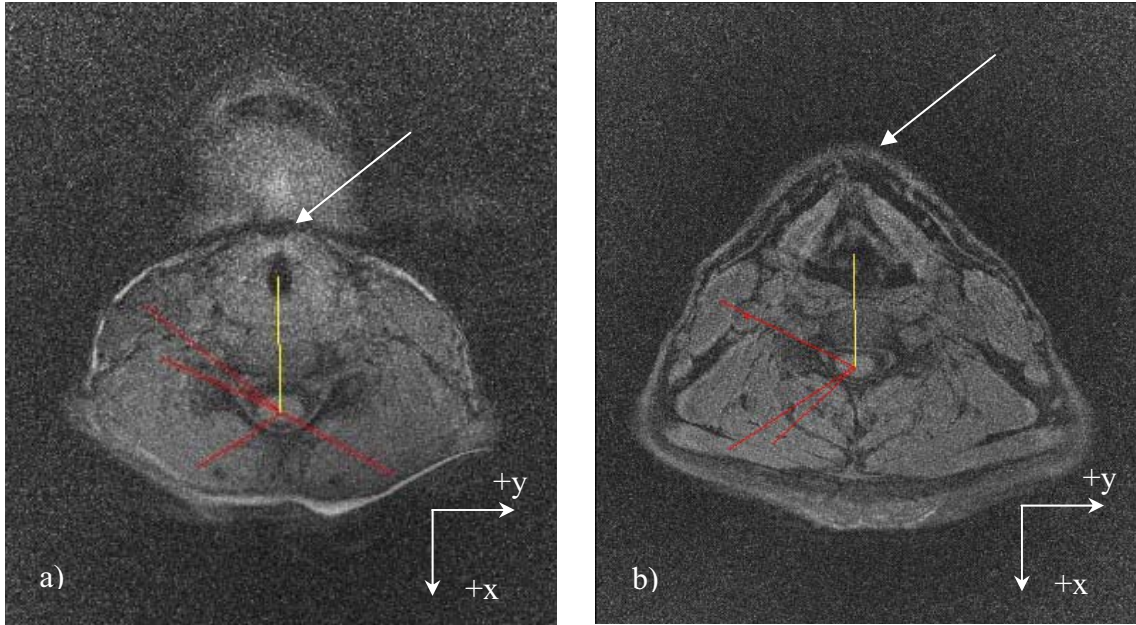


Figure 4-11: Transverse slice at C4-vertebra (a) 10-year old boy; (b) 50th percentile adult male. Arrow indicates the larynx in both subjects. Changes in the size, shape, and proportion of the thyroid cartilage of the larynx changes the relative position of the SCM in the anterior-posterior direction – the x-component of the SCM moment arm remains constant in spite of increased overall neck CSA.

The moment arms of the neck muscles vary depending on the movement of the neck – flexion/extension, lateral bending or torsion [Ackland, 2011]. They also vary with the state of muscle contraction [Vasavada, 1998]. This study considered only forces generated in flexion/extension. To that end, moment arms were measured at the C4-plane from MR-images taken with subjects in the supine position. The average moment arms for adults in this study from the centroid of the intervertebral disc at C4/5 to the centroid of the muscle/muscle group were as shown in Table 4-1 – SCM = 49.44 +/-3.15 mm; TRAP = 59.98 +/- 5.09 mm; SPL = 51.98 +/- 5.09 mm and SCAL = 36.36 +/-3.36 mm. Few studies have been conducted which explicitly measure neck muscle moment arms in the axial plane. Most studies involving neck muscle moment arms are computer

models and as such use muscle length from origin to insertion. However, in a recent study comparing the neck muscle morphometry of subjects whose necks were imaged in an upright MR-imager to those whose neck muscles were imaged in the more traditional supine position, Stemper et al. [2010] measured neck muscle radius from the centroid of the each neck muscle to the centroid of the intervertebral disc at C4/C5. Measurements of muscle cross-sectional area at this location were also measured. The approximate measurements of muscle radii for their study included, SCM = 48mm; and TRAP = 55mm. Subjects in the study were larger than 50th percentile adult males, weighing 81kg (178.2lbs) and measuring 180cm (72in) in height. In this study, the average adult subject had a height of 172.57cm (69.03in) and weighed 74kg (163lbs). In spite of differences in the height and weight of the respective study groups, the difference in moment arms is minimal - less than 10% difference for both the sternocleidomastoid and the trapezius. Comparative moment arm data in children was not found.

In 1998, Kamibayashi et al., reported on their study in which the neck muscles of 14 cadavers were dissected. Measures of muscle mass, angle of pennation, sarcomere length and fascicle length and muscle physiologic cross-sectional area (PCSA) were recorded. Reported average PCSA's for the SCM = $3.72 \pm 0.91 \text{cm}^2$; trapezius = $1.96 \pm 0.62 \text{cm}^2$; and anterior scalene = $1.45 \pm 1.23 \text{cm}^2$. In a similar study VanEe et al. [2000] determined neck muscle PCSA through a combination of cadaveric dissection and subject MRI. The dissection provided muscle origin and insertion locations and sarcomere and fiber lengths. MRI was used to determine in-vivo muscle volume from the base of the skull to

T4 in 2mm slices. Muscle volume was multiplied by the mass ratios obtained from the cadaveric dissections. Their reported PCSAs were 4.92cm^2 for the SCM, 3.77cm^2 for the cervical trapezius, 3.09cm^2 for the splenius capitis and 1.88cm^2 for the anterior scalene for a 50th percentile adult male. Gzik et al. [2008] measured the PCSA of both male and female volunteers as part of their study to determine mechanical properties of the cervical spine. In their study, muscle PCSA was determined using 3-D MRI. Values of muscle volume and PCSA were taken directly from the image data. Results of their study found the following PCSA values - SCM R: 3.64cm^2 –L: 3.96cm^2 . In their 1997 paper, van der Horst et al. referenced the neck muscle PCSA results, determined using MRI, in the doctoral dissertation of M. Jager, from the University of Eindhoven. The PCSA results from the Jager dissertation reported PCSA's of 3.7cm^2 for the SCM, 1.8cm^2 for the trapezius, 1.55cm^2 for the splenius capitis and 2.8cm^2 for the scalene muscles.

This study relied entirely on MR-images to determine physiologic cross-sectional area. The ability to determine PCSA was thus dependant on the clarity of the muscle boundary in every image along its origin to insertion length. Although it was possible to determine the anatomical cross-sectional area for each the sternocleidomastoid (SCM), the trapezius, the splenius capitis and the anterior scalene in the C4/5 axial plane, only the boundary of the SCM was consistently visible along the entire origin to insertion length. The average PCSA of the SCM of the 50th percentile adult male subjects in this study was calculated as $3.80\pm 0.94\text{cm}^2$. Relative to the Kamibayashi, Gzik, and van der Horst results,

the average SCM PCSA in this study is less than 5% different than the reported SCM PCSA values. However, compared to the results of the VanEe study, the PCSA value calculated in this study is 22.76% smaller. The difference in SCM PCSA between the VanEe study and this one can likely be attributed to the length used in the PCSA calculation. In this study, total muscle length from origin to insertion was used since muscle fascicle length is difficult to determine from MRI, and comparable morphological data is not available for children (i.e. fascicle length). The VanEe study found that muscle fibers extend through 72.6+/-9.4% of the muscle's total length. Vasavada et al. [1998] similarly reported that tendon length for the SCM can be as long as 7cm. The overestimated length in this case would reduce the overall PCSA of the muscle. Differences between the results of this study and other studies may also be due to differences in the muscle volumes calculated in each slice. This protocol was developed to provide maximum information in a short amount of time, given the child sample group used in the study. The total imaging time for all sequences was 15 minutes. This was reduced from an imaging time of 30 minutes in a pilot study.

With the notable exception of the trapezius muscle, the anatomical cross-sectional area values at C4/5 in this study are similar to those reported in the published literature.

More recently, more studies have been conducted which measure muscle cross-sectional area (CSA) at specific spinal levels. In 2010, Stemper et al. reported a CSA of 5.65cm² for the SCM and 1.25cm² for the trapezius for subjects imaged in the neutral head-neck, where the neutral head-neck

orientation was defined as a horizontal Frankfort Plane. Other studies were aimed at understanding how changes in neck muscle CSA relate to chronic pain and headaches. A 2009 study by DeLoose et al. measured neck muscle CSA of fighter pilots to determine whether an increase in the CSA of particular neck muscles showed a correlation to chronic neck pain. Subjects in their study were physical fit and were exposed to forces on the body that ordinary subjects would not likely encounter on a daily basis. The subjects in the Stemper study were matched for height and weight to the subjects in the DeLoose study. DeLoose et al. reported cross-sectional areas at C4/5 for subjects reporting no neck pain of, SCM: R: 5.93cm^2 – L: 6.28cm^2 ; trapezius R: 3.97cm^2 – L: 4.32cm^2 ; splenius capitis R: 2.73cm^2 – L: 2.89cm^2 ; and the scalene muscles R: 1.17cm^2 - L: 1.16cm^2 . Subjects were imaged in the traditional supine position. Oksanen et al. [2007] also looked at morphological differences in the neck muscles of subjects with chronic pain. In their study, the neck muscle CSA of adolescents suffering from recurring migraines and tension headaches was compared to that of adolescents without recurring headaches. Subjects in the study were both male and female with an average age of 17 years old. The average height and weight of all subjects, both male and female, was 173cm (69.2”) and 63kg (138.6lbs). The cross-sectional areas for subjects without recurring headaches were SCM: R: 5.02cm^2 – L: 5.26cm^2 ; trapezius R: 1.46cm^2 – L: 1.68cm^2 ; splenius capitis R: 2.84cm^2 – L: 2.94cm^2 ; and the scalene muscles R: 1.13cm^2 - L: 1.20cm^2 . The results of muscle cross-sectional area calculated at C4/5 in this study were, SCM: $5.26\pm 0.76\text{cm}^2$; trapezius: $3.16\pm 1.03\text{cm}^2$; splenius capitis: $2.54\pm$

0.32cm²; and the scalene muscles: 1.25+/-0.20cm². Table 4-5, below shows a summary of reported cross-sectional areas for the SCM, trapezius, splenius capitis and scalene muscles, including the PCSA of the SCM.

Study/Reference	CSA (cm ²)			
	SCM	Trapezius	Splenius Capitis	Scalene Muscles
Physiologic Cross Sectional Area				
Kamibayashi et al. [1998]	3.72 +/-0.91	1.96 +/-0.62		*1.45 +/-0.90
VanEe et al. [2000]	4.92	3.77	3.09	*1.88
Gzik et al. [2008]	R: 3.64 L: 3.96			
from van der Horst paper [1997]	3.7	1.55	2.8	
Dawson study Data (PCSA)	3.81 +/-0.83			
Anatomic Cross Sectional Area				
Oksanen et al. [2007]	R: 5.02 +/-0.68 L: 5.26 +/-0.61	1.46 +/-0.71 1.68 +/-0.79	2.84 +/-0.34 2.94 +/-0.35	1.13 +/-0.27 1.2 +/-0.26
DeLoose et al. [2009]	R: 5.93 +/-1.07 L: 6.28 +/-1.09	3.97 +/-1.05 4.32 +/-1.40	2.73 +/-0.77 2.89 +/-0.70	1.17 +/-0.29 1.16 +/-0.32
Stemper et al. [2010]	5.65	1.25		
Dawson study Data (ACSA at C4/C5)	5.26 +/-0.76	3.16 +/-1.03	2.54 +/-0.32	1.25 +/-0.20

Table 4-5: Cross-sectional area (cm²) of the sternocleidomastoid, trapezius, splenius capitis and scalene muscles as reported in the literature for adult males compared to results measured in this study. Bold type values are the results of this study. *Denotes values for the anterior scalene muscle.

With the exception of the trapezius, the values of cross-sectional area at C4/5 calculated in this study were similar to those in the published literature. The sternocleidomastoid shows the smallest percent difference relative to the published data. Percent difference ranged from no difference to less than 5% difference relative to the left-side Oksanen data. The subjects in the Okasanen study were reported to be approximately the height and weight as the subjects in this study, so in spite of the difference in the average age of the subjects (17 vs. 35 year old) and the inclusion of female subjects in the Oksanen data, the results

are comparable. Relative to the DeLoose and Stemper data, differences in SCM cross-sectional area ranged from 7% (Stemper data) to 16% (DeLoose data). Given that the subjects in these two studies were bigger in both height and weight than the subjects in this study, muscle cross-sectional areas should be larger. In addition, the subjects in the DeLoose study were physically conditioned due to exercise and the nature of their career - fighter pilots experience "extremes of extension and rotation of the cervical spine" [DeLoose, 2009]. As a result of this conditioning, the neck muscles would exhibit an increase in cross-sectional area [Kanehisa, 1994]. Furthermore, the results from both the Stemper study [2010] and a study by Vasavada [1998] show that changes in the flexion/extension of the neck has an effect on both moment arm and muscle cross-sectional area. The subjects in the DeLoose study, although supine, were positioned such that their head and neck were in the neutral position. In neither this study nor the Oksanen study was the position of the head-neck specified.

Similarly, percent differences between the reported cross-sectional area values of the splenius capitis ranged from 11-14% when compared to the Oksanen data, and 7-12% when compared with the DeLoose data. The results of the scalene muscles are similar to those of the splenius capitis. The ACSA of the scalene muscles in this study ranged from 5-10% greater than those reported by Oksanen. The differences in results may be as a result of differences in clarity with which the muscle boundaries used to calculate CSA. As with the SCM, the difference in the stature of the subject was expected to increase the cross-

sectional area of the muscle, however, the reported values of the splenius capitis CSA in the Oksanen study were greater than that of the DeLoose study.

By comparison, the CSA results of the trapezius in this study are greater by 50-150% than the results of both the Stemper and Oksanen studies. Compared to DeLoose study, the CSA of the trapezius is 20-27% smaller than their reported trapezius cross-sectional area. Although differences in height and weight could be cited, the subjects in the Stemper study were matched to the subjects in the DeLoose study for height and weight – the difference between trapezius CSA value between these two studies is greater than 150%. The trapezius muscle boundary is generally visible, however, it is possible that the CSA of this study includes other posterior neck muscles. This study's imaging protocol was developed to maximize the data discernable from the image while reducing the time spent in the magnet since there were child subjects involved in the study. Other studies were not faced with the same restriction which would enable longer scan times and clearer images.

The results of muscle cross-sectional area at C4/5 calculated in this study are comparable to the results published in the literature. Results of this study are smaller than the values reported in the DeLoose [2009] and Stemper [2010] data where the subjects were bigger than the subjects in this study. In the case of the Oksanen [2007] study where the subjects were the same height and weight, the results of this study were within 10% of their study's results, with the exception of the trapezius CSA. The PCSA of the SCM was closer in magnitude to the results of the Kamibayashi [1998] cadaveric study. However since their study did not

include any in-vivo measurements, their results appear to be underestimated. Although Gzik et al. and van der Horst report no use of cadaveric data it is possible that results are also underestimated if the origin to insertion muscle length was used in the calculation rather than fascicle length. Relative to the SCM PCSA value published by VanEe [2000], the value calculated in this study was approximately 25% smaller. This can be attributed to using the origin-to-insertion muscle length rather than the muscle fascicle length in the PCSA calculation.

The PCSA of the SCM in the 10-year old male subjects, and ACSAs calculated from the MR-images were a SCM PCSA of $2.13 \pm 0.30 \text{ cm}^2$. The anatomical cross-sectional areas at C4/5 were $3.33 \pm 0.37 \text{ cm}^2$ for the SCM, $2.89 \pm 0.96 \text{ cm}^2$ for the combined area of trapezius and splenius capitis; and $0.92 \pm 0.17 \text{ cm}^2$ for the scalene. The value for the SCM PCSA is likely underestimated since the origin-to-insertion muscle length was used in the calculation. The muscle differentiation of the 10 year-old male subjects was limited, particularly for the posterior muscles (figure 4-11). The interstitial fat of the adult male neck shows a pronounced boundary around the large muscles. Children, unless obese, have little to no interstitial fat. Other types of imaging sequences for muscles have been developed since this study which provide for better muscle differentiation. However these studies focused on extremities. There is also no data on the fascicle length of the muscles in children.

CHAPTER 5: DETERMINATION OF NECK MUSCLE FORCE AND STRESS AT C-4 VERTEBRAE DURING A MAXIMAL VOLUNTARY CONTRACTION

5.1 INTRODUCTION

The force generated during an individual muscle contraction is difficult to measure due to the complexity of the musculoskeletal system. Numerous assumptions are required to make an indeterminate mechanical system into one in which discrete values of muscle force can be calculated.

Early optimization models [Crownshield, 1978] simplified an otherwise indeterminate system by scaling the muscle response by normalizing based on physiologic characteristics. Crownshield's model reduced the number of model variables by assuming that the muscle with the largest product of muscle cross-sectional area and moment arm produced the greatest moment. The remaining muscles produced a percentage of this force value. While this model was effective, it didn't fully consider the activation patterns of each muscle in a given contraction direction. In the cervical spine, the trapezius muscle has the largest product of moment arm and cross-sectional area but doesn't maximally contract in all directions. Optimization models based on electromyography seek to similarly simplify the joint model by normalizing the muscle's response to its maximal voluntary response [Cholewicki, 1994; Amarantini, 2004; Staudenmann, 2005]. In their 2001 study, Gagnon et al. concluded that an EMG-assisted optimization model was the best model that "simultaneously satisfied mechanical and physiological validity". EMG-assisted optimization models have been used to estimate the muscle force developed in the lumbar muscles [Gagnon, 2001];

cervical spine [Moroney, 1998; Lu, 1996; Choi, 2003]; lower extremity muscles [Amarantini, 2004; Bogey, 2005; Erdemir, 2007; Staudenmann, 2007; Heintz, 2007], and upper extremity [Laursen, 1998; Staudenmann, 2005].

Many studies have been conducted to determine the difference in muscle strength and response between adults and children. Most studies use load studies to make strength comparison between adults and children [Ikai, 1968; Kanehisa, 1994, 1995; Halin, 2003]. These studies were conducted using the muscles of the upper and lower extremities. Results showed a significant difference in the strength between adults and children. In all of the above studies, when strength data was normalized to muscle cross-sectional area, the difference between adults and children was decreased, but was still significant. The cause of the lesser strength and normalized strength in children is not fully understood. During puberty, skeletal muscles are not only affected by physical and hormonal changes but studies show that skeletal muscles are also affected by neuronal changes [Blimkie CJR, 1989, in Lambertz, 2003]. In the 2003 study by Lambertz et al., the increased musculotendinous stiffness of the triceps surae with age was attributed not only to increase maturity of the elastic tissues but to changes in the activation capacity of the muscles. Their study showed that the muscle activation required to maintain a specific level of torque was greater in 7 year olds than in 11-year olds. Further their study showed that younger children also showed a greater level of muscle co-activation, all of which was attributed to an immaturity in the neural mechanisms that control the muscle in children. Grosset et al. [2008] suggested that the immaturity was to the central pattern

generator governing recruitment of the muscles. Their 2008 study showed that the neuromuscular efficiency, expressed as the ratio of applied torque to %MVC, was lower in children than in adults. The results of a study by Halin R., et al. [2003], also suggested a lower level of neuromuscular activation in children may cause them to be unable to fully recruit Type I (slow twitch) muscle fibers.

Understanding how a muscle generates force and how much force it can generate is important for developing understanding injury patterns and developing rehabilitation programs as well as developing accurate human surrogates. The physiologic muscle data most readily available is that of an adult. Understanding the differences in muscle strength and responses between adults and children would provide valuable information for the development of child-specific safety equipment and human surrogates to assess safety equipment and motor vehicles. To that end, this study was performed to calculate the force and stress generated in the neck muscles of 50th percentile adults and 10 year old boys under static loading using an EMG assisted optimization model.

5.2 METHODOLOGY

5.2.1 Force and EMG Data Collection:

5.2.1.1 Instrumentation

Surface electromyography (EMG) was used to record the muscle activity of sternocleidomastoid (SCM), the trapezius (TRAP), the splenius capitis (SPL) and the scalene (anterior, middle and posterior) muscles (SCAL). Signals were collected bi-laterally using a pair of V91-02 AgCl 4mm diameter reusable electrodes (Coulbourn Instruments, Whitehall, PA) (figure 5-1). Signals were

input to a differential AC amplifier of 110db common mode rejection ratio, with a 10-2500Hz analogue bandpass filter (Bortek Biomedical Ltd., Calgary, AB, Canada). Signals were sampled at 5000Hz with a gain of 500. Data was recorded and stored using a LabVIEW program specifically written for this application (LabVIEW 7.1, National Instruments Corp, Austin, TX).

Electrodes were attached to the skin by means of double-sided, disposable, adhesive rings and additional adhesive tape as required. A generic brand, non-irritating, water-based electrode gel covering the electrode/skin interface was used to reduce the impedance of the skin, thus allowing for better signal collection. Two electrodes were placed on the belly of the muscle, 1cm apart. The ground electrode was placed on the right clavicle. Seventeen electrodes were used on each subject.

A single axis 1000lb load cell sensor number 2077-075 (Humanetics Innovative Solutions, Inc., formerly Denton ATD, Plymouth, MI) was used to collect force data. The load cell had been calibrated in 2000 by Denton ATD. Load cell data was input to a single channel of a TDAS data collection system. Data was sampled at 10,000Hz and recorded using TDAS Control v.6.81g2 (Diversified Technical Systems, Seal Beach, CA). All data was stored on a computer.

5.2.1.2 Electrode Placement

The subject's skin was cleaned with rough paper towel and rubbing alcohol to remove any oil from the skin prior to attaching the electrode. The ground

electrode was attached to the subject on the skin over the right clavicle. Only the most superficial muscles, responsible for flexion, extension and lateral bending of the neck were instrumented in this study. The sternocleidomastoid was identified by having the subject turn his/her head to one side -right or left depending on the side being instrumented - with the chin resting on the opposite shoulder. The belly of the muscle is easily palpated from this position. The trapezius is identified by asking the subject to raise his shoulders against the resistance of the tester's hand pushing down. The levator scapula is the most superficial muscle in the upper portion of the posterior triangle, formed by the junction of the sternocleidomastoid and the trapezius. This junction can be palpated when the subject holds his head in the neutral position. The anterior, middle and posterior scalene muscles cannot be distinguished one from the other by external palpation; therefore, the response of the scalene muscles was measured as a single group. The scalenes lie at the base of the posterior triangle of neck and can be located by palpating above the clavicle.

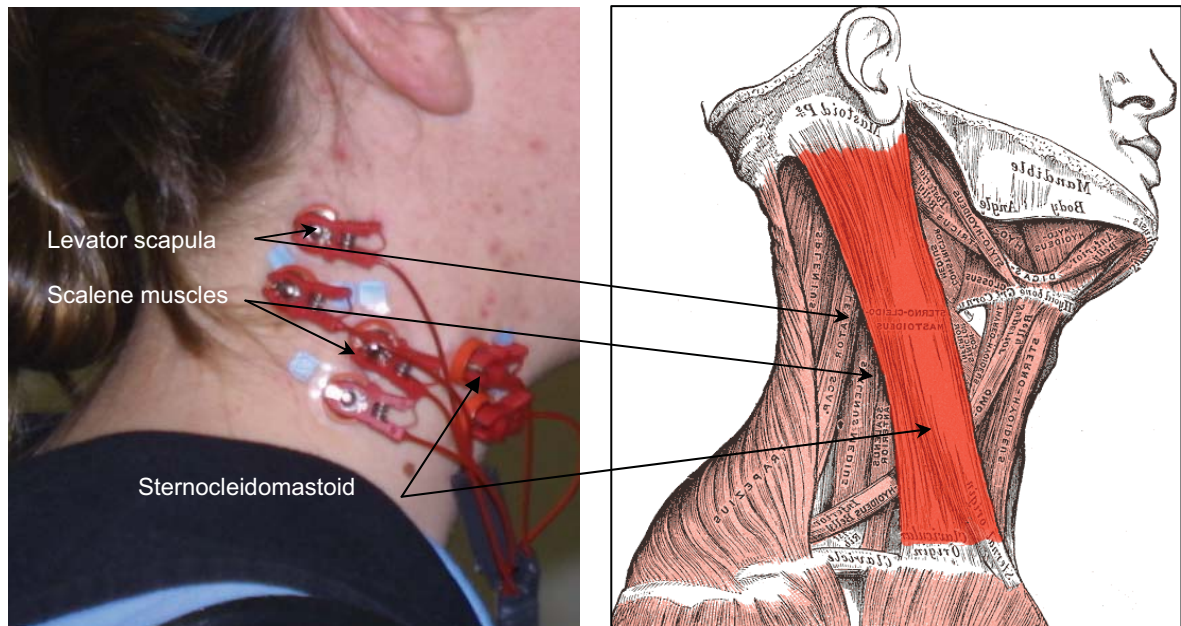


Figure 5-1: (a) Placement of EMG electrodes over the sternocleidomastoid, levator scapula and scalene muscles, and (b) drawing of the superficial musculature of the neck and the muscles of the posterior triangle of the neck [Gray, 1918]. The 4mm diameter of the electrodes made instrumenting the smaller surface area of the 10 year-old male subject's neck possible.

Proper placement of the electrodes on the muscles helped to prevent cross-talk between the muscles. The group **Surface Electromyography for the Non-Invasive Assessment of Muscles** (SENIAM) and other similar groups have developed a series of guidelines for proper electrode placement, which include placing the electrodes on the belly of the muscle, away from the neuromuscular junctions – the location in which the axon of the motor neuron meets the motor endplate for muscle stimulation - and placing the electrodes such that they are parallel to the direction of the muscle fibers. These guidelines were followed in this study. However, while they don't completely eliminate cross-talk between muscles, they do limit the interference.

5.2.1.3 Maximal Voluntary Contraction Data Collection Set-up

The static test fixture consisted of a load cell attached to an adjustable, rigid arm (figure 5-2).

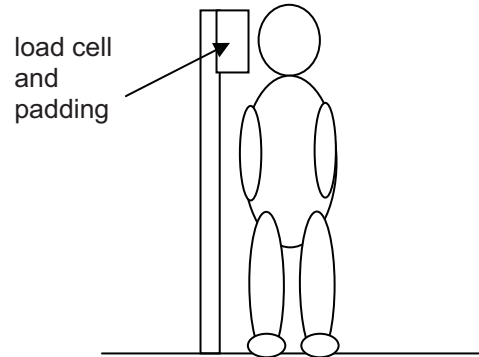


Figure 5-2: Static test fixture. The position of the load cell was adjustable to align with the center of gravity of the subject's head.

The set-up is similar to the fixture described in the studies conducted by Kumar et al. [2001, 2001, 2002, 2003, 2004], Subjects in those studies were seated, rather than standing. In other studies Seng et al. [2002] used an isokinetic dynamometer to determine the static force generated in the neck muscles of adult male military recruits. However, their study did not collect EMG data. Kanehisa et al. [1994, 1995] also used an isokinetic dynamometer for testing the strength of the elbow flexors and knee extensors in adult males and females as well as children. Maganaris et al. [2001] used both MR-imaging and the force data collected using an isokinetic dynamometer to measure the tendon length of the ankle plantar and dorsi-flexors of the ankle in adults.

Tests for maximal voluntary contraction were conducted with the subject standing. In flexion/extension, the padded load cell was positioned so that its

center coincided with the midline of the subject's forehead, approximately halfway between the eyebrows and the hairline. A 1cm thick fabric pad was secured to the load cell using high strength tape to provide a buffer between the subject's head and the hard edges of the load cell. In adult subjects the bottom of the load cell was in line with the bridge of the nose. The load cell was not repositioned for testing in extension, the subject turned to face the opposite direction. In lateral bending, the load cell was adjusted so that its center coincided with the auditory canal. The surface area of the load cell was large, particularly relative to the child's head, to encompass a large portion of the pushing surface. External moment arms from the center of the load cell of the head to the C4 vertebra were measured and recorded during testing. The center of gravity of the head is approximately 2cm above and 2cm forward of the auditory canal [Beier et al., 1980]. In flexion/extension, the load cell was positioned approximately in line with the CG. The moment arm of the applied moment at C4 was measured from the center of the load cell to C4. The C4 vertebra was determined by palpating the subject's neck along the spinous processes. The spinous process of C7 was located first. C4/5 was determined by palpating up from C7.

Prior to the start of data collection, subjects were given a short training and warm-up session to familiarize themselves with the equipment and procedure. A baseline noise signal was collected for 10 seconds. The subject were then asked to exert a maximum voluntary contraction by pushing as "hard as possible" [Kumar, 2001, 2002] using only their head against the test fixture's

rigidly fixed lever arm. The contractions were recorded during each of three consecutive repetitions of the test. Each contraction lasted for 5 seconds. A relaxation period of 2 minutes was given in between contractions to prevent muscle fatigue and to maintain consistency with other similar studies [Kumar, 2000, 2001, 2002, 2004; Choi, 2000]. Data was collected for contractions in flexion, extension and right and left lateral bending in order that the true MVC for each muscle was recorded.

5.2.2 Data Processing

5.2.2.1. Data Filtering

The baseline noise signal and the Maximal Voluntary Contraction (MVC) signals were processed, using a custom-built LabVIEW program. A baseline EMG signal was collected for ten seconds prior to the beginning of the test session. Subjects were asked to stand completely still during this period. The data processing protocol used by Staudenmann et al, [2007] was followed since their study indicated that it provided the best signal for force estimation. The baseline noise signal collected for each subject at the beginning of the data collection was processed first. The signal was high-pass filtered using a second order Butterworth filter with a 250Hz cut-off frequency. The signal was rectified and then low passed filtered using a second order Butterworth filter with a 10Hz cut-off frequency. The mean of the rectified, filtered signal was calculated and saved. The mean was calculated from the point at which the sustain contraction was achieved for a duration of 4.5 seconds. The MVC signals were processed using the same protocol as described above. The MVC signal was zeroed after

filtering by subtracting the mean of the filtered baseline. Figure 5-3 shows the raw and filtered muscle contraction signal.

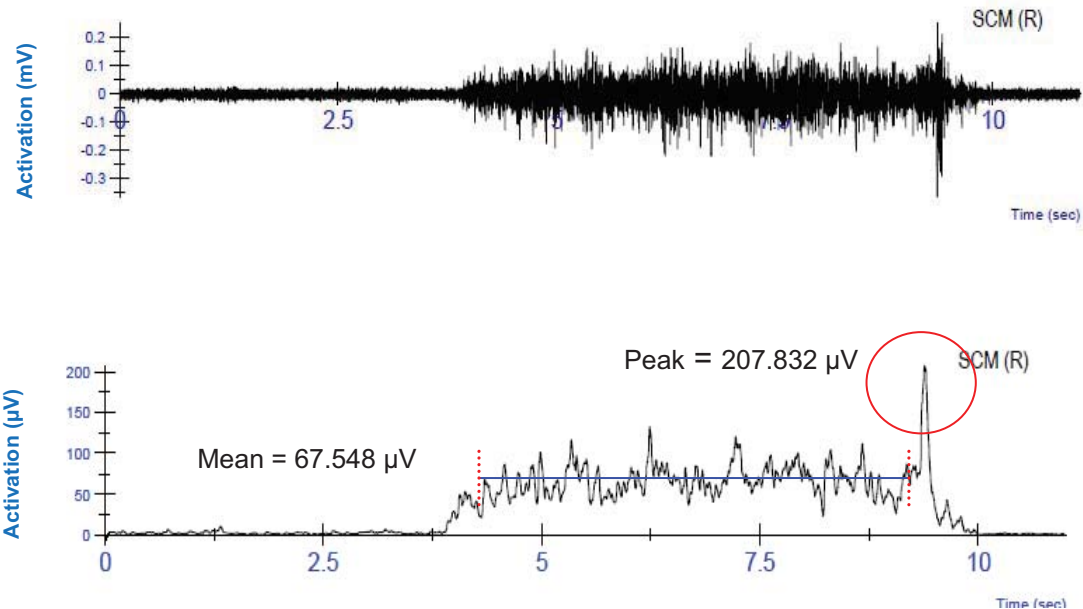


Figure 5-3: EMG recording of the right SCM in flexion (a) raw data; (b) filtered/rectified data. Red circle denotes peak EMG (mV), blue line shows the average EMG value (μV) for the muscle contraction. The mean muscle contraction was calculated for the sustained muscle contraction for a duration of 4.5 -5s.

The peak and mean EMG activation values from each muscle contraction in each bending direction were obtained from the recorded EMG data.

The data from the load cell was processed using a custom built LabVIEW analysis program. Data was zeroed and filtered using a second order high pass filter with a cut-off frequency of 1000hz.. The peak and mean force values were recorded, processed in LabVIEW and stored on a personal computer.

5.2.2.2 Normalizing EMG data

The three peak filtered, rectified EMG values in mV for each muscle for a given test direction were averaged, as were the three mean values. The maximum average EMG value for a muscle, regardless of the contraction direction, was deemed the Maximal Voluntary Contraction (MVC). Table 5-1 shows the instrumented and the direction of their respective MVC.

Muscle	Direction of MVC
Sternocleidomastoid	Flexion
Posterior Muscles	Extension
Postero-Lateral muscles	Lateral Bending
Scalene muscles	Lateral Bending

Table 5-1: Direction of Maximal Voluntary Contraction for SCM, posterior muscles, posterior-lateral muscles and scalene muscles.

The averaged mean EMG values for each muscle in all tested directions were normalized by dividing by their respective MVC peak value. Force values were not normalized.

5.2.3 Force Calculations

The force developed in each of the eight instrumented muscle groups was calculated for the MVC test condition using force and moment equations of motion taken in the C4/5 vertebral plane. Although muscle activation values recorded using surface EMG pertains to the muscle nearest to the skin, it was assumed that the muscle activation value was the same for all muscles within the muscle group [Moroney, 1988; Lu, 1996; Choi, 2004]. The muscle groupings were as follows,

- 1) Posterior muscles (electrodes attached over the trapezius) – trapezius, splenius capitis, splenius cervicis, semispinalis capitis, semispinalis cervicis and multifidus.
- 2) Postero-lateral muscles (electrodes placed in the superior aspect of the posterior triangle) – longissimus and levator scapula.
- 3) Scalene muscles (electrodes placed in the lower aspect of the posterior triangle) – scalene muscles and longus colli and cervicis.
- 4) Sternocleidomastoid

Figure 5-1, above, shows the external placement of the electrodes. Figure 5-4 shows the muscle groupings in an axial view of the neck at C4. Table 5-2 gives the values of posterior and postero-lateral muscle cross-sectional area and the percent of the CSA of the combined trapezius and splenius capitis. For muscles like the scalene muscles that cannot be individually identified, their CSA was estimated as a percentage of the combined muscle group CSA. Based on the VanEe et al [2000] and the Oi et al. [2004], the CSA of the middle scalene comprises approximately 24% of the combined CSA of the anterior, posterior, and middle scalene, the longus colli and the longus cervicis.

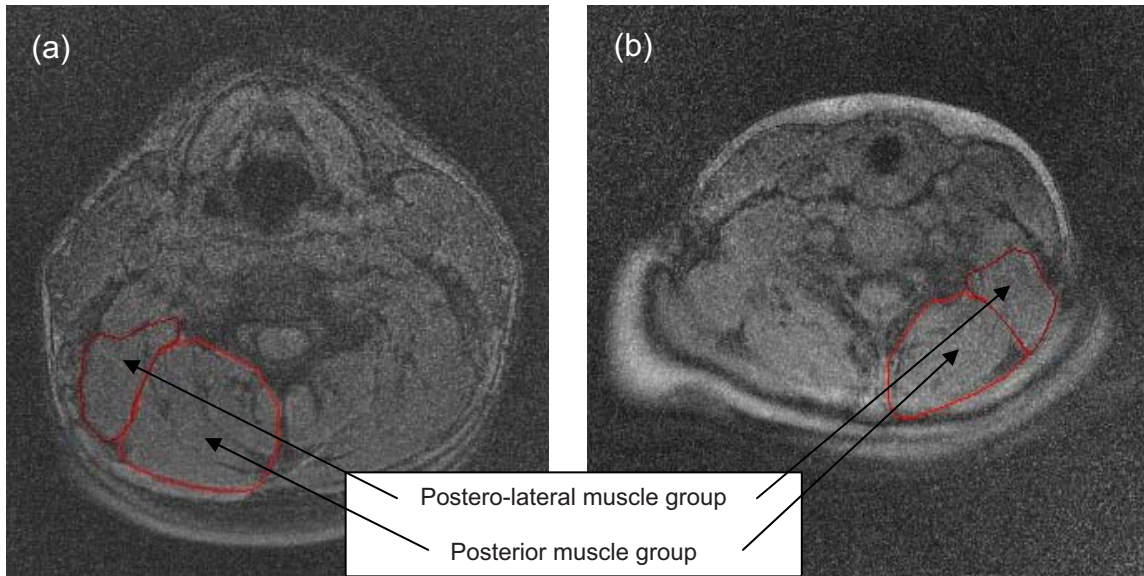


Figure 5-4: Axial MR-image at C4/5 for (a) 50th percentile adult male and (b) 10-year-old boy. The boundaries show the muscle or muscle groups recorded by a pair of electrodes – SCM, SCAL, POST and P-L. Moment arms were taken from the centroid of the muscle group to the centroid of the neck. The centroid of the neck was calculated using ImageJ, as described in Chapter 4 - **Muscle Cross-sectional Area and Moment Arms based on Magnetic Resonance Imaging measurements**

Average 10-year boys

Subject	Anatomic CSA at C4 (cm ²)		%CSA			Neck CSA (cm ²)
	POST	P-L	TRAP	SPL	TRAP+SPL	
K01	6.15	3.10			55.91	65.22
K03	8.58	3.88			53.53	98.37
K04	5.68	2.66			40.53	62.29
K05	6.30	2.92			57.48	77.62
K06	8.08	3.61			42.19	77.83
K07	7.45	3.37			21.20	76.88
K08	9.31	3.61			18.90	77.82
K09	8.15	2.41			43.05	70.51
K10	7.35	2.93			33.49	65.02
K11	6.88	2.44			31.98	54.91
average	7.39	3.09			39.83	72.65
SD	1.16	0.51			13.59	12.01

Average Adult Males

Subject	Anatomic CSA at C4 (cm ²)		%CSA			Neck CSA (cm ²)
	POST	P-L	TRAP	SPL	TRAP+SPL	
S08	13.02	8.42	38.09	23.67	61.76	133.88
S09	11.54	5.38	23.45	21.67	45.12	108.07
S10	13.13	7.28	38.73	19.60	58.33	145.66
S11	10.30	4.35	24.09	29.09	53.18	109.85
S13	13.38	4.72	18.90	18.19	37.08	122.52
S14	11.94	5.79	25.65	21.80	47.45	109.27
S15	12.69	4.23	21.30	17.47	38.77	107.99
S16	9.83	4.45	20.96	25.60	46.57	101.33
S17	14.47	5.47	22.03	17.06	39.10	147.93
S20	13.95	5.54	20.11	14.29	34.39	128.95
average	12.42	5.56	25.33	20.84	46.18	121.55
SD	1.51	1.35	7.17	4.44	9.24	16.82

Table 5-2: Cross-sectional area of the posterior and postero-lateral muscles for both 10-year old male and 50th percentile adult male subject groups. The trapezius and splenius capitis are shown as a percent of the posterior cross-sectional area for the adult male subject group. The trapezius+splenius capitis is shown as a percent of the posterior cross-sectional area for both subject groups. Anatomic CSA values for the trapezius, splenius capitis and TRAP+SPL are shown in Table 4-3.

Figure 5-5 (a) shows the Free Body Diagram for a maximal voluntary contraction in flexion. The standard body coordinate system was applied in this study - Z-axis is vertical, the X-axis is perpendicular to the coronal plane and the Y-axis is perpendicular to the sagittal plane. The flexion and extension contractions will result in moments about the Y-axis, while the lateral left and right bending will result in moments about the X-axis. The force and moment equations are based on the free body diagram below. Figure 5-5 (b) shows the Free Body diagram of a section taken at C4/C5 where the acting muscle forces generate the moment M_y shown in Fig 5-5 (a).

The applied moment, M_y , was calculated relative to the center of gravity of the head, where the cg of the head is approximately 2cm above and 2cm forward of the auditory canal [Beier et al., 1980]. The moment arm of the applied moment, d_{head} , was measured from the center of gravity of the head to the C4 vertebra. The C4 vertebra was determined by first locating the C7 vertebra using palpation, and then palpating up from C7 to C4.

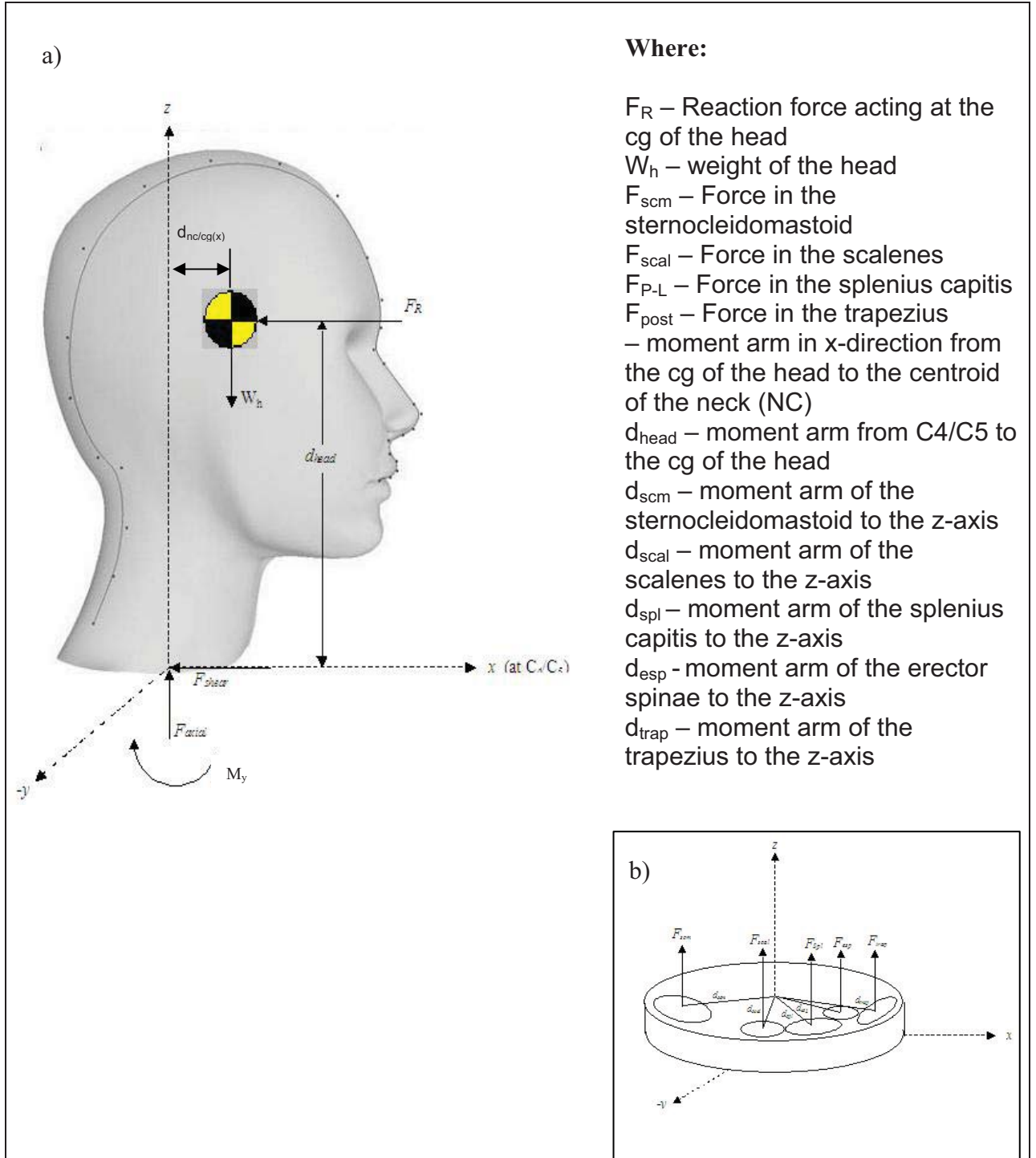


Figure 5-5: Free Body Diagram of (a) the Head/Neck to C4; (b) section at C4/C5 showing the forces and moment arms contributing to M_y
 Consider first the equations of motion in flexion:

$$\Sigma M_x = 0 \quad (5-1)$$

$$\Sigma M_y = 0 \quad (5-2)$$

$$\Sigma M_z = 0 \quad (5-3)$$

Where, from the FBD,

$$\Sigma M_y = 0 = -F_R \times d_{head} \quad (5-4)$$

and

$$\Sigma M_{y(flex)} = -W_h \times d_{nc/cg(x)} + 2 * [-F_{SCM(z)} \times d_{SCM(x)} - F_{SCAL(z)} \times d_{SCAL(x)} + F_{P-L(z)} \times d_{P-L(x)} + F_{POST(z)} \times d_{POST(x)}] \quad (5-5)$$

Where:

$-W_h \times d_{nc/cg(x)}$ = the moment due to the mass of the head. This is the baseline moment experienced by the muscles as they work to resist the mass of the head in the neutral position. The muscle activity is represented by the baseline EMG activity which is subtracted from the EMG signal when it is zeroed.

The effects of the tendons and ligaments were assumed to be negligible in this portion of the testing. It was assumed that the muscle response from one side of the neck to the other is symmetrical as denoted by the factor of 2 multiplying the muscle forces. The force balance equations in flexion are as follows:

$$\Sigma F_{x(flex)} = 0 = -F_R + 2(F_{SCM,F(x)} + F_{P-L,F(x)} + F_{SCAL,F(x)} + F_{POST,F(x)}) + F_{shear} \quad (5-6)$$

$$\Sigma F_{y(flex)} = 0 \quad (5-7)$$

$$\Sigma F_{z(flex)} = 0 = F_{axial} - W_{head} + 2(F_{SCM,F(z)} + F_{P-L,F(z)} + F_{SCAL,F(z)} + F_{POST,F}) \quad (5-8)$$

Where:

F_R = the resisting force of the head recorded by the load cell during the MVC.

F_{axial} = the resisting force produced by the inter-vertebral discs and the bony structure of the vertebral column.

F_{shear} = the shear force acting in the anterior-posterior direction in C4/5 axial plane of the neck

The equations in extension are similar to those in flexion, a sign change denotes the different bending direction. Equations (5)-(8) become,

$$\sum M_{y(ext)} = 2 * [F_{SCM(z)} \times d_{SCM(x)} + F_{SCAL(z)} \times d_{SCAL(x)} - F_{P-L(z)} \times d_{P-L(x)} - F_{POST(z)} \times d_{POST(x)}] \quad (5-9)$$

$$\sum F_{x(ext)} = 0 = F_R + 2(F_{SCM,E(x)} + F_{P-L,E(x)} + F_{SCAL,E(x)} + F_{POST,E(x)}) - F_{shear} \quad (5-10)$$

$$\sum F_{y(ext)} = 0 \quad (5-11)$$

$$\sum F_{z(ext)} = 0 = F_{axial} - W_{head} - 2(F_{SCM,E(z)} + F_{P-L,E(z)} + F_{SCAL,E(z)} + F_{POST,E(z)}) \quad (5-12)$$

The equations (5)-(12) are indeterminate. Using an EMG assisted optimization model, equations (5-13) – (5-15) [Choi, 2000],

$$F_i = \left(\frac{emg}{emg_{max}} \right)^{1/1.3} a_i \sigma_{max} \quad (5-13)$$

Where:

F_i = the individual muscle force.

a_i = the cross-sectional area of the individual muscle

σ_{\max} = maximum muscle stress

$\left(\frac{emg}{emg_{\max}}\right)^{1/1.3}$ = the muscle mean rectified EMG signal normalized to its maximal EMG value, i.e. %MVC. The exponent, used in the EMG optimization neck study by Choi et al. [2004] is a power function relationship which describes the relationship between muscle force and the ratio of the mean, rectified EMG to the maximum EMG activation for a particular muscle. The power relationship was developed using data from studies by Stokes et al. [1987], Vink et al. [1987] and most recently Cholewicki et al. [1995]. The power relationship better approximates the relationship of EMG and muscle force than the linear relationship used in other studies [Kumar, 2002, 2003].

Since the force calculated is the total force of the muscle grouping,

$$F_i = \left(\frac{emg}{emg_{\max}}\right)^{1/1.3} F_{\max} \quad (5-14)$$

Where:

$F_{\max} = a \cdot \sigma_{\max}$ = maximum muscle force

Using the above relationship (5-14), the number of unknowns and equations were reduced to six. Equation 5-13 was also used to resolve the group muscle

force – i.e. POST, P-L, and SCAL - into individual muscle forces – i.e. trapezius, splenius capitis and scalene (M). For this equation 5-13 is re-written as:

$$F_i = \left(\frac{emg}{emg_{max}} \right)^{1/1.3} \%CSA * F_{max} \quad (5-15)$$

Where %CSA values are shown in Table 5-2, and:

$$F_i = F_{trap}, F_{spl}, F_{trap+spl} \text{ or } F_{scal(M)}$$

$$F_{max} = F_{post}, F_{p-l}, \text{ or } F_{scal}, \text{ as calculated from equations 5-16 through 5-21.}$$

$$M_{y(ext)} = -F_{R,ext} \times d_{head} = 2 * (\%MVC_{ext})^{1/1.3} * F_{SCM(MVC)} * d_{SCM(x)} \sin \theta_{SCM} \quad (5-16)$$

$$\begin{aligned} & - 2 * (\%MVC_{ext})^{1/1.3} * F_{POST(MVC)} * d_{POST(x)} \sin \theta_{POST} \\ & - 2 * (\%MVC_{ext})^{1/1.3} * F_{P-L(MVC)} * d_{P-L(x)} \sin \theta_{P-L} \\ & + 2 * (\%MVC_{ext})^{1/1.3} * F_{SCAL(MVC)} * d_{SCAL(x)} \sin \theta_{SCAL} \end{aligned}$$

$$F_{x(ext)} = -F_{R,ext} = 2 * (\%MVC_{ext})^{1/1.3} * F_{SCM(MVC)} * \cos \theta_{SCM} \quad (5-17)$$

$$\begin{aligned} & + 2 * (\%MVC_{ext})^{1/1.3} * F_{POST(MVC)} * \cos \theta_{POST} + 2 * (\%MVC_{ext})^{1/1.3} * F_{P-L(MVC)} * \cos \theta_{P-L} \\ & + 2 * (\%MVC_{ext})^{1/1.3} * F_{SCAL(MVC)} * \cos \theta_{SCAL} - F_{shear} \end{aligned}$$

$$m_{head} * g = -2 * (\%MVC_{ext})^{1/1.3} * F_{SCM(MVC)} * \cos \theta_{SCM} \quad (5-18)$$

$$\begin{aligned} & - 2 * (\%MVC_{ext})^{1/1.3} * F_{POST(MVC)} * \cos \theta_{POST} \\ & - 2 * (\%MVC_{ext})^{1/1.3} * F_{P-L(MVC)} * \cos \theta_{P-L} - 2 * (\%MVC_{ext})^{1/1.3} * F_{SCAL(MVC)} * \cos \theta_{SCAL} \\ & + F_{axial} \end{aligned}$$

$$M_{y(flex)} = F_{R,flex} \times d_{head} = -2 * (\%MVC_{flex})^{1/1.3} * F_{SCM(MVC)} * d_{SCM(x)} \sin \theta_{SCM} \quad (5-19)$$

$$\begin{aligned} & + 2 * (\%MVC_{flex})^{1/1.3} * F_{POST(MVC)} * d_{POST(x)} \sin \theta_{TRAP} \\ & + 2 * (\%MVC_{flex})^{1/1.3} * F_{P-L(MVC)} * d_{P-L(x)} \sin \theta_{P-L} \\ & - 2 * (\%MVC_{flex})^{1/1.3} * F_{SCAL(MVC)} * d_{SCAL(x)} \sin \theta_{SCAL} \end{aligned}$$

$$F_{x(flex)} = F_{R,flex} = 2 * (\%MVC_{flex})^{1/1.3} * F_{SCM(MVC)} * \cos \theta_{SCM} \quad (5-20)$$

$$\begin{aligned} & + 2 * (\%MVC_{flex})^{1/1.3} * F_{POST(MVC)} * \cos \theta_{POST} \\ & + 2 * (\%MVC_{flex})^{1/1.3} * F_{P-L(MVC)} * \cos \theta_{P-L} + 2 * (\%MVC_{flex})^{1/1.3} * F_{SCAL(MVC)} * \cos \theta_{SCAL} \\ & - \%F_{shear(ext)} \end{aligned}$$

$$m_{head} * g = -2 * (\%MVC_{flex})^{1/1.3} * F_{SCM(MVC)} * \cos \theta_{SCM} \quad (5-21)$$

$$\begin{aligned} & - 2 * (\%MVC_{flex})^{1/1.3} * F_{POST(MVC)} * \cos \theta_{POST} \\ & - 2 * (\%MVC_{flex})^{1/1.3} * F_{P-L(MVC)} * \cos \theta_{P-L} - 2 * (\%MVC_{flex})^{1/1.3} * F_{SCAL(MVC)} * \cos \theta_{SCAL} \\ & - \%F_{axial(ext)} \end{aligned}$$

The recorded values of applied moment and the moment arms used in these calculations are shown in Table 5-2. The values for %MVC^{1/1.3} are shown in Table 5-3.

An online, matrix solver from Pennsylvania State University was used to calculate the values of each unknown:

[http://mac6.ma.psu.edu/lin_equations/index.html].

5.2.4 Statistical Analysis

A student's t test was used to determine the statistical significance of the difference in means between the 50th percentile adult male and 10 year old boy subject groups. A p value <0.05 was considered significant. Linear regression analysis was used to determine if correlation existed between age and force and stress generated in the neck muscles. A p value <0.05 was considered significant P values <0.10 were also noted.

5.3 RESULTS

5.3.1 Force and EMG

Using the recorded and calculated data, comparisons between 50th percentile adult males and 10 year-old boys for applied moments and forces; peak and mean EMG values; calculated muscle forces and muscle stress generated under maximal voluntary contraction. Five subjects were removed from this portion of the analysis, although the data collected from their MR-images and dynamic tests was used in later portions of the study. Both K08 and

S10 were removed from the analysis since one or more EMG channels did not record. K01, K05 and S08 were removed from the study, and analysis of their EMG values indicated that the subjects were leaning into the load cell. The applied load was reasonable compared to other subjects however there was little or no EMG activity.

Muscle forces in flexion and extension were calculated using the applied forces and moments collected during maximal voluntary contraction. Values of applied moments, applied forces and the moment arms used in the calculation of individual muscles forces are shown below in Table 5-3.

10 Year Old Boys

Subject	Mean Applied Load (N)		Mean Applied Moment (Nm)		Moment Arms (mm)				
	Extension	Flexion	Extension	Flexion	d _{SCM(x)}	d _{POST(x)}	d _{P-L(x)}	d _{SCAL(A,M,P)}	d _{head}
K03	24.6	6.6	3.0	0.8	22.3	21.5	5.9	9.9	120.0
K05	13.0	19.9	1.8	2.8	18.9	23.1	7.0	4.2	140.0
K06	37.0	22.9	5.2	3.2	21.0	24.8	11.3	6.1	140.0
K07	27.5	27.8	3.7	3.8	13.0	25.7	10.2	2.3	120.0
K09	20.4	4.9	2.4	0.6	17.3	22.1	6.1	3.4	120.0
K10	12.3	19.0	1.5	1.6	12.6	23.3	10.7	0.6	120.0
K11	13.7	10.3	1.7	1.3	14.5	23.3	8.3	0.8	125.0
Average	21.2	15.9	2.7	2.0	17.1	23.4	8.5	3.9	126.4
Std. Dev.	9.2	8.7	1.3	1.2	3.8	1.5	2.2	3.3	9.4

50th Percentile Adult Males

Subject	Mean Applied Load (N)		Mean Applied Moment (Nm)		Moment Arms (mm)				
	Extension	Flexion	Extension	Flexion	d _{SCM(x)}	d _{POST(x)}	d _{P-L(x)}	d _{SCAL(A,M,P)}	d _{head}
S09	33.5	14.8	5.7	2.5	14.2	27.6	12.3	4.7	170.0
S11	21.3	9.9	3.8	1.8	16.1	26.4	13.3	4.5	180.0
S13	44.4	23.6	7.5	4.0	14.0	33.3	21.2	0.7	170.0
S14	30.6	35.0	4.9	5.6	19.3	24.1	9.4	6.6	160.0
S15	18.8	9.5	2.8	1.4	11.8	27.5	11.1	0.8	150.0
S16	55.8	38.0	9.1	5.9	14.3	30.3	10.3	5.3	155.0
S17	15.0	15.3	2.5	2.5	14.6	24.3	8.5	13.3	165.0
S20	66.7	50.4	8.7	6.6	14.4	25.1	11.2	11.4	130.0
Average	35.7	24.5	5.6	3.8	14.8	27.3	12.2	5.9	160.0
Std. Dev.	18.5	15.0	2.6	2.0	2.1	3.2	4.0	4.5	15.4

Table 5-3: Mean applied forces, mean applied moments and moment arms for both 10-year-old male and 50th percentile adult male subject groups. The mean values refer to the average of the sustained muscle contraction force for all three trials.

The peak and mean applied forces the adult subjects were able to exert on the load cell in extension was significantly greater than that of children ($p < 0.02$). In flexion, the difference in the applied load was only significant to 90% ($p < 0.10$). The adult subject group was able to apply a significantly greater moment at C4/5 in both flexion and extension ($p < 0.02$) than the 10-year-old boys.

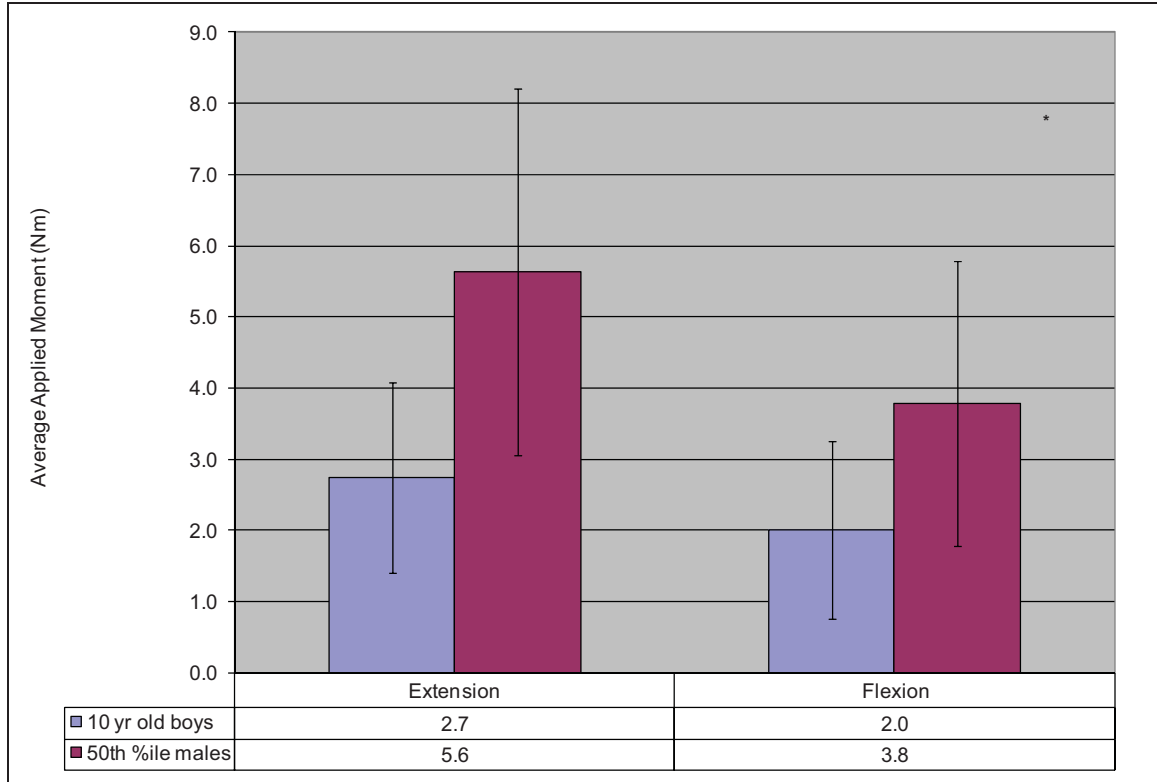


Figure 5-6: Comparison of average applied moments in 3 bending directions between 50th percentile adult males and 10-year old boys. Adults produced significantly higher moments ($p < 0.02$) than the 10-year old boys.

The processed rectified EMG muscle contraction signals showed the expected characteristic trapezoidal shape for a sustained, maximal contraction (see figure 5-3). In the direction of their maximum contraction – SCM (flexion) and TRAP (extension) – the mean EMG activation values were approximately 30% of the peak MVC values. Percent MVC in the remaining muscles ranged from 10% to 25% of peak values for both the adult and child sample groups. The difference between the mean EMG values of the adults and 10-year old boys was not significant in this study with the exception of the SCM (R) which was significant to $p = 0.05$ in extension, and the SCAL (R) which was significant to

p=0.10 in extension. The difference in peak and mean EMG values was not significant between adult and 10-year-old boy subject groups.

10 Year Old Boys

	Extension			Flexion			Lateral (L)	Lateral (R)
	Average Peak (μ V)	Average Mean (μ V)	Average %MVC	Average Peak (μ V)	Average Mean (μ V)	Average %MVC	Average Peak (μ V)	Average Peak (μ V)
SCM(R)	38.1	5.3	0.03	163.4	59.5	0.34	62.3	97.6
SCM(L)	55.5	11.1	0.10	174.3	54.5	0.29	43.4	64.0
POST(R)	84.0	27.2	0.32	42.9	7.3	0.07	62.1	119.0
POST(L)	82.2	22.0	0.26	61.4	7.8	0.11	65.8	96.7
P-L(R)	122.5	27.2	0.15	105.3	31.1	0.16	56.7	79.3
P-L(L)	102.8	23.8	0.18	82.3	17.8	0.14	81.9	32.2
SCAL(R)	83.4	21.5	0.19	76.3	20.6	0.26	102.5	81.3
SCAL(L)	78.4	18.3	0.18	62.1	13.3	0.14	95.6	47.0

50th Percentile Adult Males

	Extension			Flexion			Lateral (L)	Lateral (R)
	Average Peak (μ V)	Average Mean (μ V)	Average %MVC	Average Peak (μ V)	Average Mean (μ V)	Average %MVC	Average Peak (μ V)	Average Peak (μ V)
SCM(R)	85.7	29.2	0.11	150.9	51.1	0.37	73.9	180.0
SCM(L)	99.6	32.0	0.11	136.2	43.5	0.33	107.2	72.9
POST(R)	39.8	13.1	0.27	17.9	3.2	0.08	43.7	70.2
POST(L)	26.9	9.4	0.31	13.3	2.5	0.08	39.7	79.6
P-L(R)	105.8	33.6	0.24	55.1	17.6	0.17	72.8	79.3
P-L(L)	56.2	16.3	0.20	38.2	9.2	0.15	50.3	20.9
SCAL(R)	120.8	37.6	0.20	83.6	25.3	0.20	64.8	85.2
SCAL(L)	50.6	16.3	0.20	35.1	8.8	0.16	60.1	31.4

Table 5-4: Maximum and average EMG activation values (mV) and normalized %MVC values for extension and flexion, and peak EMG activation values (mV) in lateral bending. Values highlighted in blue represent the direction of the maximal voluntary contraction (MVC) for the SCM and trapezius. The direction of MVC for the SPL and SCAL is in lateral bending.

The calculated muscle forces generated during the flexion and extension contractions, as well as the calculated shear and axial forces in the C4/5 vertebral segment during loading are shown below in Table 5-5. The calculated stress values in extension and flexion are shown in Table 5-6.

In the 10-year old subject group, the muscle force of the trapezius and splenius capitis were grouped together since the cross-sectional area of the individual muscles could not be reliably distinguished in the MR-images of each subject. The average calculated muscle force in the TRAP+SPL for 10-year-old boys in extension was 36.3 ± 52.0 N. This calculated force was greater for the TRAP+SPL in this direction than in the SCM ($F_{scm(e)} = 9.9 \pm 9.1$ N) or middle scalene ($F_{scal(m)(e)} = 21.9 \pm 28.1$ N). However, due to the high variability the difference was not significant. In adults, the combined trapezius and splenius force was calculated to be 77.6 ± 81.6 N. Unfortunately, due to the large variability in the data, there was no significant difference between the force calculated in the combined trapezius and splenius capitis when compared to the force in the SCM ($F_{scm(e)} = 28.4 \pm 24.4$ N) and middle scalene ($F_{scal(m)(e)} = 33.3 \pm 20.3$ N). Between subject groups, the difference between the calculated force values of the SCM was significant, but only to 90% ($p < 0.10$). With respect to calculated muscle stress, there was no significant difference between the muscle stress generated in any of the muscle groups.

10 Year Old Boys

(a)	Calculated Muscle Force (N)									
	F_{SCM}		$F_{TRAP+SPL}$		$F_{SCAL(M)}$		F_{shear}		F_{axial}	
	Extension	Flexion	Extension	Flexion	Extension	Flexion	Extension	Flexion	Extension	Flexion
K03	13.9	78.8	154.7	52.5	83.5	70.4	118.6	31.6	137.3	36.6
K05	28.7	98.9	18.1	7.9	7.6	6.6	38.1	66.1	36.0	90.4
K06	9.3	80.2	24.6	4.0	12.3	14.2	124.8	41.0	18.8	6.2
K07	4.3	76.5	10.0	1.8	15.9	22.7	261.9	264.8	511.5	517.2
K09	2.6	19.5	24.9	4.7	3.4	3.6	10.8	1.8	157.0	25.7
K10	6.0	18.1	12.1	12.4	5.5	4.5	19.0	29.3	18.1	27.9
K11	4.7	59.2	9.7	0.8	25.5	30.9	151.2	114.5	348.8	264.0
Mean	9.9	61.6	36.3	12.0	21.9	21.8	103.5	78.4	175.3	138.3
St.Dev	9.1	31.4	52.6	18.3	28.1	23.7	89.5	89.5	188.7	189.0

50th Percentile Adult Males

(b)	Calculated Muscle Force (N)									
	F_{SCM}		$F_{TRAP+SPL}$		$F_{SCAL(M)}$		F_{shear}		F_{axial}	
	Extension	Flexion	Extension	Flexion	Extension	Flexion	Extension	Flexion	Extension	Flexion
S09	50.9	32.2	39.8	13.4	45.9	13.8	66.2	29.3	125.7	29.3
S11	6.7	63.3	10.6	4.5	44.5	22.9	104.1	36.8	250.6	88.7
S13	9.9	42.9	170.2	59.4	19.4	10.3	133.6	91.0	12.9	8.8
S14	44.7	448.6	237.7	113.4	52.3	137.0	18.1	15.8	40.0	35.0
S15	67.7	92.4	47.0	41.3	-5.8	-7.4	-29.6	-15.0	64.0	32.4
S16	33.8	343.5	48.3	12.2	54.6	79.4	16.3	11.1	306.3	208.9
S17	12.8	23.1	13.7	16.9	26.9	9.5	7.3	7.1	76.3	74.1
S20	0.9	9.2	53.8	11.7	28.7	11.2	70.7	53.4	20.7	15.7
Mean	28.4	131.9	77.6	34.1	33.3	34.6	48.3	28.7	112.1	61.6
St.Dev	24.4	167.4	81.6	36.9	20.3	48.7	54.6	32.5	109.6	65.6

Table 5-5: Calculate force values in flexion and extension for the SCM, trapezius./splenius capitis, and middle scalene muscles for (a) 10 year old boys and (b) 50th percentile adult males. Calculated values of anterior-posterior shear and axial (compression) force are also shown.

10 Year Old Boys

(a)	Calculated Muscle Stress (N/cm ²)					
	σ_{SCM}		$\sigma_{TRAP+SPL}$		$\sigma_{SCAL(M)}$	
	Extension	Flexion	Extension	Flexion	Extension	Flexion
K03	4.2	24.0	33.7	11.4	69.4	58.6
K05	7.9	27.1	5.0	2.2	7.8	6.8
K06	2.5	21.3	7.2	1.2	15.7	18.2
K07	1.1	20.4	6.3	1.1	22.6	32.2
K09	0.7	5.5	7.1	1.3	4.3	4.5
K10	1.8	5.5	4.9	5.0	5.3	4.4
K11	1.3	17.1	4.4	0.4	32.5	39.4
Mean	2.8	17.3	9.8	3.2	22.5	23.4
St.Dev	2.5	8.6	10.6	3.9	23.1	20.8

50th Percentile Adult Males

(b)	Calculated Muscle Stress (N/cm ²)					
	σ_{SCM}		$\sigma_{TRAP+SPL}$		$\sigma_{SCAL(M)}$	
	Stress (N/cm ²)		Extension	Flexion	Extension	Flexion
S09	10.5	6.6	7.6	2.6	34.7	10.5
S11	1.1	10.6	1.9	0.8	37.6	19.3
S13	1.8	7.8	34.3	12.0	12.2	6.5
S14	8.3	83.2	41.9	20.0	44.6	116.8
S15	13.9	19.0	9.6	8.4	-4.0	-5.1
S16	8.1	82.5	10.6	2.7	52.7	76.6
S17	2.5	4.5	2.4	3.0	28.0	9.9
S20	0.2	1.8	11.2	2.4	22.5	8.8
Mean	5.8	27.0	14.9	6.5	28.5	30.4
St.Dev	5.1	34.8	14.9	6.6	18.2	42.8

Table 5-6: Calculate stress (N/cm²) values in flexion and extension for the SCM, trapezius/splenius capitis, and middle scalene muscles for (a) 10 year old boys and (b) 50th percentile adult males. Stress values were calculated in the C4/5 plane using the anatomic cross-sectional area of the muscle or muscle group.

In flexion, the SCM generated higher force values than the other muscles for both subject groups. Due to the variability in the adult data, however, the force in the SCM was only significantly greater in the 10-year-old subject group ($p < 0.05$). Average calculated force values for the 10-year old–male subject

group were $F_{scm(f)} = 61.6 \pm 31.4$ N; $F_{trap+spl(f)} = 12.0 \pm 18.3$ N and $F_{scal(m)(f)} = 21.8 \pm 23.7$ N. In the adult subject group average calculated muscle force for the same muscles were $F_{scm(f)} = 131.9 \pm 167.4$ N; $F_{trap+spl(f)} = 34.1 \pm 36.9$ N; and $F_{scal(m)(f)} = 34.6 \pm 48.7$ N. Comparing the results between subject groups, in spite of the empirical difference between the forces generated by the adults and children, there was no significant difference between the muscle forces of these two subject groups. The variability of the results was too great to determine if a significant difference existed.

Axial and shear neck forces in the C4 vertebral segment were calculated in flexion and extension. In the 10 year-old male group, average anterior-posterior shear force ranged from 103.5 ± 89.5 N in extension to 78.4 ± 89.5 N in flexion; average axial force in compression ranged from 138.3 ± 189.0 N in flexion to 175.3 ± 188.7 N in extension. Similarly, average anterior-posterior shear force ranged from 28.7 ± 32.5 N in flexion to 48.3 ± 54.6 N in extension; average axial force in compression ranged from 61.6 ± 65.6 N in flexion to 112.1 ± 109.6 N in extension for the adult male subject group. Results were not statistically significant between subject groups.

5.4 DISCUSSION

The objective of this study was to determine the force and stress generated in the neck muscles and the difference in these values between 50th percentile adult males and 10 year old boys.

The muscle forces calculated for the 50th percentile adult males in this study were consistent with the results published by Choi et al. [2000] and Moroney et al. [1998], although the results calculated in this study are likely higher than the actual individual muscle forces produced for the average applied extension/flexion moments. Both the Choi and Moroney studies calculated muscle force using the combination of an EMG-assisted optimization model and muscle cross-sectional areas as was done in this study. The number of muscles included in the other two studies was greater than the number included in this study. The MR-images did not provide the resolution required to accurately differentiate all the muscles of a particular muscle group, therefore, the %CSA used to resolve the individual muscle forces may be larger in this study than in the Choi et al., and Moroney et al. studies. Furthermore, in both the previously mentioned studies the platysma, and hyoid muscle responses were included in the muscle force calculations. This was not the case in the calculations of this study. The muscle forces in extension calculated using the optimization model of this study were as follows, $F_{scm(e)} = 28.4 \pm 24.4$ N, $F_{trap(e)} = 50.7 \pm 61.1$ N, $F_{spl(e)} = 27.0 \pm 25.2$ N, and $F_{scal(m)(e)} = 33.3 \pm 20.3$ N. Similarly, the muscle forces calculated in flexion for the 50th percentile adult males were $F_{scm(f)} = 131.9 \pm 167.4$ N; $F_{trap(f)} = 16.8 \pm 19.3$ N, $F_{spl(f)} = 17.3 \pm 18.1$ N; and $F_{scal(m)(f)} = 34.6 \pm 48.7$ N. The results of the Choi et al. and Moroney et al. studies are shown in Table 5-7.

The results of this study show a high degree of variability, associated with the load applied by each subject. In this study, the load was applied by having

the subject push against the load cell as hard as they were able, but since there was no mechanism to provide feedback to the subject, the load considered to be maximal to one subject was lower than the maximal load of another subject.

No comparative data was found for the force found in the neck muscles of 10-year old boys.

Study/Reference	Calculated Muscle Force (N)				
	SCM	TRAP	SPL	SCAL	
Extension					
Moroney et al. [1988]		73+/-32	61+/-27	39 +/-17(m)	
Choi et al. [2000]	22+/-12	68+/-16	56+/-13	104+/-19	
Dawson study [2011]	50th percentile adult males	28.4+/-24.4	50.7+/-16.8	27.0+/-17.3	33.3+/-20.3
	10-year-old males	9.9+/-9.1	36.3+/-52.6		21.9+/-28.1
Flexion					
Moroney et al. [1988]	145 +/- 106			36+/-27 (ant)	
Choi et al. [2000]	292+/-145	38+/-16	14+/-9	29+/-24	
Dawson study [2011]	50th percentile adult males	131.9+/-167.4	16.8+/-19.3	17.3+/-18.1	34.6+/-48.7
	10-year-old males	61.6+/-31.4	12.0+/-18.3		21.8+/-23.7

Table 5-7: Published muscle force values calculated using an EMG-assisted optimization model compared with the results of this study (Dawson, 2011).

The anterior-posterior shear force in extension predicted by this model, $F_{\text{shear}} = 48.3+/-54.6$ N is lower than the anterior-posterior force reported by both Choi et al. (162+/-110N) and Moroney et al., (135N). Similarly, the compression force reported by this model, $F_{\text{axial}} = 112.1+/-109.6$ N is also less than the reported compression force reported by Choi et al. (1654+/-308N). The difference between the predicted anterior-posterior shear force and compression of this

model and the Choi et al. is consistent with the lower applied moments produced by the adult subjects in this study. In this study, the average applied moment in extension for adult males was 5.6 ± 2.6 Nm. Reported values of average applied moment in extension range from 25.9 ± 13.4 Nm [Moroney, 1998] to 53 ± 12 Nm [Mayoux-Benhamou, 1989].

The difference in applied load would suggest that either the subjects in this study were not producing a maximal contraction or that the difference in applied load is due to the method of applying the load. In this study, subjects were asked to apply a load by pushing against a load cell. In other studies an isokinetic dynamometer was used to measure the load [Seng et al., 2002] or subjects were asked to resist the load applied to the head by means of a rope and pulley system [Mertz et al., 1971; Foust et al., 1973]. The latter two methods may in fact produce higher applied loads since the subject is resisting a load rather than trying to generate the load.

For the purposes of comparison between genders and various age groups, muscle force is often normalized to the cross-sectional area of the muscle, or in some cases to the cross-sectional area of the limb being evaluated. Most often, these comparisons are made using the forces and moments generated in the extremities. Few studies have studied the force and stress values in the neck. In this study, the muscle stress for adult male subjects in extension ranged from 5.8 ± 5.1 N/cm² for the SCM to 14.9 ± 14.9 N/cm² for the TRAP+SPL to 28.5 ± 18.2 N/cm² for the middle scalene. In flexion the adult male stress values ranged from 6.6 ± 6.5 N/cm² for the TRAP+SPL to 27.0 ± 34.8

N/cm² for the SCM to 34.6±48.7 N/cm² for the middle scalene. In the Mayoux-Benhamou study [1989] the stress in the extensor muscles was reported to be 10.17 N/cm². The difference between the Mayoux-Benhamou results and the results of this study can mostly be attributed to the variability in the data, and the partitioning of the muscles as explained above.

In the upper extremities, muscle stress ranged from 7.15 ±0.50N/cm² [Halin, 2003] to 13.19±0.40N/cm² [Kanehisa, 1994] for the elbow flexors and extensors. In the lower extremities, muscle stress ranged from 5.34±0.21N/cm² [Kanehisa, 1994] to 15.5N/cm² [Maganaris, 2001]. Only studies by Narici et al. [1988] and Miller et al. [2003] reported high muscle stress values. Narici reported muscle stress values of 70.5±7.0N/cm² in the knee flexors and 80.1±15.5N/cm² in the knee extensors. Miller et al. reported 72.7N/cm² for the elbow flexors of the adult male.

The results of the child muscle stress calculation from this study found stress values ranging from 2.8±2.5 N/cm² in the SCM to 9.8±10.6 N/cm² for the TRAP+SPL to 22.5±23.1 N/cm² for the middle scalene in extension. In flexion the calculated stress values ranged from 3.2±3.9 N/cm² for the TRAP+SPL to 17.3±8.6 N/cm² for the SCM to 23.4±20.8 N/cm² for the middle scalene. In children, specifically 10-year old boys, stress data is limited to the elbow flexor muscles. Halin et al. reported on the elbow muscle stress of 10-year old boys in two separate studies. Muscle stress from these studies ranged from 4.6±0.7N/cm² to 6.48±0.5N/cm². Miller et al. [2003] reported an elbow muscle stress value of 59.3N/cm².

In both the adult and child results, it is likely that the stress reported for the middle scalene is overestimated. As mentioned previously, the partitioning of the muscle force for the middle scalene is based on that muscle's percentage of the entire SCAL muscle group. Due to the quality of the MR-image it is likely that the force in the muscle was overestimated, while the cross-sectional area was underestimated, resulting in a higher muscle stress value.

The results of the study showed a significant difference between the applied moments in flexion and extension ($p < 0.05$) of the adult and 10-year old boy subject groups. There was no statistical difference in the muscle forces and stresses between the subject groups. The stress results agree with the scaling model proposed by Wolanin et al. [1982] and supported by Irwin et al. [1997] where the ratio of muscle stress between 50th percentile adult males and other subject groups, regardless of age and gender, is 1.0. From **Chapter 1 – Background and Significance**, the Wolanin et al. relationship is as follows,

$$M_C = M_A * \frac{A_C * D_C * \sigma_C}{A_A * D_A * \sigma_A} \quad (5-22)$$

Where,

M_A = Moment of the adult head about the neck

M_C = Moment of the child head about the neck

A_A = cross sectional area of the adult neck

A_C = cross sectional area of the child neck

D_A = the moment arm of the adult neck

D_C = the moment arm of the adult neck

σ_A = physiologic stress of the adult muscle

σ_C = physiologic stress of the child muscle

Using the linear relationship of the neck anthropometry developed by Snyder et al. [1972] the equation was reduced to

$$M_C = M_A * \lambda_{NC}^3 \quad (5-23)$$

Where

$\lambda_{NC}^3 =$ is the scalar of $(A_c \times D_c)/(A_a \times D_a)$

If the scaling model, as proposed by Wolanin et al. is applied to predict both applied moments and muscle moments of the 10-year old male subject group using the moments of the adult group recorded in this study, the results are greater than the actual moments calculated as part of this study. Using the average adult applied moment values for extension ($M_{ext} = 5.632 \pm 2.583 \text{ Nm}$; $M_{flex} = 3.785 \pm 2.008 \text{ Nm}$) and the average neck circumference values for the 10-year boys ($NC_C = 30.05 \pm 1.53 \text{ cm}$) and adult males ($NC_A = 38.17 \pm 2.34 \text{ cm}$) as shown in **Chapter 3 – Anthropometrics and Subject Selection**, predicted applied moments for the child subject group should be as shown below in Table 5-8.

Muscle/Muscle Group	Adult Muscle Moments (Nm)		Predicted 10 yo Moments (Nm)		Actual 10-yo Muscle Moments		% Difference	
	Extension	Flexion	Extension	Flexion	Extension	Flexion	Extension	Flexion
SCM	0.33	2.20	0.16	1.08	0.12	0.79	-41.0	-36.3
TRAP+SPL	3.17	1.50	1.55	0.73	0.87	0.29	-78.3	-155.0
SCAL(M)	0.23	0.25	0.11	0.12	0.08	0.08	-48.9	-48.8

Table 5-8: Predicted applied moment values for 10-year old boys using the Wolanin et al. [1982] scaling model, assuming equal muscle stress. Moments were calculated using the average muscle forces shown in Table 5-4 and moment arms shown in Table 5-3.

While this relationship may hold for dynamic moments where the effects of muscle contraction are limited, the above comparison would indicate that in a static loading situation, the difference in muscle forces and moments between adults and children is due to more than anthropometry. Under static loading conditions, the difference in muscle force and moment between adults and children is likely due not only to anthropometric differences, but to an immaturity in the neuromuscular response pathways.

In spite of the differences in applied load, the peak and mean EMG activation values recorded for each subject group showed no significant difference. Based on the results of a fatigue study in which the EMG of the arm muscles of adult males and young boys was monitored over an extended period, Halin et al., [2003] concluded that adult males engaged more Type II muscle fibers than the young boys during a muscle contraction. Type II fibers are those fibers primarily associated with generating power in the muscle. These muscle fibers contract quickly but also fatigue quickly, unlike the Type I muscle fibers which contract more slowly, and are the fibers responsible for muscle endurance [Vander, 1990]. Their results suggest that adults are more fully recruiting their muscle fibers during a contraction. In their 2000 study, Gerdle et al., found that EMG amplitude correlated with the proportion of Type II fibers found in the muscle. Lambertz et al., [2003] also concluded, based on an EMG study on the musculotendinous stiffness of the triceps surae, that immaturity in the neural mechanisms of children was responsible for differences in a muscle's ability to generate and maintain torque. Their study found that the muscle activation

required to maintain a certain level of applied torque was significantly higher in 7-year olds than it was in 10-year olds. Although these results could be due to difficulties in detecting EMG activation voltage, the authors concluded that results were due to immaturity in the neural mechanisms since co-activation of the triceps anterior was also greater in younger children. In a later, similar study, Grosset et al. [2008], also concluded that children were less able to fully activate their muscles. Their conclusion is based on calculating the neuromuscular efficiency (NME_{max}) of the contraction. The neuromuscular efficiency is defined as the neuromuscular system's ability to recruit muscle fibers and generate muscle tension [Clark et al., 2008]. Grosset et al. [2008] calculated neuromuscular efficiency according to the following relationship,

$$NME_{max} = \frac{Moment_{max} (Nm)}{normalizedEMG_{max} (\%)} \quad [Grosset, 2008] \quad (5-24)$$

Where:

Moment_{max} = the maximum moment generated in the muscle, and

Normalized EMG_{max} = the %MVC of the muscle.

The results in the Grosset et al., study were not significant between 10-year boys and adult males, however, when compared with younger children, the adult male subjects had a significantly higher NME_{max} ($p < 0.05$). Applying a similar analysis to the results of this study, in extension, adults had a significantly greater NME_{max} ($p < 0.05$) than the 10-year old boys. In flexion the difference was only significant to 90%. Table 5-9 shows the calculated NME_{max} values for the subjects in this study.

10 Year Old Boys

Subject	Peak Moment (Nm)		Max %MVC		NME _{max}	
	Extension	Flexion	Extension	Flexion	Extension	Flexion
K03	4.2	2.2	0.3	0.4	13.5	5.8
K05	3.8	6.1	0.3	0.8	12.8	7.4
K06	6.8	5.7	0.3	0.4	19.9	15.6
K07	5.3	5.6	0.4	0.4	13.8	12.7
K09	3.7	1.0	0.5	0.5	7.8	2.1
K10	2.9	1.0	0.4	0.3	7.6	3.0
K11	2.2	1.9	0.2	0.2	12.2	7.9
Average	4.1	3.3	0.3	0.4	12.5	7.8
Std. Dev.	1.5	2.3	0.1	0.2	4.2	4.9

50th Percentile Adult Males

Subject	Peak Moment (Nm)		Max %MVC		NME _{max}	
	Extension	Flexion	Extension	Flexion	Extension	Flexion
S09	8.1	7.6	0.5	0.2	17.6	38.7
S11	8.1	3.3	0.2	0.4	39.6	8.8
S13	9.0	5.2	0.4	0.3	23.8	18.1
S14	6.7	6.7	0.3	0.4	26.7	17.7
S15	3.6	2.2	0.4	0.4	8.9	5.0
S16	11.4	7.1	0.4	0.6	27.2	12.0
S17	3.1	3.1	0.4	0.4	8.2	7.1
S20	13.0	9.8	0.3	0.4	44.3	23.6
Average	7.9	5.6	0.3	0.4	24.5	16.4
Std. Dev.	3.4	2.6	0.1	0.1	13.0	11.0

Table 5-9: Results of neuromuscular efficiency for the 10-year old male and 50th percentile males based on the Grosset et al. [2008] relationship. Efficiency in extension was significantly greater for adult males than boys ($p < 0.05$).

The duration of the muscle activation in this study was too short to look at the ability of the child to maintain a prescribed moment. However, for similar or lower EMG activation voltage the adults were able to generate a similar or higher amount of force than the children, further suggesting that the 10 year-old males are inefficient in generating muscle force.

5.5 CONCLUSIONS

The force results of the study were consistent with the conclusions of other studies in which adult muscle strength was compared with that of children. Adults are able to generate higher applied forces and moments than children and consequently higher muscle forces. The results of this study and others indicates that the difference in muscle force is due to the immaturity of the neural mechanisms governing muscle recruitment. This is the first such study to compare neck muscles in adults and children. In this study, the 10-year old male subjects showed a significantly lower ($p<0.05$) neuromuscular efficiency during maximal muscle contractions than the adult male subjects of this study.

CHAPTER 6: THE NECK MUSCLE RESPONSES OF 50TH PERCENTILE ADULT MALES AND 10 YEAR OLD BOYS IN LOW SPEED FRONTAL IMPACTS

6.1 INTRODUCTION

Dynamic studies are frequently used to measure the kinematic and physiologic responses of the body to imposed loads. High speed, high load studies are typically conducted using post-mortem human subjects in order to determine biomechanical response, injury mechanism and injury tolerance. Low speed dynamic testing, below levels of injury often use human volunteers in order to understand the in-vivo mechanical and physiologic responses at dynamic low loads. Few impact studies have been done to understand the responses of children.

Research studies characterize the velocity in one of two ways – 1) closing velocity, which refers to the difference in velocity between the “bullet” vehicle/sled and the target vehicle just prior to impact. For example, if the bullet vehicle is moving at a speed of 25mph (40.23km/h) prior to impact with a stationary object, the closing velocity is 25mph. If however, the bullet vehicle is 25mph and the target vehicle is moving at 15mph (24.14km/h) in the same direction, the closing velocity is (25mph – 15mph) = 10mph. The change in velocity, the more common characterization, refers to the change in velocity during the impact of the bullet or target vehicle, where change in velocity is described by Newton’s second law. [Eppinger, 2001]

$$\Delta V = (F \cdot \Delta T) / M$$

Relative to the occupant of the bullet vehicle, the risk of injury is not only affected by the change in velocity, but the time over which that change occurs, as shown in the equation above. Also significant is the energy transferred to the occupant from the vehicle during an impact event. Consider the example provided by Eppinger in his paper on “Occupant Restraints Systems” [2001]. In a normally braking vehicle, the internal energy of the vehicle, that is the energy transferred to the occupant, is essentially zero. The kinetic energy of the vehicle during braking is transformed into work as the vehicle slows down. During an impact, assuming no pre-braking, the kinetic energy of the vehicle is transferred to the occupant – the greater the change in velocity, the greater the energy transferred to the occupant. The role of the restraint system is to then reduce the force transferred to the occupant, by increasing the time over which the change in velocity is experienced. In order to design effective restraint systems, the responses of the human body relative to these changes in velocity must be understood.

Many studies have been conducted on adult volunteer subjects using dynamic test devices at varying magnitudes of acceleration and change in velocity (Δv) and in various impact directions. Siegmund et al. [2004] conducted a study on a linear sled in which participants were subjected to 36 consecutive rear-impacts ranging in acceleration from 0.5-1.3 gs. No injuries were reported. Ono et al. [1997] used a specially designed, gravity driven, ramp to determine the head/neck response of volunteer subjects in low speed rear-impacts. Test

speeds ranged from 1.1 - 2.2m/s (4-8km/h). Only one of the 12 subjects reported neck discomfort after testing. The symptoms of this impact disappeared within a few days and no other symptoms were reported. Szabo et al. [1996] used car-to-car impacts to determine the neck response of volunteer subjects in rear-impact with a change in struck car velocity of 2.78m/s (10km/h). There were no reports of volunteer pain or discomfort. Mertz and Patrick [1967, 1971] and Patrick and Chou [1976] characterized the response of the human neck in rear, frontal and side impact using a linear sled. Test speeds ranged from 4.5-8.94m/s (16-32km/h) with a range of accelerations from 5-9g's. The volunteers reported pain and discomfort after a 9g test when the subject had an additional mass attached above the center of gravity of the head. Symptoms included minor neck, shoulder and back muscle soreness lasting less than one week. No actual injuries have been reported in these test series on human volunteers, but higher speed tests produced ligamentous neck injuries in cadavers [Mertz and Patrick, 1967, 1971]. A study by the University of Pennsylvania measured the acceleration levels of three high g-force roller coasters and found that the highest g levels were 6g's for 1 second. Although there have been some fatal injuries associated with roller-coasters, the University of Pennsylvania study concluded that death and/or injury was not as a result of the acceleration levels of the roller coasters in their normal mode of operation [Smith, 2002].

In recent years, kinematic studies have been conducted using children. Since the responses of the child crash test dummies (ATD's) are based, primarily, on scaled adult responses, the intent of these studies was to either

validate or improve the biofidelity of the child ATD by comparing the kinematics of child volunteers to adult volunteers or to the ATD. A 2009 study by Arbogast et al. [2009] compared the kinematics of children to that of adults in low speed impacts ($a=4.9g$, $\Delta v = 2.3m/s$). The purpose of the study was to determine whether the child Hybrid III ATD spine, scaled from adult spine data, was representative of actual children. Further to this study, a study by Seacrist et al. [2010] compared the kinematics of 6-9 year old males to the Hybrid III 6-year old ATD. Results of their study showed that Hybrid III had significantly higher head angular acceleration, but less forward excursion of the naison, external auditory meatus and the C4 and T1 vertebrae than a similar size child. The results of the Seacrist study are similar to an older study by Cassan et. al. [1993] where the kinematic responses of the Hybrid III 3-year old were compared to child cadavers, matched for size and weight. Results of the Cassan study and others [Newman, 1993; Wismans, 1979] showed that the neck and torso of the child ATD's are stiffer than the neck and torso of children. In their studies, children had greater forward excursion of the head, neck and torso than the ATD's when similarly restrained in tests of the same speed.

Kinematic studies done at low speeds are particularly important for understanding and interpolating to responses at high speeds. In high speed impacts, muscle response is due, in large part, to its tissue properties rather than contractile response. At low speeds, muscles have the opportunity to contract and provide resistance to the applied forces and moments. Unfortunately, data relating to muscle response in children is based, for the most part, on static

studies. **Chapter 5 - Determination of Neck Muscle Force and Stress at C-4 Vertebrae During a Maximal Voluntary Contraction** – compared the neck muscle forces and stresses of the 50th percentile adult male to those of the 10 year-old boy under static loading conditions. The static responses were determined using an EMG assisted optimization model. EMG has also been used to determine muscle responses in dynamic situations, although most studies use EMG to quantify muscle response time rather than to determine muscle force. Kumar et al., evaluated muscle activation levels during both low speed frontal impacts [2003] and low speed rear impacts [2002]. The results of these studies showed that during a dynamic event, the EMG of some neck muscles exceeded the EMG recorded during a maximal voluntary contraction. In a rear impact at 13.7m/s², Kumar reported that the SCM had EMG values were, on average, 179% MVC. These results are similar to the results reported by Szabo et al. [1996]. In their study, the EMG value of the trapezius ranged from 17.5% MVC to 254.9% MVC. No muscle force was calculated in any of the above mentioned studies.

The objective of this study is to determine the responses of the neck muscles and the resulting kinematics under low speed frontal impacts for 50th percentile adult males and 10-year old boys, - both aware and unaware of the coming impact. A better understanding of muscle contraction types (eccentric vs. concentric), force generated and the neural pathways used to stimulate muscle contractions during low speed impacts, and how these differ in children will provide insights into injury mechanisms, rehabilitation programs and preventative

measures. This is particularly important in the head and neck region, where children are most often injured.

6.2 METHODS

6.2.1 Instrumentation

The EMG set-up described in **Chapter 5 - Determination of Neck Muscle Force and Stress at C-4 Vertebrae During a Maximal Voluntary Contraction** - was also used in this study. In addition to measuring muscle response, swing acceleration and head acceleration were measured. The nine-accelerometer 3-2-2-2 array was used to measure the acceleration of the head, while a single linear accelerometer was used to measure swing acceleration. All accelerometers were Endevco 7764 200g accelerometers (Endevco, San Juan Capistrano, CA) Acceleration data was collected at 10,000Hz with a TDAS system (Diversified Technical Systems, Seal Beach, CA). A single high Kodak HG1000 speed camera, was set-up perpendicular to the motion of the fixture to capture the kinematics of the head during impact. Video was recorded at 1000Hz. A TDAS PRO Timed Output Module (TOM), connected to the TDAS system was used to simultaneously trigger the collection of acceleration data and both the camera and released the solenoid holding the swing in its raised position. The TDAS system was manually triggered. The differential AC amplifier (Bortek Biomedical Ltd., Calgary, AB, Canada) used to collect EMG activation voltage was also manually triggered, independently of the TDAS system. At the time of the TDAS system trigger, a 5V pulse was sent from the TDAS system to the AC amplifier to synchronize the two data collection systems. The swing

release and camera trigger were delayed by 2seconds to ensure that any delay in the acquisition of the 5V pulse by differential AC amplifier did not affect the synchronization of the two data collection systems. Figure 6-1 shows a schematic of the data collection systems.

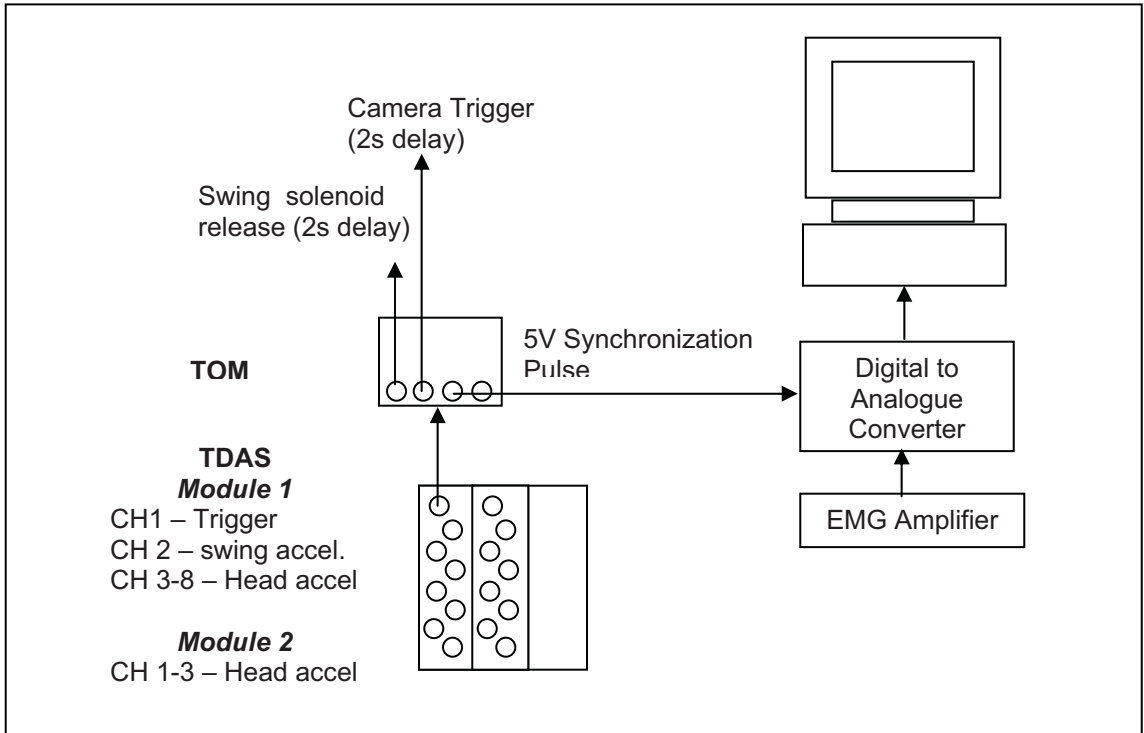


Figure 6-1: Schematic of data collection systems.

The 3-2-2-2 accelerometer mount was attached to a 2mm thick metal mounting plate, held between the subject's teeth with the aid of SPLASH, a quick setting dental impression material [Cuson, 2004]. The mounting plate was cut in two different sizes – an adult size and a child size – both sizes were cut using an appropriately sized mouth guard as a template. The putty was bound top to bottom through holes drilled in the plate. The putty was new for each subjects

and the mounting plate autoclaved to ensure sterility. Figure 6-2 shows a drawing of the metal plate, and complete mouth-piece assembly.

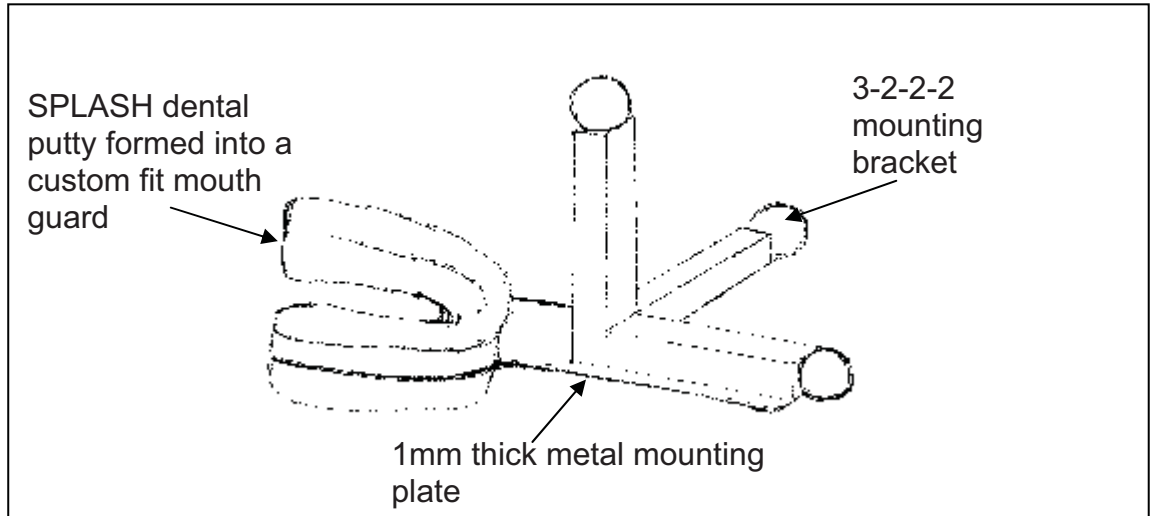


Figure 6-2: Drawing of completed mouthpiece assembly.

Subjects were given headphones to wear and listen to music during testing. The headphones served two purposes. First, a marker was attached to the headphones so that the displacement of the head could be traced using the high speed video footage. The marker was located over the ear rather than the center of gravity of the head. The center of gravity of the head in the sagittal plane is located 2cm up and forward 2cm of the Frankfurt Plane for adults [Beier et al., 1980]. In children these dimensions are slightly less. Loyd et al., gives the location in the 9-year old relative to the centroid of the occipital condyles as $x=19.2\text{mm}$ and $z=-49.0\text{mm}$ [Loyd, 2010]. The surface area of the headphones is sufficiently large that it encompassed the CG.

The headphones were also used to reduce any external cues to the swing's release which might cause the subject to tense their muscles during the

untensed muscle test condition. During this test condition, each subject listened to relaxing music.

6.2.2 Test Fixture

A gravity driven swing capable of a maximum speed of 5-8km/h was used to simulate a low speed, frontal impact event. A schematic of the test fixture is shown below in Figure 6-3. The test speed was limited to 3 mph (4.5 km/h) which is the speed attained in normal walking. Peak swing g's was limited to 3+/- 0.25g's, one quarter to one half of the value that has been used in many previous studies with adults. A study at the Children's Hospital of Philadelphia (CHOP) in which bumper cars were used to study the kinematics of adults and children used an acceleration pulse of 3.62+/-0.29g's to 3.82+/-0.17g's with a rise time range of 59+/- 2ms to 63+/-12ms [Arbogast, 2009].

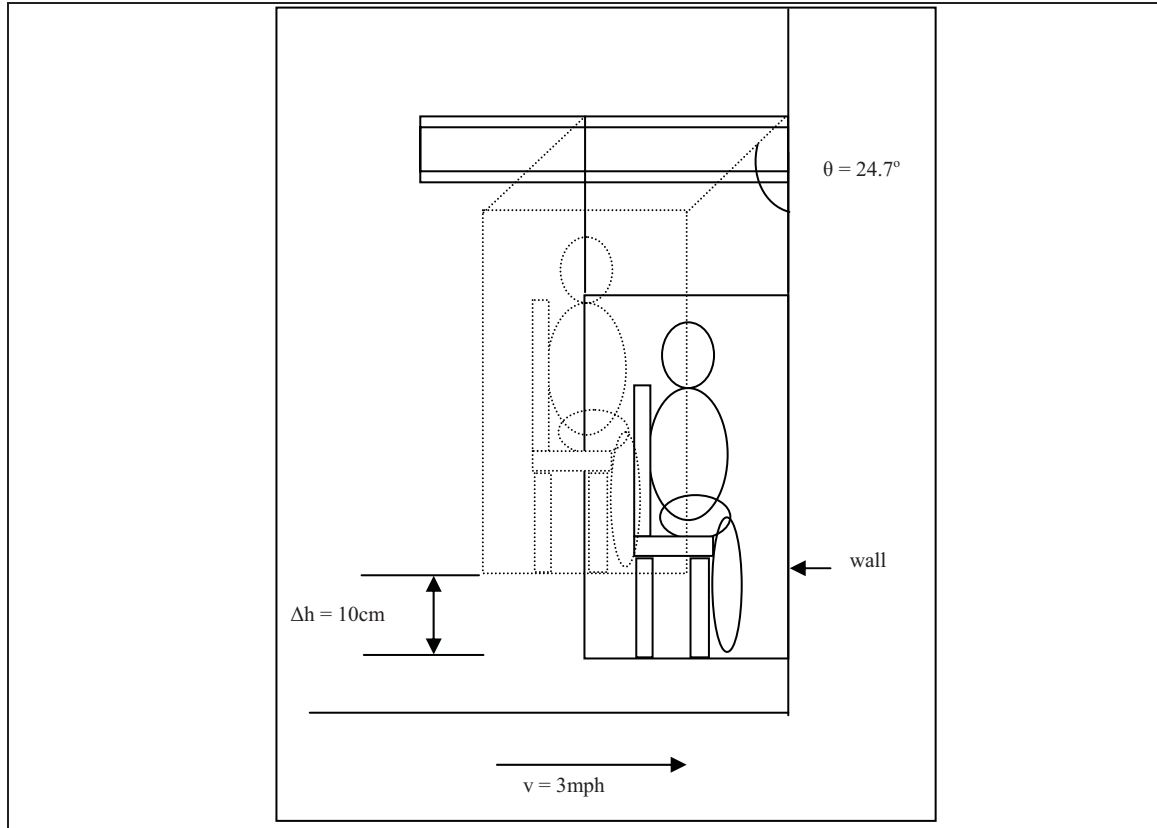


Figure 6-3: Schematic of the dynamic test fixture swing

The swing was constructed such that the position of the seat can be adjusted to achieve any impact direction. In this study, the direction of impact was limited to frontal impacts. The swing was suspended from two beams made of Unistrut, using chains and was cross-braced with 3/8" spectra core, marine grade rope. Chains were adjusted so that the swing was level, eliminating inclination of the swing base about the z-axis during the forward motion of the swing. The cross-bracing of the ropes provided an additional mechanism against twisting. The swing was designed to behave as a simple pendulum. Since the impact occurred at the bottom of the pendulum swing arc, the impact was linear.

The acceleration of the swing was modulated by four ACE MC 3325-3 shock

absorbers [ACE Controls Inc., Detroit, MI], placed in line with the bottom of the swing on the risers of the suspension fixture. The second two shock absorbers were placed on the suspension fixture to contact the swing at approximately 2/3 its total height. This was to prevent rotation of the swing about the y-axis due to contact with the bottom shock absorbers. The shock absorber was sized per the ACE catalogue specifications for a weight with no propelling force. The specifications for the MC3325-3 include, a stroke length of 0.91 inches, an impact velocity range of 0.5-16.5 ft/s (0.35 -11.25 mph) and an effective weight range of 230-920 lbs. The estimated total mass of the fixture plus adult occupant was 500lbs. The recommended uses for this shock absorber include crash testers and emergency stops.

Figure 6-4 below show images of the swing assembly and its various components.

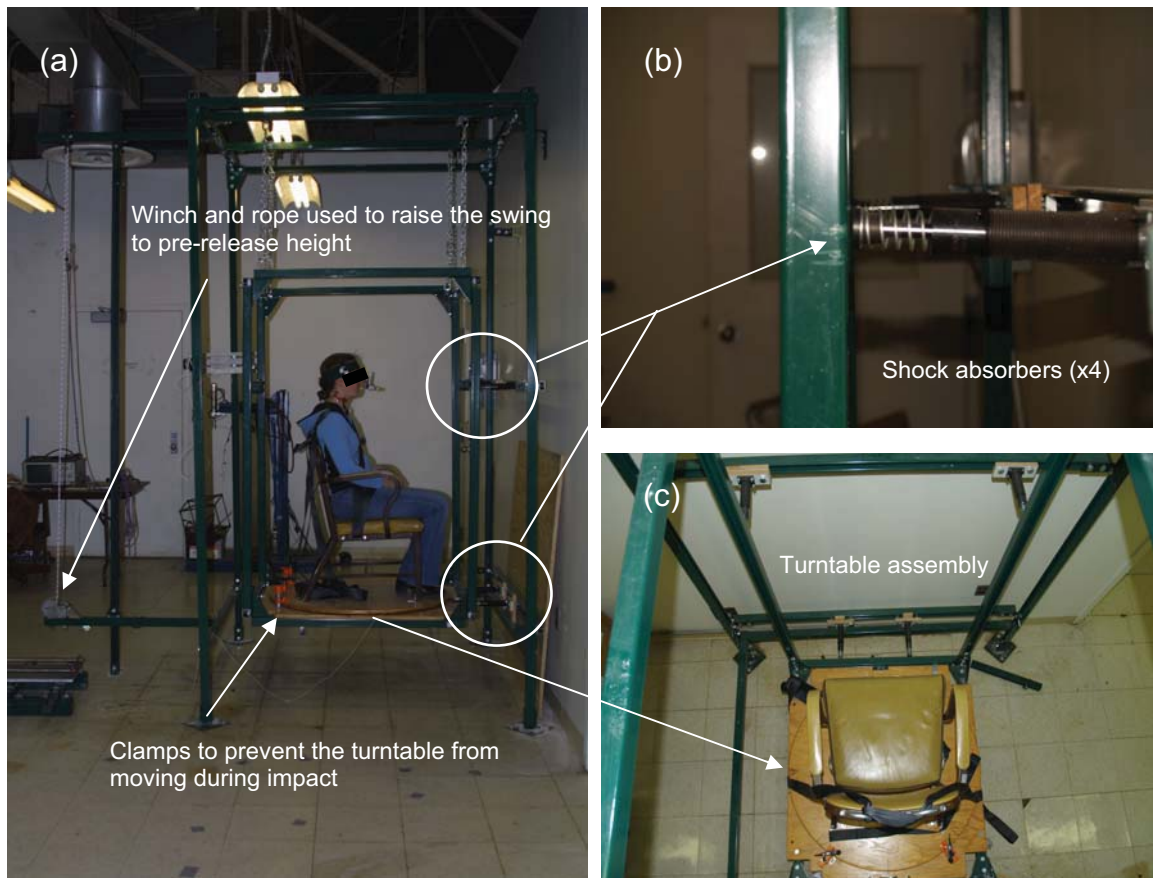


Figure 6-4: Photographs showing (a) the swing fixture and its component parts (b) the shock absorbers and (c) the chair and turntable assembly.

The subject was seated on the swing with his torso and pelvis restrained to the seat by means of Velcro straps so that the measured response was that of the head and neck only. The straps were made of 48mm wide seat belt webbing. Velcro strips were sewn onto the seat belt webbing using a canvas sewing machine. The straps were attached to fixed loops on the seat back of the seat used in the swing. The webbing restrained the occupant in a single, continuous loop, starting across the shoulder from right to left where it was threaded through a fixed loop attached to the left hand side of the seat. The webbing then passed across the lap, through a loop affixed to the right hand side of the seat, and

across to the top of the left shoulder where it was threaded through a final loop attached to the top of the seat back. The restraint was secured with a Velcro strip. The straps were tightened such that only one finger width of space was available between the strap and the subject's chest.

Each adult subject participated in a total of six dynamic frontal impact tests. The 10-year-old male subjects only participated in a total of 4 tests. After each test, participants were asked if they wished to continue with the next test. In the case of the child participants, most indicated they wished to stop after the fourth test. Many found the blindfolded, unaware tests frightening. For the child participants, the tests were conducted in a 2-aware, 2-unaware sequence so that if the subject wished to stop, a repeat test was obtained for both test conditions. Subject K03 was content to continue for all 6 tests in the protocol, subject K07 asked to stop after the first two tensed muscle impact tests. All participants were asked after each test whether they were experiencing any neck soreness or pain. Neither was reported by any subject.

During three of the tests (two tests in children), the subjects were blindfolded and asked to keep their muscles as relaxed as possible. Subjects were asked to keep their hands relaxed resting on either their laps or on the arm rests for this test configuration. Relaxing music was played during this portion of the testing so that no external cues were given to the subject so as to avoid muscle tenseness due to anticipation of the impact event. This was to simulate an occupant unaware of the impending impact. In the other three tests (two tests in children), subjects were asked to tense their muscles in anticipation of the

impact. In this case, muscle tenseness was aided by having the subjects make a fist with their hands. A countdown to impact was given so that subjects were fully aware of the impending impact.

This research plan was approved by the Wayne State University Human Investigations Committee (HIC) on February 1, 2005. Re-approval was obtained in December 2006. The approval number for the study is 121204M1F. The pediatric HIC was approved April 3, 2007, HIC approval number 026307MP4F.

6.2.3 Data Analysis

The 10 second baseline noise signal collected for each subject and processed as part of the static test protocol, was used to zero the dynamic EMG data. The dynamic EMG signal was high-pass filtered using a second order Butterworth filter with a 250Hz cut-off frequency. The signal was rectified and then low passed filtered using a second order Butterworth filter with a 10Hz cut-off frequency. The mean of the rectified, filtered signal was calculated and saved.

The accelerometer data was filtered according to SAE J211 standard using a CFC 1000Hz filter. A custom Diadem (Diadem v.9.1, National Instruments Corp, Austin, TX) program was used to calculate the angular acceleration of the center of gravity of the head and the linear acceleration at the center of gravity of the head from the 3-2-2-2 acceleration data.

The mass of the head and neck and the mass moment of inertia of head/neck were not calculated in this study. The mass of the head and the mass moment of inertia, I_{yy} , used in this study were those published by Yoganandan et

al. [2009] for a 25th –75th percentile male where the mass of the head $m_{\text{head}} = 4.54\text{kg}$, and $I_{yy} = 2.55\text{e-}2 \text{ kg-m}^2$. The mass and inertial properties presented in the Yoganadan et al. study are based on data compiled from studies published between 1857 and 2005. The mass moment of inertia of the head and neck and the mass of the head for the children used in this study was taken from the results of a study by Lloyd et al. [2010]. The mass and inertial properties of the pediatric head of children ages 1-month to 120-months in the Lloyd et al study were developed using a series of CT scans. From this study the $m_{\text{head}} = 3.62\text{kg}$, $I_{yy} = 1.64\text{e-}2 \text{ kg-m}^2$. Child values are estimates for a 9-year old.

Moment arms for calculating the moment at the occipital condyles were measured from the MR-images discussed in Chapter 4. Using anatomical landmarks, the coordinates for the occipital condyles were marked. The Frankfurt Plane was marked from the upper canal of the external auditory meatus to the lower boundary of the orbital of the eye [Beier, 1980]. Figure 6-5 shows the MR-images of an adult subject, the anatomical landmarks and planes of measurement are shown. Table 6-1 gives the moment arms to the occipital condyles. The moment arm to C4 was measured during static testing.

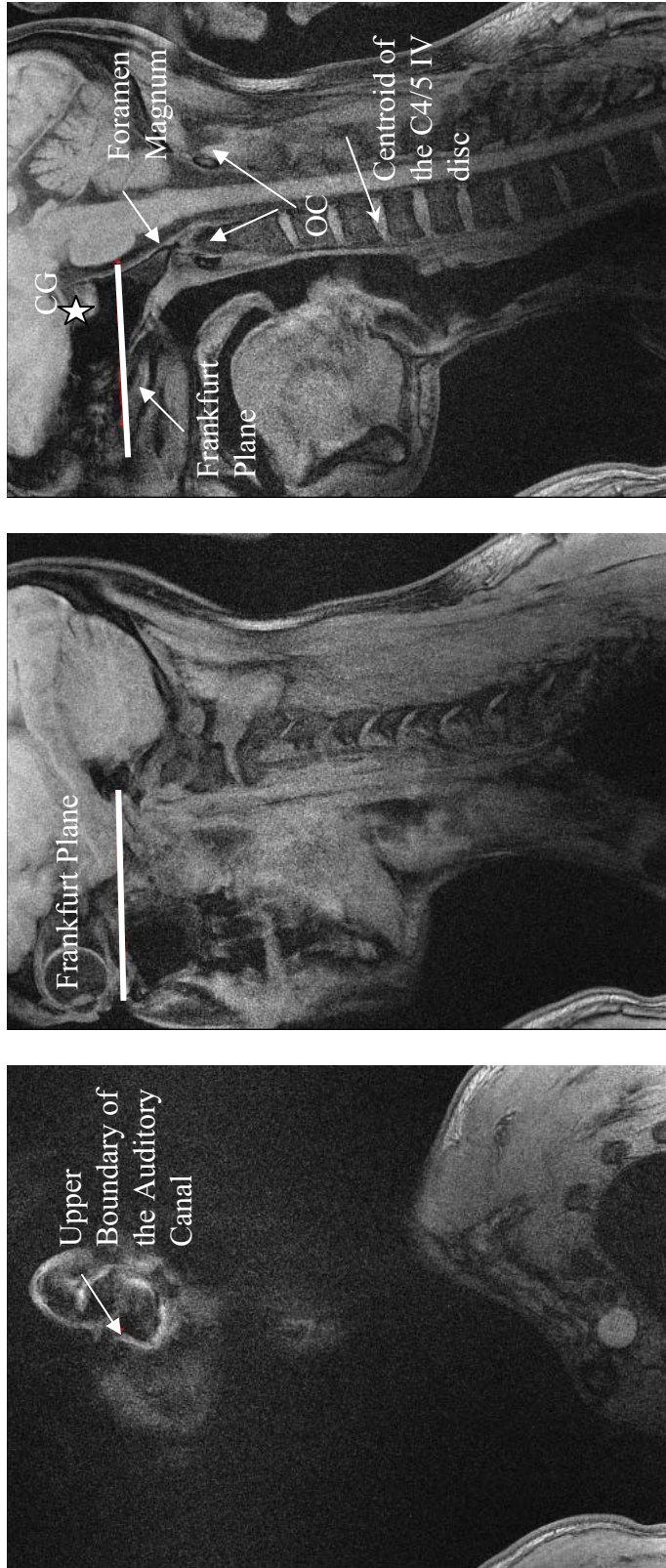


Figure 6-5: MR-images of adult subject S08 showing the anatomical landmarks used to determine the moment arms to the occipital condyle (OC). The center of gravity was determined to be 2cm above the Frankfurt plane and 2cm anterior of the auditory meatus.

10 Year Old Boys

(a)	Center of Gravity of Head		C4/5 IV Disc Centroid (coord)		Moment Arm to C4 (mm)	Moment Arm to C4/5 IV disc (mm)	
	x	z	x	z		x	z
K01	165	98	210	298	115	22.5	100.0
K03	154	69	196	258	120	21.0	94.5
K04	144	51	199	258	135	27.5	103.5
K05	160	108	216	275	140	28.0	83.5
K06	173	56	220	241	140	23.5	92.5
K07	151	80	186	268	135	17.5	94.0
K09	150	79	200	259	120	25.0	90.0
K10	175	88	217	270	120	21.0	91.0
K11	150	99	203	268	125	26.5	84.5

mean

23.6 92.6

St.Dev

3.5 6.5

50th Percentile Adult Males

(b)	Center of Gravity of Head		C4/5 IV Disc Centroid (coord)		Moment Arm to C4 (mm)	Moment Arm to C4/5 IV disc (mm)	
	x	z	x	z		x	z
S13	158	42	194	268	170	36	226
S14	151	43	176	245	160	25	202
S15	164	61	171	273	150	7	212
S16	178	76	195	303	155	17	227
S17	176	51	184	275	165	8	224
S18	187	71	206	265	165	19	194
S20	175	44	177	272	130	2	228

mean

16.3 216.1

St.Dev

11.8 13.7

Table 6-1: Coordinates of the intervertebral (IV) disc centroid and the Center of Gravity (CG) of the head measured from the MR-images of Chapter 4; The coordinates are taken relative to the top left hand corner of the MR-image, this is the images (0,0) point. Moment arms in x and z are from the CG to the IV disc centroid – moment arms in mm were calculated by multiplying by the pixel length of 0.5mm; moment arms from the CG to C4, measured in static test set-up.

6.2.4 Dynamic Force Calculations

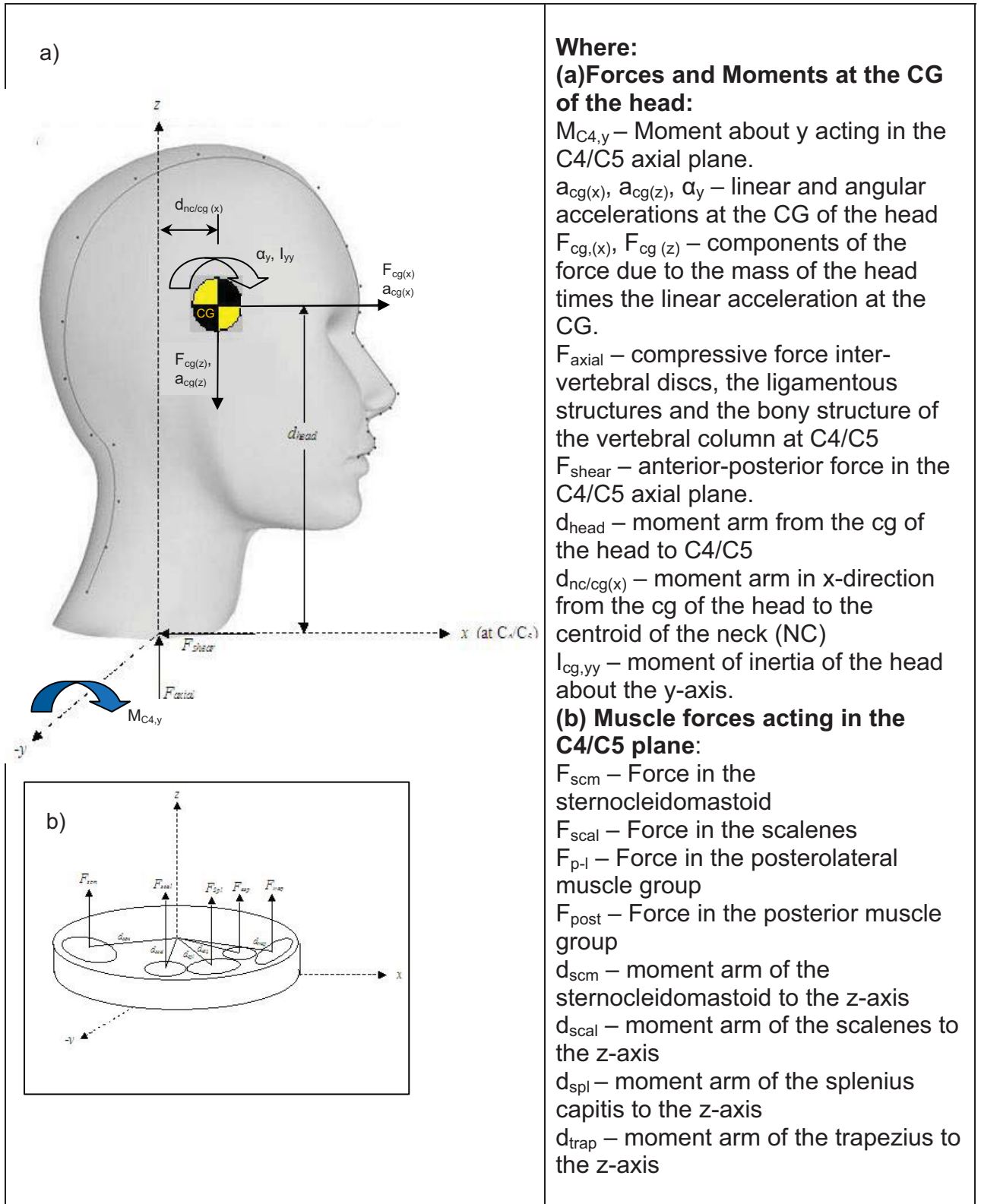


Figure 6-6: Free Body Diagram of (a) the Head/Neck to C4; (b) section at C4/C5 showing the forces and moment arms contributing to $M_{cg,y}$

The equations of motion of the head were developed from the same free body diagram used in Chapter 5 - **Determination of Neck Muscle Force and Stress at C-4 Vertebrae During a Maximal Voluntary Contraction**, shown above in Figure 6-6. Also from Chapter 5, the force and moment equilibrium equations are as follows, except in the dynamic situation, the forces and moments are those acting on the head due to the acceleration of the swing.

Consider first the equations of motion in flexion

$$\Sigma M_x = 0 \quad (6-1)$$

$$\Sigma M_{C4,y} = F_{cg/C4,x} \times d_{head} + F_{cg,z} \times d_{cg/oc,x} + I_{yy,cg} * \alpha_y \quad (6-2)$$

$$\Sigma M_z = 0 \quad (6-3)$$

and

$$\Sigma M_{C4,y} = 2 * [-F_{SCM(z)} \times d_{SCM(x)} - F_{SCAL(z)} \times d_{SCAL(x)} + F_{P-L(z)} \times d_{P-L(x)} + F_{POST(z)} \times d_{POST(x)}] \quad (6-4)$$

It was assumed that the muscle response from one side of the neck to the other is symmetrical as denoted by the factor of 2 multiplying the muscle forces. The force equilibrium equations in flexion are as follows:

$$\Sigma F_x = m_h * a_{x,cg} = -2(F_{SCM,F(x)} + F_{P-L,F(x)} + F_{SCAL,F(x)} + F_{POST,F(x)}) - F_{shear} \quad (6-5)$$

$$\Sigma F_y = 0 \quad (6-6)$$

$$\Sigma F_z = -m_h * a_{z,cg} = F_{axial} + 2(F_{SCM,F(z)} + F_{P-L,F(z)} + F_{SCAL,F(z)} + F_{POST,F}) \quad (6-7)$$

Where:

F_{axial} = the resisting force produced by the inter-vertebral discs, the ligamentous structures and the bony structure of the vertebral column.

F_{shear} = the shear force acting in the anterior-posterior direction in the coronal plane of the neck

$a_{x,cg}$, $a_{z,cg}$ and α_y = the accelerations of the CG of the head as calculated from the 3-2-2-2 accelerometer data using the equations developed by Padgaonkar [1975] Equations 6-8 through 6-10 give the equations for calculating angular acceleration using the accelerometers of the 3-2-2-2 accelerometer mount.

$$\dot{\omega}_x = (a_{z1} - a_{z0})/2\rho_{y1} - (a_{y3} - a_{y0})/2\rho_{z3} \quad (6-8)$$

$$\dot{\omega}_y = (a_{x3} - a_{x0})/2\rho_{z3} - (a_{z2} - a_{z0})/2\rho_{x2} \quad (6-9)$$

$$\dot{\omega}_z = (a_{y2} - a_{y0})/2\rho_{x2} - (a_{x1} - a_{x0})/2\rho_{y1} \quad (6-10)$$

Where:

$\dot{\omega}_x, \dot{\omega}_y, \dot{\omega}_z$ = calculated angular acceleration in x, y and z-directions

$a_{x,y,z,i}$ = data recorded from the accelerometers of the 3-2-2-2 mount. The subscript indicates direction of the acceleration (x,y or z) and the bar (i) on which the accelerometer is located, where 0 is the origin, 1 is in the x-direction, 2 is in the y-direction and 3 is in the z-direction.

$\rho_{x,y,z,i}$ = is the distance from the origin of the 3-2-2-2 mount to the center of the accelerometer.

Values of angular velocity were integrated from the calculated values of angular acceleration. Linear velocity and acceleration of the head were calculated using the equations of relative motion of a rigid body. In this study, two assumptions were made with respect to the motion of the occupant/swing.

1. The angular acceleration about the CG is the same as that calculated at the mount location (ie. $\dot{\omega} = \dot{\Omega}$)
2. In the ideal case, angular velocity (ω_x, ω_z) and angular acceleration (α_x, α_y) about x and z are negligible.

Considering first velocity at the CG:

$$v_{cg} = v_M + (\omega \times r_{cg/M}) \quad (6-11)$$

In component form:

x-component:

$$(v_{cg})_i = (v_{x,M} \cos \theta - v_{z,M} \sin \theta)_i + (\omega_y \times r_{cg/M,z})_i + (\omega_z \times r_{cg/M,y})_i \quad (6-12)$$

where from the assumptions,

$$(\omega_z \times r_{cg/M,y})_i \approx 0$$

so equation 6-12 becomes

$$(v_{cg})_i = (v_{x,M} \cos \theta - v_{z,M} \sin \theta)_i + (\omega_y \times r_{cg/M,z})_i \quad (6-13)$$

y-component:

$$(v_{cg})_j \approx 0 \quad (6-14)$$

z-component:

$$(v_{cg})_k = (v_{z,M} \cos \theta + v_{x,M} \sin \theta)_k + (\omega_y \times r_{cg/M,x})_k + (\omega_x \times r_{cg/M,y})_k \quad (6-15)$$

where

$$(\omega_x \times r_{cg/M,y})_k \approx 0$$

so equation 6-15 becomes

$$(v_{cg})_k = (v_{z,M} \cos \theta + v_{x,M} \sin \theta)_k + (\omega_y \times r_{cg/M,x})_k \quad (6-16)$$

Again using the equations of relative motion, the equations of linear acceleration are as follows,

$$a_{cg} = a_M + \alpha \times r_{cg/M} - \omega^2 r_{cg/M} \quad (6-17)$$

In component form:

x-component:

$$(a_{cg})_i = (a_{x,M} \cos \theta - a_{z,M} \sin \theta)_i + (\alpha_y \times r_{cg/M,z})_i + (\alpha_z \times r_{cg/M,y})_i - (\omega_x^2 \bullet r_{cg/M,x})_i \quad (6-18)$$

where

$$(\alpha_z \times r_{cg/M,y})_i \approx 0$$

$$(\omega_x^2 \bullet r_{cg/M,x})_i \approx 0$$

the acceleration at the center of gravity of the head in the x-direction becomes

$$(a_{cg})_i = (a_{x,M} \cos \theta - a_{z,M} \sin \theta)_i + (\alpha_y \times r_{cg/M,z})_i \quad (6-19)$$

y-component:

$$(a_{cg})_j = (a_M)_j + (\alpha_x \times r_{cg/M,z})_j + (\alpha_z \times r_{cg/M,x})_j - (\omega_y^2 \bullet r_{cg/M,y})_j \quad (6-20)$$

where

$$(a_M)_j \approx 0$$

$$(\alpha_x \times r_{cg/M,z})_j \approx 0$$

$$(\alpha_z \times r_{cg/M,x})_j \approx 0$$

the acceleration at the center of gravity of the head in the y-direction becomes

$$(a_{cg})_j = -(\omega_y^2 \bullet r_{cg/M,y})_j \quad (6-21)$$

z-component:

$$(a_{cg})_k = (a_{z,M} \cos \theta + a_{x,M} \sin \theta)_k + (\alpha_x \times r_{cg/M,y})_k + (\alpha_y \times r_{cg/M,x})_k - (\omega_z^2 \bullet r_{cg/M,z})_k \quad (6-22)$$

where

$$(\alpha_x \times r_{cg/M,y})_k \approx 0$$

$$(\omega_z^2 \bullet r_{cg/M,z})_k \approx 0$$

the acceleration at the center of gravity of the head in the z-direction becomes

$$(a_{cg})_k = (a_{z,M} \cos \theta + a_{x,M} \sin \theta)_k + (\alpha_y \times r_{cg/M,x})_k \quad (6-23)$$

Where:

$a_{x,y,z,M}$ = acceleration recorded at the mouth using 3-2-2-2 mounting configuration

$r_{cg/M}$ = the distance from the origin of the 3-2-2-2 mount to the CG of the head.

This was measured at the time of testing.

$\dot{\omega}, \omega$ = Calculated using the equations developed by Padgaonkar et al., [1975],

shown in equations 6-8 through 6-10.

6.3 RESULTS

The crash pulse in this study was governed by gravity since a swing device was used to create the impact. Since the mass of the adult and child subjects differed, the peak values of the impact pulse, measured at lower right hand corner of the swing cage, also differed. Although the shock absorbers were sized according to the ACE Control sizing guidelines, the stroke length of the shock absorbers was not sufficiently long to effectively absorb the energy of the adult impact. The shock absorber bottomed out, confirmed by video analysis, resulting in a high peak acceleration for adult test subjects. For the lighter children, the stroke length was sufficient to absorb the impact energy, resulting in a lower peak acceleration than the adult test subjects. The crash pulse, for adult testing, had a peak acceleration of $3.2 \pm 0.2g$. Due to the reduced mass of the child subjects the peak acceleration of the child impact was $2.6 \pm 0.2g$'s. The shape and duration of the pulse were the same, only peak amplitude differed. Both pulses, overlaid with the acceleration traces of all tests are shown below in figure 6-7 (a) and (b). Figure 6-7 (c) shows the average acceleration pulse for each of the subject groups.

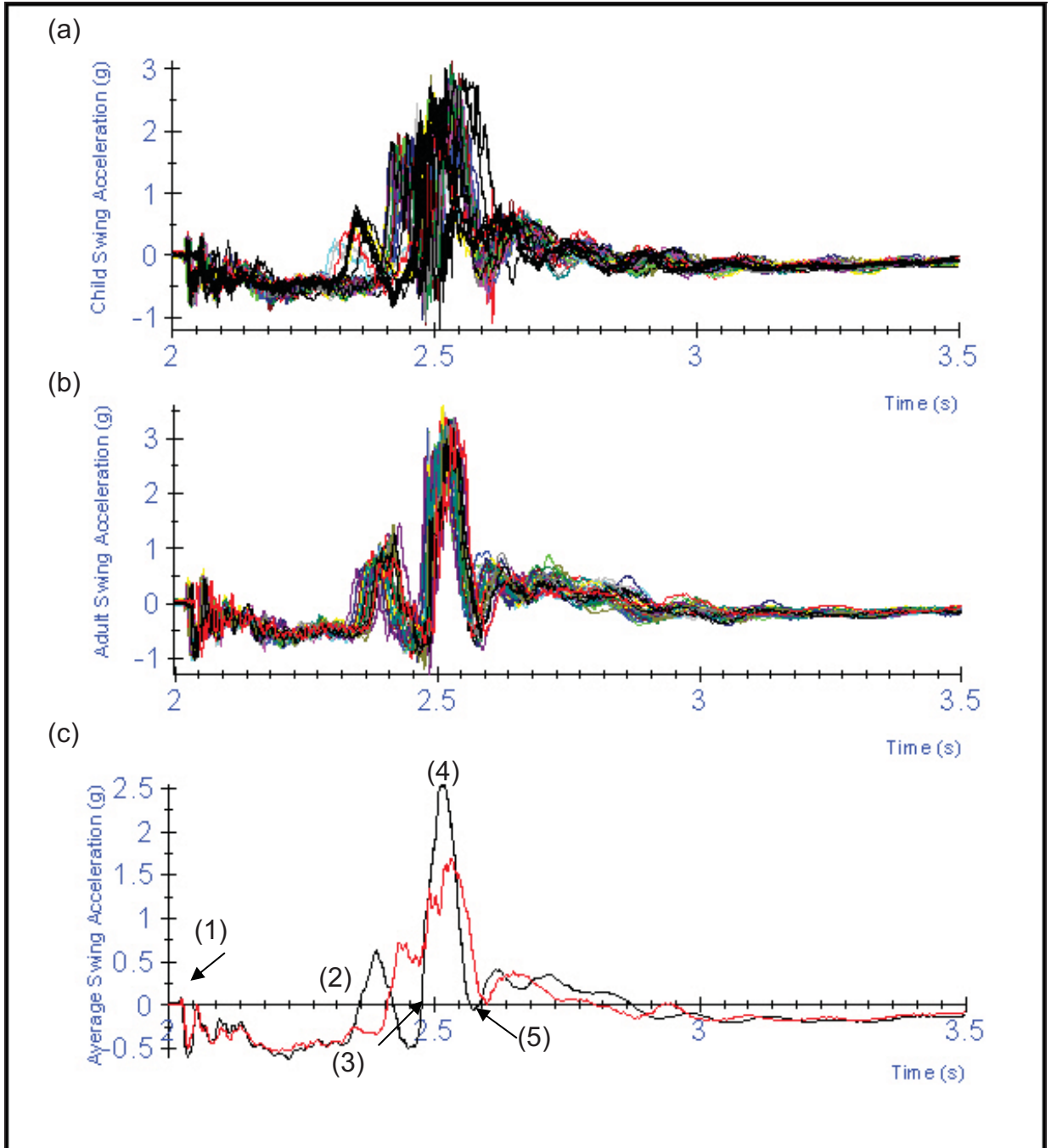


Figure 6-7: Acceleration trace for (a) 10-year male (b) 50th percentile male dynamic tests and (c) the average acceleration for each subject group – 10-year olds (black), adult males (red). Figure (c) gives the time and a description of each peak: 1) Swing release at t=2.0s. 2) Rear occupant cage chains engage, swing begins the linear portion of its arc. 3) First contact with shock absorbers at t=2.461s. 4) Peak swing deceleration at t=2.523s, rebound begins. 5) Swing disengages from shock absorbers at t=2.612s. The total duration of the deceleration with the shock absorber was $\Delta t = 250\text{ms}$.

As a result of the difference in crash pulses, direct quantitative comparisons cannot be made between subject groups as intended in this study.

6.3.1 Dynamic Moment

Linear and angular accelerations at the center of gravity of each subject were calculated using the equations developed by Padgaonkar [1975], shown as equations (6-9), and from the equations of relative motion for a rigid body, shown as equations (6-19) and (6-23). Data for the calculations was collected using the 3-2-2-2 accelerometer mount. Figures 6-5(a) and (b) – 10-year old boy; and Figures 6-6 (a) and (b) – 50th percentile adult male, show the raw 3-2-2-2 acceleration data, the linear acceleration of the CG of the head in the x- and z- directions and the angular acceleration of the head about the y-axis. As discussed in Section 6.2.4 – Dynamic Force Calculations, it was assumed that the acceleration in the y-direction was negligible and that the angular accelerations about the x and z-axes were zero. The data in figures 6-8 and 6-9 show that measured acceleration in the y-direction was less than 0.5g's. Data shown below is for a tensed muscle test.

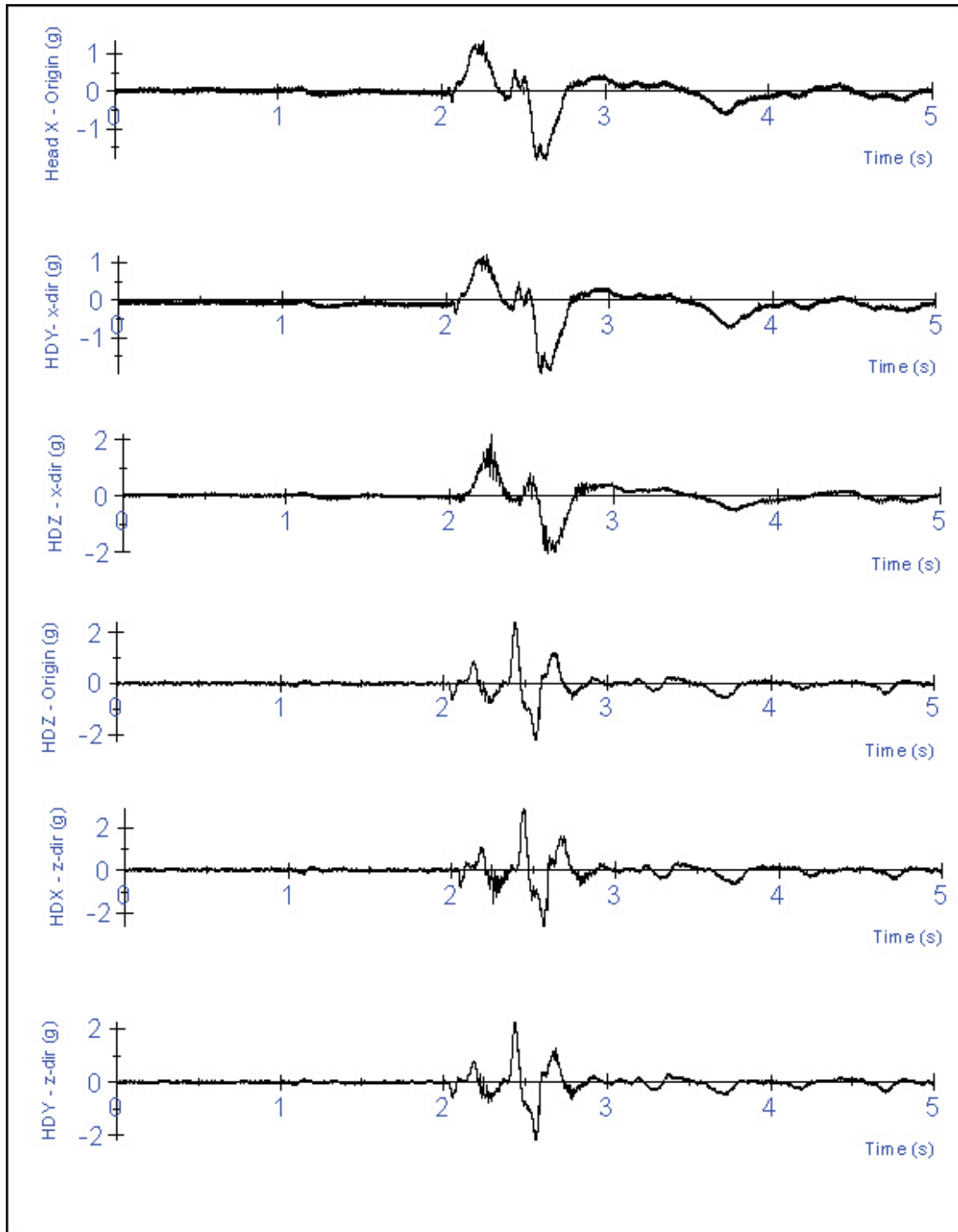


Figure 6-8(a): Acceleration data from 3-2-2-2 for accelerometers in the x and z-directions for a 10-year old boy during a tensed muscle impact. HDX, Y, Z denote the bar on which the accelerometer was attached, and x, y, z-dir denotes the direction of acceleration measured.

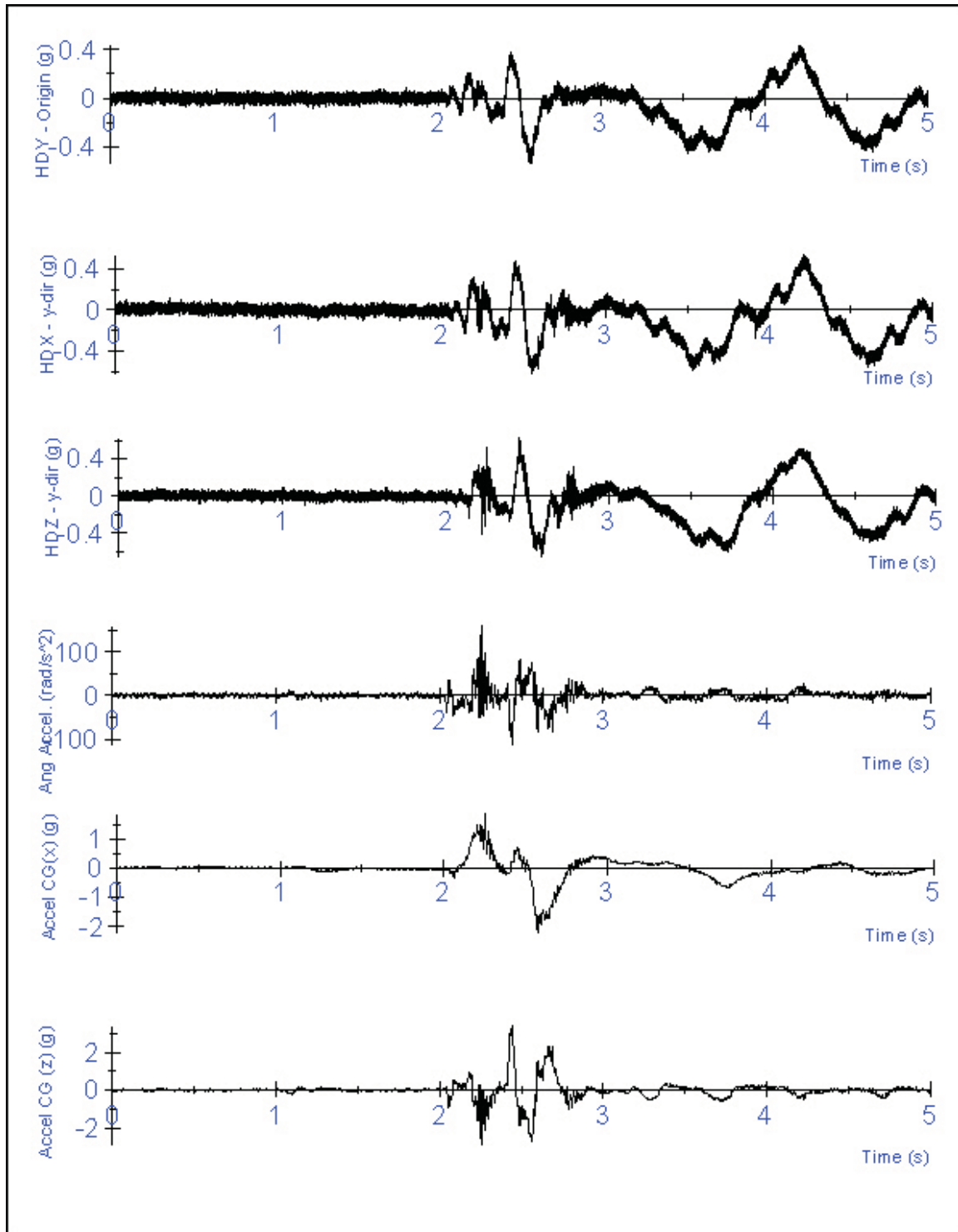


Figure 6-8(b): Acceleration data from 3-2-2-2 for accelerometers in the y-direction, and the calculated acceleration at the CG of the head in the x and z-directions and the angular acceleration about the y-axis for a 10-year old boy during a tensed muscle impact.

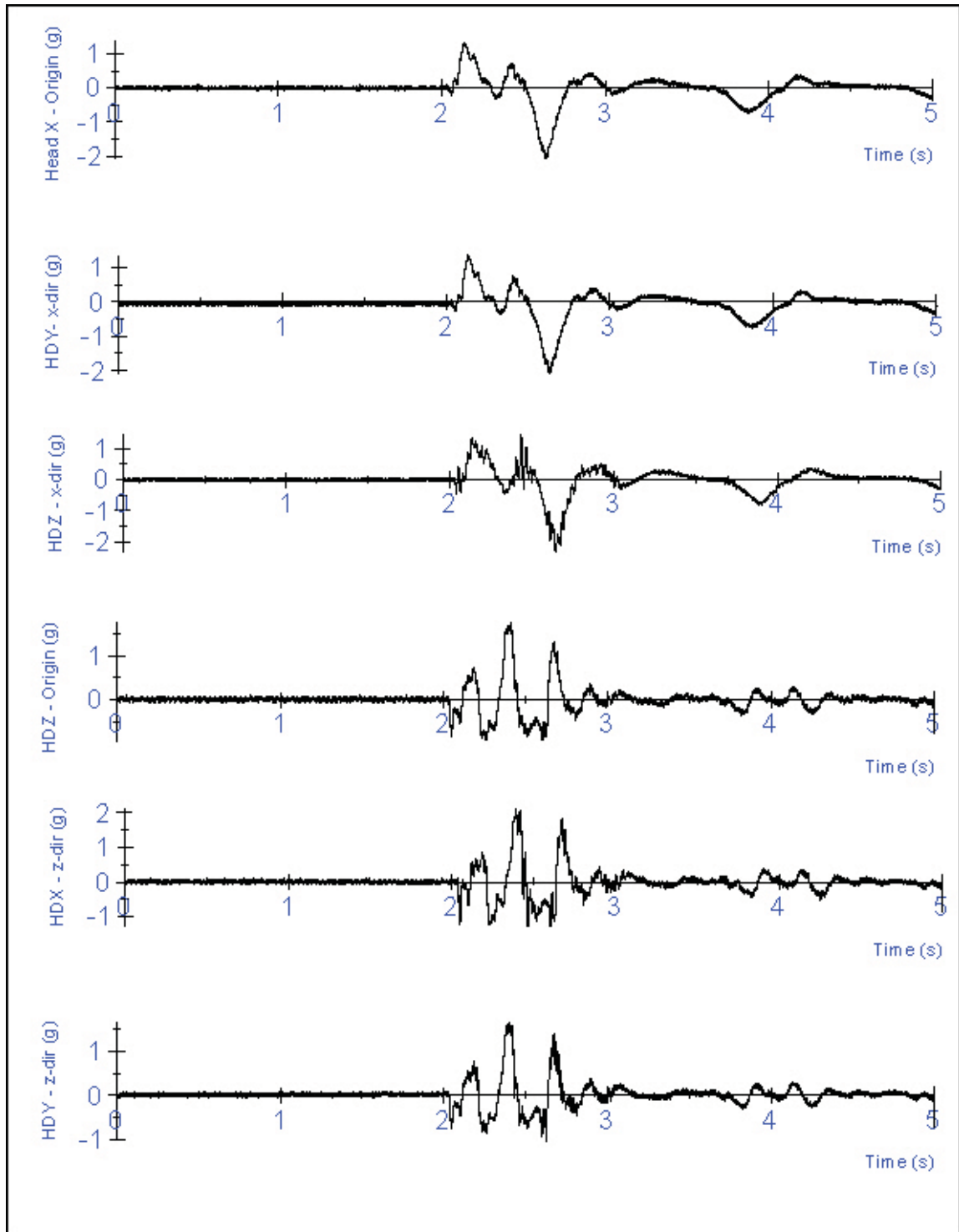


Figure 6-9(a): Acceleration data from 3-2-2-2 for accelerometers in the x and z-directions for a 50th percentile male during a tensed muscle impact. HDX,Y,Z denote the bar on which the accelerometer was attached, and x,y,z-dir denotes the direction of acceleration measured

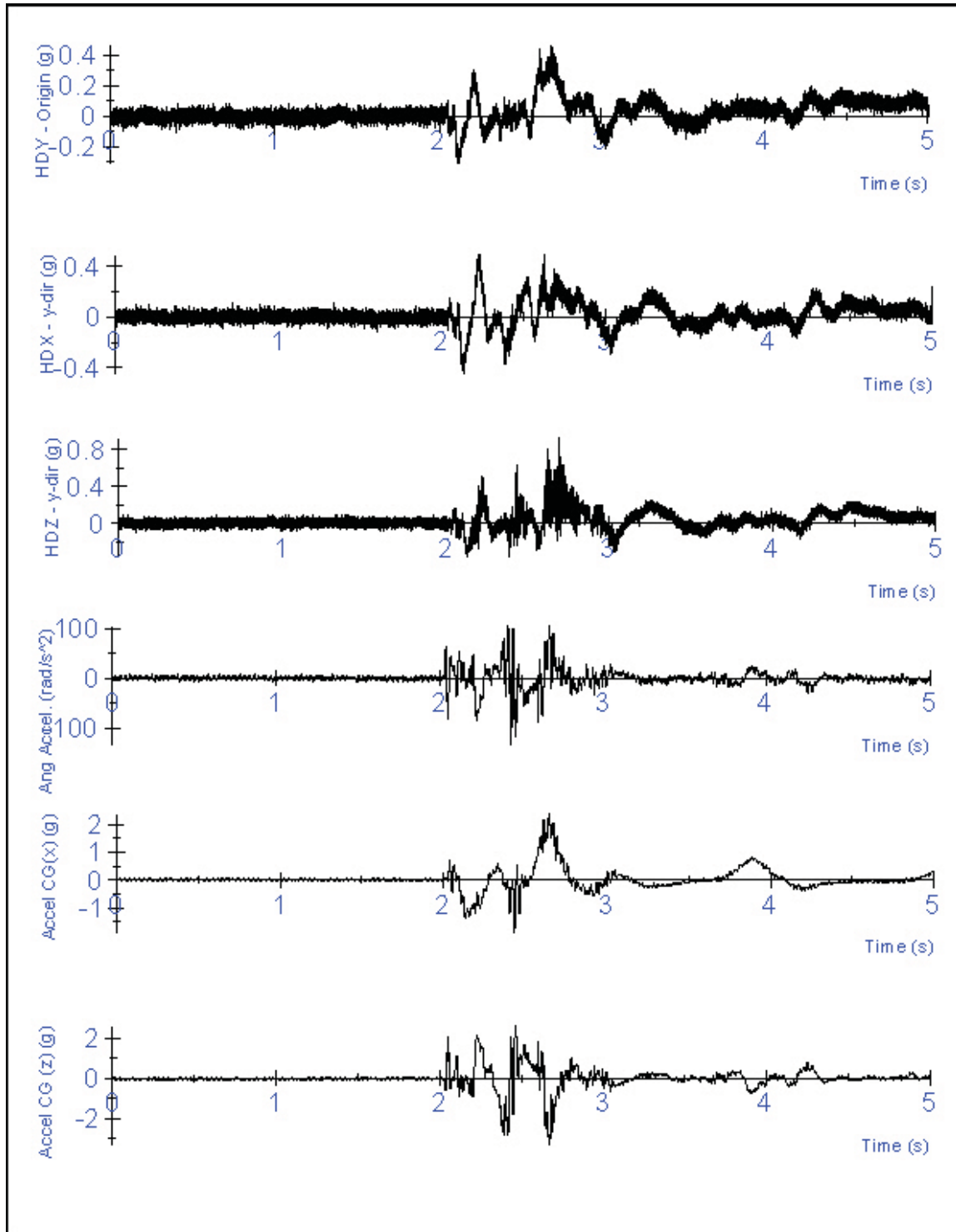


Figure 6-9(b): Acceleration data from 3-2-2-2 for accelerometers in the y-direction, and the calculated acceleration at the CG of the head in the x and z-directions and the angular acceleration about the y-axis for a 50th percentile male during a tensed muscle impact

The linear and angular accelerations calculated at the CG of the head for the 10-year old male subjects using the data from the 3-2-2-2 accelerometer array are shown below in Table 6-2. For the tensed muscle impact, average acceleration in the x-direction was $2.3 \pm 0.3g$'s; average acceleration in z was $4.1 \pm 1.2g$'s with an average resultant acceleration of $4.5 \pm 1.0g$'s. The average angular acceleration was $148.3 \pm 45.2 \text{ rad/s}^2$. In the untensed muscle impact average linear accelerations were x: $2.6 \pm 0.2g$'s; z: $-4.0 \pm 2.0g$'s with a resultant of $5.0 \pm 1.6g$'s. Angular acceleration about the y-axis for the untensed muscle impact was $210.4 \pm 107.5 \text{ rad/s}^2$. There was no significant difference in acceleration between test conditions.

10 Year Old Boys

(a)	Tensed Muscle Impact Mean Acceleration				Untensed Muscle Impact Mean Acceleration			
	a_x (g)	a_z (g)	a_{res} (g)	α_y (rad/s ²)	a_x (g)	a_z (g)	a_{res} (g)	α_y (rad/s ²)
K01	2.3	-3.4	4.4	130.5	2.7	-0.5	4.7	179.7
K03	2.3	-3.0	3.4	97.9	2.5	-3.1	3.3	129.8
K04	2.4	-4.9	5.4	183.6	2.8	-7.0	8.1	220.4
K05	2.5	-5.6	5.9	180.5	No Data Available			
K06	2.1	-5.2	5.3	157.2	2.7	-4.5	4.5	425.0
K07	1.7	-2.6	2.9	108.4	No Data Available			
K09	2.7	-5.1	5.3	237.3	2.5	-4.6	6.1	255.0
K10	2.2	-2.8	3.6	120.3	2.4	-3.5	3.6	106.2
K11	2.0	-4.3	4.5	119.4	2.4	-4.8	4.9	156.4
mean	2.3	-4.1	4.5	148.3	2.6	-4.0	5.0	210.4
St.Dev	0.3	1.2	1.0	45.2	0.2	2.0	1.6	107.5

Table 6-2: Acceleration of the cg of the head calculated for the 10-year old male subjects using the 3-2-2-2 acceleration data. Linear acceleration in the y-direction was assumed to be zero.

The linear and angular accelerations calculated at the CG of the head for the 50th percentile adult male subjects using the data from the 3-2-2-2 accelerometer array are shown below in Table 6-3. For the tensed muscle

impact, average acceleration in the x-direction was $2.7\pm 0.7g$'s; average acceleration in z was $-4.0\pm 0.5g$'s with an average resultant acceleration of $4.5\pm 0.8g$'s. The average angular acceleration was $170.0\pm 41.2\text{rad/s}^2$. In the untensed muscle impact, average linear accelerations were x: $2.0\pm 0.4g$'s; z: $-4.0\pm 0.6g$'s with a resultant of $4.3\pm 0.7g$'s. Angular acceleration about the y-axis for the untensed muscle impact was $169.2\pm 29.1\text{rad/s}^2$. The difference in linear acceleration in the x-direction was significantly greater in the tensed muscle condition as compared to the untensed muscle condition ($p < 0.05$).

50th Percentile Adult Males

(b)	Tensed Muscle Impact Mean Acceleration				Untensed Muscle Impact Mean Acceleration			
	a_x (g)	a_z (g)	a_{res} (g)	α_y (rad/s ²)	a_x (g)	a_z (g)	a_{res} (g)	α_y (rad/s ²)
S13	2.9	-4.7	4.8	188.2	1.6	-3.6	3.6	129.1
S14	2.4	-4.0	4.4	134.1	2.3	-4.4	5.2	192.9
S15	2.0	-3.9	3.9	145.6	1.9	-4.7	4.8	195.9
S16	2.8	-3.9	4.3	167.5	2.5	-4.1	4.1	178.8
S17	4.2	-4.4	6.0	254.4	No Data Available			
S18	2.1	-3.2	3.6	155.0	1.7	-3.2	3.6	149.3
S20	2.7	-3.7	4.7	145.2	No Data Available			
mean	2.7	-4.0	4.5	170.0	2.0	-4.0	4.3	169.2
St.Dev	0.7	0.5	0.8	41.2	0.4	0.6	0.7	29.1

Table 6-3: Acceleration of the cg of the head calculated for the 50th percentile adult male subjects using the 3-2-2-2 acceleration data. Linear acceleration in the y-direction was assumed to be zero.

Although no direct comparison was made between the adult and child subject groups, the peak acceleration values of the head are similar between the two groups, in spite of a lower test acceleration for the 10-year old males.

Moments were calculated over the entire impact event using equation (6-2), from section 6.2.4 – Dynamic Force Calculations, shown again below.

$$\Sigma M_y = F_{cg,x} \times d_{head} + F_{cg,z} \times d_{oc,x} + I_{yy, cg} \cdot \ddot{\alpha}_y \quad (6-2)$$

Moments were calculated for the duration of the impact. In response to the onset of swing acceleration, the subject's neck went into extension. Peak moment in extension was greater in both subject groups during the untensed muscle impact than in the tensed muscle impact ($p < 0.05$). In response to the swing's peak deceleration, the subjects' neck went into flexion. In the case of the 10-year old male subjects, the peak moment in flexion was greater in the untensed muscle impact than in the tensed muscle impact ($p < 0.05$). For the adult male subjects the opposite was true – flexion moment was greater in the tensed muscle impact than in the untensed muscle impact. Figure 6-10 (a) and (b) show the moment time histories for both the 10-year old subject group and the 50th percentile adult male subject group during both a tensed muscle impact and an untensed muscle impact.

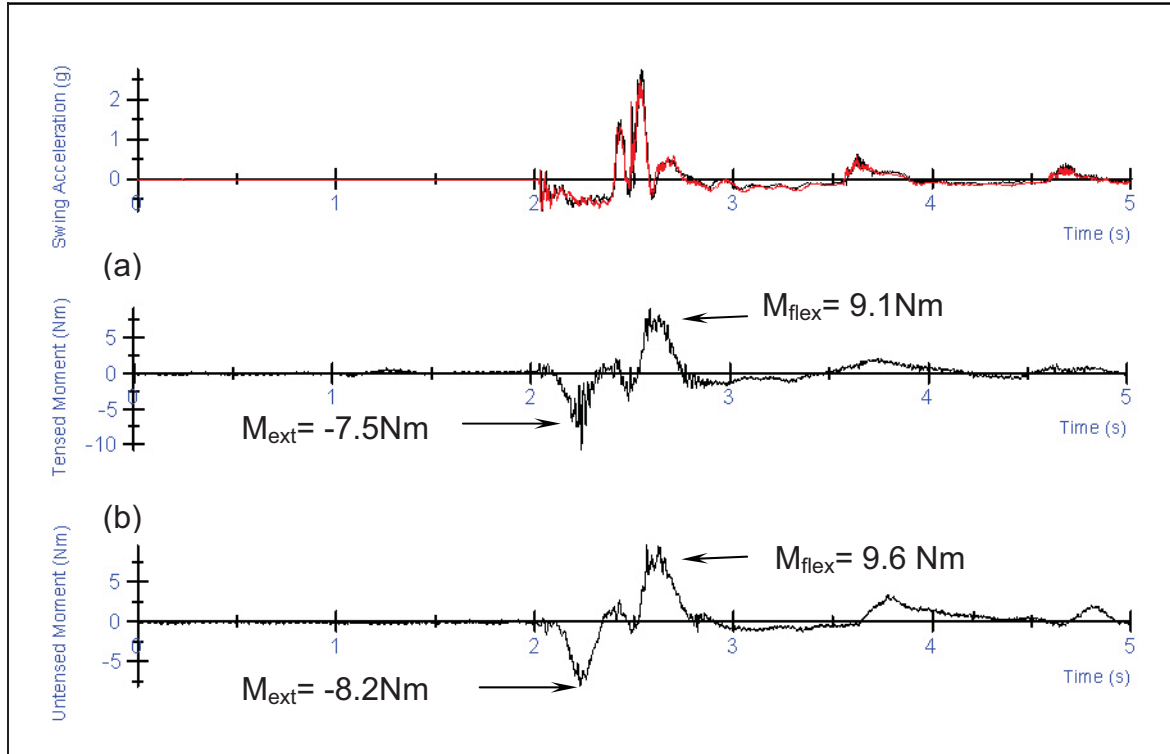


Figure 6-10(a): Total moment at C4 for (a) Tensed Muscle Impact and (b) Untensed muscle impact for a 10-year old male subject.

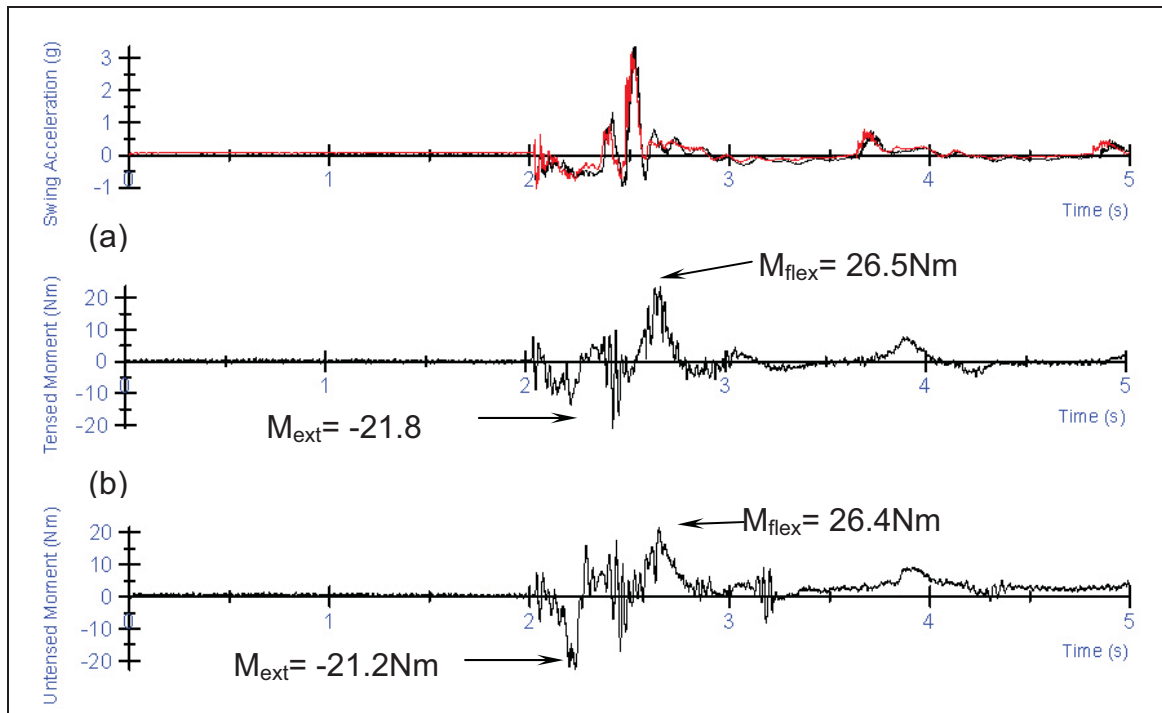


Figure 6-10(b): Total moment at C4 for (a) Tensed Muscle Impact and (b) Untensed muscle impact for a 50th percentile adult male subject.

During the tensed impact the 10 year old boys had an average peak moment in extension of 7.5 ± 1.2 Nm at $t = 2.3 \pm 0.1$ s after the onset of swing acceleration. After peak swing acceleration, at $t = 2.6 \pm 0.1$ s the average moment at C4 in flexion was 10.4 ± 2.2 Nm. During the untensed muscle impact, the average moment in extension 9.6 ± 3.6 Nm at $t = 2.4 \pm 0.4$ s after the onset of swing acceleration. The average peak flexion moment for an untensed muscle impact was 12.6 ± 28.5 Nm at $t = 2.6 \pm 0.1$ s. The difference in the time to peak moments between the tensed and untensed muscle impacts was not significant for either extension or flexion moments, nor was the difference in the extension and flexion moments between the tensed and untensed muscle impacts. Table 6-4 shows the mean moments in flexion and extension for both the tensed and untensed muscle impacts of 10-year old boys.

10 Year Old Boys

(a)	Tensed Muscle Condition Mean Moments (Nm)				Untensed Muscle Condition Mean Moments (Nm)			
	Ext	Time	Flex	Time	Ext	Time	Flex	Time
K01	-6.8	2.22	9.6	2.59	-8.0	2.26	9.5	2.64
K03	-8.6	2.24	9.0	2.59	-9.5	2.23	9.8	2.58
K04	-7.3	2.24	13.8	2.62	-17.4	2.21	15.7	2.64
K05	-9.8	2.19	12.3	2.62	No Data Available			
K06	-8.4	2.15	10.0	2.63	-8.1	2.17	15.2	2.70
K07	-6.6	2.19	7.4	2.59	No Data Available			
K09	-6.9	2.42	13.1	2.88	-9.6	2.63	15.5	2.75
K10	-6.1	2.50	9.5	2.58	-7.2	3.32	10.0	2.56
K11	-7.2	2.21	8.7	2.57	-7.2	2.23	12.6	2.60
Mean	-7.5	2.26	10.4	2.63	-9.6	2.43	12.6	2.64
St. Dev	1.2	0.12	2.2	0.09	3.6	0.42	2.9	0.07

Table 6-4: Mean peak moments in extension and flexion for tensed and untensed muscle impacts for 10-year old boys.

The extension moment in response to the onset of swing acceleration, for the 50th percentile adult male subject group was also significantly greater for the untensed muscle impact ($p < 0.05$). During the tensed muscle impact, the extension moment was 18.5 ± 2.3 Nm, occurring at $t = 2.4 \pm 0.1$ s from swing drop. In the untensed muscle impact, the extension moment was 22.1 ± 4.3 Nm, occurring at $t = 2.3 \pm 0.1$ s from swing drop. The maximum flexion moment occurred in response to peak swing acceleration. For the tensed muscle impact, the average peak moment in flexion was 27.1 ± 8.8 Nm occurring at $t = 2.7 \pm 0.1$ s from swing drop. In the untensed muscle impact, average peak moment in flexion was 20.3 ± 5.0 Nm, occurring at $t = 2.6 \pm 0.1$ s from swing drop. Table 6-5 shows the mean moments and time to peak moment for the 50th percentile adult male for both muscle conditions.

50th Percentile Adult Males

(b)	Tensed Muscle Condition Mean Moments (Nm)				Untensed Muscle Condition Mean Moments (Nm)			
	Ext	Time	Flex	Time	Ext	Time	Flex	Time
S13	-20.7	2.28	28.4	2.62	-19.4	2.21	15.5	2.64
S14	-21.8	2.58	26.5	2.86	-27.2	2.24	26.4	2.53
S15	-19.4	2.43	18.4	2.65	-17.0	2.45	15.3	2.65
S16	-17.1	2.25	23.0	2.64	-21.2	2.37	20.4	2.67
S17	-18.9	2.30	45.6	2.56	-25.8	2.17	24.0	2.65
S18	-15.6	2.27	24.5	2.63	No Data Available			
S20	-16.5	2.31	23.4	2.64				
mean	-18.6	2.35	27.1	2.66	-22.1	2.29	20.3	2.63
St.Dev	2.3	0.12	8.8	0.10	4.3	0.12	5.0	0.06

Table 6-5: Mean peak moments in extension and flexion for tensed and untensed muscle impacts for 50th percentile adult males. The untensed muscle impact extension moments were significantly greater ($p < 0.05$) than the tensed muscle impact extension moments. The flexion moments were greater ($p < 0.05$) for the tensed muscle condition. The time to peak moment was not different between test conditions.

For the 50th percentile male subjects, the moment in flexion was greater for the tensed muscle condition than for the untensed muscle conditions ($p < 0.05$). The extension moment was greater ($p < 0.05$) in the untensed muscle impact than the tensed muscle impact. There was no significant difference in the time to peak moments in either flexion or extension between muscle conditions. There was no difference in either of the moments between the tensed and untensed muscle impacts for the 10-year old male subjects.

6.3.2 Electromyography Results

A baseline EMG recording was taken prior to the start of the dynamic phase of testing. During this recording the subject was biting down on the plate holding the accelerometer array. The mean of the filtered, rectified baseline signal with the subject holding the bite plate was significantly greater in all muscles ($p < 0.02$) than the baseline recording made prior to the static MVC test series where the subjects were not holding a bite plate. The increase in the baseline was due to muscle activation in response to the subject biting down on the 3-2-2-2 mouthpiece. The increased baseline had negligible effect on the overall results since it was subtracted from the EMG recorded during the impact testing in order to zero the signal. Furthermore, during the tensed muscle testing, subjects were asked to tense their muscles in preparation for impact. In both the tensed and untensed test conditions, the muscle activation was significantly higher ($p < 0.05$) than the baseline signal collected prior to dynamic testing with the subject holding the bite plate.

For the 10-year old male subjects, in dynamic loading conditions the EMG values of the muscles and muscle groups examined in this study all exceeded the EMG values recorded during the static maximal voluntary contraction - %MVC was greater than 100%, with the exception of the right postero-lateral muscle group and the right scalene muscle group. Both these muscle groups were under 100% MVC at 92.4% and 99.2% MVC respectively. The SCM recorded average EMG values of 111.3%-162.6% MVC. The posterior muscle group had average recorded EMG values of 115.2%-135.3% MVC, as shown in Table 6-6. There was no difference in the muscle activation between the tensed and untensed muscle dynamic conditions.

10 Year Old Boys

	Tensed Muscles					
	Peak EMG (μV)		Time to Peak (s)		%MVC	
	Mean	stdev	Mean	stdev	Mean	stdev
SCM (R)	195.3	88.9	2.29	0.19	1.10	0.43
SCM (L)	206.4	102.9	2.27	0.17	1.41	1.04
POST (R)	100.6	87.6	2.52	0.24	1.22	0.56
POST (L)	94.0	38.1	2.45	0.24	1.39	0.91
P-L (R)	211.6	252.1	2.51	0.30	1.19	1.04
P-L (L)	150.5	57.0	2.43	0.26	1.28	0.88
SCAL (R)	135.2	47.1	2.48	0.20	1.22	0.62
SCAL (L)	116.6	56.1	2.43	0.25	1.26	0.70

10 Year Old Boys

	Untensed Muscles					
	Peak EMG (μV)		Time to Peak (s)		%MVC	
	Mean	stdev	Mean	stdev	Mean	stdev
SCM (R)	195.2	99.4	2.22	0.16	1.11	0.44
SCM (L)	240.5	122.2	2.17	0.03	1.63	1.08
POST (R)	84.4	42.3	2.54	0.13	1.15	0.52
POST (L)	106.6	88.5	2.43	0.22	1.35	0.98
P-L (R)	139.2	56.3	2.42	0.21	0.92	0.52
P-L (L)	126.4	37.6	2.31	0.19	1.06	0.52
SCAL (R)	111.9	45.8	2.38	0.20	0.99	0.50
SCAL (L)	121.9	54.3	2.42	0.21	1.20	0.54

Table 6-6: EMG values and %MVC values for the 10 year old male subjects in both the dynamic tensed and untensed conditions.

As shown in figure 6-11 (a) and (b) below the peak EMG activation voltage for the SCM occurs in response to the swing's release and the extension moment, rather than the peak swing acceleration. The posterior muscles, by contrast, reach their peak activation voltage in response to the swing's peak acceleration and the flexion moment.

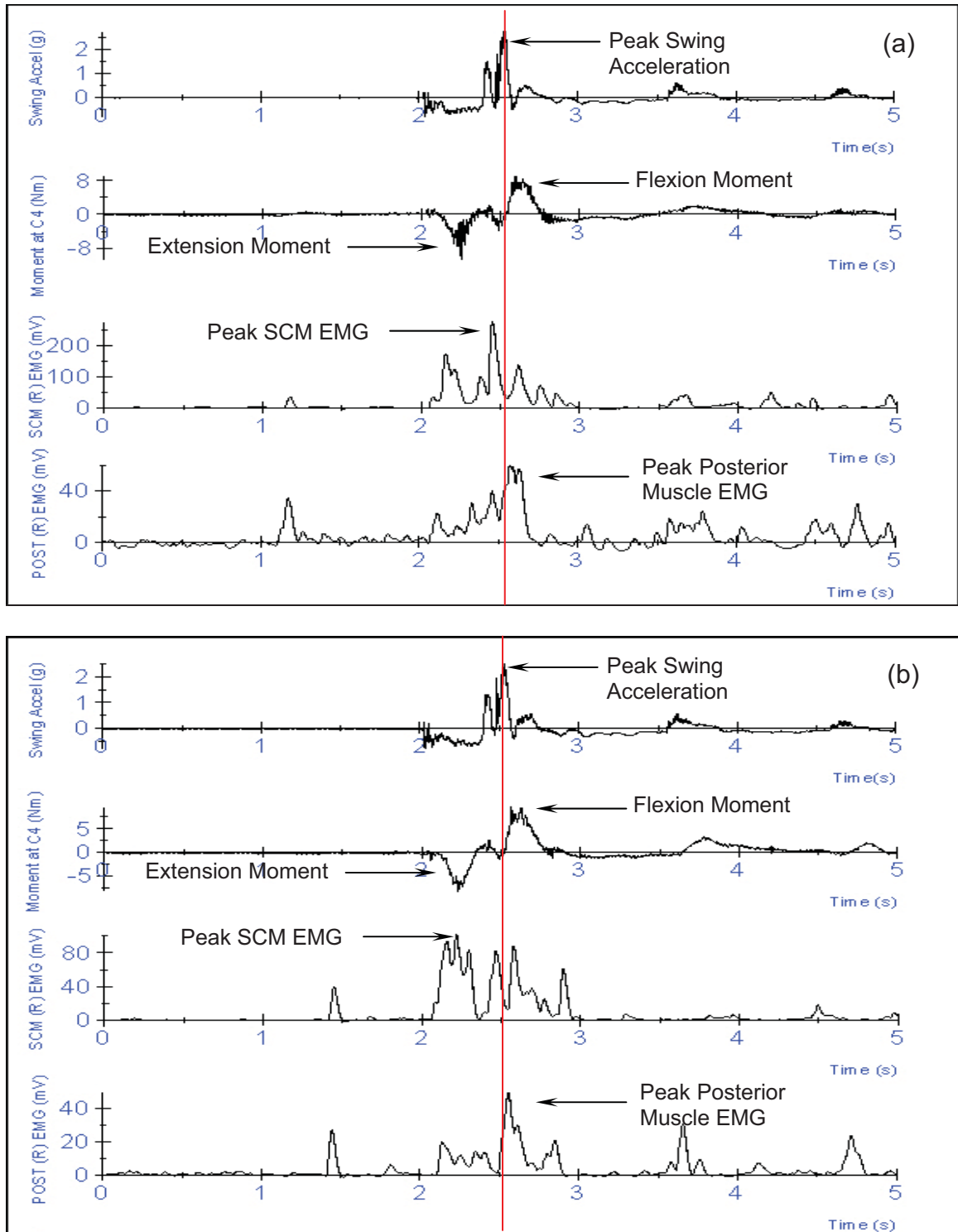


Figure 6-11: The EMG activation trace of both the SCM and posterior muscle group for the (a) tensed muscle impact, and (b) untensed muscle impact for a 10-year old male relative to the swing's acceleration and the moment at C4. On average, the SCM's peak EMG occurs prior to the swing's peak acceleration while the posterior muscles' peak EMG occurs after the swing's peak acceleration, regardless of the muscle condition.

The response of the scalene muscles and the postero-lateral muscles showed no distinct activation pattern. There was no significant difference in the time to peak activation between the tensed and untensed muscle impact conditions. This is consistent with the results detailed in **Chapter 7 - Latency of Neck muscle response and Head displacement during Dynamic Loading**. Figures 6-12 (a)-(d) show the raw and rectified, filtered EMG traces for both a tensed and untensed muscle impact for a 10-year old male subject.

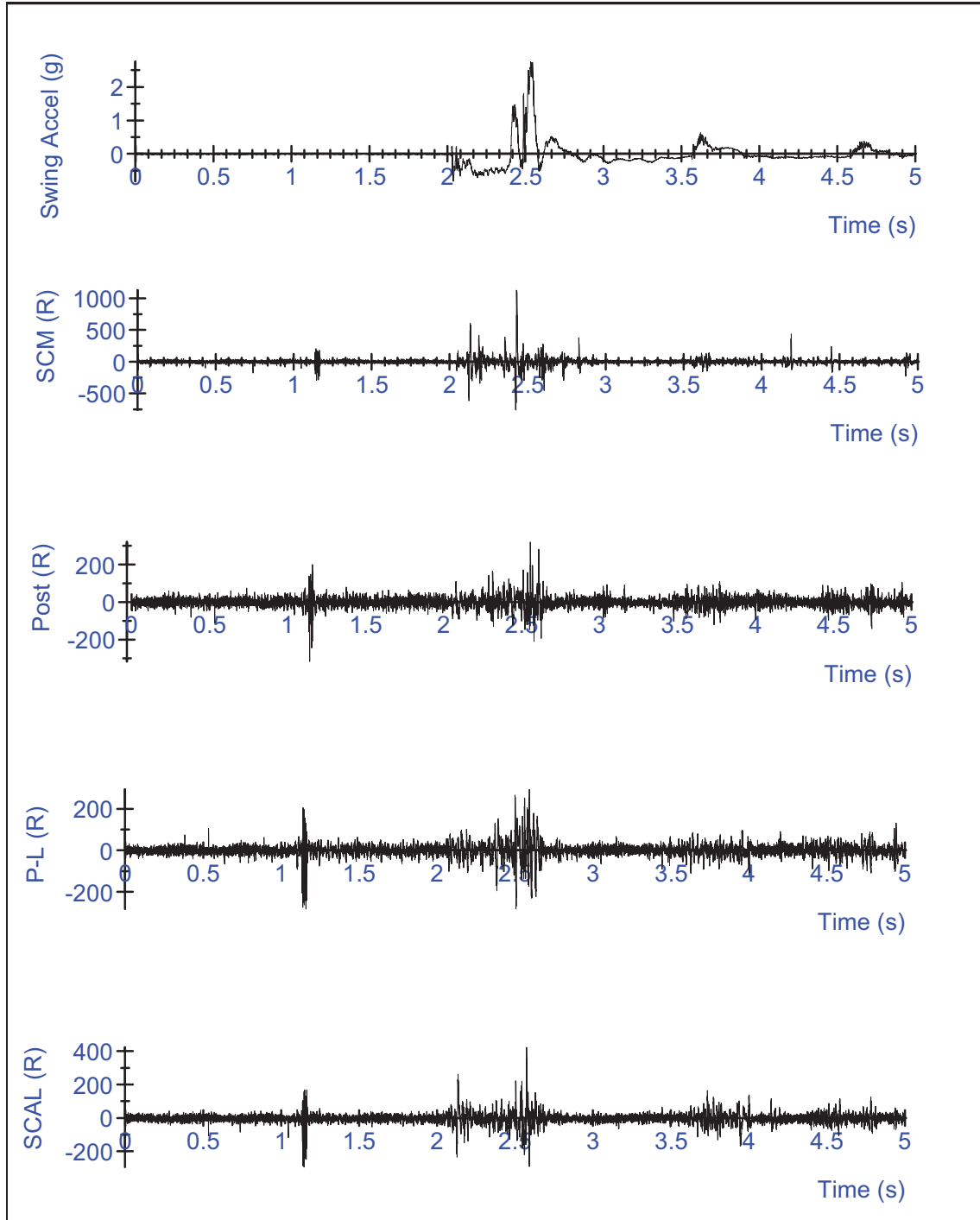


Figure 6-12(a): Raw EMG data for the right hand side muscles for a 10-year old male subject in a tensed muscle impact. The units for the y-axis are in mV. Where on the y-axis SCM refers to the EMG of the sternocleidomastoid, POST refers the EMG of the posterior muscle group, P-L refers to the EMG of the postero-lateral muscle group and SCAL refers to the EMG of the scalene muscle group.

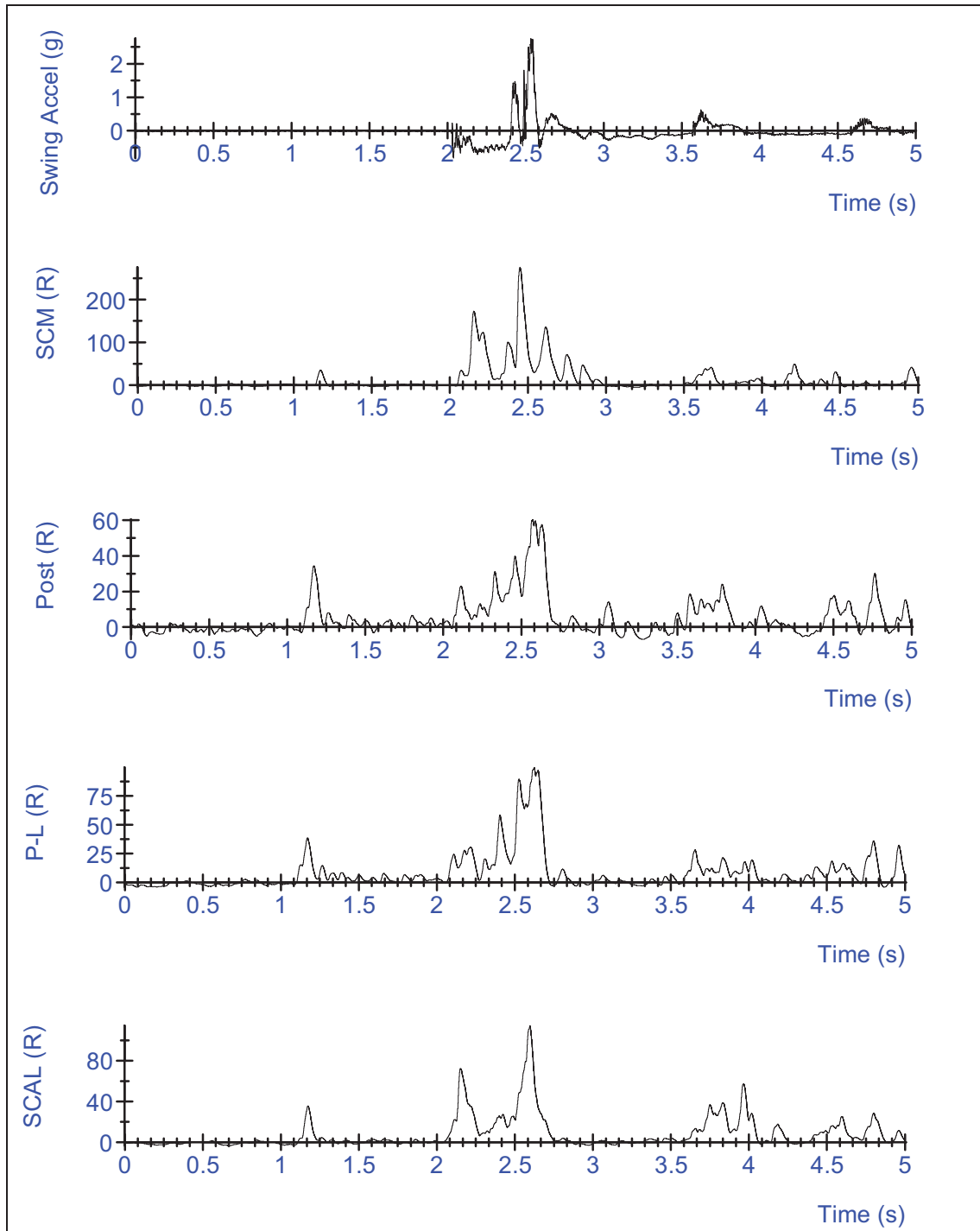


Figure 6-12(b): Filtered rectified EMG data for the right hand side muscles for a 10-year old male subject in a tensed muscle impact. The units for the y-axis are in μV . Where on the y-axis SCM refers to the EMG of the sternocleidomastoid, POST refers the EMG of the posterior muscle group, P-L refers to the EMG of the postero-lateral muscle group and SCAL refers to the EMG of the scalene muscle group.

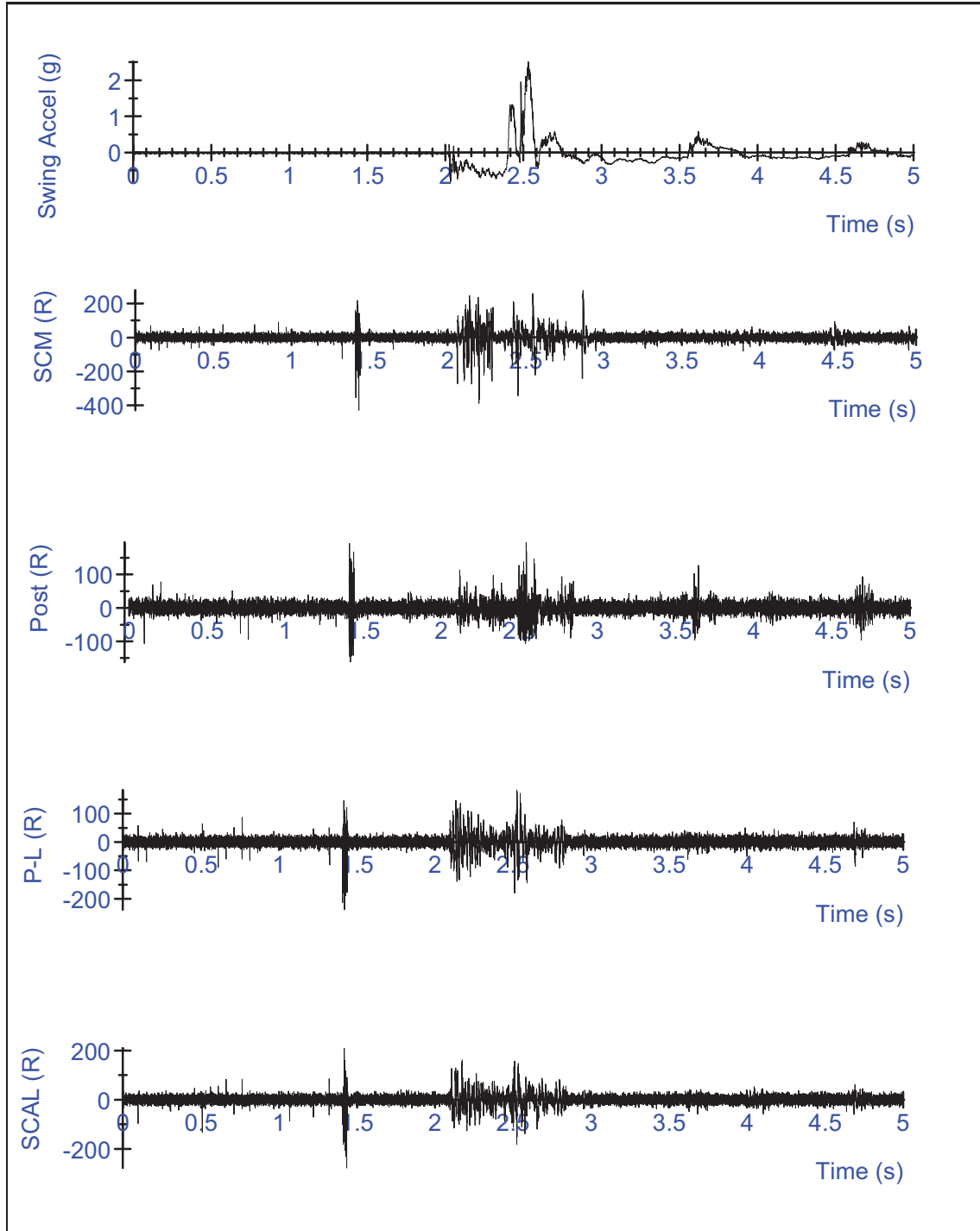


Figure 6-12(c): Raw EMG data for the right hand side muscles for a 10-year old male subject in an untensed muscle impact. The units of the y-axis are in mV. Where on the y-axis SCM refers to the EMG of the sternocleidomastoid, POST refers the EMG of the posterior muscle group, P-L refers to the EMG of the postero-lateral muscle group and SCAL refers to the EMG of the scalene muscle group.

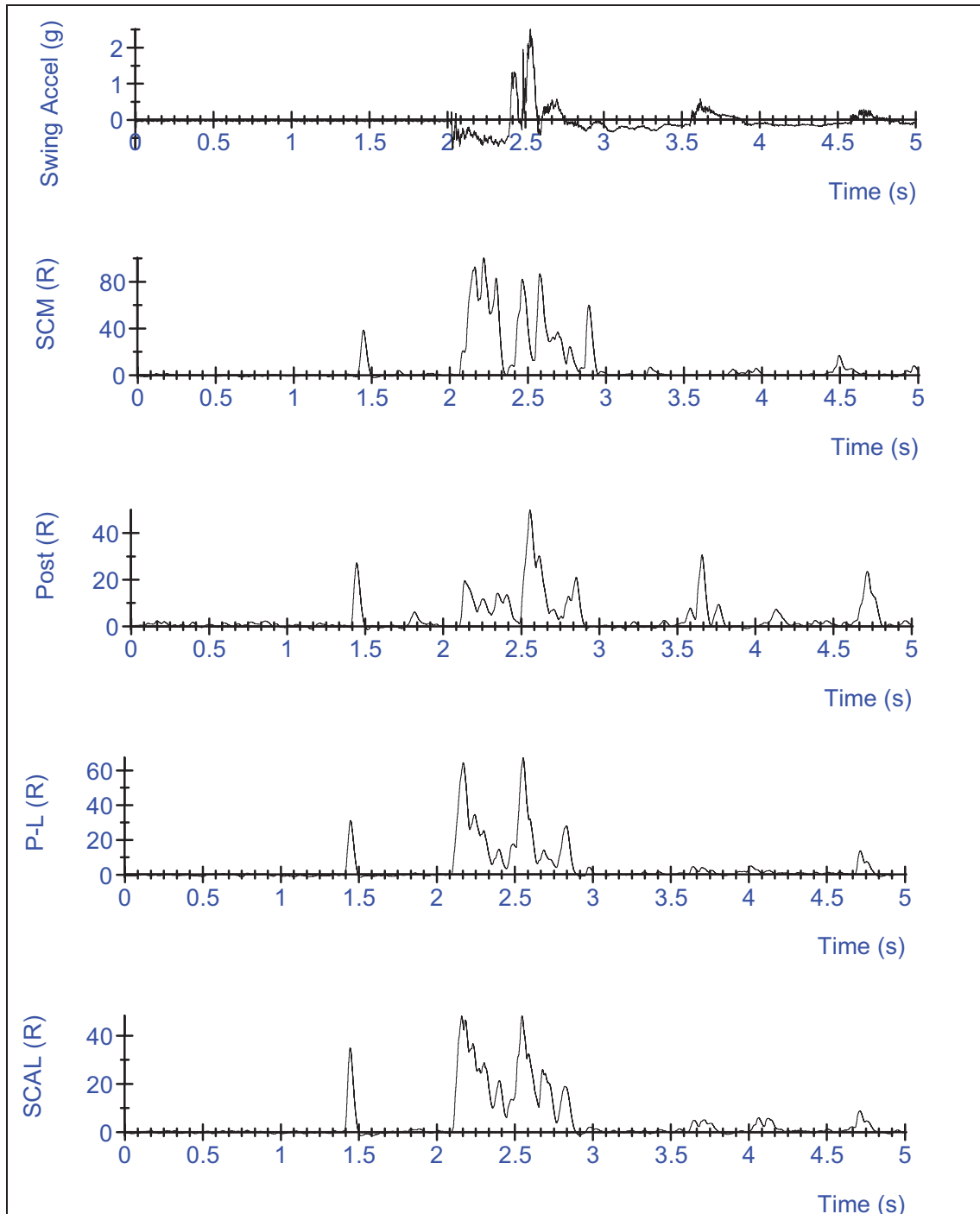


Figure 6-12(d): Rectified, filtered EMG data for the right hand side muscles for a 10-year old male subject in an untensed muscle impact. The units for the y-axis are in μV . The difference in the time scale between the raw and filtered data is due to synchronization with acceleration data. Where on the y-axis SCM refers to the EMG of the sternocleidomastoid, POST refers the EMG of the posterior muscle group, P-L refers to the EMG of the postero-lateral muscle group and SCAL refers to the EMG of the scalene muscle group.

The adult data followed a similar pattern to the children. There was no significant difference between the EMG activation values of the muscles and muscle groups examined in the study, but in all cases when activation was expressed as %MVC, the muscle activation was greater than 100%, with the exception of the postero-lateral muscles in the untensed muscle condition. In the untensed muscle impact condition, the postero-lateral muscles had an activation range of 83.4%-94.0% MVC. The muscle activation values in μV and expressed as %MVC and the time to peak muscle activation are shown below in Table 6-7.

50th Percentile Adult Males

	Tensed Muscles					
	Peak EMG (μV)		Time to Peak (s)		%MVC	
	Mean	stdev	Mean	stdev	Mean	stdev
SCM (R)	193.1	118.6	2.30	0.25	1.42	0.65
SCM (L)	182.3	98.5	2.31	0.26	1.62	0.71
POST (R)	60.1	61.7	2.59	0.29	2.26	1.71
POST (L)	42.8	23.9	2.63	0.37	1.98	0.96
P-L (R)	105.1	88.3	2.41	0.58	1.00	0.63
P-L (L)	92.2	58.2	2.49	0.41	1.29	0.41
SCAL (R)	123.3	76.3	2.45	0.48	1.81	1.64
SCAL (L)	81.8	56.6	2.29	0.47	1.10	0.43

50th Percentile Adult Males

	Untensed Muscles					
	Peak EMG (μV)		Time to Peak (s)		(%MVC)	
	Mean	stdev	Mean	stdev	Mean	stdev
SCM (R)	195.9	99.4	2.21	0.16	1.32	0.57
SCM (L)	206.1	93.7	2.25	0.18	1.88	1.08
POST (R)	59.1	49.4	2.60	0.11	2.21	1.46
POST (L)	35.9	20.8	2.56	0.20	1.56	0.79
P-L (R)	108.0	89.6	2.40	0.25	0.83	0.51
P-L (L)	61.9	31.1	2.48	0.24	0.94	0.61
SCAL (R)	100.3	61.1	2.33	0.21	1.08	0.86
SCAL (L)	68.1	28.0	2.41	0.22	1.02	0.51

Table 6-7: EMG values and %MVC values for the 50th percentile adult male subjects in both the dynamic tensed and untensed conditions.

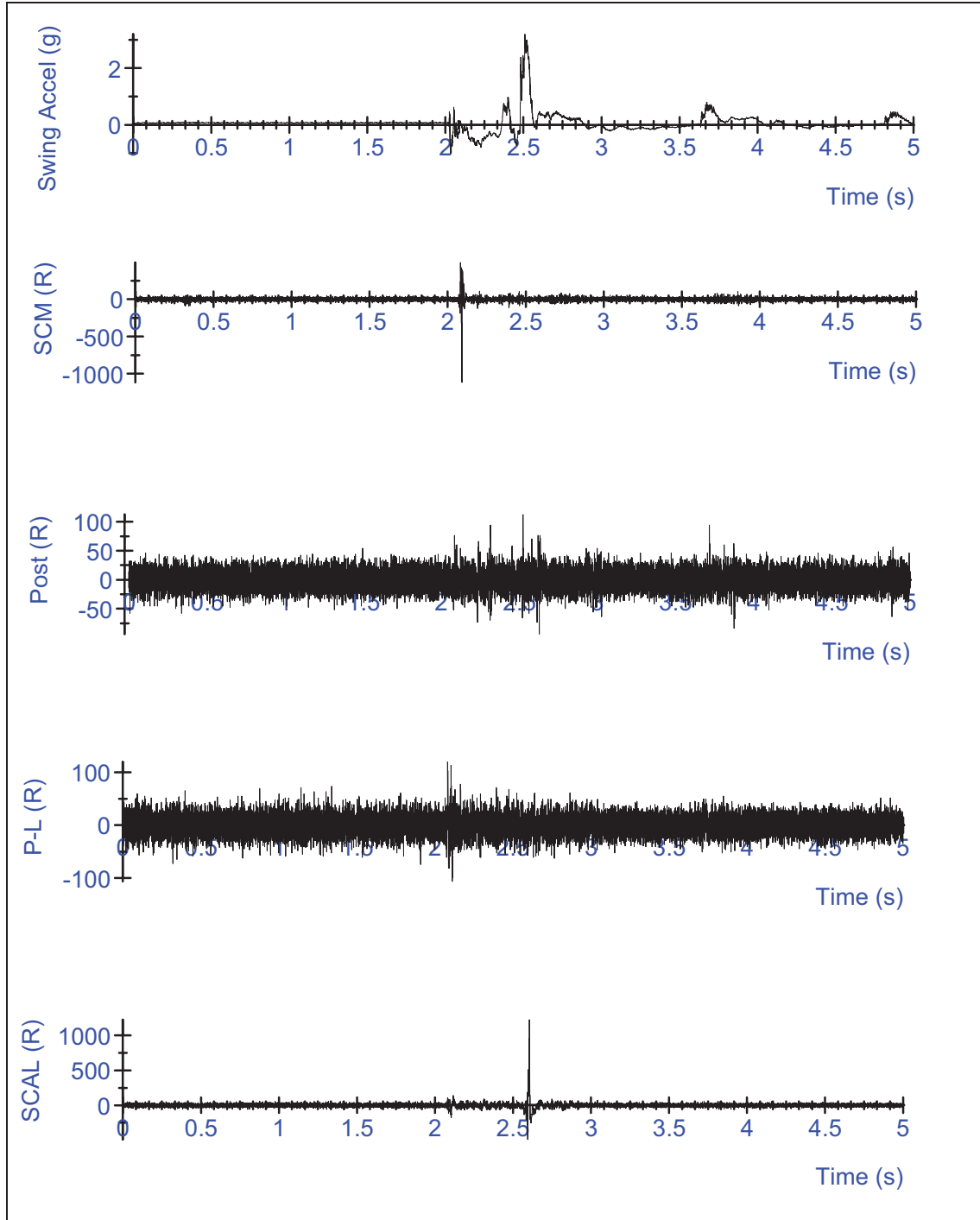


Figure 6-13(a): Raw EMG data for the right hand side muscles for a 50th percentile adult male subject in a tensed muscle impact. The units of the y-axis are in mV. Where on the y-axis SCM refers to the EMG of the sternocleidomastoid, POST refers the EMG of the posterior muscle group, P-L refers to the EMG of the postero-lateral muscle group and SCAL refers to the EMG of the scalene muscle group.

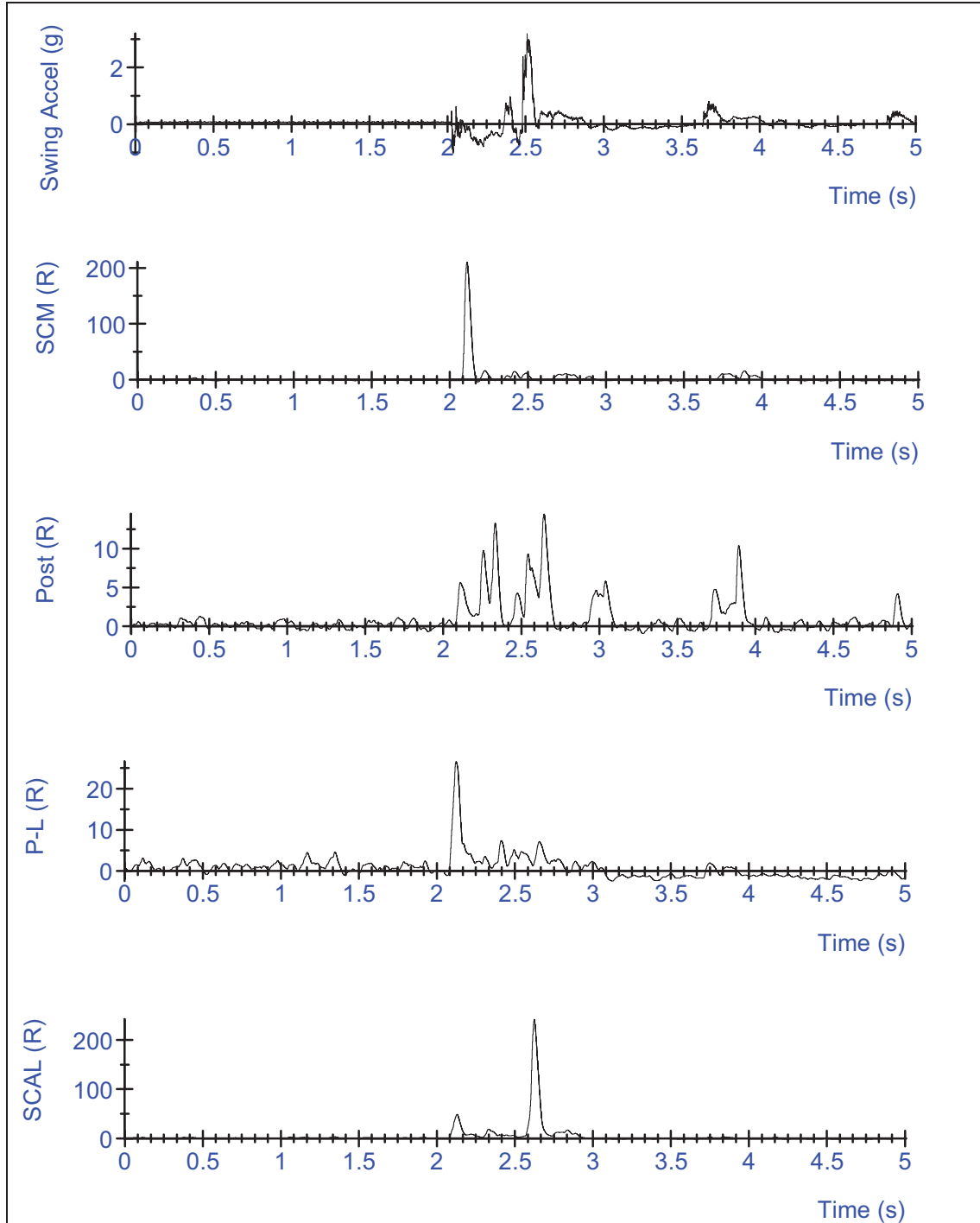


Figure 6-13(b): Rectified, filtered EMG data for the right hand side muscles for a 50th percentile adult male subject in an untensed muscle impact. The units for the y-axis are in μV . The difference in the time scale between the raw and filtered data is due to synchronization with acceleration data. Where on the y-axis SCM refers to the EMG of the sternocleidomastoid, POST refers the EMG of the posterior muscle group, P-L refers to the EMG of the postero-lateral muscle group and SCAL refers to the EMG of the scalene muscle group.

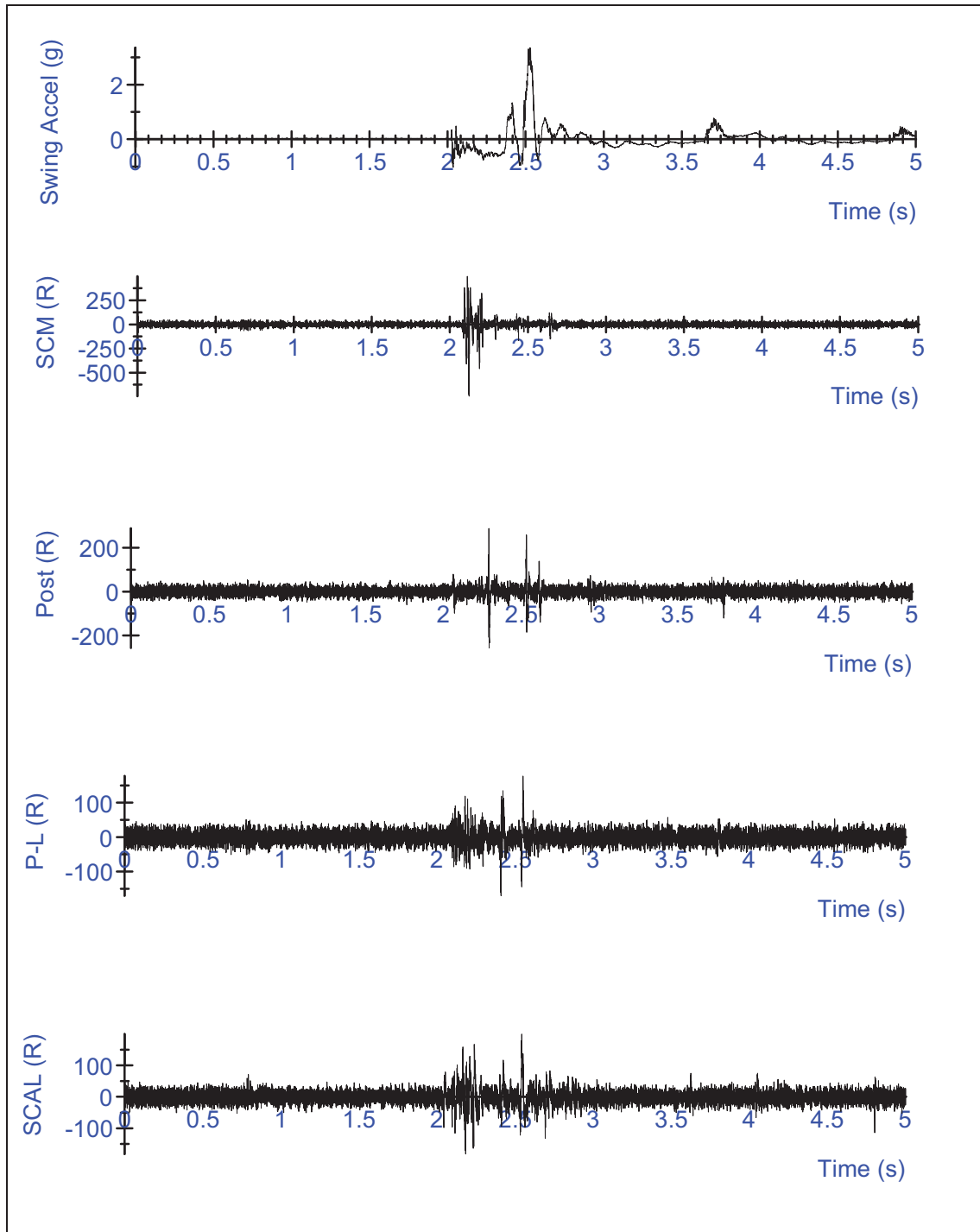


Figure 6-13(c): Raw EMG data for the right hand side muscles for a 50th percentile adult male subject in an untensed muscle impact. The units of the y-axis are in mV. Where on the y-axis SCM refers to the EMG of the sternocleidomastoid, POST refers the EMG of the posterior muscle group, P-L refers to the EMG of the postero-lateral muscle group and SCAL refers to the EMG of the scalene muscle group.

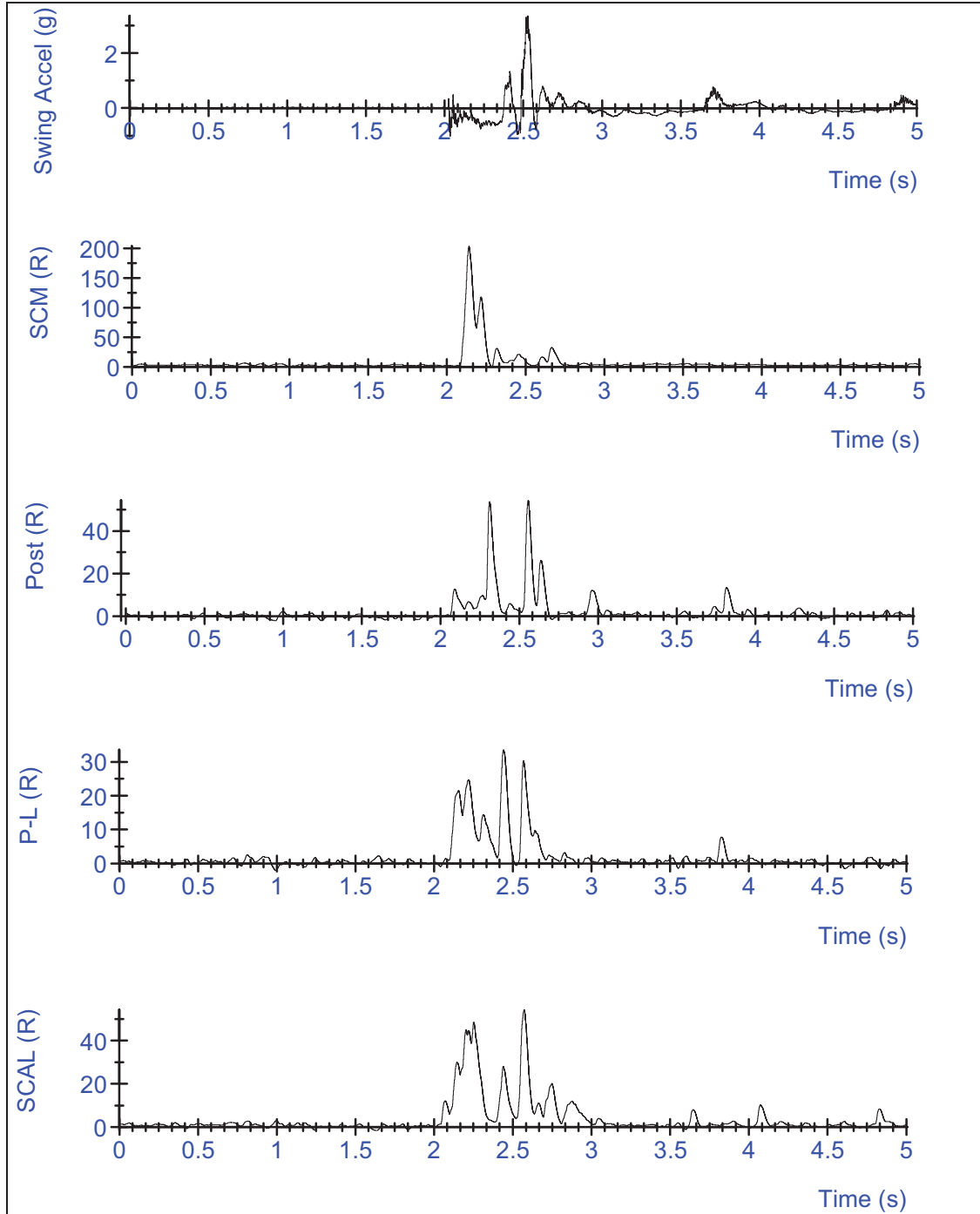


Figure 6-13(d): Rectified, filtered EMG data for the right hand side muscles for a 50th percentile male subject in an untensed muscle impact. The units for the y-axis are in μV . The difference in the time scale between the raw and filtered data is due to synchronization with acceleration data. Where on the y-axis SCM refers to the EMG of the sternocleidomastoid, POST refers the EMG of the posterior muscle group, P-L refers to the EMG of the postero-lateral muscle group and SCAL refers to the EMG of the scalene muscle group.

Figures 6-13 (a)-(d), above show the raw and rectified, filtered data for a 50th percentile male subject in both muscle impact conditions. Similar to the results of the 10-year old male subjects, the peak muscle activation for the SCM corresponds with the swing release and the extension moment, occurring before the swing's impact with the shock absorbers. The peak activation value for the posterior muscles occurs after the swing's impact with the shock absorbers, corresponding the flexion moment (figure 6-14 (a) and (b)).

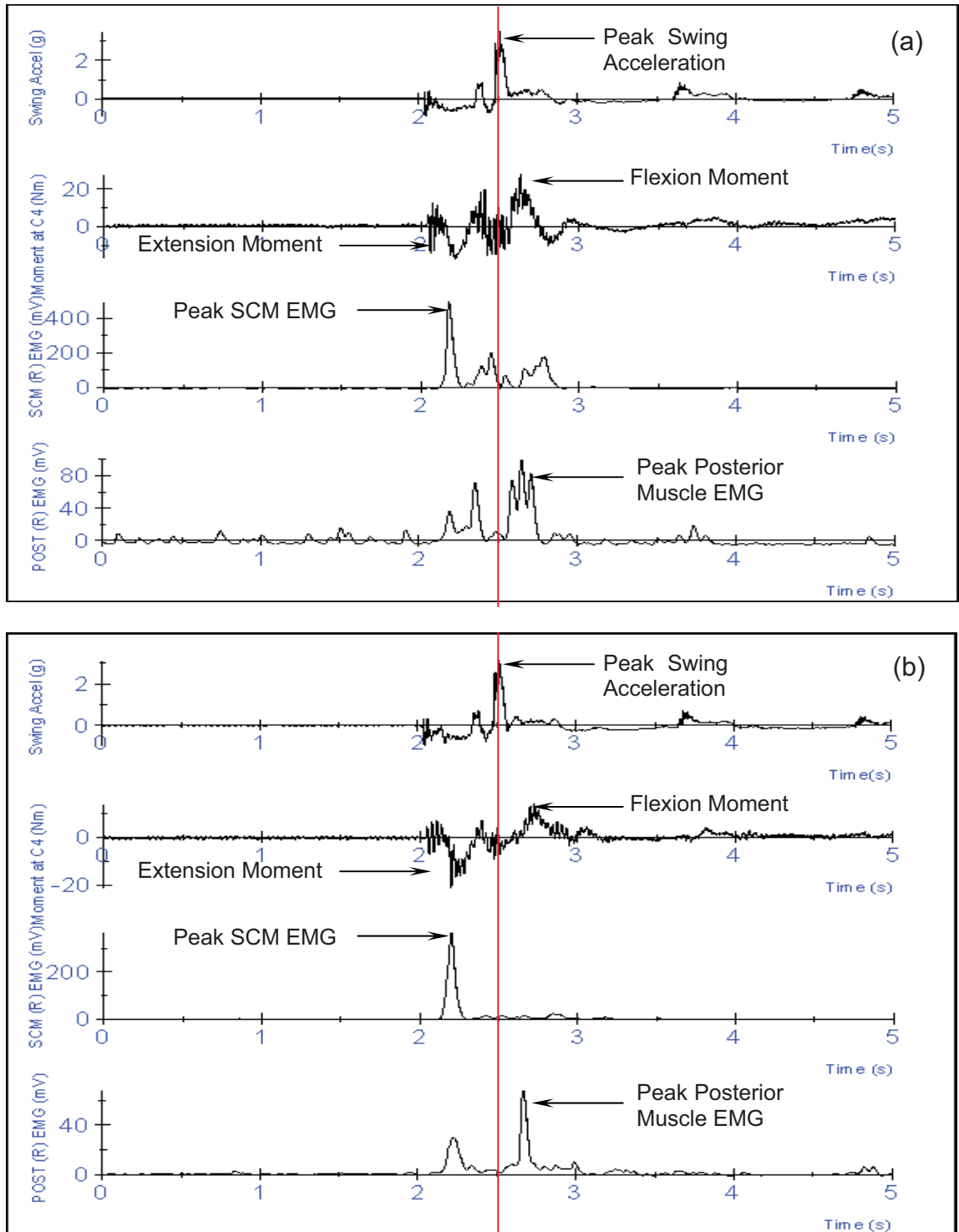


Figure 6-14: The EMG activation trace of both the SCM and posterior muscle group for the (a) tensed muscle impact, and (b) untensed muscle impact for a 50th percentile adult male relative to the swing's acceleration and the moment at C4. On average, the SCM's peak EMG occurs prior to the swing's peak acceleration while the posterior muscles' peak EMG occurs after the swing's peak acceleration, regardless of the muscle condition.

There was no difference in the time to peak EMG activation between the tensed and untensed muscle condition. However, as discussed in **Chapter 7 - Latency of Neck muscle response and Head displacement during Dynamic Loading**, the onset of muscle activity in response to the swing's maximum acceleration differed between muscle conditions.

6.4 DISCUSSION

The physiologic response of children to various types of perturbations provides insight into their potential injury tolerance. At low speed, the neck muscles have a more significant role in the response of the neck than at high speeds where injuries are related to the tolerances of the tissues. At low speeds the activation of and force generation in the neck muscles has an influence on the injury of the subject. The results reported in this chapter and in **Chapter 7 - Latency of Neck muscle response and Head displacement during Dynamic Loading** show that tensing the neck muscles, bracing for impact does not affect the peak moment generated at C4 by the excursion of the head. Nor does awareness affect the timing for initiating muscle activation in response to a perturbation. The role of awareness from the perspective of latency of muscle activation and displacement is discussed in detail in Chapter 7.

The role of awareness for adults and its effect on the forces and moments generated in the muscles of the neck, is not consistent in all studies. Kumar et al. [2003] found that subjects who were aware of the impact had lower head acceleration and showed earlier muscle activation than subjects who were

unaware prior to impact. Kuramochi et al., [1996] found no significant difference between the peak head acceleration of subjects aware of a coming head perturbation and those who were not. However, their study showed that subjects who were aware responded to the perturbation sooner than those who were not, similar to the EMG latency results that Kumar et al. reported. The results of studies by Siegmund et al. [2003], Magnussen et al. [1999] and Mertz and Patrick [1971] show that the role of awareness is not a factor affecting the acceleration or moment of the head in response to an impact. The results of this study showed that the extension moment due to the swing's release was significantly smaller when the subject was aware of the coming impact than when he was unaware and relaxed ($p < 0.05$).

The acceleration pulse of the swing produced both flexion and extension moments. For the 50th percentile males subjects, the extension moment at C4, in response to the swing's release was $M_{\text{ext}(u)} = -22.1 \pm 4.3 \text{ Nm}$ for the untensed muscle impact and $M_{\text{ext}(t)} = -18.6 \pm 2.3 \text{ Nm}$ for the tensed muscle impact. Van den Kroonenberg et al. [1998] reported similar moments at the occipital condyle in their whiplash study. The average extension moment reported in their whiplash study was 25Nm at the occipital condyle for a rear impact of a 9.5km/h Δv . Relative to the occipital condyle, the moments reported in this study would be reduced. Since this acceleration from this study was directed in the +Gx direction instead of the -Gx as was the case in the van den Kroonenberg study, a lower extension was expected. A flexion moment was generated at C4, in response to the peak swing acceleration. For the 50th percentile adult males in this study, the

flexion moments were $M_{\text{flex}(u)} = 20.3 \pm 5.0 \text{ Nm}$ for the untensed muscle impact and $M_{\text{flex}(t)} = 27.1 \pm 8.8 \text{ Nm}$. These results are similar to those reported by Mertz and Patrick [1971] in their study on the strength and response of the human neck in a +Gx direction. For sled accelerations ranging from 2.9-3.3g's the flexion moment at the occipital condyle of a helmeted subject with relaxed muscles ranged from 11.66Nm to 13.287Nm. For the same subject with tensed muscles, the flexion moment at the occipital condyles ranged from 12.20Nm to 14.19Nm for the same range in acceleration. The moments in this study are higher due to the different location at which the moments are calculated – the influence of the moment arm from the CG to C4 causes a larger total moment.

The flexion moment in the tensed muscle impact was significantly greater than that of the untensed muscle impact ($p < 0.05$). While this result seems to be counter-intuitive, the high speed video shows that in the untensed muscle condition, unlike the tensed muscle condition, there is a large head displacement in the $-x$ -direction. At the point of maximum swing acceleration, the energy of the head, due to the larger extension moment and larger head displacement must be overcome. In response to the swing's peak acceleration, the change in direction of the head may cause the reduction in the head's acceleration. In the tensed muscle condition, the extension moment is reduced due to the existing muscle tension. At impact, the energy of the head is in the direction of the swing acceleration resulting in a larger moment. Unlike the results of the 50th percentile adult male subjects, there is no difference for either the extension moments or the flexion moments between the tensed and untensed muscle conditions. The

moments in extension were, $M_{\text{ext}(u)} = -11.5 \pm 6.3 \text{ Nm}$ in the untensed muscle condition and $M_{\text{ext}(t)} = -7.5 \pm 1.2 \text{ Nm}$ in the tensed muscle condition. Similarly, the moments generated in flexion were $M_{\text{flex}(u)} = 12.6 \pm 2.9 \text{ Nm}$ for the untensed muscle condition and $M_{\text{flex}(t)} = 10.4 \pm 2.2 \text{ Nm}$. This is consistent with the results of the Grosset et al. [2008] and Lambertz [2003] studies, in which they concluded that due to the immaturity of the central neural pathways of muscle activation, pre-pubescent children are unable to fully activate their muscles, nor are they able to maintain a prescribed moment. The study by Grosset et al. [2008] based their conclusion on the lower neuromuscular efficiency (NME_{max}) of the muscle contraction. The NME_{max} , shown in equation (5-24) in **Chapter 5 - Determination of Neck Muscle Force and Stress at C-4 Vertebrae During a Maximal Voluntary Contraction**, is defined as

$$NME_{\text{max}} = \frac{\text{Moment}_{\text{max}} (\text{Nm})}{\text{normalized} - EMG_{\text{max}} (\%)} \quad [\text{Grosset, 2008}] \quad (5-24)$$

Calculating the NME_{max} will enable a comparison of the results between adults and children, even though the test accelerations differed between subject groups. Using the values of peak extension and flexion moments, and the %MVC values for the SCM in extension and posterior muscles in flexion, the NME values were calculated. The %MVC value of the SCM was used in extension, since its peak activation was in response to the extension moment. Similarly, the %MVC of the posterior muscles was used, since their activation was in response to the flexion moment. The activation of the postero-lateral and scalene muscles

showed no specific time to activation pattern. The values of peak EMG and %MVC for the SCM and posterior muscles are shown in Tables 6-4 and 6-5. For the 10-year old male subjects, average values of peak EMG for the SCM and posterior muscles during the untensed muscle impact ranged from 195.2+/-99.4 μ V to 240.5+/-122.2 μ V (1.1+/-0.4 %MVC to 1.6+/-1.1 %MVC) for the SCM, and from 84.4+/-42.3 μ V to 106.6+/-88.5 μ V (1.2+/-0.5 %MVC to 1.4+/-1.0 %MVC) for the posterior muscles. For the tensed muscle impact, peak EMG values ranged from 195.3+/-89.0 μ V to 206.4+/-102.9 μ V (1.1+/-0.4 %MVC to 1.4+/-1.0 %MVC) for the SCM and 94.0+/-38.1 μ V to 100.6+/-87.6 μ V (1.2+/-0.6 %MVC to 1.390+/-0.907 %MVC) for the posterior muscles. For the 50th percentile adult males, the peak EMG values during the untensed muscle impact ranged from 182.3+/-98.5 μ V to 193.1+/-118.6 μ V (1.4+/-0.7 %MVC to 1.6+/-0.7 %MVC) for the SCM and 42.8+/-23.9 μ V to 60.1+/-61.7 μ V (2.0+/-0.10 %MVC to 2.3+/-1.7 %MVC) for the posterior muscles. During the tensed muscle impact, the peak EMG values for the SCM ranged from 195.9+/-99.4 μ V to 206.1+/-93.7 μ V (131.9+/-57.1 %MVC to 187.7+/-108.3 %MVC) and for the posterior muscles peak EMG values ranged from 35.9+/-20.8 μ V to 59.1+/-49.4 μ V (155.6+/-0.790 %MVC to 220.6+/-146.3 %MVC). There was no significant difference between the peak EMG values of the adult male and 10-year male subjects, in spite of the increased swing acceleration for the adult male subjects. The greater than 100% MVC values for the dynamic event is similar to results reported by Kumar et al., [2003] where values of 179% MVC were reported for the trapezius muscle in a 1.5g frontal impact. Szabo et al. [1996] also reported values greater than 100%

MVC in their low speed rear impact study. Their study reported %MVC values of over 200% for the trapezius muscle. Values of %MVC may be attributed to the muscle lengthening during an eccentric muscle contraction, as suggested by Loeb and Gans [1986].

The calculated values for NME_{max} , shown below in Table 6-8, are similar to the NME_{max} values of Chapter 5. The 50th percentile adult male subjects have a higher muscle contraction efficiency than the 10-year old male subjects ($p < 0.05$). There was no difference between the efficiency of the tensed and untensed muscle impacts for either subject group.

10 Year Old Boys

(a)	Tensed Muscle Condition						Untensed Muscle Condition					
	Peak Moment (Nm)		Max %MVC		NME _{max}		Peak Moment (Nm)		Max %MVC		NME _{max}	
	Ext	Flex	SCM	Post	Ext	Flex	Ext	Flex	SCM	Post	Ext	Flex
K01	-6.8	9.6	1.0	1.5	6.6	6.4	-8.0	9.5	1.0	1.5	7.6	6.4
K03	-8.6	9.0	1.3	0.8	6.7	11.6	-9.5	9.8	0.7	0.9	12.9	11.2
K04	-7.3	13.8	1.7	1.1	4.3	12.4	-17.4	15.7	1.8	1.8	9.5	8.7
K05	-9.8	12.3	0.9	1.3	11.5	9.4	No Data Available					
K06	-8.4	10.0	0.4	1.8	20.6	5.5	-8.1	15.2	0.7	0.6	11.8	25.1
K07	-6.6	7.4	0.9	0.9	7.3	8.1	No Data Available					
K09	-6.9	13.1	1.4	1.4	5.0	9.2	-9.6	15.5	1.6	1.1	6.0	13.6
K10	-6.1	9.5	1.4	1.1	4.5	8.3	-7.2	10.0	1.1	0.7	6.6	14.2
K11	-7.2	8.7	0.9	1.2	8.0	7.3	-7.2	12.6	1.2	0.9	6.0	13.5
Mean	-7.5	10.4	1.1	1.2	8.3	8.7	-9.6	12.6	1.2	1.1	8.6	13.2
St. Dev.	1.2	2.2	0.4	0.3	5.1	2.3	3.6	2.9	0.4	0.4	2.8	6.0

50th Percentile Adult Males

(b)	Tensed Muscle Condition						Untensed Muscle Condition					
	Peak Moment (Nm)		Max %MVC		NME _{max}		Peak Moment (Nm)		Max %MVC		NME _{max}	
	Ext	Flex	SCM	Post	Ext	Flex	Ext	Flex	SCM	Post	Ext	Flex
S13	-20.7	28.4	1.1	0.7	19.1	38.4	-19.4	15.5	1.5	1.0	13.1	14.8
S14	-21.8	26.5	1.2	1.1	18.8	25.0	-27.2	26.4	1.5	1.1	17.8	24.8
S15	-19.4	18.4	0.5	1.5	35.6	12.3	-17.0	15.3	0.6	1.7	27.5	9.1
S16	-17.1	23.0	2.3	2.3	7.6	10.1	-21.2	20.4	1.5	1.5	14.2	13.5
S17	-18.9	45.6	1.9	1.0	9.7	44.7	-25.8	24.0	2.1	1.2	12.3	19.4
S20	-16.5	23.4	1.1	1.4	14.6	16.6	No Data Available					
Mean	-19.1	27.5	1.4	1.3	17.6	24.5	-22.1	20.3	1.4	1.3	17.0	16.3
St. Dev.	2.0	9.5	0.6	0.5	10.0	14.3	4.3	5.0	0.5	0.3	6.3	6.0

Table 6-8: Results of the dynamic neuromuscular efficiency for the 10-year old male and 50th percentile males based on the Grosset et al. [2008] relationship. Efficiency in tensed muscle extension and flexion and untensed muscle extension was significantly greater for adult males than boys ($p < 0.05$).

The results of the efficiency calculation are further support to the hypothesis that the 10-year old boys are unable to fully activate their muscle in response to an applied moment.

6.5 CONCLUSIONS

The moments generated at C4 during a low speed dynamic event for a 50th percentile adult male are consistent with the moment values reported in the literature. For the 10-year old boys, this study is the first to evaluate the moments generated in the neck during a dynamic event. The results of this study show that the awareness of the adult prior to impact affects the moment generated in the neck. Adults tensing their muscles in preparation for impact had a significantly lower extension moment ($p<0.05$) and higher flexion moment ($p<0.05$) than when they were relaxed and unaware of the impact. For the 10-year old boys, there was no difference between the moments generated in the tensed and untensed muscle impacts. In spite of this difference in response, both the adult males and the 10-year boys showed a similar muscle activation pattern - the peak activation of the SCM occurred in response to the extension moment in both test conditions, while the peak activation of the posterior muscles occurred in response to the flexion moment in both test conditions.

The results of this dynamic moment study are also consistent with the findings of Chapter 5 - in dynamic loading conditions, like static loading conditions, children are significantly less efficient in generating muscle force than adults ($p<0.05$).

CHAPTER 7 LATENCY OF NECK MUSCLE RESPONSE AND HEAD DISPLACEMENT DURING DYNAMIC LOADING

7.1 INTRODUCTION

Muscle activation is facilitated through a variety of neural strategies involving both the central and peripheral nervous system. Measurements of muscle response times provide information not only on these muscle activation strategies but also on neuromuscular development and neuromuscular disorders. Head displacement and the magnitude of the moment of the head for a given speed are regulated by the cervical and thoracic spinal muscles ability to respond to an applied load. Latency is the time it takes for the muscle to activate in response to the applied load..

There are several motor-neural pathways through which a muscle is stimulated, including the stretch-reflex [Snyder, 1975; Grosset, 2008; Baker, 2009], the startle reflex, and vestibular-collic response [Ito, 1997; Kuramochi, 2004; Siegmund, 2007]. Each neural pathway has a different response timing [Vander, 1990] which depends on the mechanism of stimulation. The stretch reflex is a spinal reflex. Muscle response is stimulated by the stretching of the spindle fiber embedded in the muscle, or by the speed at which that spindle fiber is stretched [Vander, 1990]. Vestibular-collic response is stimulated by the vestibular organs – the inner ear. Vestibular-collic stimulation occurs in the neck muscles, generally in response to the onset of head acceleration [Szabo, 1996; Ito, 1997; Kuramochi, 2004]. The neural-response pathway is affected by the

position of the subject and the type and perturbation. Horak et al. [1994] showed in their study that EMG neck response amplitudes differed between a direct hit to the head, and head motion due to platform movement even though the induced head motion was the same.

Muscle response may be stimulated by one or a combination of neural regulatory strategies. In their 1997 study, Ito et al., concluded that neck muscle response was due to a combination of stretch reflex and vestibular-collic response. Their study compared the active and passive head-righting responses of healthy adults to labyrinthine-defective (LD) subjects in a head drop test. In healthy subjects, response time (24.5ms) was significantly sooner than in the LD subjects (67.4ms). Since the inner ear of LD subjects is affected, their response was attributed to only a stretch reflex response, while the healthy adult subject response time was attributed to a combination of the vestibular colic reflex acting first, followed by the stretch reflex. Voluntary response was not initiated until 100ms. In a similar study by Kuramochi et al. [2004], neck muscle response was determined by a direct perturbation of the head (ball-drop). The subjects were tested in both aware and unaware test conditions. Their findings indicate the stretch response is reduced ($p < 0.05$) when the subject is aware of the coming blow. There was no difference in the vestibular-collic response. In a 1996 rear impact vehicle-to-vehicle impact study using human volunteers, Szabo et al., found that the muscle activity onset occurred in various parts of the body at the same time, coinciding with the onset of head acceleration. Although their study did not specifically examine the neural pathways of muscle response, they

surmised that the response was due to a centrally (CNS) generated mechanism, not a stretch reflex, although they conceded that a stretch response may play a role later in the event. In their study, full muscle tension did not develop until 60-70ms after onset of muscle activity.

In children, the role of awareness in impact testing, the latency of muscle response and the neural pathways involved in these responses have not been tested. Grosset et al. [2008] tested the change in stretch reflex with age and tissue stiffness. They used a tendon jerk to elicit response. Their study found an increase in reflex response with age. The findings of their study correlate with the results of the recent low-speed, frontal impact sled test study by Arbogast et al. [2009], which compared the normalized displacements of the head, cervical and thoracic spine and the pelvis of children to that of adults. The studies showed that normalized displacement decreases with increasing age. Studies of the developmental changes of the cervical spine have shown that children have lower tensile and bending stiffness of the cervical spine than adults [Nuckley et al., 2005; Ouyang, 2005; Nuckley and Ching, 2006]. Arbogast et al. concluded that increased stiffness in adult tissues was one of the contributing factors to the lower displacement values of the adult subjects.

Given the continued high rate of fatal and non-fatal head injuries in children involved in motor vehicle accidents, biofidelic human surrogates of children are important. Head displacement is a simple, effective method of assessing the kinematics of the head, cervical, thoracic and lumbar spine. In an early study, Wismans and Maltha [1979] showed a significant difference in the

head excursion of a child cadaver (37cm) matched for weight and size to a child surrogate (29cm). Cassan et al. [1993] found similar results in their 1994 study comparing the 3-year old ATD to child cadavers matched for weight and size and restrained in child restraint systems. The cadavers showed high displacements in both the x- and z-directions.

This portion of the study was conducted in tandem with the dynamic study. The purpose of this portion of the study was to determine if there was a difference in neural regulatory strategies in children by comparing latency of muscle response and head excursion in a dynamic tensed and untensed muscle condition to the responses of adults similarly tested.

7.2 METHODOLOGY

7.2.1 Test Set-up

Latency of muscle response was determined from the EMG and acceleration data collected during the dynamic study. Head displacement was evaluated using the high speed video captured during the same study. Details of the test set-up, execution, and data processing are discussed in **Chapter 6 - The Neck Muscle Responses of 50TH Percentile Adult Males and 10 Year Old Boys in Low Speed Frontal Impacts.**

7.2.2 Data Analysis

7.2.2.1 Latency of Muscle Response

The latency of muscle response was calculated from the filtered, rectified electromyography (EMG) data collected during the tensed and untensed dynamic impact events described in Chapter 6 - **The Neck Muscle Responses of 50TH Percentile Adult Males and 10 Year Old Boys in Low Speed Frontal Impacts**. The digitized, un-rectified EMG data collected during the tensed and untensed impact events was band-pass filtered with a frequency range of 10-1000Hz [Forssberg et al., 1994] using LabVIEW. Latency in this study was calculated at two instances in the dynamic event – 1) initial muscle response, which corresponds to the start of swing motion, and 2) muscle response to peak swing acceleration. The time of the onset of sustained muscle activity above the baseline signal was determined by visual inspection [Forssberg et al., 1994; Siegmund et al., 2008] from the EMG traces displayed in LabVIEW. Latency relative to the peak swing acceleration was also determined by visual inspection and corresponded to the onset of the first EMG peak (either maximum or minimum since the signal was unrectified) after maximum swing acceleration as determined from the swing's acceleration trace (Figure 7-1).

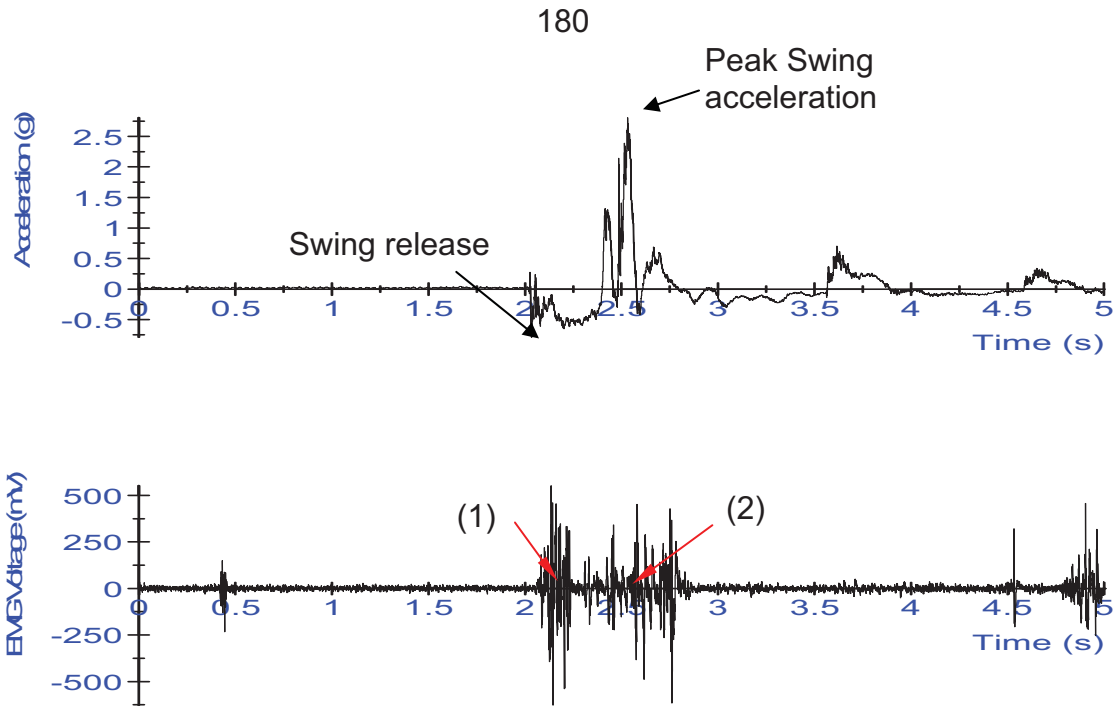


Figure 7-1: Swing pulse and EMG activation trace for SCM showing the two instances where latency was calculated – (1) response to swing release and (2) response to peak swing acceleration.

Latency was calculated according to,

$$L = (t_{swing} - t_{EMG, onset}) * 1000 ms / s \quad 7-1$$

Where t_{swing} represents either the time of swing release or the time of peak swing acceleration depending on which calculation is being carried out. Latency calculations were carried out at two distinct times to determine which of the neural pathways described above (i.e. a central pattern generator, vestibular collic, or a combination of these) were responsible for triggering the muscles' response to the perturbations. LabVIEW was used to determine the time of swing release, peak swing acceleration, and the EMG onset times. For the swing,

$$t_{swing} \text{ (in seconds)} = (\text{sample\# of release/peak}) / 10,000\text{Hz} \quad 7-2$$

Acceleration data was sampled at 10,000Hz. Similarly, for EMG

$$t_{EMG} \text{ (in seconds)} = (\text{sample\# of EMG onset at release/peak})/5000\text{Hz} \quad 7-3$$

EMG data was sampled at 5000Hz.

7.2.2.2 Head Displacement

A single high-speed camera, set perpendicular to the direction of the swing's arc was used to record the impact event. Video data was recorded at 1000 frames/second. A marker was placed on the headphones the subjects wore during testing. This approximated the center of gravity of the head. See Chapter 6 for a full description of measurement of the CG of the head. The marker was a two inch square with alternating black and white one-inch squares. Using Image J, the NIH freeware software, the x- and z-pixel coordinates of the head and the x-pixel coordinate of the swing were recorded every 0.01 seconds from the time of the swing's first contact with the shock absorber until its release. Measurements in Image J are based on a 640x480 pixel grid. Each pixel is located on the grid using (x,z) coordinates – the x and z axes correspond to the body coordinate system shown in figure 7-2.

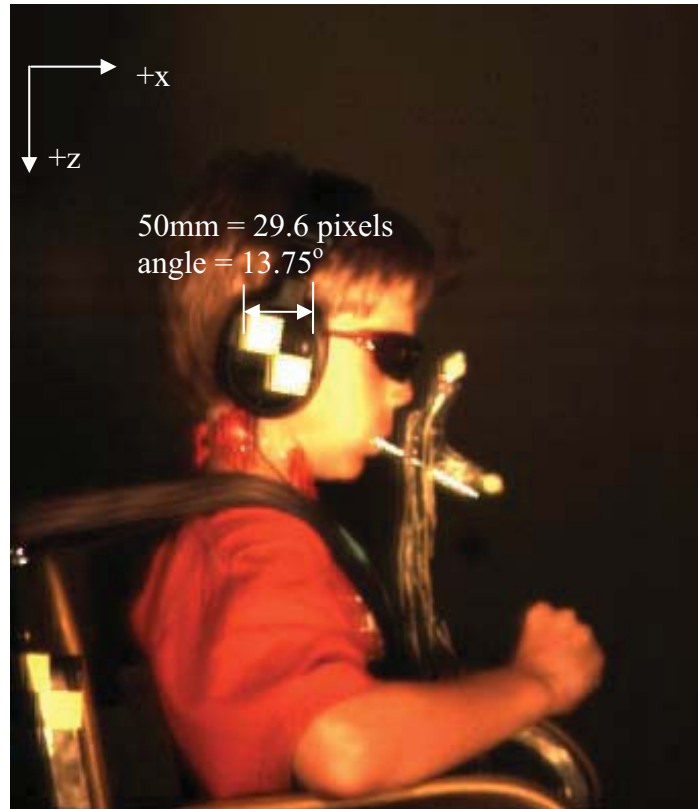


Figure 7-2: Positive direction of the coordinate system of video image used for measuring head displacement. The measurement shows the calibration of distance measurements.

On the video, the 1x1 inch black and white squares corresponded to a measured number of pixels (shown above in Figure 7-2). The calibration measurements for all subjects are shown below in Table 7-1.

Subject	Calibration Measurement (pixel/mm)	Subject	Calibration Measurement (in/pixel)
K01	0.59	S14	0.59
K03	0.47	S15	0.59
K04	0.47	S16	0.59
K05	0.47	S17	0.59
K06	0.47	S18	0.60
K07	0.47	S20	0.47
K09	0.47		
K10	0.47		
K11	0.47		

Table 7-1: Measurements of the head marker from the calibration shot of the high speed video camera.

The maximum head excursion during both the tensed and untensed dynamic events were determined using video analysis. Image J, and Motion Central v.3.0.8.0, by Redlake MASD Inc. were used to do the analysis. The video data was first viewed using Motion Central to determine the period of the start of impact - the time at which the swing makes initial contact with the shock absorbers - until the time at which the shock absorbers are completely re-extended. Timing of both initial shock absorber contact and the subsequent shock absorber re-extension was determined through visual inspection. The video data was analyzed frame by frame, initial contact was the frame prior to shock absorber compression when no gap between the swing frame and the black end of the shock absorber was visible. Similarly, the point at which the shock absorbers were considered to be fully re-extended was the frame prior to the reappearance of a gap between the swing frame and the black end of the shock absorber (Figure 7-3).

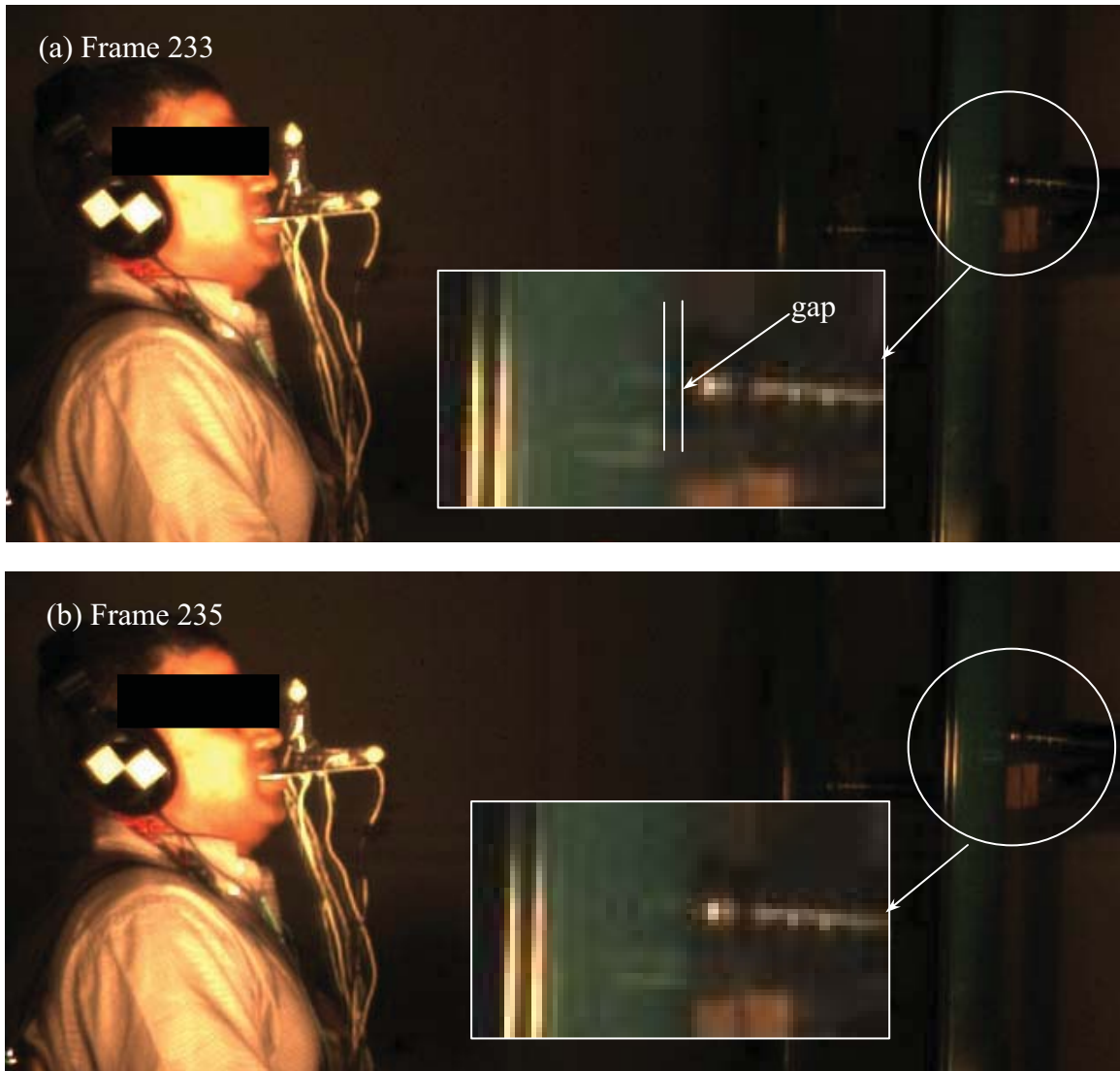


Figure 7-3: Timing of shock absorber contact – (a) Frame 233 ($t=464\text{ms}$) shows a gap between the shock absorber and the swing frame. (b) Frame 235 ($t=468\text{ms}$), no gap remains. Figure 7-3 (b) shows what was considered to be initial swing contact with the shock absorber.

The x- and z-displacements of the head were calculated according to the formulae shown below.

$$Displ_x = x_i + (dx_i - dswing_i) \quad 7-4$$

$$Displ_z = z_i + dz_i \quad 7-5$$

Where

$Displ_x$ = total head displacement in x-direction

$Displ_z$ = total head displacement in the z-direction

$dx, dz, dswing$ = incremental position change between frames

The displacement values were converted to mm using the calibration values shown in Table 7-1. Displacement was normalized to the seated erect height of each subject. This measurement was taken prior to the first dynamic test and was taken from the top of the seat cushion to the top of the head.

In addition to measuring head displacement, the video data was analyzed to determine if there was any displacement of the 3-2-2-2 accelerometer mount and any motion of the head marker during the impact event. Displacement of the head marker relative to the forehead was determined by measuring the distance between the forehead of the subject and the center of the head marker 1) prior to the impact, 2) at the point of initial impact, 3) at the point of maximum head excursion, 4) at the initiation of swing rebound and 5) at the point of complete swing release from the shock absorber. Similarly, the displacement of the top of the z-arm of the 3-2-2-2 accelerometer mount was measured relative to the forehead for the same five instances. These distances were determined using

Image J.

7.2.3 Statistical Analysis

Student's t tests were used to compare the difference in muscle response time between the tensed and untensed dynamic test conditions within each subject group, as well as between subject groups. The same statistical analysis was applied to head displacement.

7.3 RESULTS

7.3.1 Latency

The time to muscle response (latency) was calculated from 1) the time of onset of swing acceleration and 2) the time of peak swing acceleration (the time of maximum shock absorber compression) for both the adult and child subject groups. Comparisons were made between the tensed and untensed dynamic conditions within each group. Since the crash pulses differed between subject groups, only the latency of muscle activation for the tensed and untensed muscle conditions at the time of swing release was compared between adults and child subject groups.

Figure 7-4 shows a comparison between the EMG traces of the right side muscles in 10-year old boys. In figure 7-4(a), the muscle activity prior to the swing's release shows the subjects were tensing their muscles in preparation for impact. The same is shown for the adults in Figure 7-5(a). The muscle activity due to tensing prior to swing release was not considered when determining

latency – only the muscle activity after swing release was deemed relevant.

Latency results for the 10 year old male subjects showed that there was no significant difference in the activation times of the muscles in this study in either the tensed or untensed muscle impact conditions. Nor was there a significant difference in the time to muscle activation between the tensed and untensed muscle impact conditions with the exception of the SPL which showed an increase in time to muscle activation during the untensed muscle impact condition ($p < 0.05$). During the tensed muscle impact condition $L_{spl,T} = 82.1 \pm 16.9$ ms while in the untensed muscle impact condition $L_{spl,U} = 92.4 \pm 18.8$ ms. Latency results for all muscles at swing release for both muscle conditions are shown in Table 7-2. Average latency values for the remaining muscles for the 10-year old male subject group were, $L_{scm,T} = 85.9 \pm 13.6$ ms, $L_{trap,T} = 90.0 \pm 49.7$ ms, and $L_{scal,T} = 81.2 \pm 20.69$ ms for the tensed muscle condition. Average latency values for the untensed muscle condition were $L_{scm,U} = 90.6 \pm 14.9$ ms, $L_{trap,U} = 84.5 \pm 21.7$ ms and $L_{scal,U} = 91.2 \pm 21.9$ ms.

In response to peak swing acceleration (Table 7-3) in the tensed muscle condition, the TRAP, SPL and SCAL responded at similar times $L_{trap,T} = 20.0 \pm 9.9$ ms, $L_{spl,T} = 21.0 \pm 11.9$ ms, and $L_{scal,T} = 23.2 \pm 12.9$ ms. In the untensed condition the trapezius responded sooner than the other muscles ($p < 0.05$) with a latency of $L_{trap,U} = 23.0 \pm 12.5$ ms.

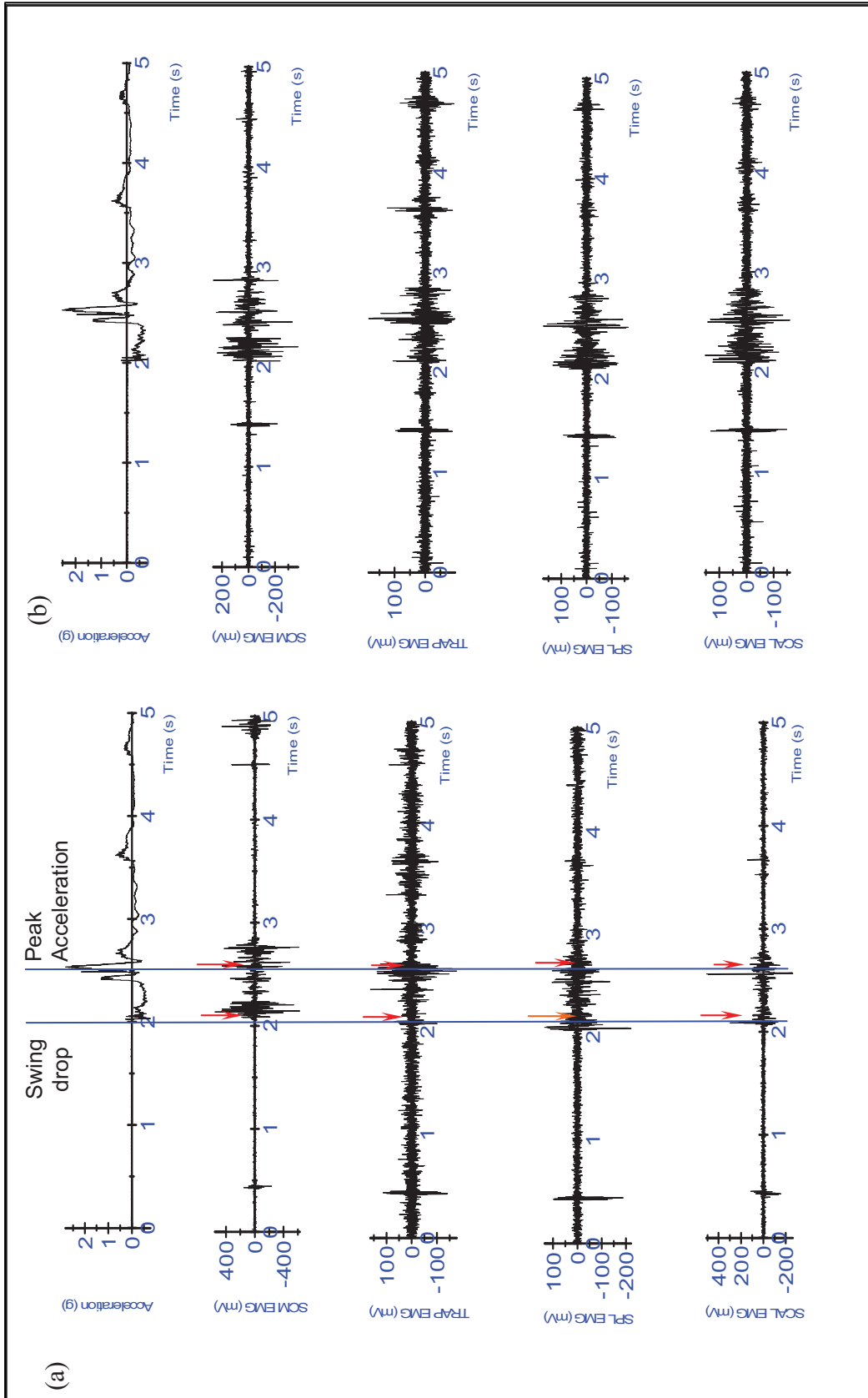


Figure 7-4: Acceleration pulse and EMG traces for the right-side muscles in (a) tensed and (b) untensed muscle dynamic tests for 10-year old male subject. Arrows indicate the time of EMG onset for (1) swing release and (2) peak acceleration. Latency values are shown in tables 7-2 and 7-3 respectively.

Subject	Trial	a) Tensed Muscle Dynamic Condition - Latency (ms)							
		SCM (R)	SCM (L)	TRAP(R)	TRAP(L)	SPL(R)	SPL(L)	SCAL (R)	SCAL (L)
K01	1	79.1	79.6	87.6	76.5	82.7	85.8	82.2	85.3
	2	92.0	94.2	93.4	83.8	98.0	93.1	92.3	85.0
K03	1	No data available							
	2	82.6	76.8	75.0	78.2	66.8	71.4	82.0	72.0
	3	90.2	85.7	85.1	75.5	85.1	80.5	84.1	75.0
K04	1	95.6	97.7	56.5	49.2	100.5	44.2	97.3	97.8
	2	95.8	96.0	47.7	57.6	90.2	85.1	118.2	113.6
K05	1	92.6	88.4	112.7	88.2	105.6	79.0	79.1	84.2
	2	58.3	65.8	67.1	33.3	54.4	81.1	84.1	29.4
K06	1	89.6	87.8	85.8	101.3	82.4	81.0	74.3	78.0
	2	92.1	77.7	No Data	75.1	79.8	74.0	114.1	31.8
K07	2	83.6	79.3	49.1	90.8	47.1	77.8	83.1	No
	3	78.2	77.4	89.0	89.6	88.2	79.0	83.1	Data
K08	1	80.7	77.4	80.0	80.1	69.2	76.4	71.4	82.5
	2	84.9	86.1	98.8	95.8	87.0	83.4	87.7	89.2
K09	1	50.9	52.3	45.1	46.4	51.7	51.9	56.5	53.3
	2	97.2	89.7	99.6	92.0	95.8	97.2	39.2	100.3
K10	1	120.0	113.0	No Data	114.7	126.8	107.1	117.9	82.4
	2	87.1	98.4	92.9	100.8	85.2	88.5	78.7	97.4
	2	84.0	85.0	93.0	No Data	68.5	95.4	67.3	53.6
Mean (L/R)		86.6	85.3	79.9	79.1	82.6	81.5	84.7	77.3
St. Dev (L/R)		14.32	13.12	20.13	20.56	19.21	14.61	19.35	22.46
Subject	Trial	b) Untensed Muscle Dynamic Condition - Latency (ms)							
		SCM (R)	SCM (L)	TRAP (R)	TRAP (L)	SPL(R)	SPL(L)	SCAL (R)	SCAL (L)
K01	1	85.5	89.3	104.9	92.5	98.5	90.5	97.7	98.7
	2	86.2	90.7	96.2	102.1	86.7	89.6	95.1	102.7
K03	1	63.6	107.1	109.5	94.0	94.1	92.9	105.9	93.2
	2	92.5	103.8	34.2	95.6	120.7	93.0	103.7	91.8
	3	93.2	60.3	60.5	61.7	61.2	61.2	63.0	61.0
K04	1	101.6	100.8	101.6	101.6	105.1	97.9	103.5	118.7
	2	88.4	95.8	105.9	92.4	42.3	92.8	105.1	95.4
K05	1	80.3	80.8	84.9	80.5	82.2	72.3	79.9	72.3
	2	No data available							
K06	1	111.0	103.2	71.9	98.8	100.0	105.9	101.9	97.9
	2	116.1	109.3	61.2	92.8	115.4	89.5	109.8	130.6
K08	1	77.3	78.0	85.1	87.1	80.3	82.5	81.7	82.4
	2	77.4	76.9	77.1	82.5	70.9	76.6	75.5	90.8
K09	1	62.6	67.5	96.6	35.2	90.2	78.2	16.3	80.5
	2	99.3	103.4	109.0	38.7	105.0	121.2	39.6	117.4
K10	1	116.2	109.8	38.6	116.4	123.6	133.7	119.7	99.8
	2	97.0	100.3	91.8	82.5	109.3	96.6	101.9	92.9
K11	1	84.3	80.8	91.7	77.3	108.4	88.3	101.9	79.8
	2	86.5	83.6	102.6	86.4	86.2	84.7	91.2	85.6
Mean (L/R)		89.9	91.2	84.6	84.3	93.3	91.5	88.5	94.0
St. Dev (L/R)		15.41	14.85	23.10	20.83	21.03	16.76	26.21	16.83

Table 7-2: Latency of a) tensed and b) untensed muscles under dynamic test conditions for 10-year old boys from time of swing release. Tests showing **no data**, indicates complete tests or data channels where changes in EMG activation could not be determined either due to noise or the EMG electrodes falling off during testing.

Subject	Trial	Latency -Tensed Muscle Condition (ms)				Latency -Untensed Muscle Condition (ms)			
		SCM	TRAP	SPL	SCAL	SCM	TRAP	SPL	SCAL
K01	1	88.2	21.3	27.3	10.2	33.0	49.7	112.3	57.6
		13.6	19.9	13.9	18.5	27.7	23.6	27.9	29.7
K03	1	37.7	29.1	5.6	24.2	13.9	5.2	14.0	6.2
	2	14.5	8.7	5.2	21.9	25.7	25.7	10.0	22.9
K04	1	18.5	18.0	13.3	15.4	6.1	37.0	44.6	28.0
	2	41.7	10.3	35.5	20.7	24.0	30.9	9.8	22.8
K05	1	12.4	21.7	16.3	15.8	27.0	11.5	24.9	24.8
	2	55.3	7.9	15.8	14.7	No Data Available			
K06	1	44.1	33.8	29.7	27.3	24.9	42.7	29.0	6.8
	2	21.5	35.9	14.2	22.1	62.8	13.8	17.9	19.8
K08	1	24.2	9.3	31.4	23.1	23.4	28.8	18.8	38.4
	2	60.1	9.5	46.5	54.1	22.4	24.5	20.5	59.5
K09	1	14.7	25.7	32.0	17.5	62.6	19.3	45.2	51.9
	2	13.5	17.5	36.3	55.9	13.1	29.5	49.7	28.2
K10	1	17.0	9.4	8.1	10.7	24.6	11.8	12.1	14.4
	2	12.2	33.8	10.7	11.9	25.5	15.5	15.1	17.4
K11	1	45.2	32.7	19.8	31.8	22.2	9.9	23.7	13.3
	2	32.4	15.4	17.1	22.4	23.4	10.9	24.9	10.4

Mean 31.5 20.0 21.0 23.2 27.2 23.0 29.4 26.6

St. Dev 21.1 9.9 11.9 12.9 14.7 12.5 24.6 16.6

Table 7-3: Latency of muscle activation in response to peak swing acceleration in the tensed and untensed muscle conditions for the 10-year old male subject group. The table shows results for only the right side since, as shown in Tables 7-2 (a) and (b) there is no significant difference between the response times of the left and right sides.

The adults showed no difference between the onsets of muscle activity in response to the swing drop regardless of the subject's awareness. Nor was there any significant difference in latency of the onset of muscle activity between the adult male and 10-year old male subject groups, regardless of the subject's awareness. In the tensed muscle condition (subject aware of the time to swing drop) for adult males, average muscle activity onset was $L_{A,T} = 84.9 \pm 33.7$ ms and for 10-year old males, average muscle activity onset was $L_{C,T} = 84.8 \pm 28.7$ ms. Similarly, for the untensed muscle condition (subject unaware of the time

to swing drop), the average time to onset of muscle activity in adults was $L_{A,U} = 84.7 \pm 33.65$ ms, while the average time to onset of muscle activity for the 10-year old males $L_{C,U} = 89.68 \pm 19.56$ ms. The only exception was the SCM which showed a significantly ($p < 0.05$) earlier response time in adults during the untensed muscle impact condition.

Figure 7-5 shows the swing pulse and EMG activation traces for the right-side muscles for the tensed and untensed muscle dynamic test conditions for the adults tested.

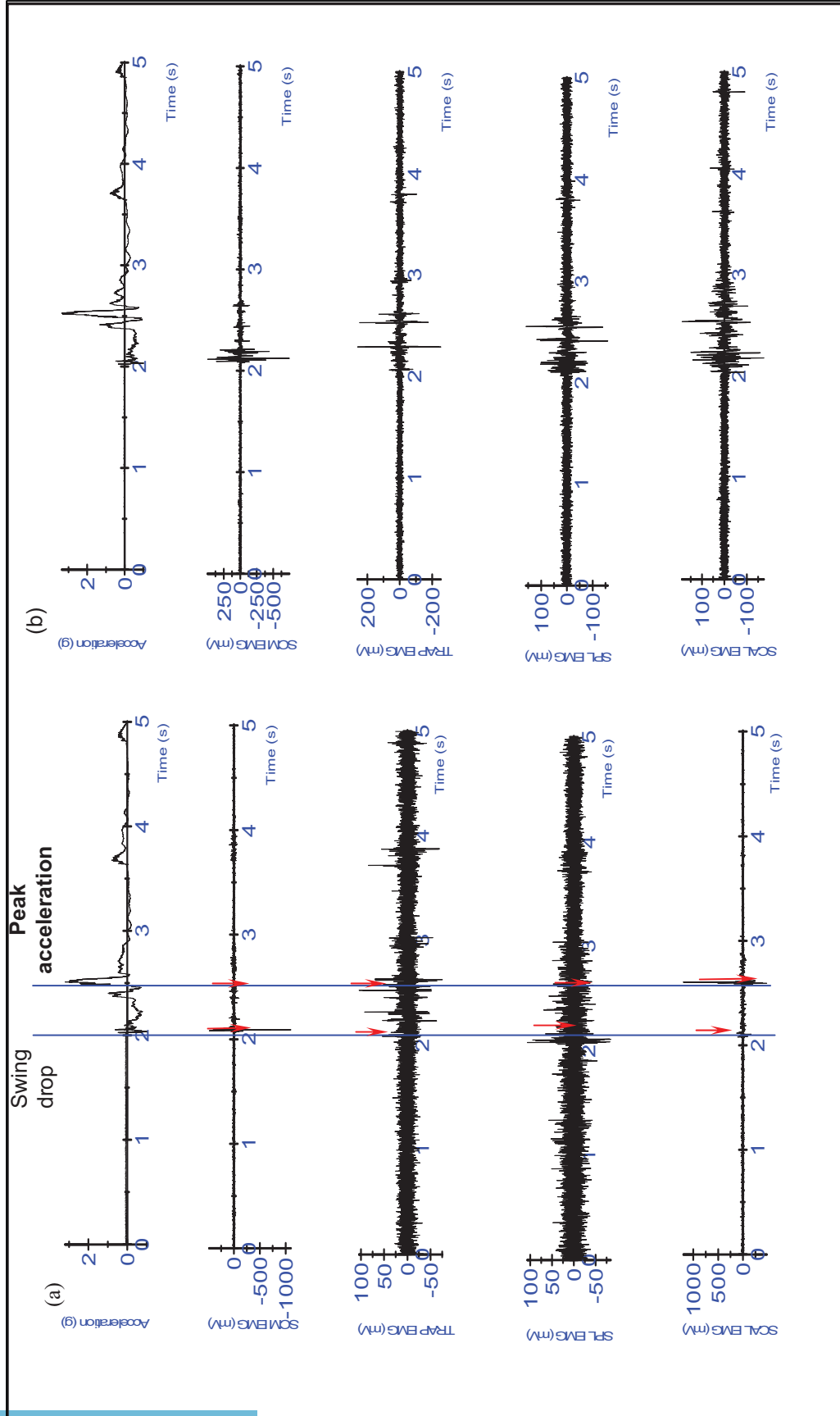


Figure 7-5: Acceleration pulse and EMG traces for the right-side muscles in (a) tensed and (b) untensed muscle dynamic tests for 50th percentile adult male subject. Arrows indicate the time of EMG onset for (1) swing release and (2) peak acceleration. Latency values are shown in tables 7-4 and 7-5 respectively.

Subject	Trial	a) Tensed Muscle Dynamic Condition - Latency (ms)							
		SCM (R)	SCM (L)	TRAP (R)	TRAP (L)	SPL (R)	SPL (L)	SCAL (R)	SCAL (L)
S13	1	106.1	101.2	123.3	76.3	97.0	77.2	81.3	78.3
	2	68.2	78.2	24.8	229.7	62.2	98.3	81.7	103.0
	3	105.5	107.4	115.9	89.2	115.2	80.0	99.0	90.3
S14	1	49.7	49.4	59.6	57.5	55.0	53.2	56.0	58.3
	2	151.9	141.3	107.4	143.7	111.1	101.8	130.4	137.9
	3	60.4	55.0	20.6	70.6	58.9	72.6	57.9	59.6
S15	1	62.7	35.4	37.5	28.8	31.0	21.0	63.5	38.9
	2	49.1	77.4	57.5	56.5	93.1	68.5	68.5	93.1
	3	52.3	81.5	114.7	55.1	85.2	56.4	69.4	42.5
S16	1	No data available							
	2	92.4	108.6	124.3	84.6	83.6	75.5	44.2	103.8
	3	89.3	83.6	78.3	111.4	151.1	126.9	95.7	73.8
S17	1	100.9	125.6	106.2	108.5	82.2	124.0	98.4	59.7
	2	No data available							
	3	115.8	114.2	56.7	96.4	53.4	124.7	54.8	25.8
S18	1	127.7	103.8	123.7	134.3	86.9	98.0	114.9	112.3
	2	77.5	109.6	121.6	97.4	95.2	69.4	119.6	119.6
	3	71.5	111.3	46.4	81.4	152.1	83.4	106.8	76.3
S20	1	35.8	69.3	78.8	72.8	86.0	85.0	69.3	79.3
	2	86.8	45.2	91.6	69.3	86.3	95.8	76.8	91.4
	3	78.7	84.5	32.8	215.4	30.1	89.3	16.6	77.3
Mean (L/R)		83.3	88.6	80.1	98.9	85.0	84.3	79.2	80.1
St. Dev (L/R)		29.88	28.85	37.08	51.64	33.18	26.22	28.50	28.74
Subject	Trial	b) Untensed Muscle Dynamic Condition - Latency (ms)							
		SCM (R)	SCM (L)	TRAP (R)	TRAP (L)	SPL (R)	SPL (L)	SCAL (R)	SCAL (L)
S13	1	108.2	103.0	123.3	129.8	110.8	103.5	90.9	92.7
	2	101.2	87.2	24.8	112.7	107.7	95.1	103.4	87.3
	3	81.3	84.5	115.9	101.5	92.5	82.5	73.2	80.3
S14	1	66.7	60.1	46.7	69.8	78.3	81.7	21.9	58.5
	2	57.7	57.9	87.9	71.4	41.4	64.5	68.2	67.9
	3	55.2	52.1	61.5	65.0	39.8	61.6	56.3	66.7
S15	1	71.0	75.5	51.9	82.0	53.1	90.5	94.6	71.8
	2	69.1	76.0	55.5	82.2	103.7	82.1	89.3	86.1
	3	73.7	70.4	85.9	0.0	84.1	119.1	95.9	98.6
S16	1	113.4	125.7	139.8	154.3	123.3	132.4	139.4	134.5
	2	104.6	102.0	82.3	89.0	111.3	116.1	103.6	54.5
	3	No data available							
S17	1	65.2	101.5	114.0	139.6	100.5	57.3	100.6	97.6
	2	63.3	103.6	82.6	104.5	100.8	68.1	91.4	107.5
	3	55.3	81.1	100.4	73.8	94.3	91.2	77.4	103.7
S18	1	92.4	68.4	105.2	102.0	84.9	80.2	81.0	77.8
	2	66.2	71.9	118.2	84.8	82.4	78.0	69.3	74.0
	3	64.7	88.8	81.9	82.7	85.5	83.7	76.5	89.8
S20	1	72.2	76.4	64.8	49.5	90.5	88.6	76.5	76.7
	2	62.9	73.7	132.2	74.3	107.2	84.0	73.4	64.4
	3	No data available							
Mean (L/R)		76.0	82.1	88.1	87.8	89.1	87.4	83.3	83.70
St. Dev (L/R)		18.60	18.61	31.71	34.10	23.03	19.61	23.53	19.48

Table 7-4: Latency of tensed and untensed muscle dynamic test conditions for 50th percentile adult males from time of swing release. Tests showing **no data**, indicates complete tests or data channels where changes in EMG activation could not be determined either due to noise or the EMG electrodes falling off during testing.

With respect to peak swing acceleration, the difference between the time to onset of muscle activity for the tensed and untensed muscle conditions for 50th percentile adult males was significant (Table 7-5) for all muscles except the SCM ($p < 0.05$). In the tensed muscle condition, the average time to muscle activity was $L_{trap,T} = 18.1 \pm 17.5$ ms, $L_{spl,T} = 19.9 \pm 13.9$ ms, and $L_{scal,T} = 19.0 \pm 16.2$ ms. In the untensed muscle condition, the time to muscle activity increased to $L_{trap,U} = 25.1 \pm 14.8$ ms, $L_{spl,U} = 29.4 \pm 19.6$ ms and $L_{scal,U} = 30.1 \pm 21.4$ ms.

Subject	Trial	Latency -Tensed Muscle Condition (ms)				Latency -Untensed Muscle Condition (ms)			
		SCM	TRAP	SPL	SCAL	SCM	TRAP	SPL	SCAL
S13	1	6.2	20.7	27.6	17.0	N/A	14.4	63.5	45.1
	2	13.8	37.6	39.4	39.9	6.5	26.5	60.5	74.4
	3	9.3	12.9	19.7	79.3	N/A	15.1	50.5	20.1
S14	1		12.9	14.3	15.4	49.9	8.7	18.9	10.0
	2	97.7	62.1	14.5	13.9	20.3	21.2	21.1	16.7
	3	82.2	64.1	54.7	20.7	14.2	8.9	10.3	15.2
S15	1	33.0	13.2	7.2	11.3	10.9	25.2	10.5	11.3
	2	16.0	6.2	11.2	5.4	34.3	47.9	34.5	18.6
	3	11.0	22.4	9.7	8.1	20.4	29.1	13.7	14.3
S16	1	34.2	16.6	14.7	11.0	70.8	38.1	50.9	36.5
	2	5.7	6.3	6.6	15.4	72.9	59.7	58.7	54.7
	3	11.1	3.0	10.5	8.6	No Data Available			
S17	1	9.7	5.9	15.5	6.4	13.1	17.1	10.3	7.0
	2	No Data Available				28.4	30.5	28.9	28.9
	3	13.9	5.1	10.2	16.2	11.2	5.8	17.6	20.6
S18	1	79.7	25.9	24.1	27.4	20.6	43.2	13.8	72.5
	2	33.1	10.8	21.4	18.3	N/A	22.5	48.2	60.0
	3	7.9	9.2	15.3	18.3	N/A	18.5	25.6	34.8
S20	1	34.0	8.3	7.1	16.6	N/A	8.2	8.9	19.8
	2	21.1	8.5	51.5	11.1	20.6	37.1	12.3	11.3
	3	55.3	10.0	22.9	20.0	No Data Available			
Mean		30.3	18.1	19.9	19.0	28.2	25.1	29.4	30.1
St. Dev.		28.3	17.5	13.9	16.2	21.6	14.8	19.6	21.4

Table 7-5: Latency of muscle activation in response to peak swing acceleration in the tensed and untensed muscle conditions for 50th percentile adult males.

7.3.2 Head Displacement

High speed videos of the dynamic events were digitized to determine head displacement. The videos where the head marker fell off the subject, or was washed out by the camera lighting were discarded. Table 7-6 gives a list of tests discarded from the results.

Subject	# of tests discarded		Subject	# of tests discarded	
	Tensed	Untensed		Tensed	Untensed
K01	1	1	S15	1	
K04		1	S17	2	
K06		1	S20	1	
K09	1				
K10	1	1			
K11	1	2			

Total Tests discarded: 14 out of 68

Table 7-6: Number of tests discarded from head displacement analysis due to fallen marker, lighting issues or swing release delay (S17).

Head displacement was compared between dynamic test conditions for both subject groups. For 10-year old boys there was no significant difference between the head displacement of the tensed condition and the untensed condition. Average displacement during the tensed muscle condition was $x=0.11\pm 0.03$ mm/mm, and $z= -0.05\pm 0.02$ mm/mm (normalized to the occupant seated erect height). In the untensed condition, average displacement values were $x=0.12\pm 0.02$ mm/mm and $z=-0.03\pm 0.02$ mm/mm. Table 7-7 shows the maximum displacement values in x and z for both the tensed and untensed dynamic conditions.

Subject	Trial	Tensed Displacement				Untensed Displacement (mm/mm)			
		Actual (mm)		Normalized (mm/mm)		Actual (mm)		Normalized (mm/mm)	
		x	z	x	z	x	z	x	z
K01	1	101.2	-40.5	0.15	-0.06	84.5	-5.3	0.13	-0.01
	2								
K03	1	74.2	-46.6	0.11	-0.07	85.1	-44.3	0.12	-0.06
	2	78.4	-55.1	0.11	-0.08	89.3	-23.2	0.13	-0.03
	3	97.5	-52.9	0.14	-0.08	85.1	-29.5	0.12	-0.04
K04	1	99.6	-29.7	0.15	-0.04	108.1	-12.7	0.16	-0.02
	2	82.6	-14.8	0.12	-0.02				
K05	1	95.3	-25.4	0.13	-0.03	82.9	-14.8	0.11	-0.02
	2	80.5	-16.9	0.11	-0.02				
K06	1	84.3	-43.8	0.11	-0.06				
	2	59.0	-40.5	0.08	-0.05				
K07	1	70.8	-32.0	0.09	-0.04				
	2	59.0	-28.7	0.08	-0.04				
	3	84.3	-37.1	0.11	-0.05				
K09	1	77.6	-13.5	0.12	-0.02	64.1	-21.9	0.10	-0.03
	2					80.9	-15.2	0.12	-0.02
K10	1	38.8	-38.8	0.05	-0.05	57.5	-27.0	0.08	-0.04
	2								
K11	1	27.0	-20.2	0.04	-0.03				
	2								
Mean		75.6	-33.5	0.11	-0.05	81.9	-21.5	0.12	-0.03
St. Dev		21.0	13.1	0.03	0.02	14.5	11.4	0.02	0.02

Table 7-7: Maximum head excursion for 10-year old boys in the dynamic tensed and untensed conditions. Table shows actual displacement values as well as displacement values normalized to seated erect height. There was no significant difference between the test conditions.

Figures 7-6 (a) and (b) show the head displacement trajectories for both dynamic conditions.

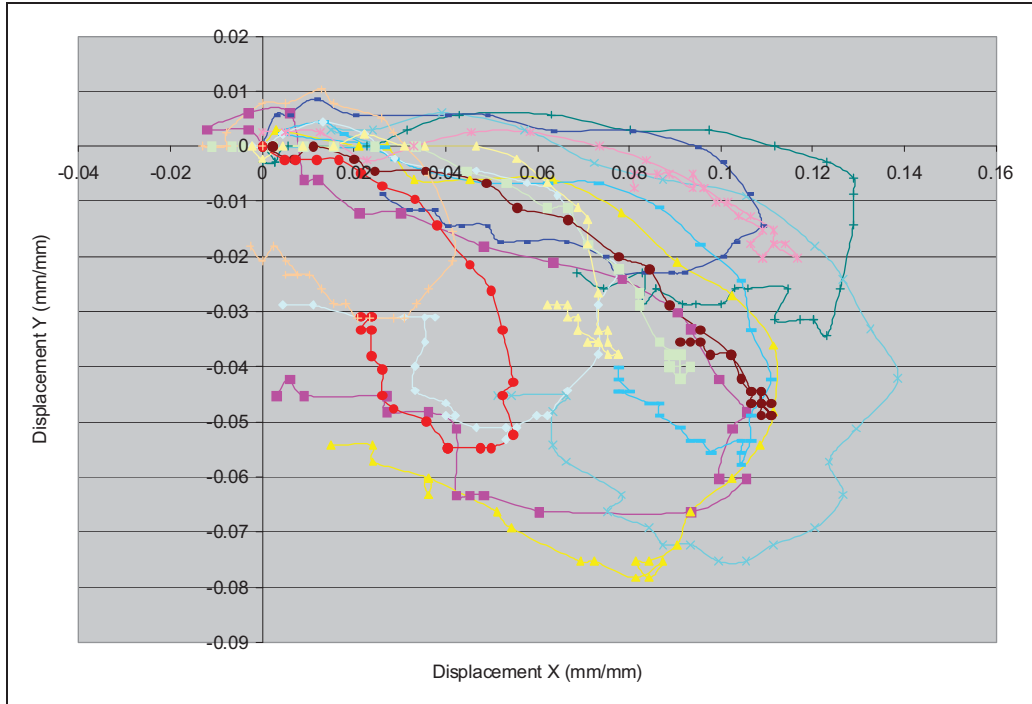


Figure 7-6(a): Trajectory of the cg of the head for 10 year old male subjects during tensed muscle, dynamic impact.

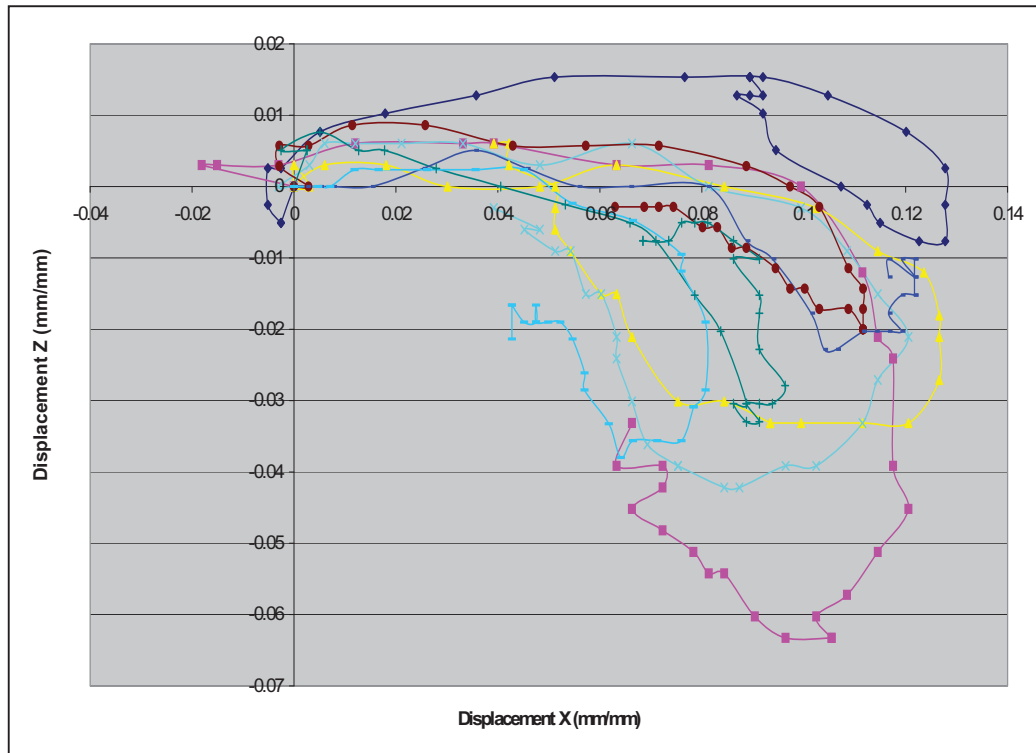


Figure 7-6(b): Trajectory of the cg of the head for 10-year-old male subjects during untensed muscle, dynamic impact.

Adult head displacement was similarly evaluated. Unlike the 10-year old boys, there was a significant difference between the head displacement of the tensed and untensed events for adults in the x-direction, with significantly greater values in the untensed condition. Average normalized displacement values for adults were $x=0.13\pm 0.02\text{mm/mm}$ and $z=-0.02\pm 0.02\text{mm/mm}$ during the tensed event, and $x=0.16\pm 0.02\text{mm/mm}$ and $z=-0.016\pm 0.01\text{mm/mm}$ during the untensed event. Maximum displacements are shown below in Table 7-8.

Subject	Trial	Tensed Displacement				Untensed Displacement (mm/mm)			
		Actual (mm)		Normalized (mm/mm)		Actual (mm)		Normalized (mm/mm)	
		x	z	x	z	x	z	x	z
S14	1	136.6	-33.7	0.16	-0.04	140.0	-11.8	0.17	-0.01
	2	126.5	-21.9	0.15	-0.03	113.0	-13.5	0.13	-0.02
	3	107.9	-15.2	0.13	-0.02	113.0	-8.4	0.13	-0.01
S15	1	102.9	-8.4	0.13	-0.01	124.8	-23.6	0.15	-0.03
	2	111.3	-3.4	0.14	0.00	143.3	-27.0	0.18	-0.03
	3					136.6	-16.9	0.17	-0.02
S16	1	113.0	-6.7	0.13	-0.01	153.5	-16.9	0.18	-0.02
	2	107.9	-6.7	0.13	-0.01	150.1	-11.8	0.18	-0.01
	3	99.5	-11.8	0.12	-0.01	145.0	-15.2	0.17	-0.02
S17	1	119.7	-50.8	0.14	-0.06	143.3	0.0	0.16	0.00
	2					111.3	-8.4	0.13	-0.01
	3					121.4	-5.1	0.14	-0.01
S18	1	86.8	-5.1	0.10	-0.01	128.5	-5.1	0.15	-0.01
	2					146.9	-5.1	0.17	-0.01
	3								
S20	1	89.0	-5.1	0.10	-0.01	135.6	-15.2	0.16	-0.02
	2	99.6	-6.7	0.12	-0.01	175.8	-13.5	0.21	-0.02
	3								
Mean		108.4	-14.6	0.13	-0.02	136.4	-12.3	0.16	-0.01
St. Dev.		14.5	14.4	0.02	0.02	17.3	7.0	0.02	0.01

Table 7-8: Maximum head excursion for 50th percentile adult male subjects in the dynamic tensed and untensed conditions. A significant difference was found in the maximum excursion in the x-direction ($p<0.02$)

Figures 7-7 (a) and (b) show the head displacement trajectories for the 50th percentile adult male subjects during the tensed and untensed test conditions.



Figure 7-7(a): Trajectory of the cg of the head for 50th percentile adult male subjects during tensed muscle dynamic impact.

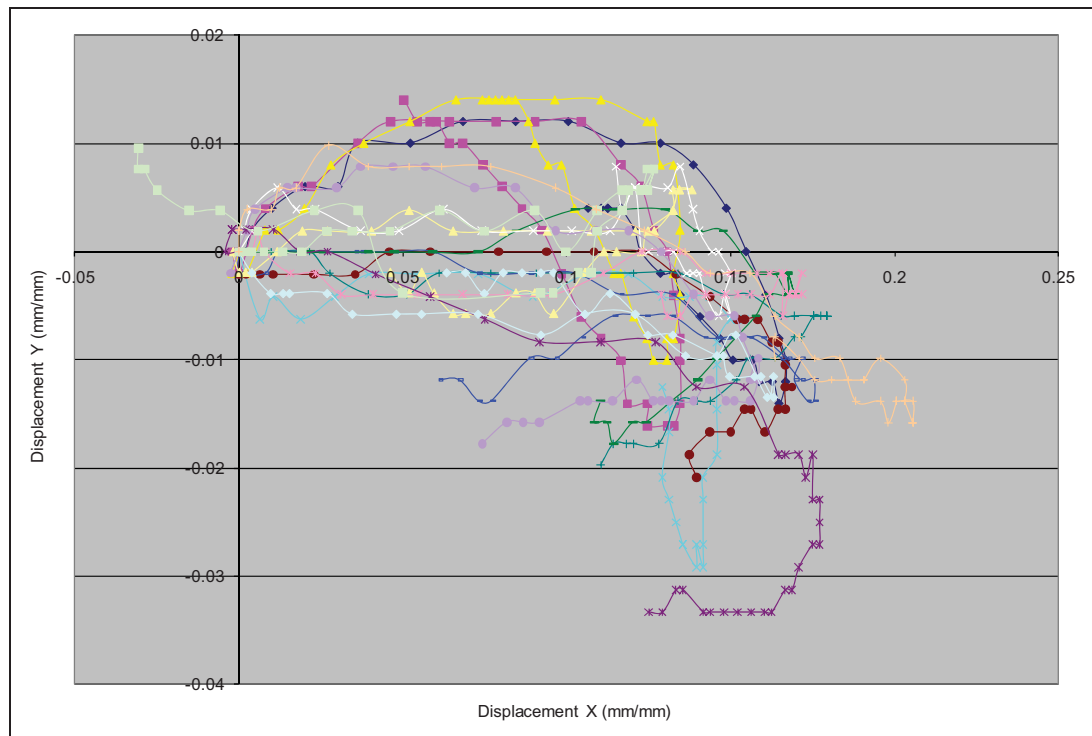


Figure 7-7(b): Trajectory of the cg of the head for 50th percentile adult male subjects during untensed muscle dynamic impact.

The results of the video analysis to determine motion of the head marker and mouthpiece showed minimal motion of the mouthpiece. In children the average mouthpiece displacement was 2.5 ± 2.3 mm. In adults, the motion of the mouthpiece was on average less than 1mm. The video analysis did show some motion of the head marker at the point of peak acceleration. In children, the displacement was greater than in adults because the headphones were looser on their head. The displacement of the head marker for both subject groups was less than the standard deviation of the head displacement results. For children, the head marker showed a displacement of 12.4 ± 8.5 mm. The standard deviation of the head displacement in the 10-year old male subject group ranged from 14.5 mm to 21.0 mm. For adults the head marker displacement was 7.4 ± 5.8 mm. The standard deviation of the head displacement of the adult subject group ranged from 14.5 mm to 17.3 mm.

7.4 DISCUSSION

7.4.1 Latency

In this study, latency of muscle response was calculated relative to distinct instances during the dynamic event: 1) swing drop - the onset of acceleration; and 2) peak swing acceleration (the point at which the shock absorbers were completely depressed) which coincided approximately with the onset of head acceleration in flexion.

Relative to swing release, the time to increased muscle activity (EMG activation above the baseline recording) ranged from 79 to 93ms after the swing's release for both subject group, regardless of muscle tension. In children

latency ranged from 81.2 \pm 20.9ms to \pm 49.7ms for the tensed muscle condition and from 84.5 \pm 21.7ms to 91.2 \pm 21.9ms for the untensed condition. In the 50th percentile adult group, latency ranged from 79.6 \pm 28.2ms to 89.5ms \pm 45.4ms in the tensed muscle condition. In the untensed muscle condition, latency ranged from 79.0 \pm 18.6ms to 88.2 \pm 21.2ms. The latencies for both subject groups were consistent with the low end of most of the latency ranges reported in published literature. Szabo et al. [1996] reported 90-120ms to onset of muscle activity in their rear-impact study. In a lower limb study, Begeman et al. [1980] reported 50-150ms from the initial sled acceleration until the onset of muscle activity. Similarly, the 2002 rear impact and the 2003 frontal impact studies by Kumar et al., report the onset of neck muscle activity occurred approximately 70-90ms from onset of sled acceleration. All studies were conducted using adult volunteers. Table 7-8 shows published values for latency of muscle activity relative to the onset of sled acceleration or perturbation and relative to peak sled acceleration/onset of head acceleration for adult subjects.

Study/Reference		Latency (ms)
<u>From onset of sled acceleration</u>		
Begeman et al. [1980]		50-150
Forsberg et al. [1994]		75-120
Szabo et al. [1996]		90-120
Kumar et al. [2002]	aware	80-94 +/-18
	unaware	77-90 +/-29
Kumar et al. [2003]	aware	73-77 +/-14
	unaware	74-91 +/-20
Siegmund et al.		120-130
Dawson study [2011]		79-93 +/- 25
<u>From peak sled acceleration/onset of head acceleration</u>		
Ito et al. [1994]		24.5
Wittek et al. [2001]		35-50
Kumar et al. [2002]	aware	11-32
	unaware	39-57
Kuramochi et al. [2003]	aware	13.7 +/- 1.4
	unaware	18.6 +/- 2.6
Dawson study [2011]	aware	21.7 +/- 19.8
	unaware	28.2 +/- 19.1

Table 7-9: Published values of muscle response latency relative to both onset of sled acceleration and peak sled acceleration.

Relative to peak impact, the adult data shows a significant difference between the test conditions ($p < 0.05$). The subjects who were aware of the impact showed an increase in EMG activity an average of 21.7 +/- 19.9ms after peak swing acceleration. Unaware subjects showed an increase in EMG activity an average of 28.2 +/- 19.1ms after peak swing impact. Wittek et al. [2001], in their

rear impact neck study reported a first wave increase in EMG activity, both in fine wire and surface EMG, at 35-50ms with respect to the onset of the impact, and a second wave 50-90ms after the start of impact, which coincided with maximum head acceleration in the x-direction. Similarly, Kumar et al., [2002] reported latencies of muscle activity from the onset of head acceleration of 39-57ms for unaware subjects and 11-32ms for subjects aware of the impact. The timing of muscle activity is similar to the timing reported by Ito et al. [1994] and Kuramochi et al. [2003]. Ito et al. reported a latency of muscle response from the time of head drop of 24.5ms. Kuramochi et al. reported latencies of muscle activity from the time of head perturbation of 13.7 +/- 1.4ms for subjects aware of the perturbation and 18.6 +/-2.6ms for subjects unaware of the perturbation.

This study found no significant difference between the muscle response time of subjects when they were aware of the swing release as compared to when they were not. The literature shows contradictory results. The Kumar et al. study [2002] reports a significant increase in onset time of muscle activity when subjects are unaware of the impact, relative to head acceleration ($p < 0.01$). However, in studies in which the head was directly perturbed, either by head drop [Ito, 1994] or direct head impact [Kuramochi, 2004], no significant difference was found in the onset of EMG activity from the time of head acceleration between subjects who were expecting the head perturbation and those who were not. The Ito et al., study found that awareness had a significant effect ($p < 0.05$) on reducing the velocity and displacement of the head after the head drop. The results of the adult subject group in this study show a similar finding; Table 7-7

shows a significantly greater head excursion ($p < 0.05$) when subjects were unaware of the impact. The adult subject group in this study also showed a significantly reduced time to maximum moment at C4/5 when the subject was tensed for impact - 264.5 ± 0.1 ms. During the impact when the subject was untensed, or unaware of the impact, the time to maximum moment at C4/5 was 267.3 ± 0.1 ms ($p < 0.05$). The results of the child studies show no difference in peak moment (Ch 6.), time to peak moment at C4/5 or head maximum head displacement between the tensed and untensed muscle conditions, in spite of higher EMG activation in the trapezius and scalene muscles and an earlier onset of muscle activity in the same muscles during the tensed muscle condition. In a 2011 study by Mathews et al., adult (ages 18-30) and child (ages 8-14) volunteers experienced a low speed (4.9g) frontal impact event. When compared with the latency of muscle response of adults, there was no significant difference between the onset times of muscle activity relative to the onset of the impact event. The average time of muscle activation of the SCM in their study was approximately 75ms, and the TRAP was approximately 80-90ms, similar to the results found in this study.

The results of this study indicate that the onset of increased muscle activity is controlled by distinct neural control pathways which depend on the point during the impact event in which muscle activity is required. In this study, there is no significant difference in the time to increase muscle activity between the muscles - all muscles respond at approximately the same time. Nor is there a significant difference between the response times of subjects who were prepared

for the swing drop (tensed muscle) as compared with those who were not (untensed muscles). These results suggest that a central pattern generator is responsible for the increased muscle activity due to the onset of swing acceleration rather than another pathway such as a stretch reflex. Although central pattern generators are typically associated with rhythmic movement such as locomotion, the results of studies by Forssberg et al. [1994] and Siegmund et al. [2008] suggest otherwise. In the 1994 Forssberg et al. study on the neural strategies responsible for postural adjustments, the muscle response timing of seated subjects was measured in response to various postural perturbations including forward translation and a legs-up rotation. Muscle response times of 75-120ms from the onset of the postural perturbation were reported regardless of the type of perturbation used to elicit the response. Forssberg et al., thus suggested that *“somatosensory signals and not vestibular information head, trigger postural responses during sitting”* [Forssberg, 1994]. Similarly, the 2008 study, Siegmund et al. used two types of perturbation to determine latency of the onset of multifidus activity. Their study compared latency due to a startle reflex to latency due to forward sled acceleration. The reported latency of onset of multifidus activity ranged from 120-130ms, again regardless of perturbation type.

The results of the child data suggest that unlike the adult data, possibly two pathways are responsible for the muscle activity in response to swing acceleration. In the tensed muscle condition there was no pattern of muscle activation, all muscles showed an increase in activity at the same time. These results are consistent with the adult data results, and would suggest a central

pattern generator is the responsible neural pathway for muscle activation. However, although there was no difference in the muscle response time between test conditions, there was a pattern of muscle activation present during the untensed test condition that was not present in the tensed muscle test condition or in the adult results. In the untensed muscle condition the trapezius muscle responds sooner ($L_{\text{trap,U}} = 84.5 \pm 21.7\text{ms}$) than any of the other muscles ($L_{\text{scm,U}} = 90.6 \pm 14.9\text{ms}$, $L_{\text{spl,U}} = 92.4 \pm 18.8\text{ms}$ or $L_{\text{scal,U}} = 91.2 \pm 21.9\text{ms}$) ($p < 0.05$). This pattern of muscle activation is consistent with the muscle activation pattern relative to the onset of head acceleration reported in the 2003 frontal impact study by Kumar et al. The Kumar paper does not discuss the neural mechanisms responsible for these findings. However in the 1996 study by Ito et al., muscle response of 67.5ms or later in labyrinthine-deficient subjects was attributed to a stretch reflex. The child response times in the untensed condition of this study are thus likely attributable to both a central pattern generator and a stretch reflex.

In response to peak impact acceleration, the results of this portion of study show shorter response times to increased muscle activity than at swing release. The results also show a pattern of muscle recruitment. In both the tensed muscle conditions in both subject groups, the trapezius was recruited prior to both the SCM and scalene muscles ($p < 0.05$). The splenius capitis increased in activity at a similar time to the trapezius. The shorter activation time and visible recruitment pattern suggest that relative to peak swing acceleration and the onset of head acceleration, the muscles are activated by a reflexive pathway. In their 1996 study, Ito et al. reported a 60ms latency for a stretch reflex, while an activation

time of 25ms is due to vestibular-collic response. The latencies of the tensed muscle condition in this study fall between these two reflexive pathways. In the 10-year old muscle group time to onset of increased muscle activity ranged from 31.2ms to 49.9ms, depending on the muscle being activated. For the 50th percentile adult subject group, time to onset of increased muscle activity ranged from 38.0ms to 44.4ms. This would suggest that the neck muscles are likely activated by a combination of the two. The decreased latency during the tensed impact may also be aided by a visual component, as suggested by Ito et al. [1996]. In the untensed muscle condition, the time to onset of muscle activity ranged from 45.8ms to 53.6ms in the 10-year old male subject group, depending on the muscle; and from 42.9ms-53.0ms for the 50th percentile adults, depending on the muscle. The onset times showed no significant difference from those of the tensed muscle condition for either subject group. While this may suggest that the visual component is less significant to the initiation of muscle response, it is more likely that in spite of the instructions to remain “relaxed” during the entire event that the subject began to tense their muscles once the swing dropped.

The 10-year old boys in this study appear to use the same neural strategies as the adults. At swing release, there is no significant difference in latency between the boys and the adult males, suggesting that the centrally regulated mechanisms are less affected by age. Since the peak swing acceleration was different between subject groups, it is difficult to compare the subjects' responses. However, the results of this study would suggest that the immaturity in neural-motor control is more likely found in the muscle ability to

generate force, as shown in Chapter 5, than in the child's ability to activate his muscles.

7.4.2 Head Displacement

There was no difference between the maximum head excursion of the 10 year old boy, regardless of their awareness of the swing impact (tensed vs. untensed muscles). The average head excursion for the 10-year old in this study, from the time of swing-to-shock absorber contact until the time of swing-to-shock absorber release was $x = 77.8 \pm 19.3\text{mm}$ and $z = -28.5 \pm 14.0\text{mm}$. When normalized to seated erect height $x = 0.11 \pm 0.03\text{mm/mm}$ and $z = -0.04 \pm 0.02\text{mm/mm}$. Arbogast et al. [2009] reported head excursion, normalized to the initial position of the top of the head, for 9-11 year olds of $x = 0.32 \pm 0.03\text{mm/mm}$; $z = -0.05 \pm 0.03\text{mm/mm}$. The results of the Arbogast study are approximately 60% greater than the results calculated in this study. Similarly, the Arbogast study reported normalized head excursion values of $x = 0.23 \pm 0.019\text{mm/mm}$ and $z = -0.043 \pm 0.091\text{mm/mm}$ for adult males. The adult male subjects in this study had an average normalized head excursion of $x = 0.13 \pm 0.02\text{mm/mm}$ and $z = -0.02 \pm 0.01\text{mm/mm}$ in the tensed muscle condition and $x = 0.16 \pm 0.02\text{mm/mm}$ and $z = -0.02 \pm 0.01\text{mm/mm}$. The results of the Arbogast study ranged from 30-45% greater than the calculated head excursion values for the 50th percentile males subject in this study. The difference in normalized head excursion results between this study and the Arbogast study can likely be attributed to the differences in the vehicle pulses and the initial sitting position of

the subject. The Arbogast study used a vehicle pulse with a peak acceleration range of $3.62 \pm 0.29g$'s to $3.82 \pm 0.17g$'s with a rise time range of $59 \pm 2ms$ to $63 \pm 12ms$. In this study, the vehicle pulse ranged from $2.644g \pm 0.183g$ to $3.234g \pm 0.155g$ with a rise time of 30ms.

In 1994, Cassan et al. reported the head excursion values for child cadavers. The cadavers in their study were matched for weight and height to the 3 year old ATD's. Both the ATD's and cadavers used in their study were restrained in a car seat or booster seat. Tests were conducted at high velocity ranging from 31-50km/h ($8.61m/s - 13.89m/s$) with an average acceleration range of 13-25g's. The average head excursion results were reported to be $x \sim 0.60m$ and $z \sim 0.20m$. Their results were significantly greater than the un-normalized values of the 10-year old boys in this study, due to the difference in sled acceleration. Average un-normalized head excursion for the 10-year old boys in this study was $x = 77.8 \pm 19.3mm$ and $z = -28.3 \pm 14.0mm$.

Szabo et al. [1996] reported head displacement in adults of $x=58-124mm$, relative to initial position of the head in rear impact. Impact velocities in the study ranged from 12.9-15km/h ($\Delta v = 3.58m/s-4.16m/s$). Un-normalized mean head displacement for adult subjects in this study was $x=108.4 \pm 14.5mm$ for the tensed muscle condition and $x=136.4 \pm 17.3mm$ for the untensed muscle condition.

In both the Arbogast study and the Szabo study, subjects were "relaxed" prior to impact. The 1984 study by Seeman et al., found that subjects who had previously participated in impact studies would "lock" their joints until the applied

forces/torques overcame the muscle force and the head began to move, resulting in reduced head excursion. Similarly, the results of this study show a reduced head excursion when the subjects were instructed to tense their muscles for impact.

CHAPTER 8: SUMMARY AND CONCLUSIONS

The objective of this study was to compare the neck responses of 10-year old boys to that of 50th percentile adult males in static and dynamic loading conditions. It was hypothesized that due to an immature neuromuscular system, pre-pubescent children would be unable to fully recruit their muscles in response to an applied load, resulting in reduced muscle reaction forces and generated muscle stress. To meet the objective of this study, 50th percentile male and 10-year old male volunteers were recruited to participate in a three-part study. In the first part of the study MRI was used to measure muscle morphology, including muscle length, muscle moment arm in the C4-axial plane and both the physiologic and anatomic cross-sectional area. In the second and third part of the study EMG was used to measure the bi-lateral muscle activation of the sternocleidomastoid, the posterior muscles, the posto-lateral muscles and the scalene muscles under both static and dynamic applied loads. An EMG assisted optimization model was used to calculate the muscle forces and stresses under static loading conditions. Neuromuscular efficiency [Grosset, 2008] was used to compare the static and dynamic responses of the 10-year old male and 50th percentile adult male subjects.

The following results were found in this study,

1. There is a linear relationship between age and moment arms ($p < 0.05$) for the sternocleidomastoid, the trapezius and the splenius capitis. There was no correlation between age and the scalene muscles.
2. There was a correlation between age, weight, height and the physiologic cross-sectional area of the sternocleidomastoid ($p < 0.02$).
3. Adults are capable of generating significantly higher muscle forces and moments in static loading conditions than 10-year old boys ($P < 0.05$).
4. The neuromuscular efficiencies for both static and dynamic loading conditions were greater for the 50th percentile adult male subjects than for the 10-year old male subjects ($p < 0.05$).
5. There was no difference in the peak EMG activation values between the 50th percentile adult males and 10-year boys in either the static or dynamic test conditions.
6. The dynamic swing impact created two distinct moments at C4 (1) an extension moment in response to the swing's release and (2) a flexion moment in response to the swing's peak impact.

- a. For the 50th percentile adult males, the extension moment was higher for the untensed muscle impact than for the tensed muscle impact ($p < 0.05$); the flexion moment was higher in the tensed muscle impact than in the untensed muscle impact ($p < 0.05$).
 - b. For 10-year old boys there was no significant difference in either moment between the tensed muscle and untensed muscle impacts.
7. The latency of muscle activation was calculated relative to two discrete events, (1) swing release and (2) peak swing acceleration.
- a. For the 50th percentile adult male, there was no difference in the time to onset of muscle activity between the tensed muscle and untensed muscle impacts relative to the swing drop.
 - b. For the 50th percentile adult male, there was a significant increase in the time to onset of muscle activation for the splenius capitis in the untensed muscle impact as compared to the tensed muscle impact. There was no difference in the onset times for the sternocleidomastoid and the trapezius muscles.
 - c. For the 10-year old boys there was a significant increase in the time to onset of muscle activation for the splenius capitis ($p < 0.05$) in the untensed muscle impact as compared to the tensed muscle impact. There was no difference in the onset times for the sternocleidomastoid and the trapezius muscles.
 - d. For the 10-year old boys there was a significant increase in the time to onset of muscle activation for the trapezius and the scalene

muscles ($p < 0.02$) in the untensed muscle impact as compared to the tensed muscle impact. There was no difference in the onset times for the sternocleidomastoid and the trapezius muscles.

8. There was no difference in the head displacement of the 10-year boys between the tensed muscle and untensed muscle impacts.
9. For the 50th percentile adult males there was a significantly greater head excursion in the untensed muscle impact than in the tensed muscle impact ($p < 0.02$).

The results of this study support the scaling relationship suggested by Wolanin et al. [1982] since no difference was found in the stress generated in the muscles of either subject group. The results also show that children are unable to fully recruit their muscles for contraction in response to an applied load, as indicated by the lower neuromuscular efficiency of the 10-year male subjects in both static and dynamic loading conditions. Given this finding, scaling the responses between adults and children would be more accurate if the Wolanin model were modified to include an additional scale factor which takes into account the difference in muscle efficiency.

8.2 LIMITATIONS

There were several, unforeseen limitations in this study.

1. Limitations of the MRI Study:

The imaging protocol for this study was initially developed using a number of volunteers, including subject S08. The sequencing time developed during this pilot study was approximately 30 minutes. In order to accommodate the ability of a 10-year-old child to remain completely still in a small, dark, loud environment, the imaging protocol was reduced to 15 minutes, in doing so, the resolution of the image was reduced. The result was that the muscle boundaries, particularly in children where there is minimum interstitial fat, were not distinguishable in all image slices. This prevented muscle volume calculations in all but the sternocleidomastoid muscle. This particular issue can be eliminated in future studies by reducing the number of imaging sequences. In this study there were a total of four imaging sequences – one in the true axial plane, parallel to ground, two along the line of action of the superficial neck muscles, and one in the sagittal plane. The same information could be recorded using a single axial sequence in combination with the sagittal sequence. Doing so would allow for an increase in the scan time of the axial sequence, thus increasing its image resolution without increasing the total image acquisition time.

2. Limitations of the Static Study:

The biggest limitation of the static study was related to the application of a maximal load to produce maximum voluntary contraction. The maximal load applied by the subject was quite subjective. The maximum applied loads varied greatly between the subjects in each group, due to what each subject perceived to be “pushing as hard as possible”. As noted in Chapter 5, **Determination of neck muscle force and stress at the C4 vertebrae during a maximal voluntary contraction**, the applied neck forces and moments of the adult male subjects in this study were significantly smaller than those reported in the published literature. The following factors likely contributed to the variation in the data:

- 1) The training session was not long enough for subjects to properly understand and execute the task required.
- 2) The lack of feedback regarding the magnitude of the applied load.
- 3) Hesitation in applying a maximum load for fear of leaning into the load cell.

Simple changes to the test protocol such as a longer training session or multiple training sessions, the addition of an LED-type indicator to provide feedback on the magnitude of the force being exerted, and restraint of the upper body, should result in higher applied force measurements and less variability in the data.

3. Limitations of the Dynamic Study

The biggest limitation of the dynamic study resulted from the differences in the peak acceleration of the swing. This difference prevented direct comparison of the magnitudes of the moments at C4/5 and the accelerations of the cg of the head between adults and children. Changes to the specifications of the shock absorbers installed on the swing fixture, and increasing the total swing mass for the child subjects to that of total swing mass of adult subjects would ensure that the peak accelerations were the same for both subject groups.

8.3 FUTURE STUDIES:

This study is the first to record and analyse the responses of the child neck in both static and dynamic loading conditions. There is still a large knowledge gap regarding the differences in neuromuscular behaviour of adults and children, and there are many potential studies which could further the understanding these differences, including the ones outlined below.

Static Studies:

1. Due to the large variability of the applied loads, a repetition of the static test described in Chapter 5, **Determination of neck muscle force and stress at the C4 vertebrae during a maximal voluntary contraction**, including the changes to the test set-up and test protocol mentioned above in section 8.2,

- would definitively determine whether the Wolanin et al. [1982] assumption of equal muscle stress between adults and children is valid.
2. In addition to the determination of muscle stress, the role neuromuscular efficiency may play in scaling response data from adults to children needs to be better understood. The development of a scale factor based on neuromuscular efficiency could be developed through a series of maximal and submaximal contractions in various bending directions. EMG assisted optimization models could once again be used to calculate individual muscle forces and moments.

Dynamic Studies:

1. A repetition of the dynamic tests as detailed in Chapter 6, **The neck muscle responses of 50th percentile adult males and 10-year old boys in low speed frontal impacts**, but ensuring that the acceleration pulse is the same for both subject groups, would enable a true comparison of the head acceleration of the cg of the head and the moments at C4/5 between adults and children. The results presented in the current study only compare patterns in responses, and the efficiency of the muscle response.
2. A low speed EMG study in which subjects experienced both frontal and rear impacts with the same acceleration pulse would enable the development of an EMG assisted optimization model, similar to the static model. From this dynamic model, the dynamic muscle forces and stresses could be calculated,

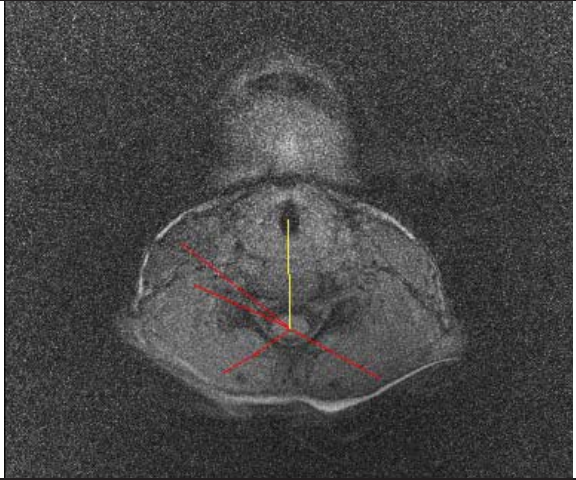
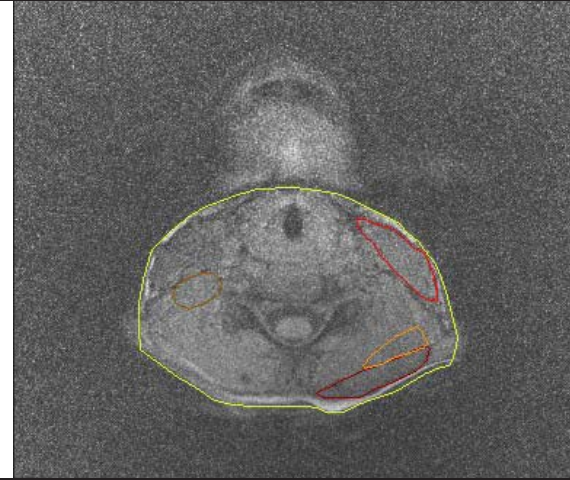
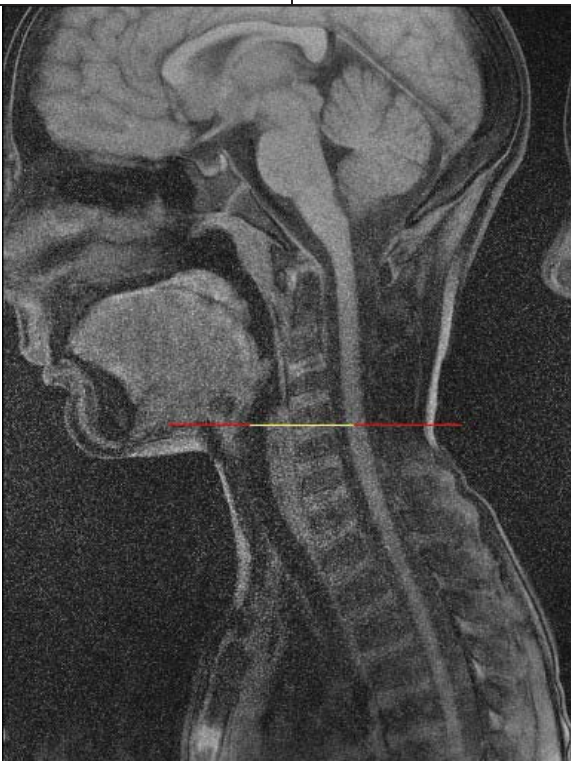
enabling further comparison of the neck muscle responses between adults and children.

3. A repeat of the dynamic study using the 50th percentile adult male and 10-year old ATD's would enable a comparison of the responses of volunteers and the current surrogates at low speeds. In addition to the testing, relating the head displacement data of the current study to the corridors developed by Mertz and Patrick [1971] would provide another means of comparing the responses of the current ATD's to human volunteers. And finally, since the current ATD's were not intended for predicting forces and moments at low speed, this data could be used to develop a mechanical neck that is representative of human response at lower impact forces and velocities.

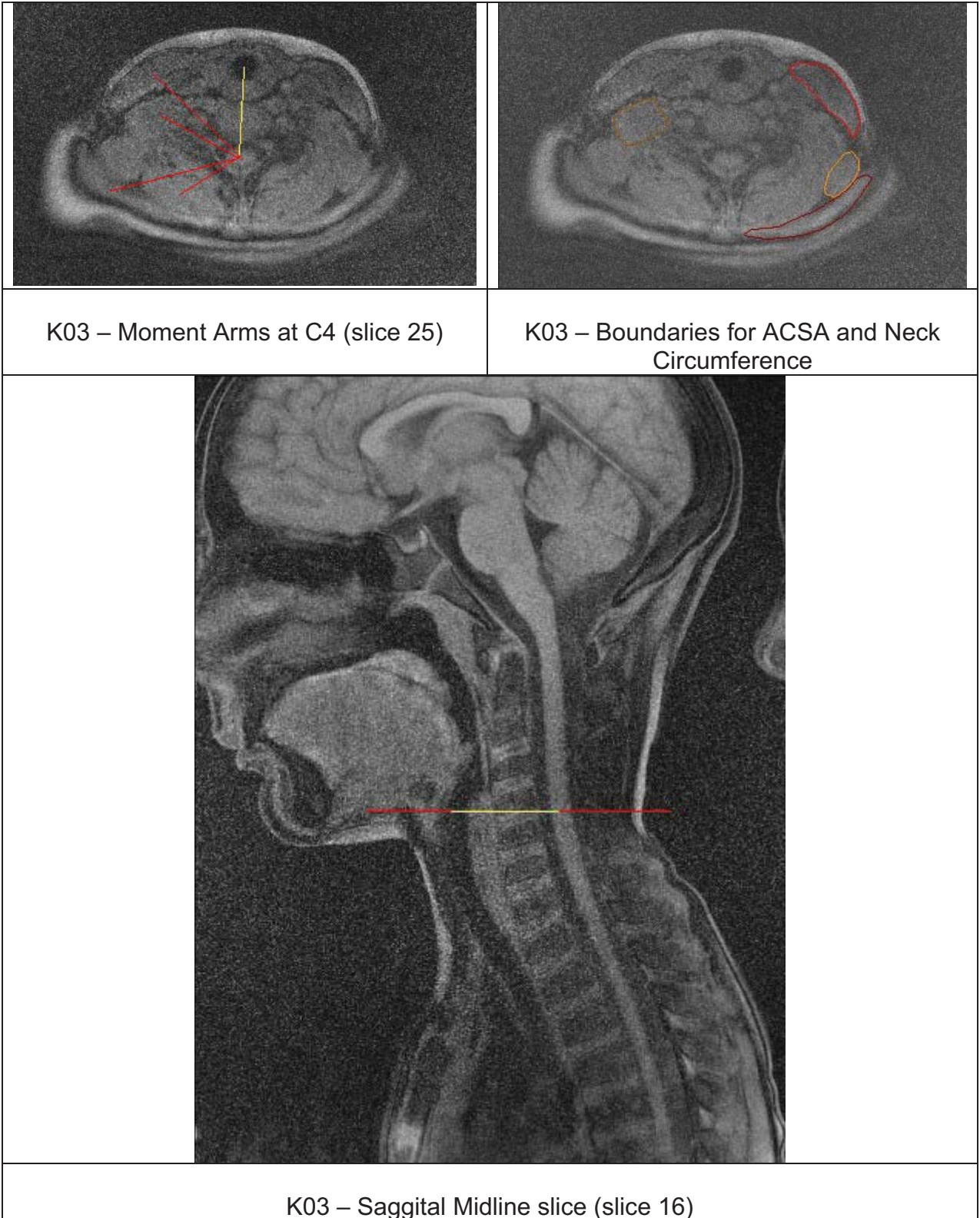
APPENDIX A

This appendix includes all images used in the calculation of muscle moment arms, and muscle cross-sectional area.

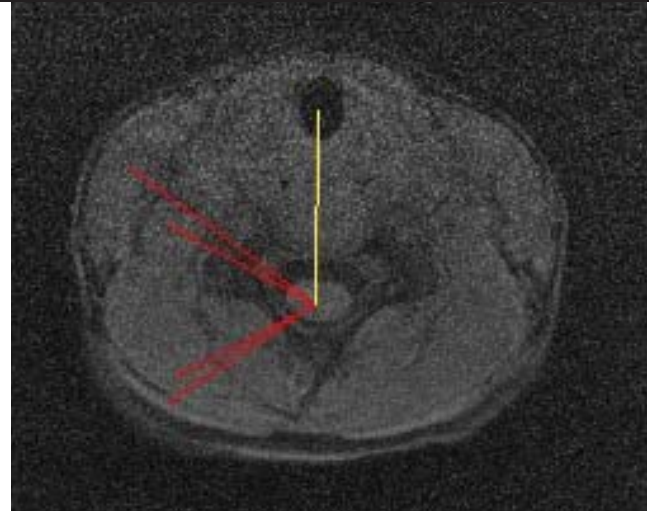
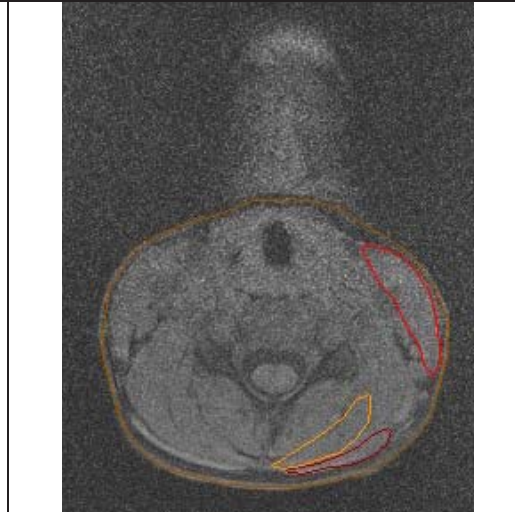

SUBJECT K01

	
<p>K01 – Moment Arms at C4 (slice 28)</p>	<p>K01 – Boundaries for ACSA and Neck Circumference</p>
	
<p>K01 – Saggital Midline slice (slice 16)</p>	

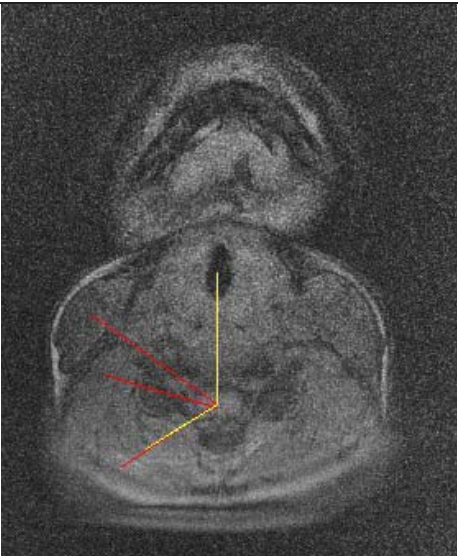
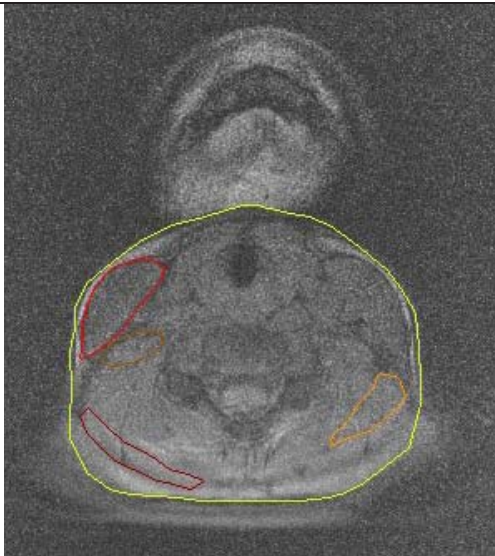

SUBJECT K03



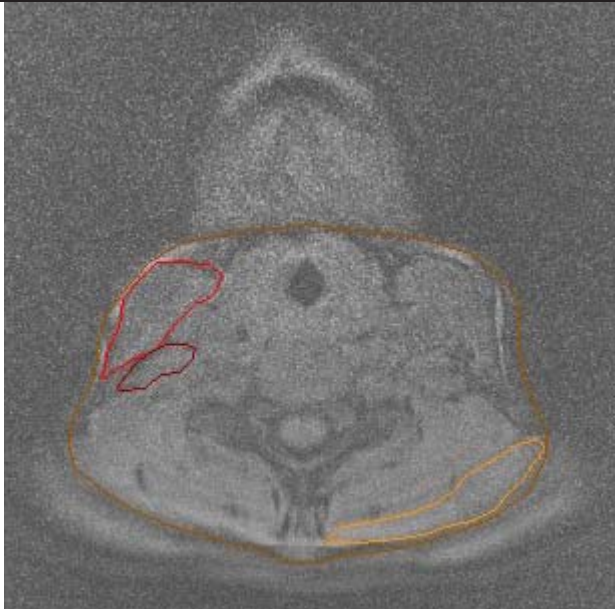

SUBJECT K04

	
<p>K04 – Moment Arms at C4 (slice 26)</p>	<p>K04 – Boundaries for ACSA and Neck Circumference (slice 30)</p>
	
<p>K04 – Saggital Midline slice (slice 17)</p>	

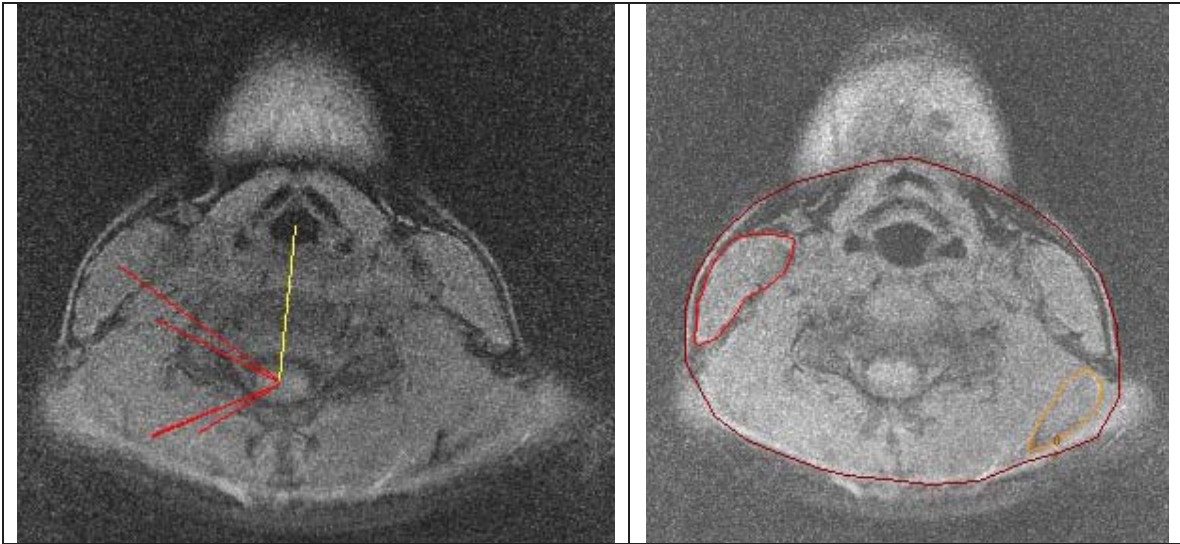
SUBJECT K05

	
<p>K05 – Moment Arms at C4 (slice 27)</p>	<p>K05 – Boundaries for ACSA and Neck Circumference</p>
	
<p>K05 – Saggital Midline slice (slice 17)</p>	

SUBJECT K06

No Image	
K06 – Moment Arms at C4 (slice 28)	K06 – Boundaries for ACSA and Neck Circumference
	
K06 – Saggital Midline slice (slice 17)	

SUBJECT K07



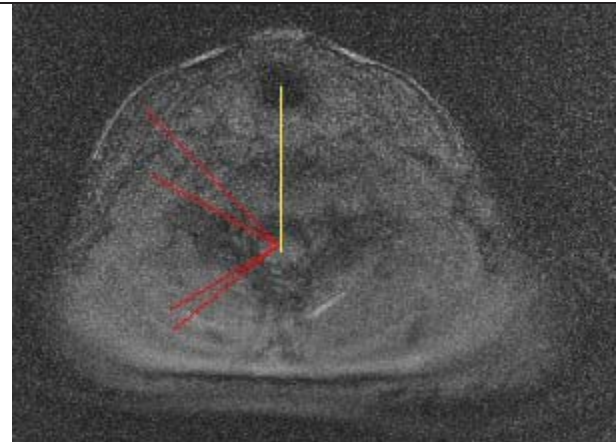
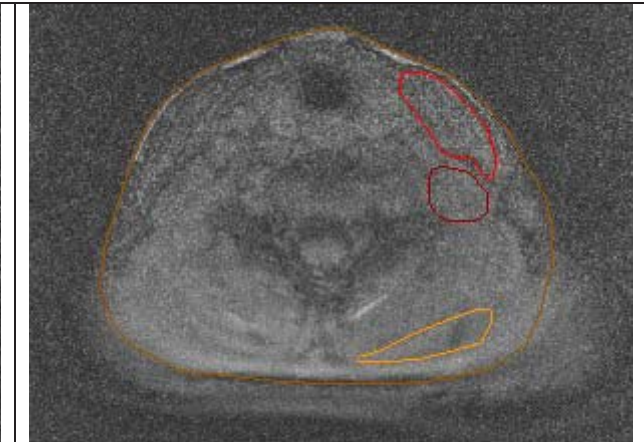
K07 – Moment Arms at C4 (slice 29)

K07 – Boundaries for ACSA and Neck Circumference

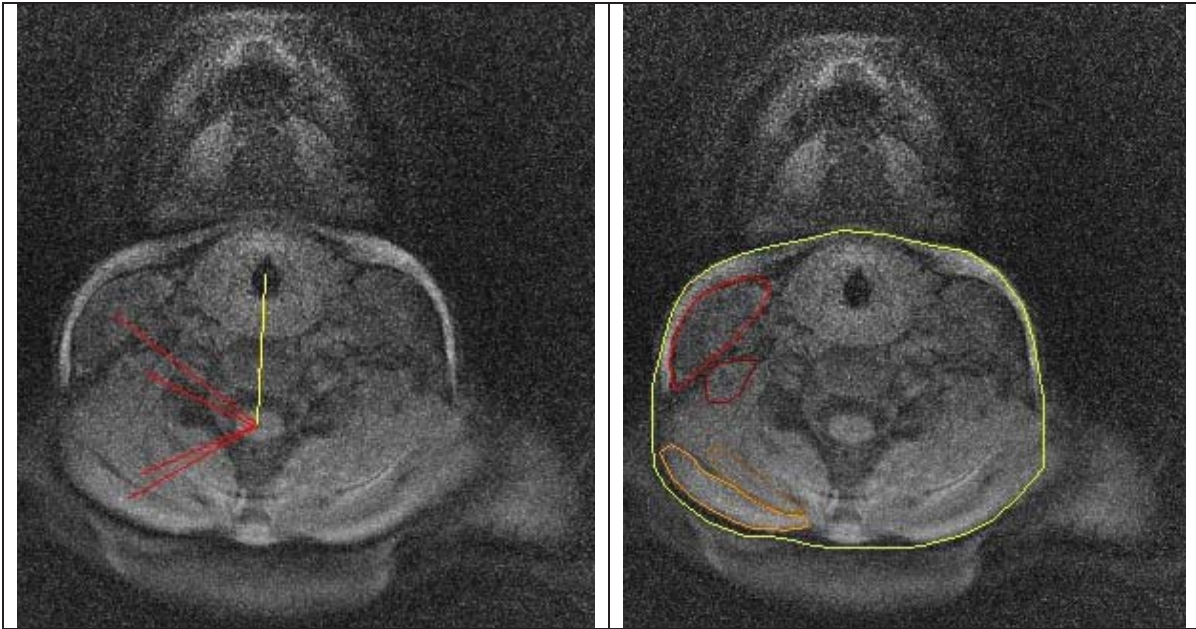


K07 – Saggital Midline slice (slice 17)

SUBJECT K08

	
K08 – Moment Arms at C4	K08 – Boundaries for ACSA and Neck Circumference
No Image	
K08 – Saggital Midline slice	

SUBJECT K09



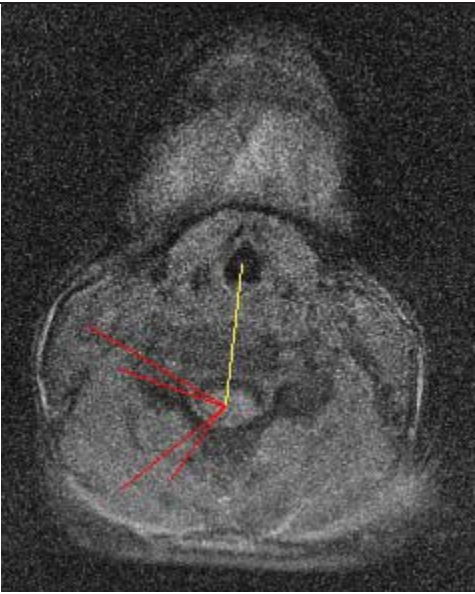
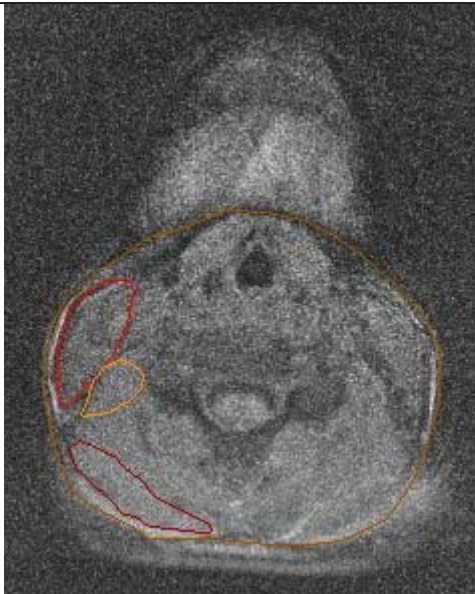

K09 – Moment Arms at C4 (slice 31)

K09 – Boundaries for ACSA and Neck Circumference

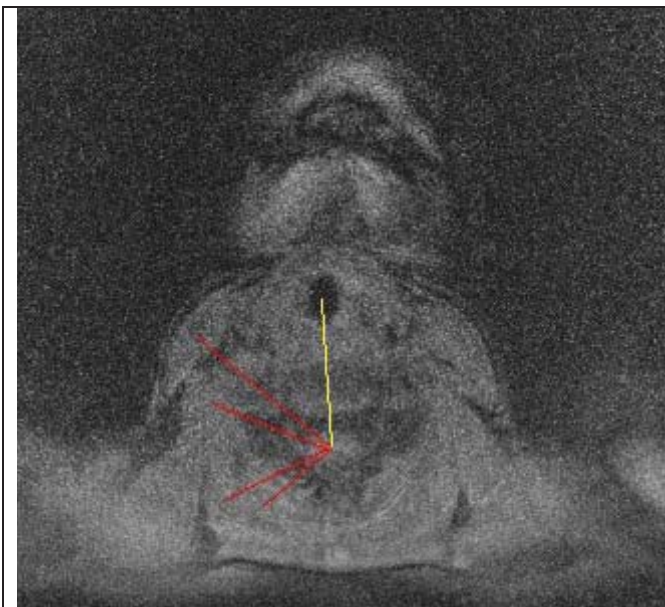


K09 – Saggital Midline slice (slice 17)

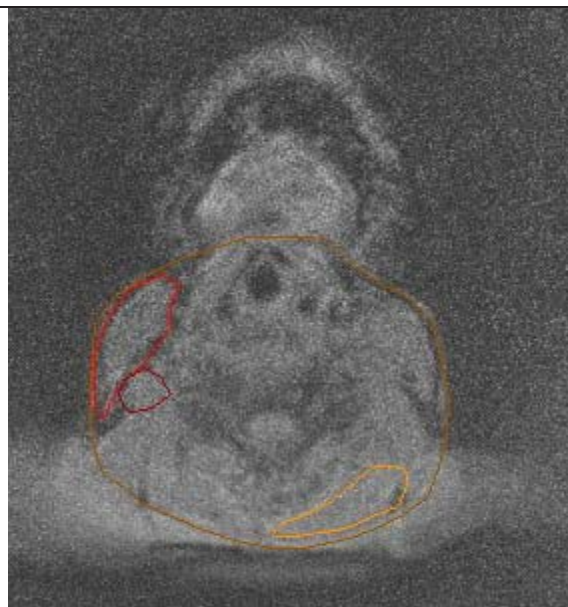
SUBJECT K10

	
<p>K10 – Moment Arms at C4 (slice 27)</p>	<p>K10 – Boundaries for ACSA and Neck Circumference</p>
	
<p>K10 – Saggital Midline slice (slice 17)</p>	

SUBJECT K11



K11 – Moment Arms at C4 (slice 28)

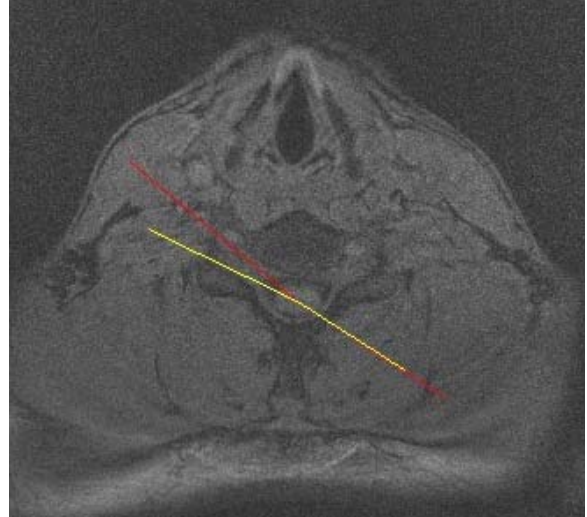
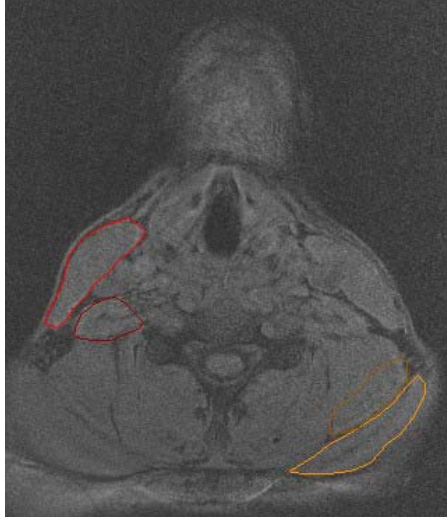
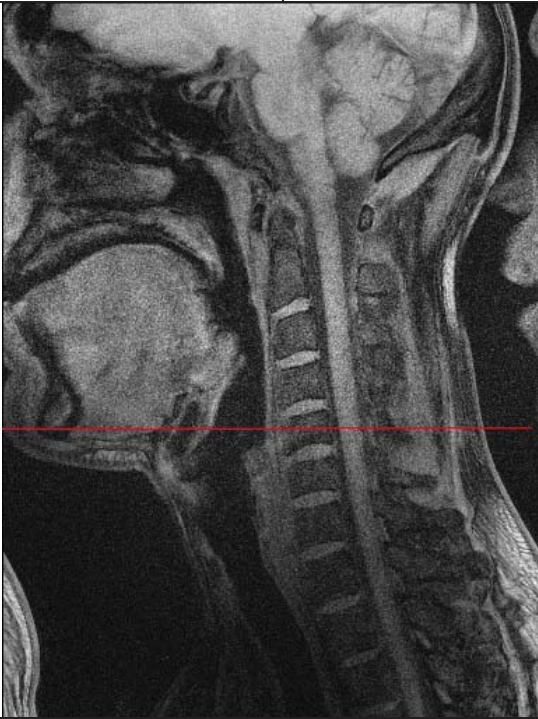


K11 – Boundaries for ACSA and Neck Circumference

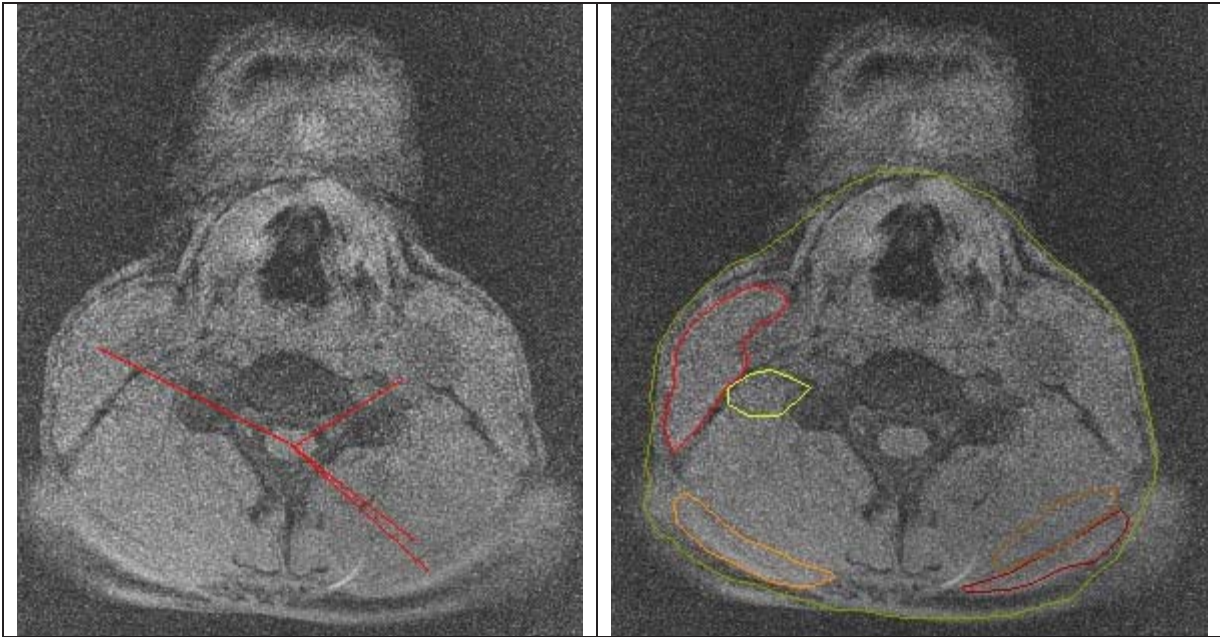


K11 – Saggital Midline slice

SUBJECT S08

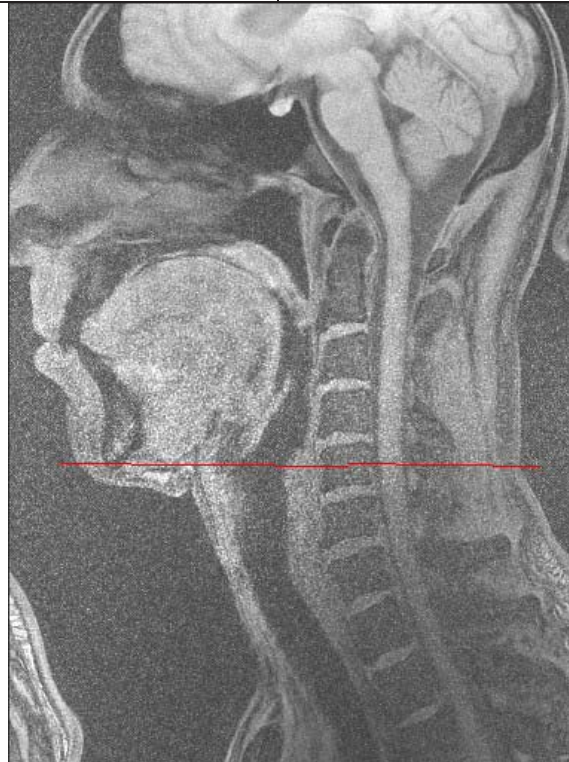
	
<p>S08 – Moment Arms at C4 (slice 25)</p>	<p>S08 – Boundaries for ACSA and Neck Circumference (Slice 26)</p>
	
<p>S08 – Saggital Midline slice (slice 16)</p>	

SUBJECT S09



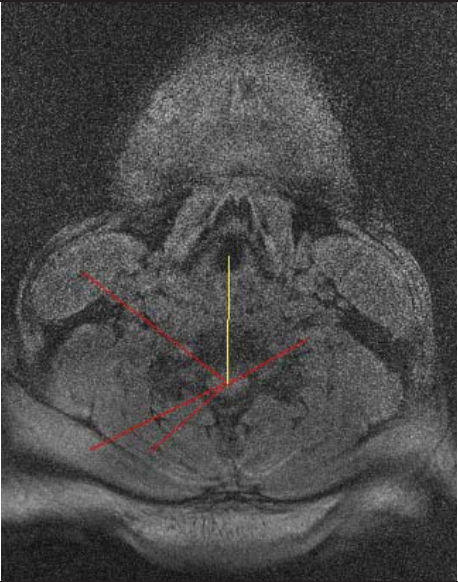
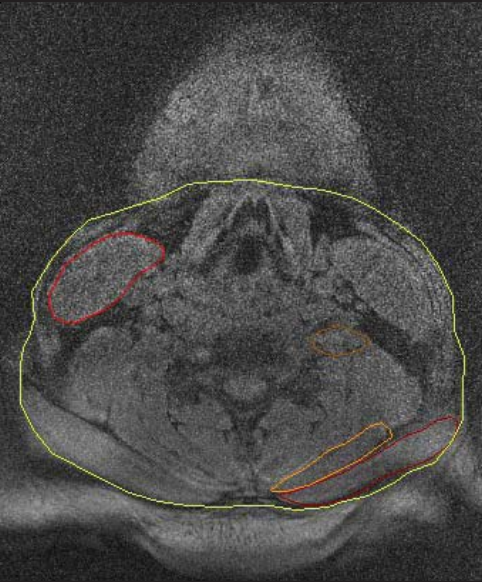
S09 – Moment Arms at C4

S09 – Boundaries for ACSA and Neck Circumference

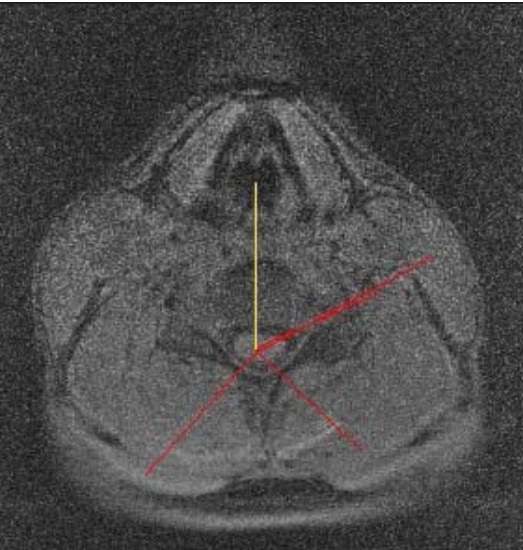
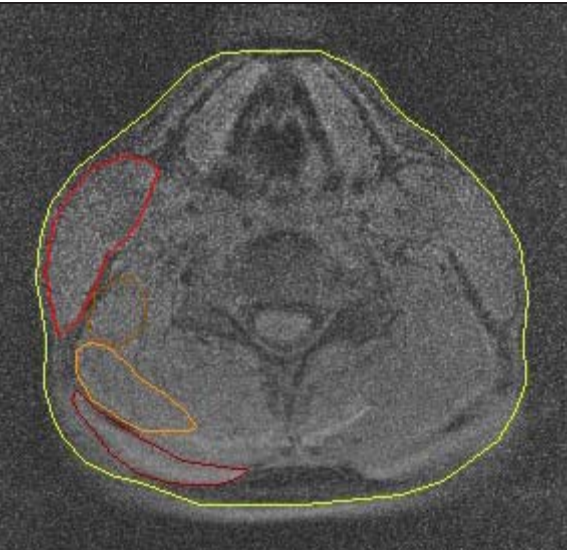



S09 – Sagittal Midline slice (slice 16)

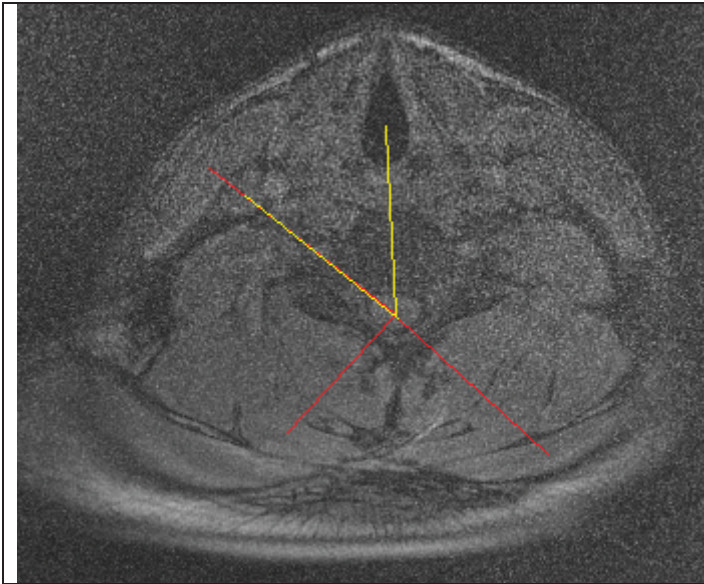
SUBJECT S10

	
S10 – Moment Arms at C4 (slice 24)	S10 – Boundaries for ACSA and Neck Circumference
No Image	
S10 – Saggital Midline slice	

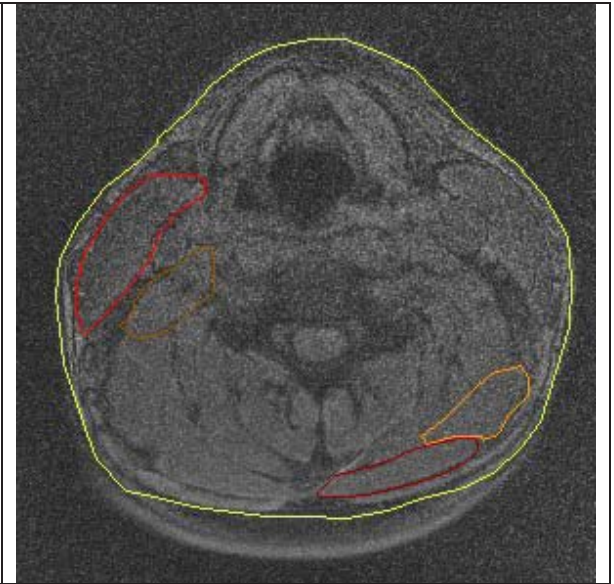
SUBJECT S11

	
<p>S11 – Moment Arms at C4 (slice 26)</p>	<p>S11 – Boundaries for ACSA and Neck Circumference</p>
	
<p>S11 – Saggital Midline slice (slice 16)</p>	

SUBJECT S13



S13 – Moment Arms at C4 (slice 27)

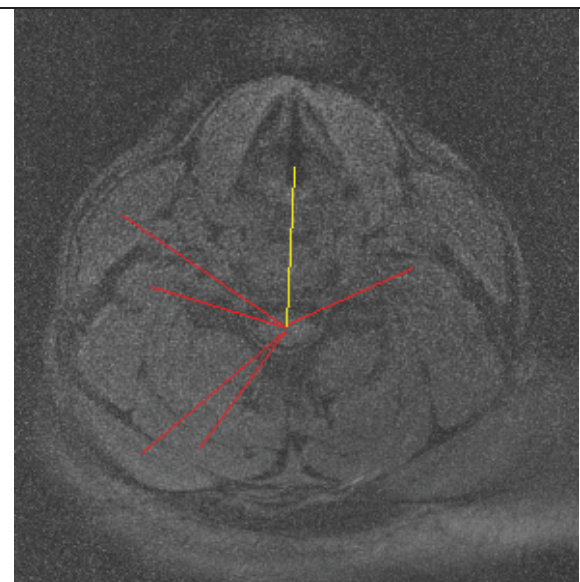
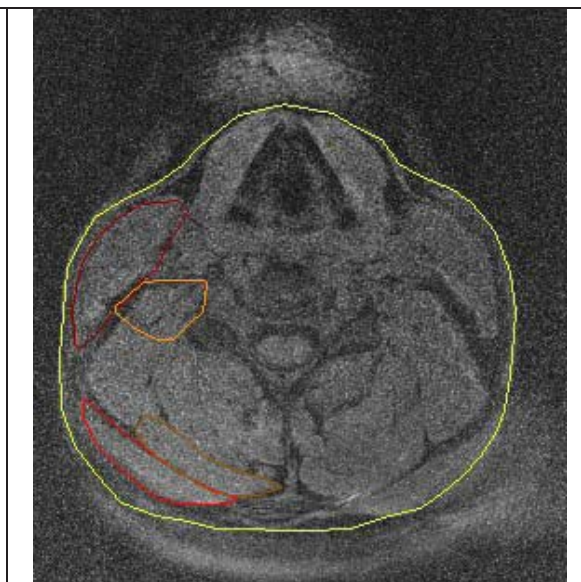
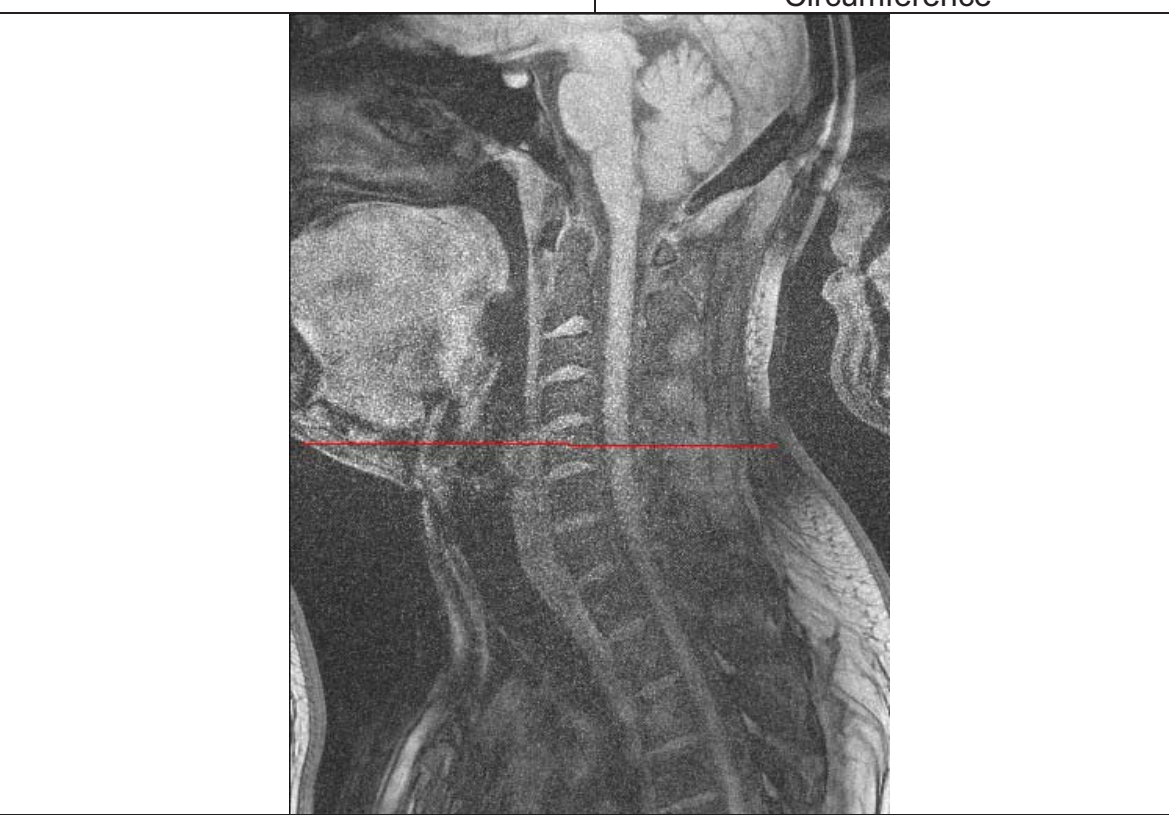


S13 – Boundaries for ACSA and Neck Circumference

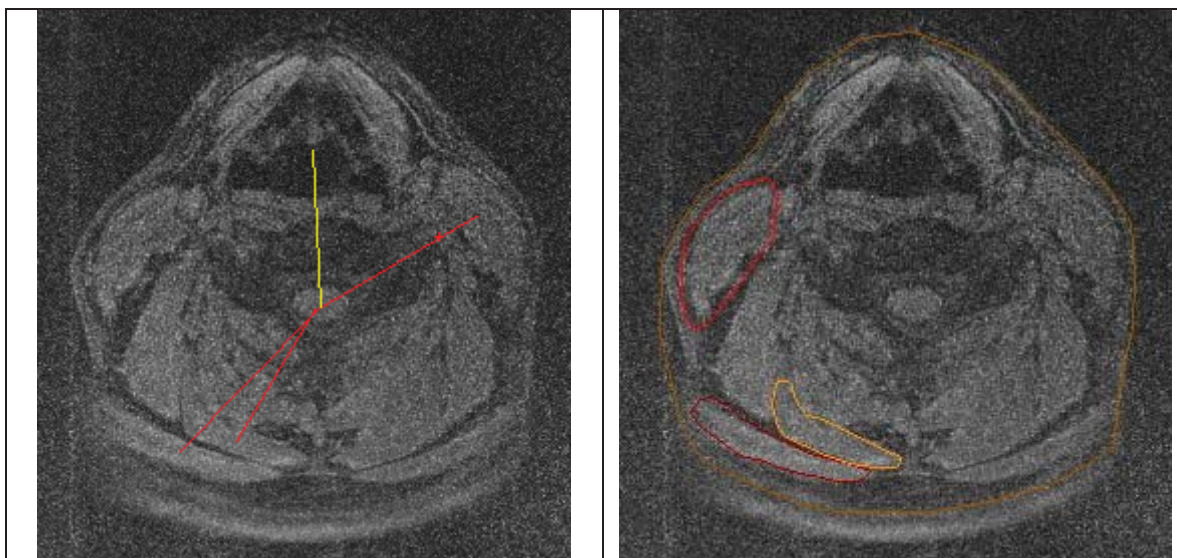


S13 – Saggital Midline slice (slice 16)

SUBJECT S14

	
S14 – Moment Arms at C4 (slice 26)	S14 – Boundaries for ACSA and Neck Circumference
	
S14 – Saggital Midline slice (slice 17)	

SUBJECT S15



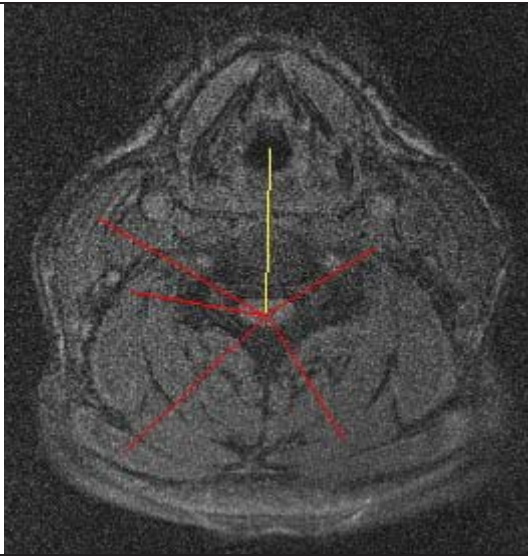
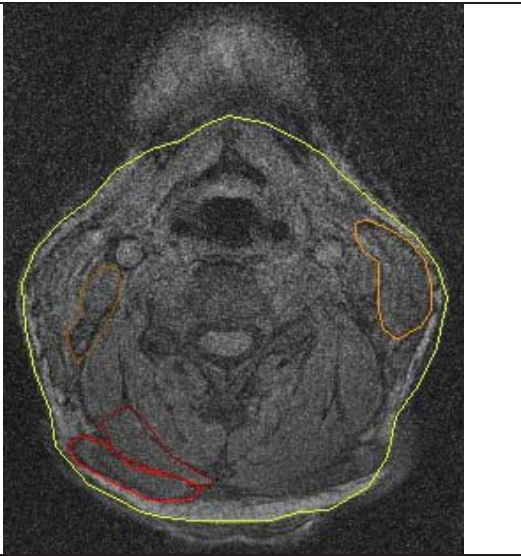

S15 – Moment Arms at C4 (slice 26)

S15 – Boundaries for ACSA and Neck Circumference

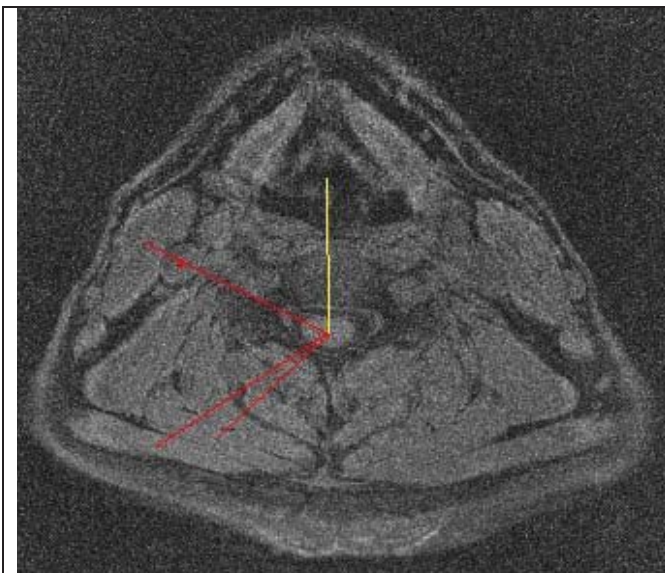


S15 – Saggital Midline slice (slice 16)

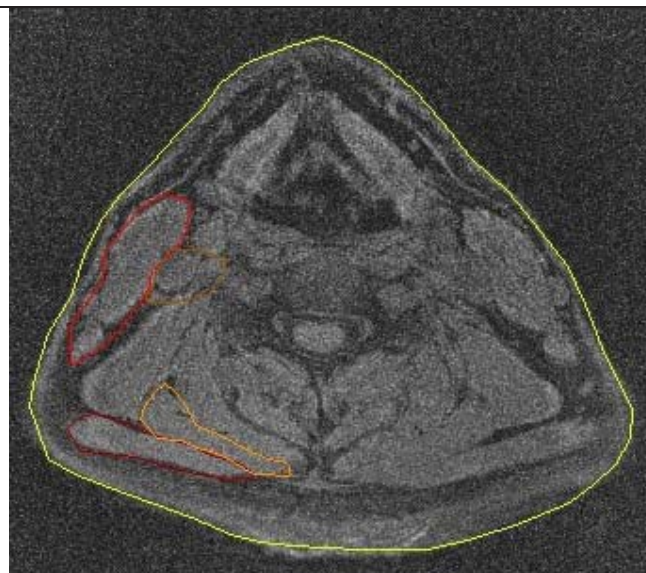
SUBJECT S16

	
<p>S16 – Moment Arms at C4 (slice 26)</p>	<p>S16 – Boundaries for ACSA and Neck Circumference</p>
	
<p>S16 – Saggital Midline slice (slice 16)</p>	

SUBJECT S17



S17 – Moment Arms at C4 (slice 28)

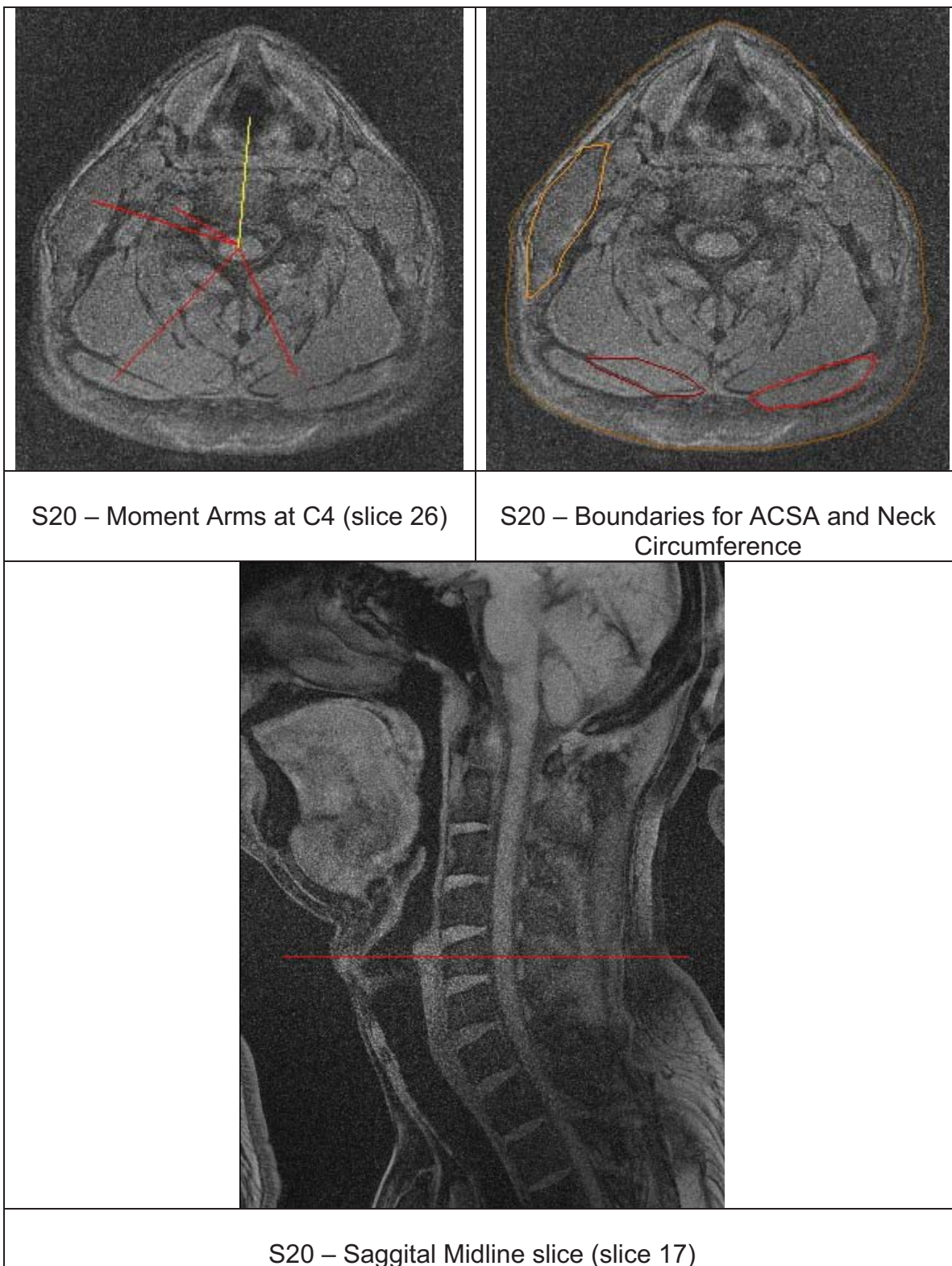


S17 – Boundaries for ACSA and Neck Circumference



S17 – Saggital Midline slice (slice 17)

SUBJECT S20



APPENDIX B

Tables and Figures for Chapter 5: Determination of Muscle Force and Stress at C-4 Vertebrae During a Maximal Voluntary Contraction

MVC - Extension							
		K03			K04		
		Peak	Mean	Mean	Peak	Mean	Mean
		(mV)	(mV)	%MVC	(mV)	(mV)	%MVC
SCM(R)	μV	8.108	1.638	0.010	15.245	0.970	0.004
SCM(L)	μV	26.638	2.474	0.010	19.916	1.076	0.005
TRAP(R)	μV	48.453	19.541	0.312	100.717	29.505	0.293
TRAP(L)	μV	71.288	18.949	0.266	54.039	19.508	0.361
SPL(R)	μV	121.924	34.032	0.182	22.280	5.402	0.022
SPL(L)	μV	80.736	20.234	0.105	64.565	17.636	0.109
SCAL(R)	μV	89.241	22.957	0.149	47.256	13.233	0.123
SCAL(L)	μV	66.621	14.573	0.139	63.026	15.446	0.133
				0.312			
MVC - Flexion							
		K03			K04		
		Peak	Mean	Mean	Peak	Mean	Mean
		(mV)	(mV)	%MVC	(mV)	(mV)	%MVC
SCM(R)	μV	156.775	58.003	0.370	233.162	101.630	0.436
SCM(L)	μV	236.143	40.111	0.170	218.142	89.811	0.412
TRAP(R)	μV	36.217	3.701	0.059	37.562	3.241	0.373
TRAP(L)	μV	55.374	5.461	0.077	28.498	1.395	0.527
SPL(R)	μV	68.291	11.089	0.059	156.170	41.551	0.650
SPL(L)	μV	65.424	9.566	0.050	112.426	31.830	0.692
SCAL(R)	μV	58.386	14.219	0.093	67.822	18.357	0.632
SCAL(L)	μV	64.880	11.676	0.111	49.594	15.794	0.428
				0.370			
MVC - Lateral (L)							
		K03		Mean	K04		Mean
		(mV)		%MVC	(mV)		%MVC
SCM(R)	μV	69.822		0.445	100.319		0.529
SCM(L)	μV	33.227		0.614	24.829		0.600
TRAP(R)	μV	81.580		0.446	43.242		0.232
TRAP(L)	μV	56.783			29.705		
SPL(R)	μV	21.928		0.437	130.826		0.180
SPL(L)	μV	123.147		1.000	82.100		1.000
SCAL(R)	μV	191.956		0.370	162.414		0.240
SCAL(L)	μV	104.943		1.000	117.775		1.000
MVC - Lateral (R)							
		K03		Mean	K04		Mean
		(mV)		%MVC	(mV)		%MVC
SCM(R)	μV	149.725		0.955	162.190		0.855
SCM(L)	μV	62.549		0.882	75.610		0.338
TRAP(R)	μV	186.656		0.840	240.409		0.706
TRAP(L)	μV	153.581		0.358	124.012		0.848
SPL(R)	μV	31.481		1.000	73.722		1.000
SPL(L)	μV	35.641		0.574	50.075		0.218
SCAL(R)	μV	110.271		1.000	35.441		1.000
SCAL(L)	μV	108.057		0.852	34.550		0.293

Table B-2: Peak and Mean EMG values and %MVC for 10 year old boys adult males in maximal bending in flexion, extension and lateral bending

MVC - Extension

		K05			K06		
		Peak (mV)	Mean (mV)	Mean %MVC	Peak (mV)	Mean (mV)	Mean %MVC
SCM(R)	μV	67.140	11.227	0.042	47.992	4.508	0.020
SCM(L)	μV	95.959	25.541	0.068	151.045	26.544	0.175
TRAP(R)	μV	66.869	20.098	0.301	139.934	42.563	0.304
TRAP(L)	μV	110.478	29.249	0.265	98.797	26.740	0.271
SPL(R)	μV	251.116	55.496	0.221	125.341	37.167	0.210
SPL(L)	μV	177.441	42.942	0.242	123.192	31.839	0.258
SCAL(R)	μV	65.139	18.836	0.263	112.425	29.693	0.205
SCAL(L)	μV	110.083	23.134	0.210	120.000	40.853	0.340
				0.301			0.340

MVC - Flexion

		K05			K06		
		Peak (mV)	Mean (mV)	Mean %MVC	Peak (mV)	Mean (mV)	Mean %MVC
SCM(R)	μV	270.211	92.096	0.341	220.372	74.123	0.336
SCM(L)	μV	374.353	127.452	0.340	151.332	49.971	0.330
TRAP(R)	μV	41.025	3.966	0.059	26.102	2.662	0.019
TRAP(L)	μV	98.621	11.301	0.102	19.737	2.833	0.029
SPL(R)	μV	130.519	19.637	0.078	176.971	64.645	0.365
SPL(L)	μV	135.244	25.568	0.144	47.525	18.249	0.148
SCAL(R)	μV	54.265	14.189	0.815	144.618	39.652	0.274
SCAL(L)	μV	85.256	19.217	0.175	82.431	29.902	0.249
				0.815			0.365

MVC - Lateral (L)

		K05 (mV)	Mean %MVC	K06 (mV)	Mean %MVC
SCM(R)	μV	77.475	0.280	83.861	0.379
SCM(L)	μV	43.718	0.386	40.544	0.158
TRAP(R)	μV	152.691	0.654	59.954	0.274
TRAP(L)	μV	109.121	0.583	70.945	0.383
SPL(R)	μV	144.461	0.542	23.962	0.501
SPL(L)	μV	69.144	0.778	46.859	0.636
SCAL(R)	μV	141.164	1.000	63.443	0.491
SCAL(L)	μV	66.960	0.589	46.341	0.365

MVC - Lateral (R)

		K05 (mV)	Mean %MVC	K06 (mV)	Mean %MVC
SCM(R)	μV	148.242	0.536	37.186	0.168
SCM(L)	μV	39.895	0.266	115.281	0.578
TRAP(R)	μV	140.556	0.597	140.282	0.780
TRAP(L)	μV	53.528	0.434	130.843	0.187
SPL(R)	μV	99.402	0.560	87.490	0.793
SPL(L)	μV	51.513	0.335	22.896	0.467
SCAL(R)	μV	60.764	0.491	46.607	0.905
SCAL(L)	μV	30.445	0.268	52.902	0.416

Table B-2: Peak and Mean EMG values and %MVC for 10 year old boys adult males in maximal bending in flexion, extension and lateral bending

MVC - Extension

		K07			K09		
		Peak (mV)	Mean (mV)	Mean %MVC	Peak (mV)	Mean (mV)	Mean %MVC
SCM(R)	μV	18.638	1.816	0.010	37.155	3.782	0.039
SCM(L)	μV	11.730	1.586	0.009	39.346	4.148	0.033
TRAP(R)	μV	110.667	36.445	0.329	42.412	20.388	0.481
TRAP(L)	μV	44.923	17.173	0.382	103.436	20.724	0.200
SPL(R)	μV	76.510	10.272	0.064	99.585	21.014	0.211
SPL(L)	μV	98.267	22.469	0.128	85.084	19.886	0.234
SCAL(R)	μV	69.936	15.115	0.103	74.500	20.483	0.193
SCAL(L)	μV	3.128	0.368	0.032	73.228	16.643	0.163
				0.382			0.481

MVC - Flexion

		K07			K09		
		Peak (mV)	Mean (mV)	Mean %MVC	Peak (mV)	Mean (mV)	Mean %MVC
SCM(R)	μV	165.283	77.326	0.426	97.316	44.167	0.454
SCM(L)	μV	179.784	78.587	0.437	124.244	57.629	0.464
TRAP(R)	μV	60.515	3.963	0.036	23.658	2.339	0.055
TRAP(L)	μV	64.078	4.838	0.230	97.602	1.706	0.016
SPL(R)	μV	0.000	22.455	0.000	101.405	23.759	0.239
SPL(L)	μV	92.808	27.377	0.156	173.348	33.452	0.393
SCAL(R)	μV	82.753	21.220	0.145	72.205	18.331	0.173
SCAL(L)	μV	6.130	0.583	0.051	75.282	10.190	0.100
				0.437			0.464

MVC - Lateral (L)

		K07 (mV)		Mean %MVC	K09 (mV)		Mean %MVC
SCM(R)	μV	94.966		0.752	41.928		0.464
SCM(L)	μV	48.895		0.703	17.465		0.638
TRAP(R)	μV	72.205		0.572	26.166		0.311
TRAP(L)	μV	100.234		0.607	21.290		0.311
SPL(R)	μV	22.057		0.329	73.084		0.311
SPL(L)	μV	49.484		1.000	24.278		0.311
SCAL(R)	μV	73.969			81.077		0.311
SCAL(L)	μV	53.565			102.362		0.311

MVC - Lateral (R)

		K07 (mV)		Mean %MVC	K09 (mV)		Mean %MVC
SCM(R)	μV	26.169		1.000	44.467		0.493
SCM(L)	μV	113.354		0.453	35.828		0.530
TRAP(R)	μV	126.244		0.573	86.572		0.639
TRAP(L)	μV	124.204		0.385	105.858		0.214
SPL(R)	μV	76.220		1.000	60.781		0.666
SPL(L)	μV	23.535		0.202	23.955		0.560
SCAL(R)	μV	45.205		1.000	59.507		1.000
SCAL(L)	μV	56.176		0.156	22.857		0.223

Table B-2: Peak and Mean EMG values and %MVC for 10 year old boys adult males in maximal bending in flexion, extension and lateral bending

MVC - Extension

		K10			K11			Average	Average	Average
		Peak (mV)	Mean (mV)	Mean %MVC	Peak (mV)	Mean (mV)	Average %MVC	Peak (mV)	Mean (mV)	Average %MVC
SCM(R)	μV	77.522	12.295	0.079	10.312	1.567	0.009	38.124	5.262	0.030
SCM(L)	μV	55.054	16.929	0.383	8.966	0.209	0.003	55.534	11.061	0.097
TRAP(R)	μV	123.223	37.243	0.302	56.100	14.094	0.182	83.951	27.196	0.316
TRAP(L)	μV	89.824	26.805	0.298	56.927	14.240	0.168	82.239	21.983	0.264
SPL(R)	μV	94.857	15.816	0.084	88.164	16.922	0.096	122.500	27.245	0.153
SPL(L)	μV	64.013	17.264	0.270	90.886	12.164	0.050	102.802	23.828	0.184
SCAL(R)	μV	87.871	27.688	0.315	84.742	15.674	0.067	83.408	21.492	0.185
SCAL(L)	μV	52.448	18.045	0.344	123.120	14.697	0.060	78.376	18.330	0.184
							0.182			

MVC - Flexion

		K10			K11			Average	Average	Average
		Peak (mV)	Mean (mV)	Mean %MVC	Peak (mV)	Mean (mV)	Average %MVC	Peak (mV)	Mean (mV)	Average %MVC
SCM(R)	μV	155.268	52.150	0.336	78.706	18.522	0.106	163.419	59.484	0.338
SCM(L)	μV	44.182	1.283	0.029	109.728	26.578	0.242	174.252	54.516	0.288
TRAP(R)	μV	86.455	32.419	0.263	26.135	2.358	0.030	42.872	7.344	0.075
TRAP(L)	μV	80.844	28.019	0.312	13.742	0.621	0.007	61.428	7.826	0.111
SPL(R)	μV	187.484	62.301	0.332	72.633	13.531	0.076	105.329	31.059	0.164
SPL(L)	μV	12.217	2.222	0.035	49.847	8.435	0.035	82.345	17.838	0.137
SCAL(R)	μV	42.318	19.045	0.217	79.273	17.863	0.077	76.260	20.645	0.256
SCAL(L)	μV	46.495	14.080	0.268	74.481	7.114	0.029	62.136	13.252	0.140
							0.242			

MVC - Lateral (L)

		K10 (mV)	Mean %MVC	K11 (mV)	Mean %MVC	Average Peak (mV)	Average Mean (mV)	Average %MVC
SCM(R)	μV	25.941	0.124	42.285	0.241	62.325		0.441
SCM(L)	μV	5.432	0.243	114.566	1.000	43.407		0.549
TRAP(R)	μV	16.543	0.098	25.459	0.329	62.085		0.354
TRAP(L)	μV	17.321	0.429	84.976	1.000	65.810		0.571
SPL(R)	μV	43.196	0.150	68.382	0.387	56.724		0.337
SPL(L)	μV	19.740	0.611	240.976	1.000	81.947		0.815
SCAL(R)	μV	51.676	0.214	113.916	0.488	102.457		0.418
SCAL(L)	μV	48.469	0.958	246.891	1.000	95.647		0.778

MVC - Lateral (R)

		K10 (mV)	Mean %MVC	K11 (mV)	Mean %MVC	Average Peak (mV)	Average Mean (mV)	Average %MVC
SCM(R)	μV	102.311	0.490	175.378	1.000	97.640		0.701
SCM(L)	μV	11.504	0.127	69.746	0.609	64.022		0.473
TRAP(R)	μV	75.218	0.209	77.338	1.000	118.981		0.668
TRAP(L)	μV	72.133	0.268	36.903	0.434	96.721		0.363
SPL(R)	μV	22.580	0.681	176.879	1.000	79.262		0.856
SPL(L)	μV	12.342	0.162	55.539	0.230	32.203		0.342
SCAL(R)	μV	13.731	0.889	233.289	1.000	81.339		0.921
SCAL(L)	μV	15.589	0.308	42.939	0.174	46.995		0.325

Table B-2: Peak and Mean EMG values and %MVC for 10 year old boys adult males in maximal bending in flexion, extension and lateral bending

MVC - Extension

		S08			S09		
		Peak (mV)	Mean (mV)	Mean %MVC	Peak (mV)	Mean (mV)	Mean %MVC
SCM(R)	μV	186.525	51.631	0.277	296.402	137.920	0.365
SCM(L)	μV	195.738	56.366	0.288	432.098	184.372	0.335
TRAP(R)	μV	76.140	26.324	0.346	50.534	23.533	0.364
TRAP(L)	μV	165.785	60.854	0.367	50.725	20.905	0.412
SPL(R)	μV	234.185	70.506	0.301	161.550	74.368	0.460
SPL(L)	μV	217.398	90.389	0.416	0.000	0.000	0.000
SCAL(R)	μV	298.937	86.130	0.288	345.851	120.453	0.340
SCAL(L)	μV	325.310	122.617	0.377	81.211	39.826	0.306
							0.460

MVC - Flexion

		S08			S09		
		Peak (mV)	Mean (mV)	Mean %MVC	Peak (mV)	Mean (mV)	Mean %MVC
SCM(R)	μV	126.966	46.645	0.250	221.696	69.763	0.185
SCM(L)	μV	101.079	31.088	0.159	294.781	108.499	0.197
TRAP(R)	μV	55.038	10.152	0.133	41.253	8.047	0.125
TRAP(L)	μV	89.229	31.347	0.189	40.593	7.407	0.146
SPL(R)	μV	140.954	51.889	0.222	48.783	8.892	0.055
SPL(L)	μV	110.752	47.299	0.218	0.000	0.000	0.000
SCAL(R)	μV	216.424	72.524	0.243	100.322	24.623	0.069
SCAL(L)	μV	222.418	42.738	0.131	37.545	8.389	0.065
							0.197

MVC - Lateral (L)

		S08			S09		
		Peak (mV)	Mean (mV)	Mean %MVC	Peak (mV)	Mean (mV)	Mean %MVC
SCM(R)	μV	15.467	0.318		251.791		0.666
SCM(L)	μV	8.147	0.168		551.097		1.000
TRAP(R)	μV	5.417	0.226		57.237		0.886
TRAP(L)	μV	17.066	0.711		39.791		0.784
SPL(R)	μV	24.297	0.530		143.122		0.886
SPL(L)	μV	45.809	1.000		143.122		1.000
SCAL(R)	μV	16.995	0.458		198.069		0.559
SCAL(L)	μV	37.101	1.000		130.024		1.000

MVC - Lateral (R)

		S08			S09		
		Peak (mV)	Mean (mV)	Mean %MVC	Peak (mV)	Mean (mV)	Mean %MVC
SCM(R)	μV	21.966	0.452		378.055		1.000
SCM(L)	μV	7.503	0.154		410.685		0.745
TRAP(R)	μV	20.567	0.857		64.629		1.000
TRAP(L)	μV	6.834	0.285		47.900		0.944
SPL(R)	μV	50.427	1.000		126.367		0.782
SPL(L)	μV	8.671	0.172		3.052		0.021
SCAL(R)	μV	27.194	1.000		354.636		1.000
SCAL(L)	μV	10.907	0.401		78.115		0.601

Table B-2: Peak and Mean EMG values and %MVC for 50th percentile adult males in maximal bending in flexion, extension and lateral bending

MVC - Extension

		S11			S13		
		Peak (mV)	Mean (mV)	Mean %MVC	Peak (mV)	Mean (mV)	Mean %MVC
SCM(R)	μV	11.181	0.556	0.015	157.587	22.122	0.063
SCM(L)	μV	12.928	0.375	0.011	80.741	7.232	0.030
TRAP(R)	μV	43.263	6.822	0.158	116.345	39.491	0.339
TRAP(L)	μV	29.056	5.541	0.191	43.238	16.283	0.377
SPL(R)	μV	58.832	11.972	0.203	339.628	91.917	0.271
SPL(L)	μV	46.842	5.253	0.112	169.878	50.059	0.286
SCAL(R)	μV	47.697	5.667	0.119	263.067	68.521	0.260
SCAL(L)	μV	30.124	3.079	0.083	118.384	32.824	0.252
				0.203			0.377

MVC - Flexion

		S11			S13		
		Peak (mV)	Mean (mV)	Mean %MVC	Peak (mV)	Mean (mV)	Mean %MVC
SCM(R)	μV	37.104	13.774	0.371	353.196	101.941	0.289
SCM(L)	μV	32.915	8.666	0.263	242.609	48.931	0.202
TRAP(R)	μV	3.266	0.114	0.003	61.939	5.040	0.043
TRAP(L)	μV	2.309	0.094	0.003	31.232	3.786	0.088
SPL(R)	μV	19.005	5.168	0.088	124.495	30.445	0.174
SPL(L)	μV	17.208	4.757	0.102	117.143	12.562	0.072
SCAL(R)	μV	14.719	5.025	0.105	125.849	32.018	0.246
SCAL(L)	μV	8.104	1.293	0.035	88.127	17.366	0.134
				0.371			0.289

MVC - Lateral (L)

		S11			S13		
		Peak (mV)	Mean (mV)	Mean %MVC	Peak (mV)	Mean (mV)	Mean %MVC
SCM(R)	μV	15.467		0.417	33.422		0.095
SCM(L)	μV	8.147		0.248	176.794		0.729
TRAP(R)	μV	5.417		0.125	83.527		0.718
TRAP(L)	μV	17.066		0.587	28.376		0.656
SPL(R)	μV	24.297		0.202	97.984		0.289
SPL(L)	μV	45.809		0.978	92.957		0.547
SCAL(R)	μV	16.995		0.356	65.877		0.250
SCAL(L)	μV	37.101		1.000	72.855		0.615

MVC - Lateral (R)

		S11			S13		
		Peak (mV)	Mean (mV)	Mean %MVC	Peak (mV)	Mean (mV)	Mean %MVC
SCM(R)	μV			0.592	361.635		1.024
SCM(L)	μV	21.966		0.228	50.788		0.209
TRAP(R)	μV	7.503		0.475	77.306		0.664
TRAP(L)	μV	20.567		0.235	16.817		0.389
SPL(R)	μV	6.834		0.420	174.802		1.000
SPL(L)	μV	50.427		0.185	24.582		0.145
SCAL(R)	μV	8.671		0.570	130.060		1.000
SCAL(L)	μV	27.194		0.294	25.092		0.212

Table B-2: Peak and Mean EMG values and %MVC for 50th percentile adult males in maximal bending in flexion, extension and lateral bending

MVC - Extension

		S14			S15		
		Peak (mV)	Mean (mV)	Mean %MVC	Peak (mV)	Mean (mV)	Mean %MVC
SCM(R)	µV	11.020	3.274	0.024	116.941	56.017	0.282
SCM(L)	µV	49.319	4.906	0.033	130.114	48.643	0.278
TRAP(R)	µV	25.420	5.005	0.197	36.171	15.287	0.348
TRAP(L)	µV	12.514	4.322	0.197	27.516	11.095	0.403
SPL(R)	µV	22.031	2.724	0.053	89.932	36.785	0.257
SPL(L)	µV	40.750	12.338	0.251	83.420	36.650	0.400
SCAL(R)	µV	12.151	4.998	0.064	197.413	68.595	0.206
SCAL(L)	µV	17.936	6.534	0.114	40.450	18.847	0.348
				0.251			0.403

MVC - Flexion

		S14			S15		
		Peak (mV)	Mean (mV)	Mean %MVC	Peak (mV)	Mean (mV)	Mean %MVC
SCM(R)	µV	136.430	45.752	0.335	198.700	83.829	0.422
SCM(L)	µV	146.744	48.799	0.333	174.949	78.107	0.446
TRAP(R)	µV	3.913	1.032	0.041	28.814	10.142	0.280
TRAP(L)	µV	5.129	1.496	0.059	19.104	5.858	0.213
SPL(R)	µV	48.017	18.430	0.358	92.642	33.242	0.232
SPL(L)	µV	42.247	13.788	0.280	77.037	31.130	0.339
SCAL(R)	µV	77.696	29.287	0.377	269.326	87.676	0.263
SCAL(L)	µV	51.073	17.119	0.298	45.212	16.580	0.306
				0.377			0.446

MVC - Lateral (L)

		S14			S15		
		Peak (mV)	Mean (mV)	Mean %MVC	Peak (mV)	Mean (mV)	Mean %MVC
SCM(R)	µV	11.311		0.666	175.639		0.838
SCM(L)	µV	59.257		0.144	51.283		0.863
TRAP(R)	µV	28.123		0.491	83.537		1.000
TRAP(L)	µV	9.873		0.172	142.043		0.845
SPL(R)	µV	32.825		1.042	160.386		0.542
SPL(L)	µV	31.494		1.000	32.674		1.000
SCAL(R)	µV	22.161		0.893	102.769		0.413
SCAL(L)	µV	24.823		1.000	65.139		1.000

MVC - Lateral (R)

		S14			S15		
		Peak (mV)	Mean (mV)	Mean %MVC	Peak (mV)	Mean (mV)	Mean %MVC
SCM(R)	µV	121.084		0.320	193.186		0.922
SCM(L)	µV	17.075		0.042	55.495		0.907
TRAP(R)	µV	26.149		0.457	154.129		1.000
TRAP(L)	µV	5.814		0.102	344.148		0.756
SPL(R)	µV	58.740		1.000	168.641		1.000
SPL(L)	µV	8.304		0.141	29.235		0.779
SCAL(R)	µV	43.877		1.000	80.063		1.000
SCAL(L)	µV	8.533		0.194	51.729		0.794

Table B-2: Peak and Mean EMG values and %MVC for 50th percentile adult males in maximal bending in flexion, extension and lateral bending

MVC - Extension

		S16			S17		
		Peak (mV)	Mean (mV)	Mean %MVC	Peak (mV)	Mean (mV)	Mean %MVC
SCM(R)	μV	7.659	0.850	0.009	39.656	10.271	0.122
SCM(L)	μV	27.649	2.060	0.021	33.826	6.161	0.160
TRAP(R)	μV	16.462	6.899	0.419	6.858	0.554	0.081
TRAP(L)	μV	14.991	6.189	0.413	15.856	3.679	0.164
SPL(R)	μV	54.884	17.686	0.217	88.334	27.661	0.280
SPL(L)	μV	28.155	7.432	0.136	37.055	10.572	0.285
SCAL(R)	μV	21.642	6.306	0.082	58.640	22.030	0.376
SCAL(L)	μV	25.001	7.377	0.087	47.249	15.464	0.327
				0.419			0.376

MVC - Flexion

		S16			S17		
		Peak (mV)	Mean (mV)	Mean %MVC	Peak (mV)	Mean (mV)	Mean %MVC
SCM(R)	μV	42.707	0.435	0.527	83.940	37.148	0.443
SCM(L)	μV	48.577	0.503	0.590	38.389	13.204	0.344
TRAP(R)	μV	0.321	0.019	0.048	1.219	0.457	0.067
TRAP(L)	μV	0.292	0.019	0.048	4.451	0.433	0.019
SPL(R)	μV	3.289	0.040	0.085	98.737	43.609	0.442
SPL(L)	μV	3.498	0.064	0.121	32.573	8.103	0.219
SCAL(R)	μV	12.535	0.163	0.248	55.014	22.056	0.382
SCAL(L)	μV	11.992	0.142	0.223	24.823	7.084	0.150
				0.590			0.443

MVC - Lateral (L)

		S16			S17		
		Peak (mV)	Mean (mV)	Mean %MVC	Peak (mV)	Mean (mV)	Mean %MVC
SCM(R)	μV	29.048		0.310	37.412		0.395
SCM(L)	μV	3.245		0.857	4.087		0.388
TRAP(R)	μV	2.869		0.080	44.300		0.277
TRAP(L)	μV	3.508		0.421	38.407		0.841
SPL(R)	μV	84.465		0.037	19.574		0.400
SPL(L)	μV	16.979		1.000	19.496		0.647
SCAL(R)	μV	54.482		0.041	28.833		0.572
SCAL(L)	μV	84.566		1.000	33.051		0.661

MVC - Lateral (R)

		S16			S17		
		Peak (mV)	Mean (mV)	Mean %MVC	Peak (mV)	Mean (mV)	Mean %MVC
SCM(R)	μV	103.036			51.419		0.542
SCM(L)	μV	16.802		0.563	5.089		0.434
TRAP(R)	μV	78.069		0.416	76.952		0.345
TRAP(L)	μV	86.157		0.141	57.730		1.000
SPL(R)	μV	55.492		1.000	21.850		0.695
SPL(L)	μV	4.889		0.102	23.175		0.663
SCAL(R)	μV	5.561		1.000	29.558		0.860
SCAL(L)	μV	10.663		0.126	25.034		0.500

Table B-2: Peak and Mean EMG values and %MVC for 50th percentile adult males in maximal bending in flexion, extension and lateral bending

MVC - Extension

		S20			Average	Average	
		Peak	Mean	Mean	Peak	Mean	Average
		(mV)	(mV)	%MVC	(mV)	(mV)	%MVC
SCM(R)	μV	45.287	2.372	0.018	85.717	29.173	0.112
SCM(L)	μV	29.863	2.286	0.021	99.567	32.004	0.111
TRAP(R)	μV	23.287	7.444	0.240	39.792	13.129	0.268
TRAP(L)	μV	21.412	7.040	0.294	26.913	9.382	0.306
SPL(R)	μV	31.304	5.978	0.191	105.812	33.636	0.242
SPL(L)	μV	43.336	8.307	0.112	56.179	16.326	0.198
SCAL(R)	μV	19.749	4.396	0.182	120.776	37.621	0.204
SCAL(L)	μV	44.533	6.708	0.084	50.611	16.332	0.200

MVC - Flexion

		S20			Average	Average	
		Peak	Mean	Mean	Peak	Mean	Average
		(mV)	(mV)	%MVC	(mV)	(mV)	%MVC
SCM(R)	μV	133.741	55.897	0.418	150.939	51.067	0.374
SCM(L)	μV	110.957	41.045	0.303	136.240	43.469	0.335
TRAP(R)	μV	2.537	0.688	0.022	17.908	3.192	0.079
TRAP(L)	μV	3.342	0.644	0.027	13.306	2.467	0.075
SPL(R)	μV	5.749	0.946	0.030	55.090	17.597	0.183
SPL(L)	μV	16.258	2.984	0.040	38.245	9.174	0.147
SCAL(R)	μV	12.993	1.713	0.071	83.557	25.320	0.220
SCAL(L)	μV	14.124	2.618	0.033	35.125	8.824	0.155

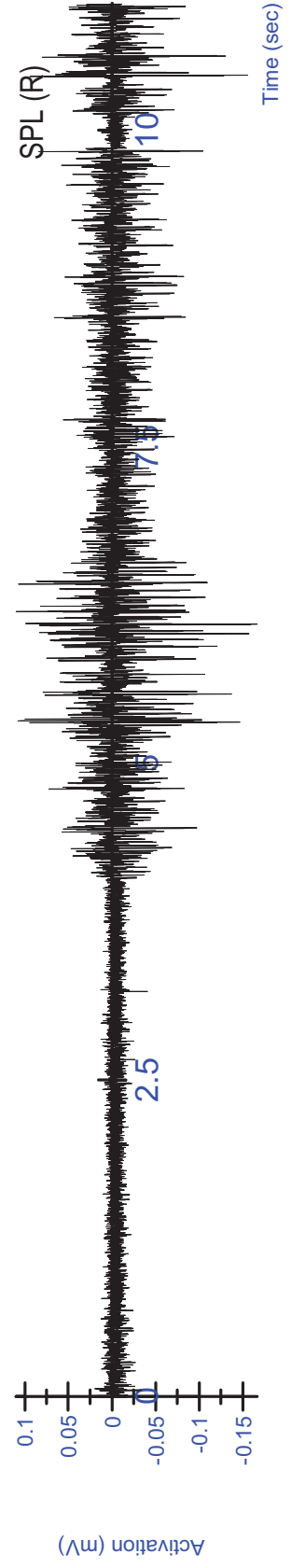
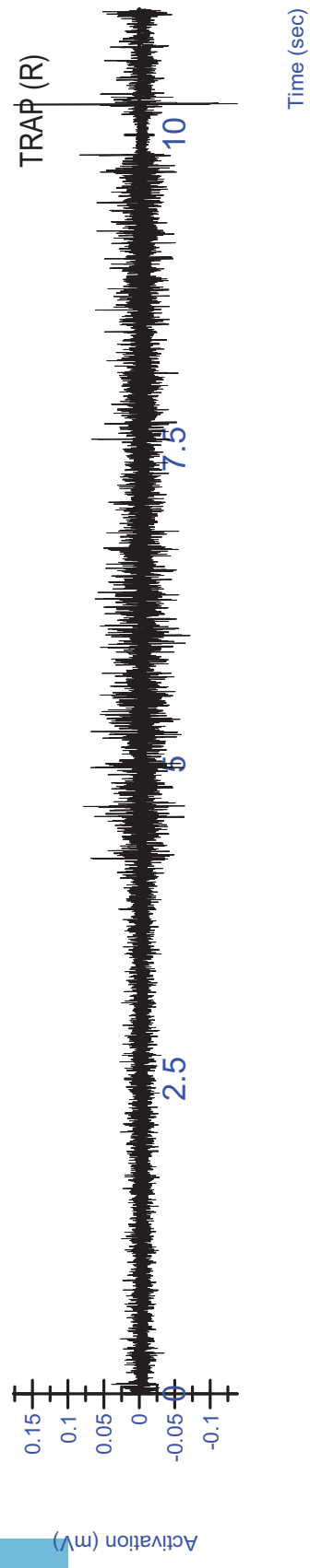
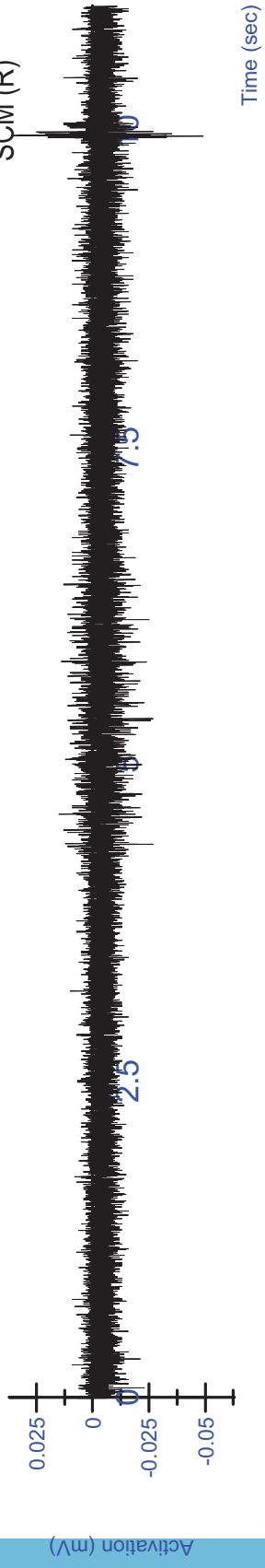
MVC - Lateral (L)

		S20			Average	Average	
		Peak	Mean	Mean	Peak	Mean	Average
		(mV)	(mV)	%MVC	(mV)	(mV)	%MVC
SCM(R)	μV	37.412		0.243	73.938	0.318	0.454
SCM(L)	μV	4.087		1.219	107.250	0.168	0.681
TRAP(R)	μV	44.300		0.383	43.664	0.226	0.495
TRAP(L)	μV	38.407		1.000	39.684	0.711	0.663
SPL(R)	μV	19.574		0.716	72.778	0.530	0.514
SPL(L)	μV	19.496		1.000	50.253	1.000	0.897
SCAL(R)	μV	28.833		0.501	64.752	0.458	0.448
SCAL(L)	μV	33.051		1.000	60.076	1.000	0.910

MVC - Lateral (R)

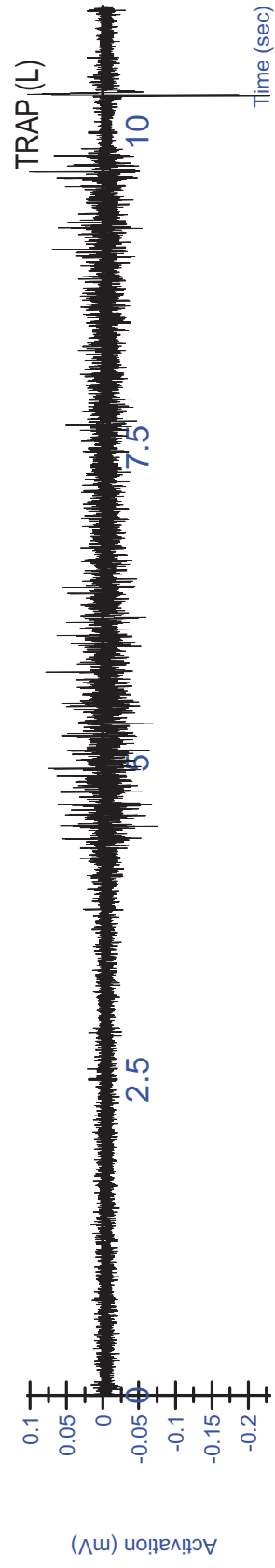
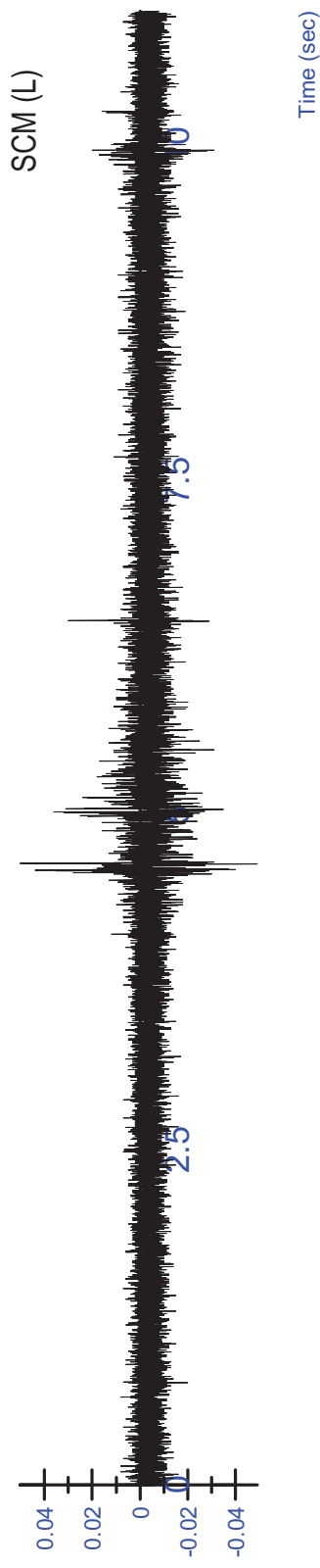
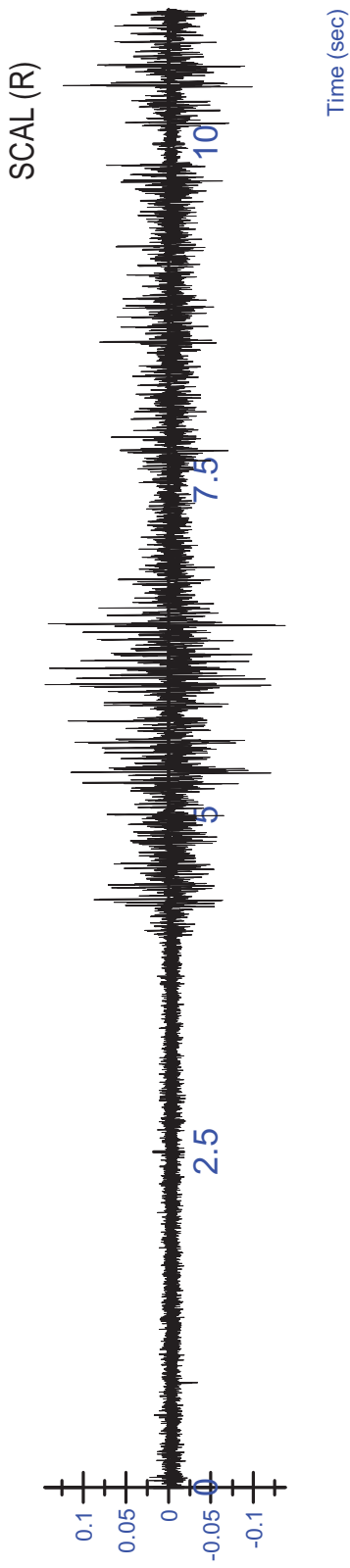
		S20			Average	Average	
		Peak	Mean	Mean	Peak	Mean	Average
		(mV)	(mV)	%MVC	(mV)	(mV)	%MVC
SCM(R)	μV	51.419		0.873	179.976	0.452	0.753
SCM(L)	μV	5.089		0.221	72.874	0.154	0.419
TRAP(R)	μV	76.952		1.000	70.211	0.857	0.670
TRAP(L)	μV	57.730		0.496	79.608	0.285	0.508
SPL(R)	μV	21.850		0.897	79.322	1.000	0.849
SPL(L)	μV	23.175		0.169	20.855	0.172	0.276
SCAL(R)	μV	29.558		1.000	85.248	1.000	0.929
SCAL(L)	μV	25.034		0.213	31.424	0.401	0.367

Table B-2: Peak and Mean EMG values and %MVC for 50th percentile adult males in maximal bending in flexion, extension and lateral bending

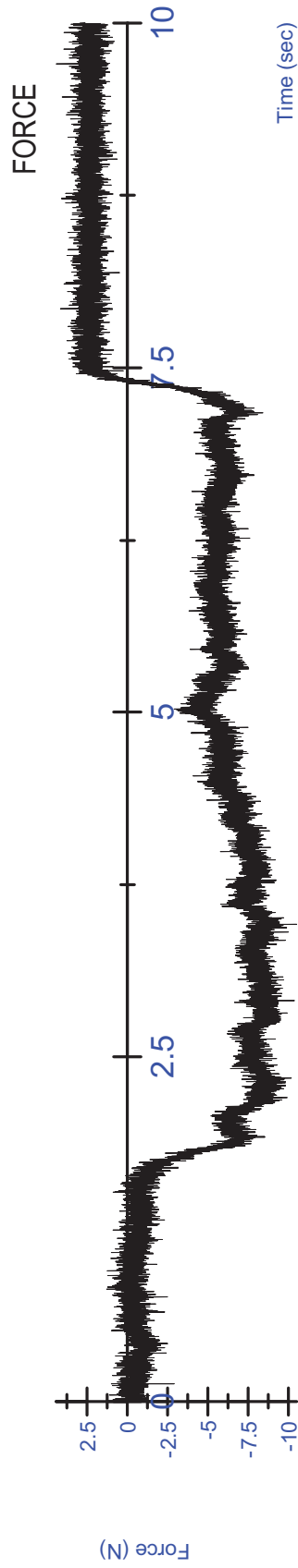
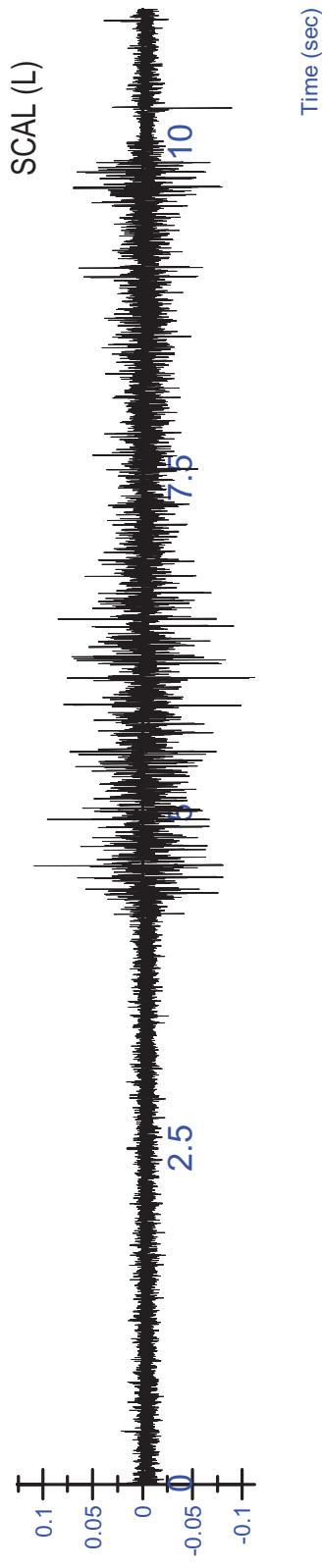
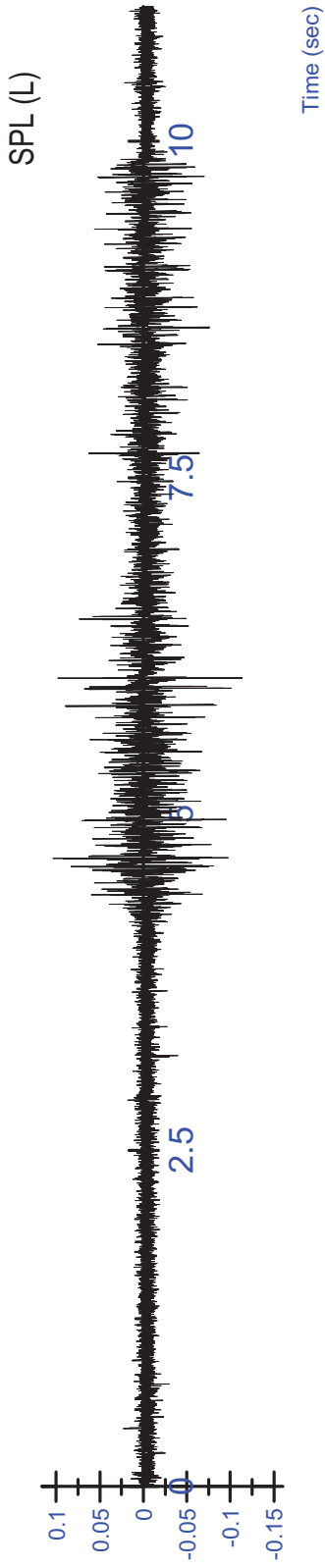


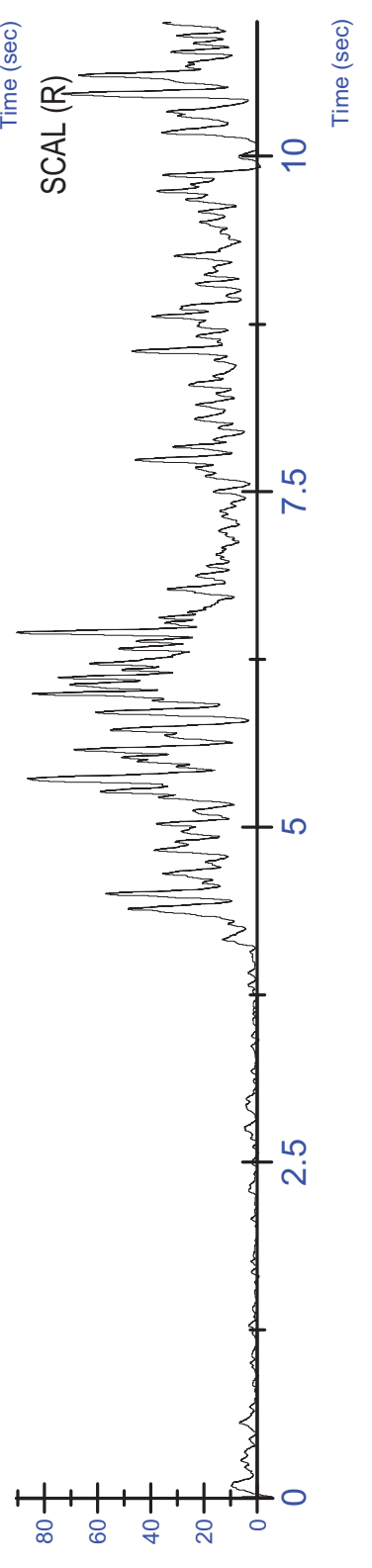
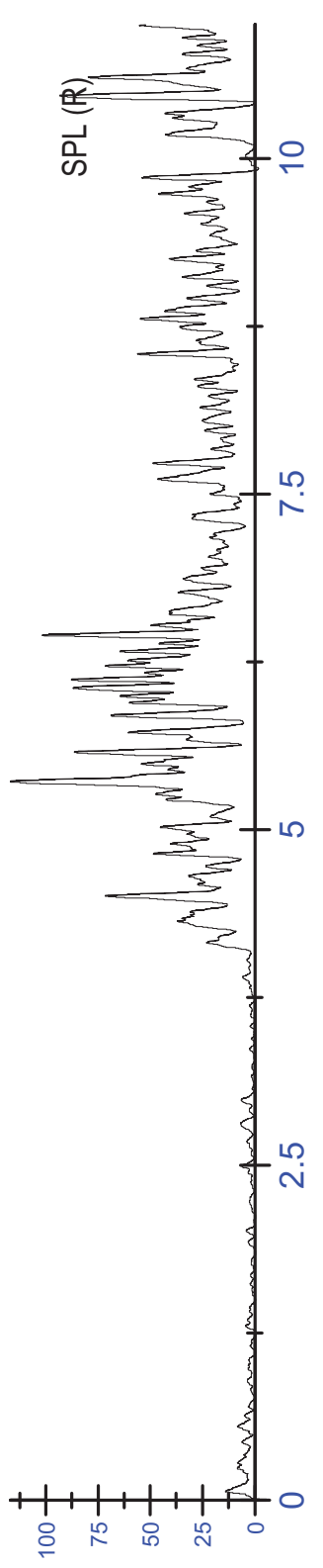
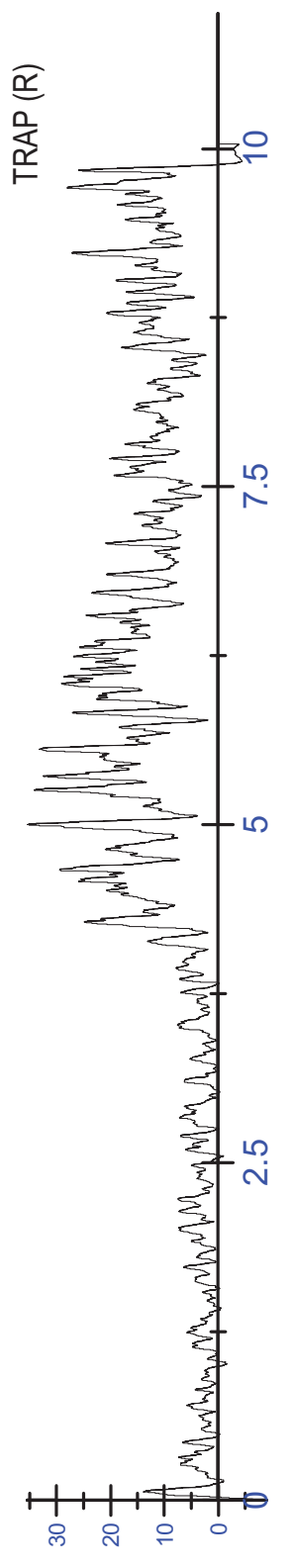
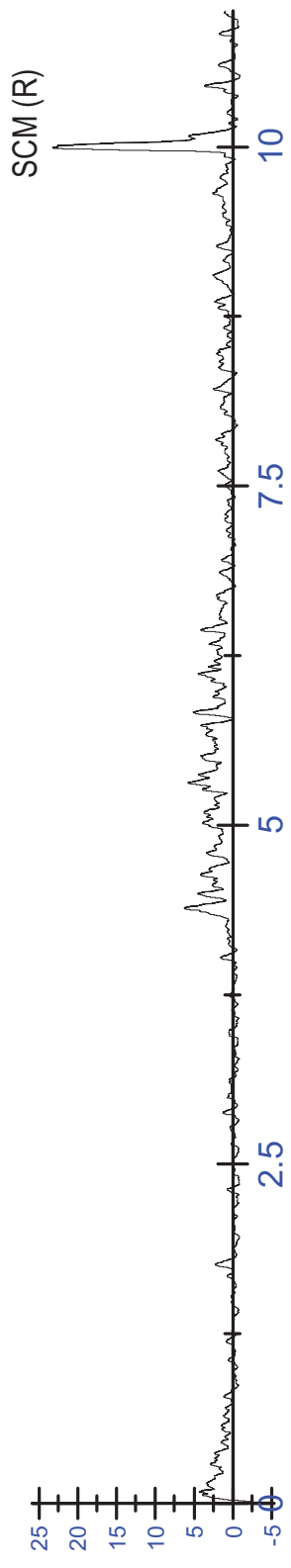
K03 MVC - Extension Trial 1 - Unfiltered

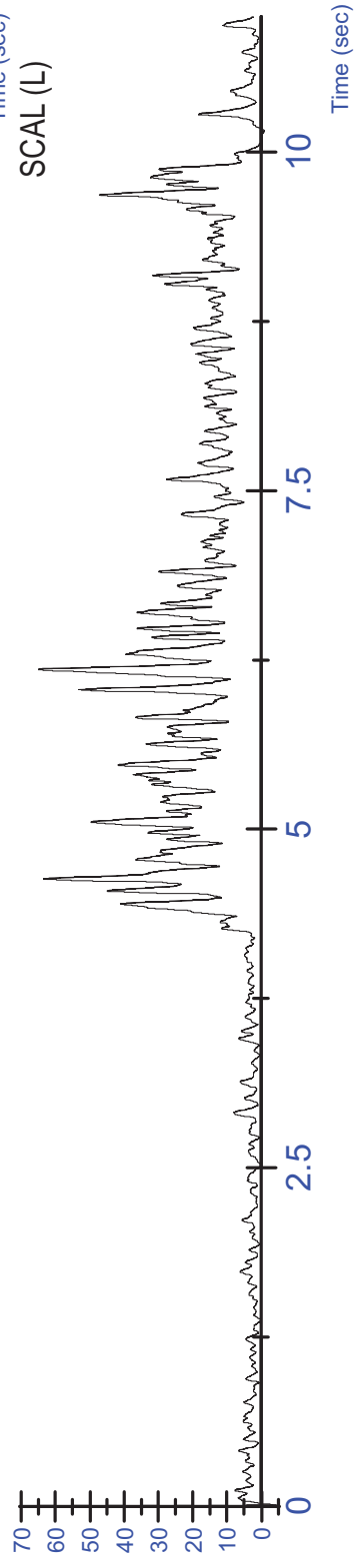
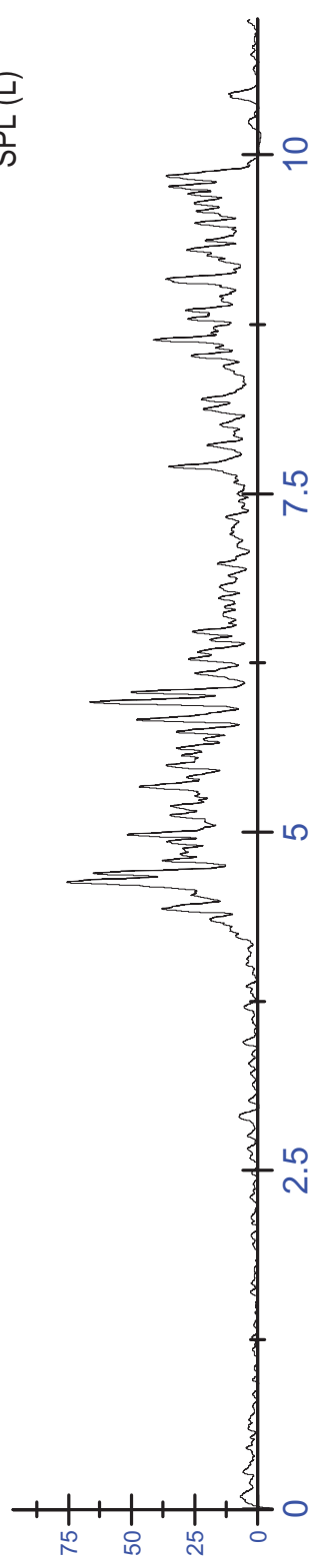
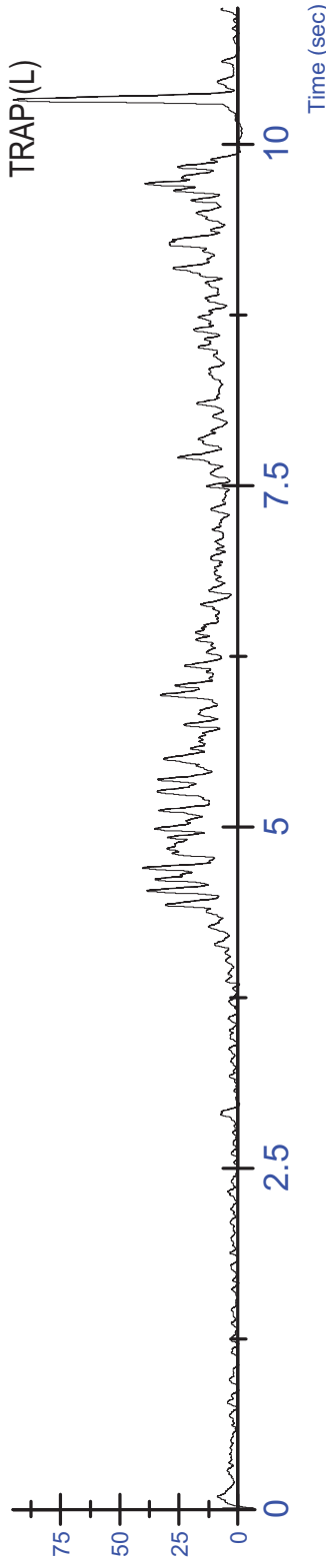
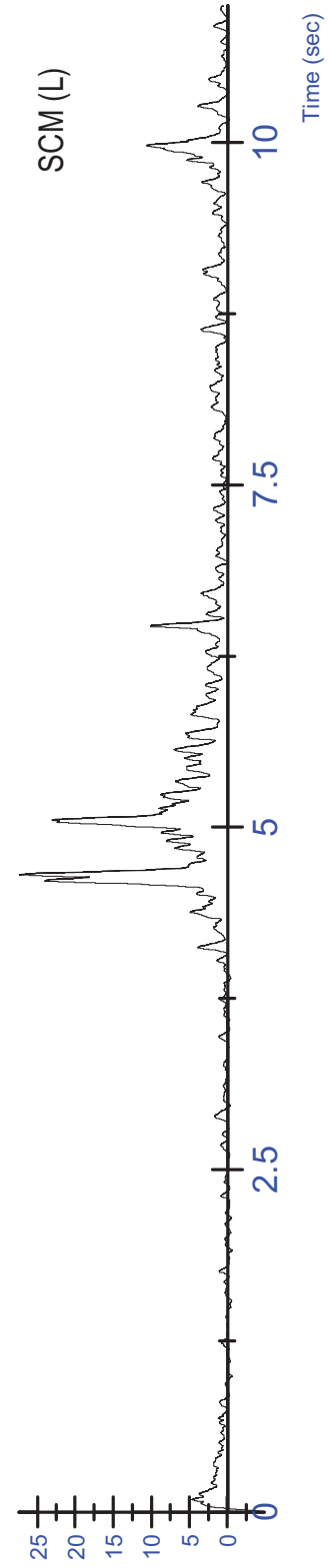
K03 MVC - Extension Trial 1- Unfiltered



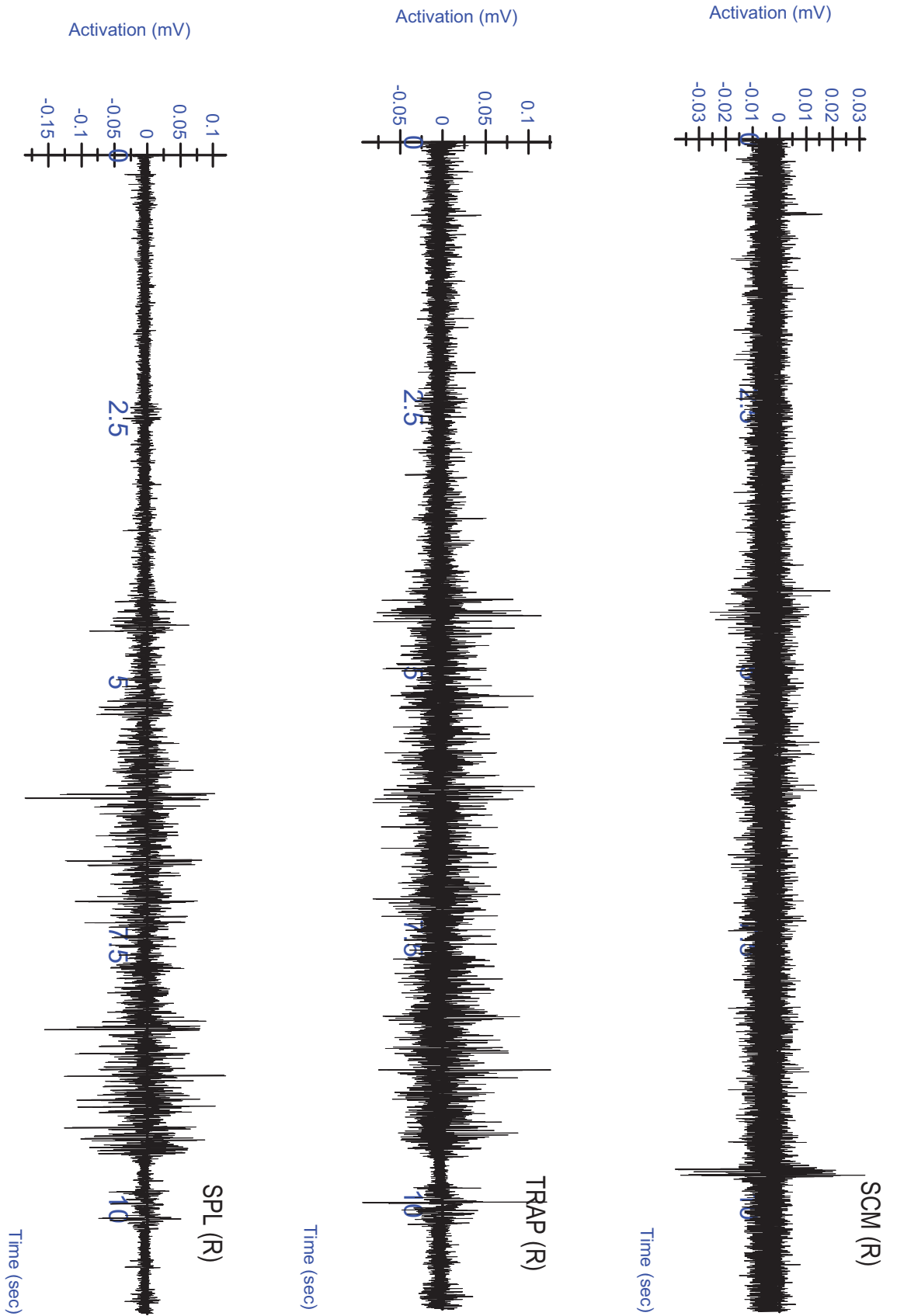
K03 MVC - Extension Trial 1- Unfiltered

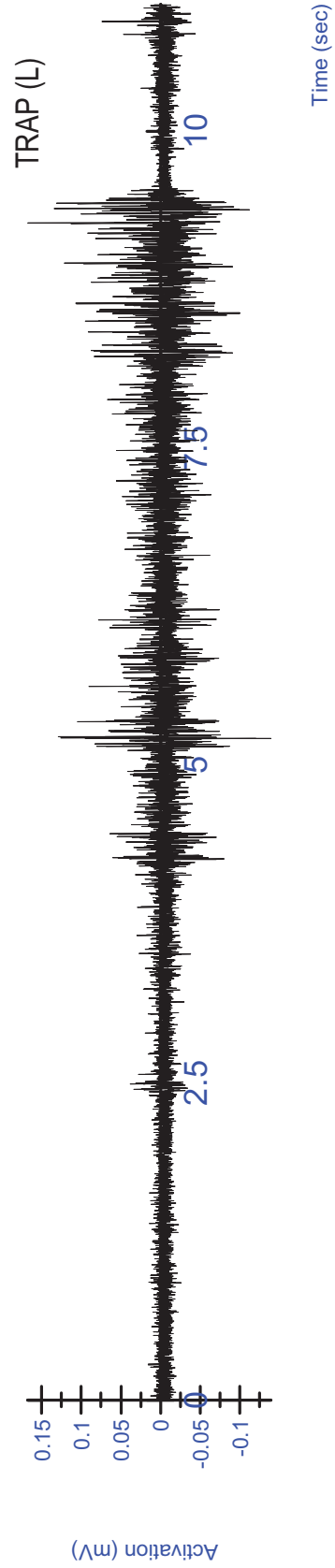
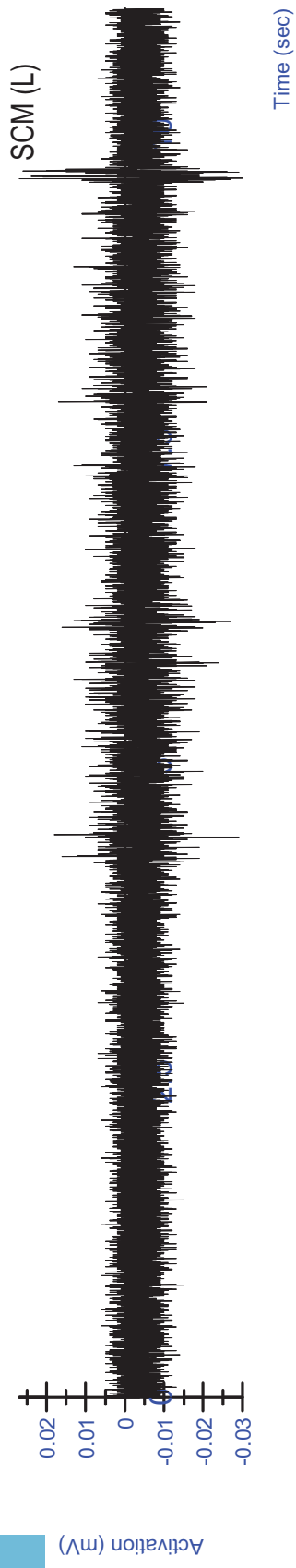
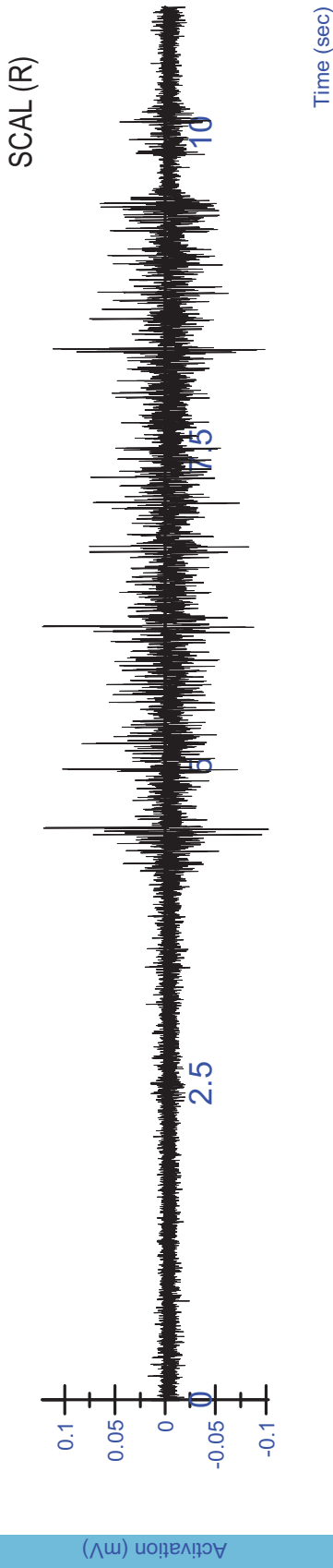




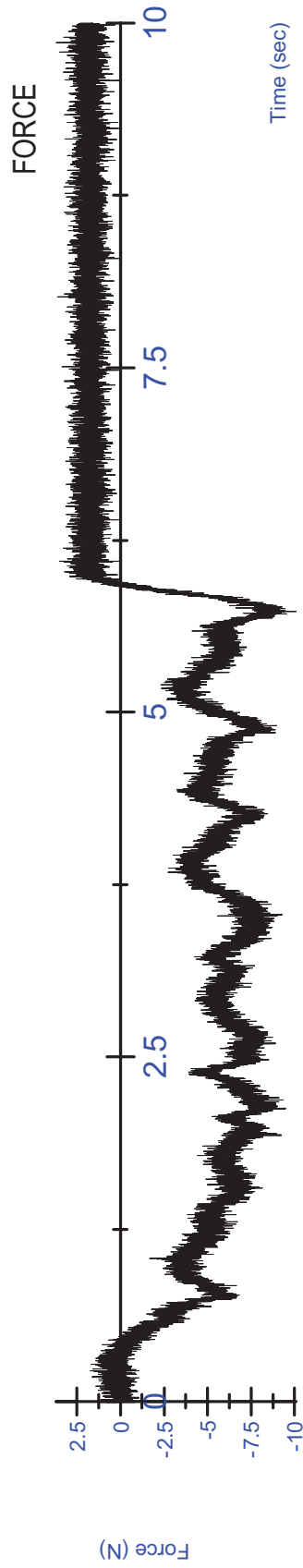
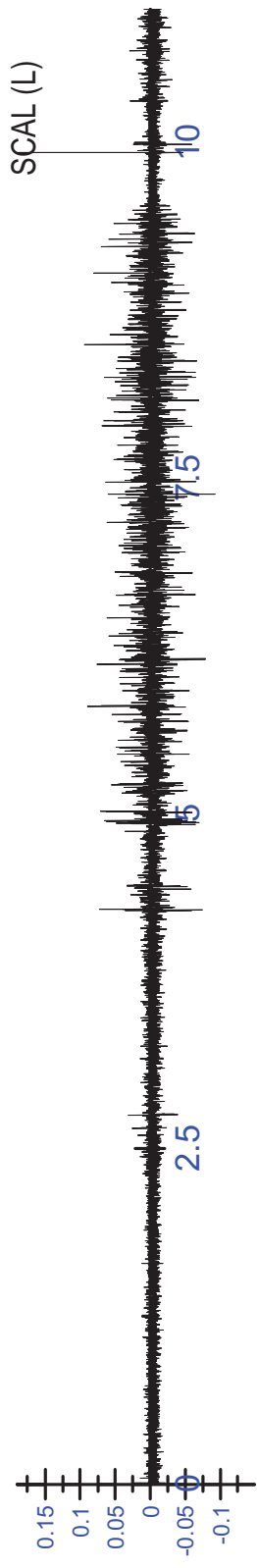
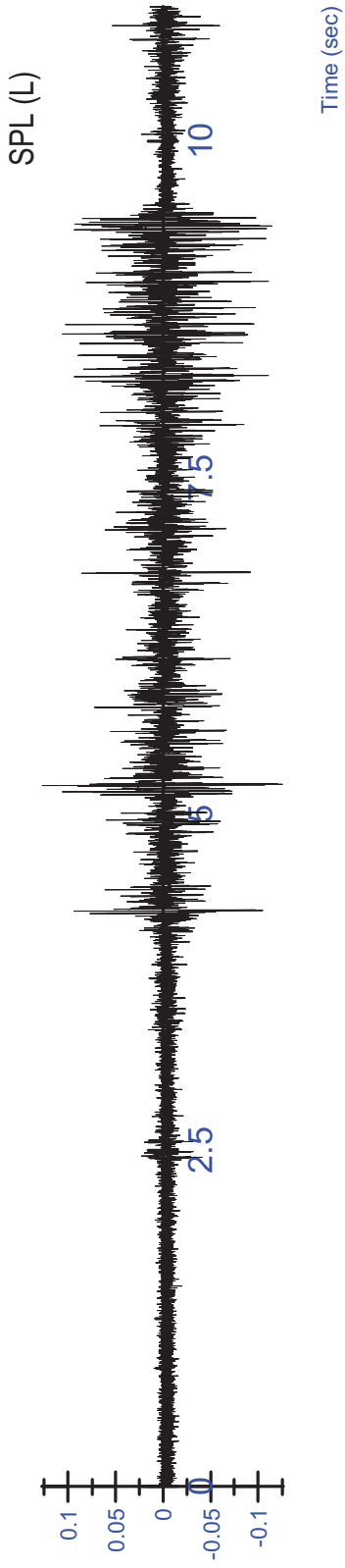


K03 MVC - Extension Trial 1 - Rectified/Filtered





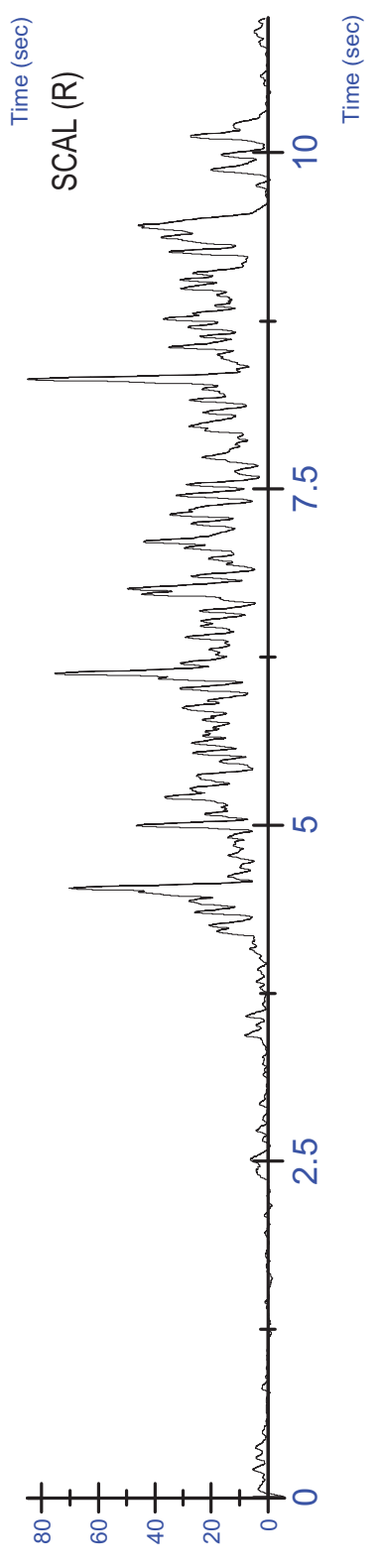
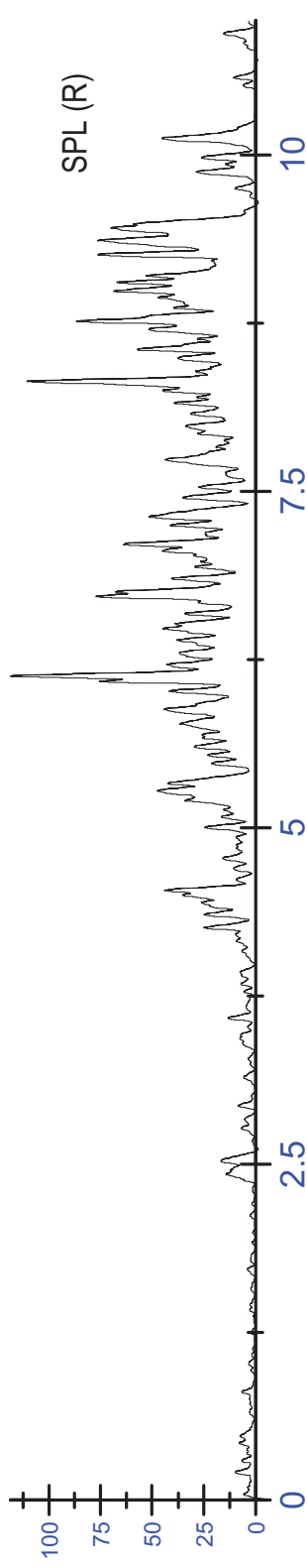
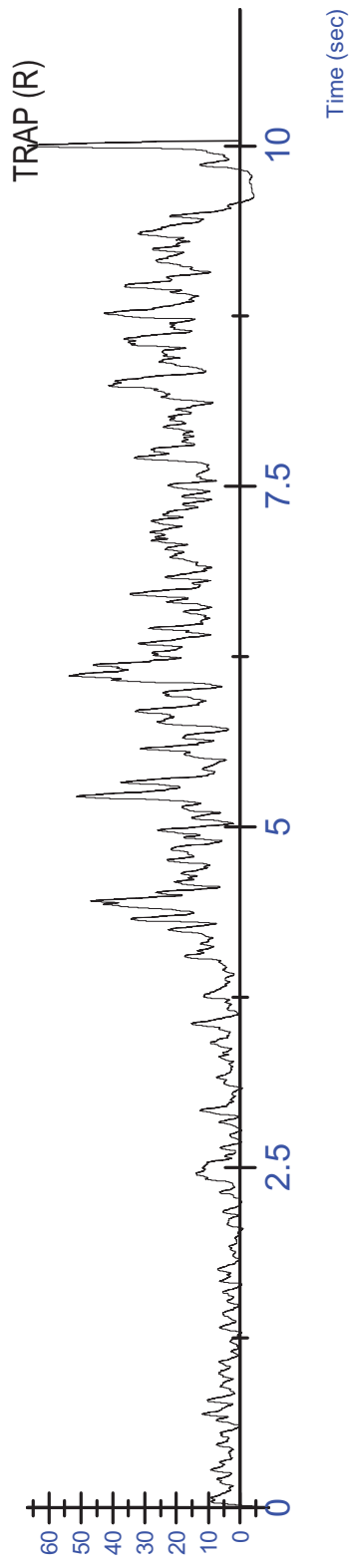
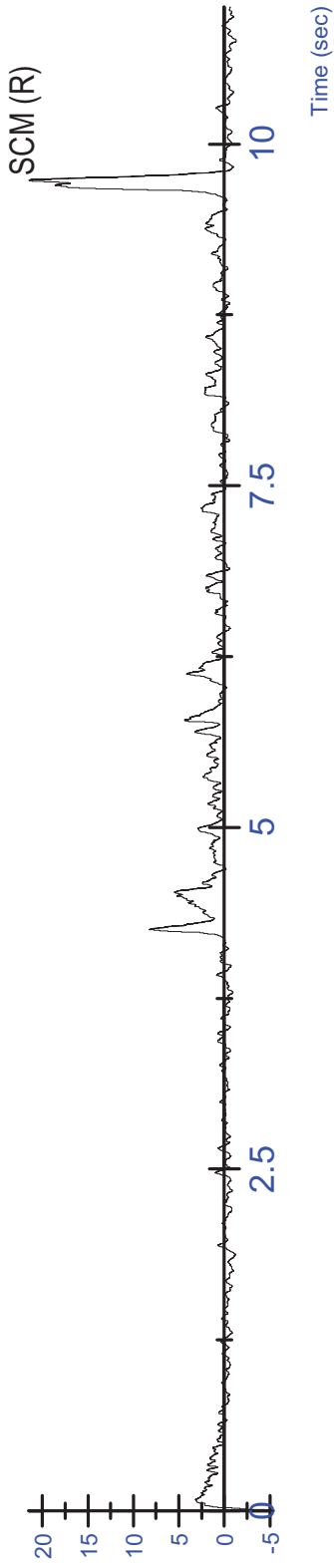
K03 MVC - Extension Trial 2- Unfiltered

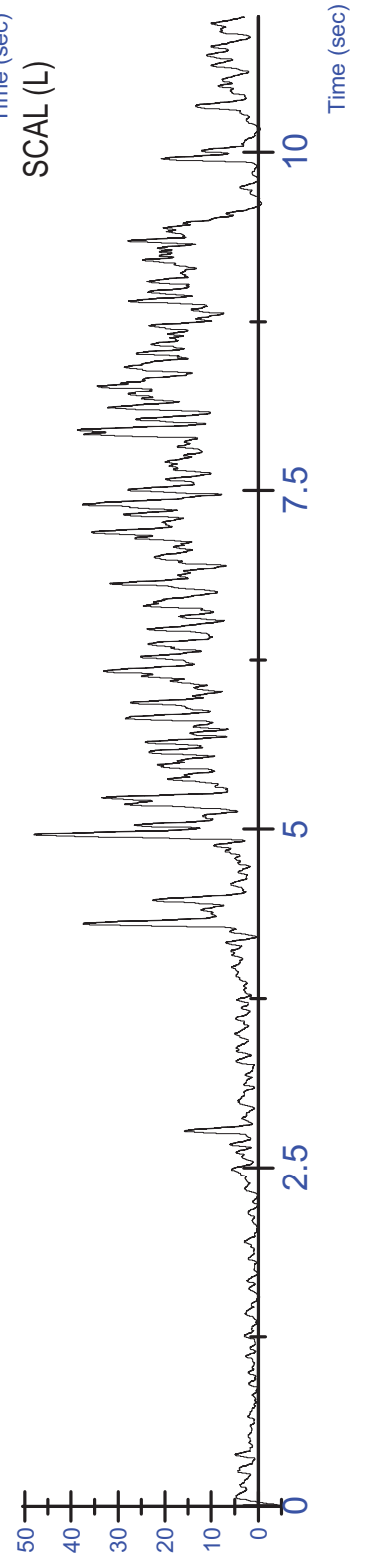
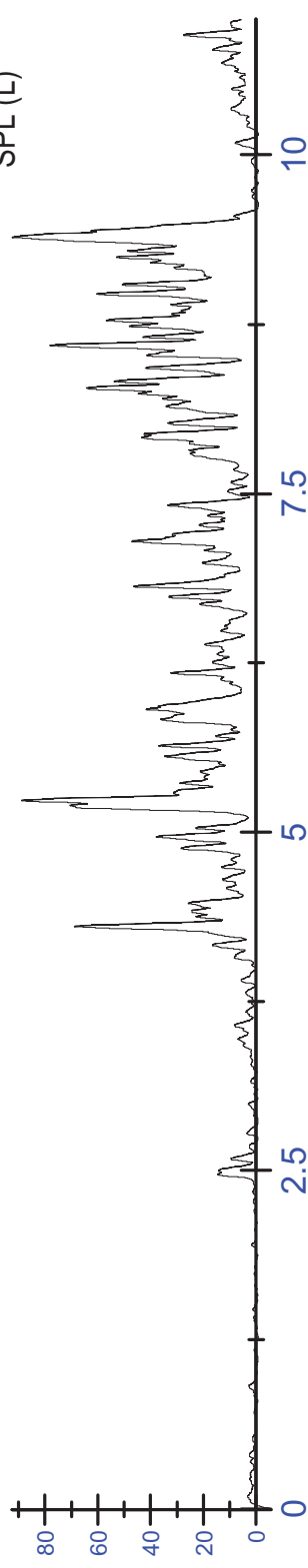
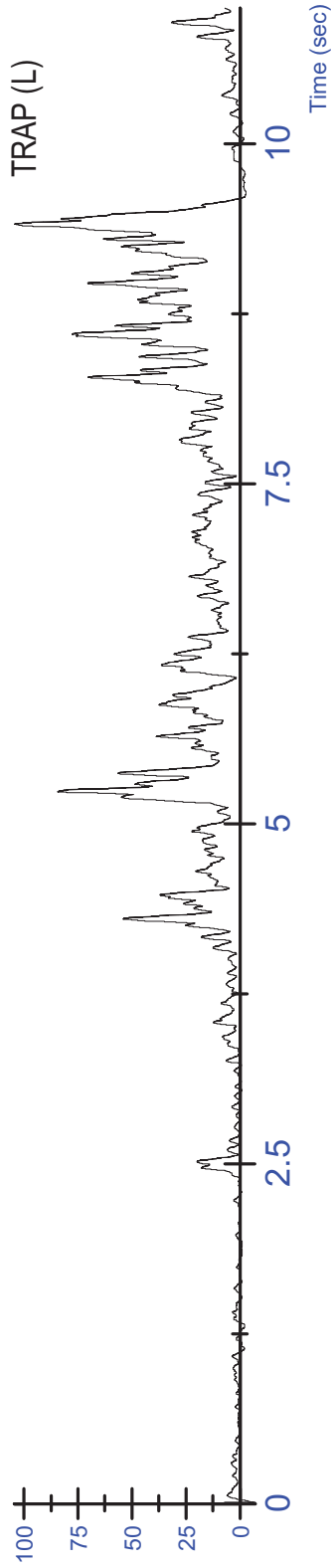
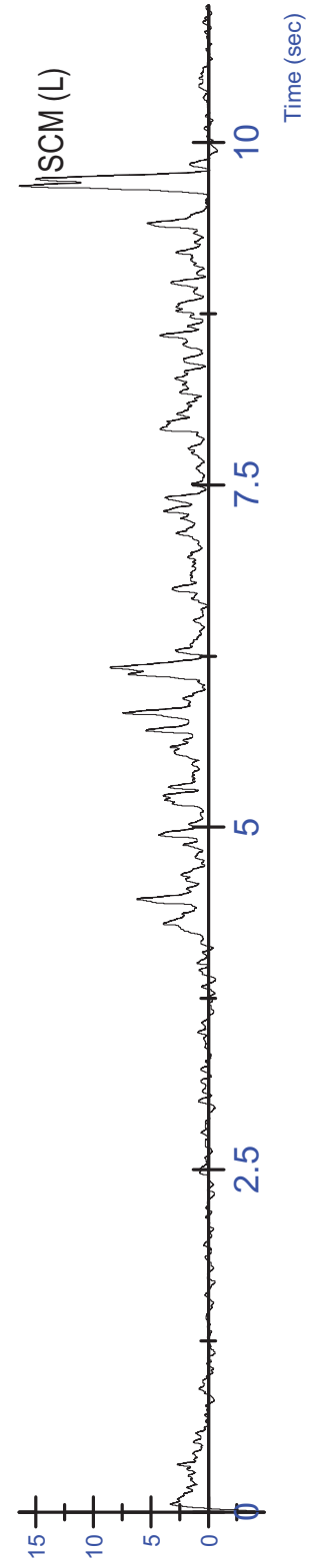


Activation (mV)

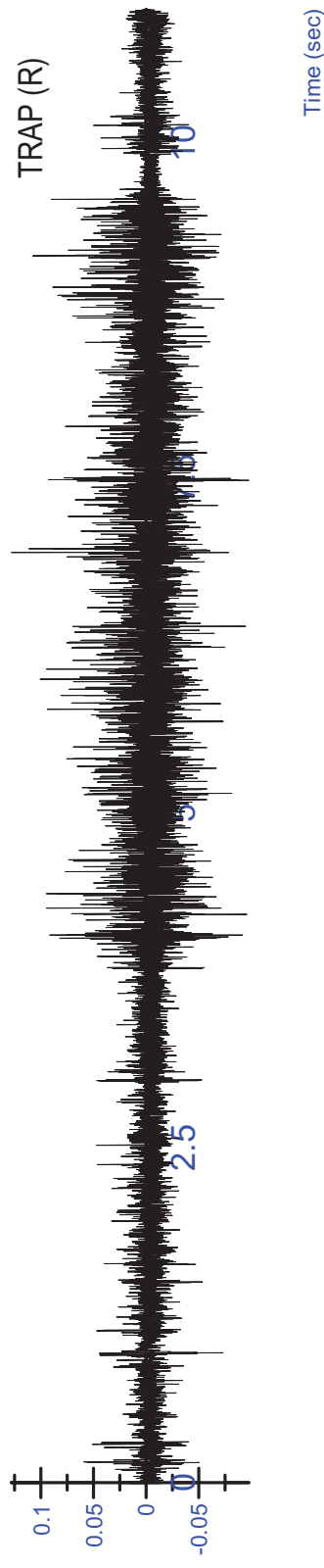
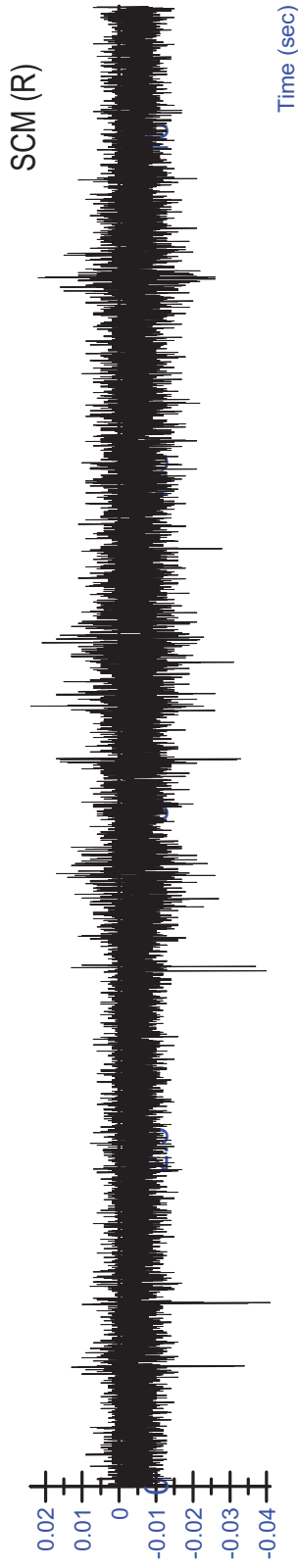
Activation (mV)

Force (N)





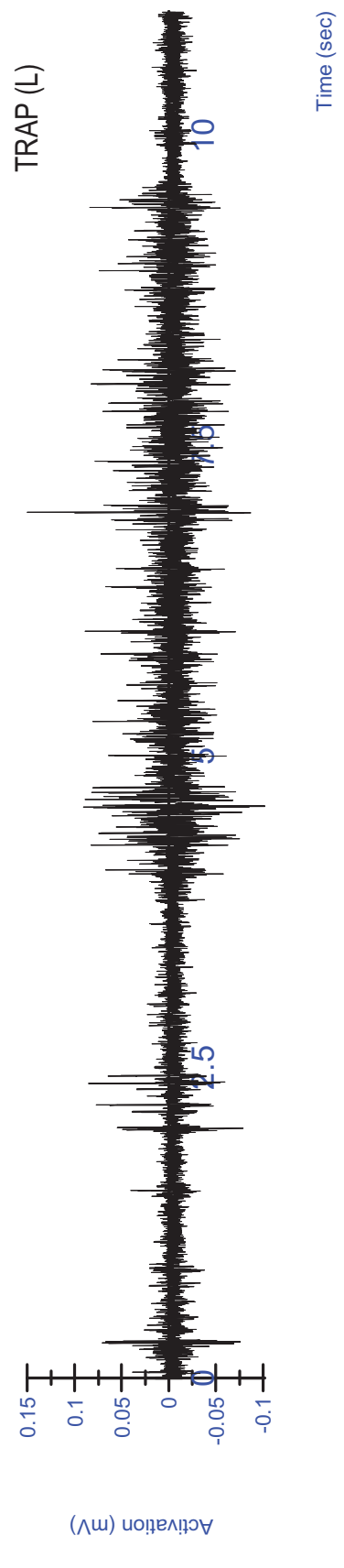
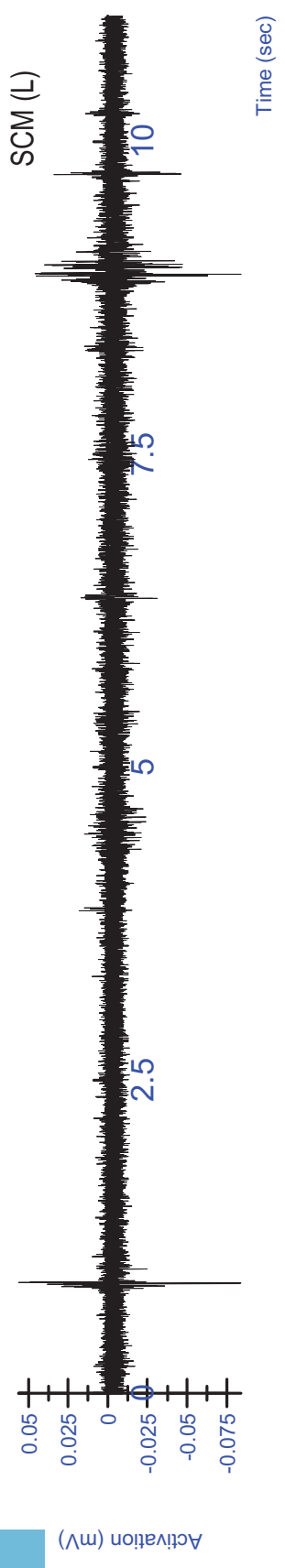
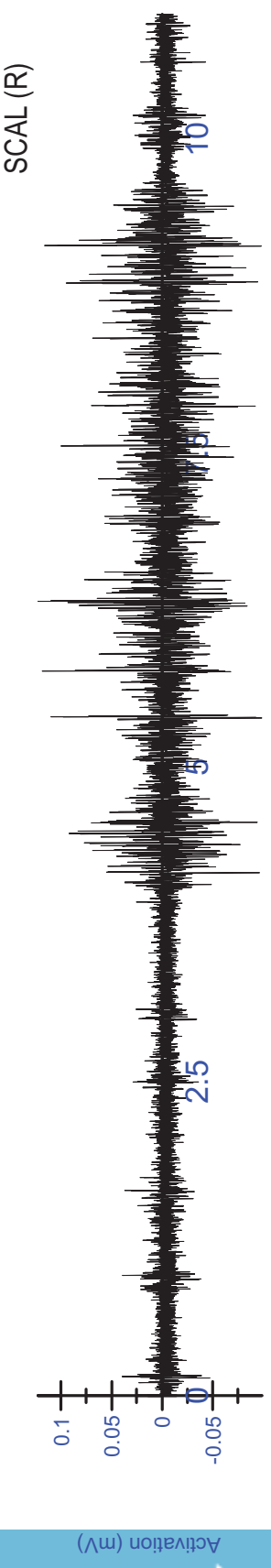
K03 MVC - Extension Trial 2 - Rectified/Filtered

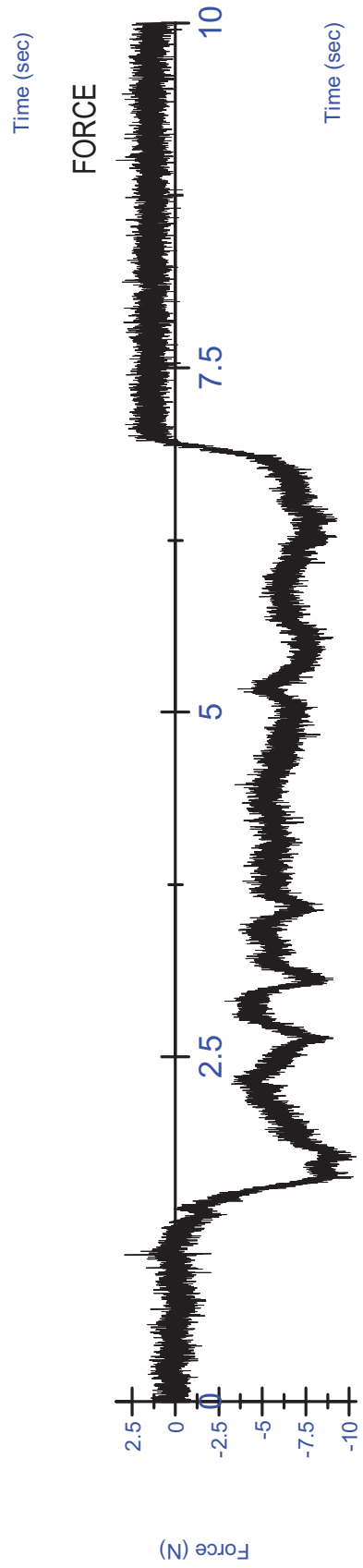
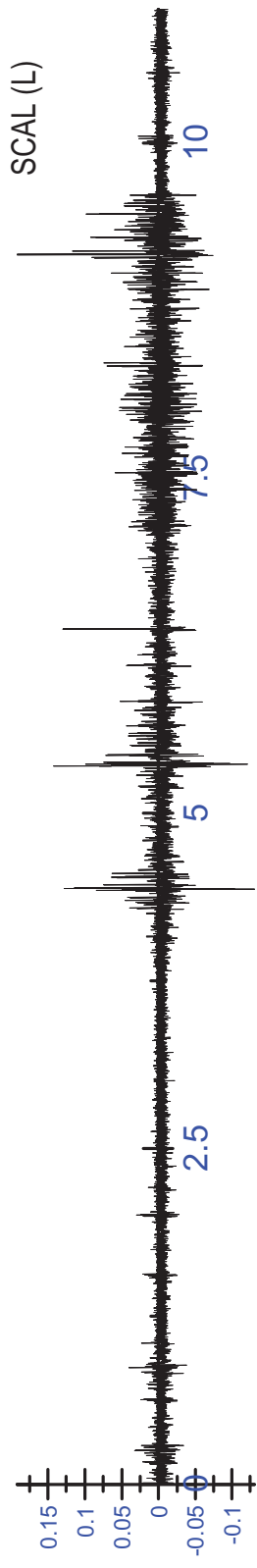
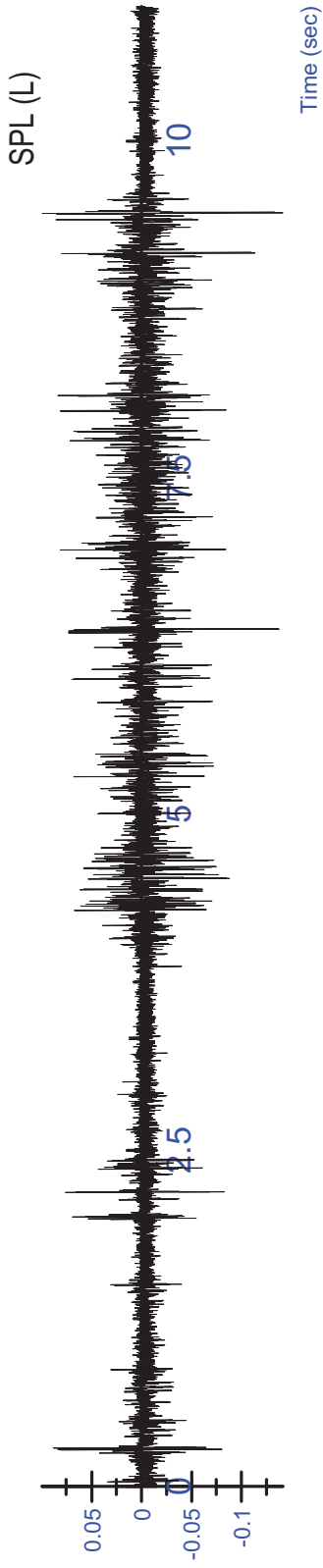


Activation (mV)

Activation (mV)

Activation (mV)

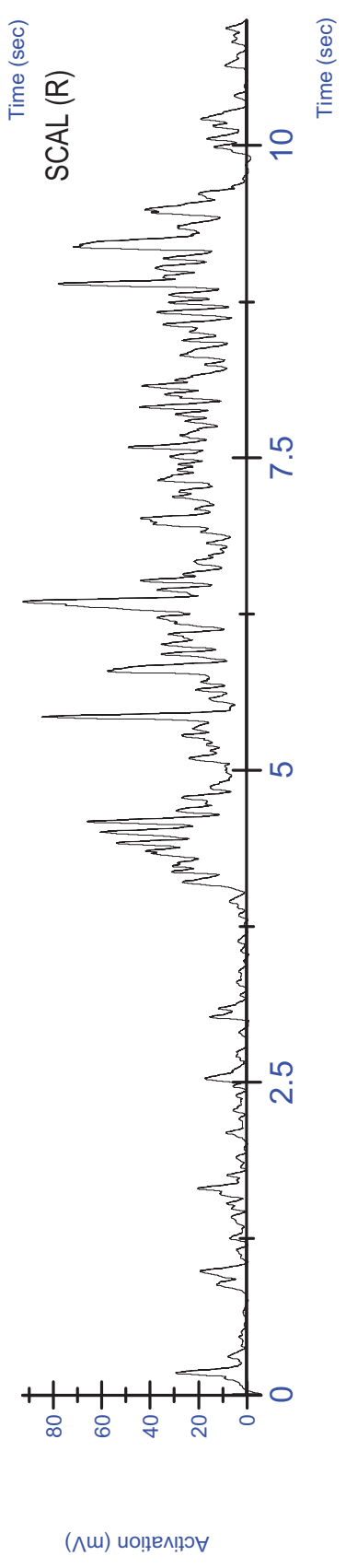
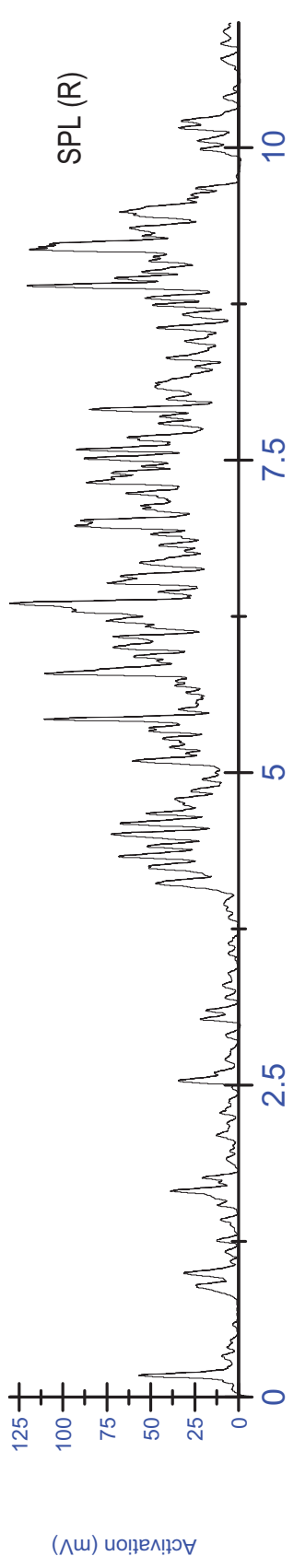
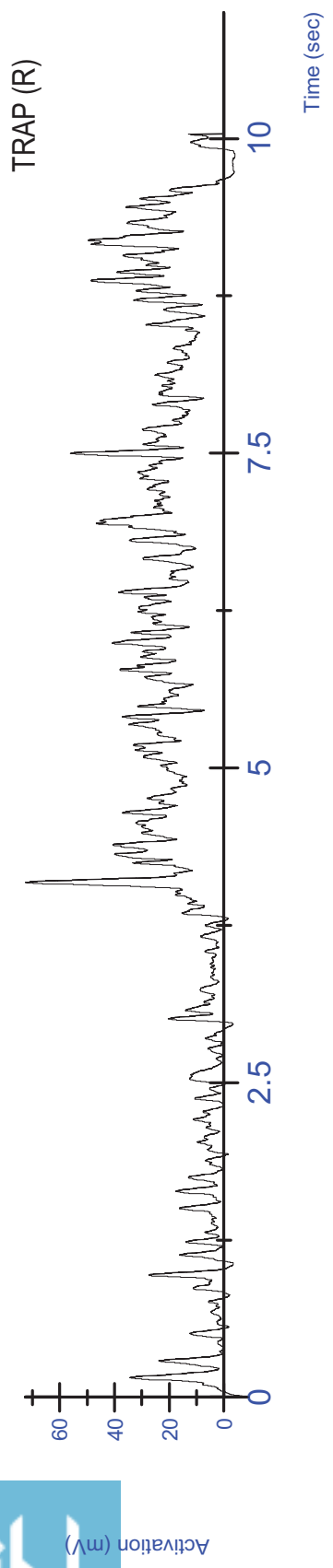
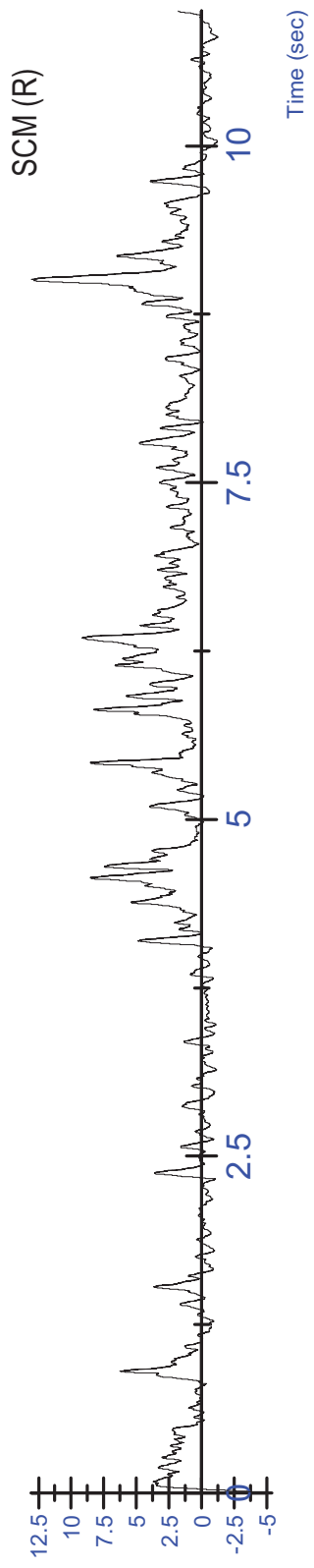




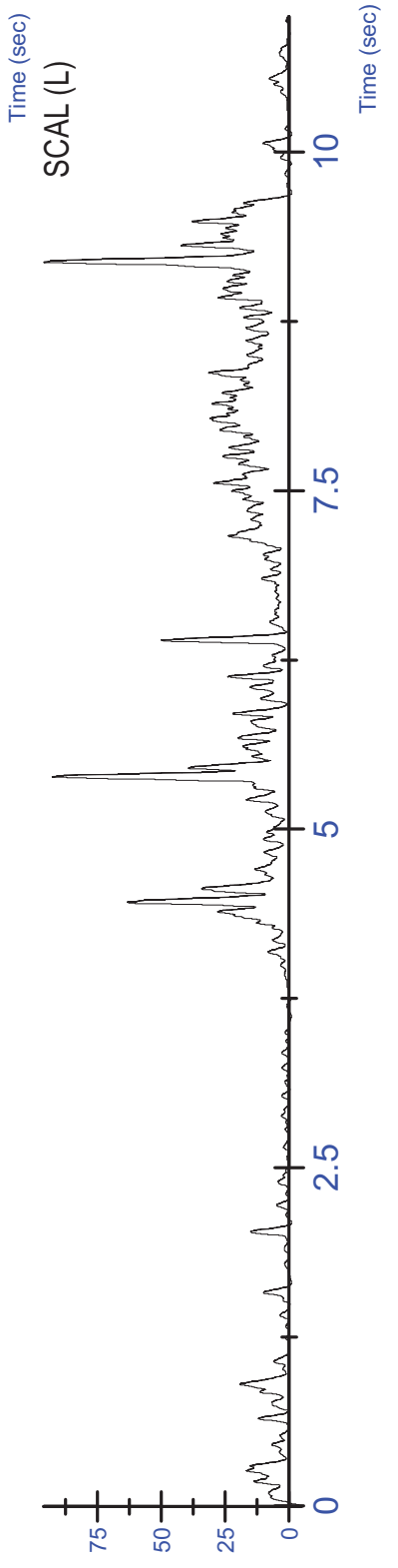
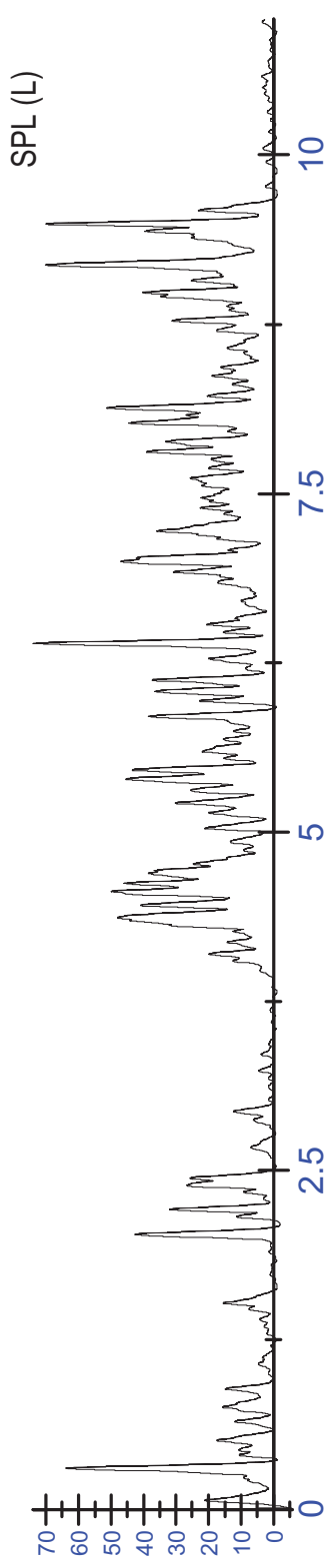
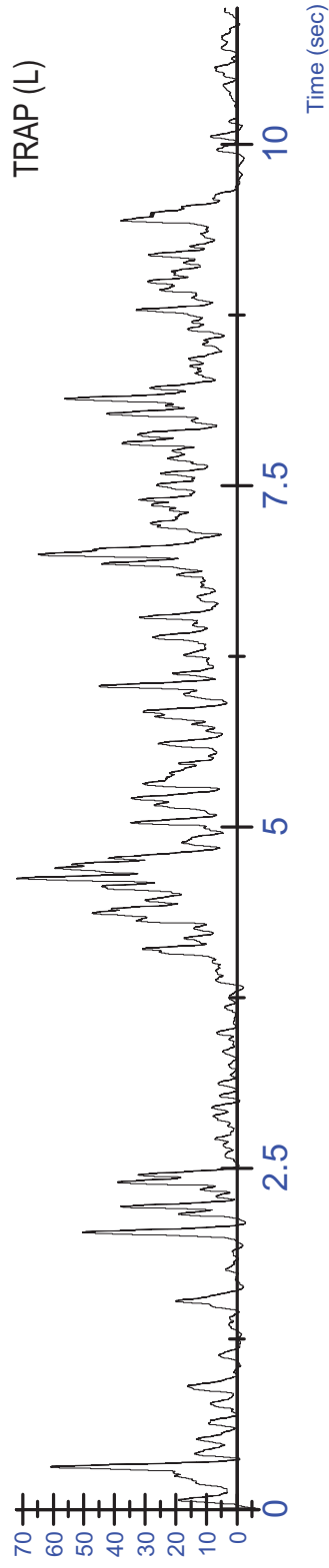
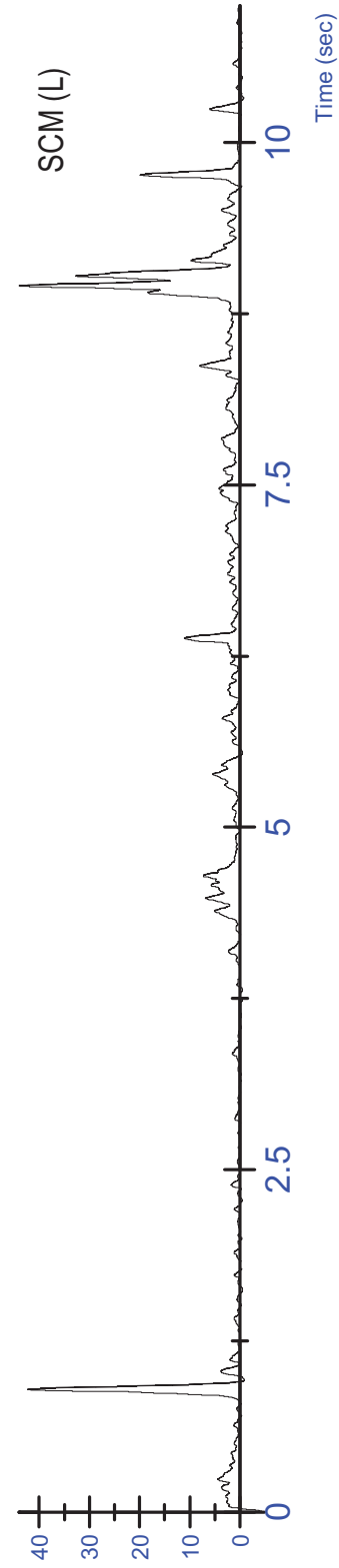
Activation (mV)

Activation (mV)

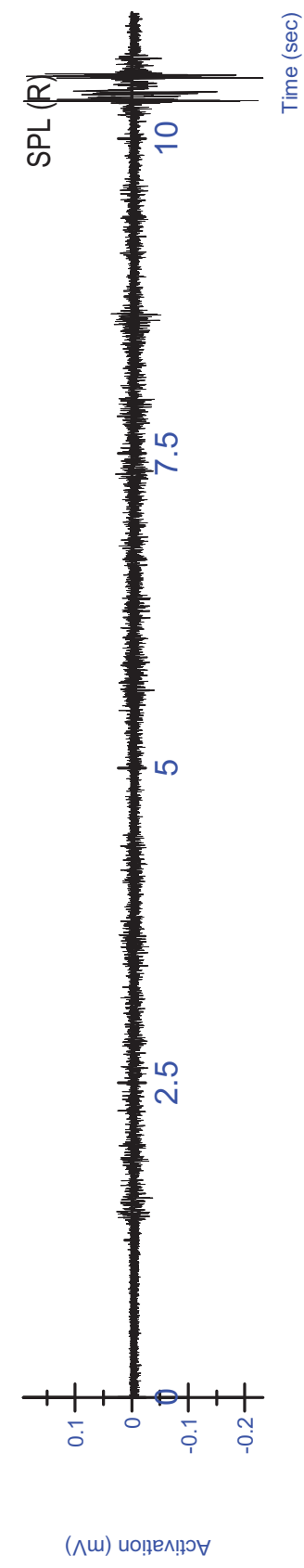
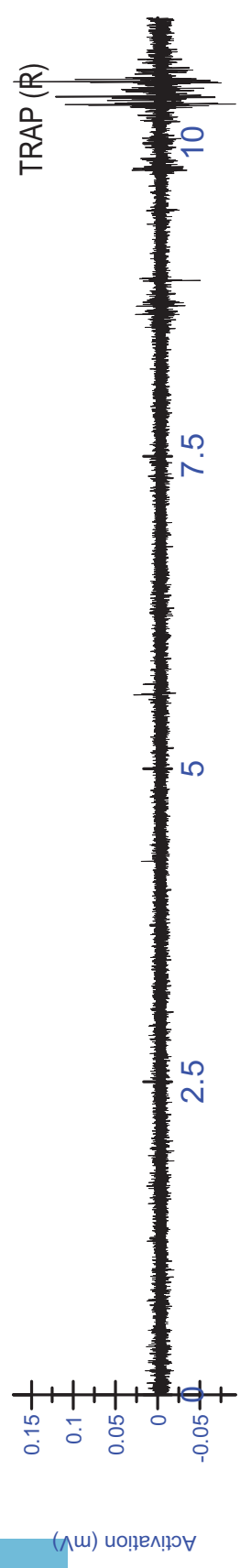
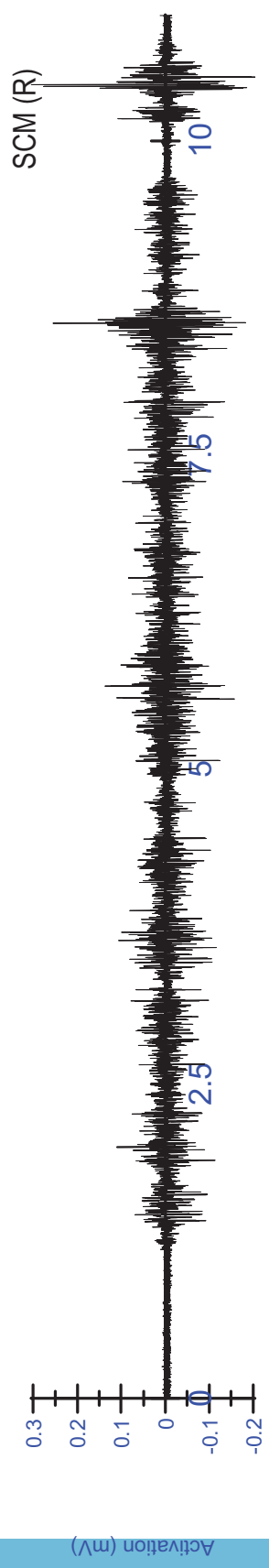
Force (N)



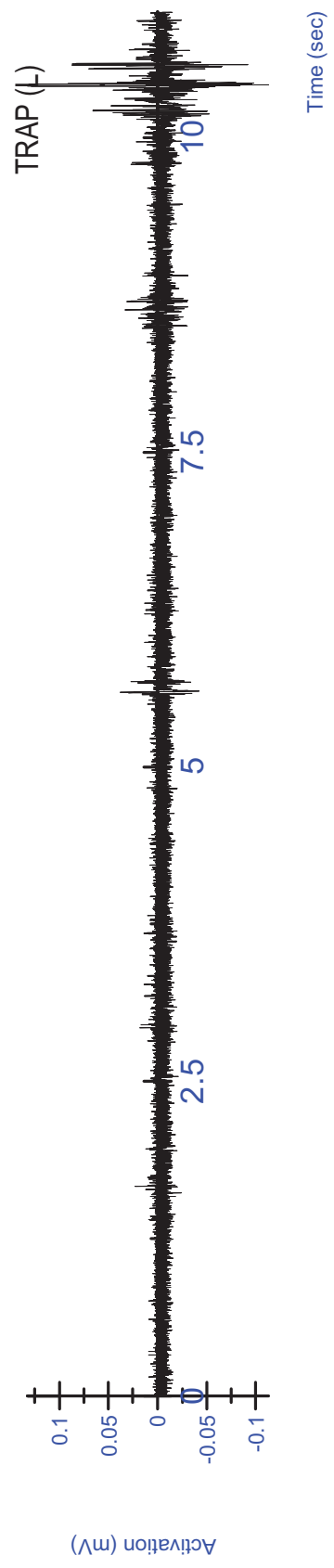
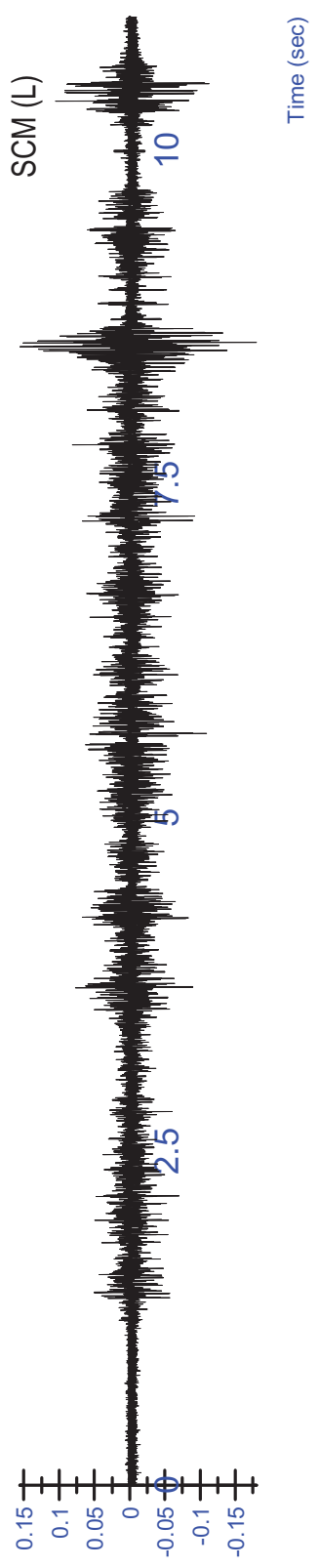
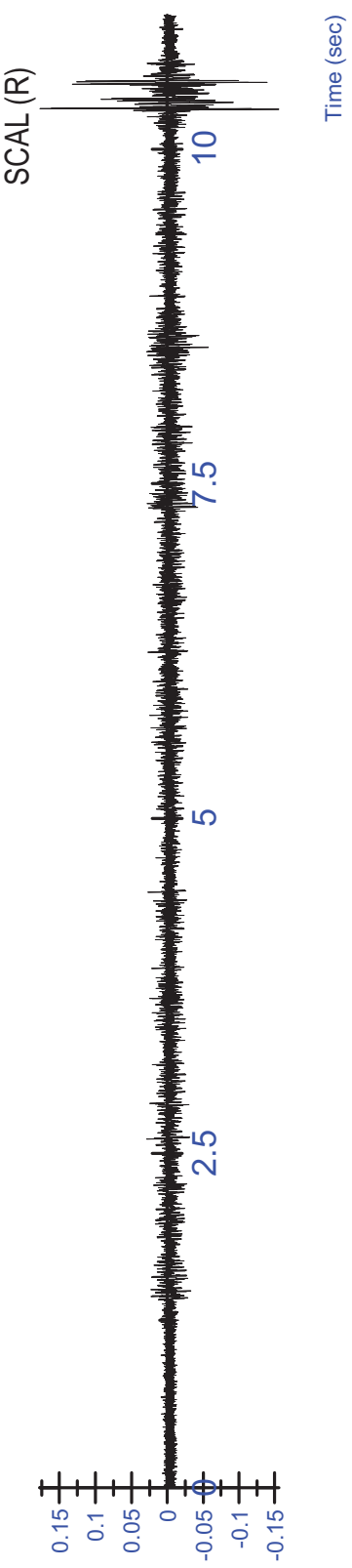
K03 MVC - Extension Trial 3 - Rectified/Filtered

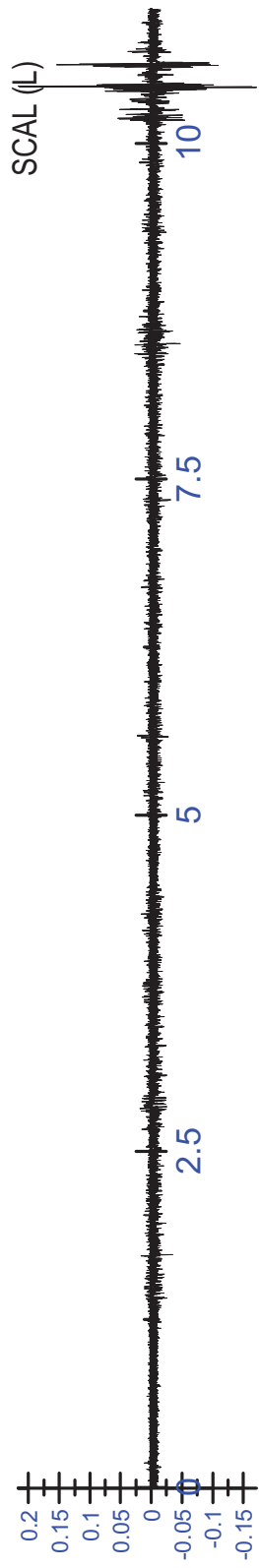
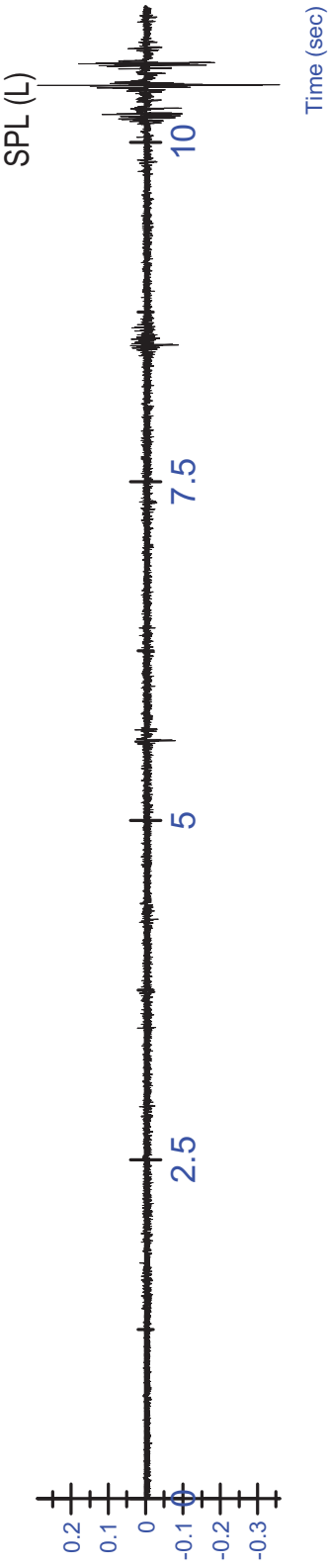


K03 MVC - Extension Trial 3 - Rectified/Filtered

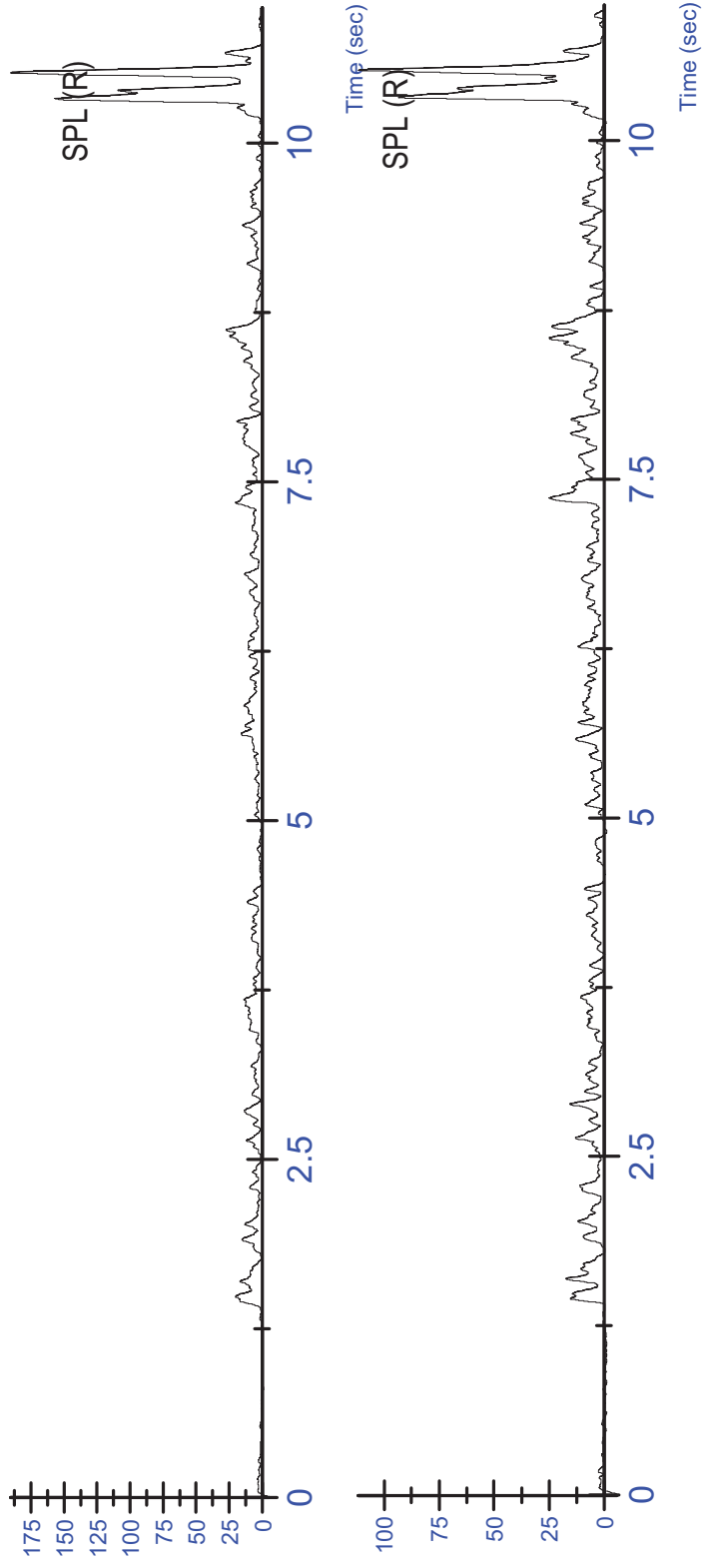
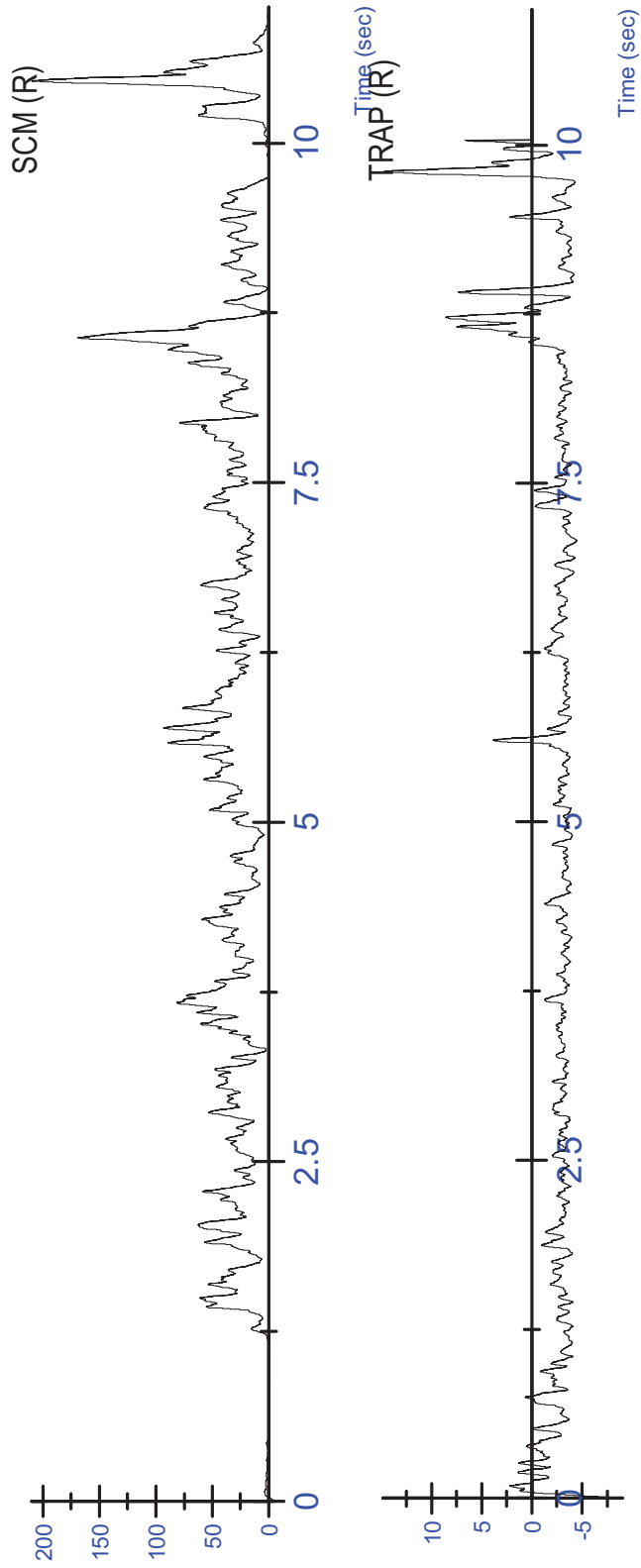


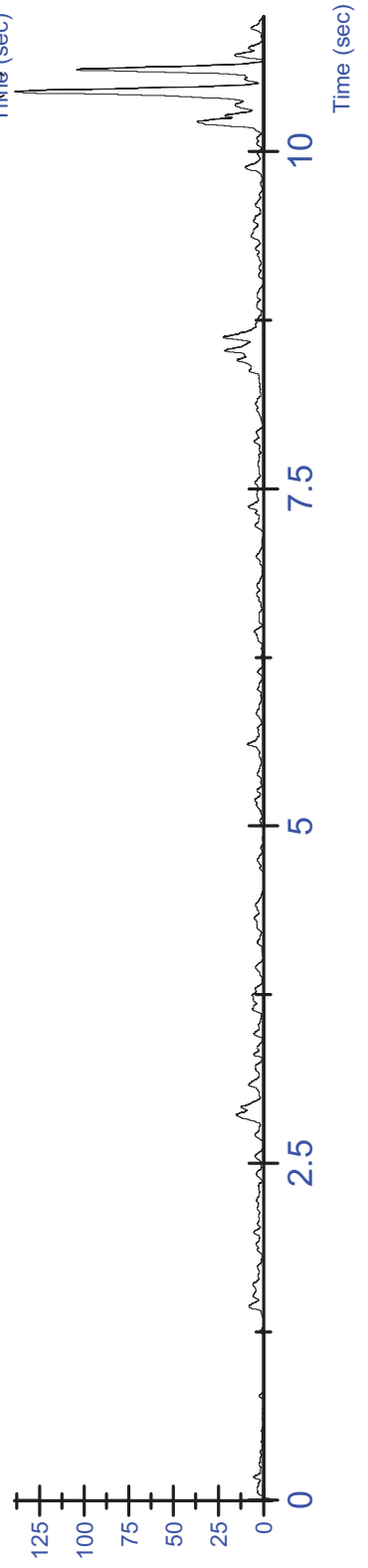
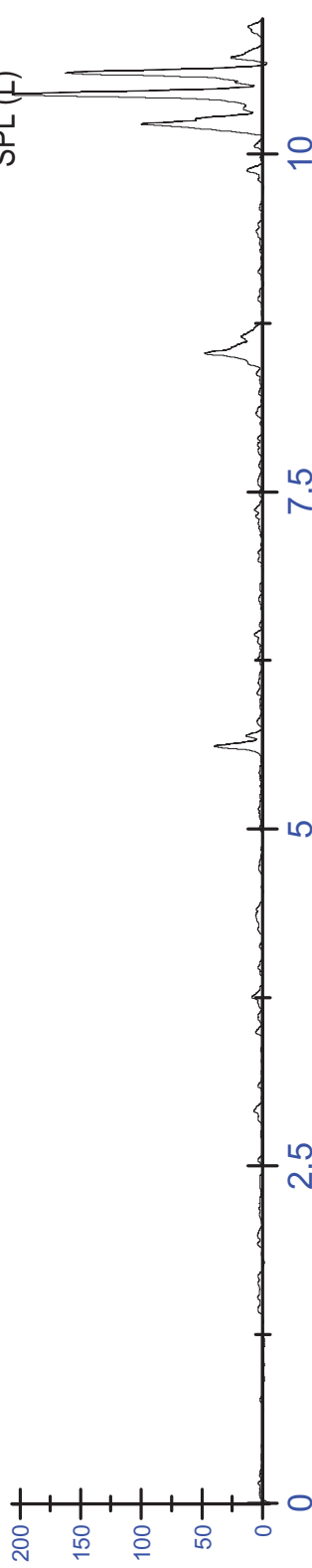
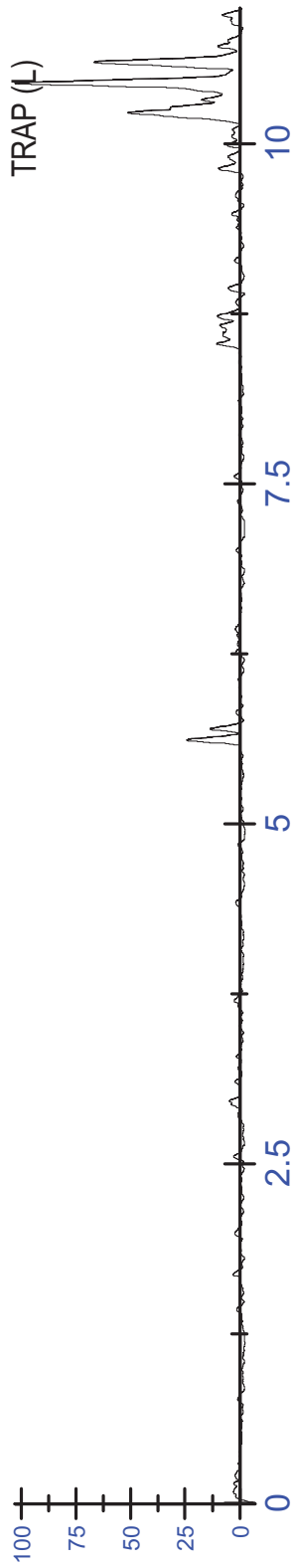
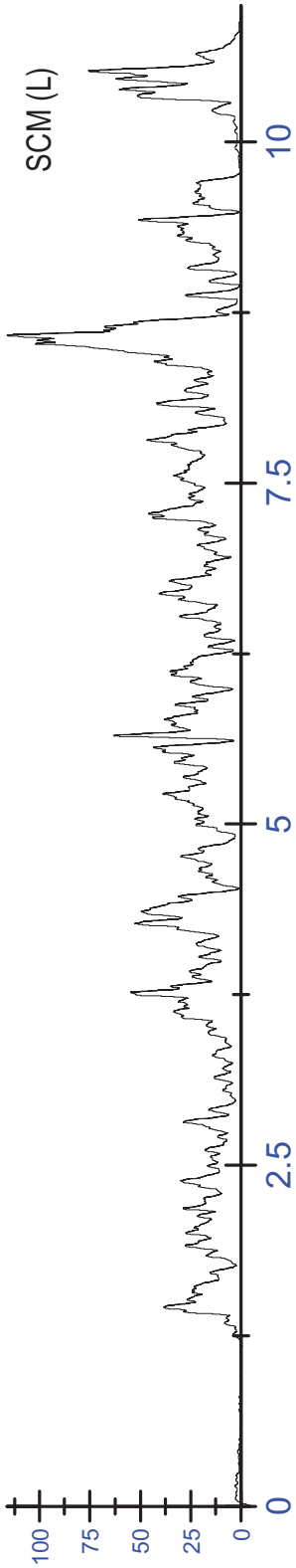
K03 MVC - Flexion Trial 1 - Unfiltered

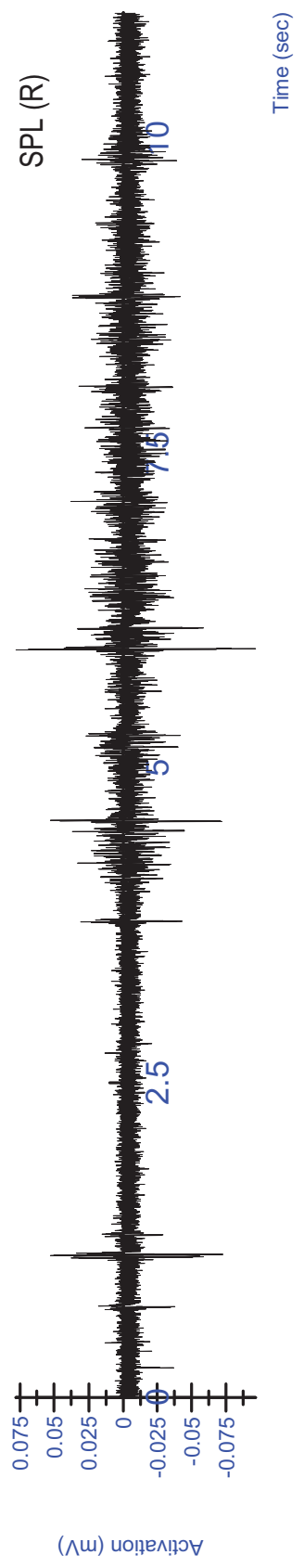
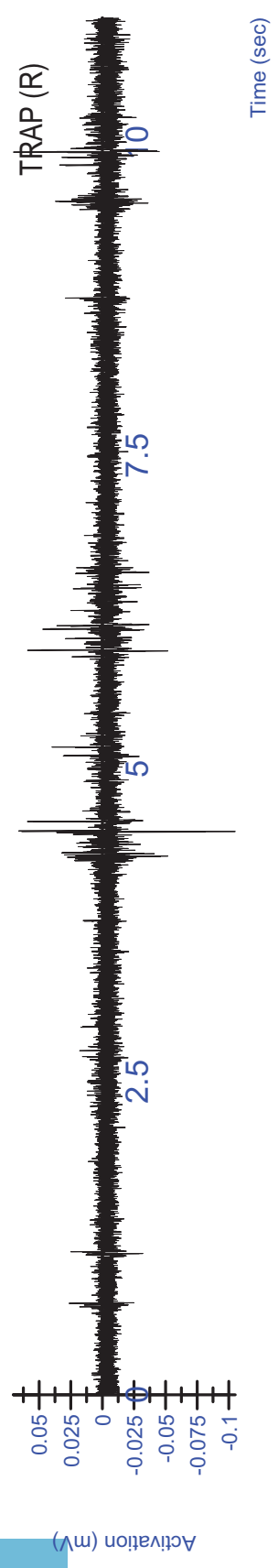
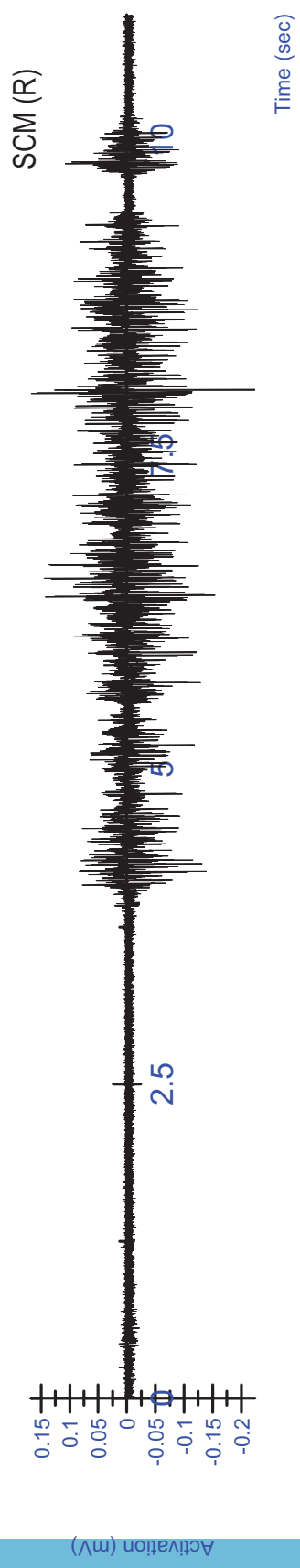


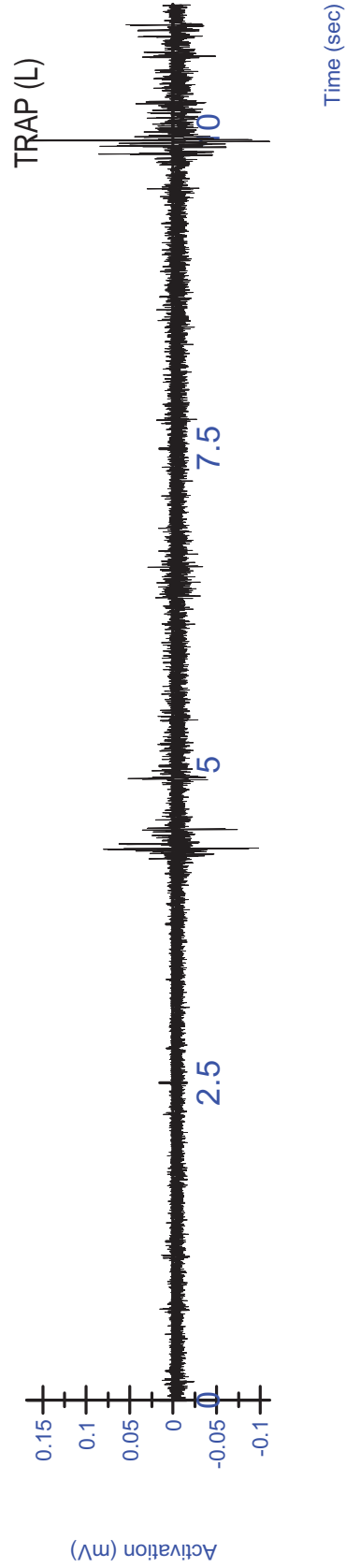
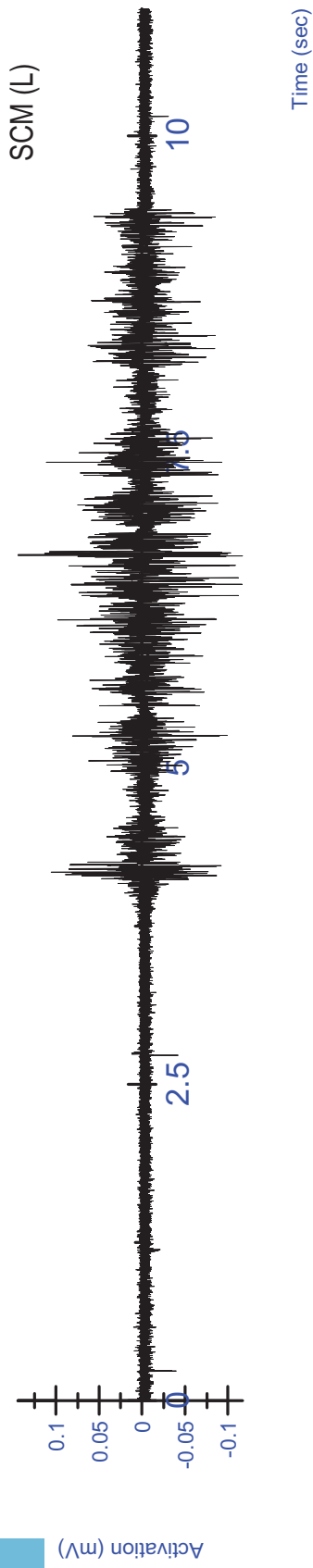
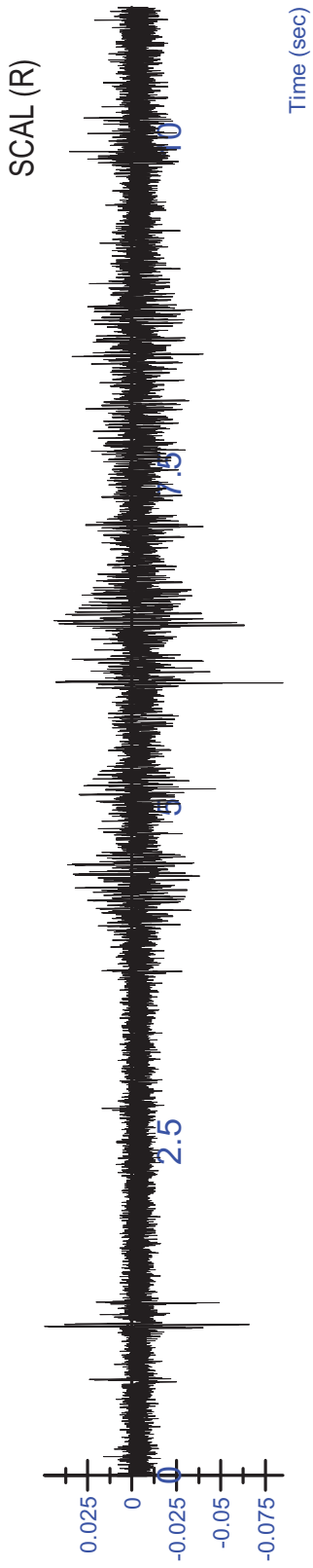


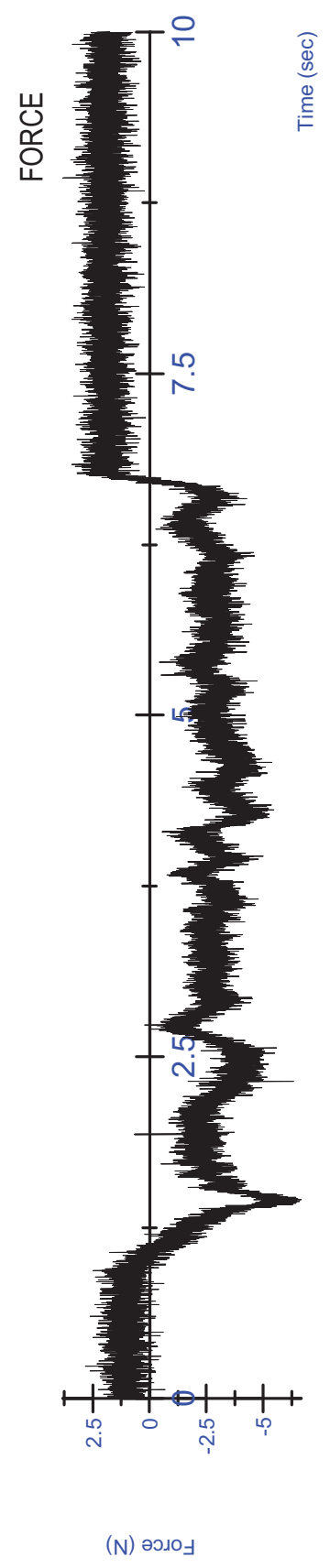
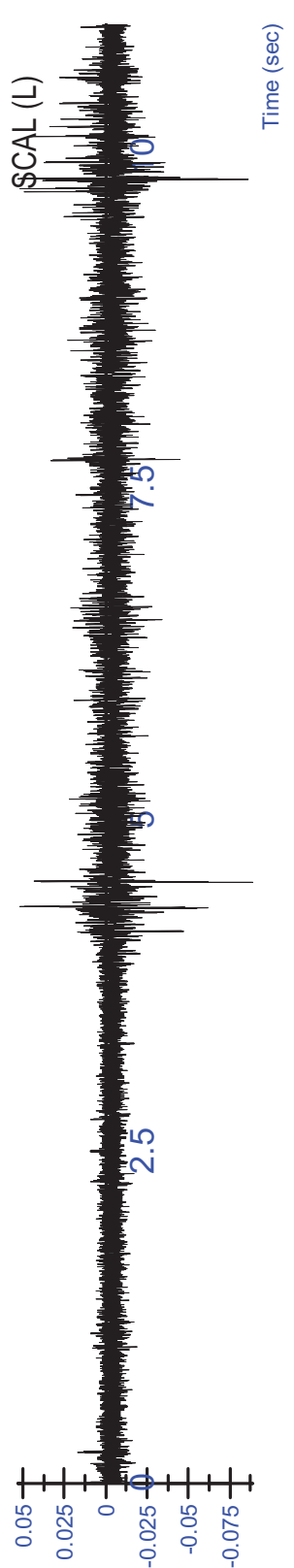
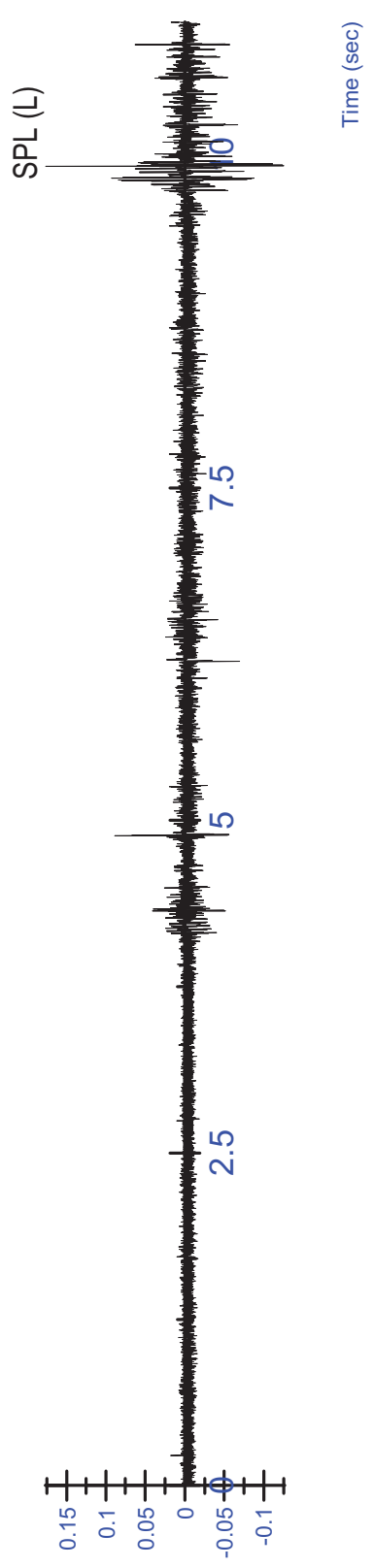
K03 MVC - Flexion Trial 1 - Unfiltered







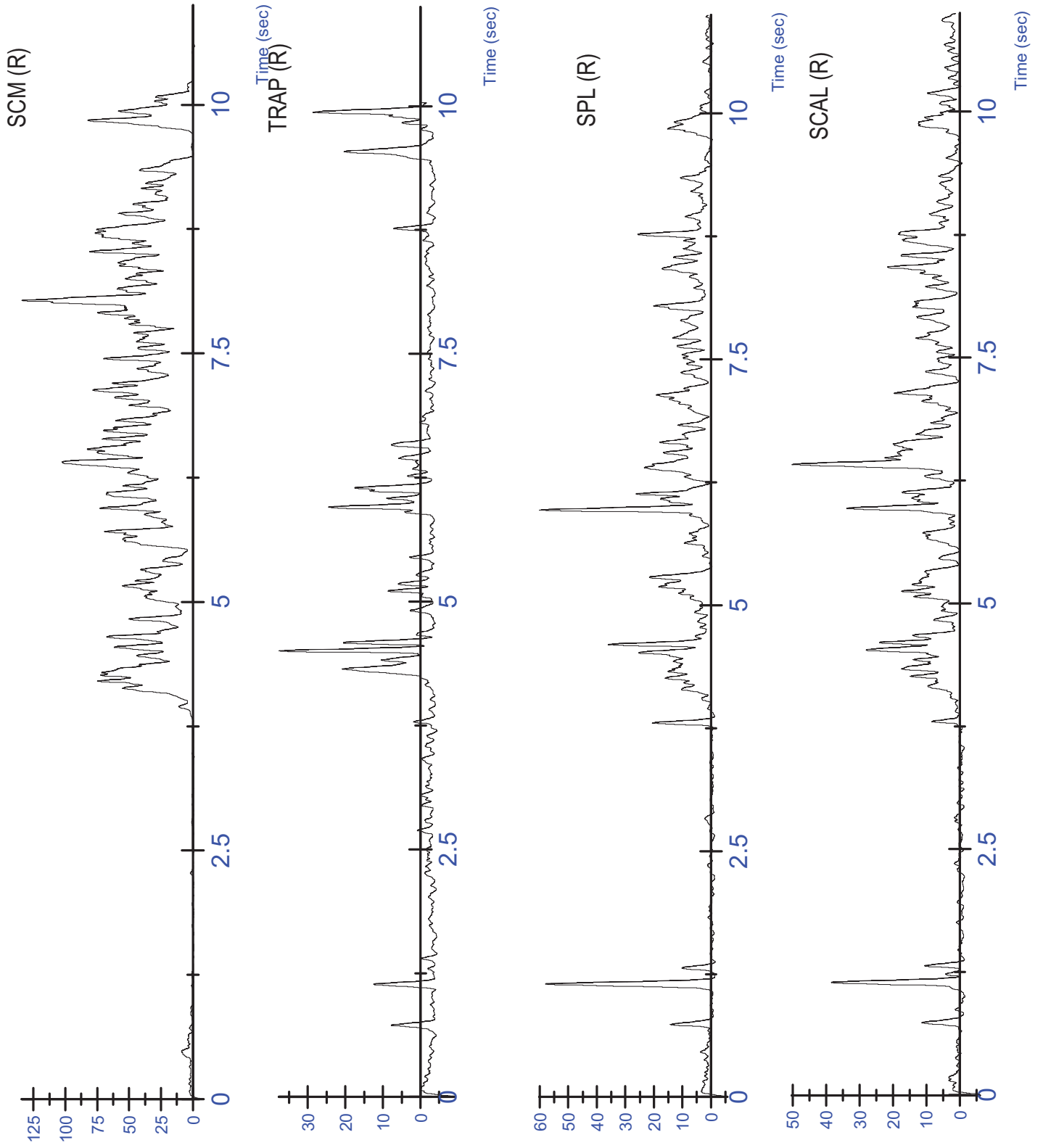


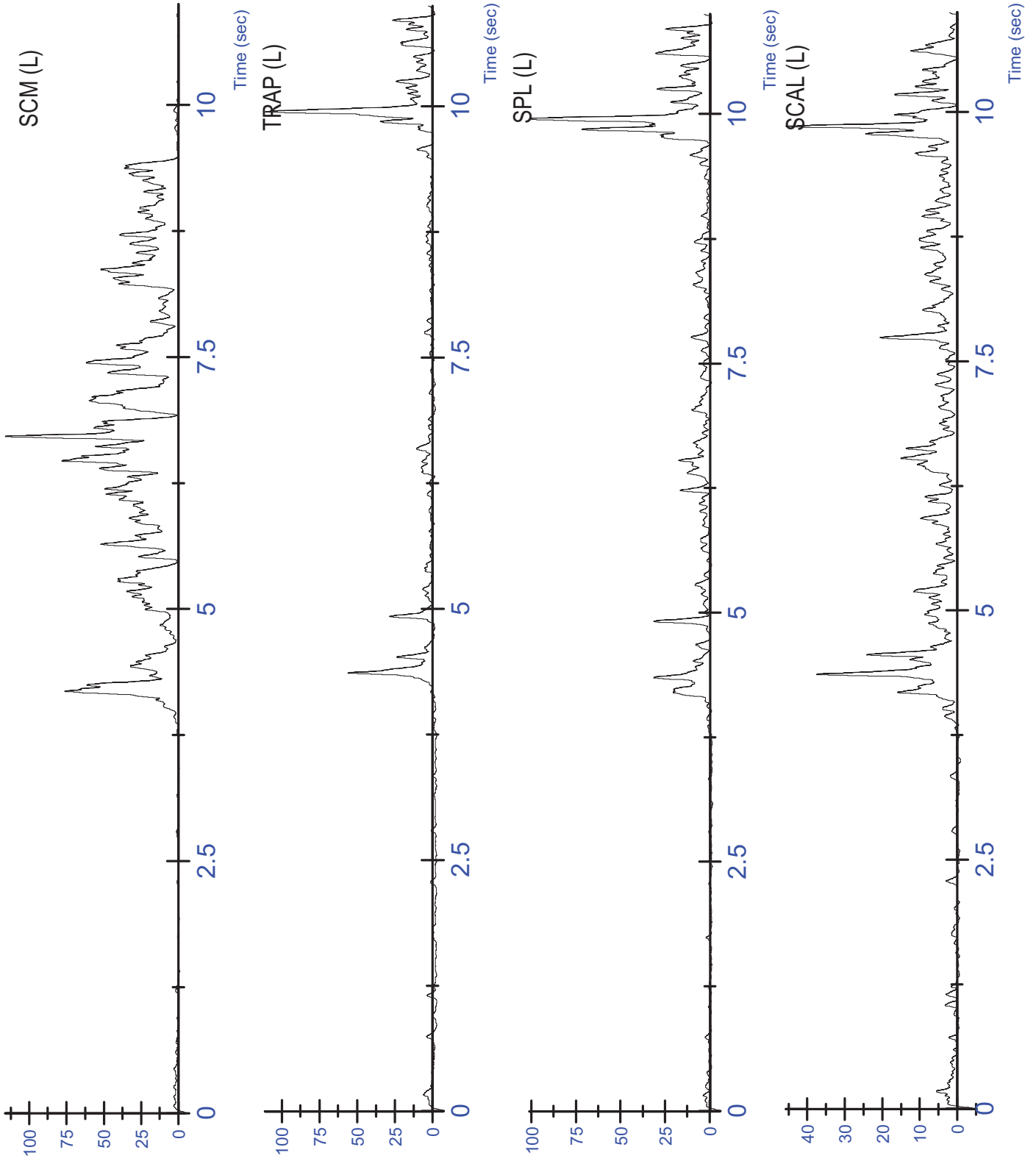


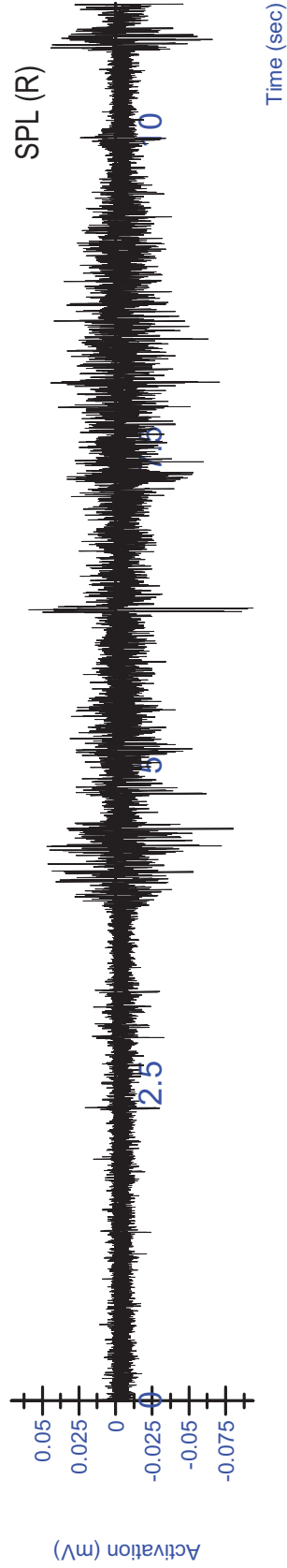
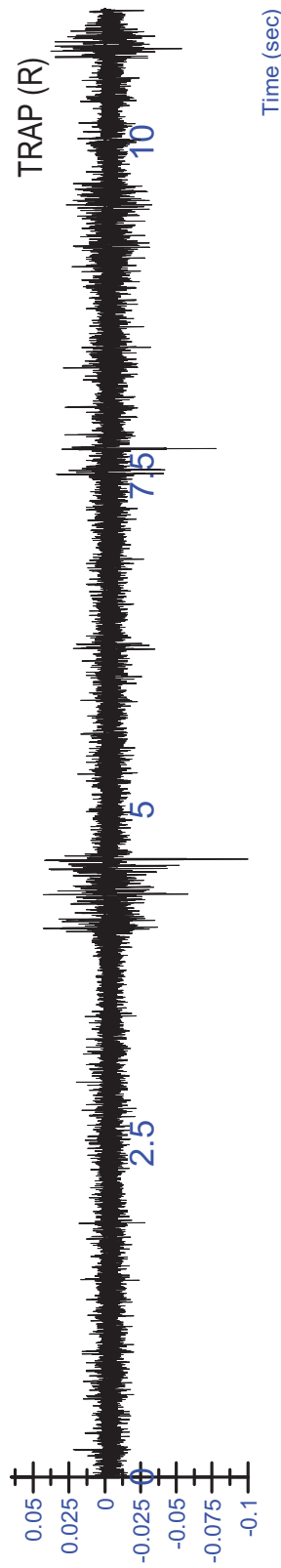
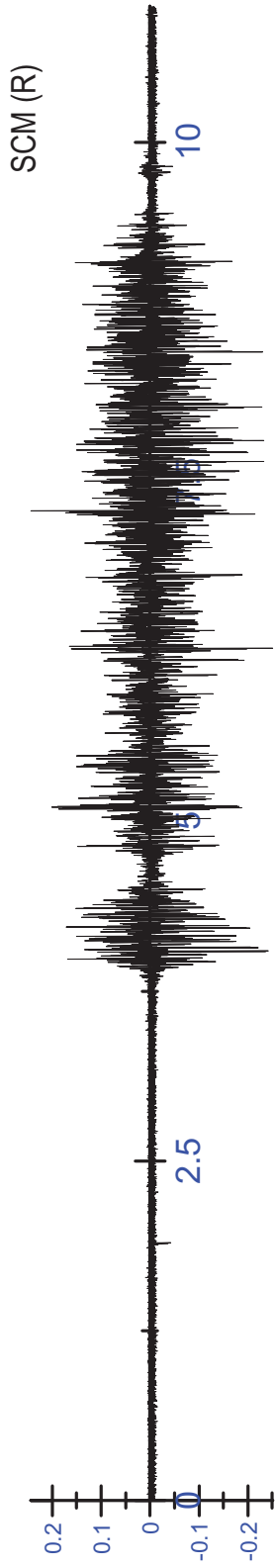
Activation (mV)

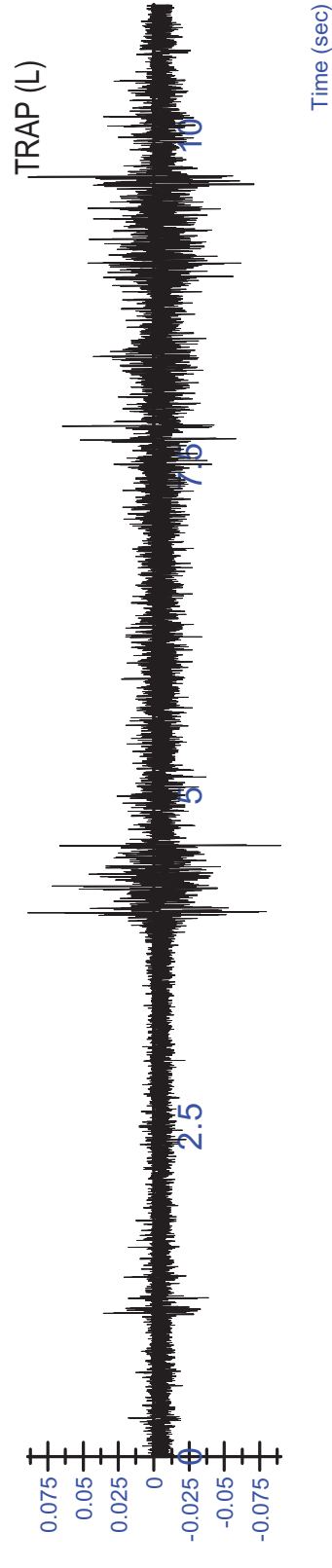
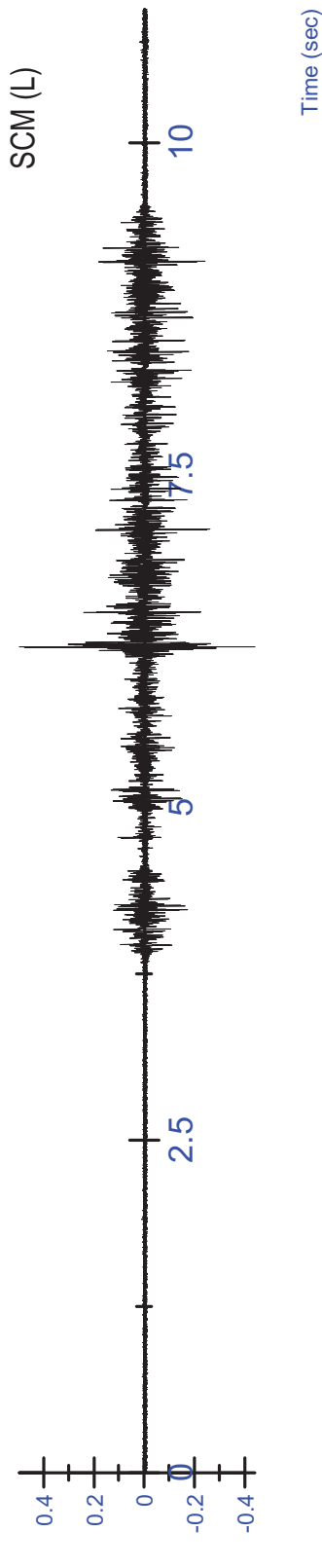
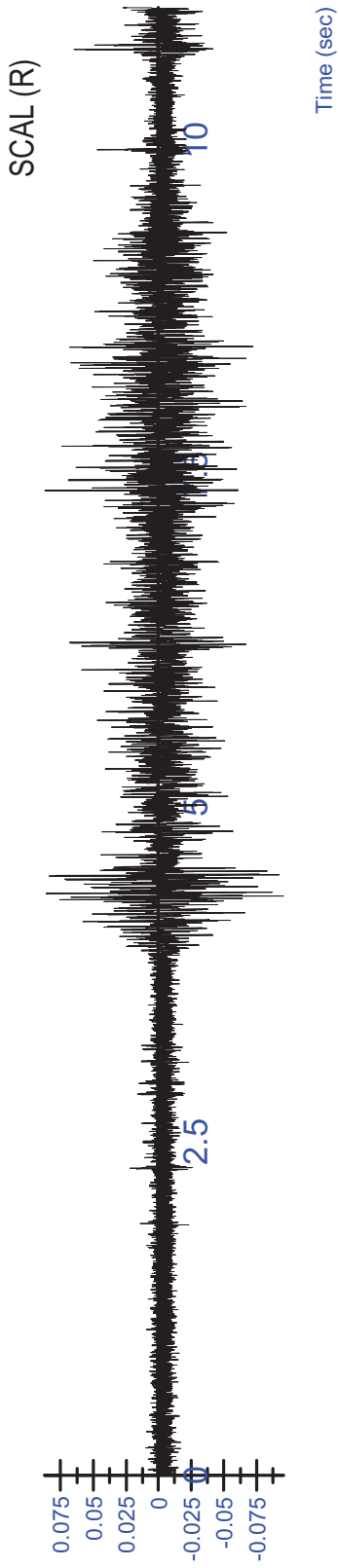
Activation (mV)

Force (N)







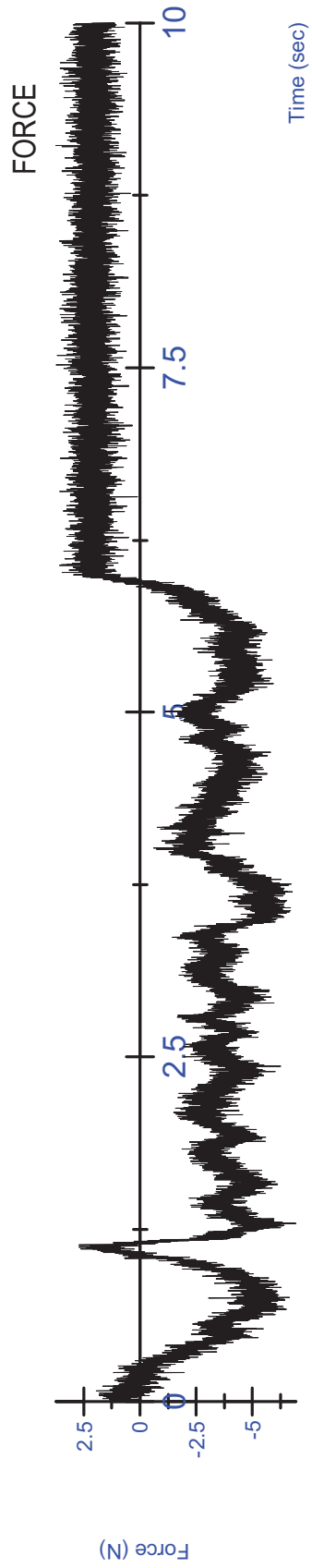
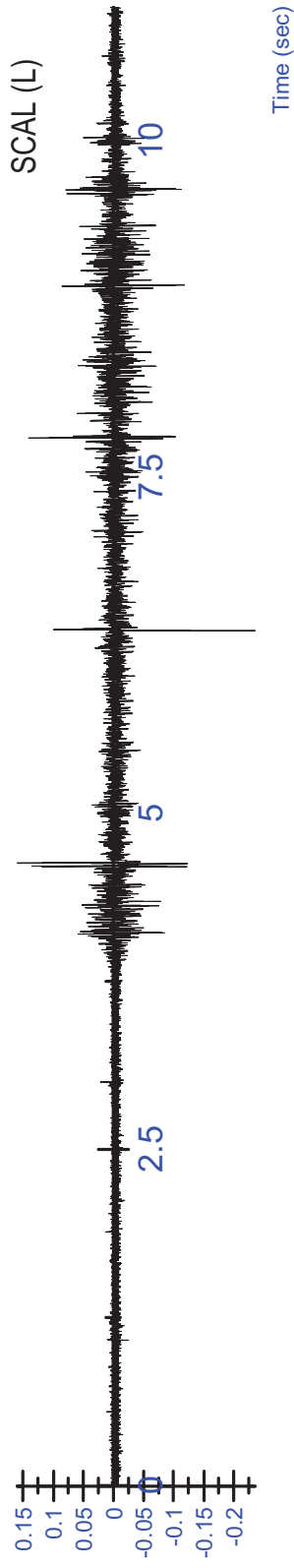
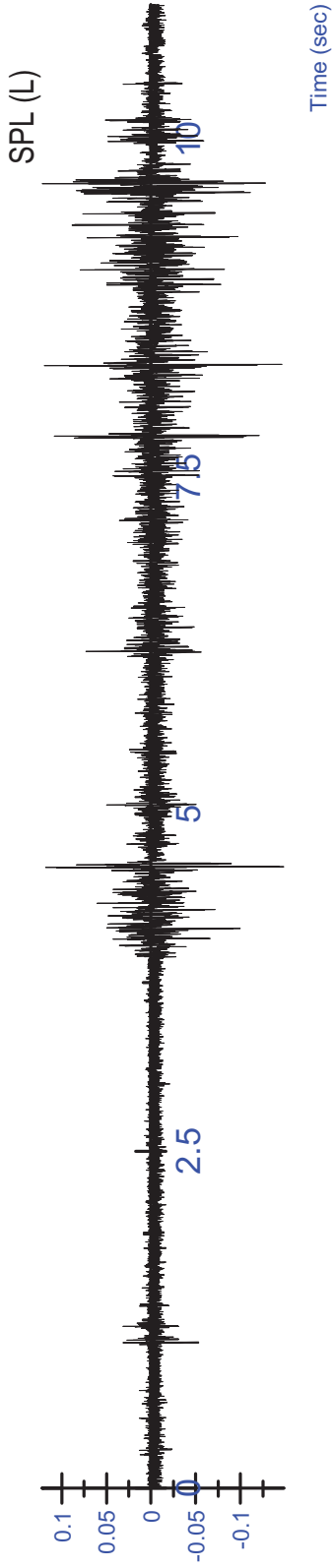


Activation (mV)

Activation (mV)

Activation (mV)

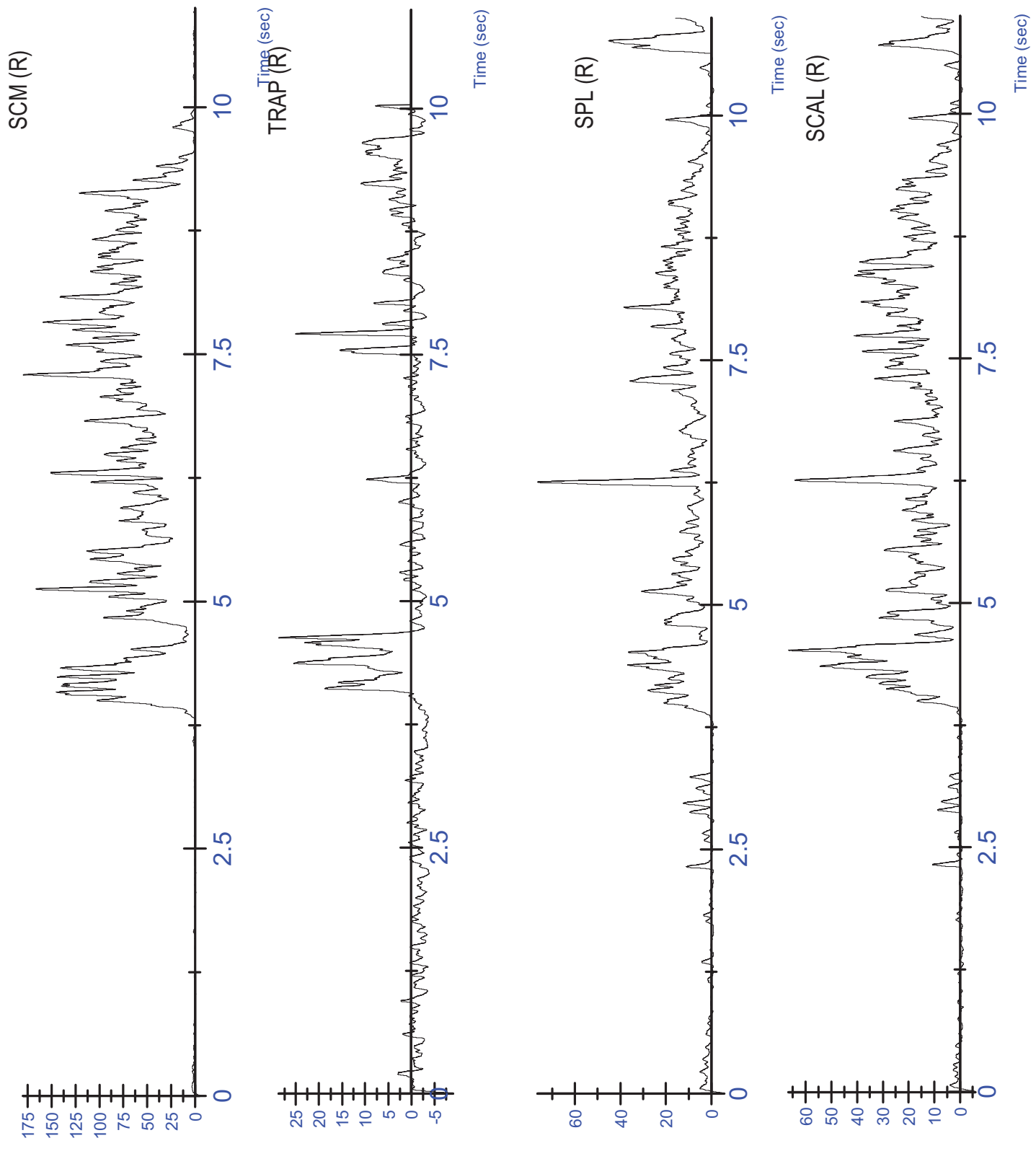
K03 MVC - Flexion Trial 3 - Unfiltered



Activation (mV)

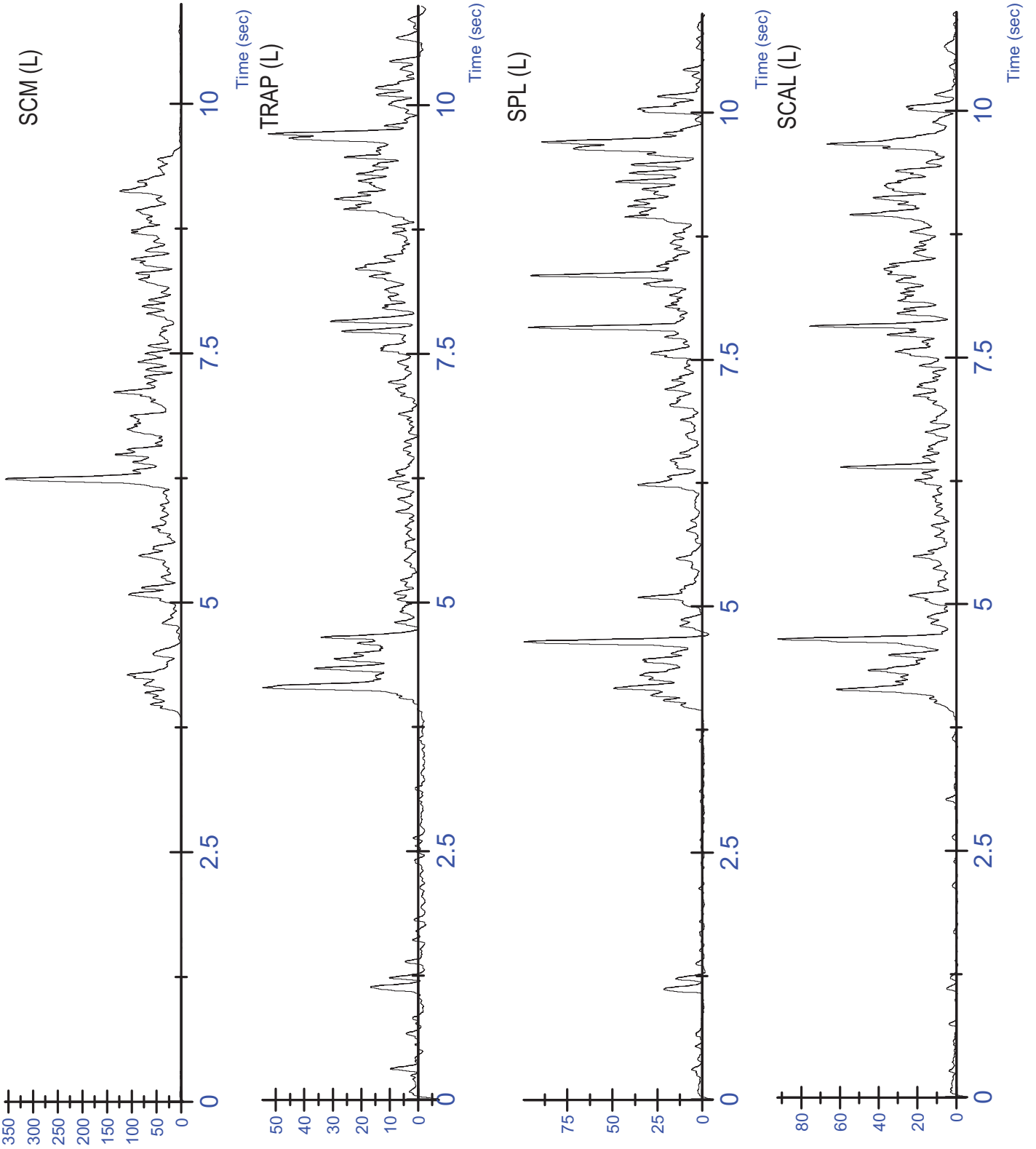
Activation (mV)

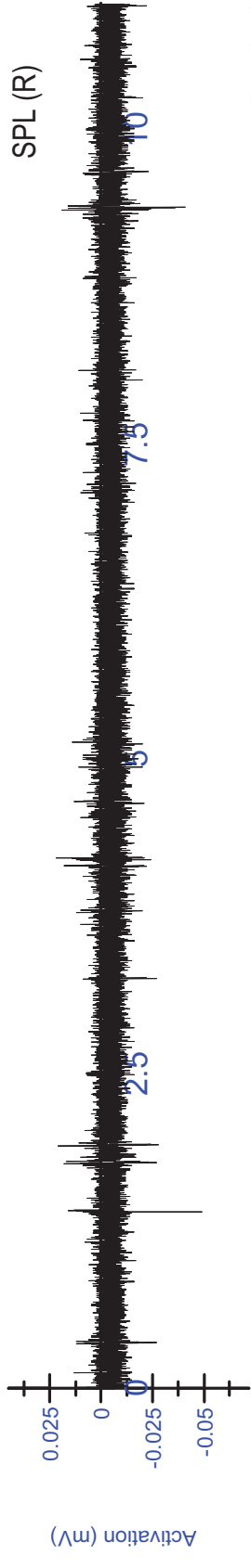
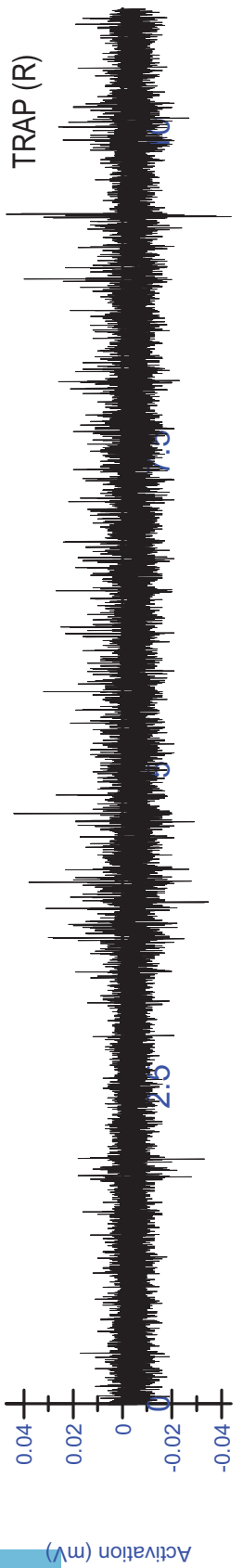
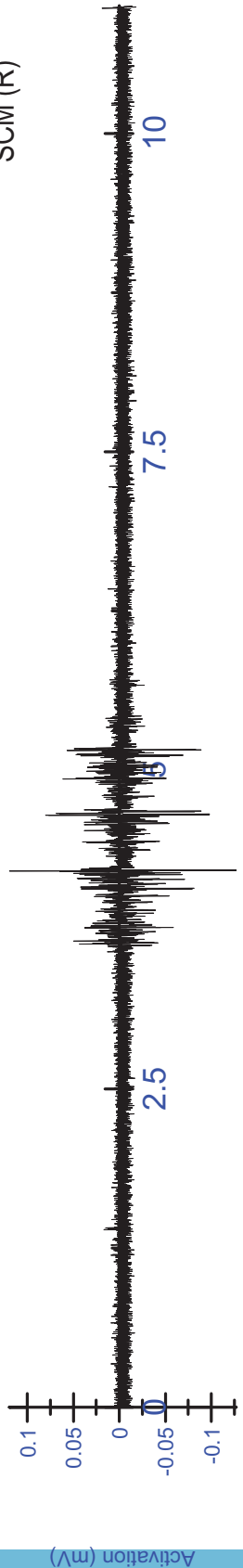
Force (N)



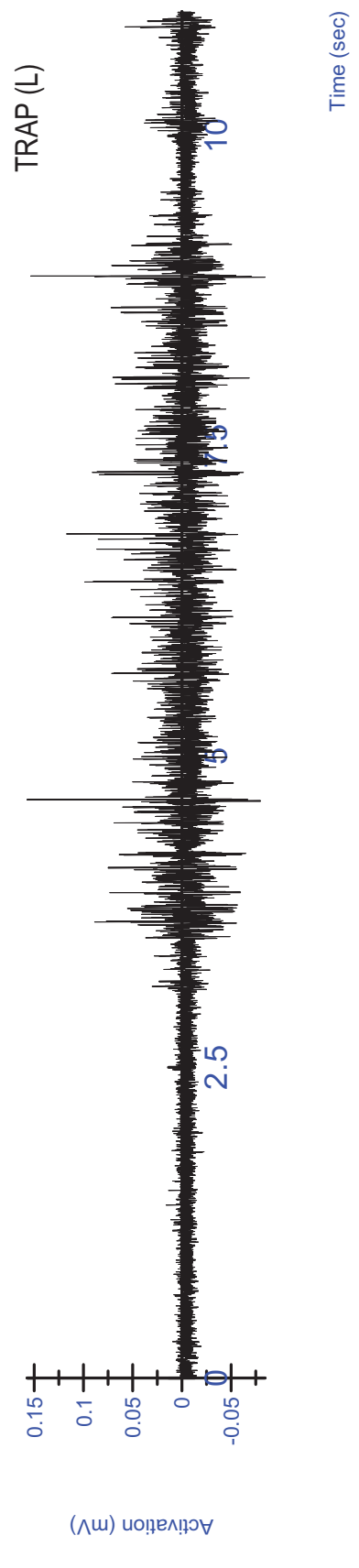
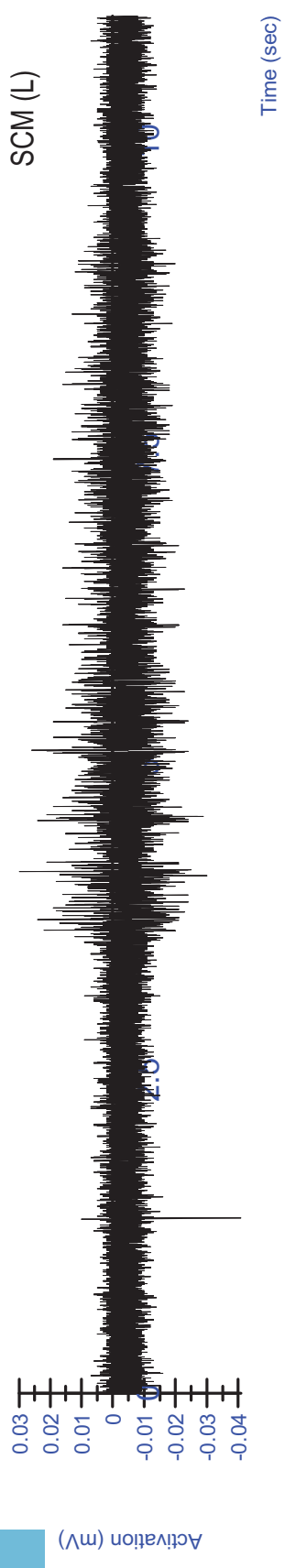
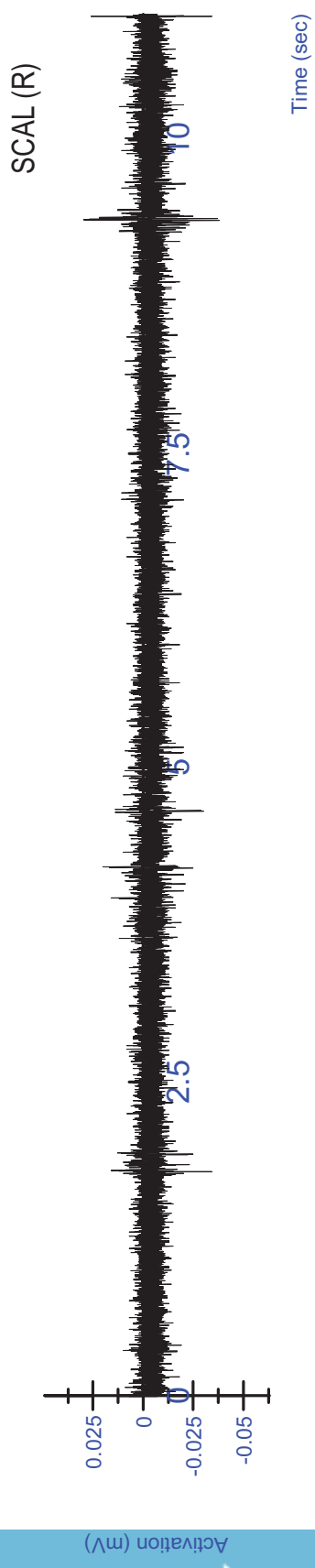
K03 MVC - Flexion Trial 3 - Rectified/Filtered

K03 MVC - Flexion Trial 3 - Rectified/Filtered

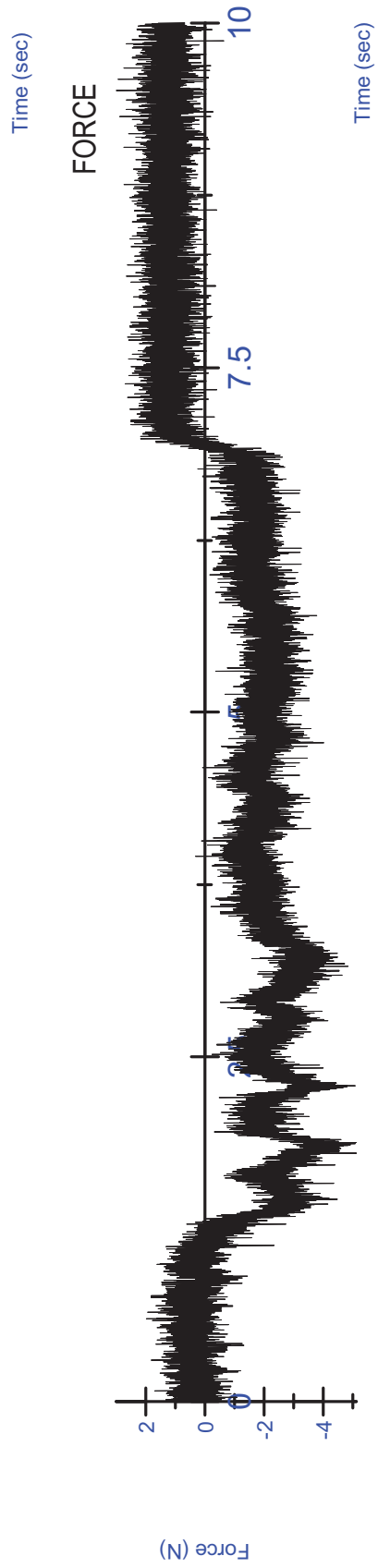
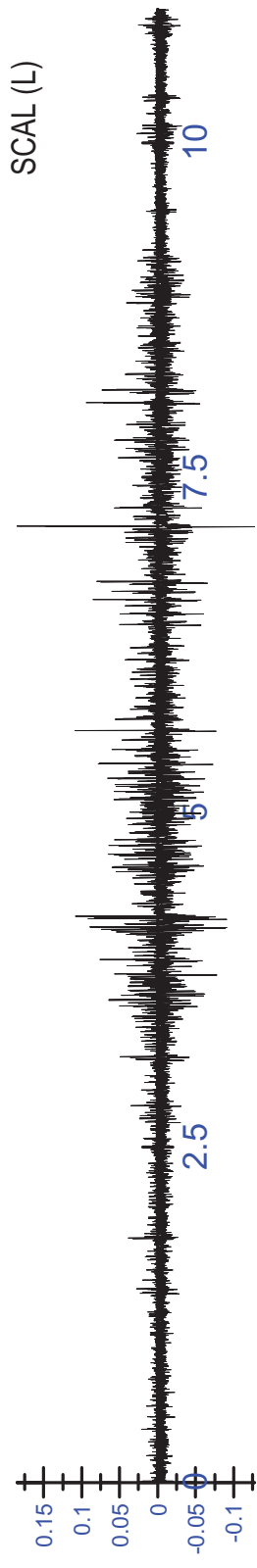
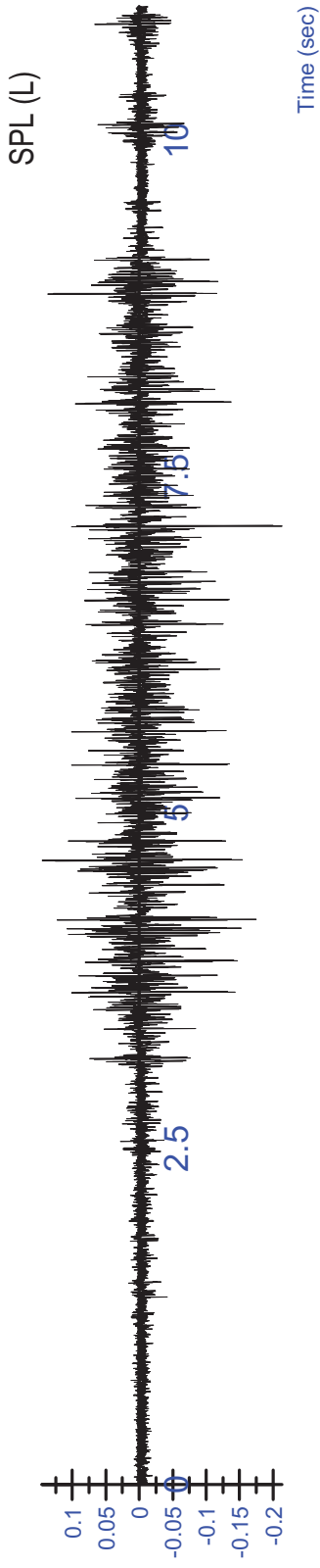


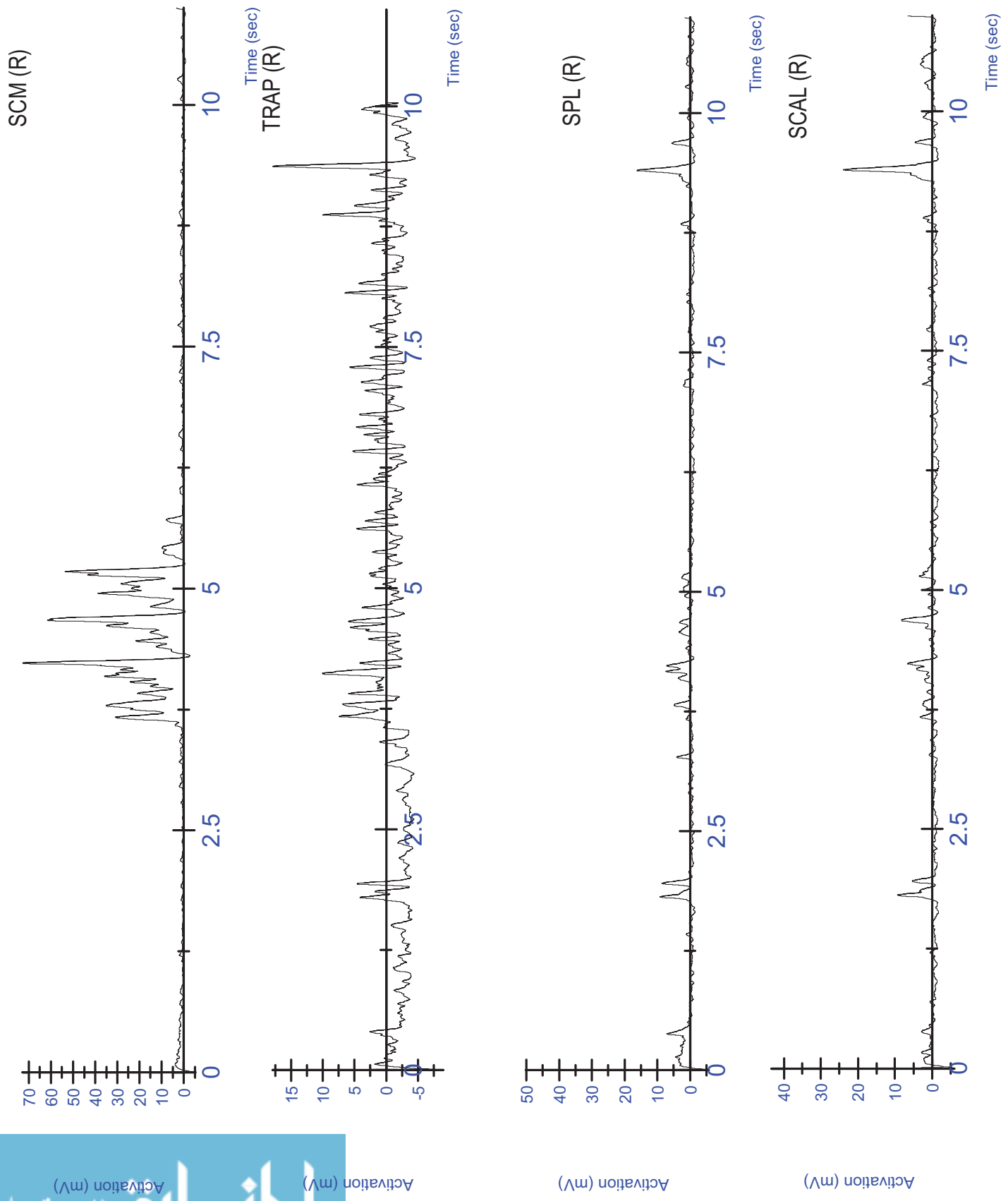


K03 MVC - Lateral (L) Trial 1 - Unfiltered

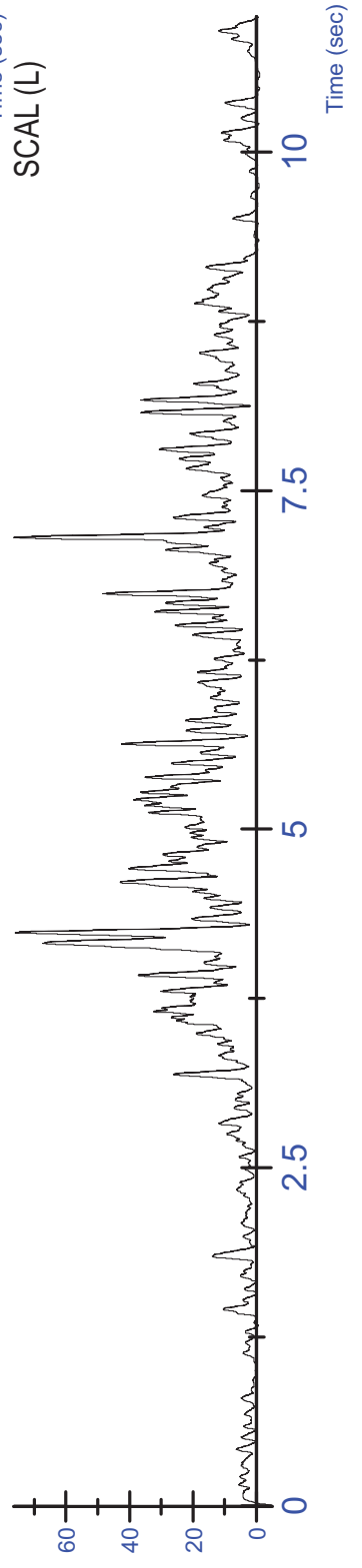
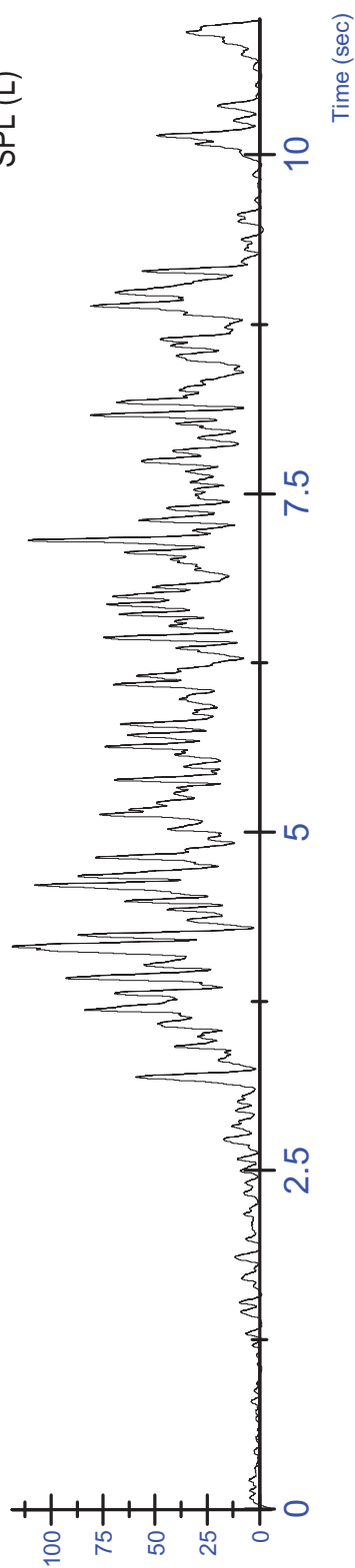
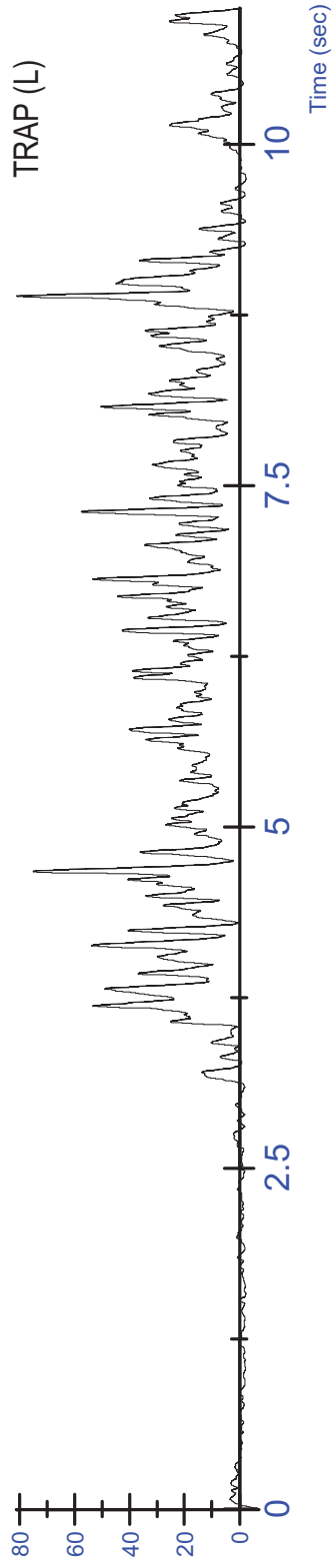
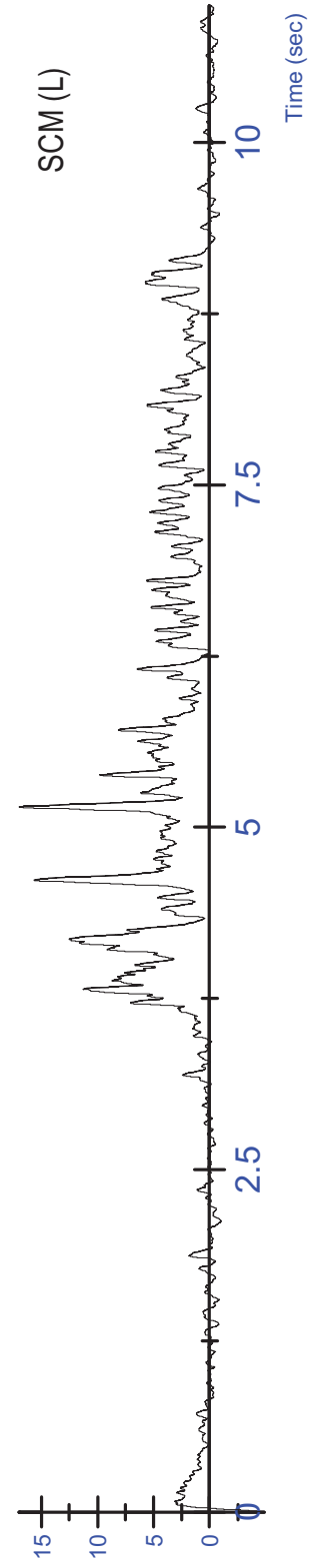


K03 MVC - Lateral (L) Trial 1 - Unfiltered

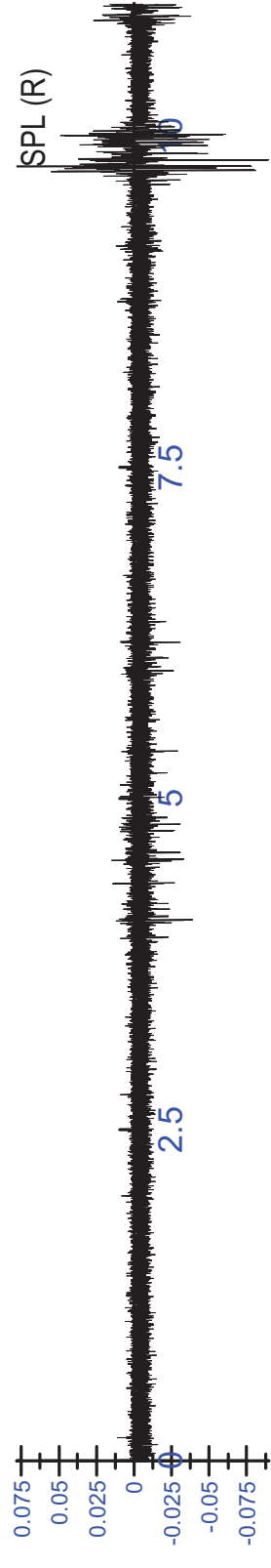
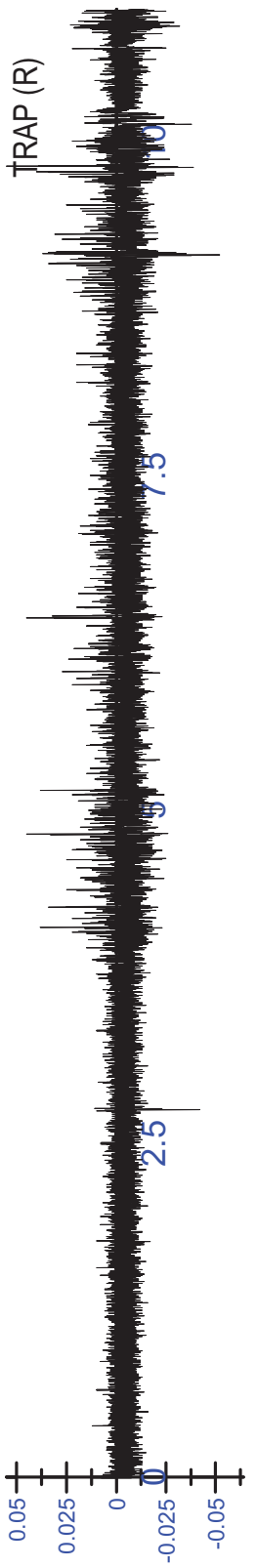
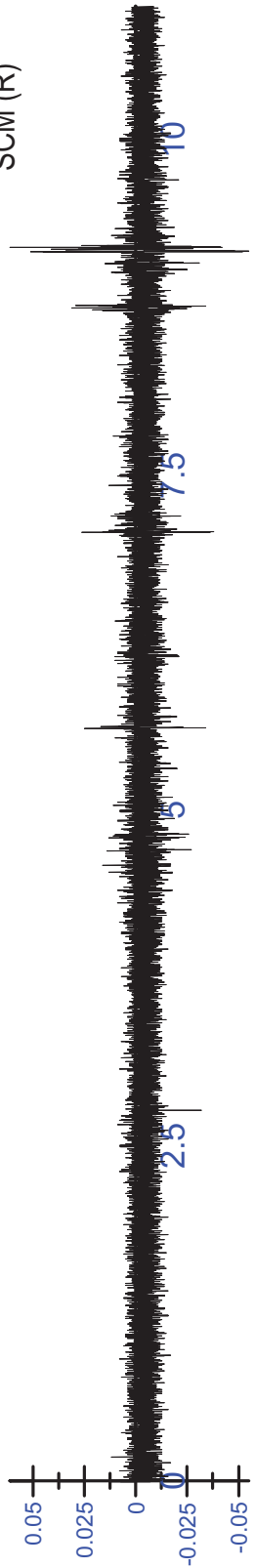




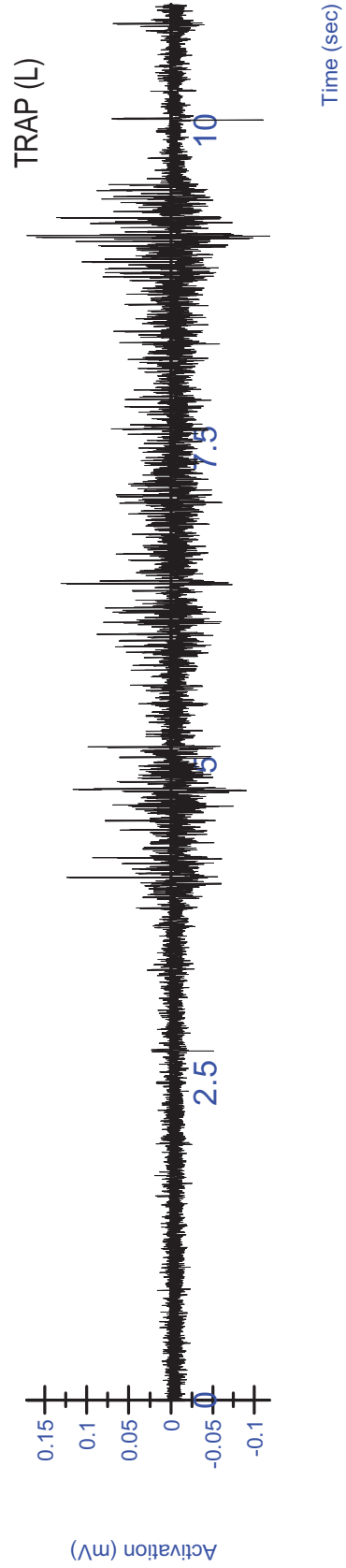
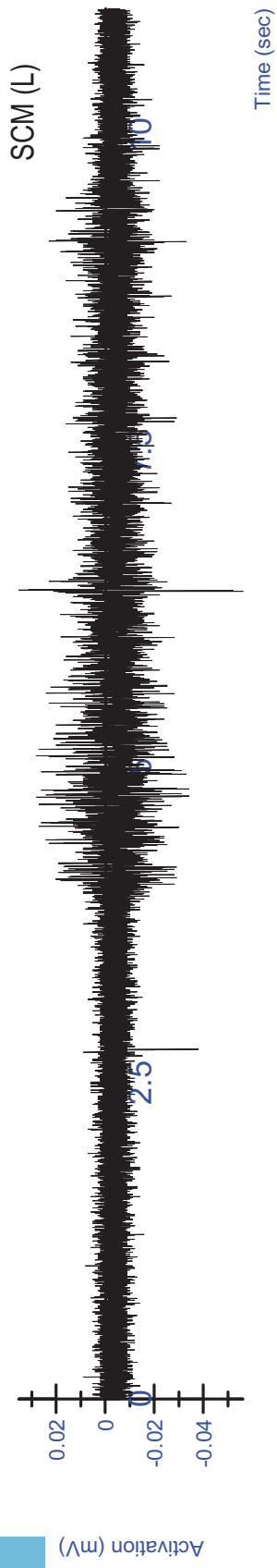
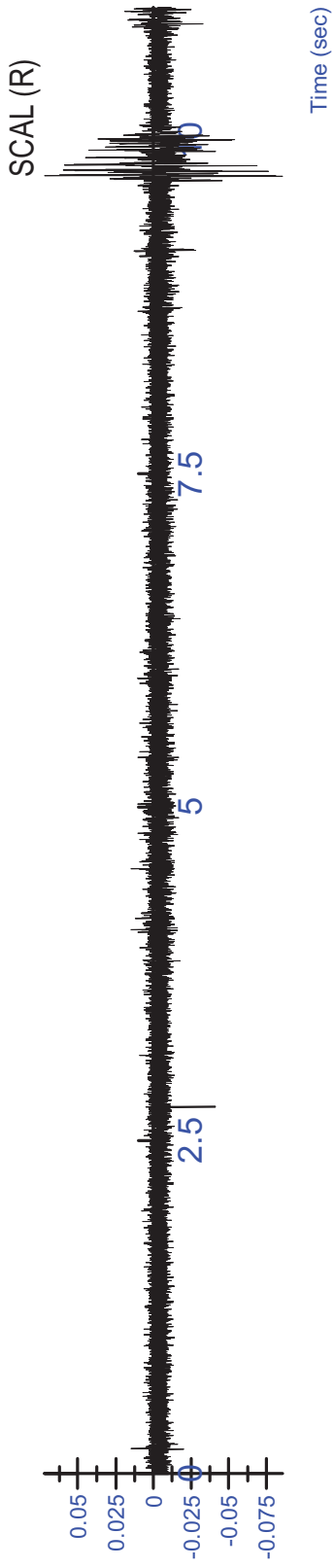
K03 MVC - Lateral (L) Trial 1 - Rectified/Filtered



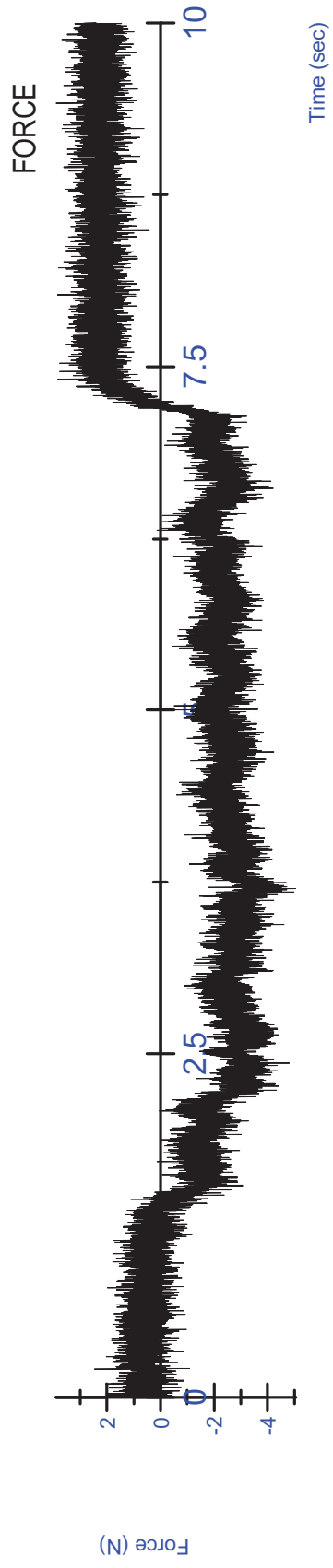
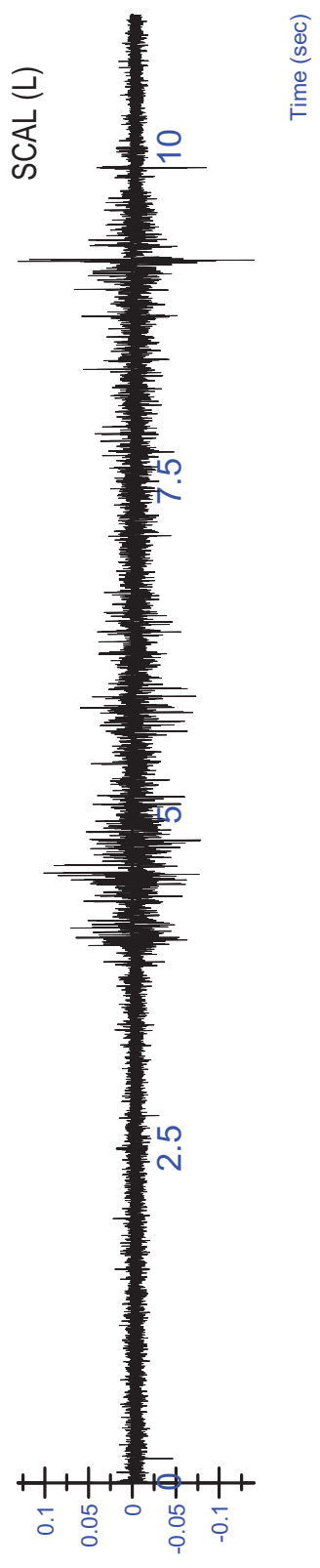
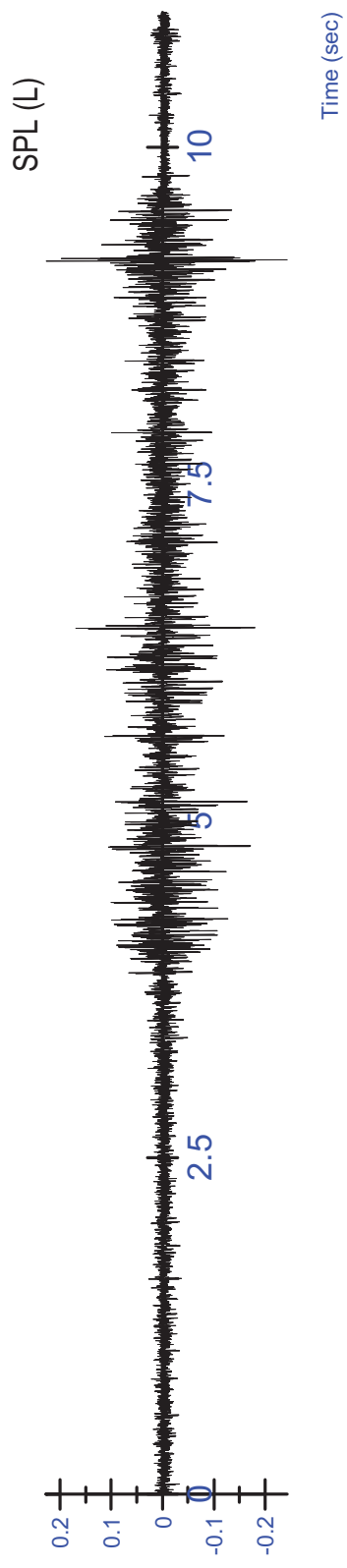
K03 MVC - Lateral (L) Trial 1 - Rectified/Filtered



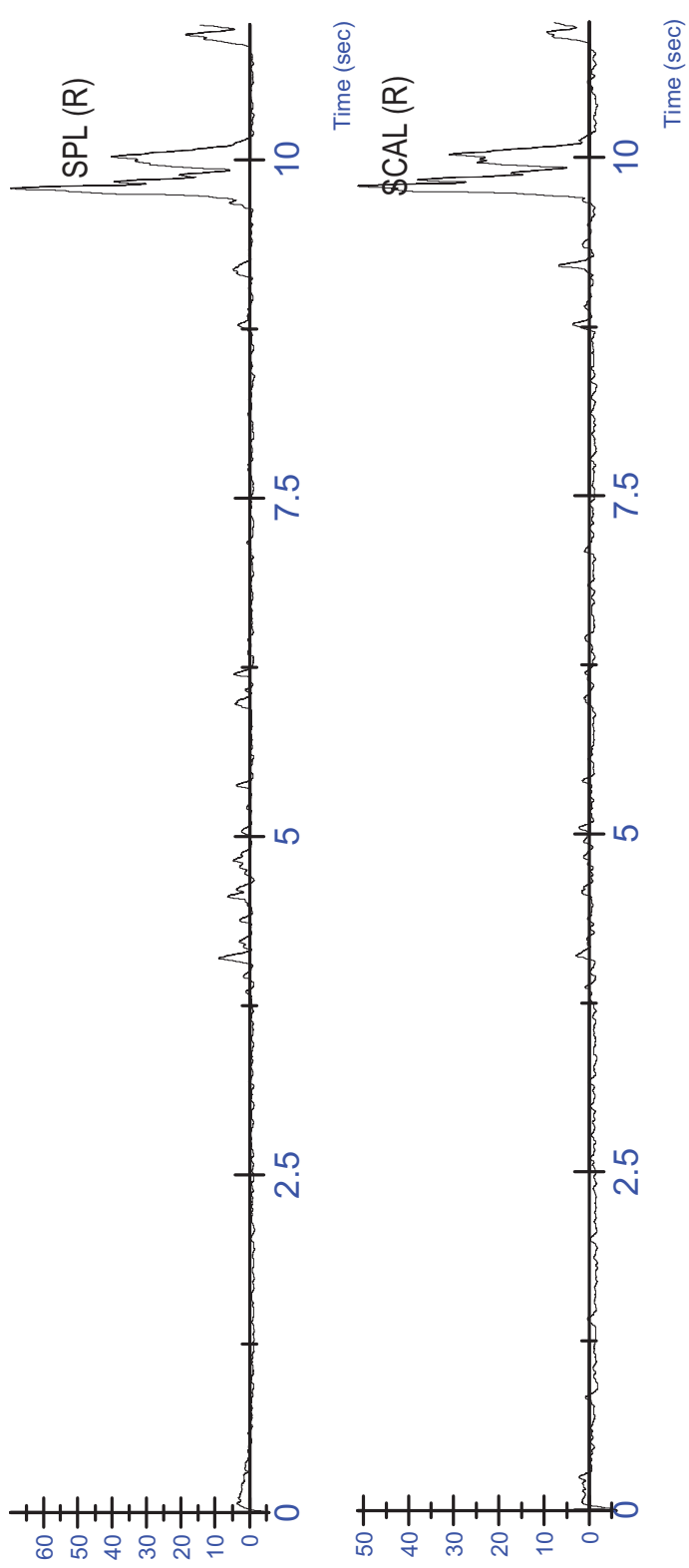
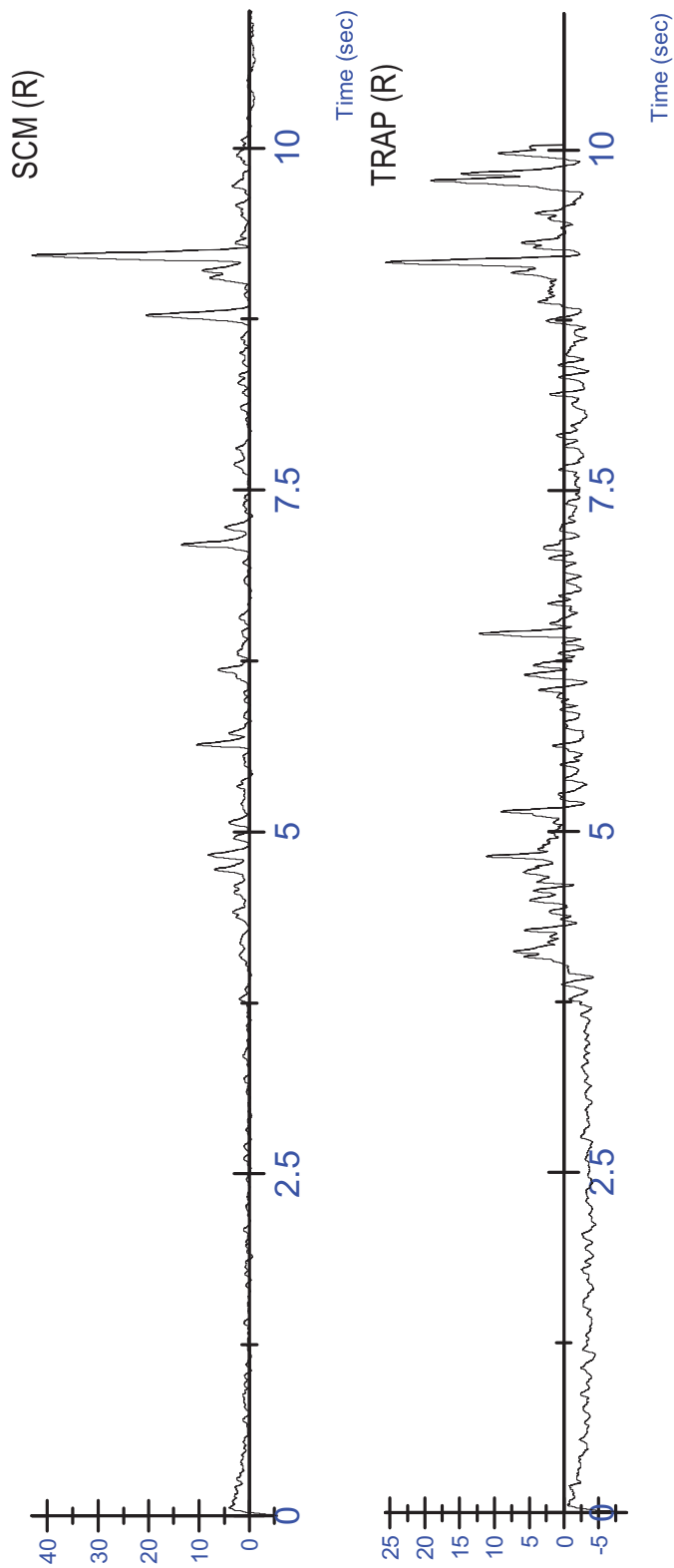
K03 MVC - Lateral (L) Trial 2 - Unfiltered

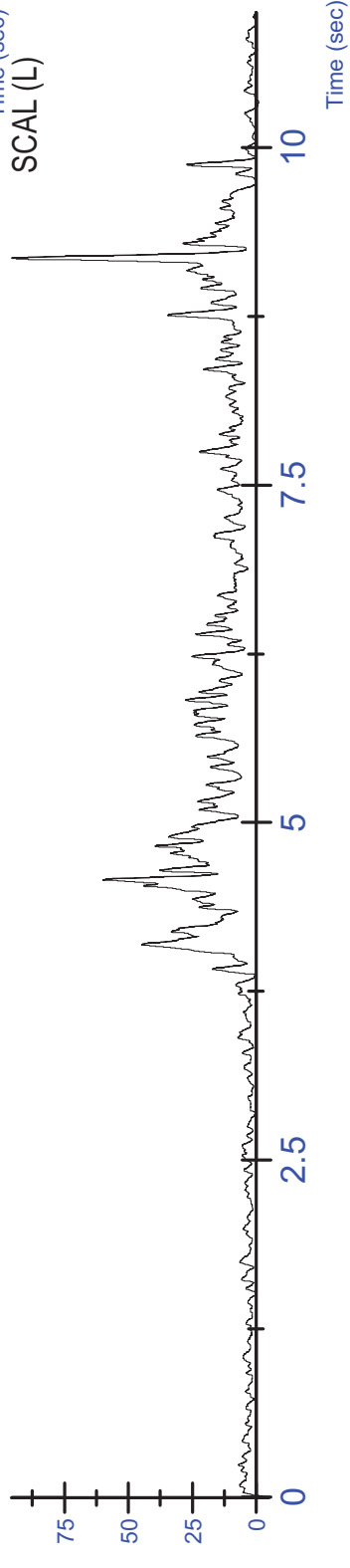
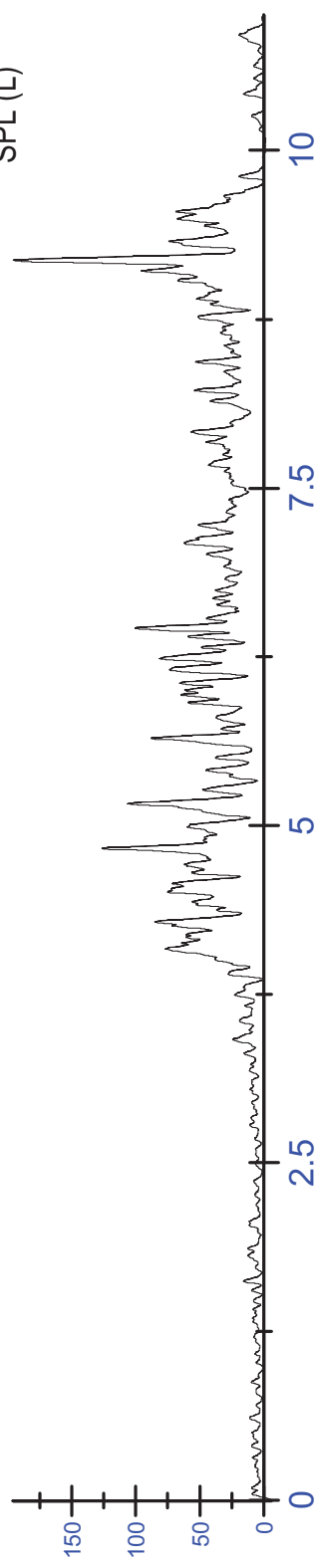
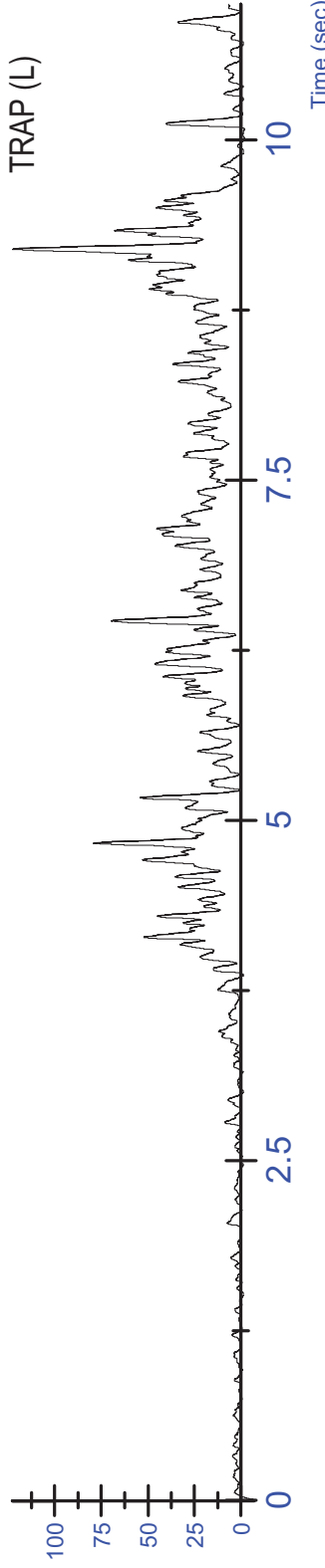
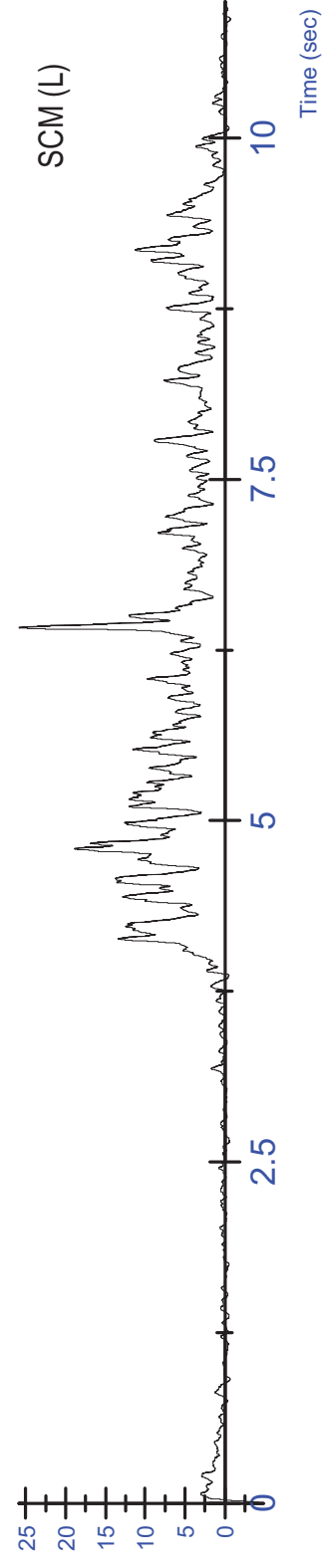


K03 MVC - Lateral (L) Trial 2 - Unfiltered

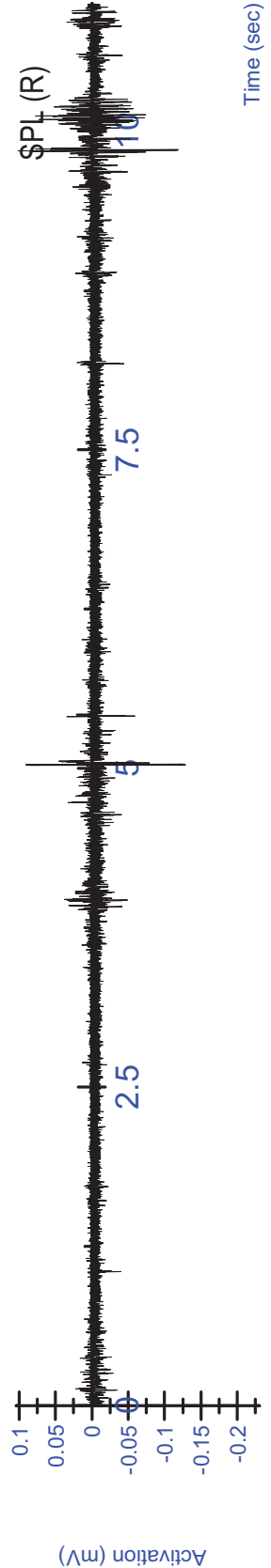
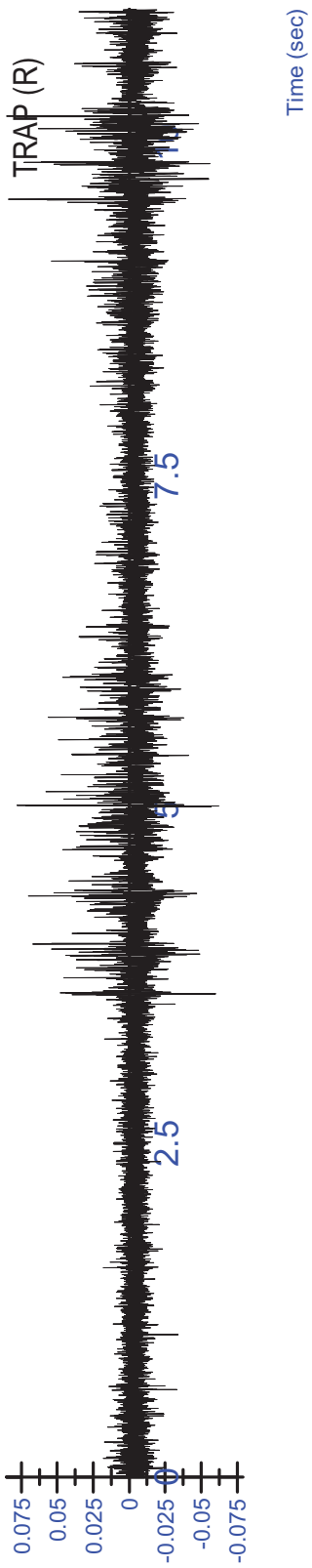
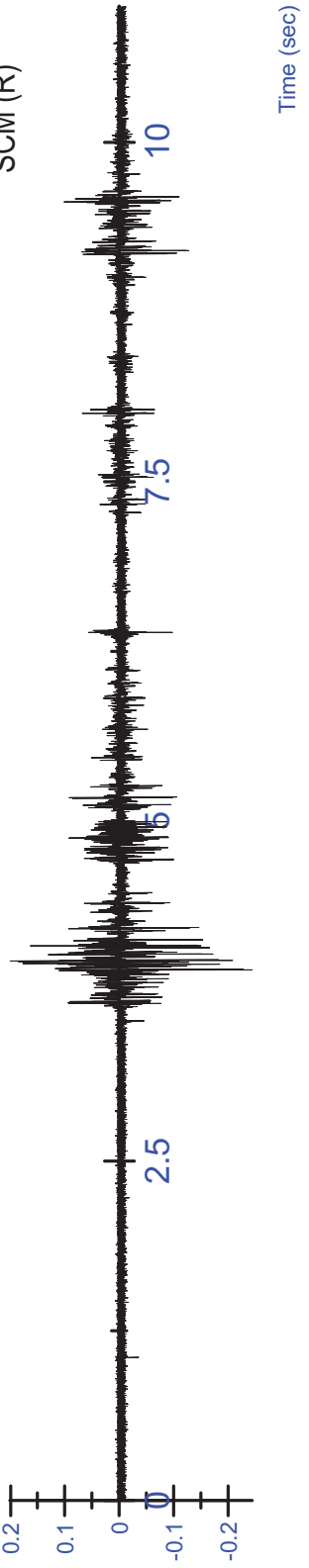


K03 MVC - Lateral (L) Trial 2 - Rectified/Filtered

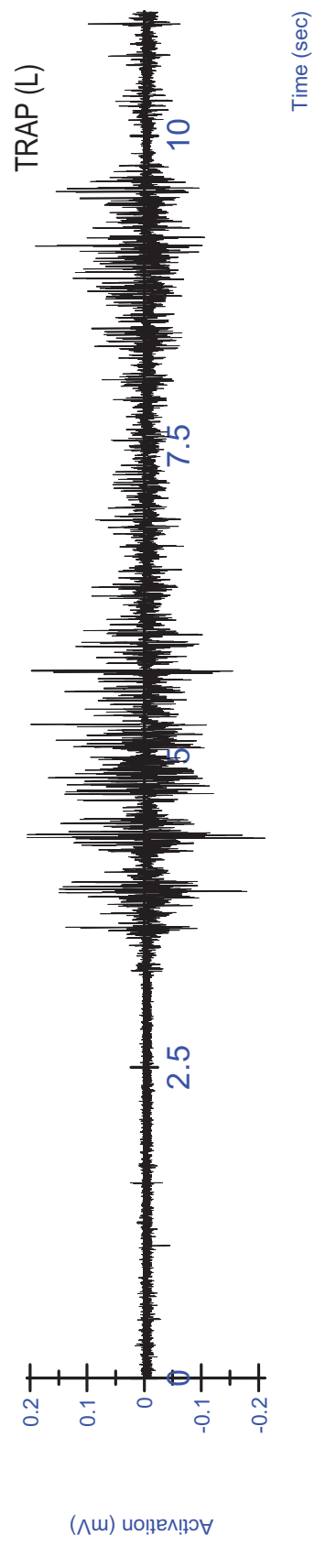
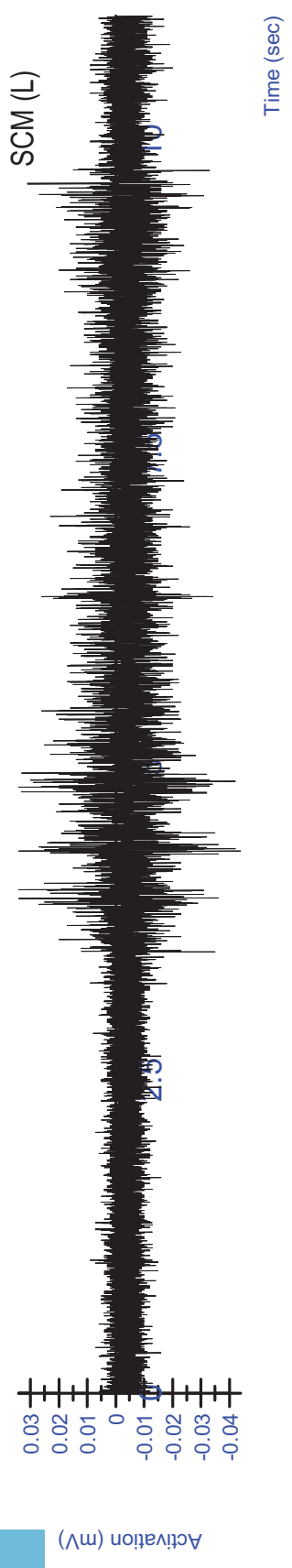
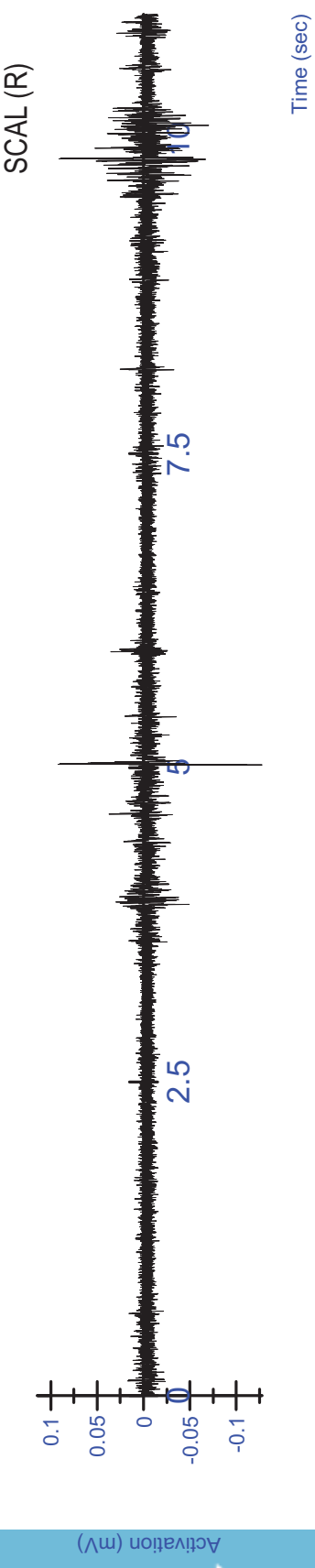




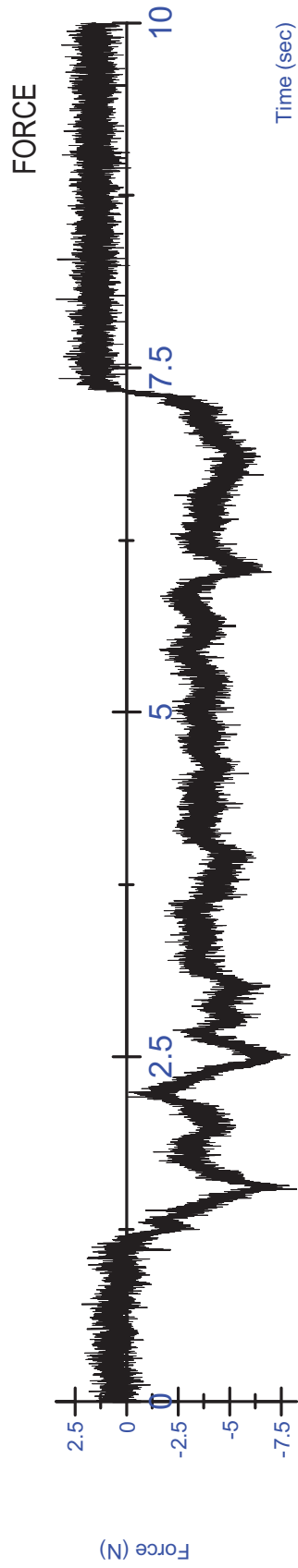
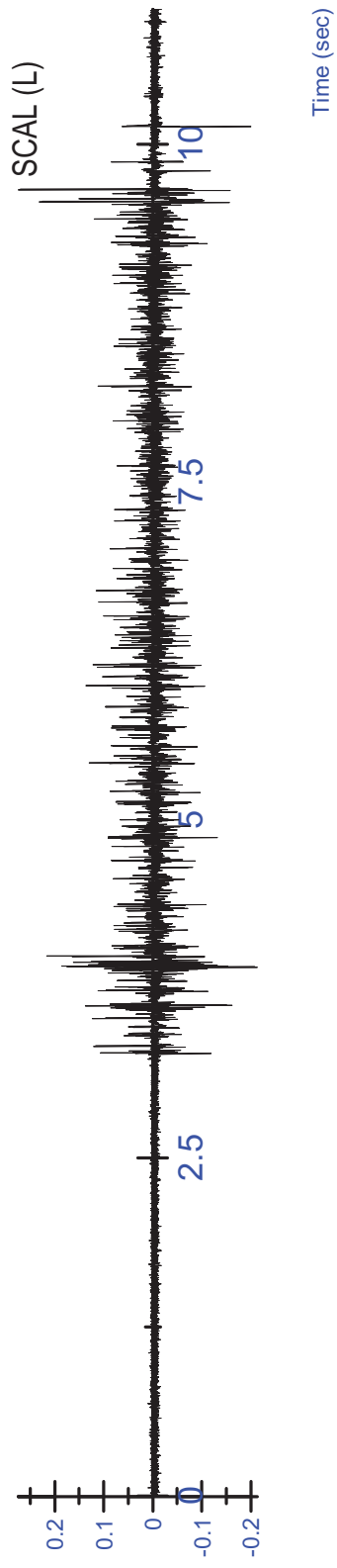
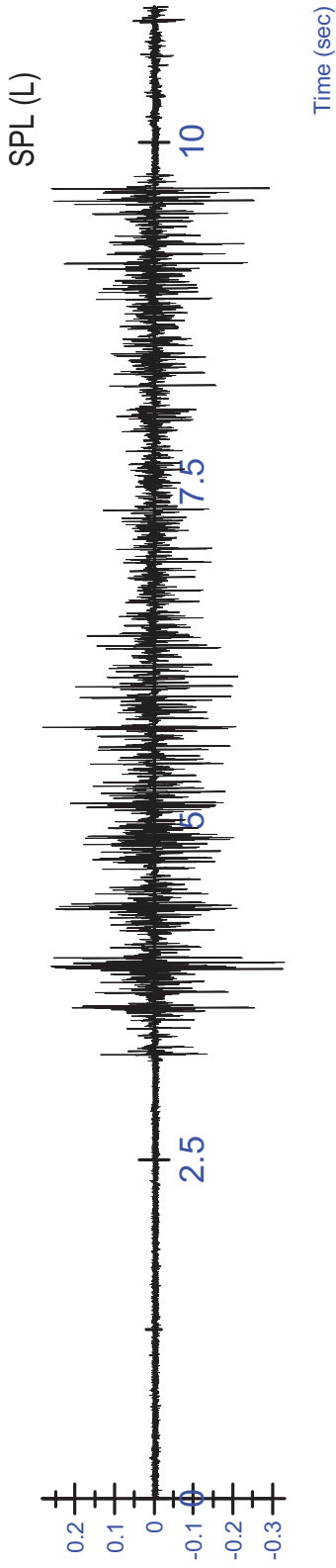
K03 MVC - Lateral (L) Trial 2 - Rectified/Filtered

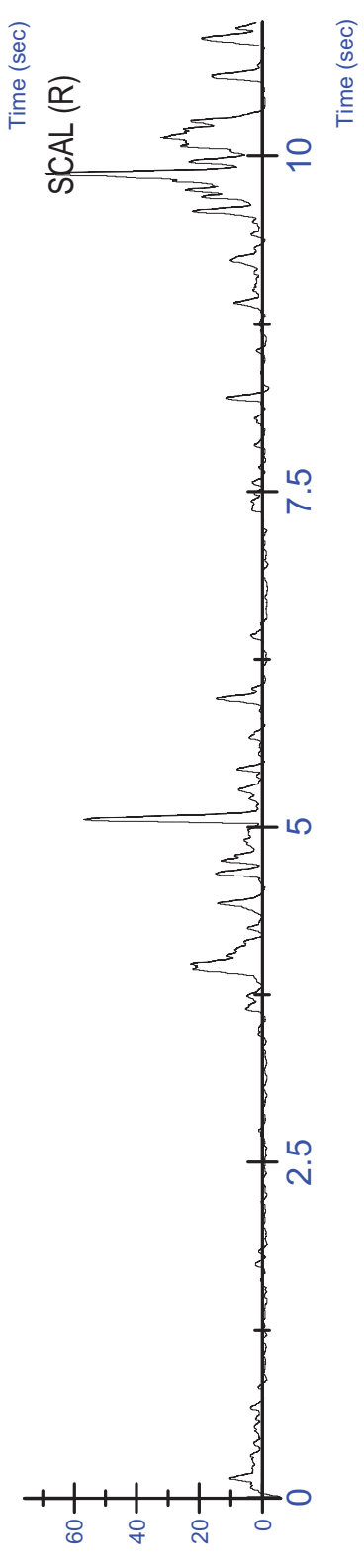
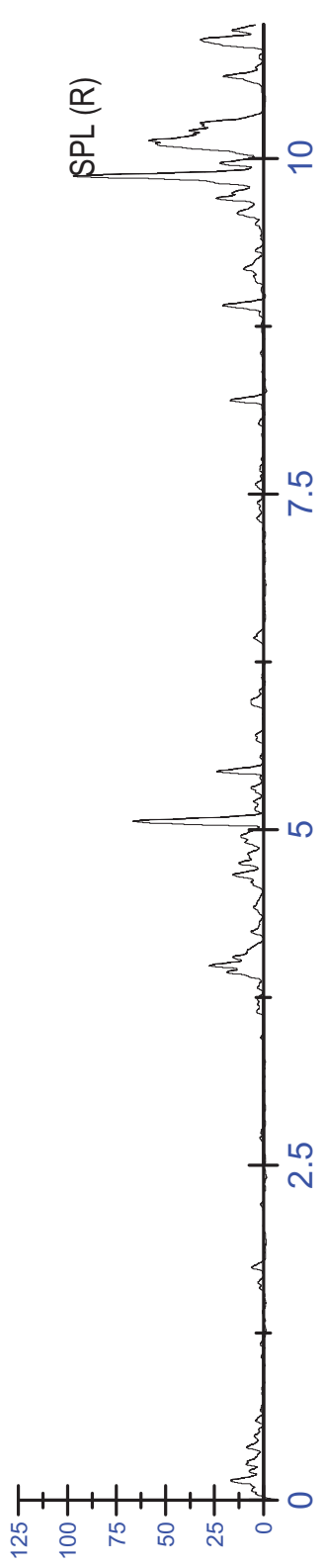
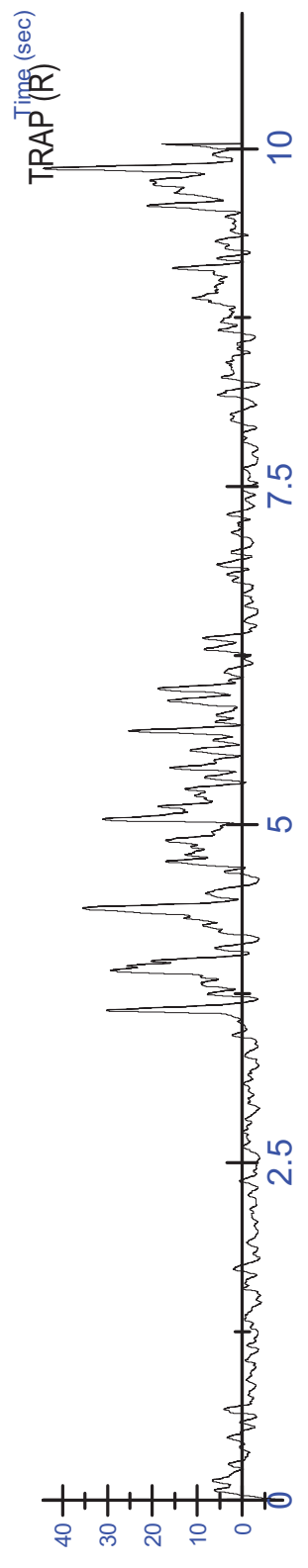
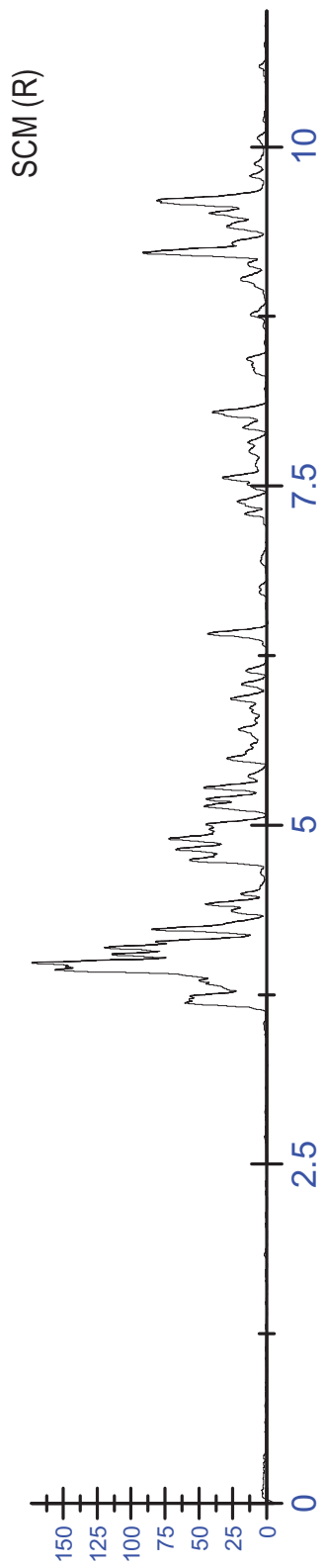


K03 MVC - Lateral (L) Trial 3 - Unfiltered

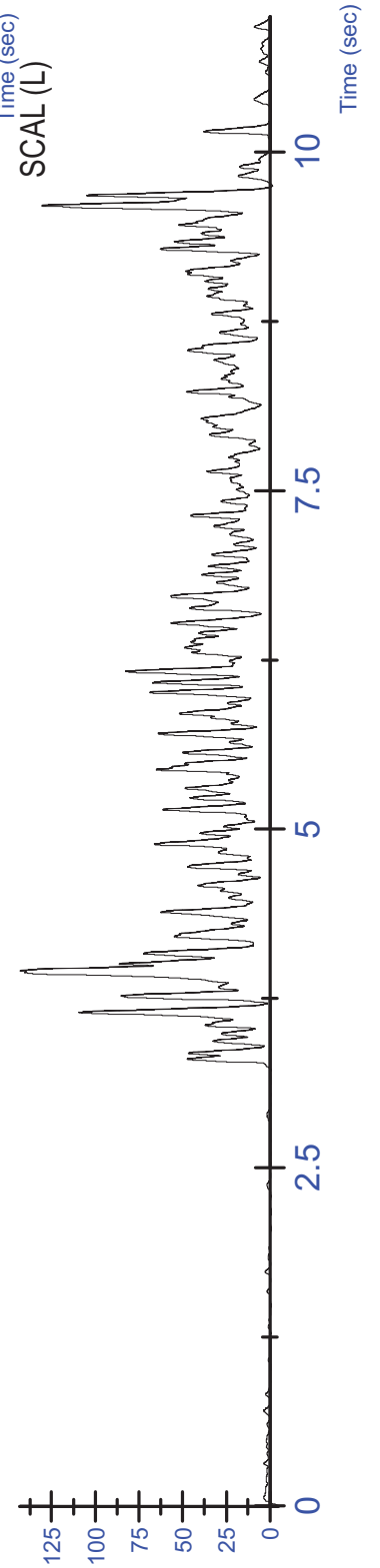
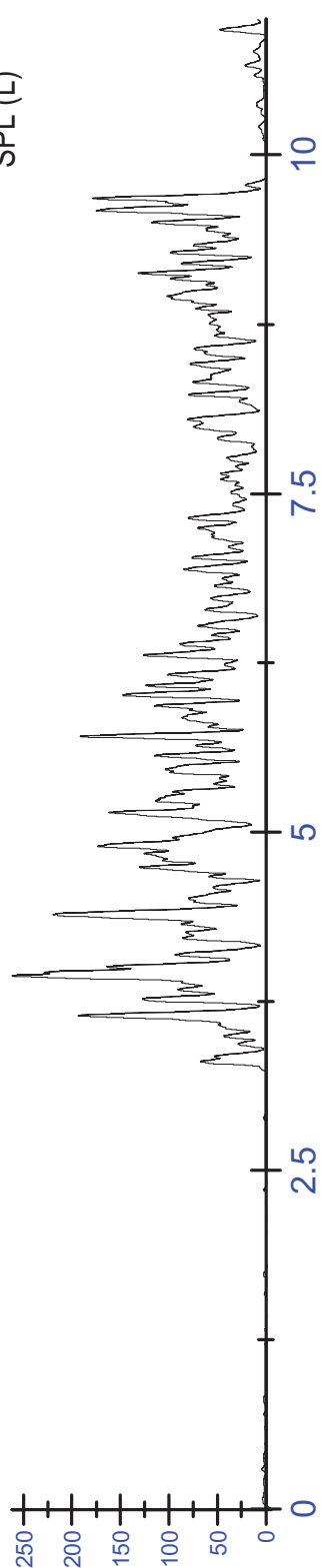
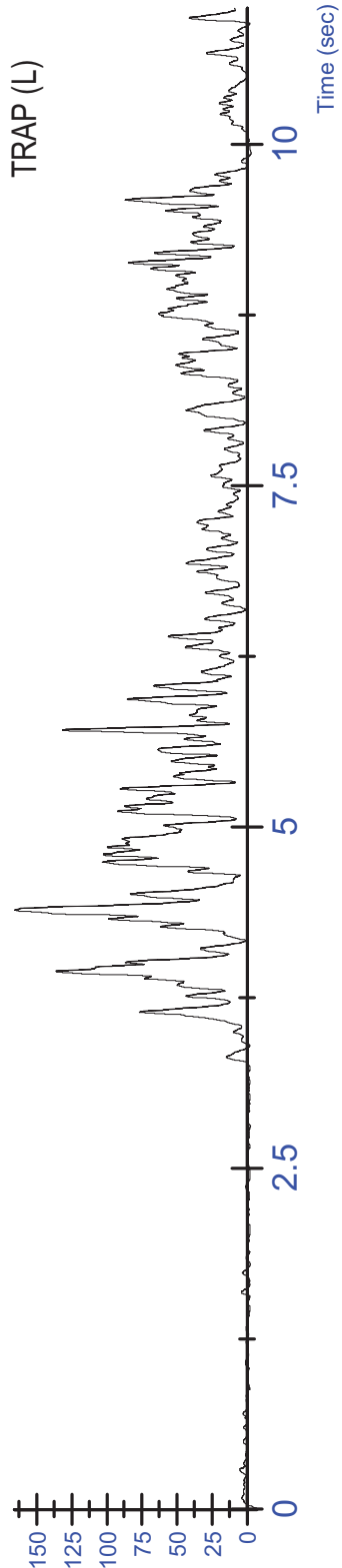
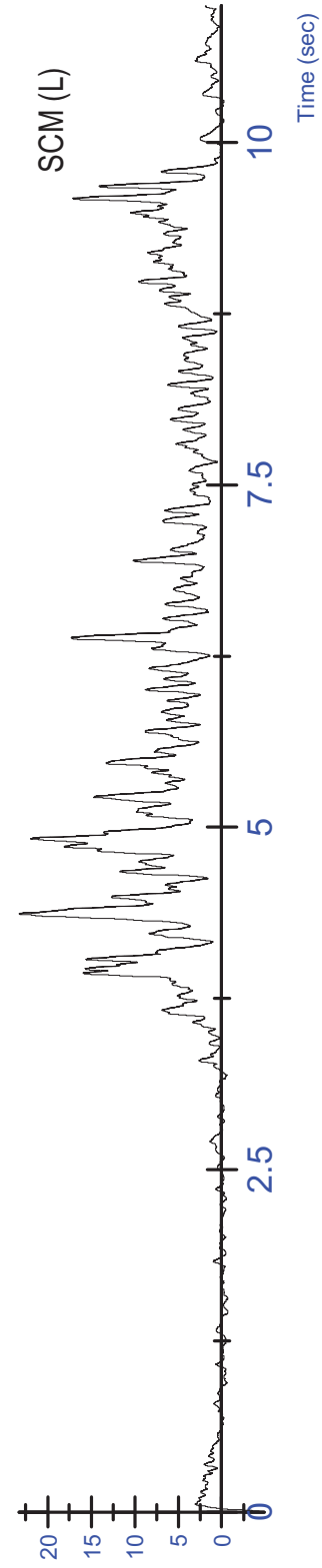


K03 MVC - Lateral (L) Trial 3 - Unfiltered



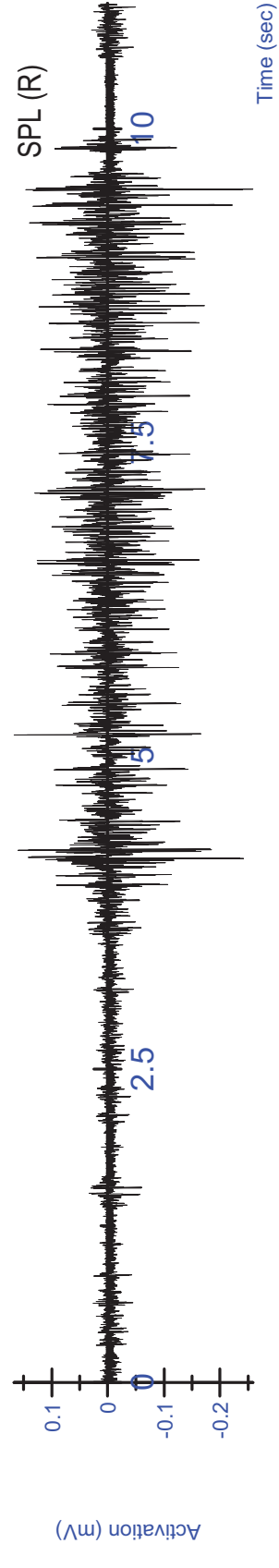
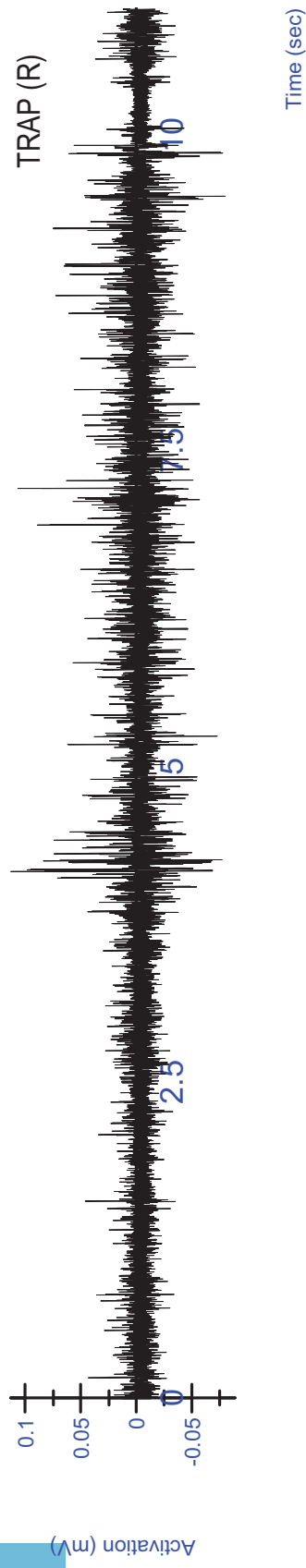
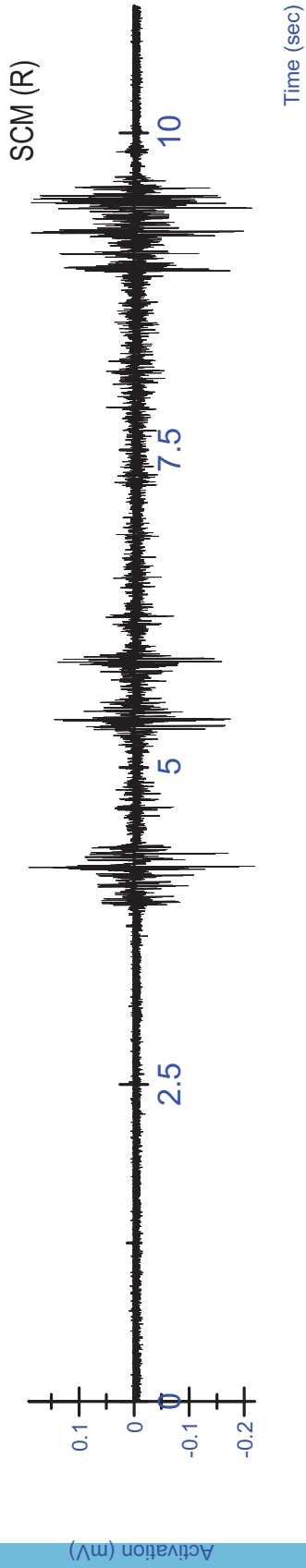


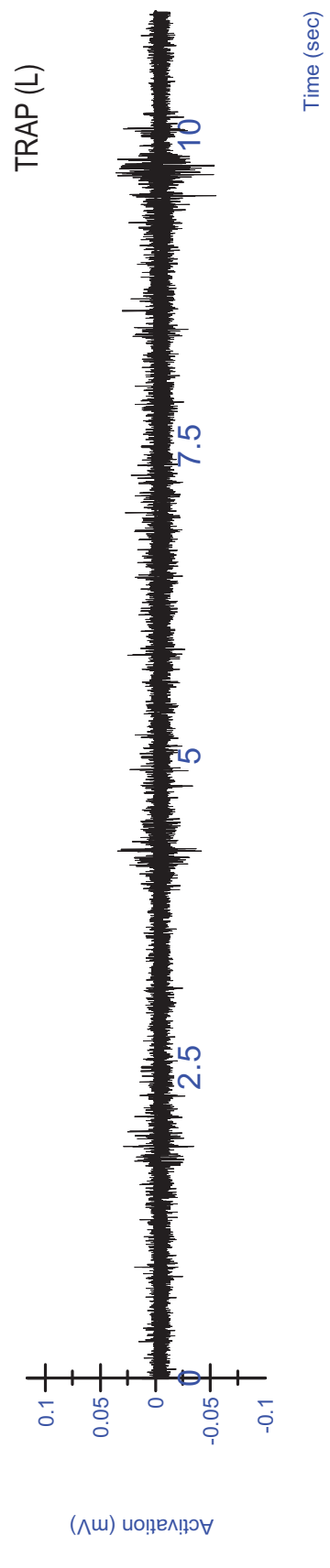
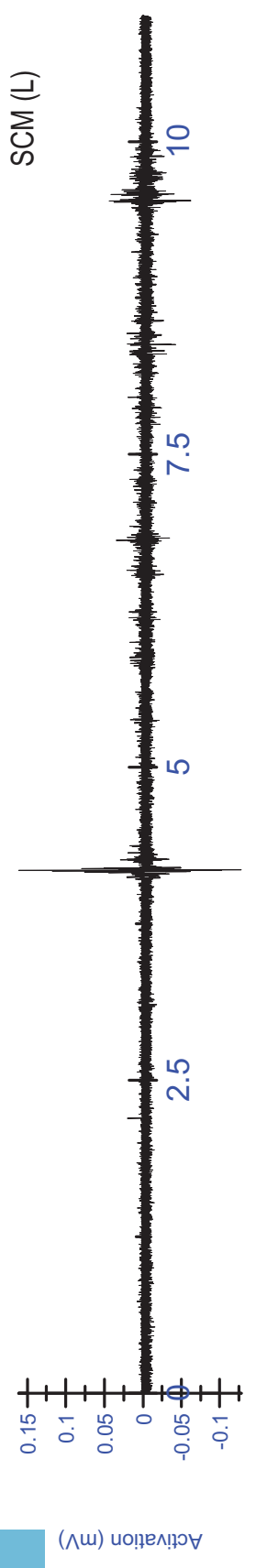
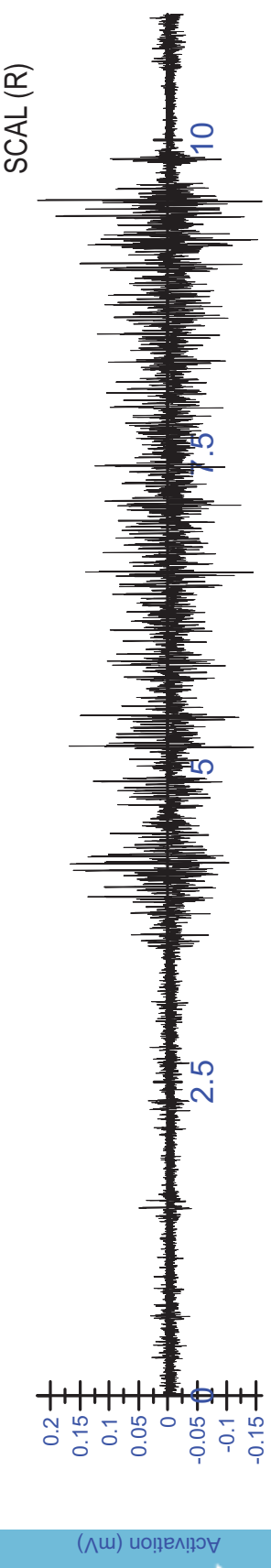
K03 MVC - Lateral (L) Trial 3 - Rectified/Filtered

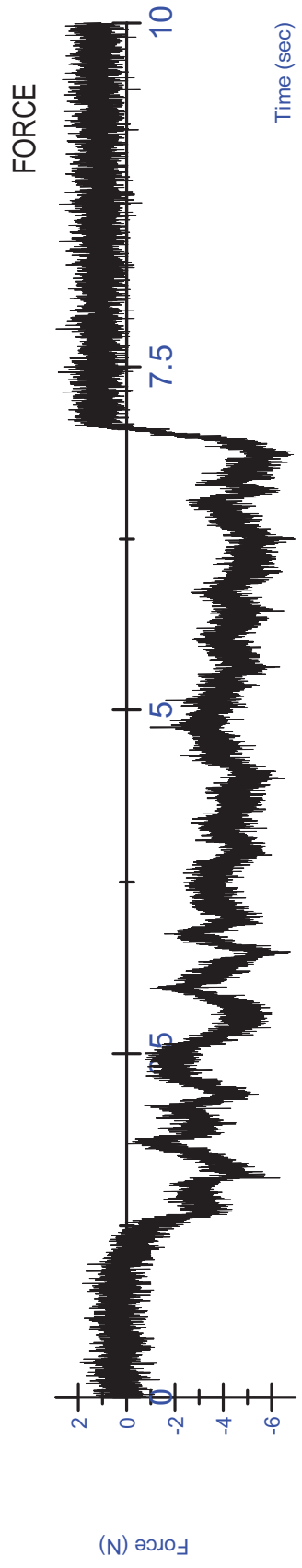
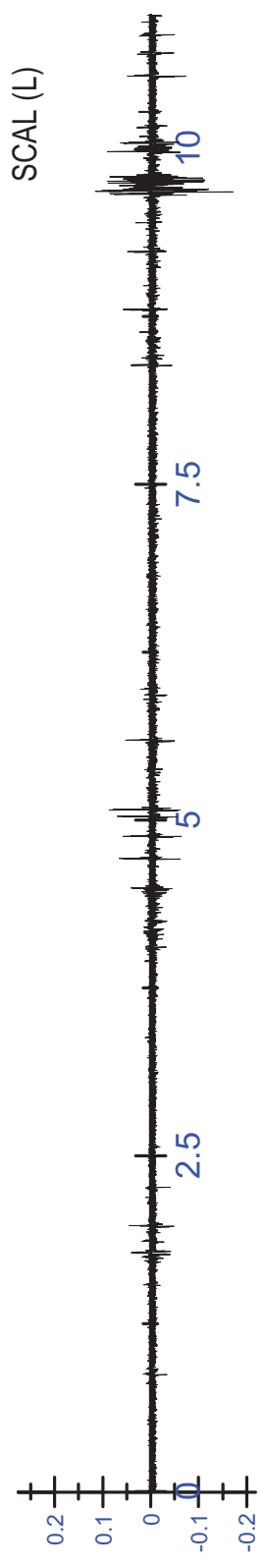
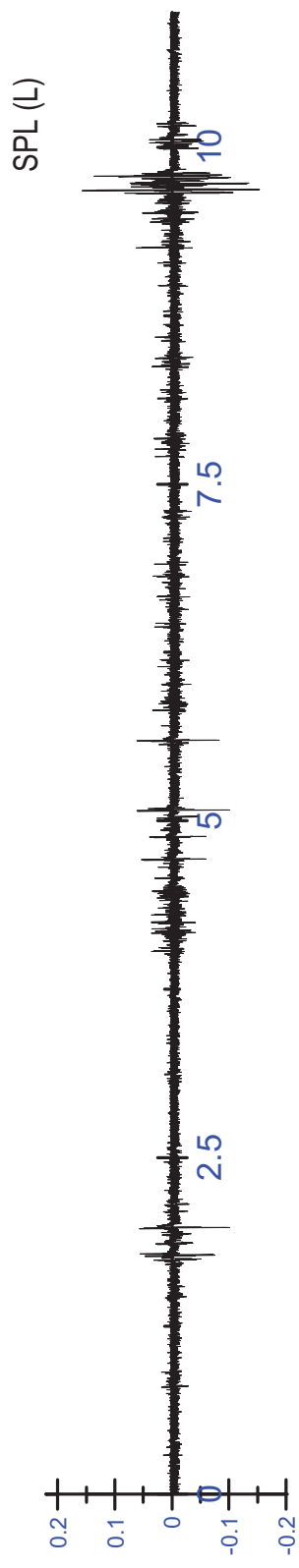


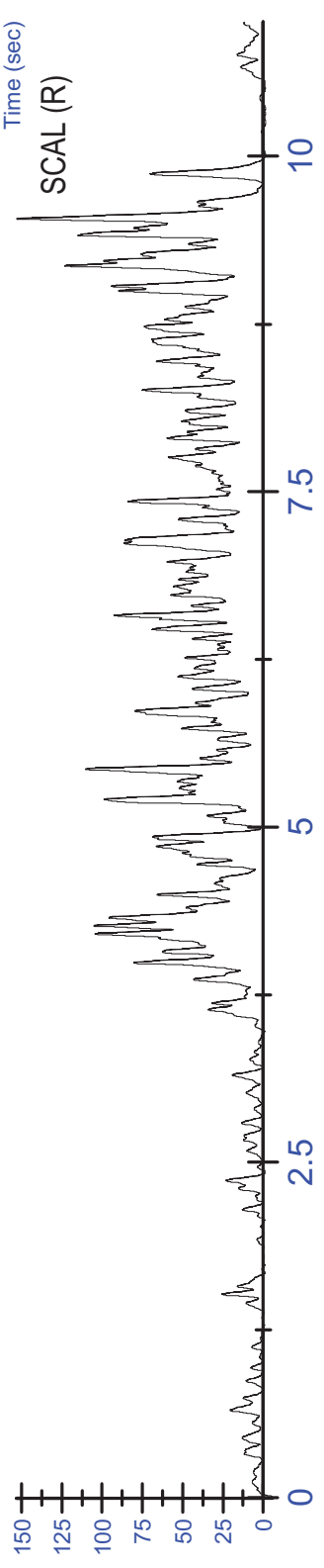
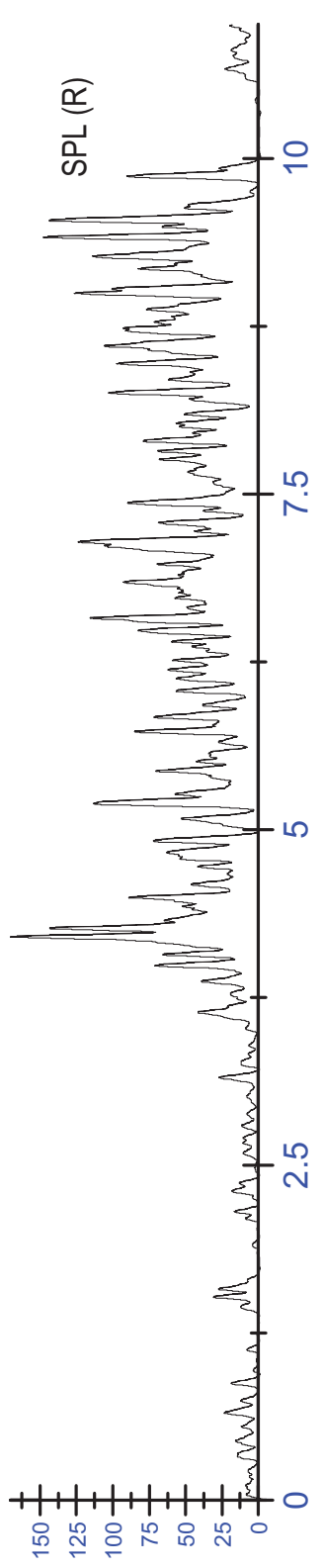
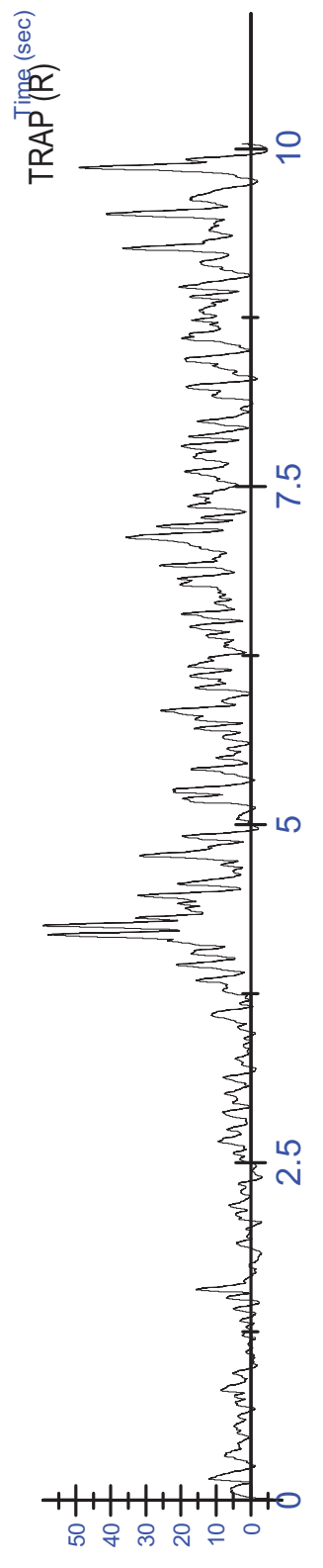
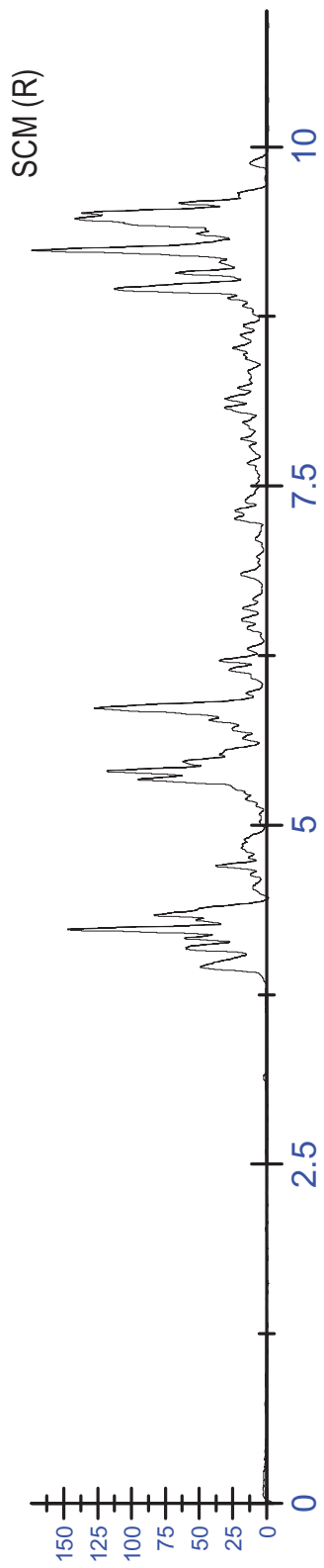
K03 MVC - Lateral (L) Trial 3 - Rectified/Filtered

K03 MVC - Lateral (R) Trial 1 - Unfiltered

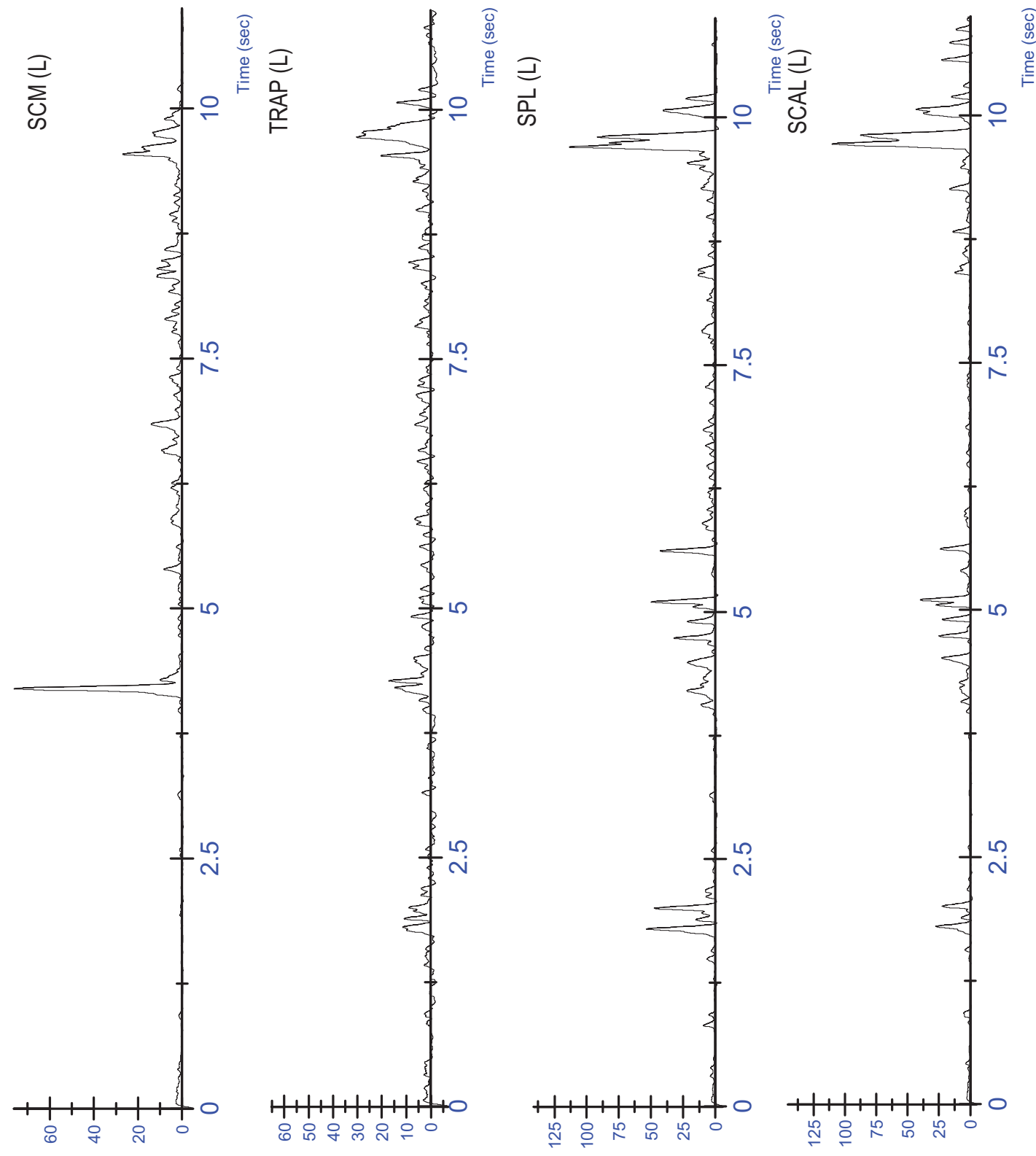




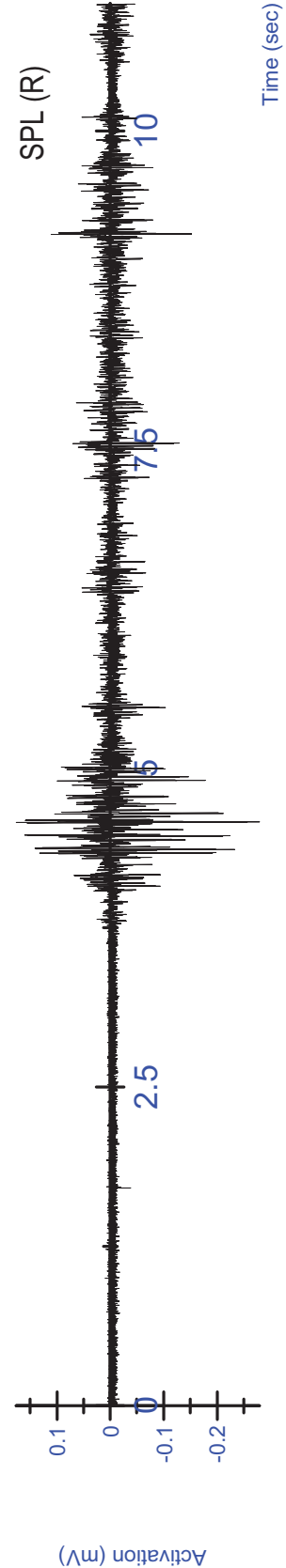
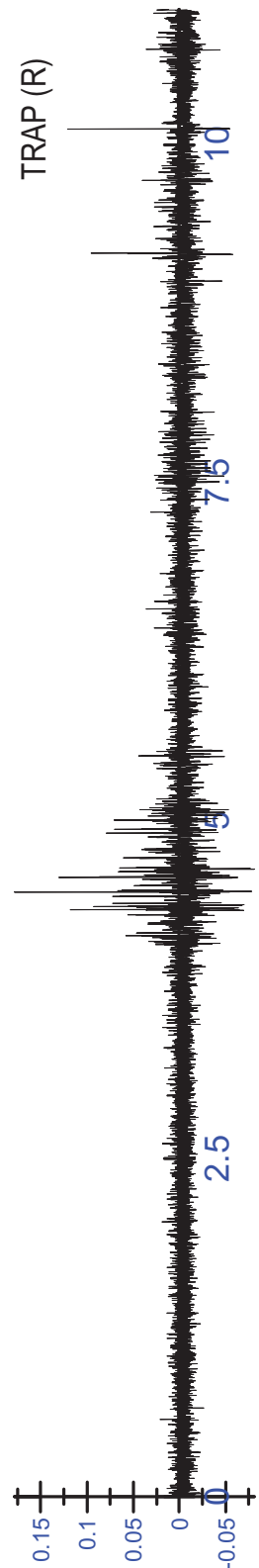
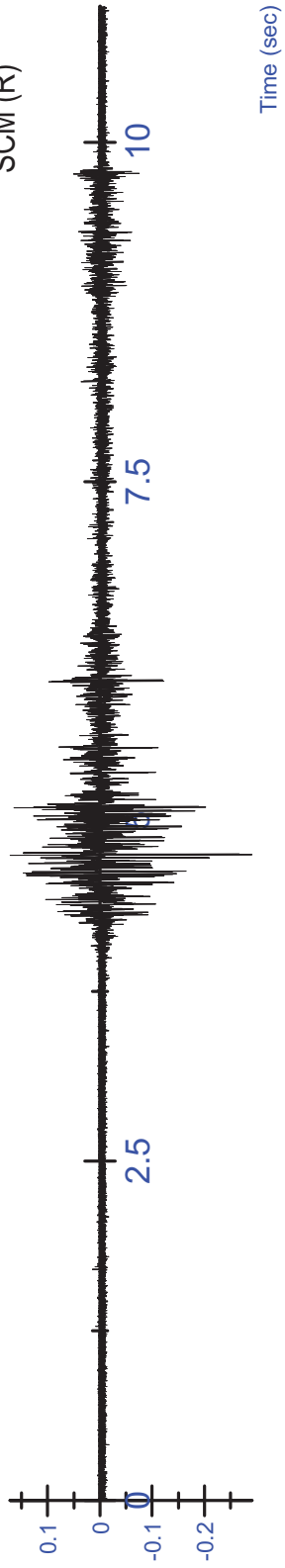




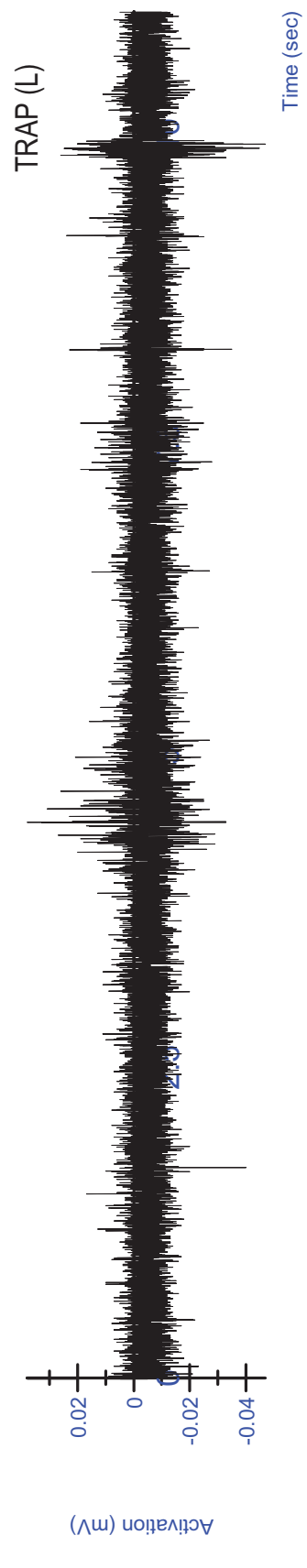
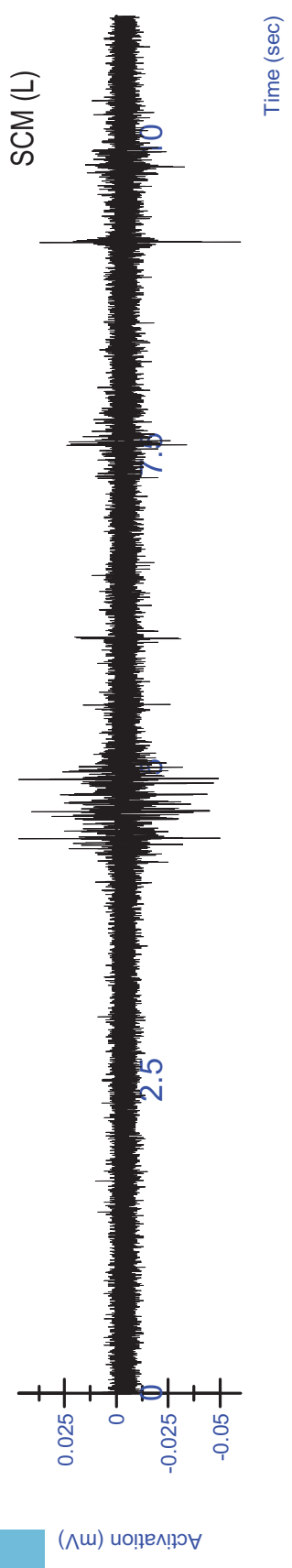
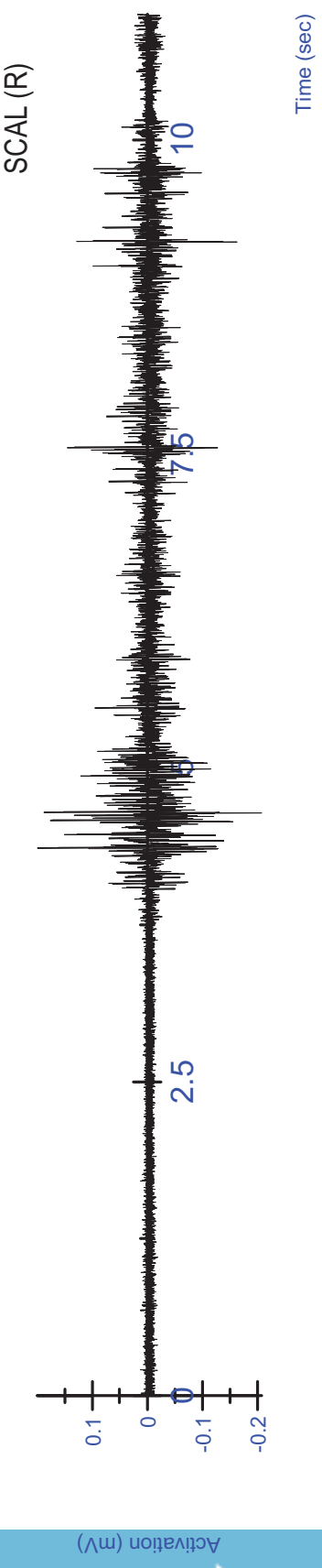
K03 MVC - Lateral (R) Trial 1 - Rectified/Filtered

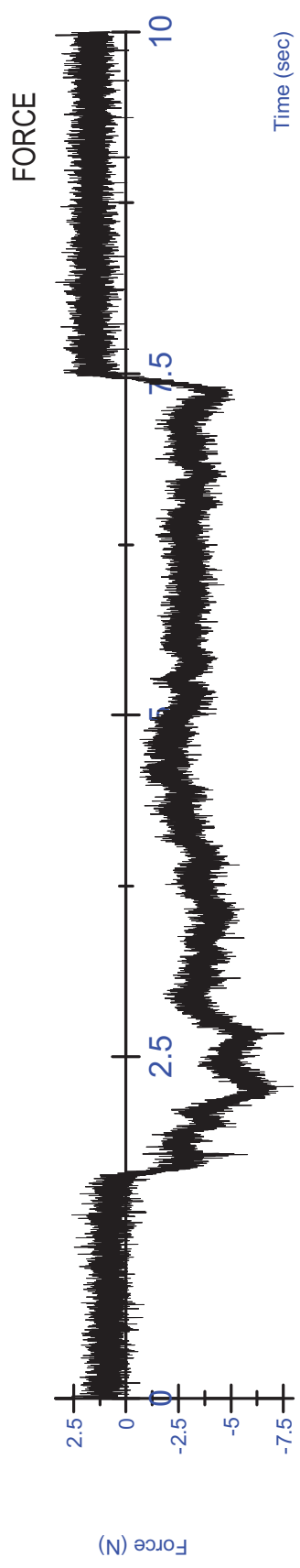
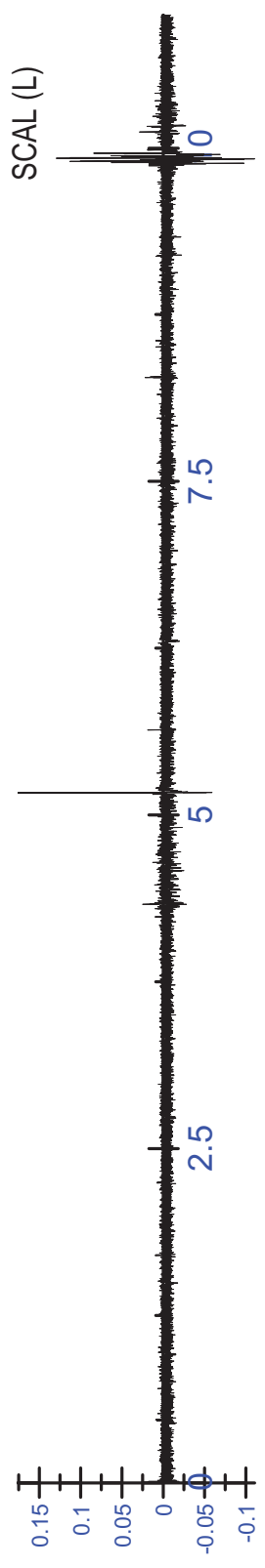
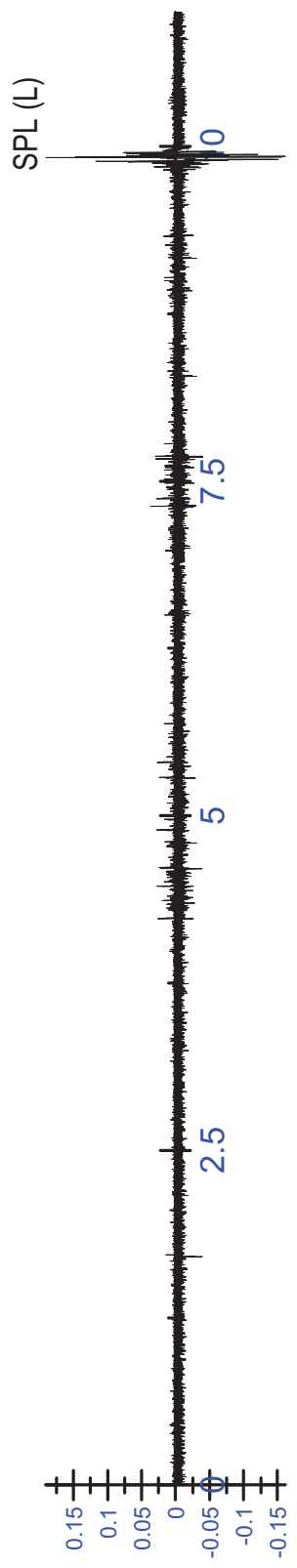


K03 MVC - Lateral (R) Trial 1 - Rectified/Filtered



K03 MVC - Lateral (R) Trial 2 - Unfiltered

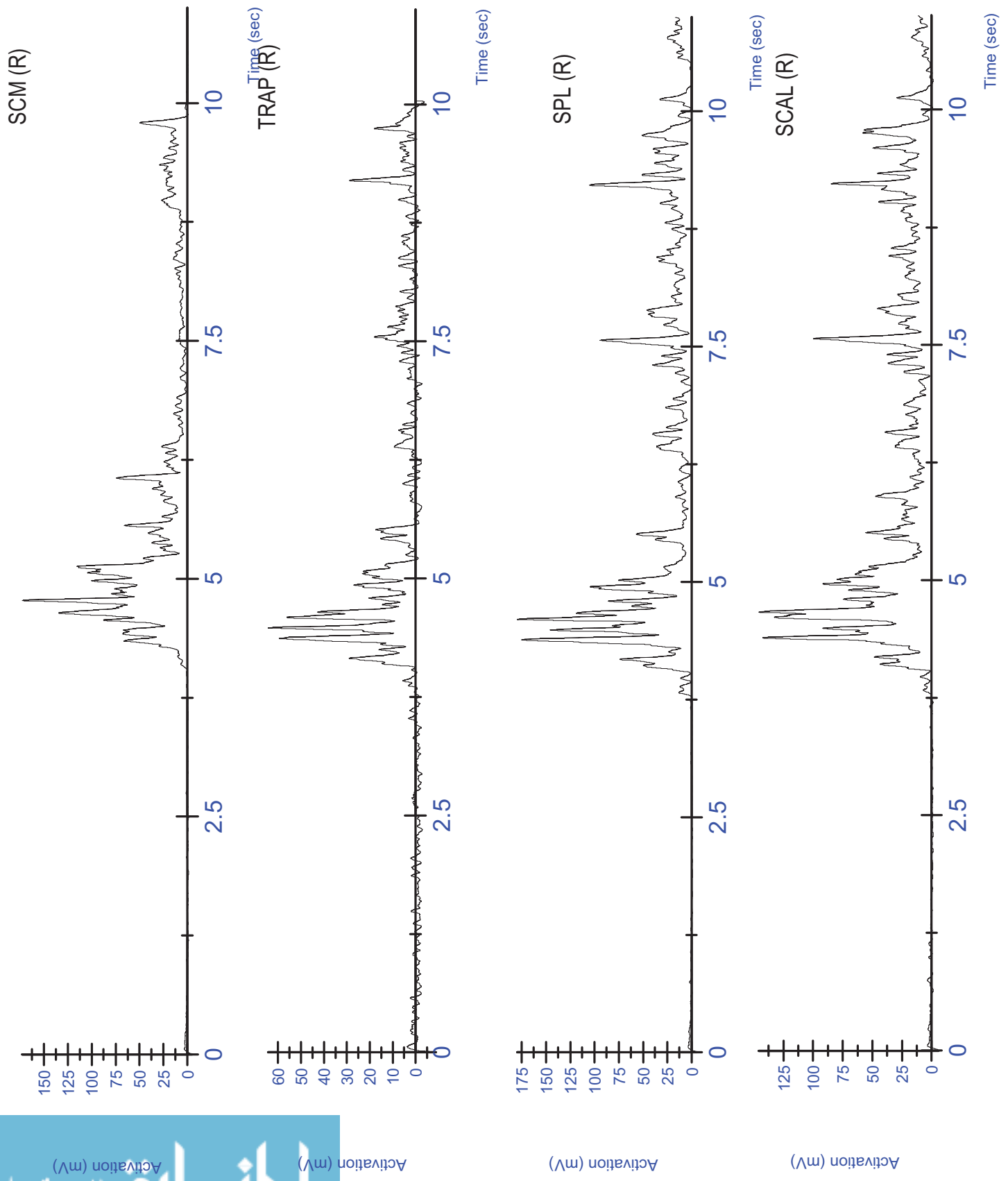




Activation (mV)

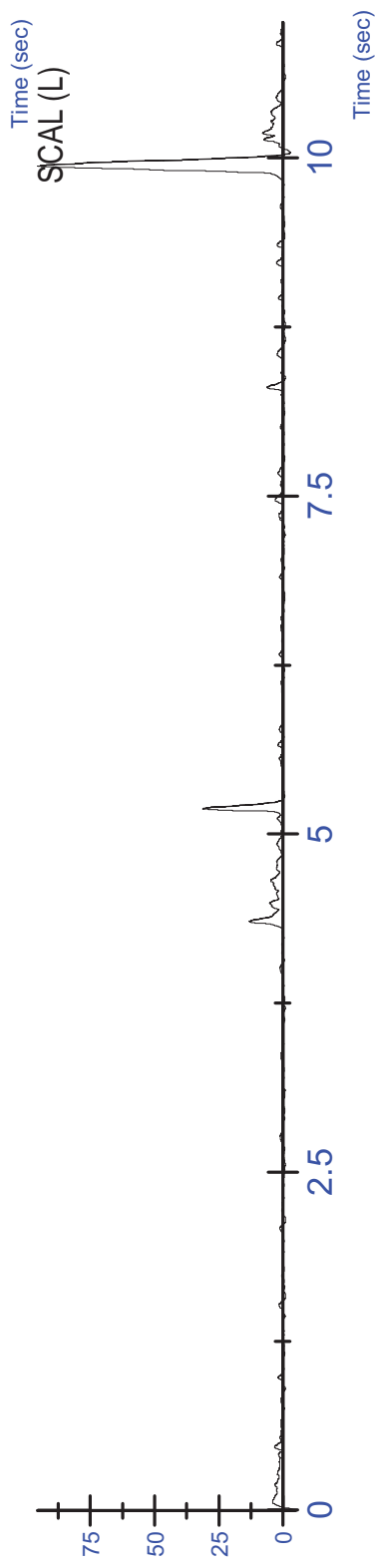
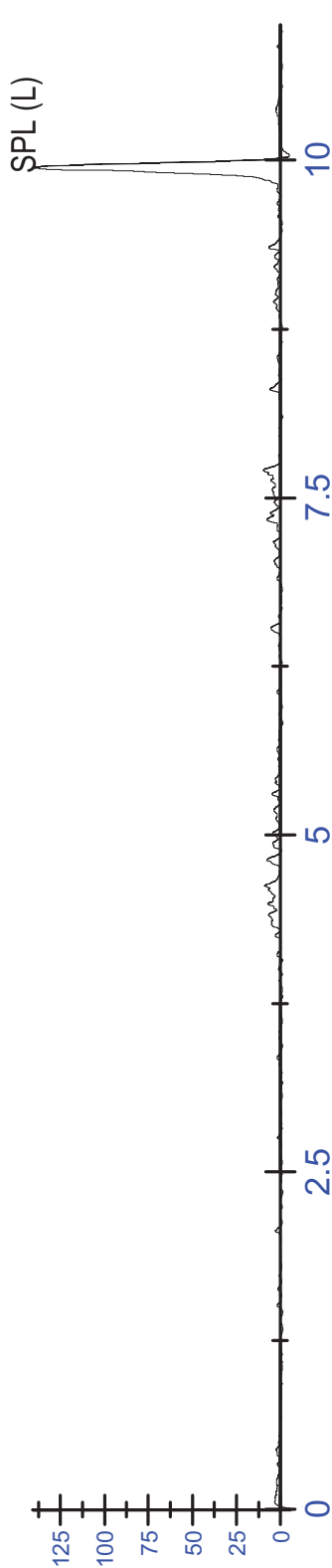
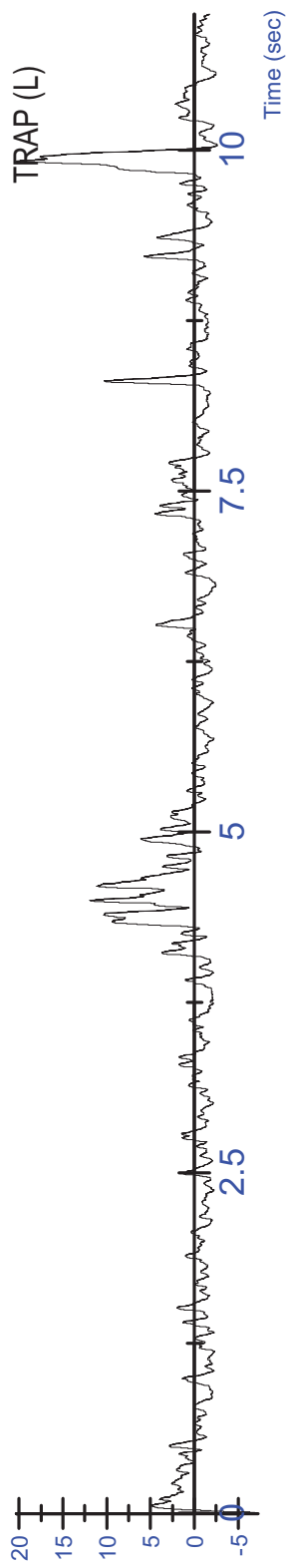
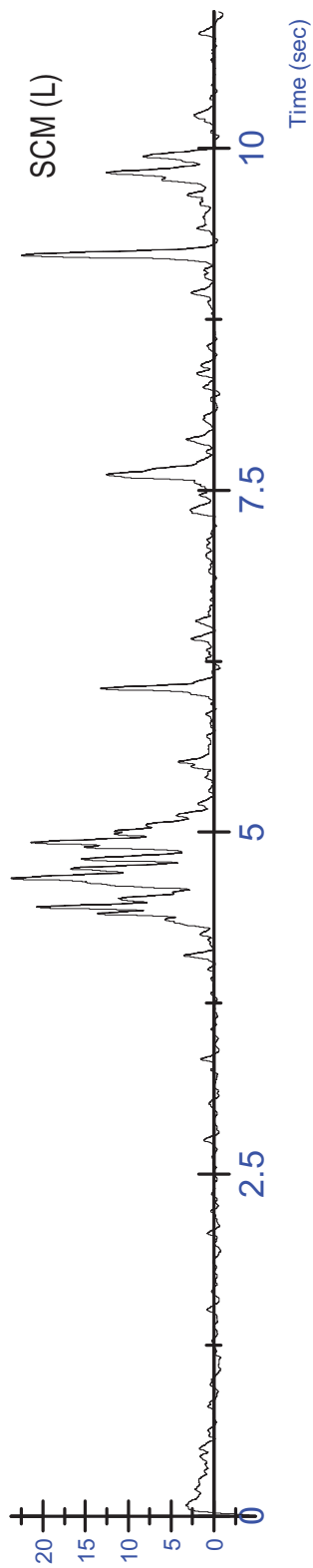
Activation (mV)

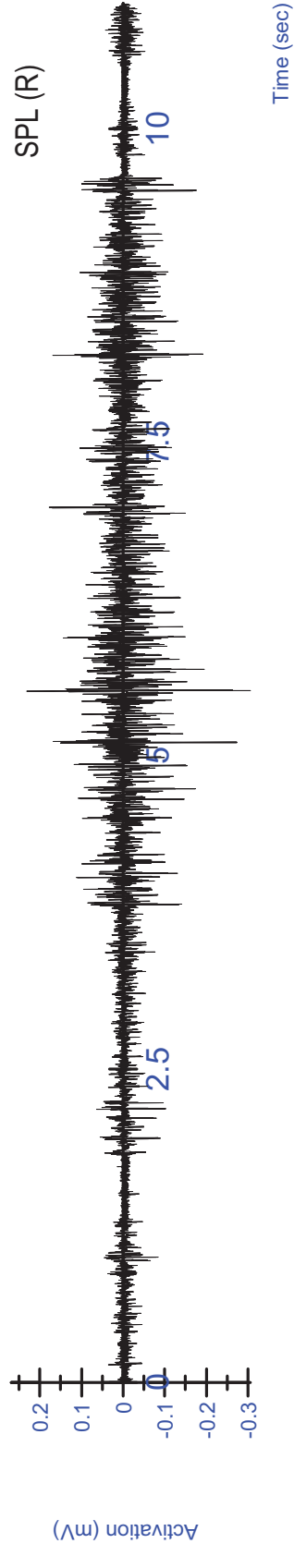
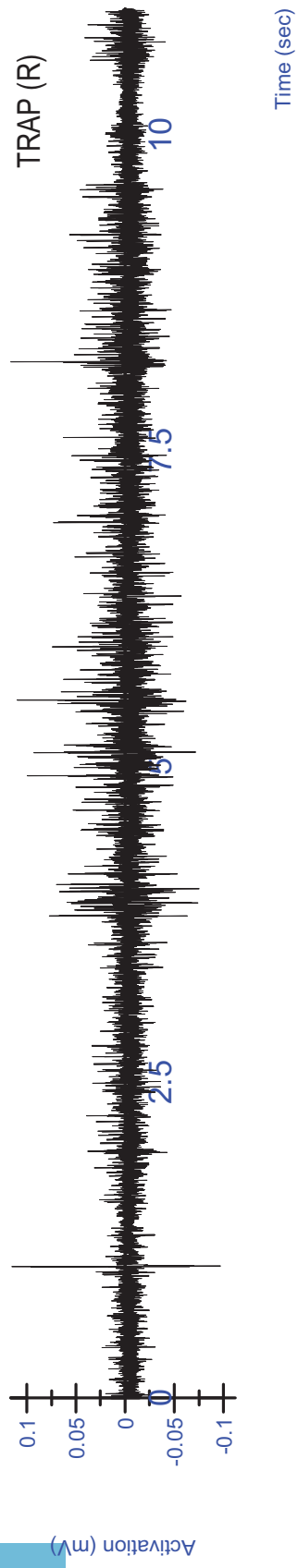
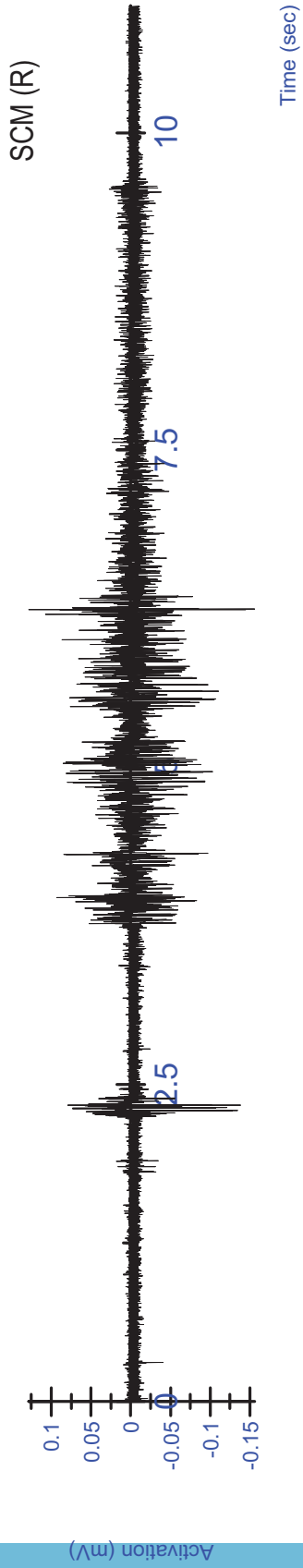
Force (N)

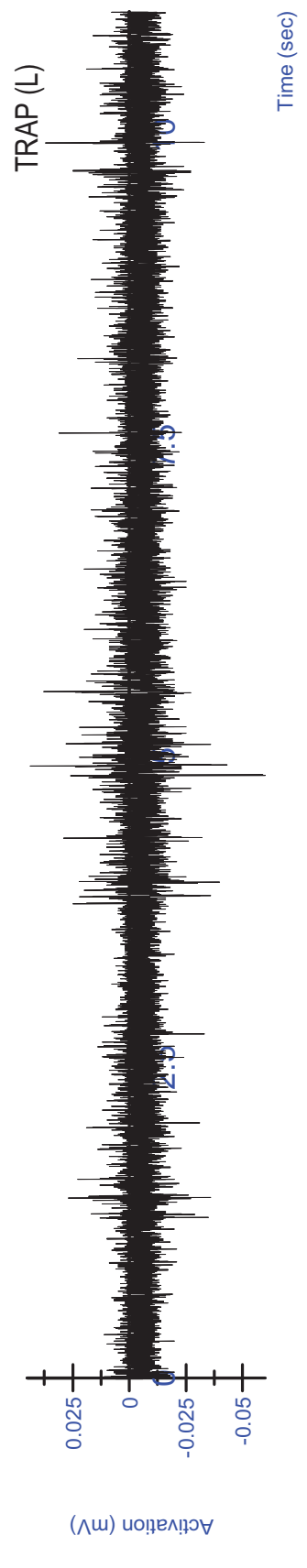
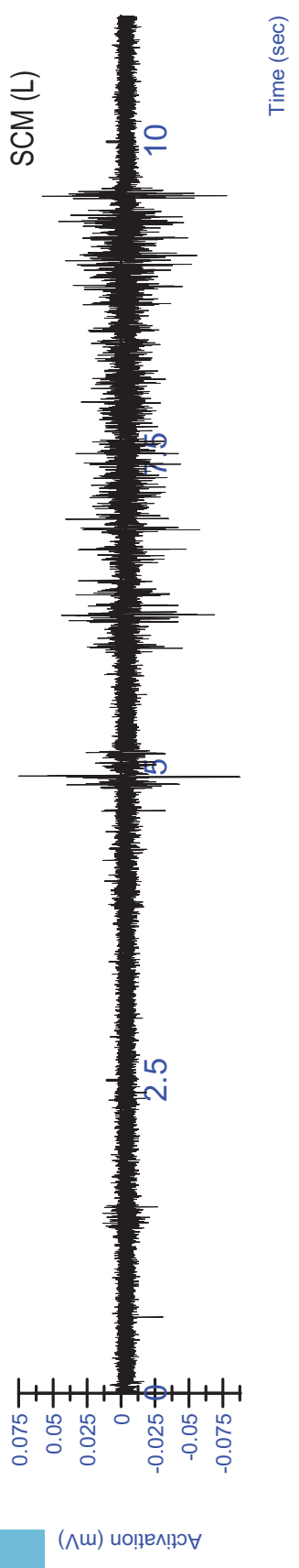
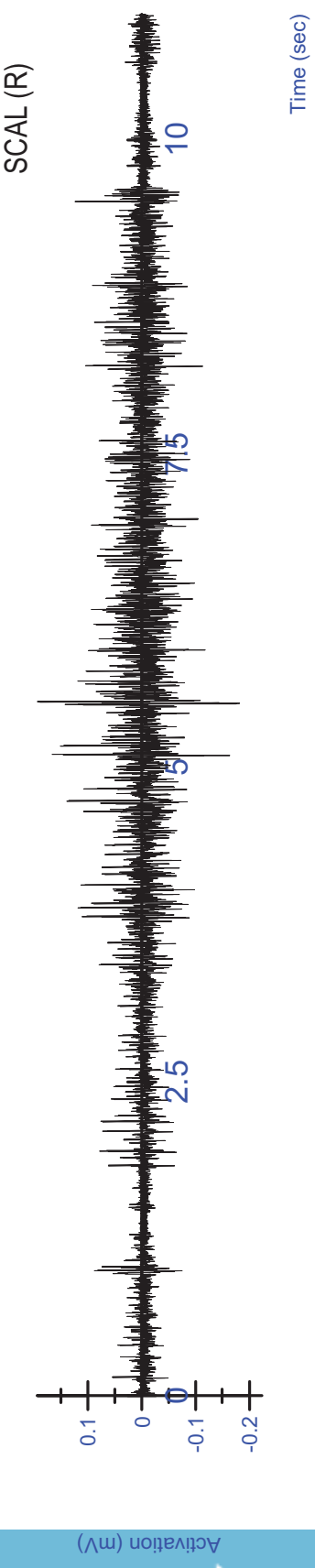


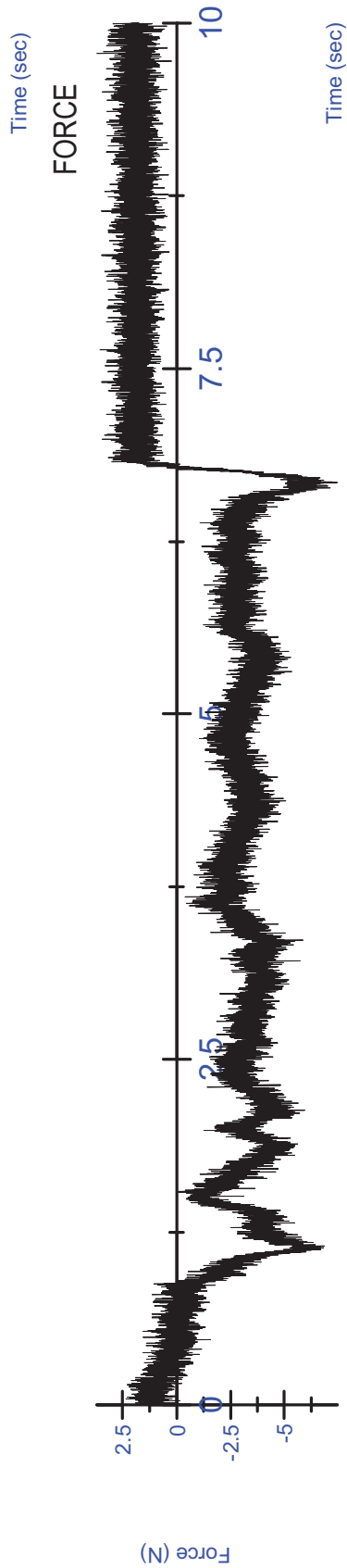
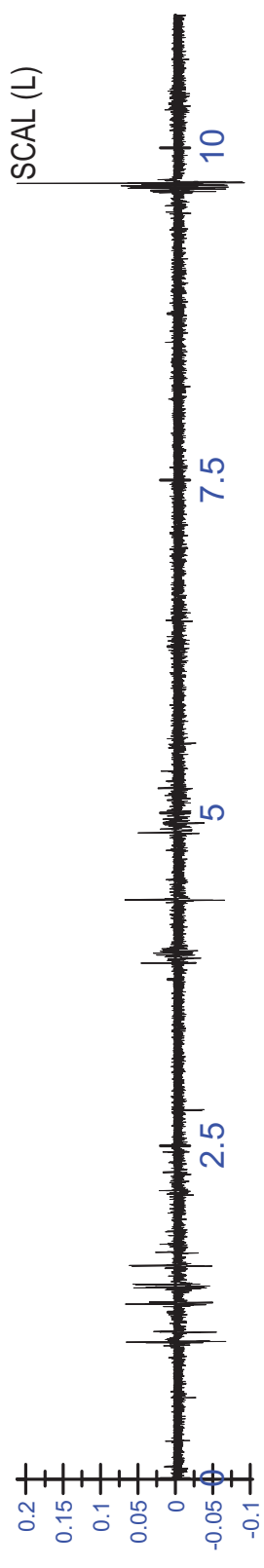
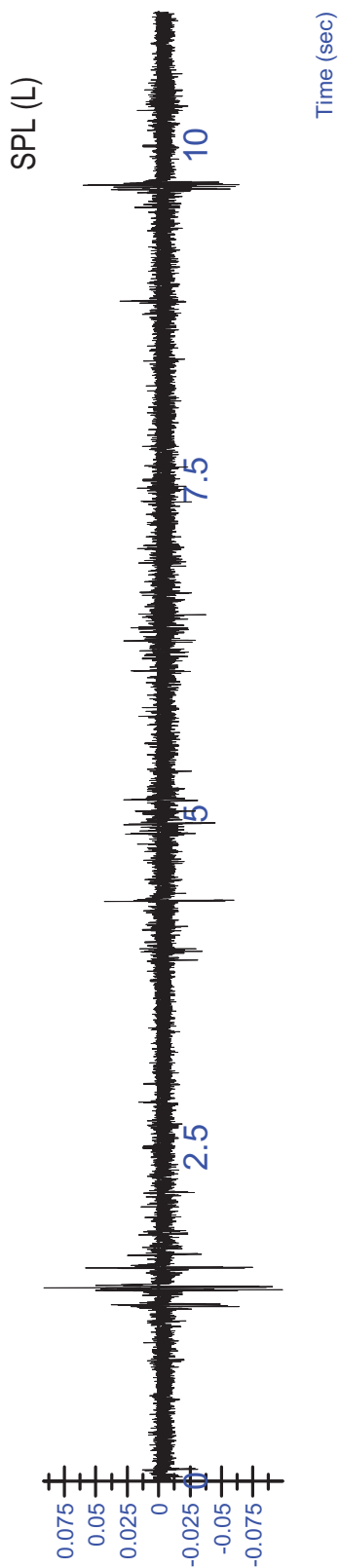
K03 MVC - Lateral (R) Trial 2 - Rectified/Filtered

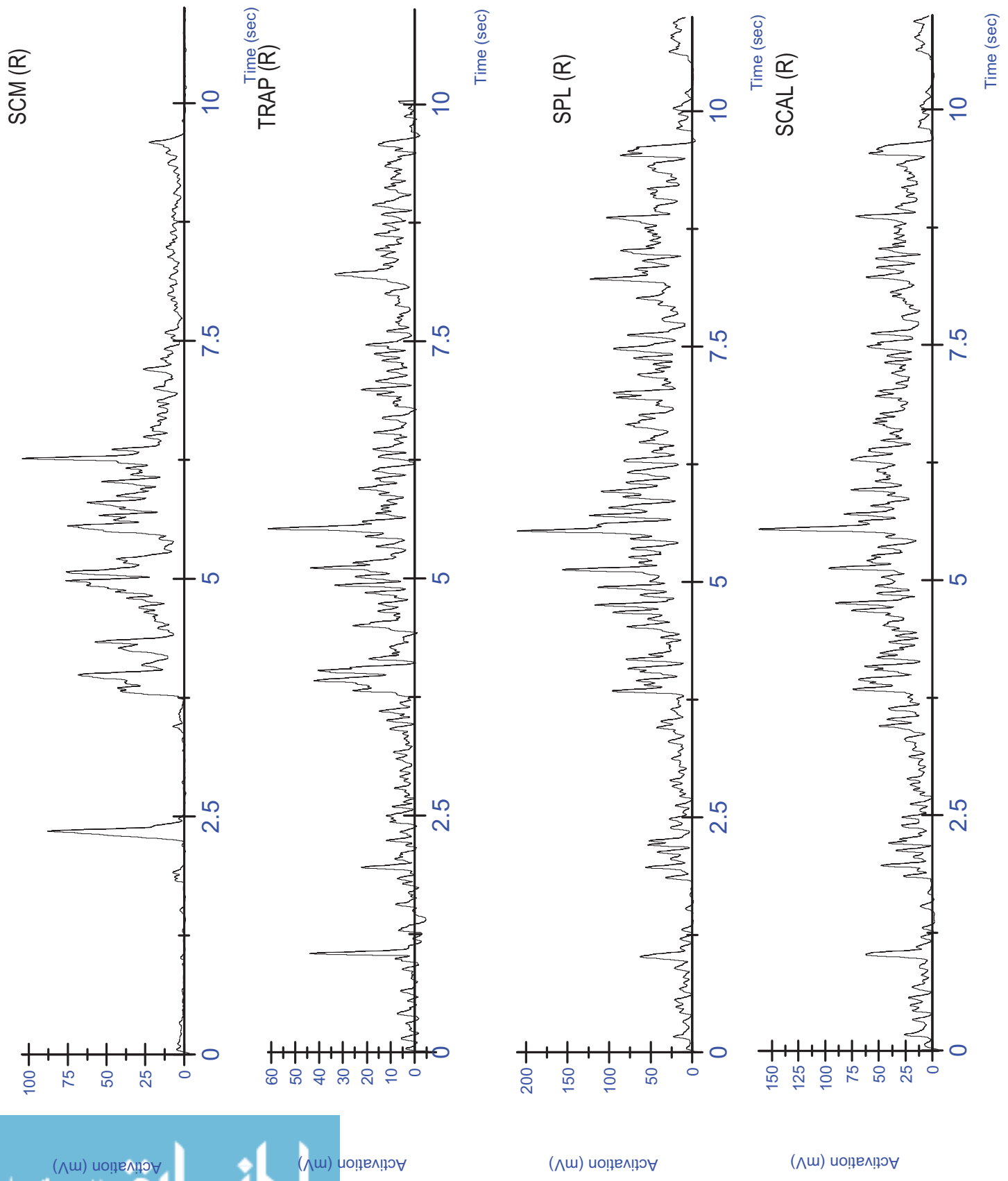
K03 MVC - Lateral (R) Trial 2 - Rectified/Filtered



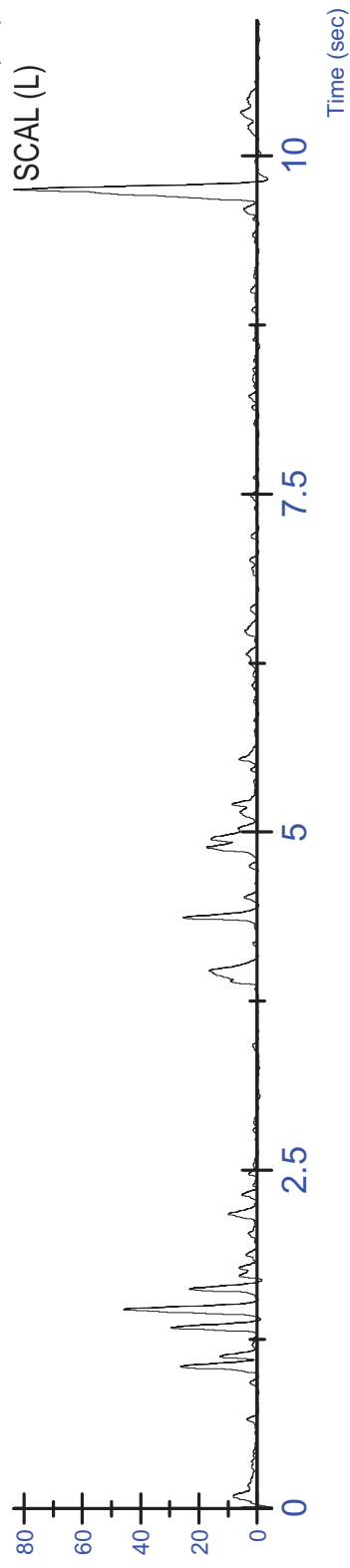
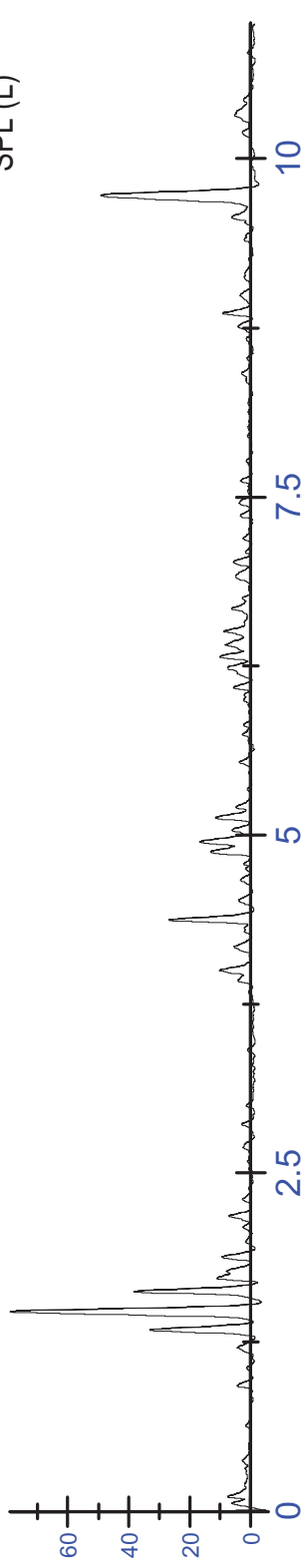
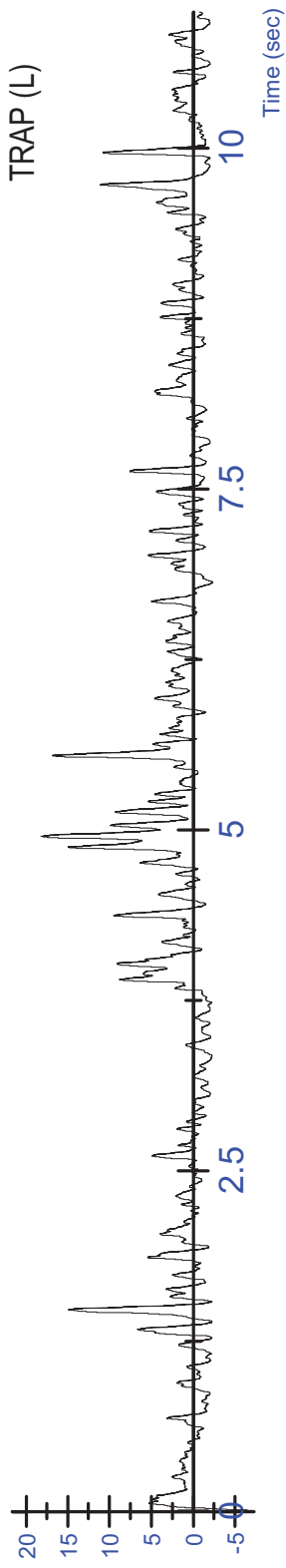
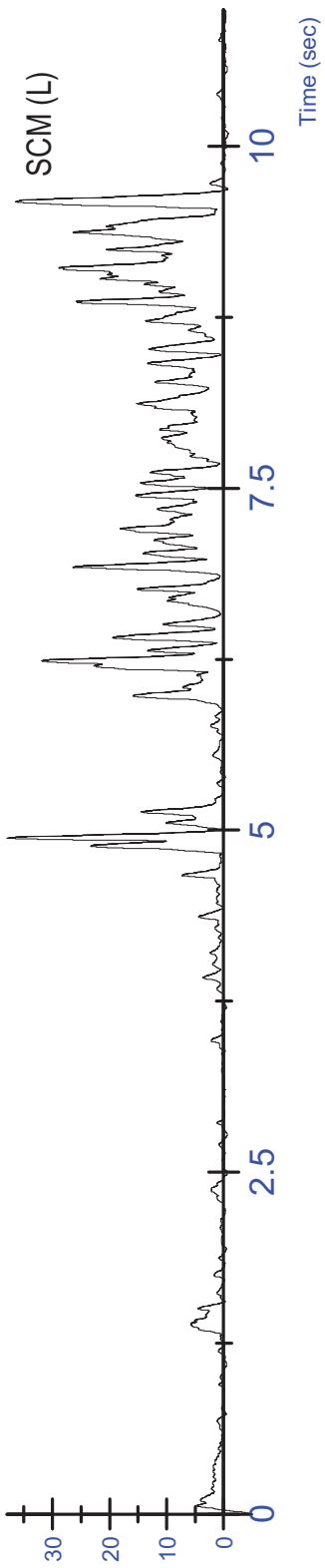


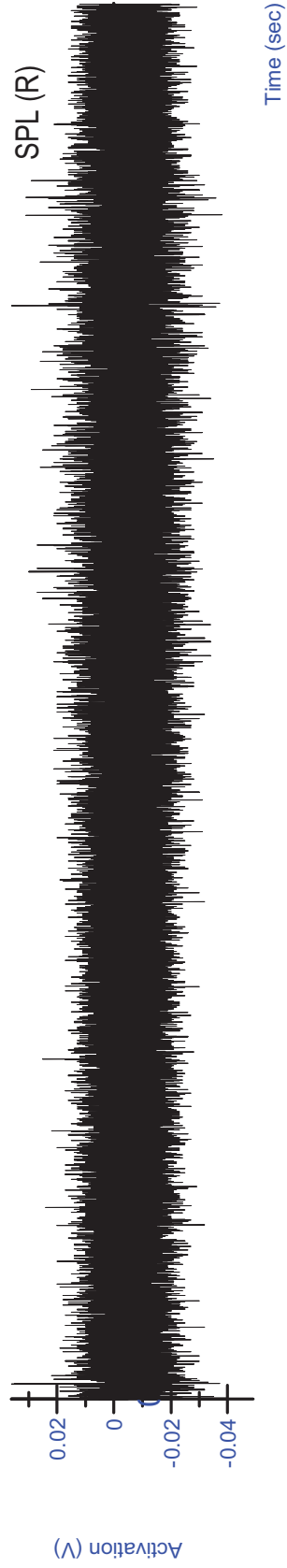
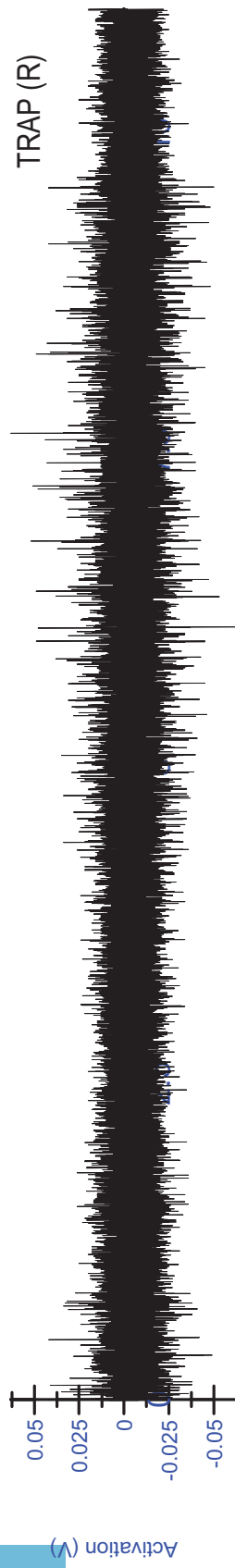
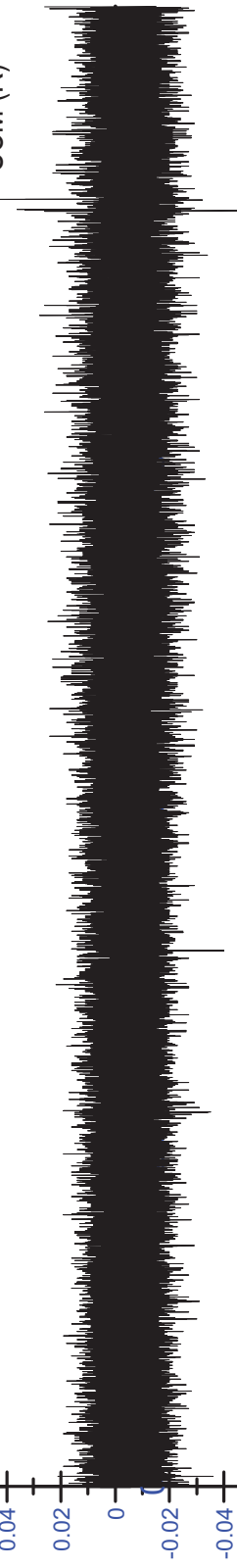




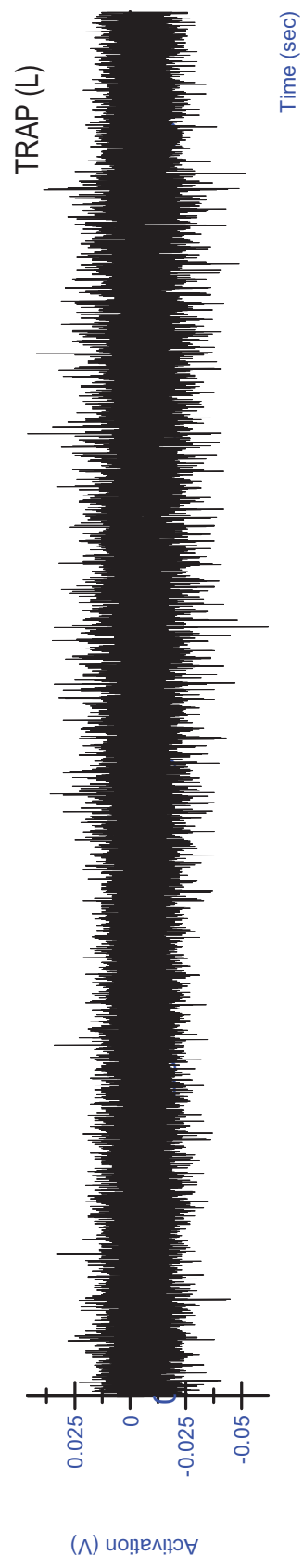
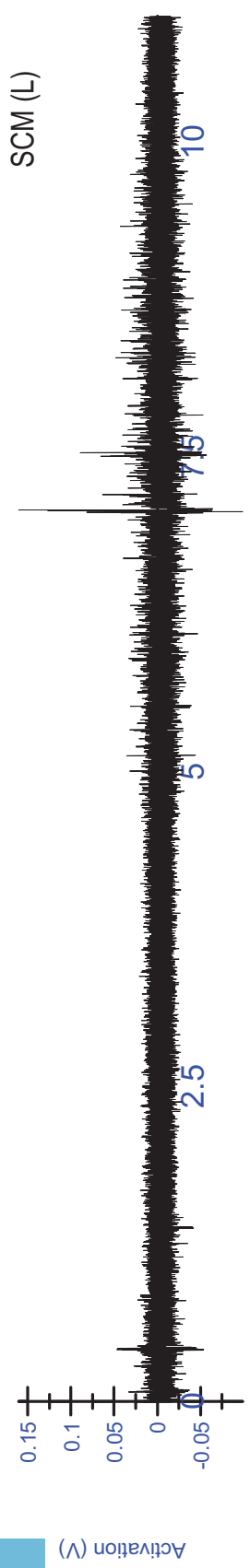
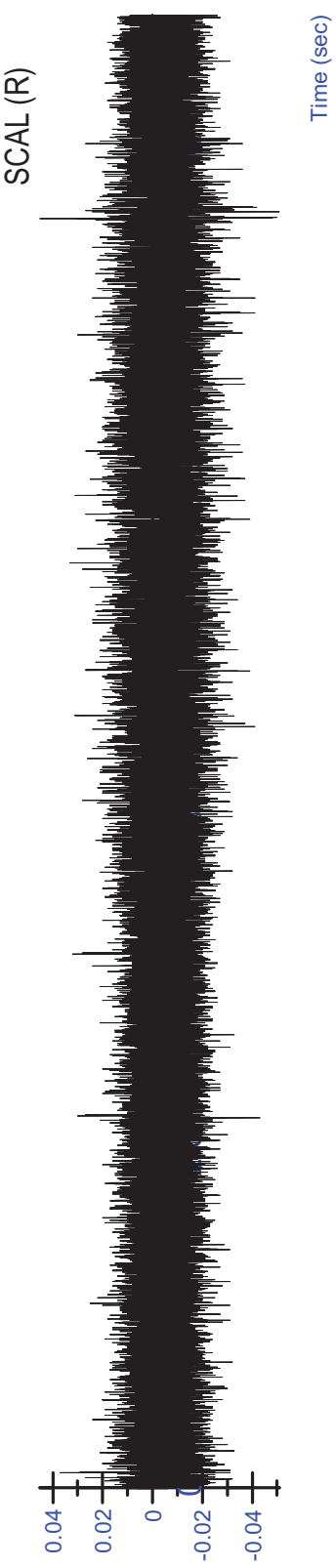


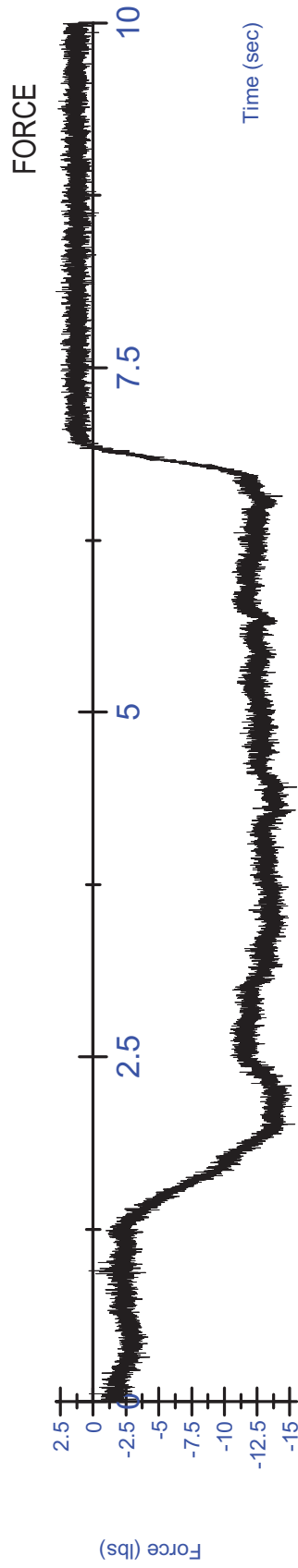
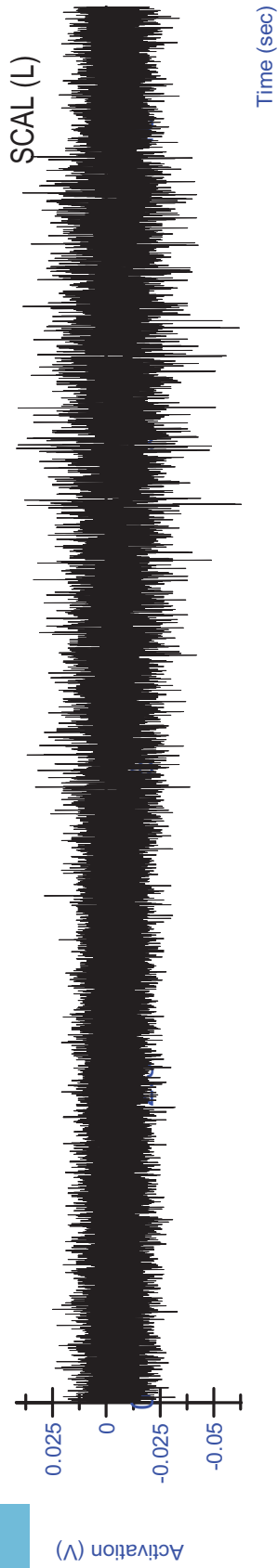
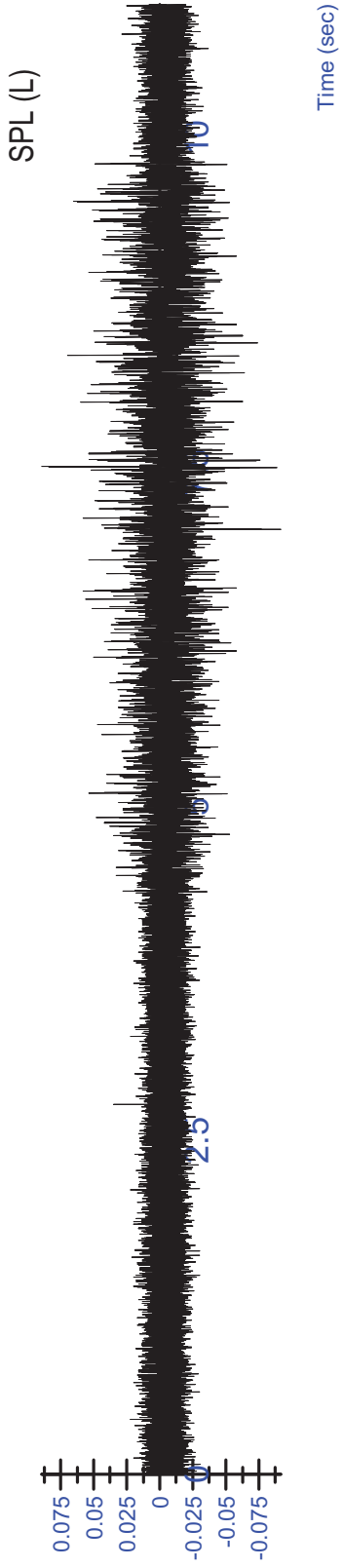
K03 MVC - Lateral (R) Trial 3 - Rectified/Filtered

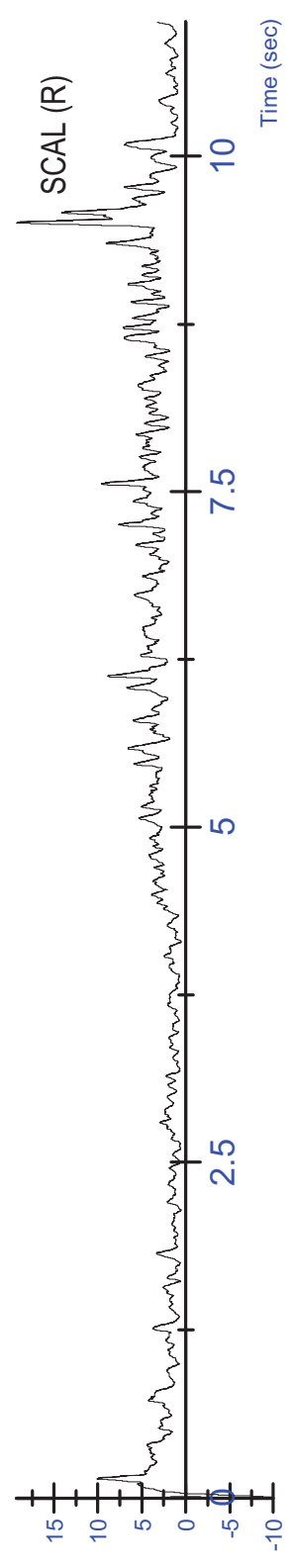
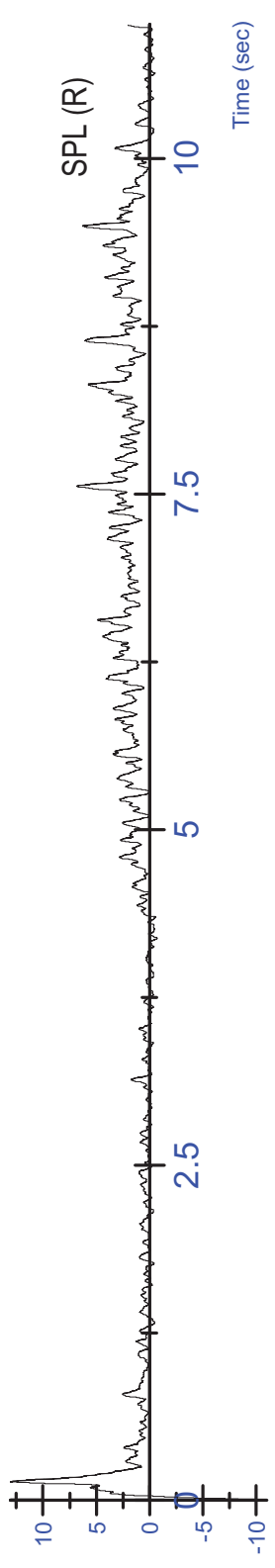
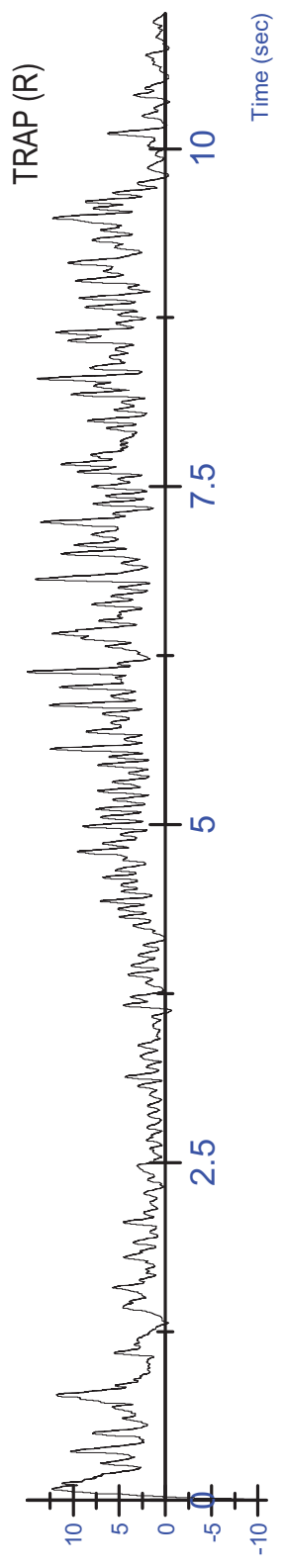
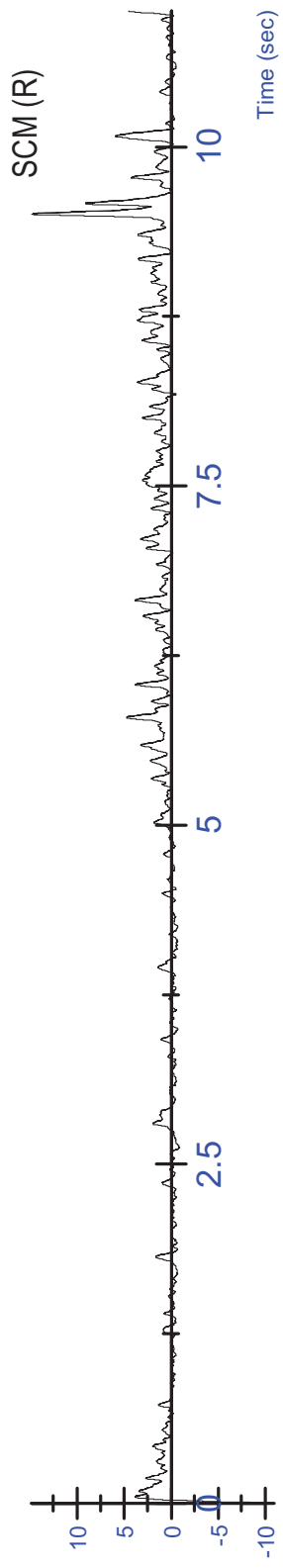


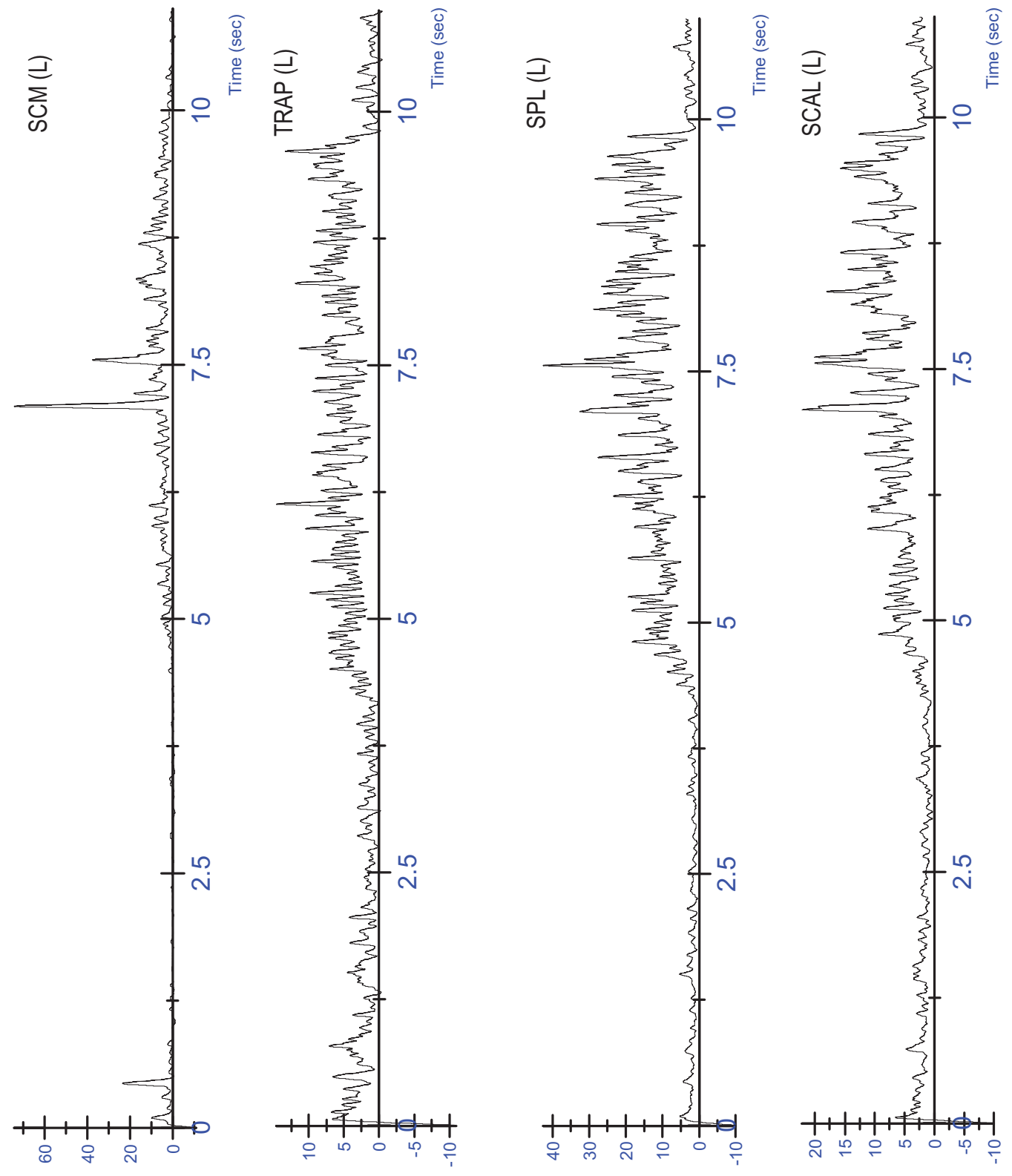


S14 MVC - Extension Trial 1 - Unfiltered

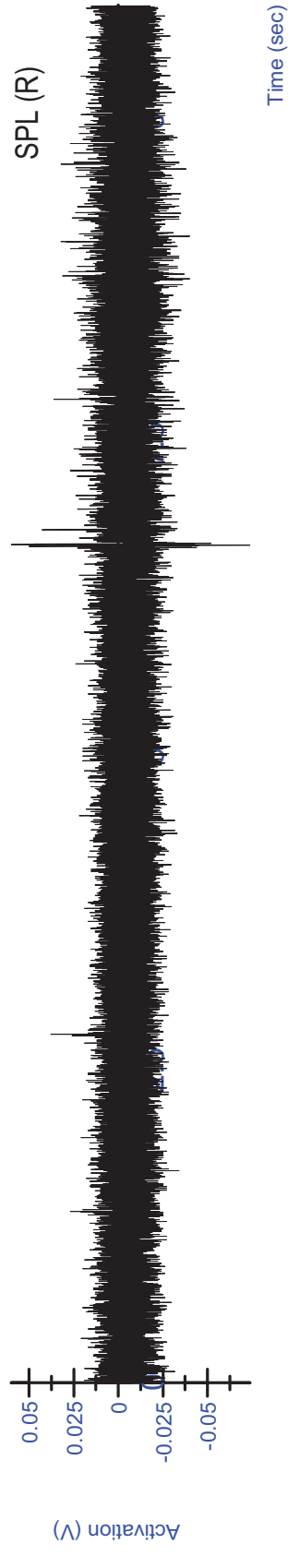
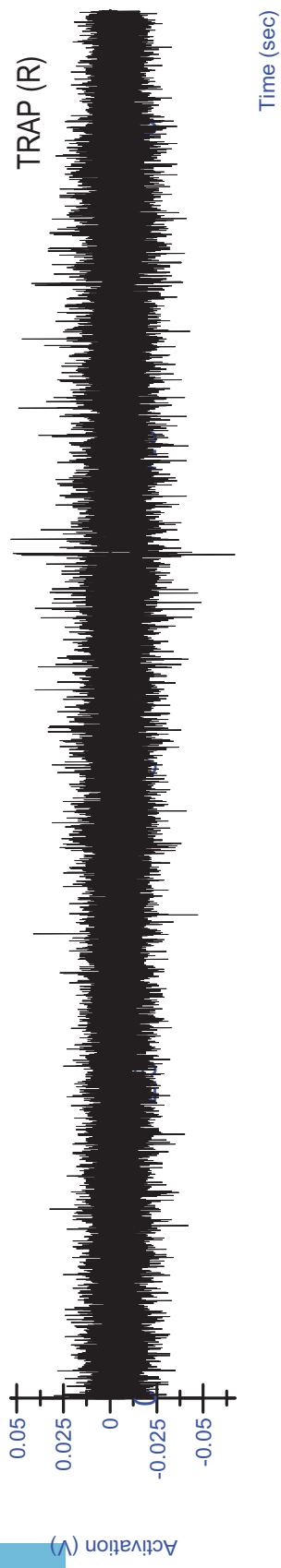
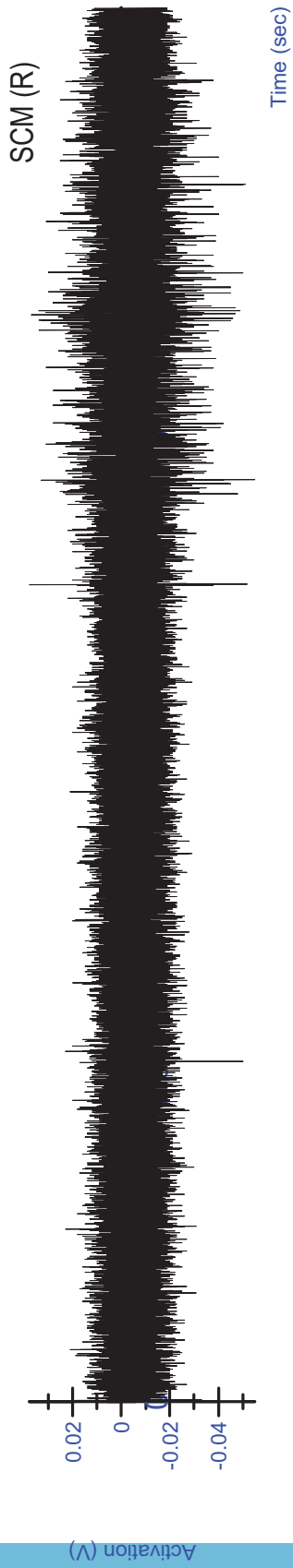


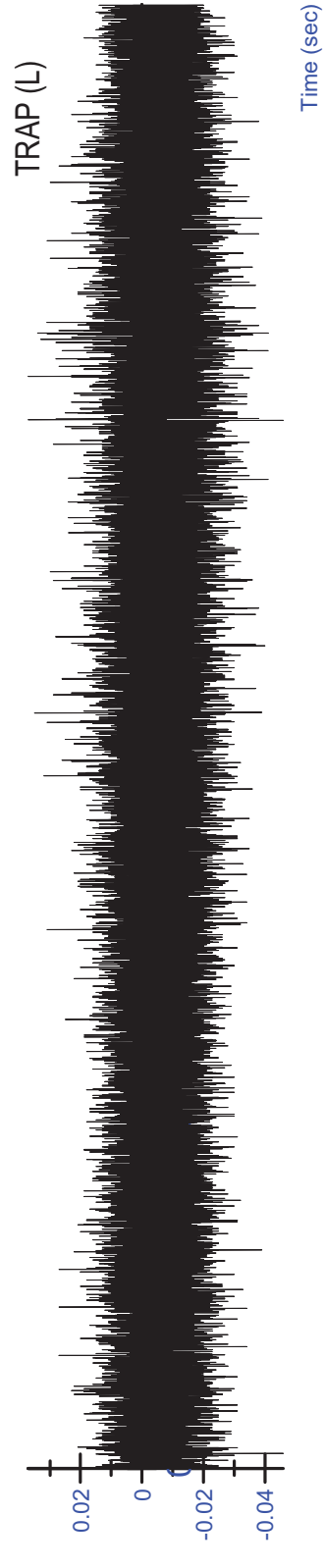
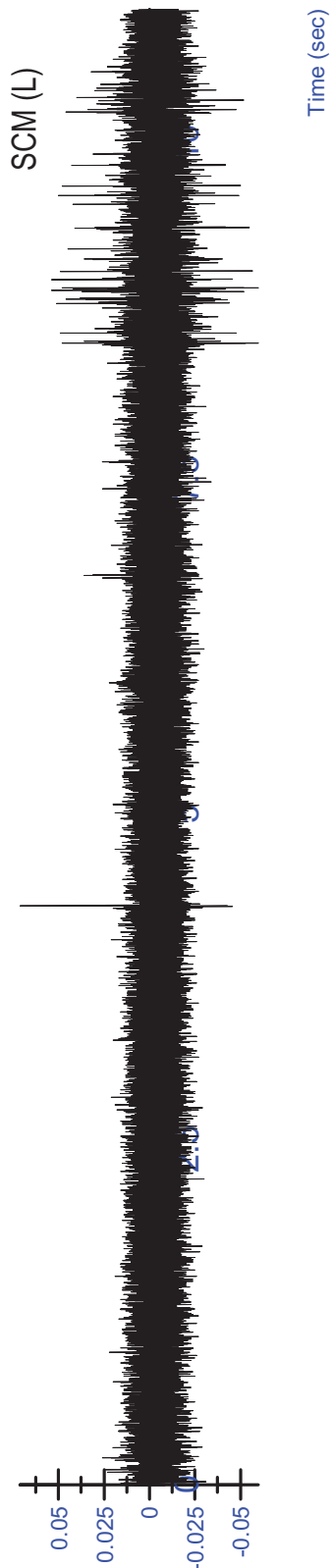
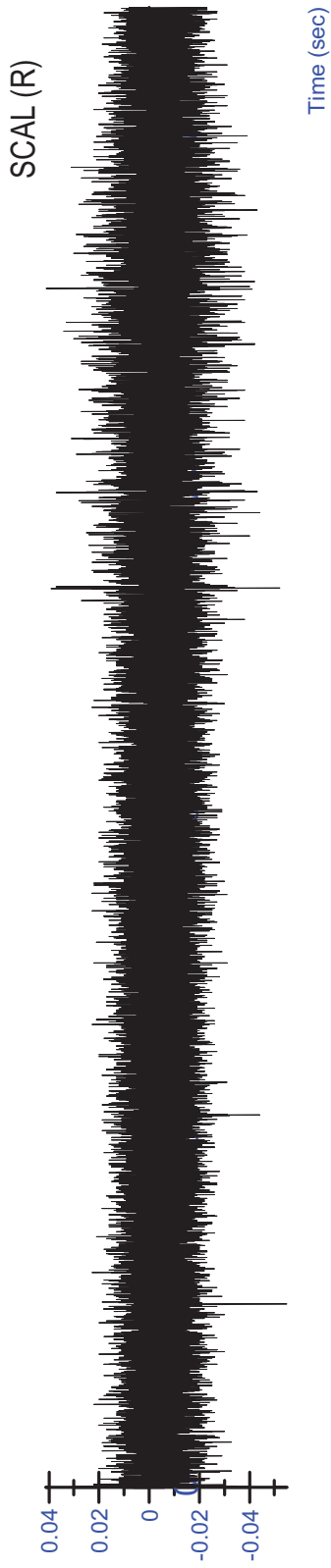




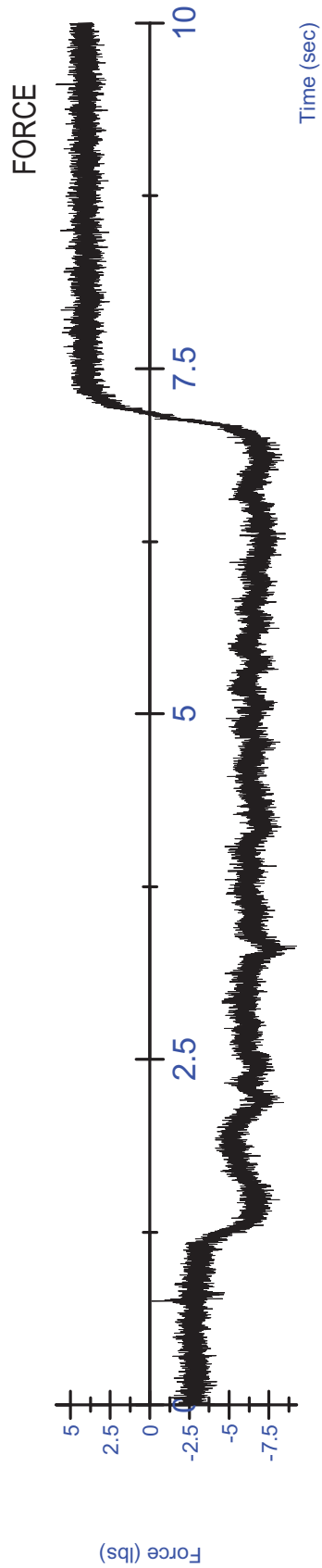
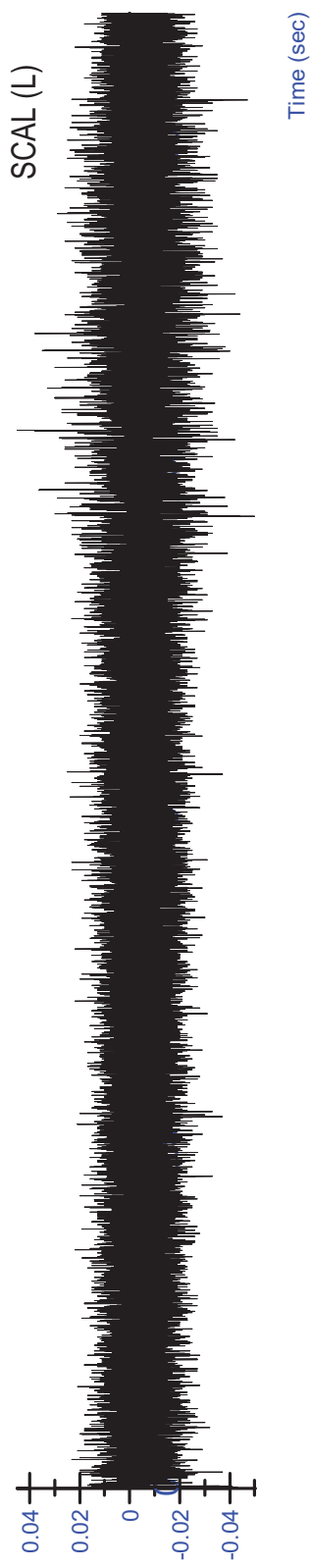
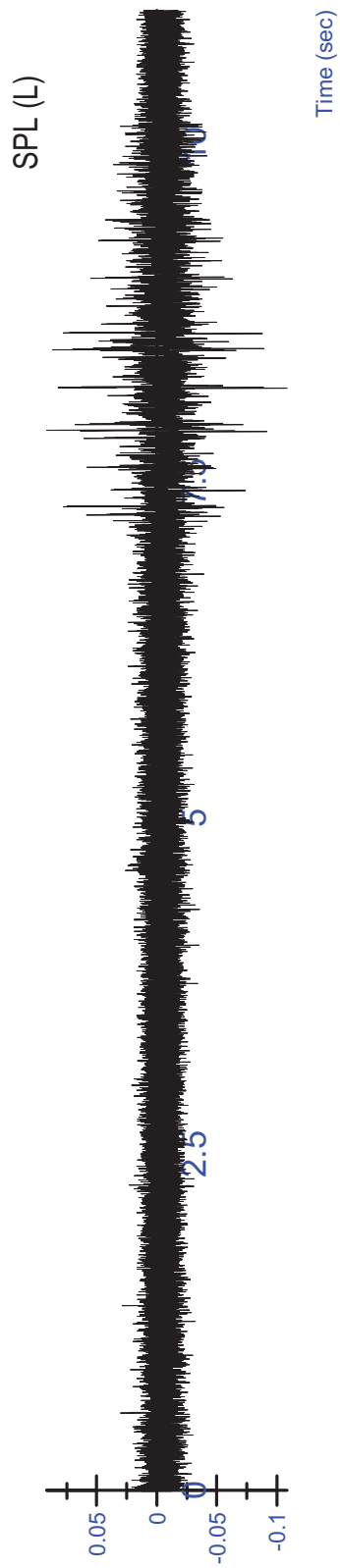


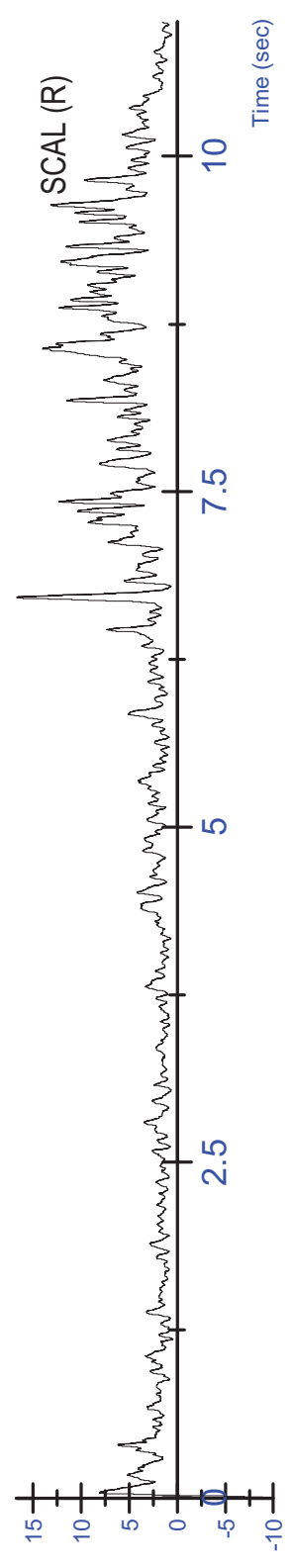
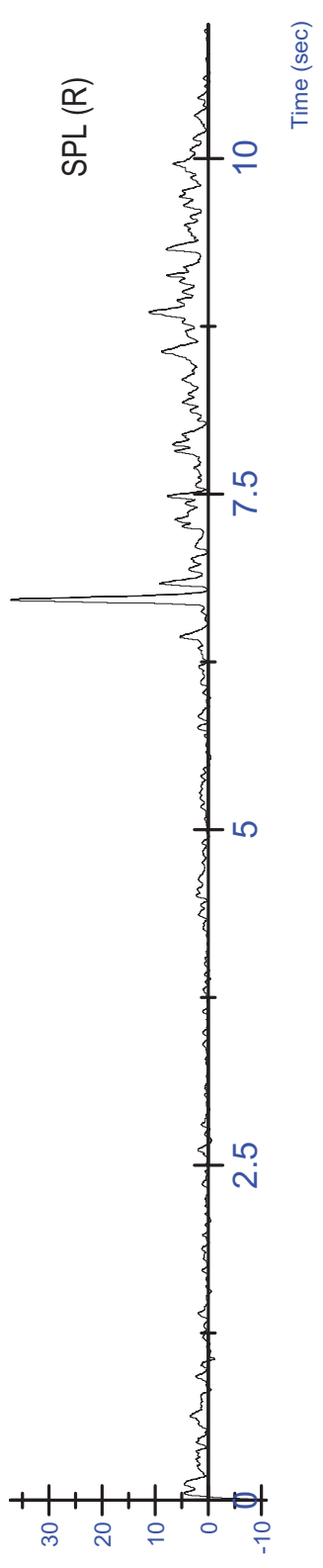
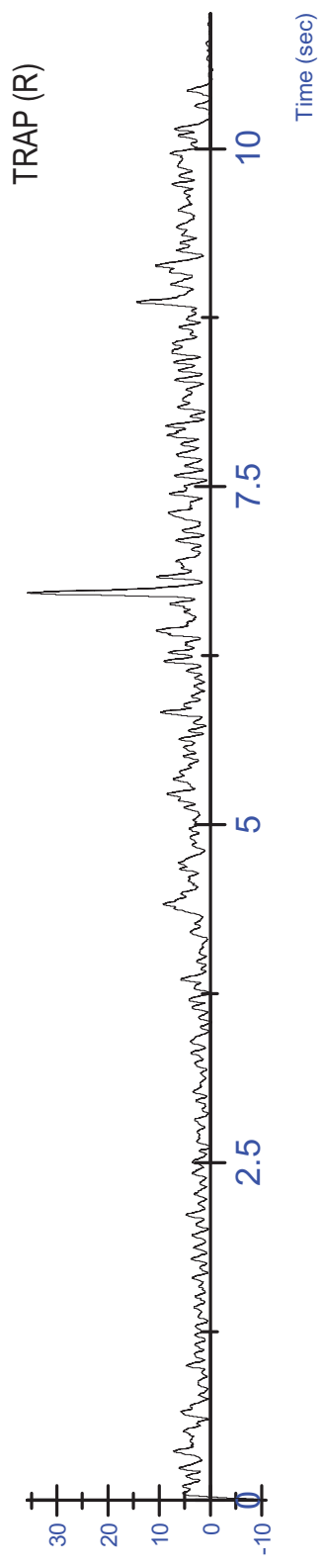
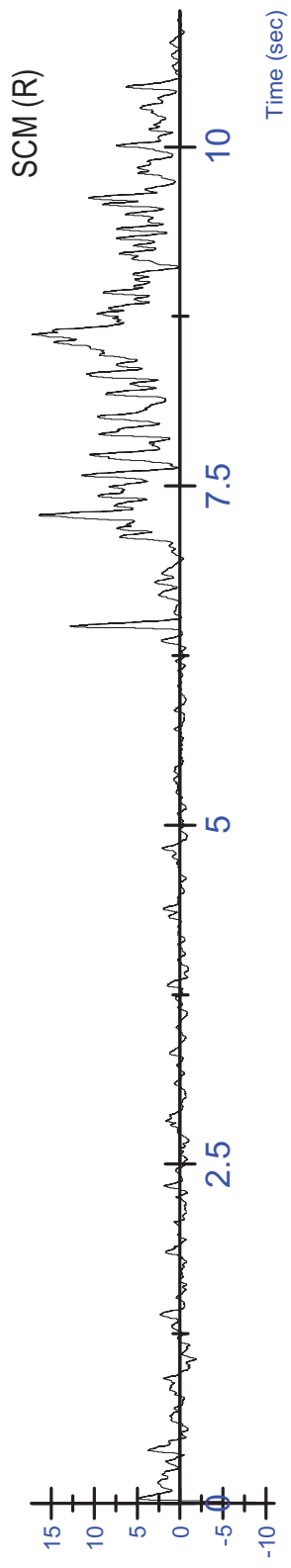
S14 MVC - Extension Trial 1 - Rectified/Filtered





S14 MVC - Extension Trial 2 - Unfiltered



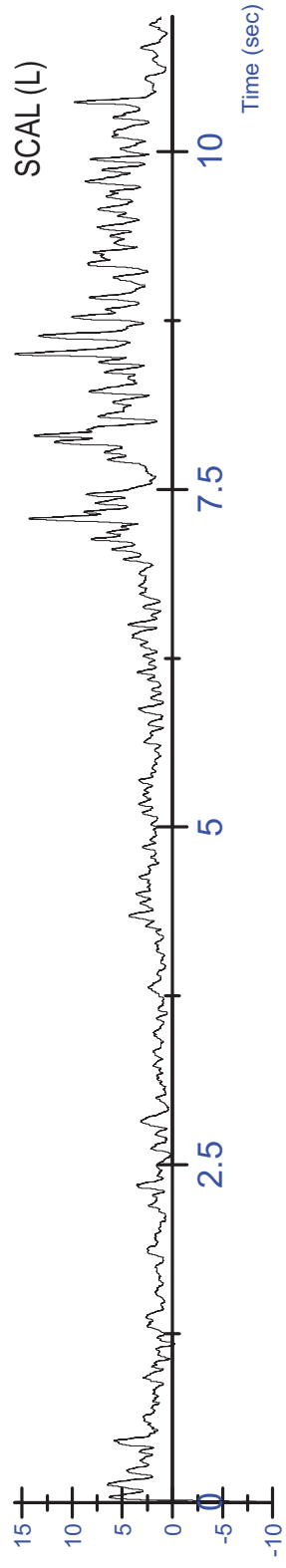
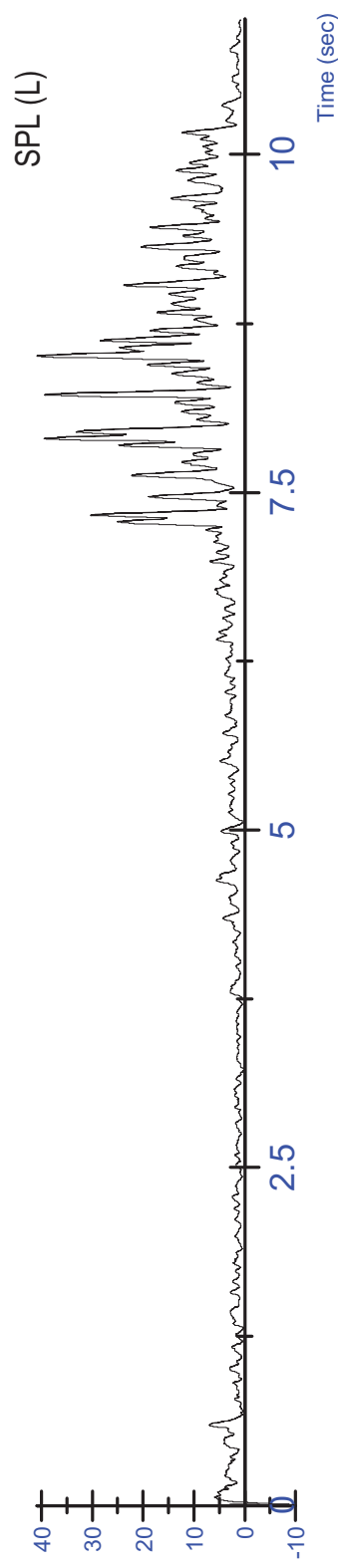
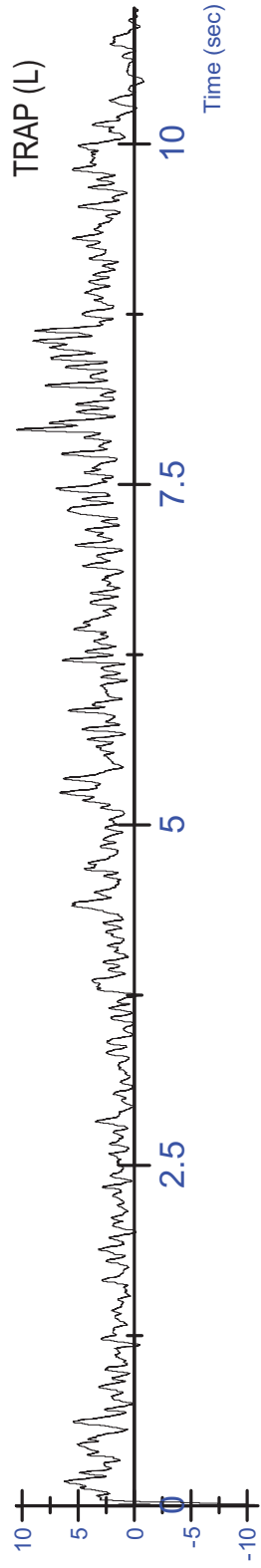
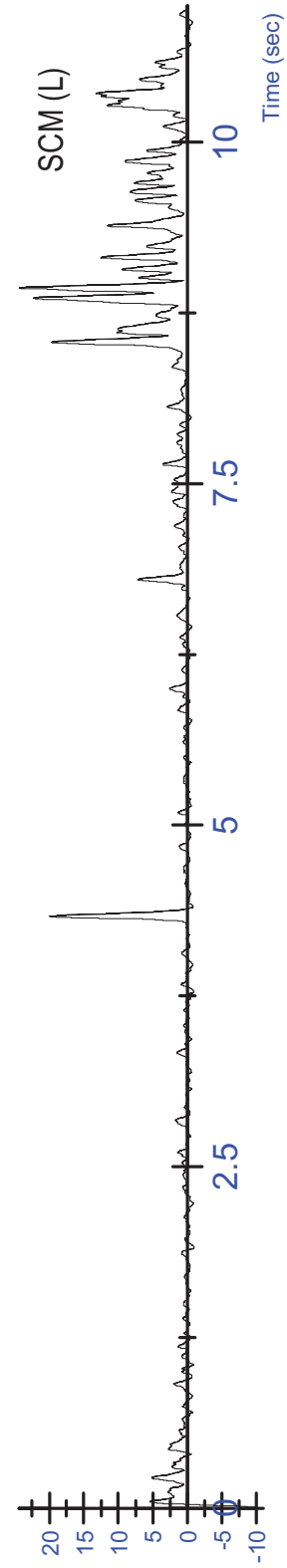


Activation (mV)

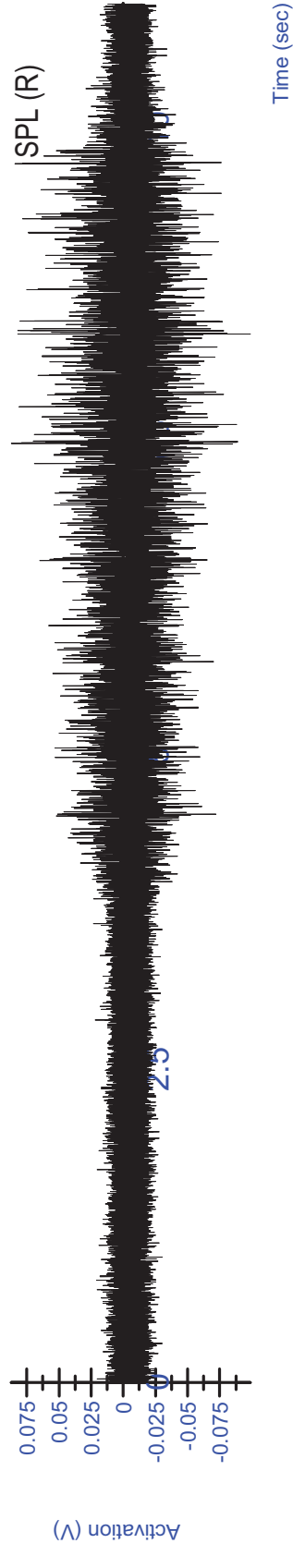
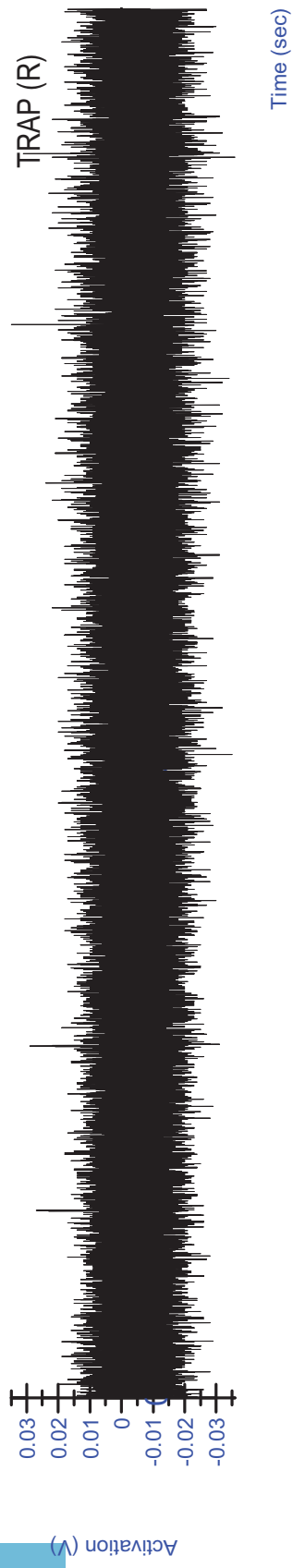
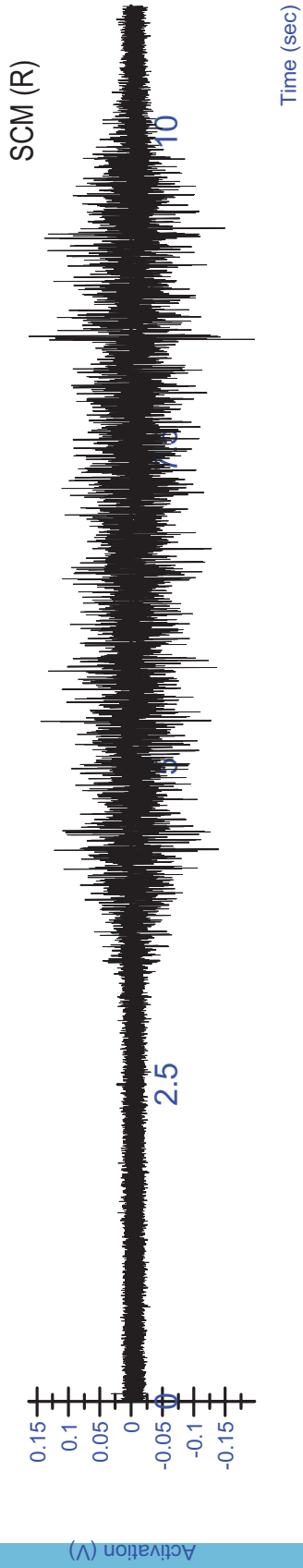
Activation (mV)

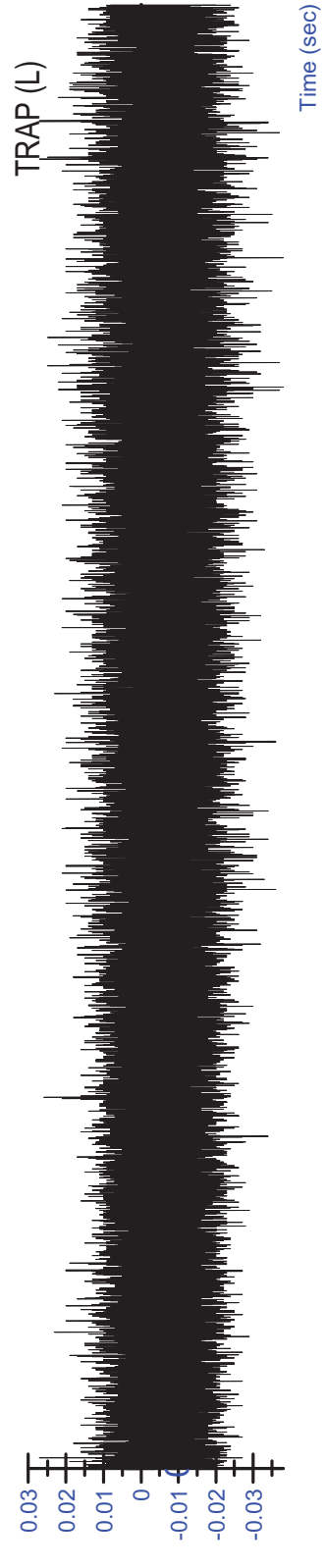
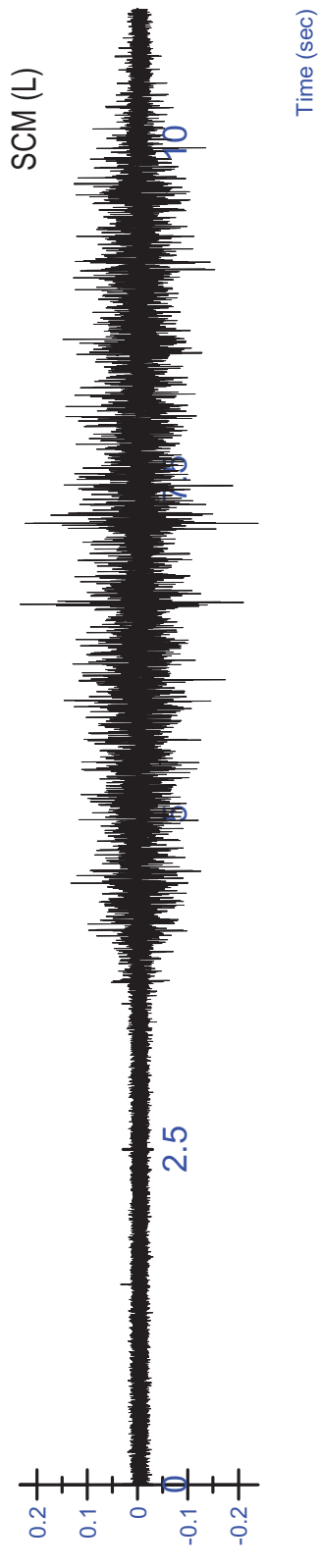
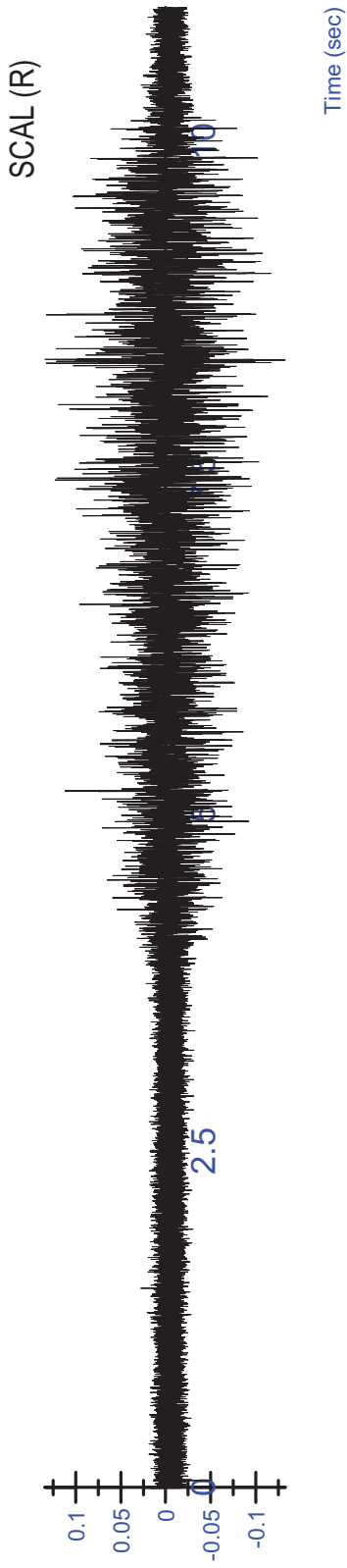
Activation (mV)

Activation (mV)

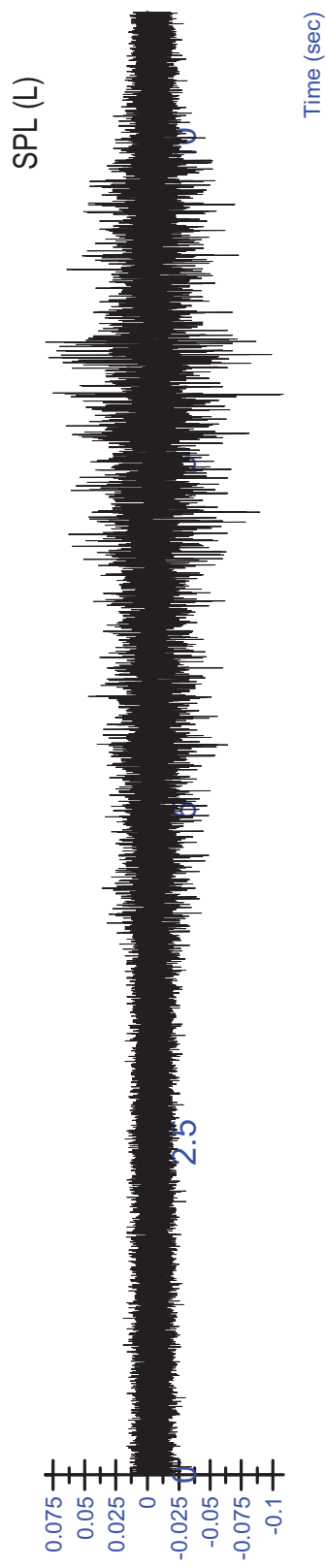


S14 MVC - Extension Trial 2 - Rectified/Filtered





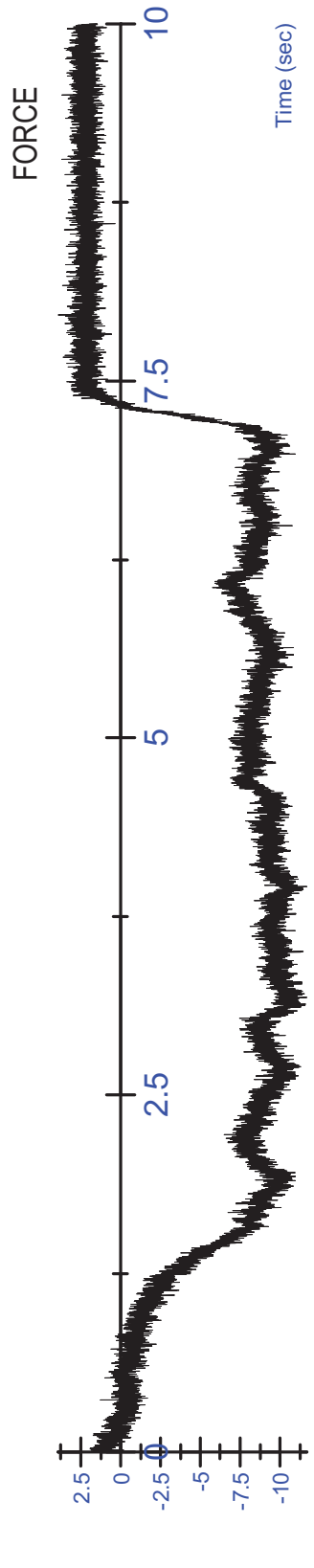
Activation (V)

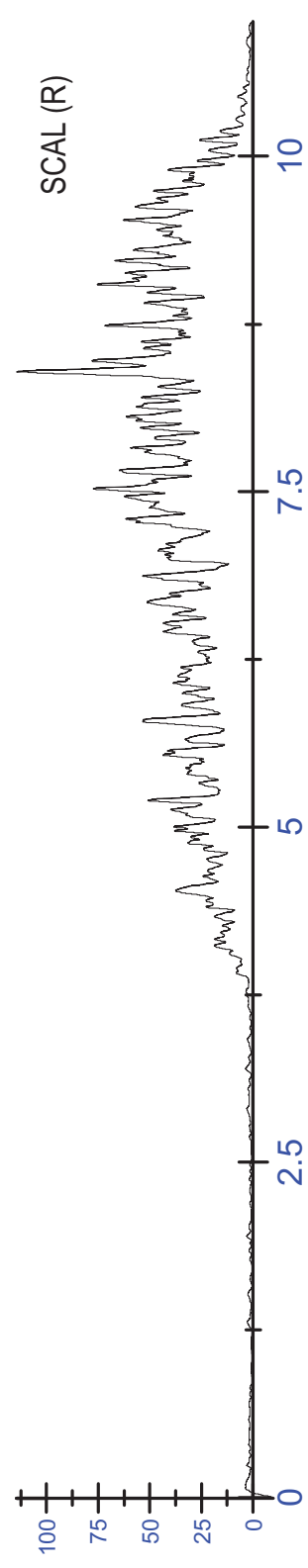
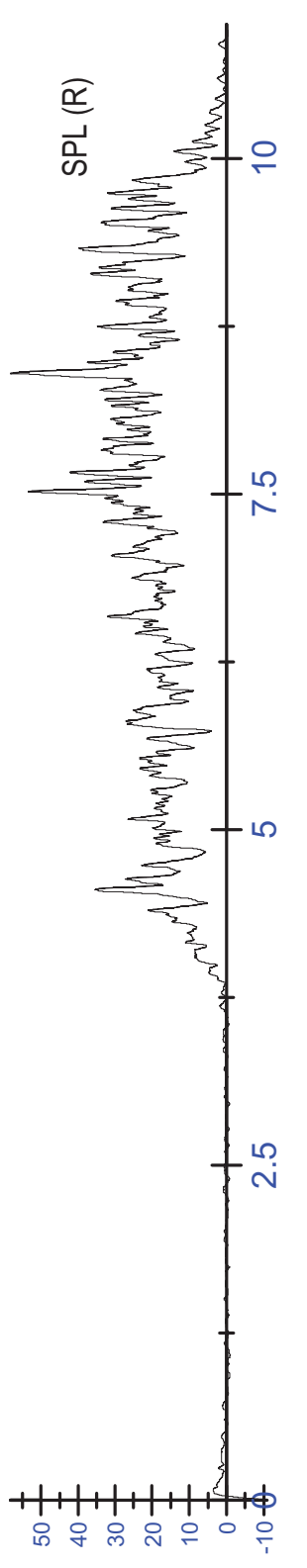
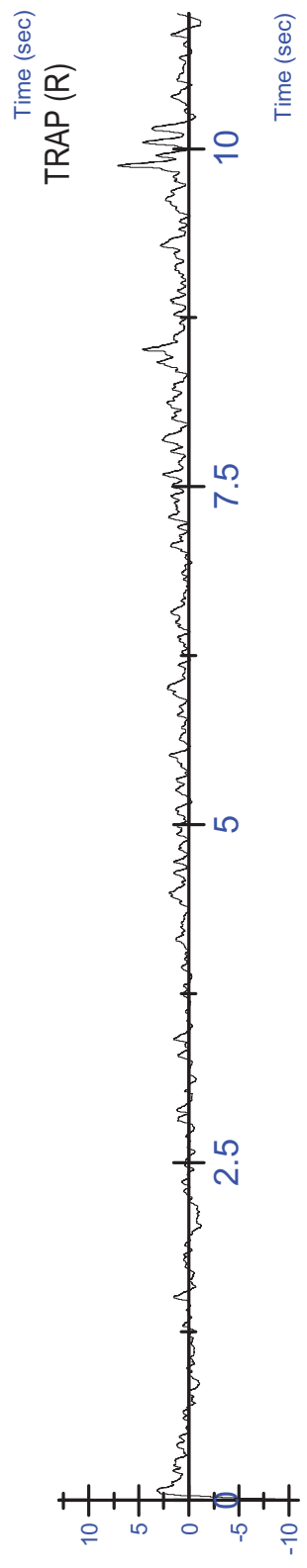
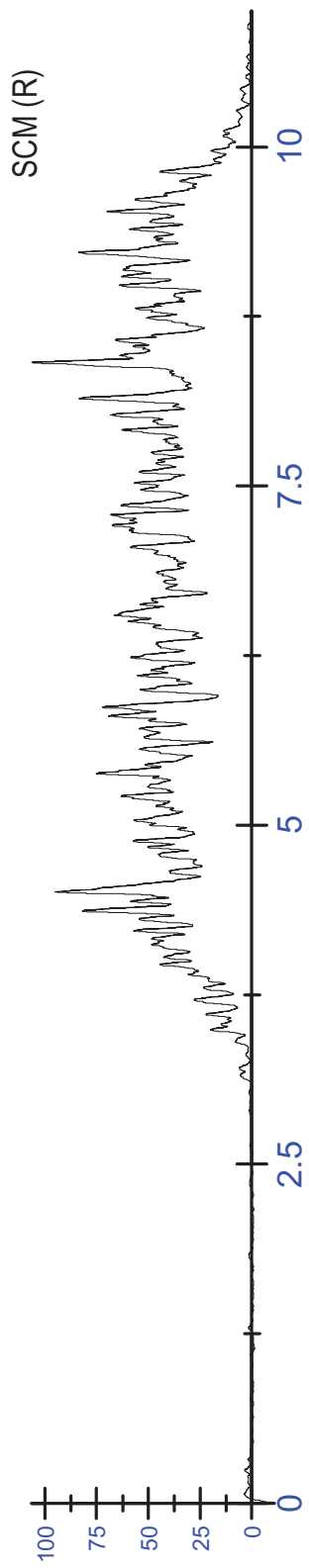


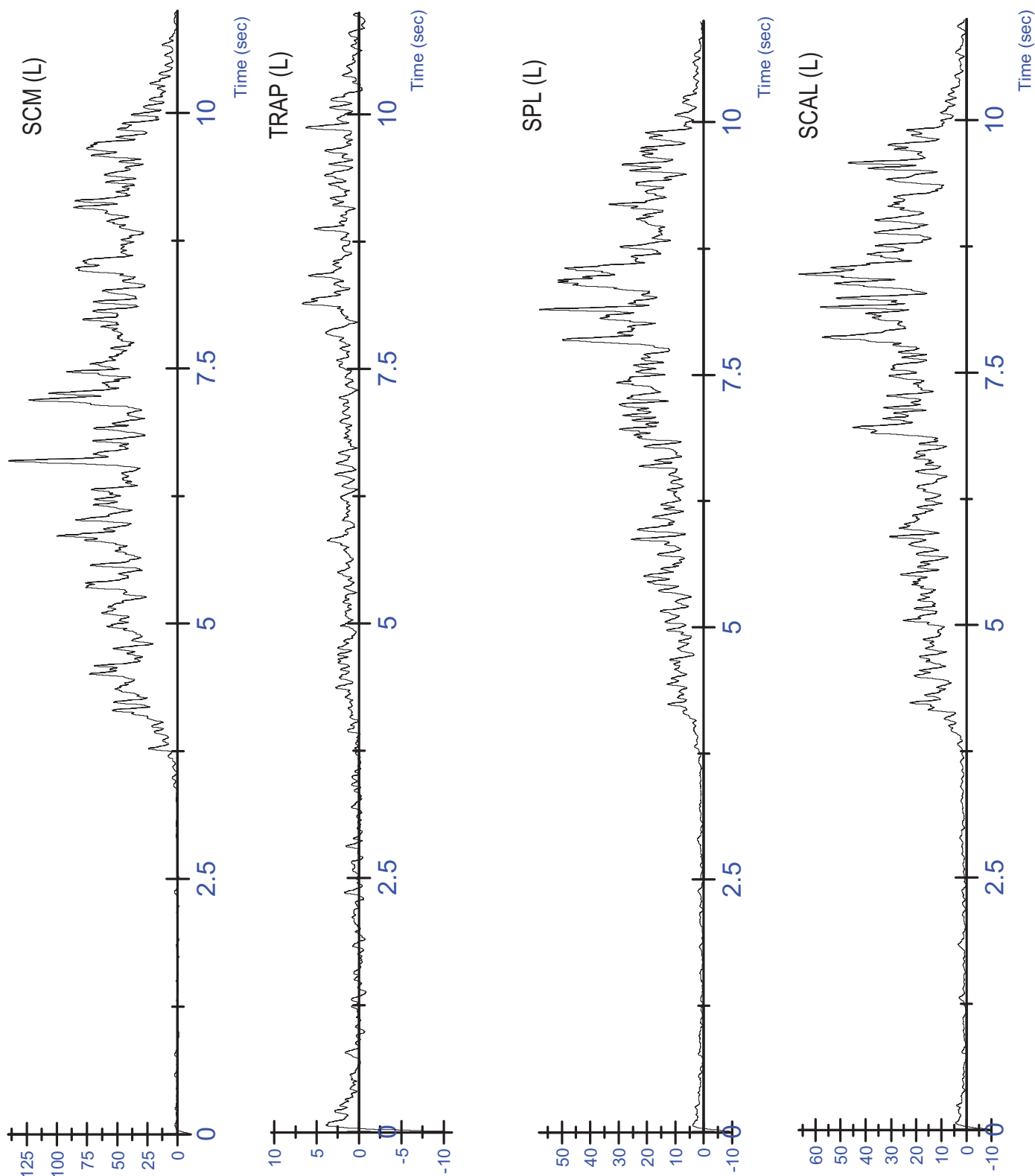
Activation (V)

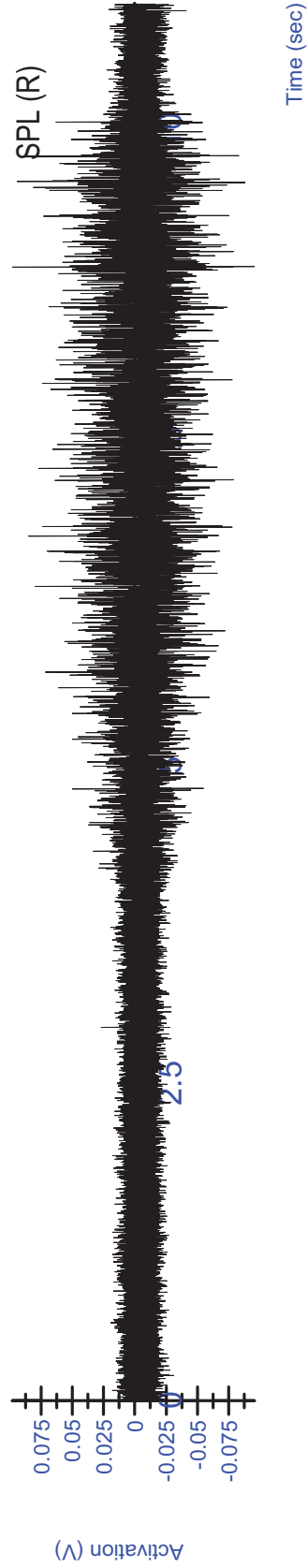
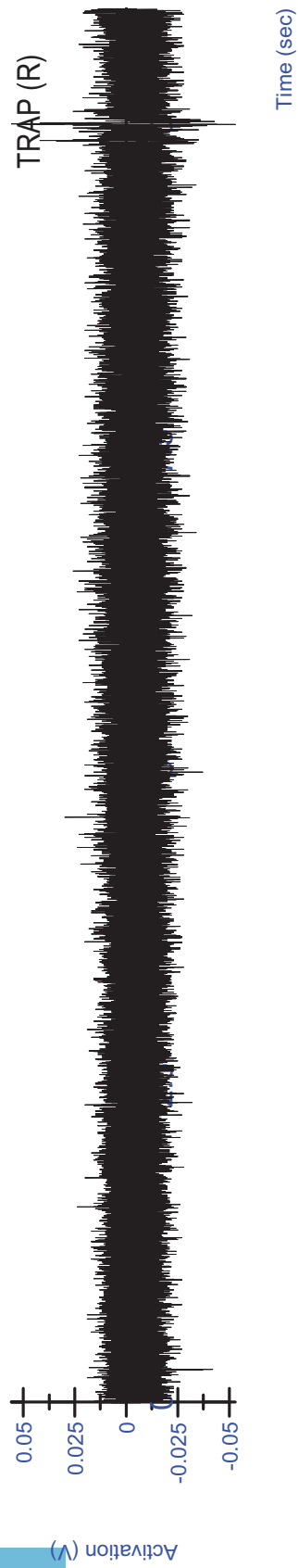
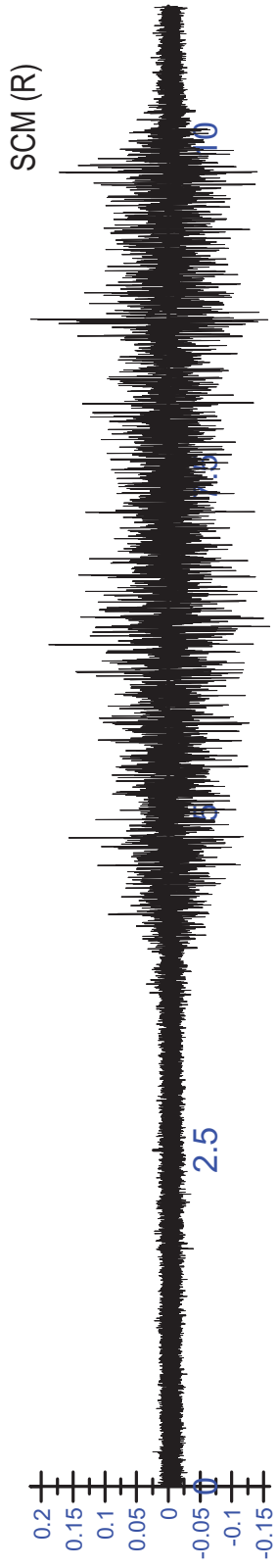


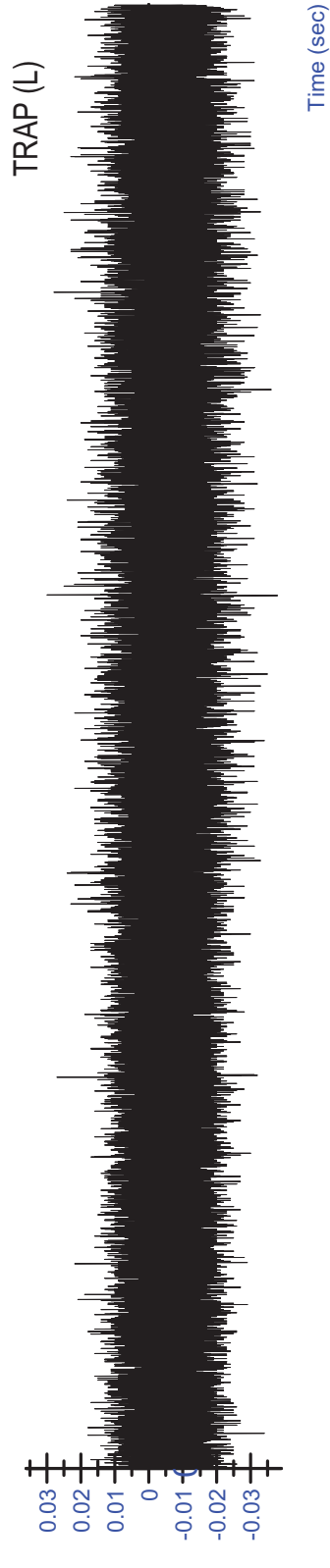
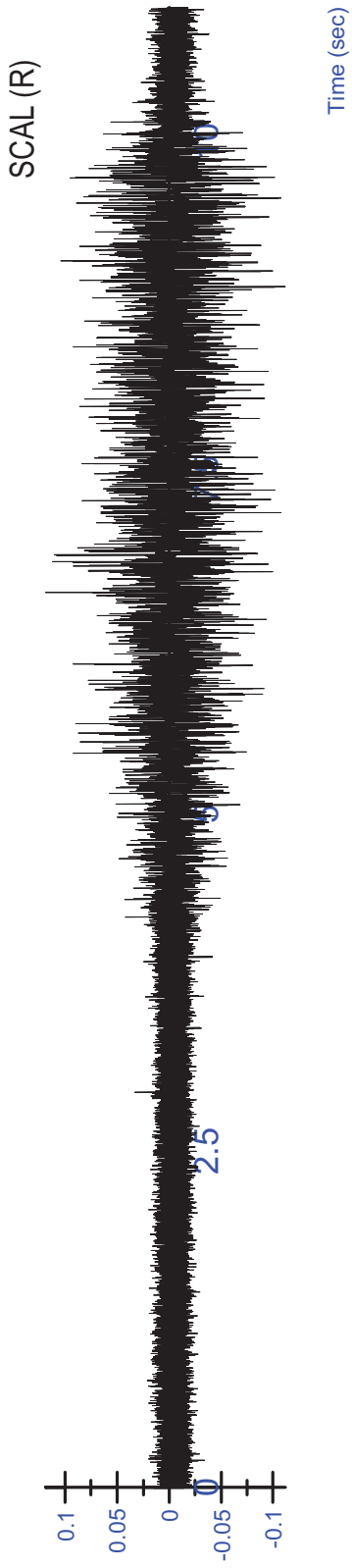
Force (lbs)

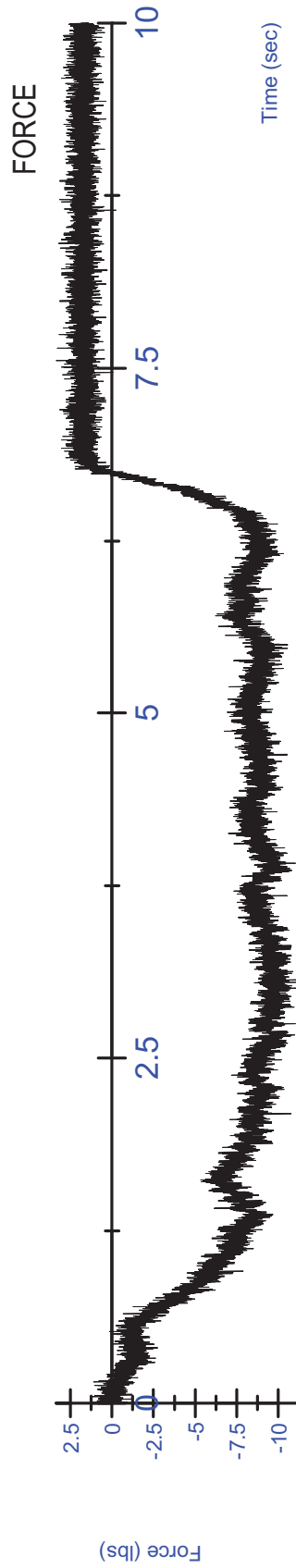
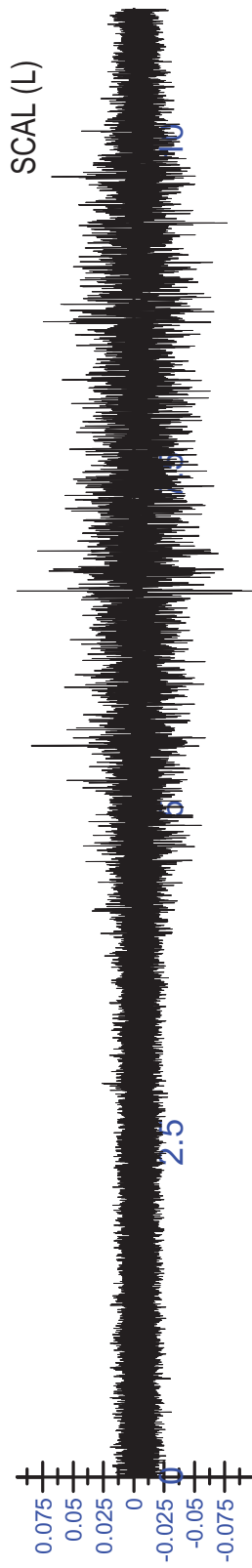
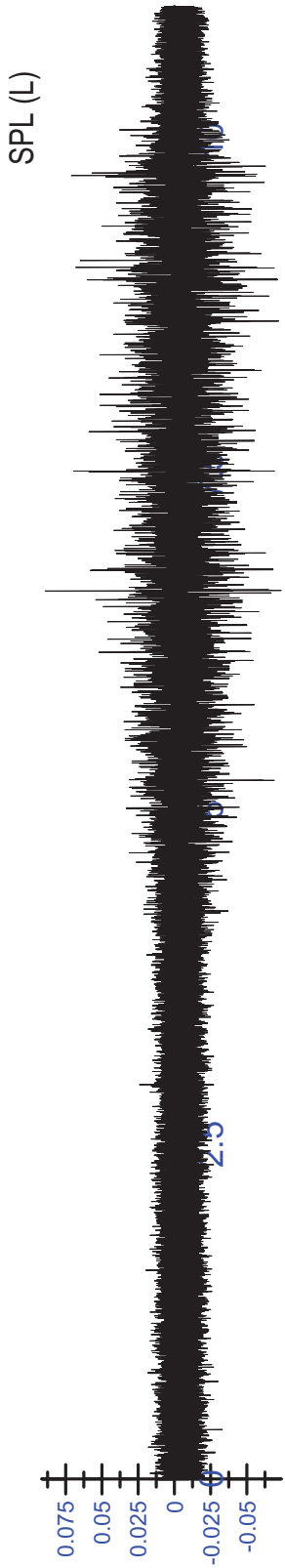


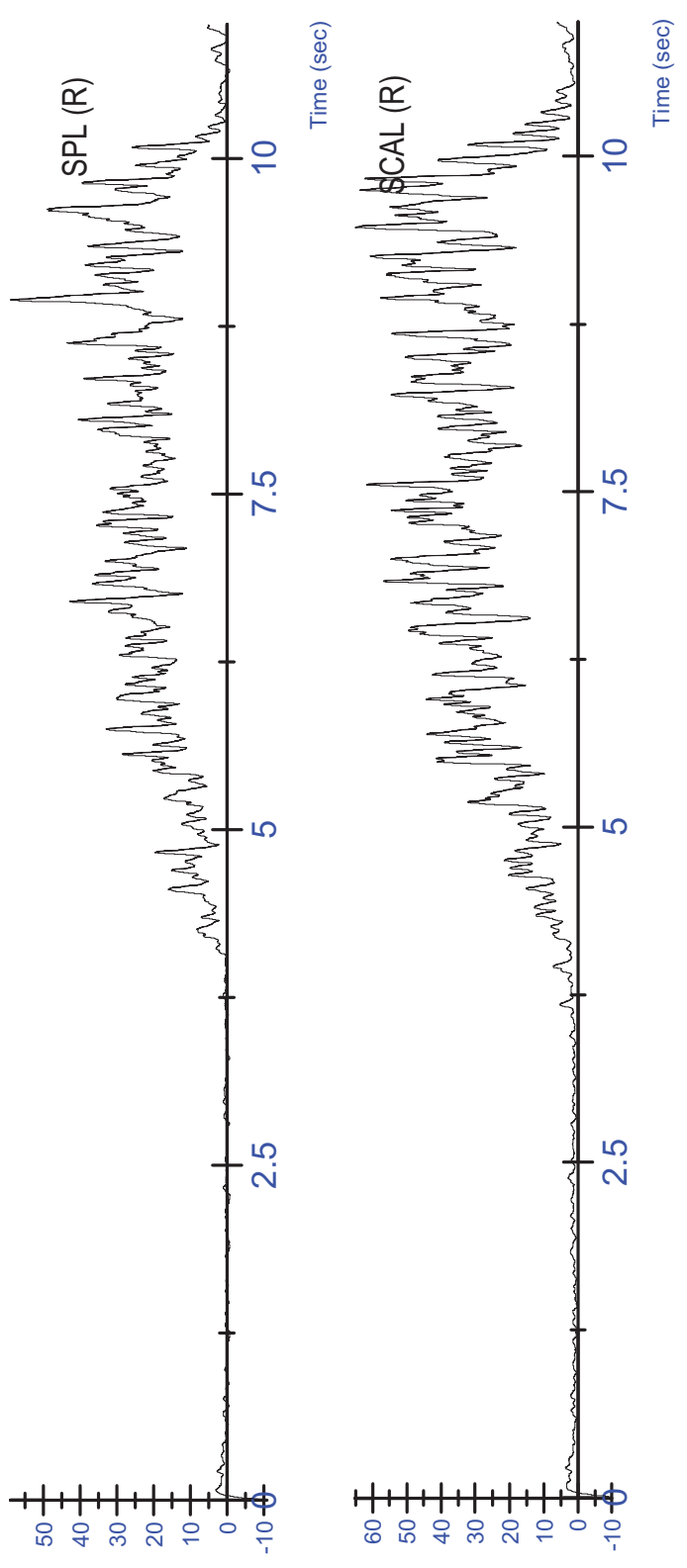
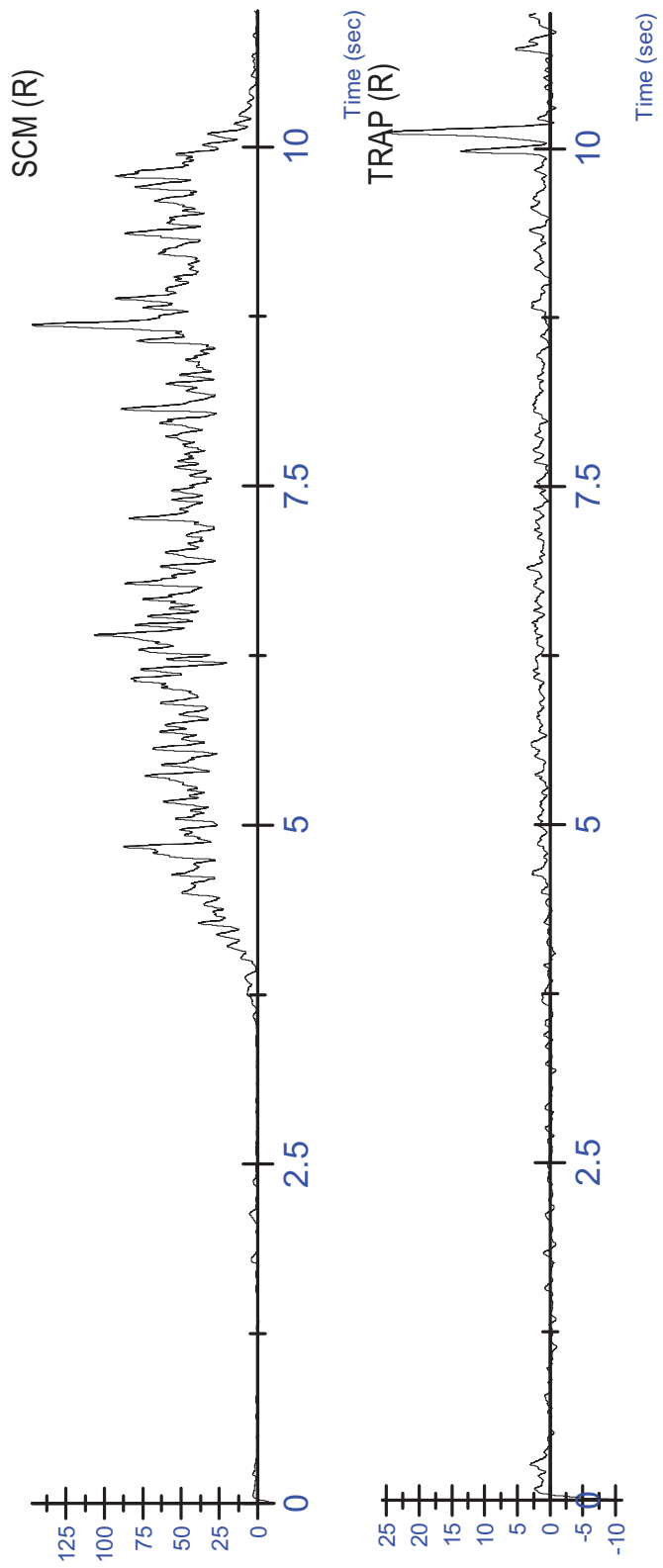


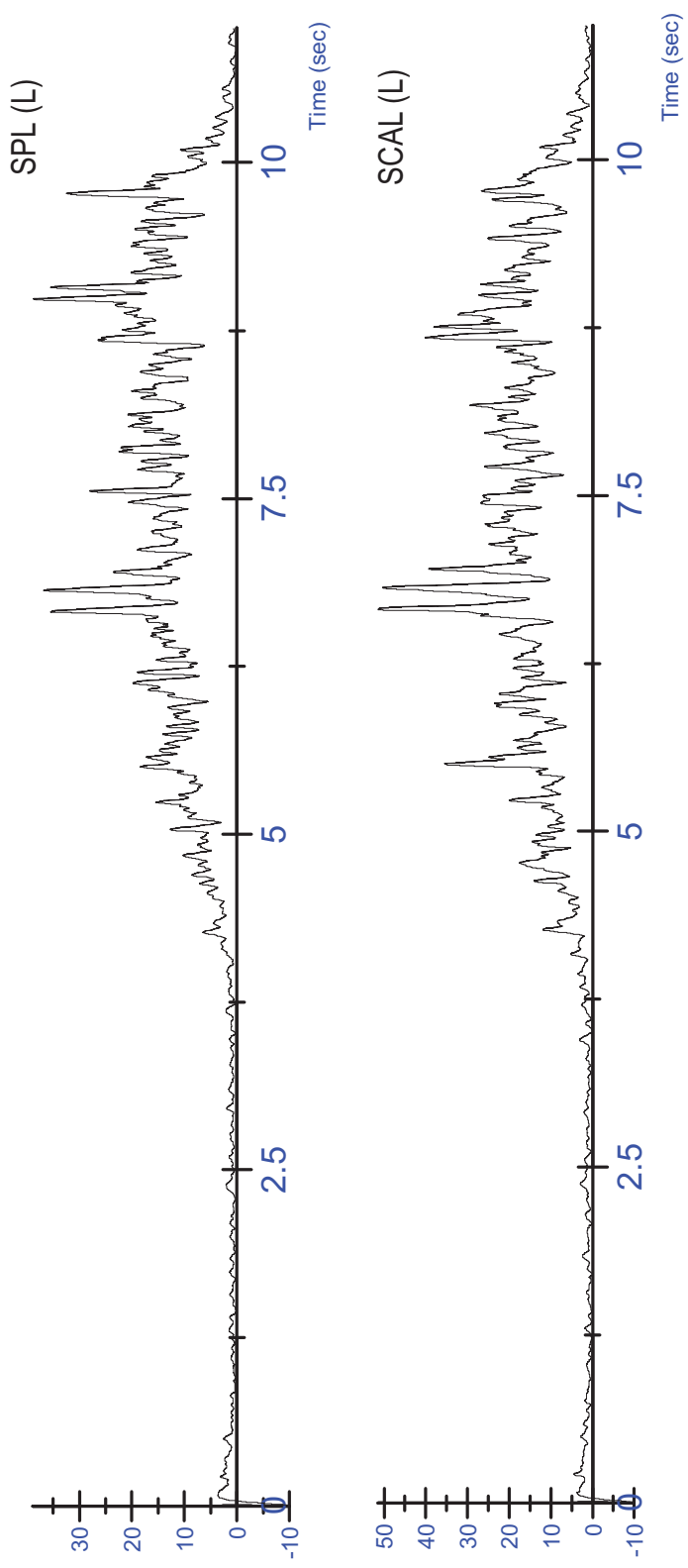
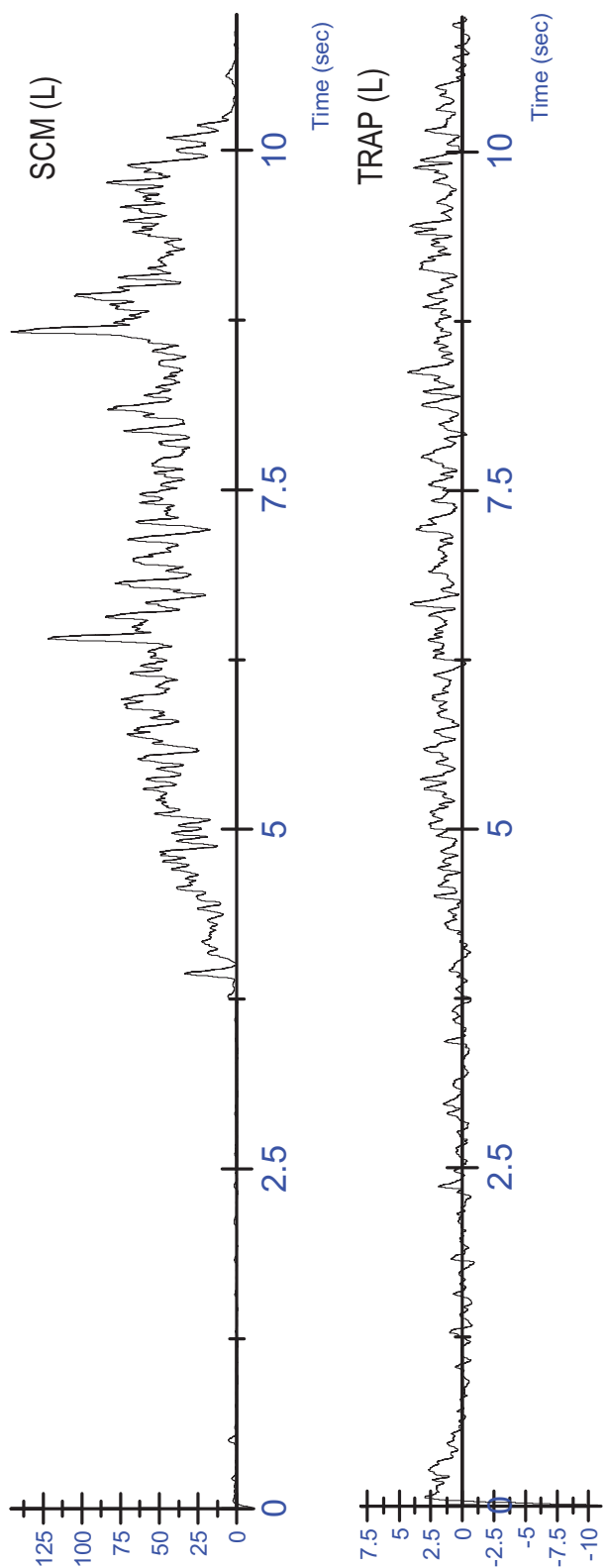


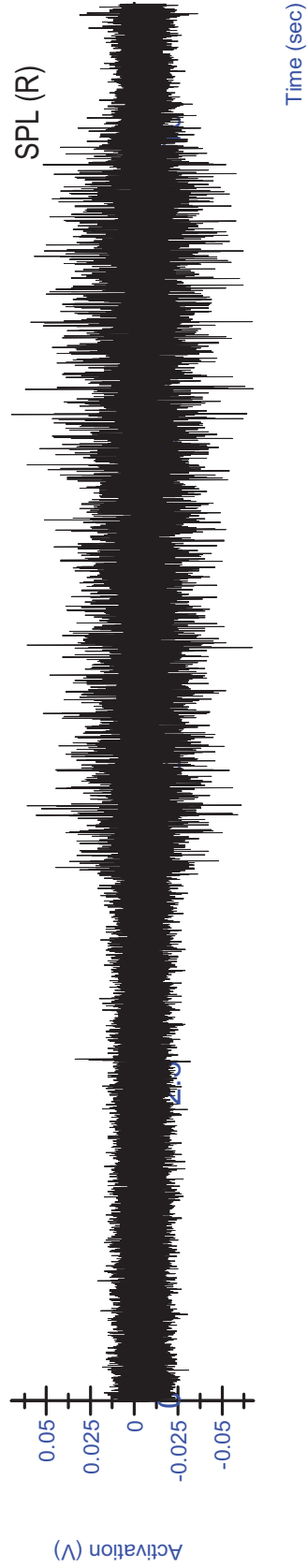
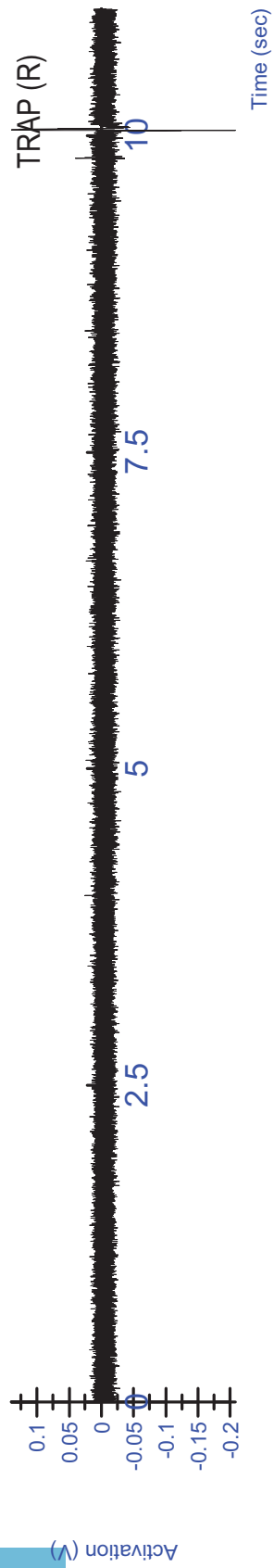
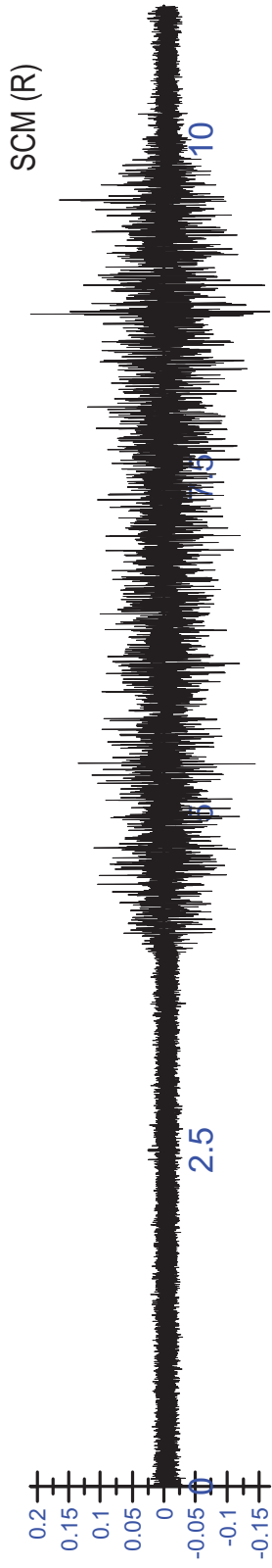


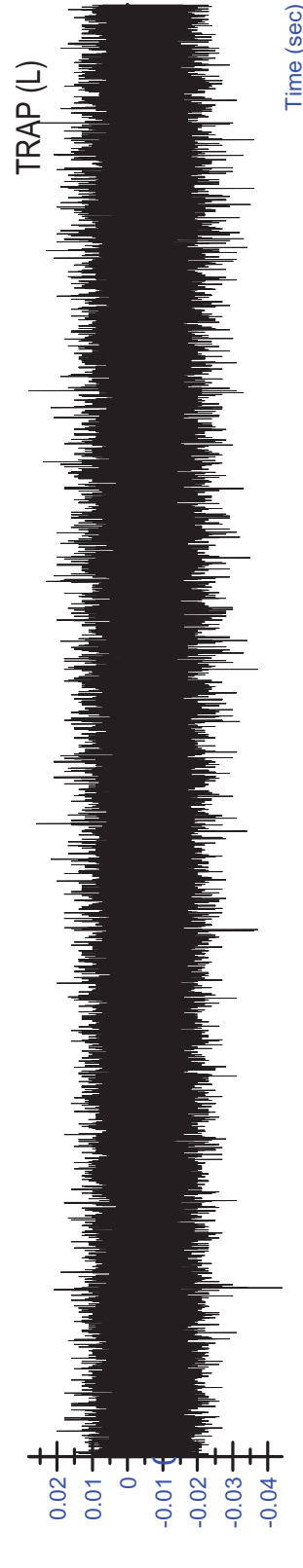
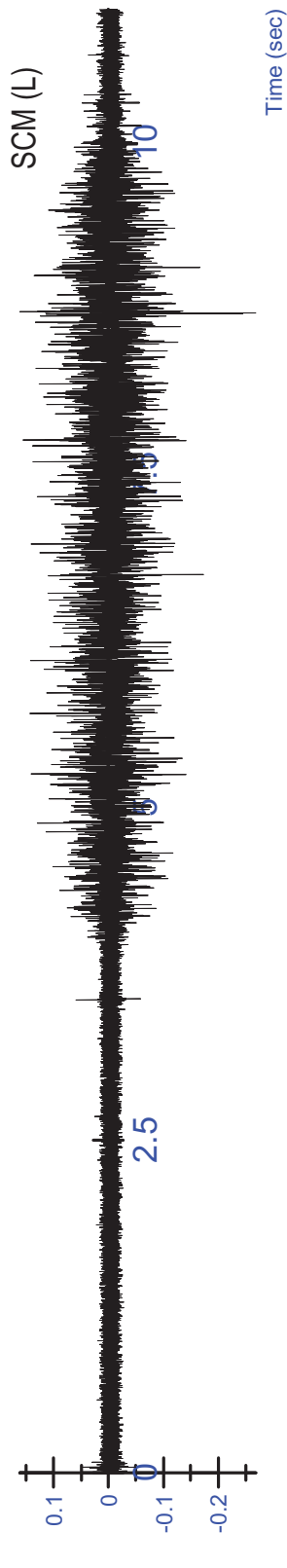


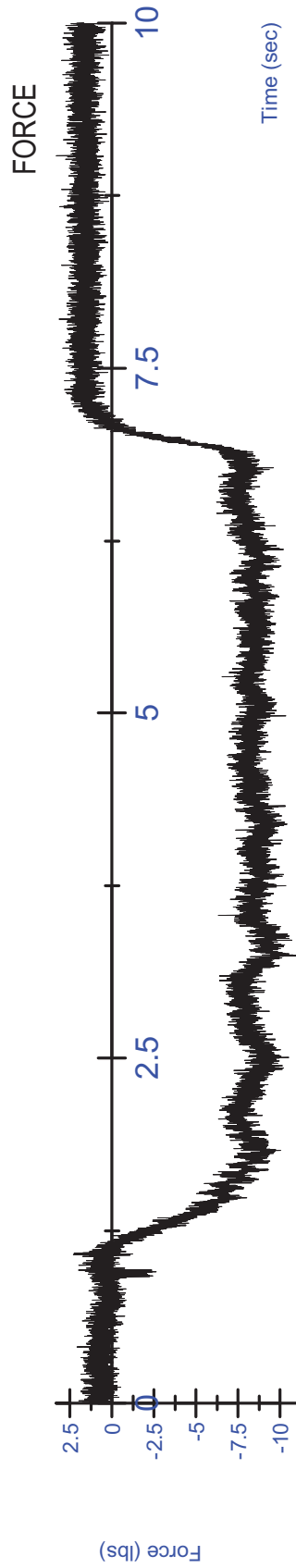
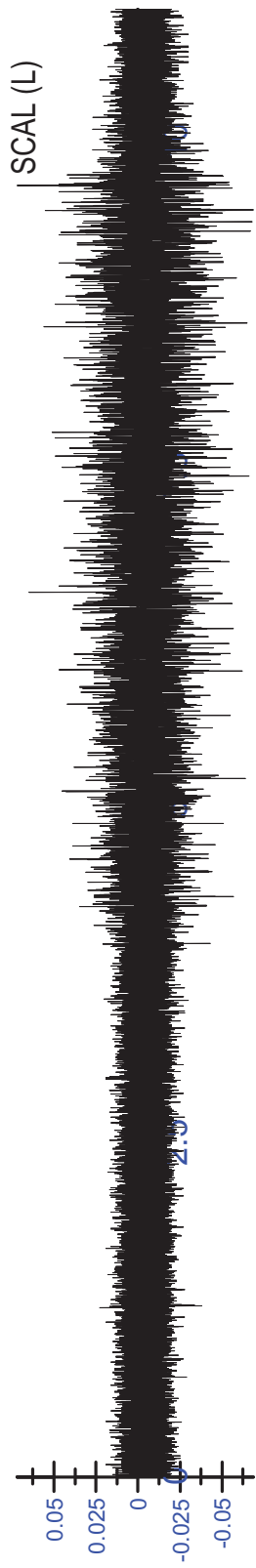
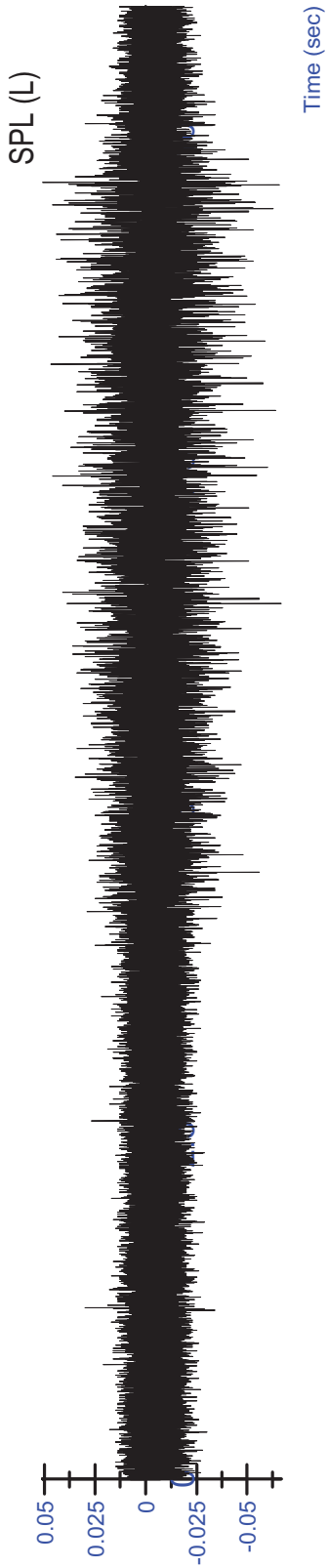


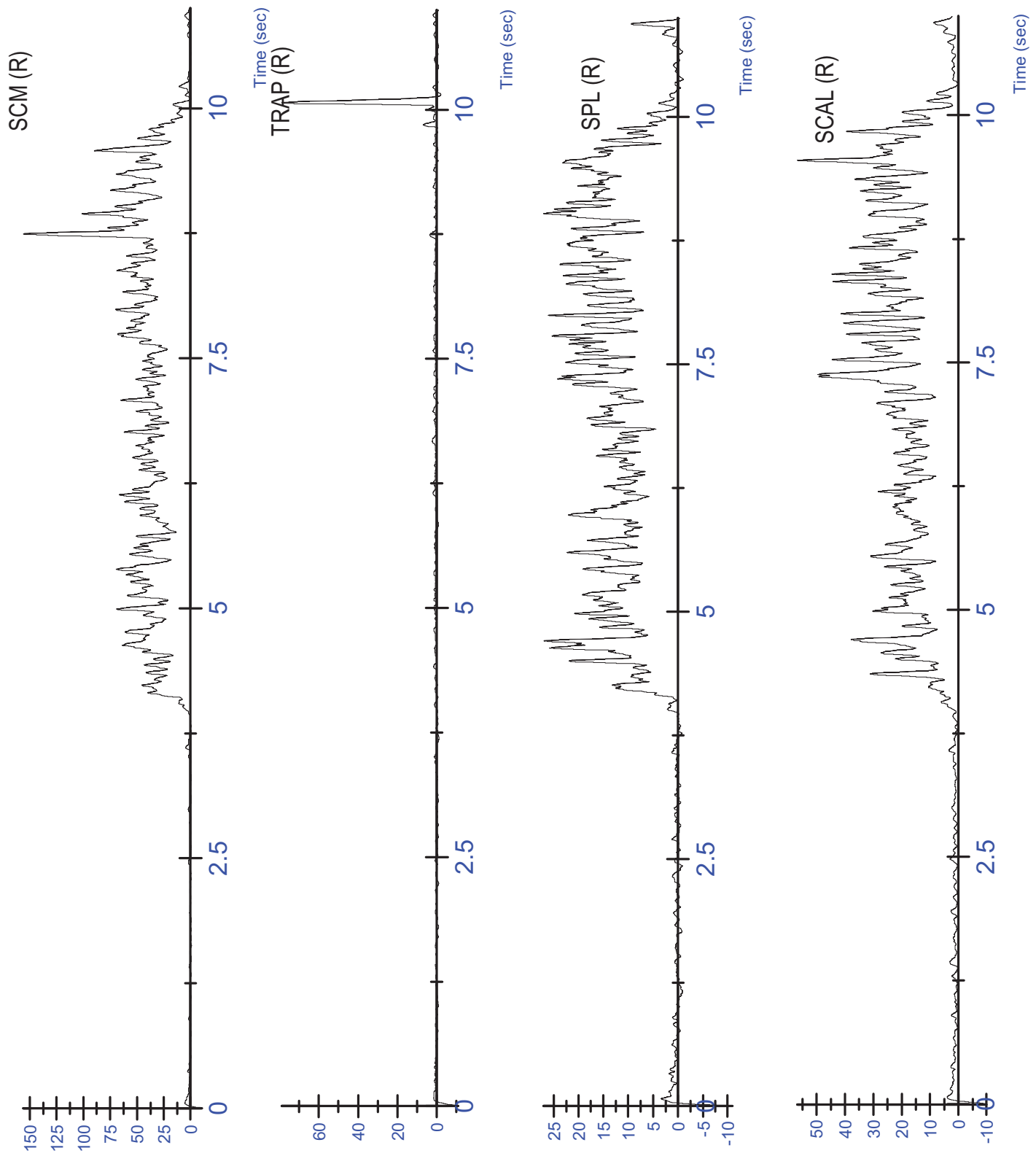


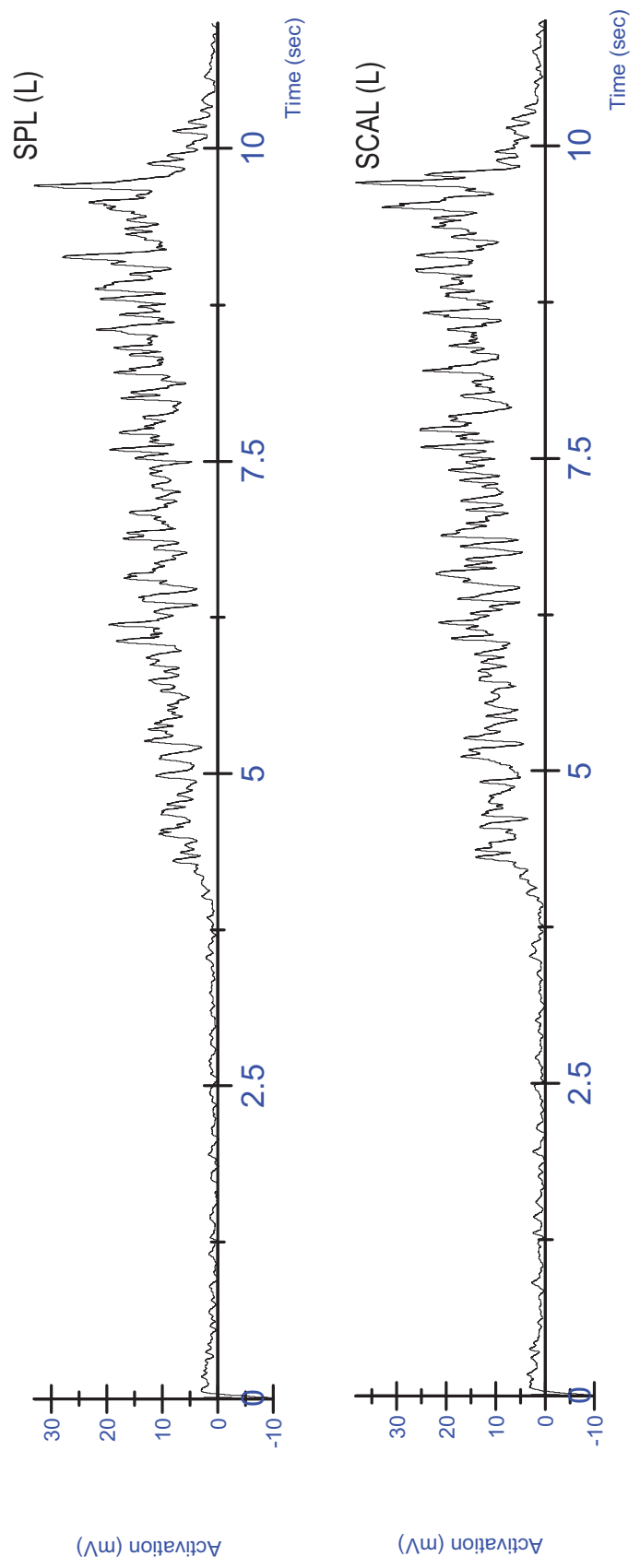
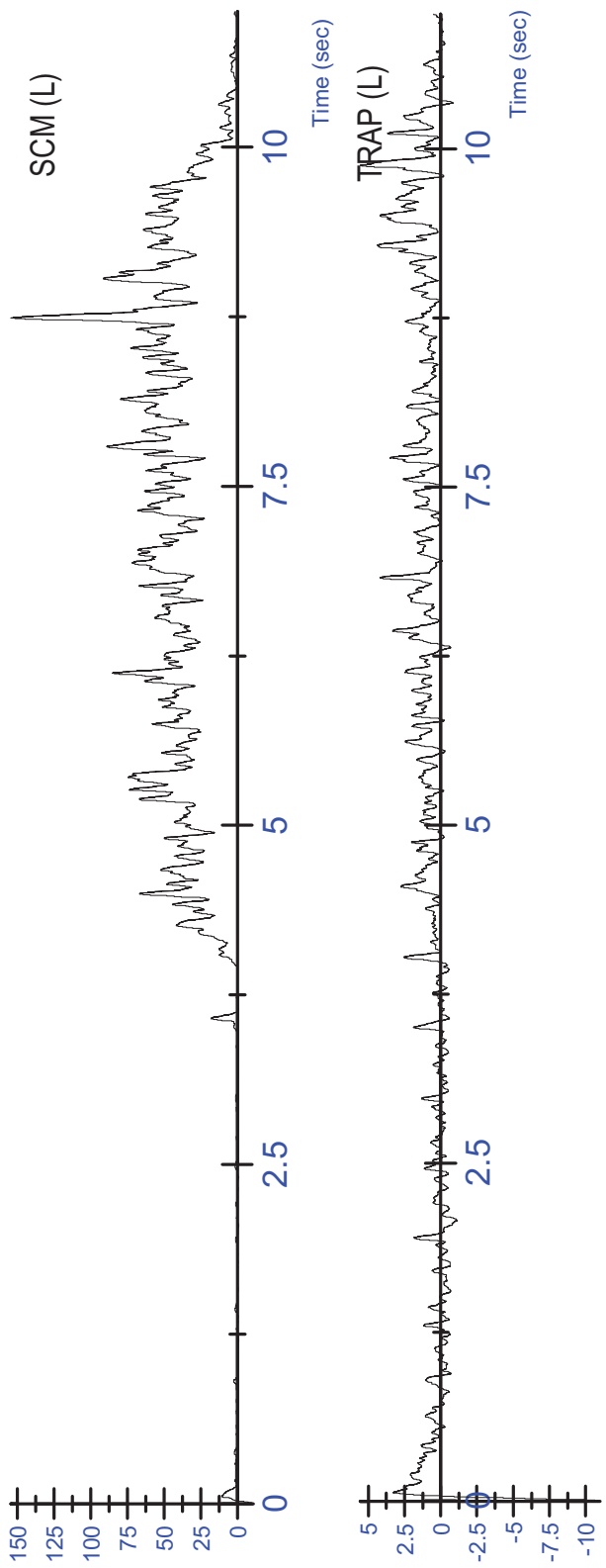






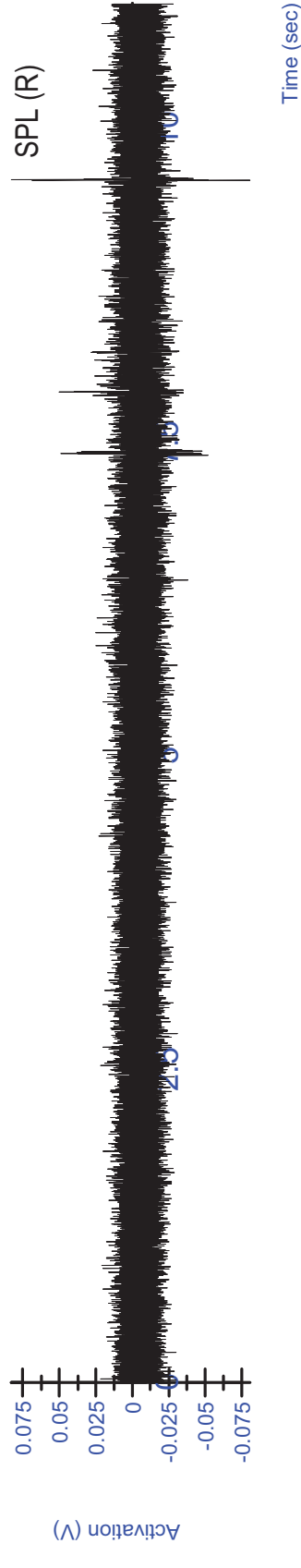
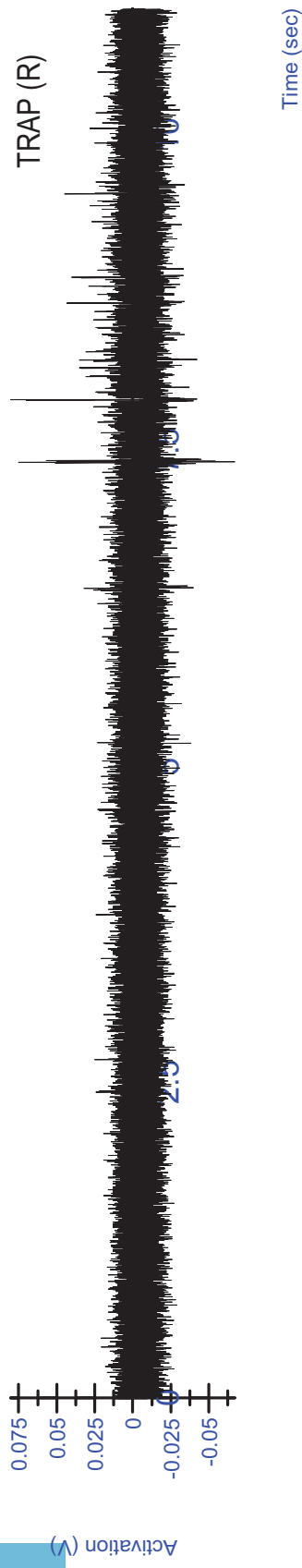
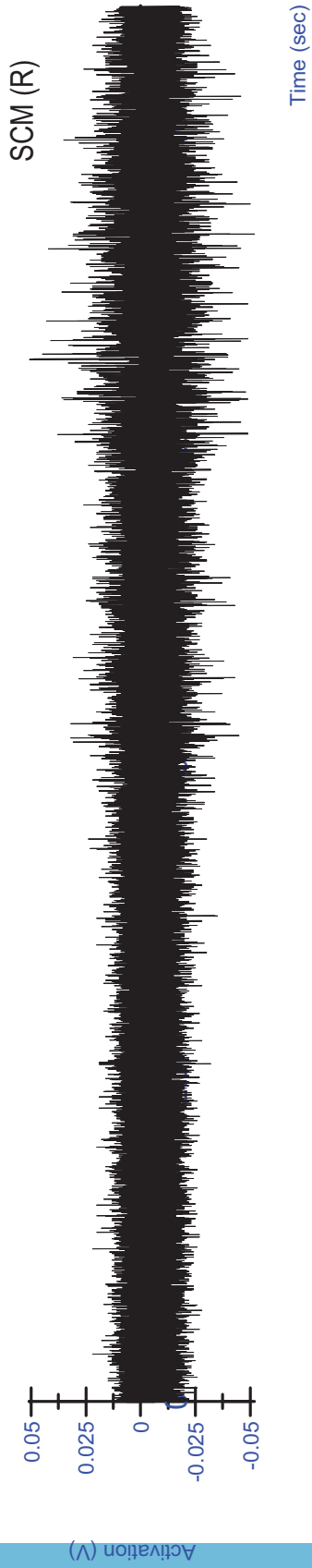


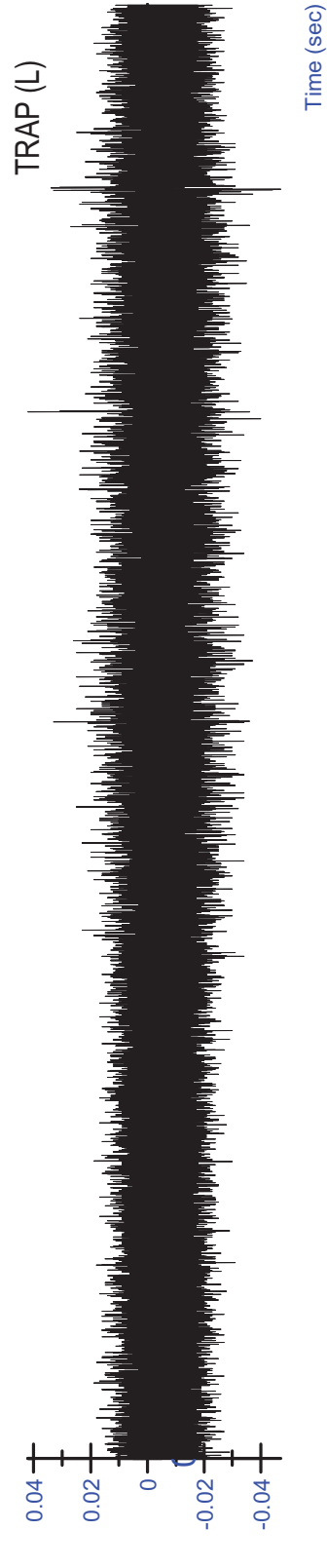
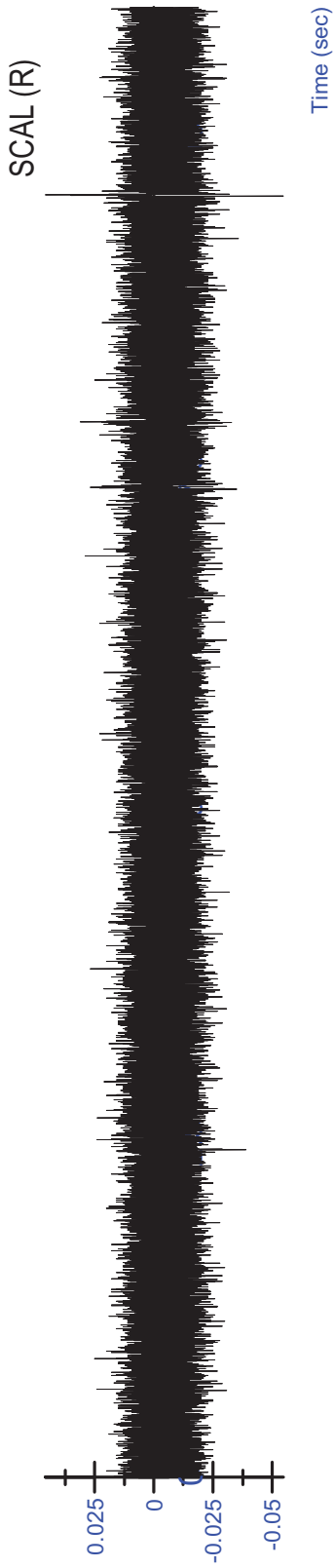




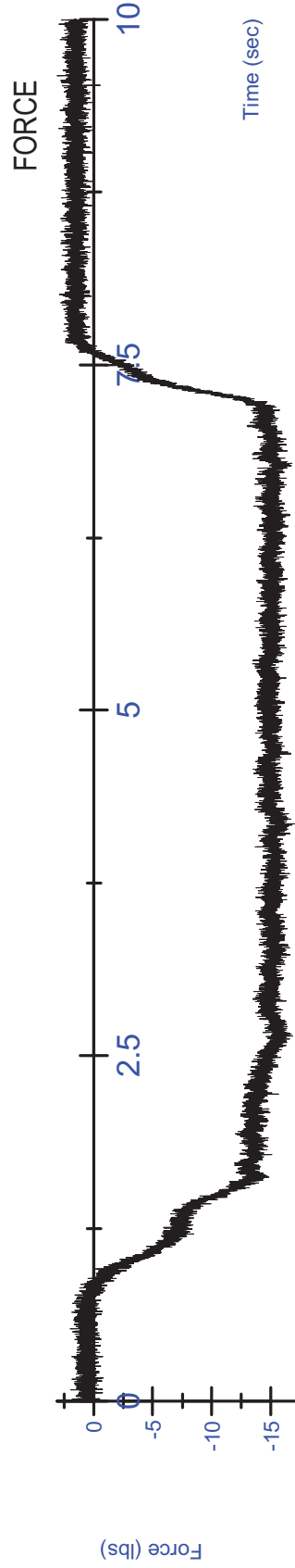
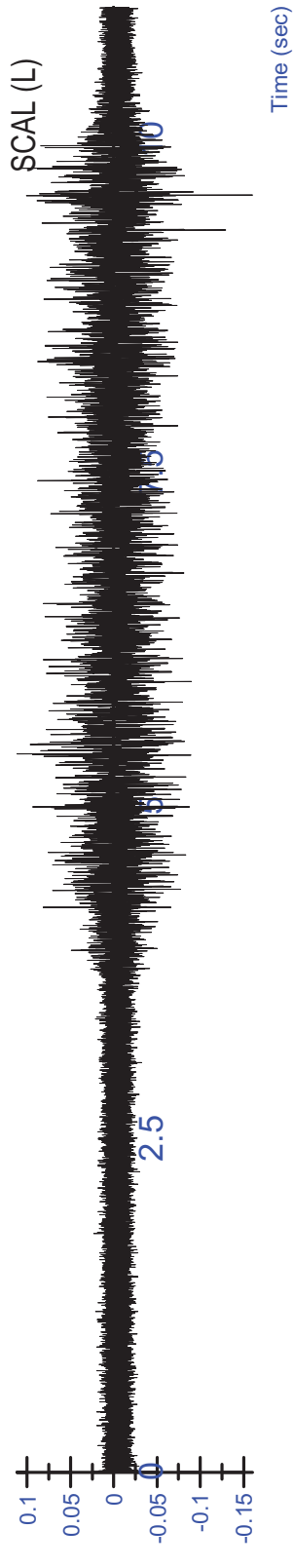
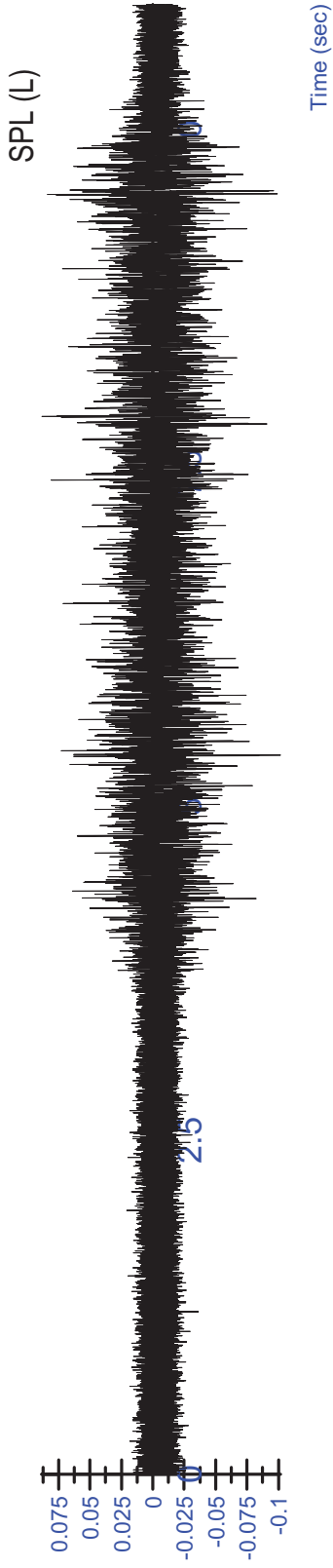
S14 MVC - Flexion Trial 3 - Rectified/Filtered

S14 MVC - Lateral (L) Trial 1 - Unfiltered

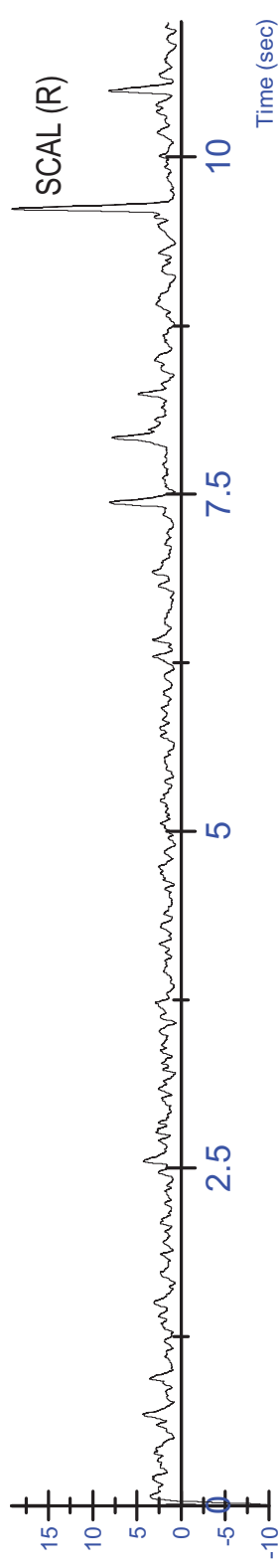
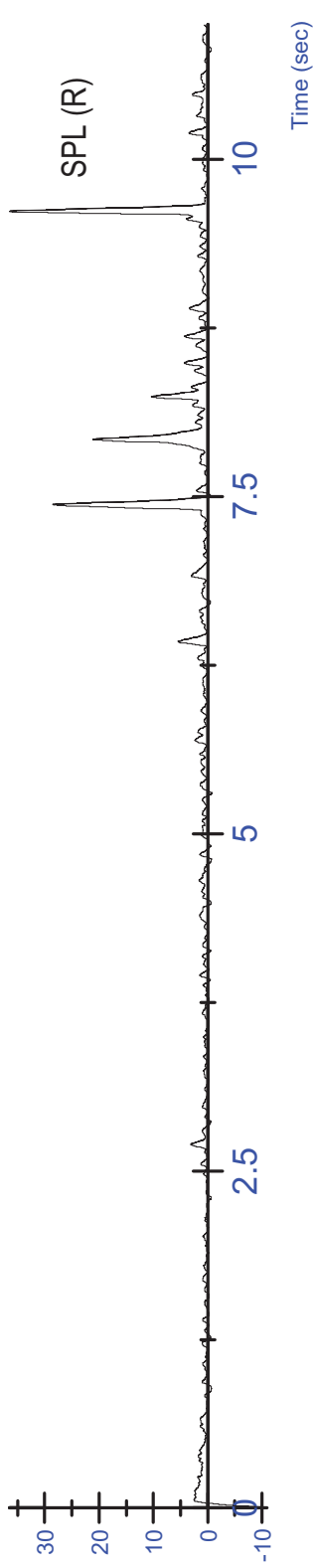
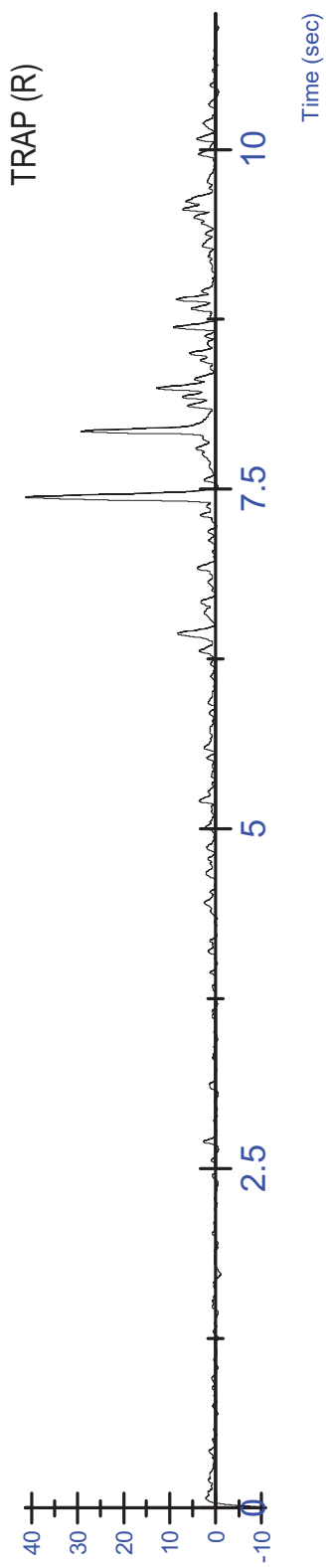
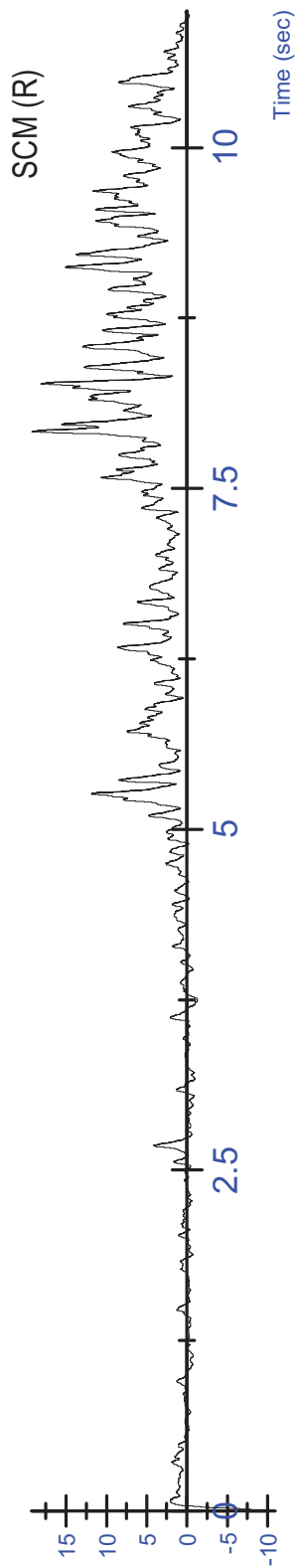




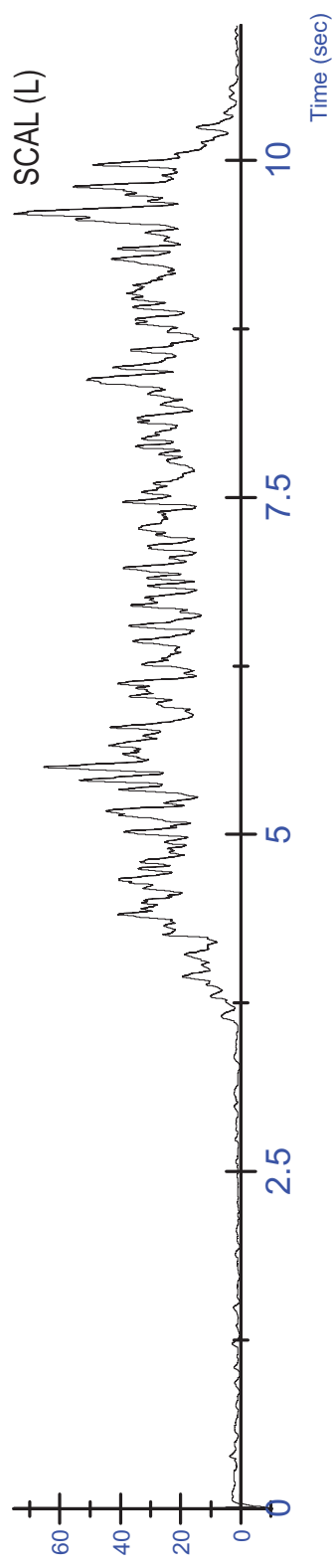
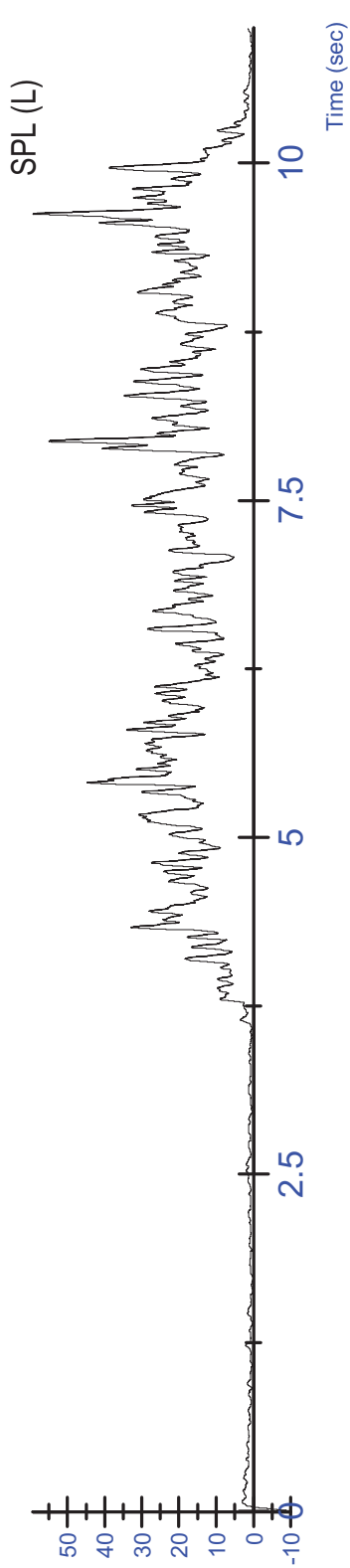
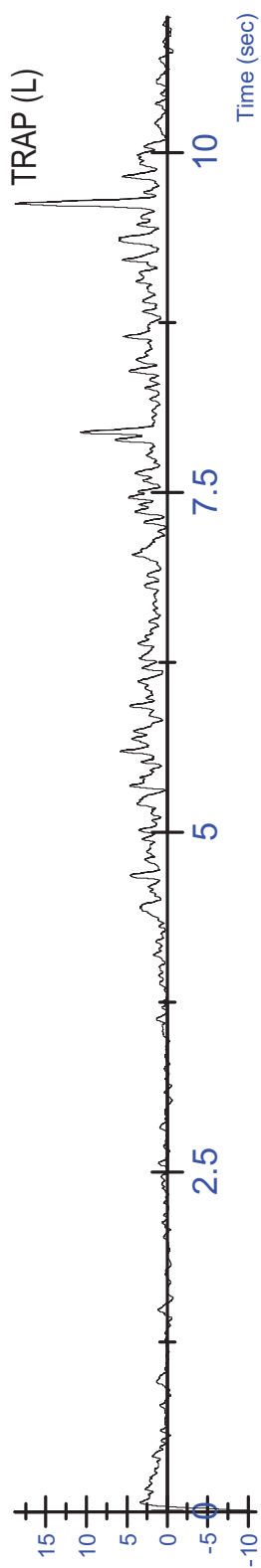
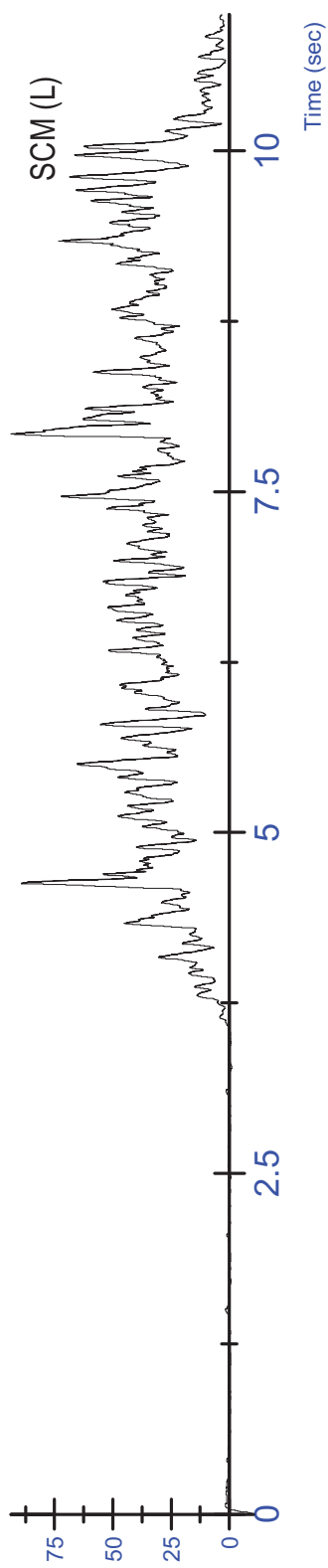
S14 MVC - Lateral (L) Trial 1 - Unfiltered

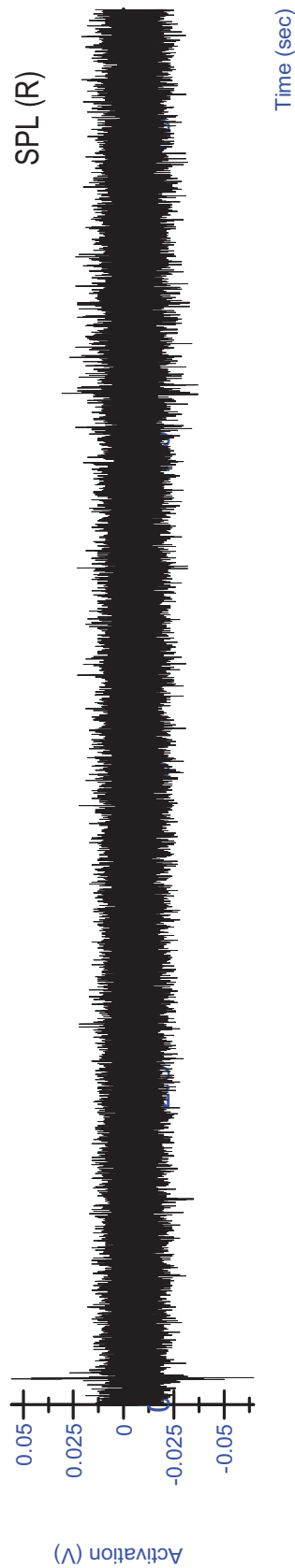
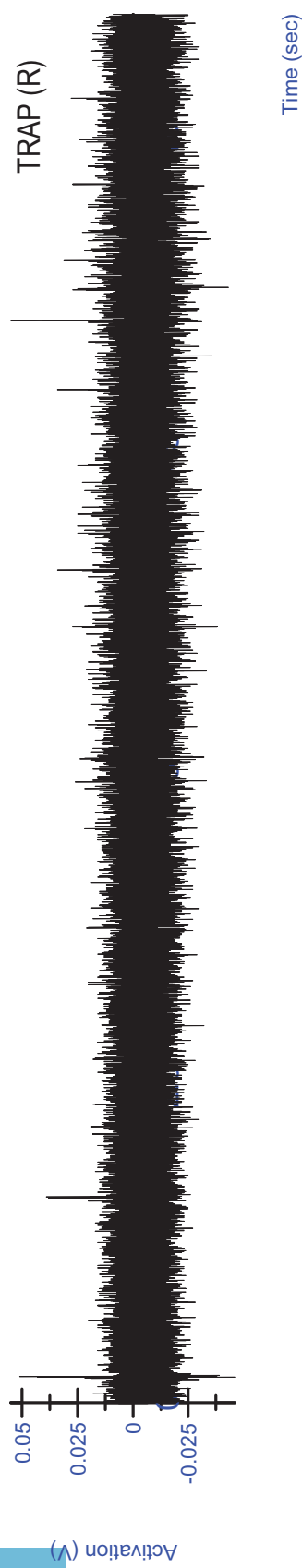
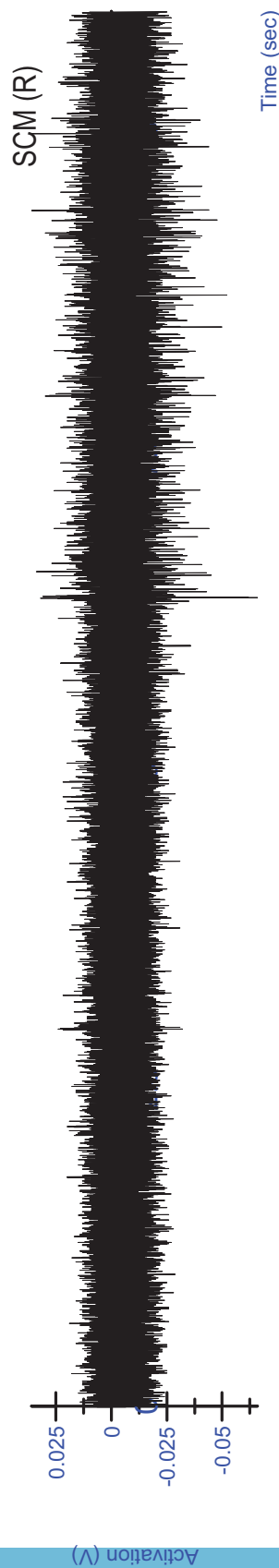


S14 MVC - Lateral (L) Trial 1 - Rectified/Filtered

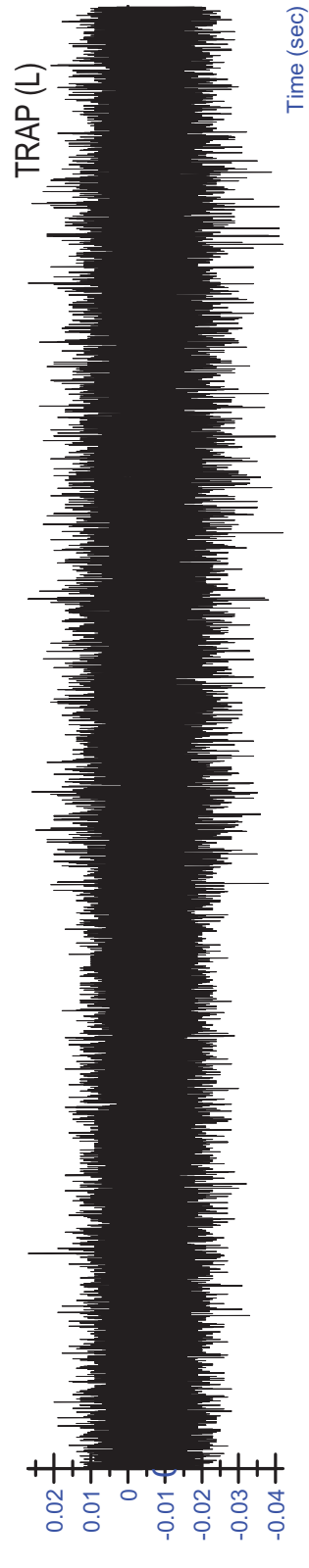
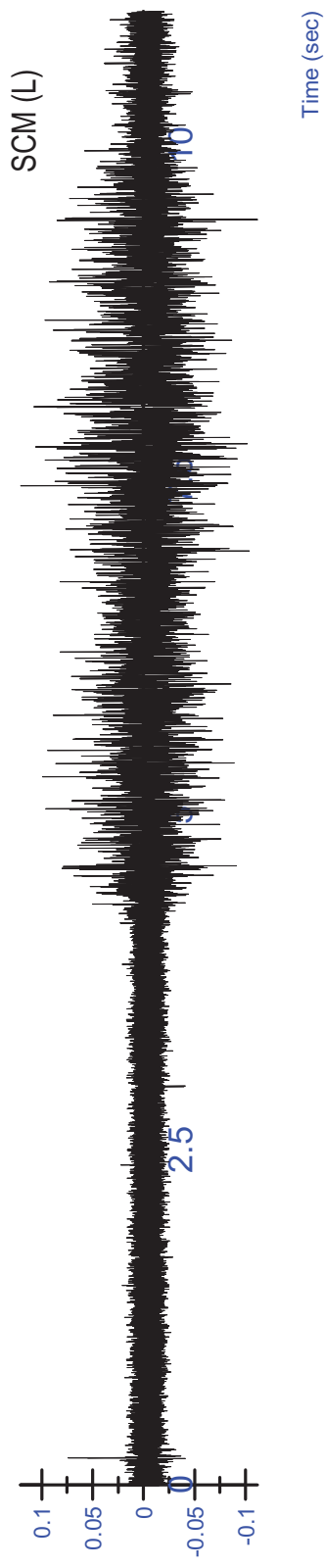
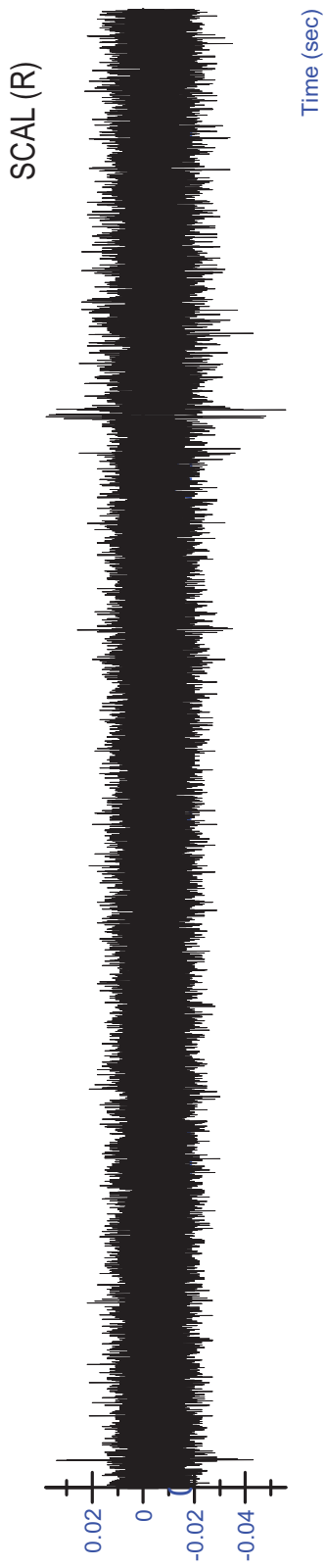


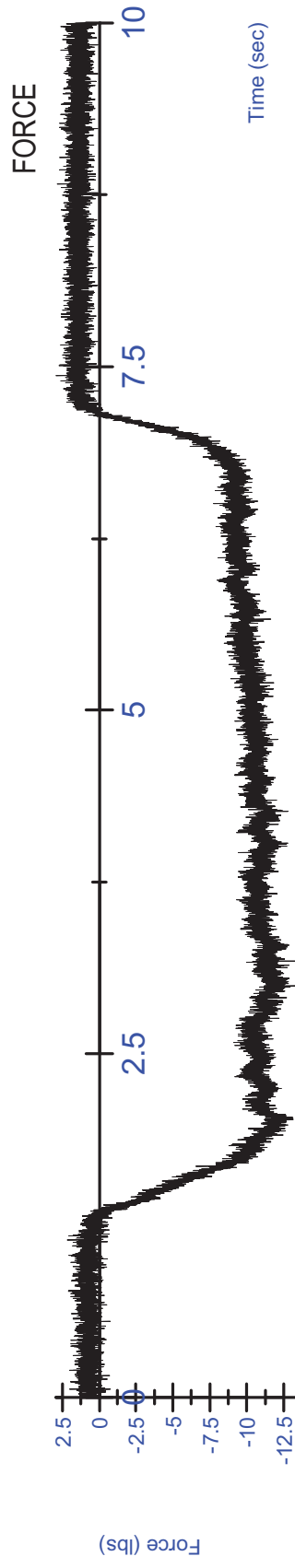
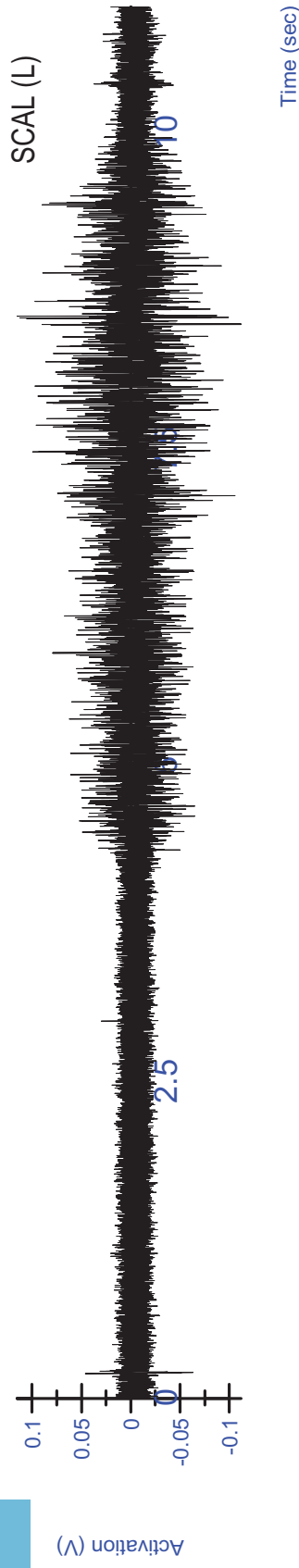
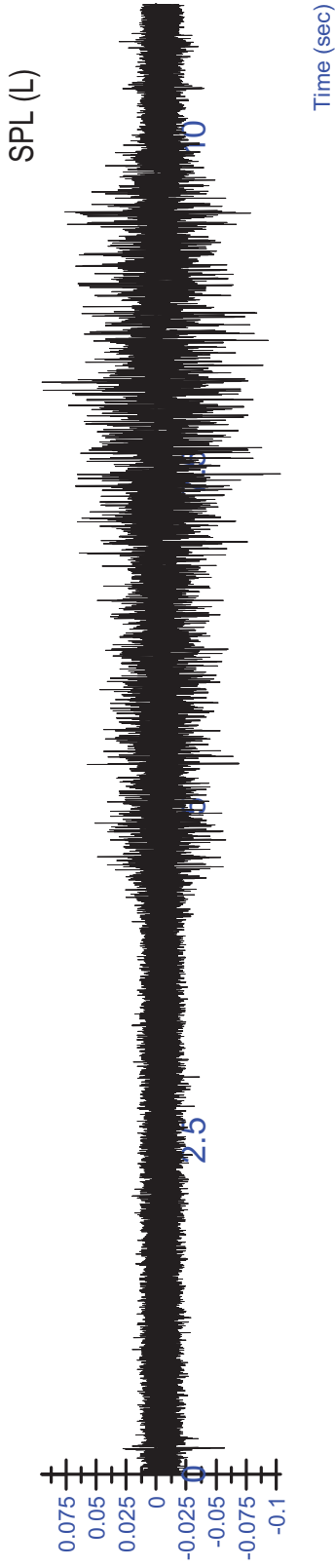
S14 MVC - Lateral (L) Trial 1 - Rectified/Filtered

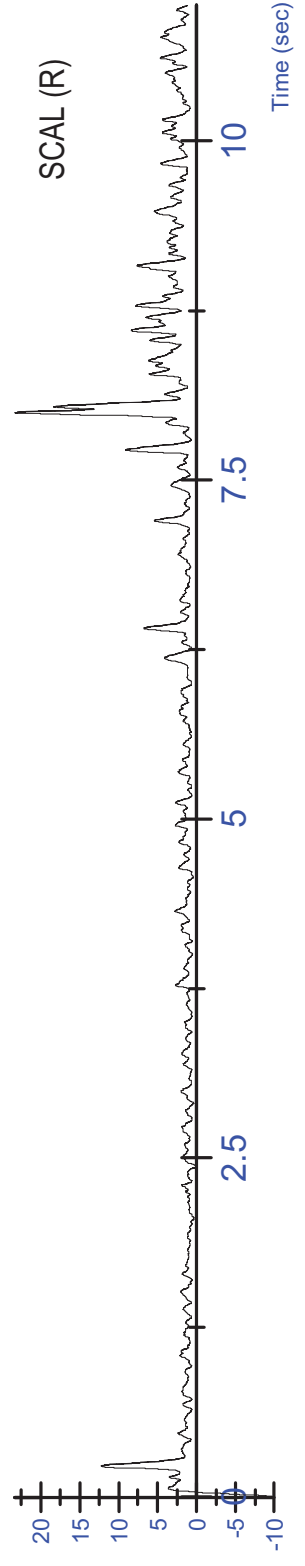
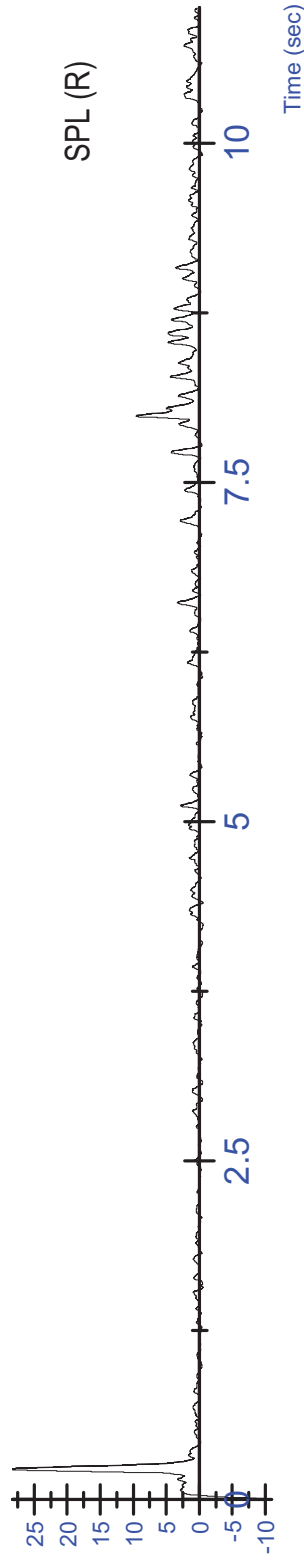
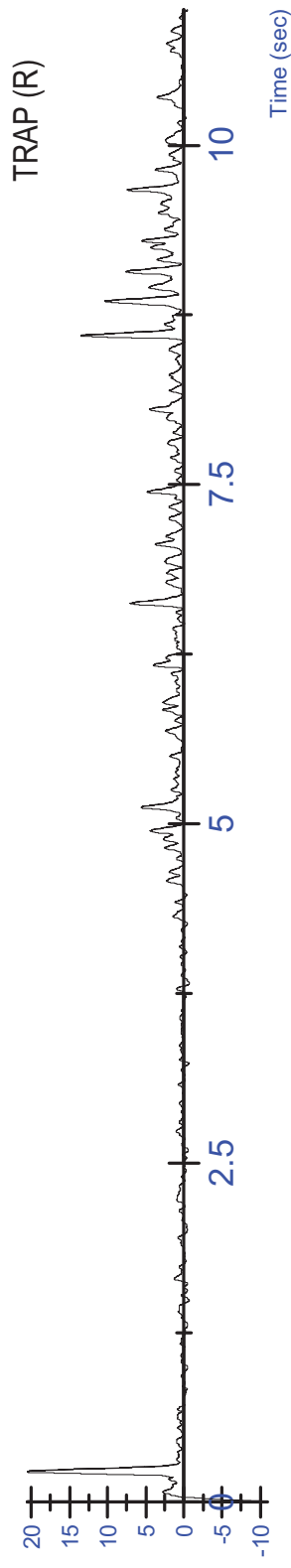
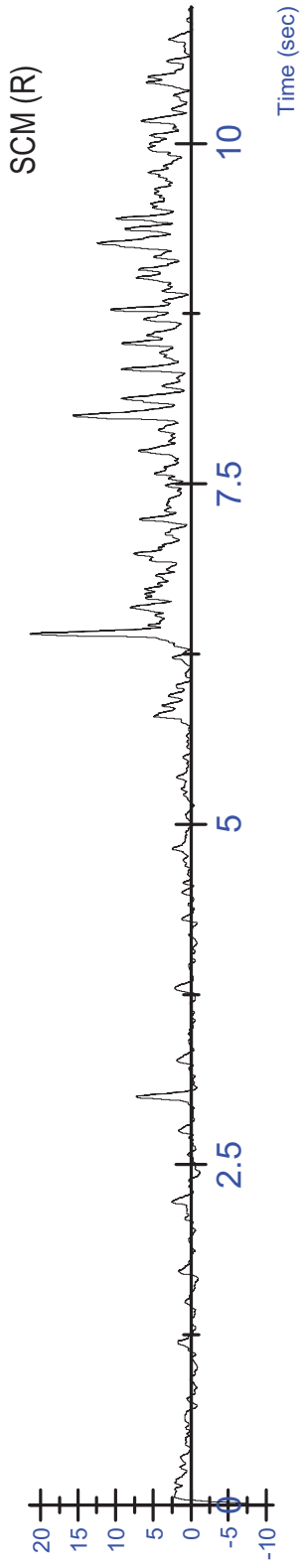




S14 MVC - Lateral (L) Trial 2 - Unfiltered





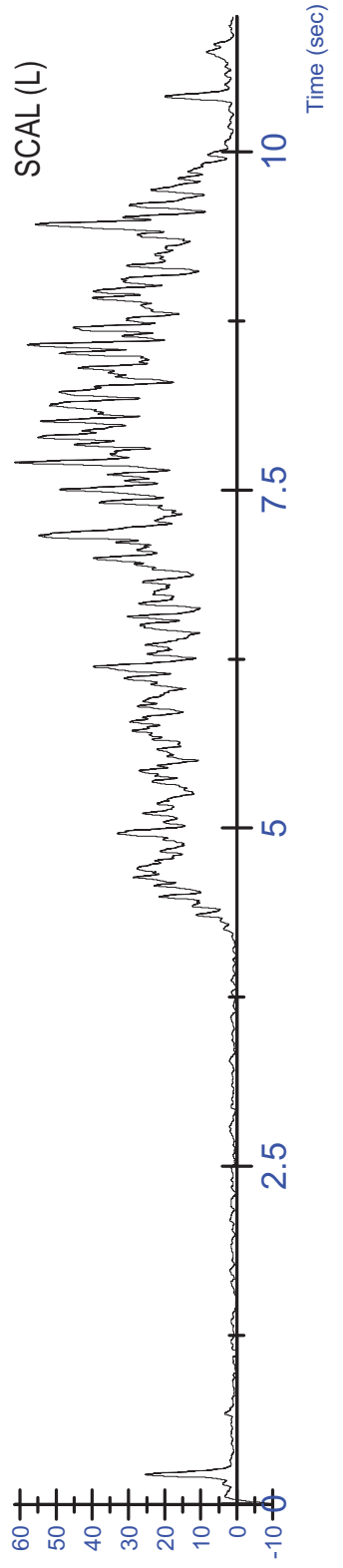
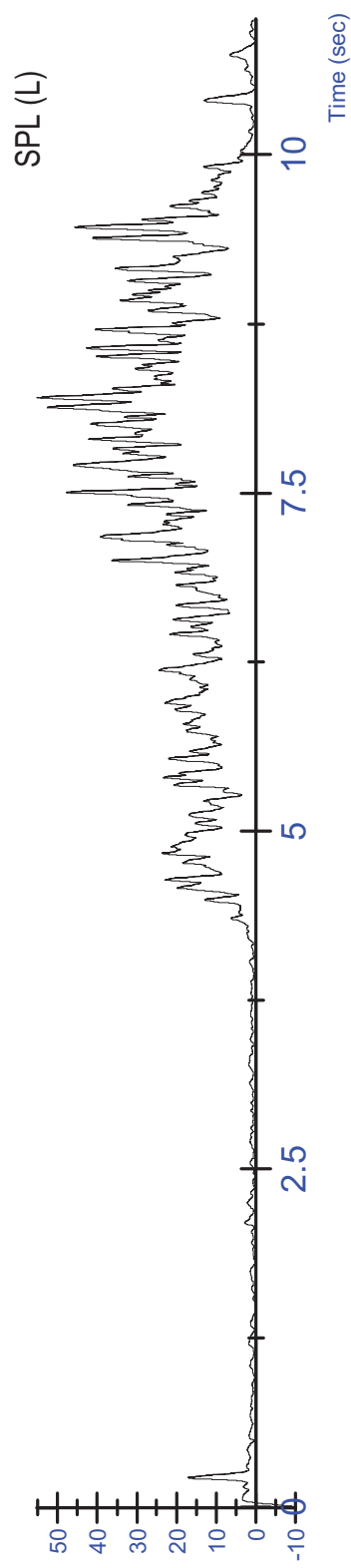
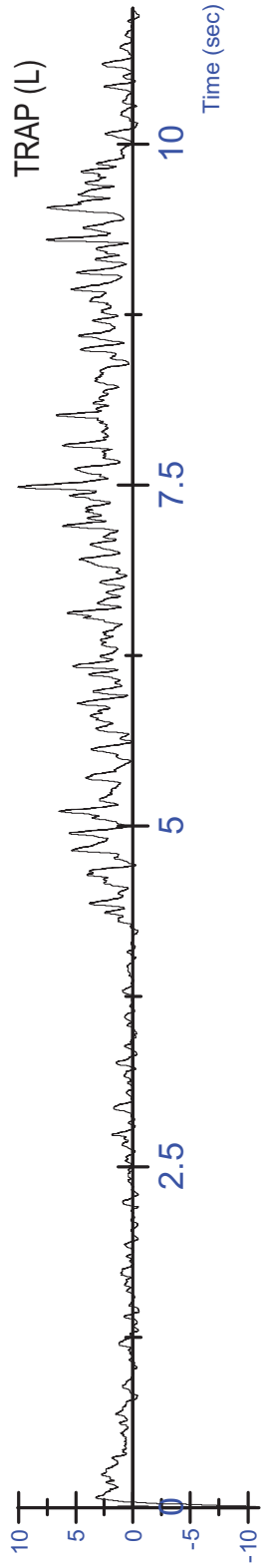
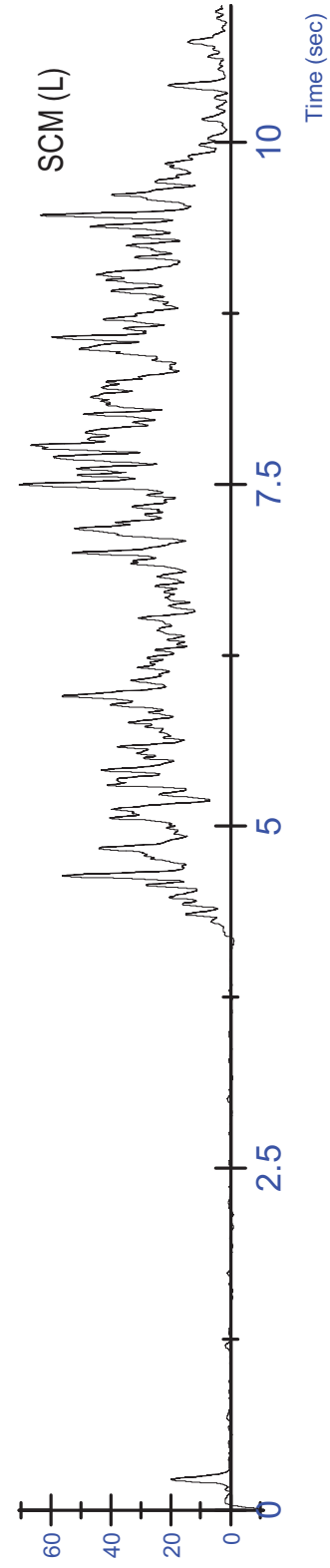


Activation (mV)

Activation (mV)

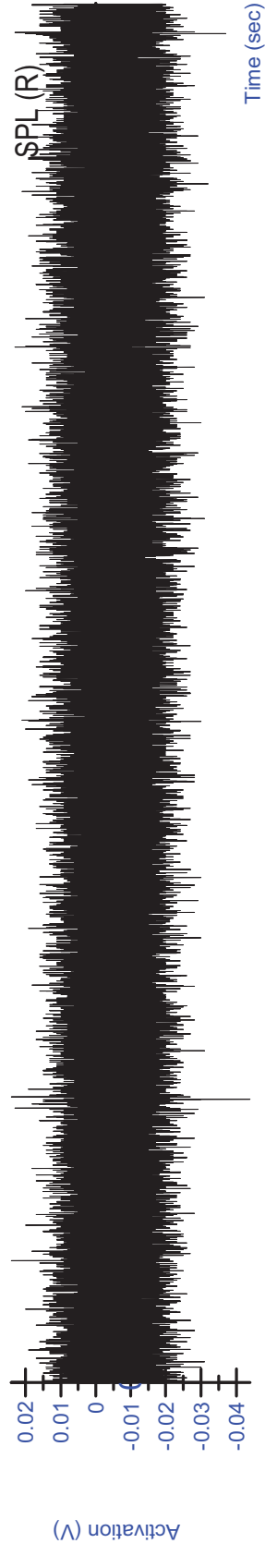
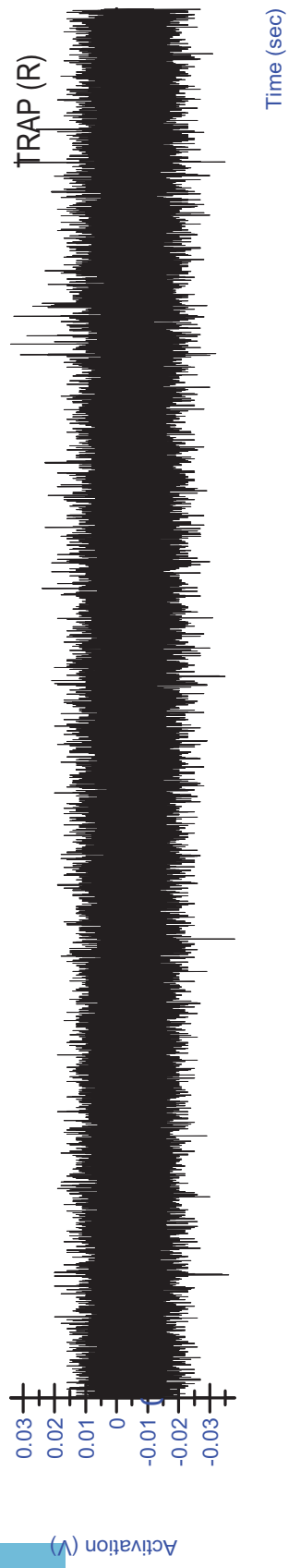
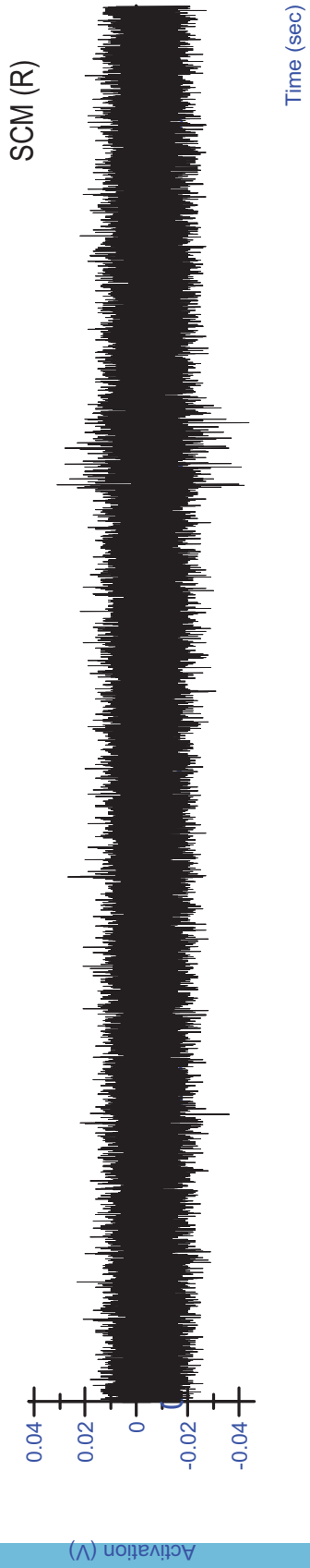
Activation (mV)

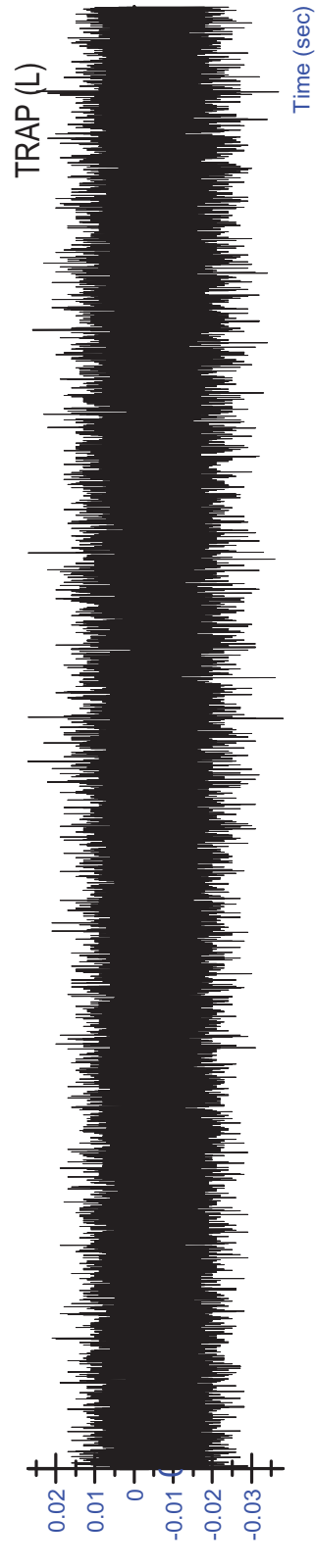
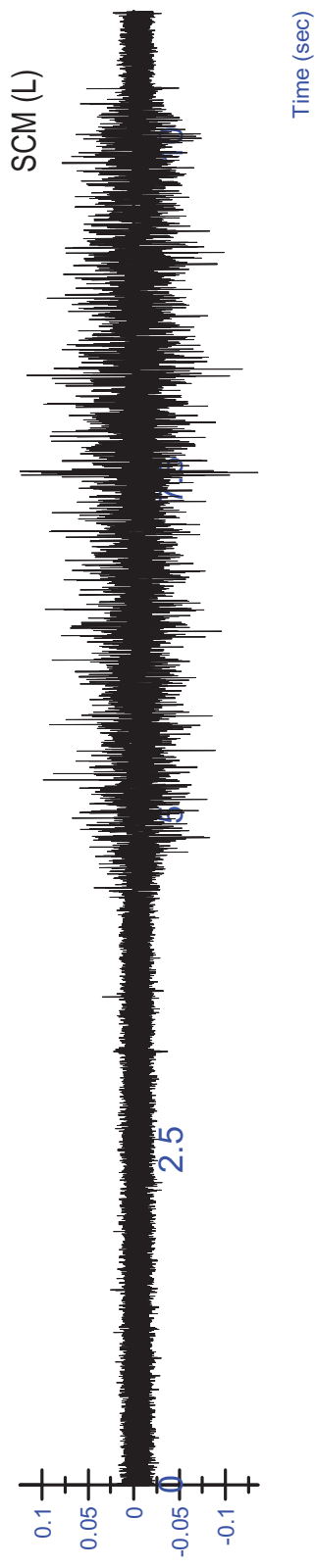
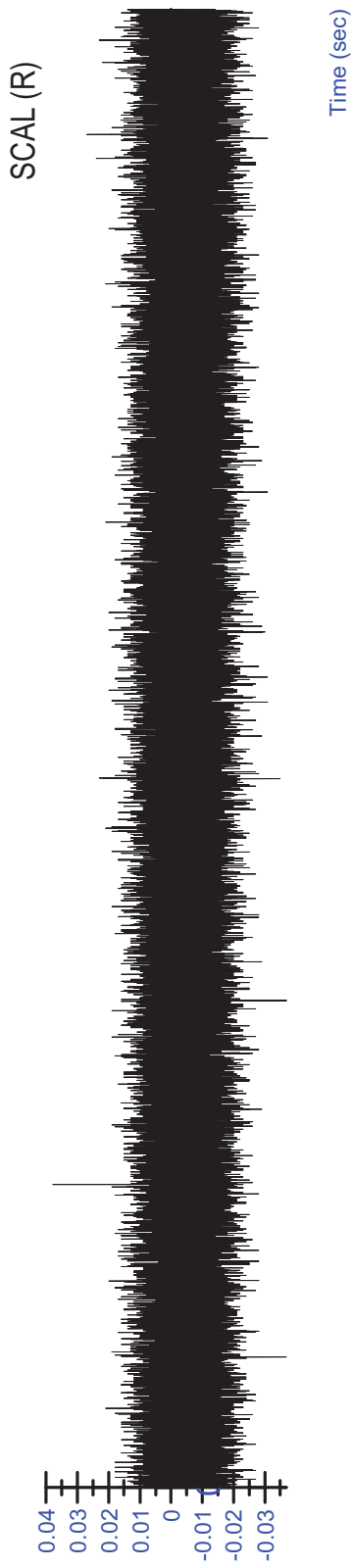
Activation (mV)

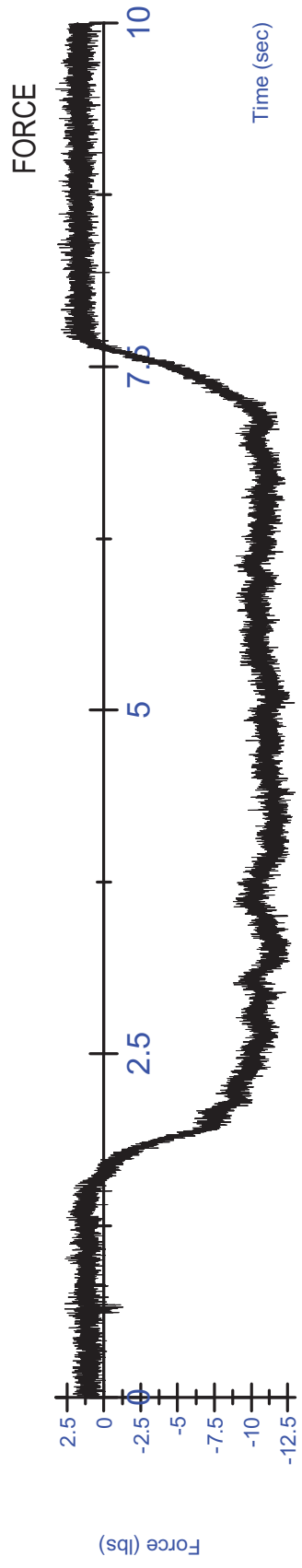
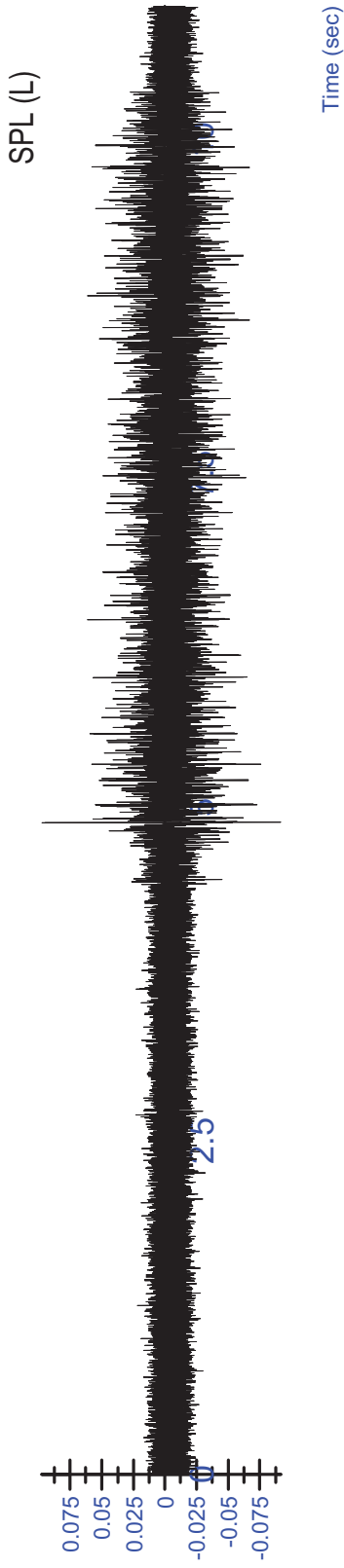


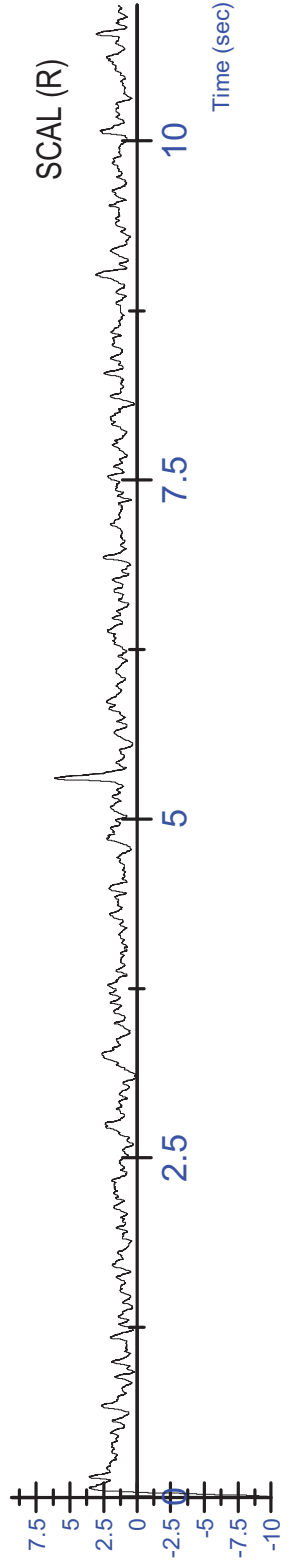
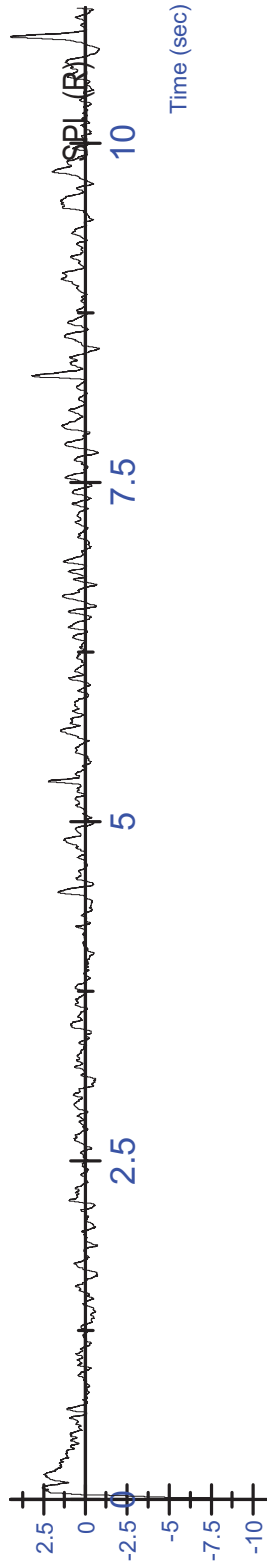
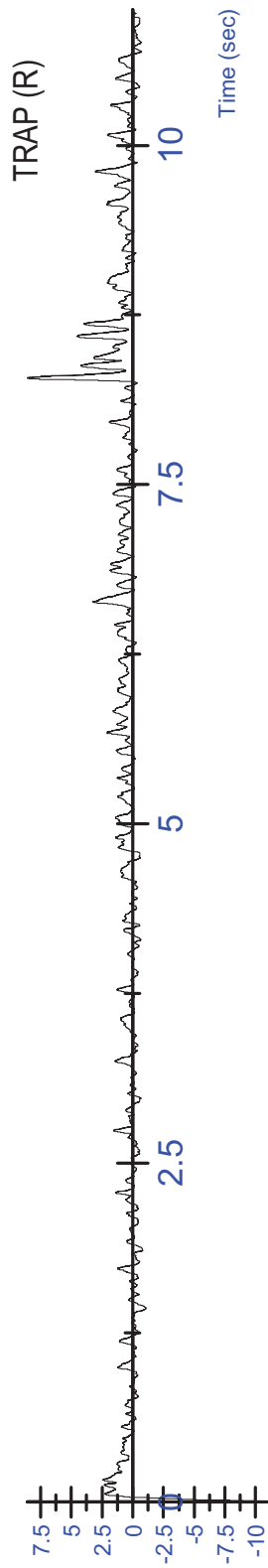
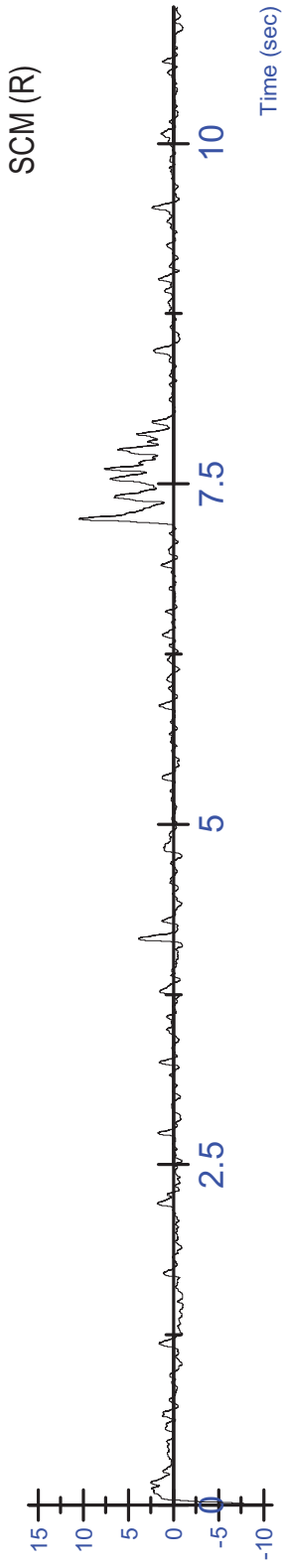
S14 MVC - Lateral (L) Trial 2 - Rectified/Filtered

S14 MVC - Lateral (L) Trial 3 - Unfiltered







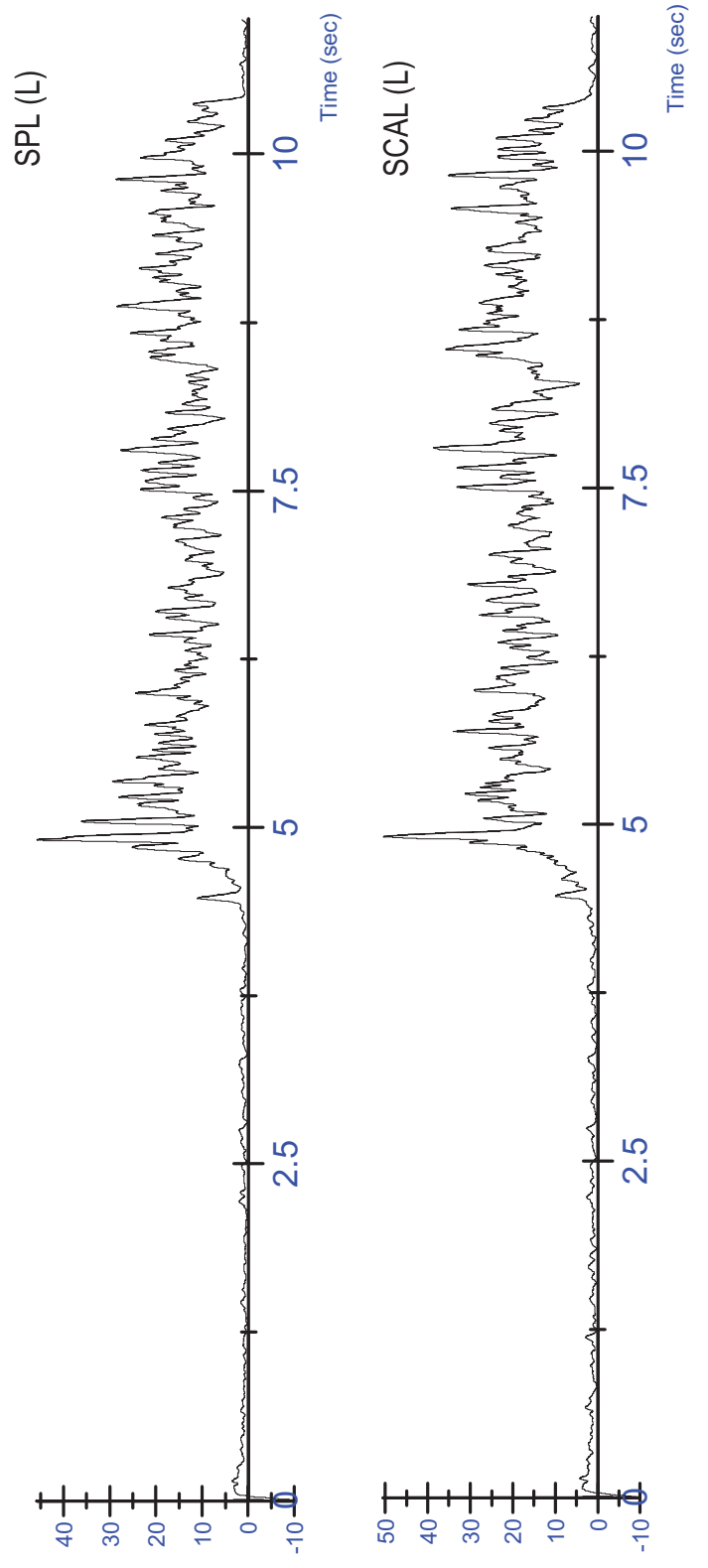
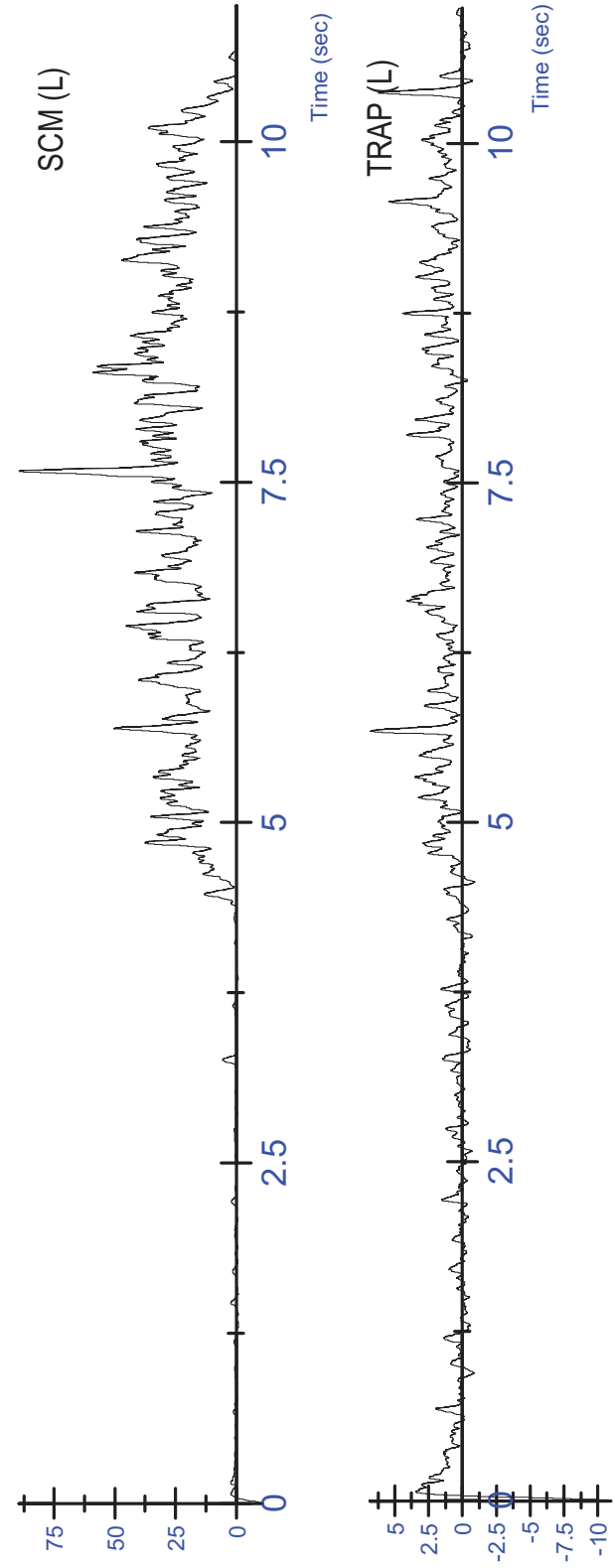


Activation (mV)

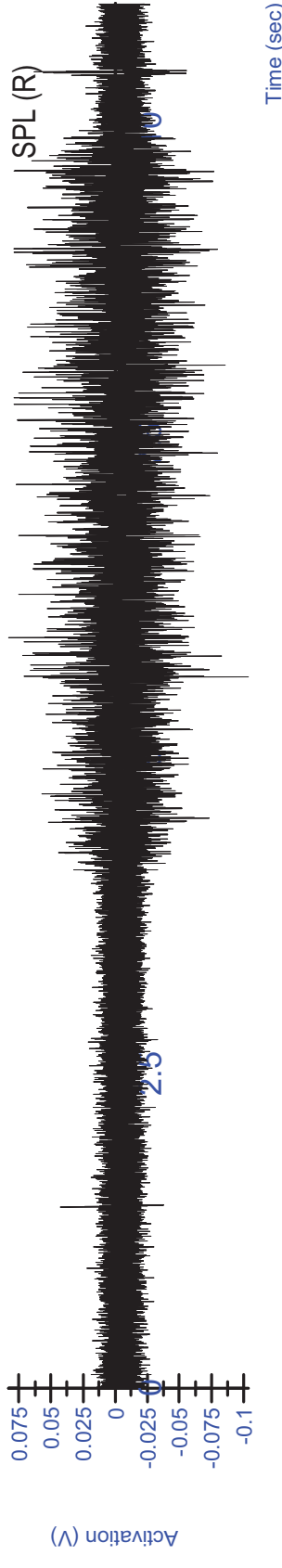
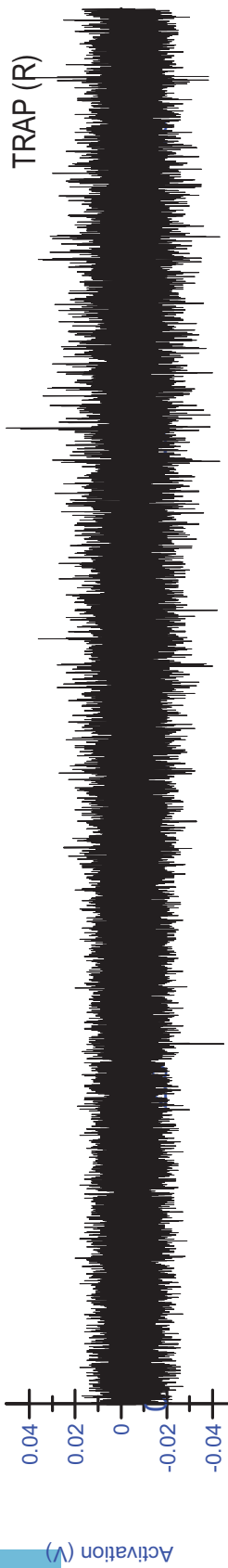
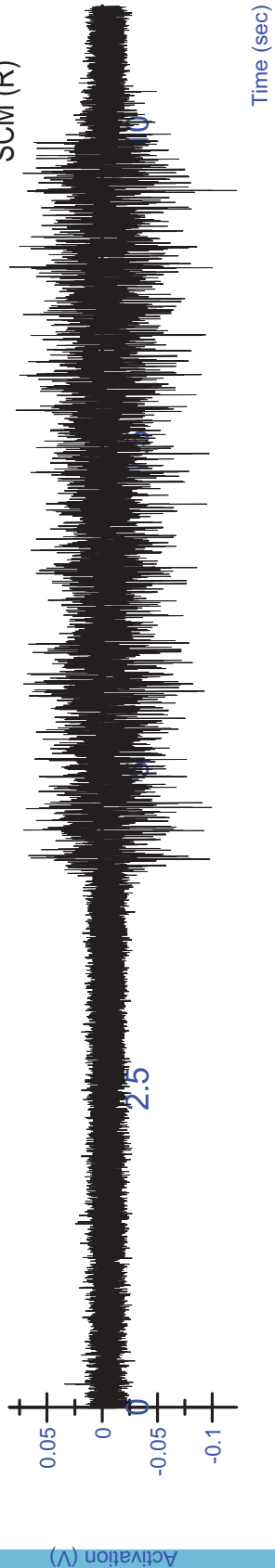
Activation (mV)

Activation (mV)

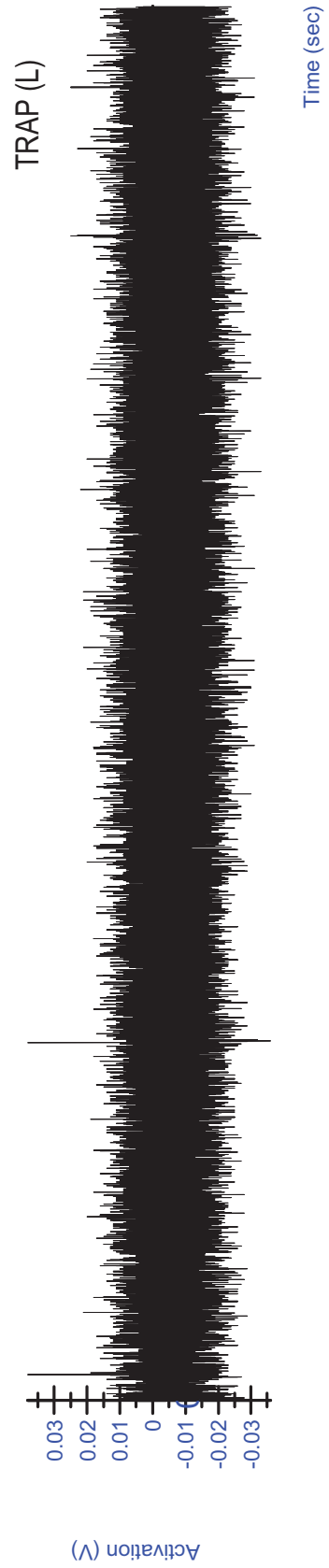
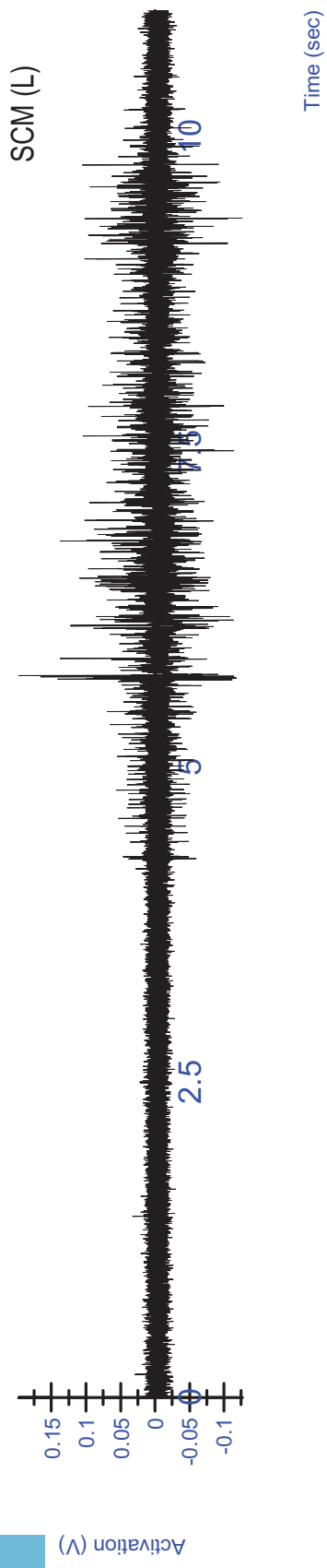
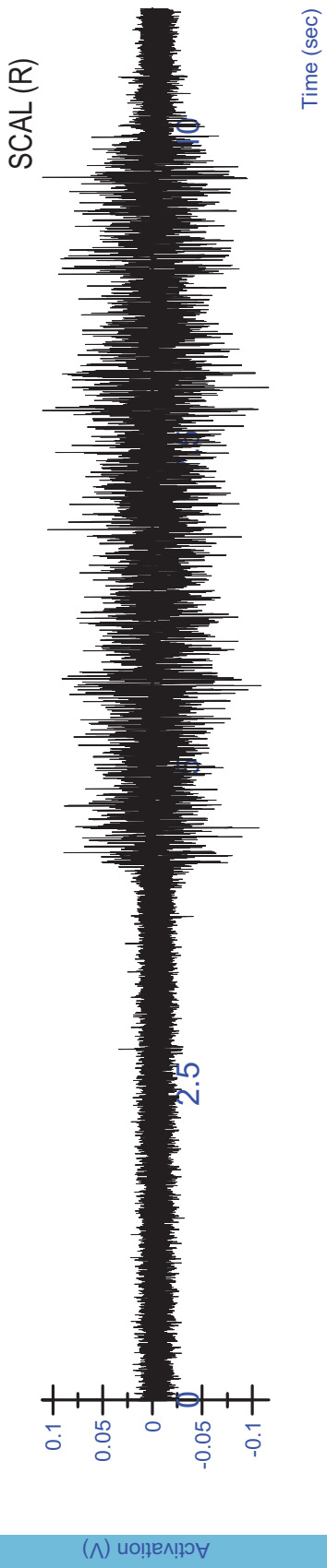
Activation (mV)

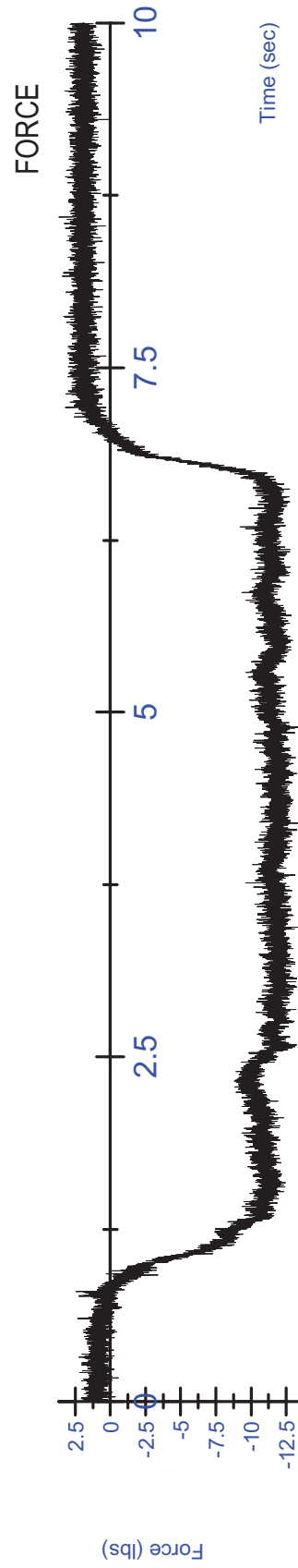
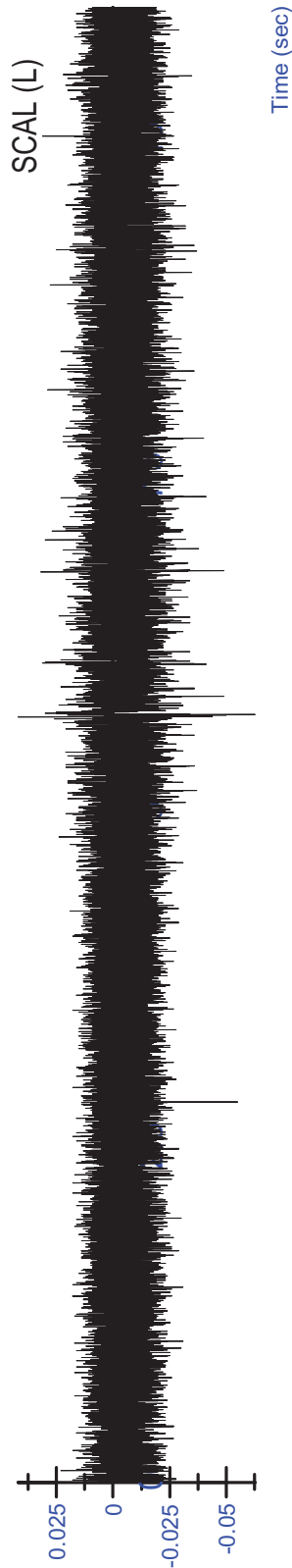
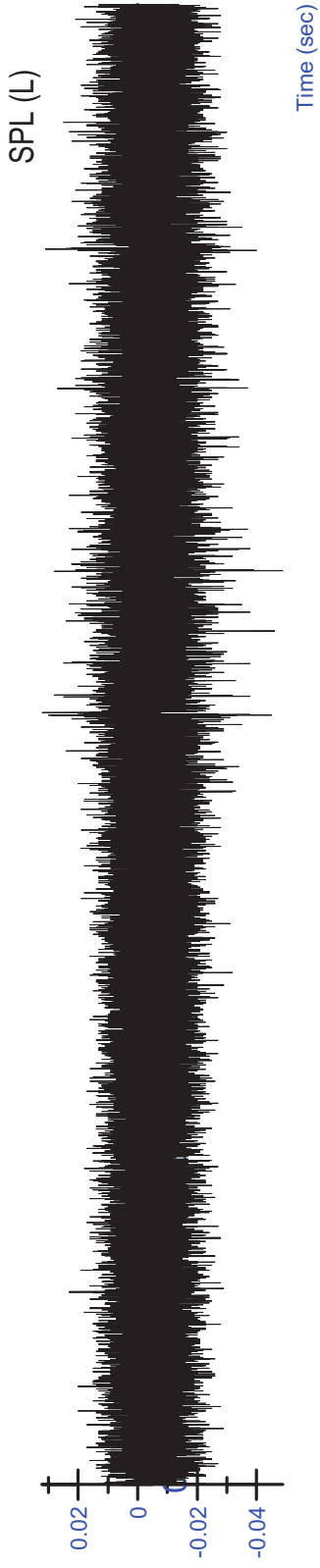


S14 MVC - Lateral (L) Trial 3 - Rectified/Filtered

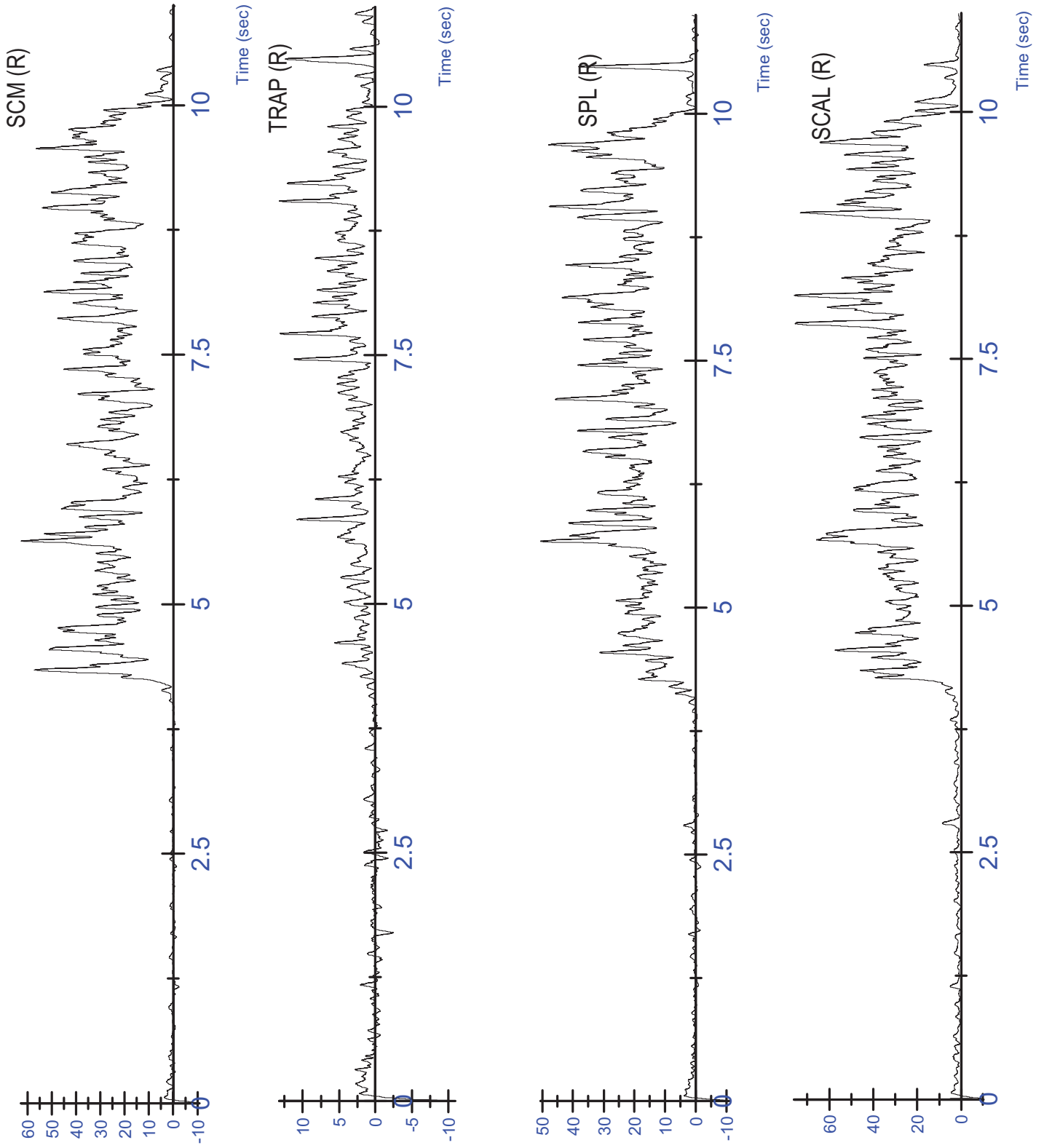


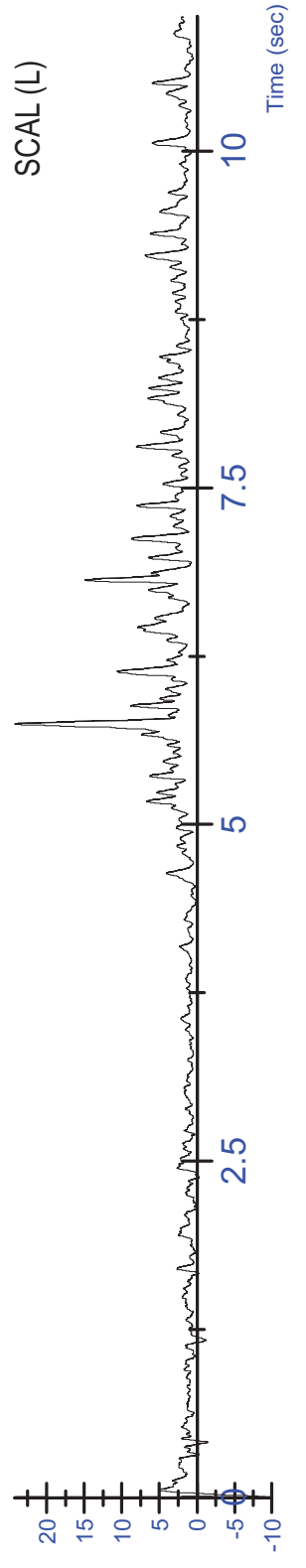
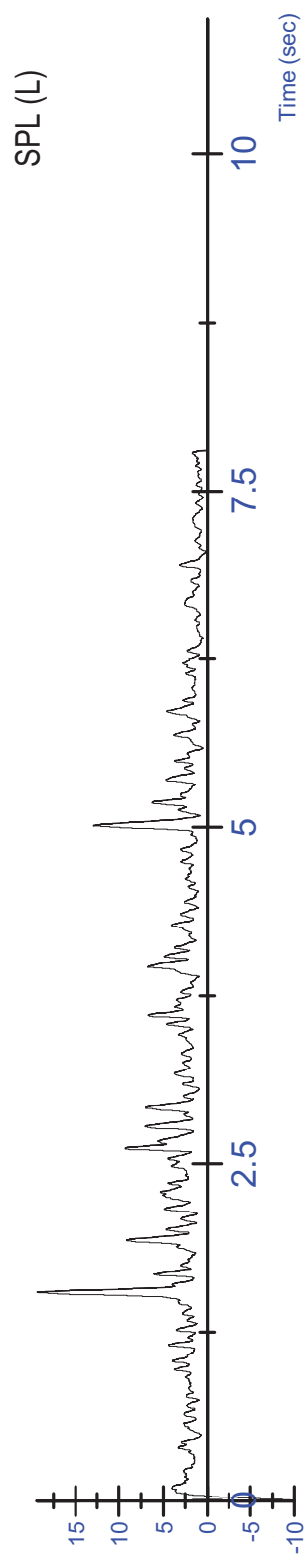
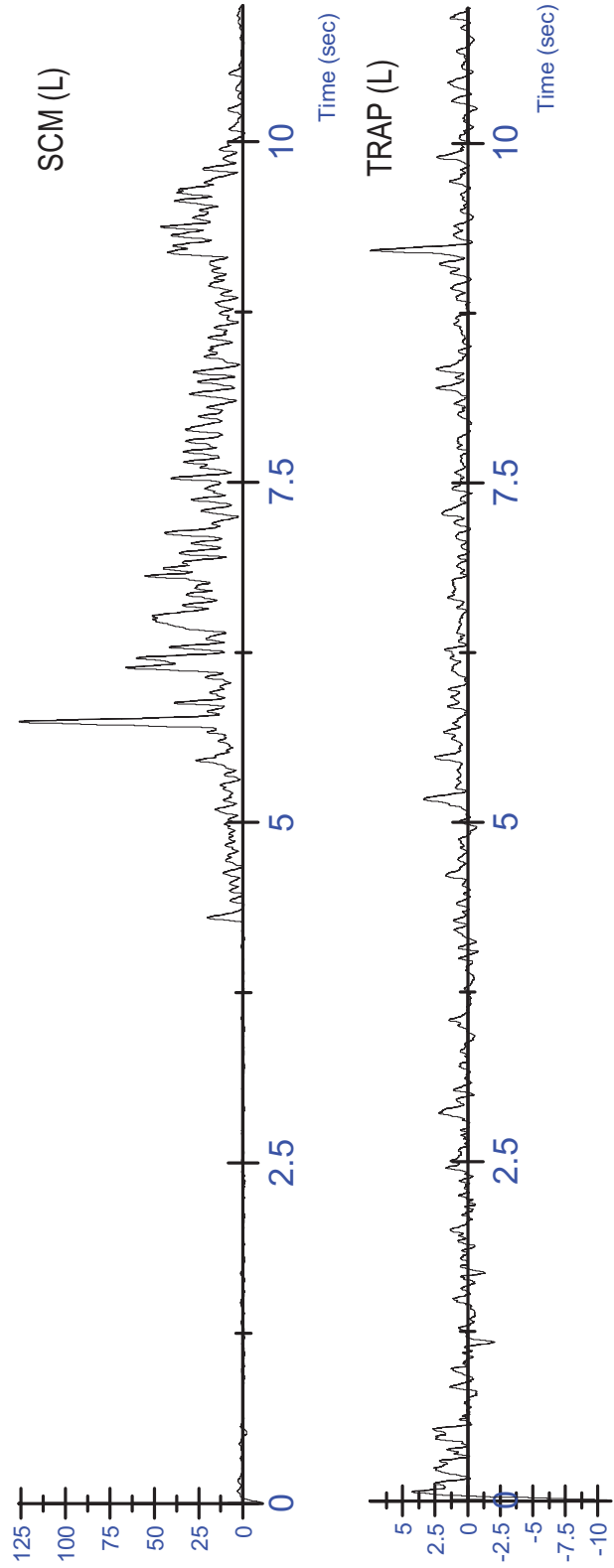
S14 MVC - Lateral (R) Trial 1 - Unfiltered





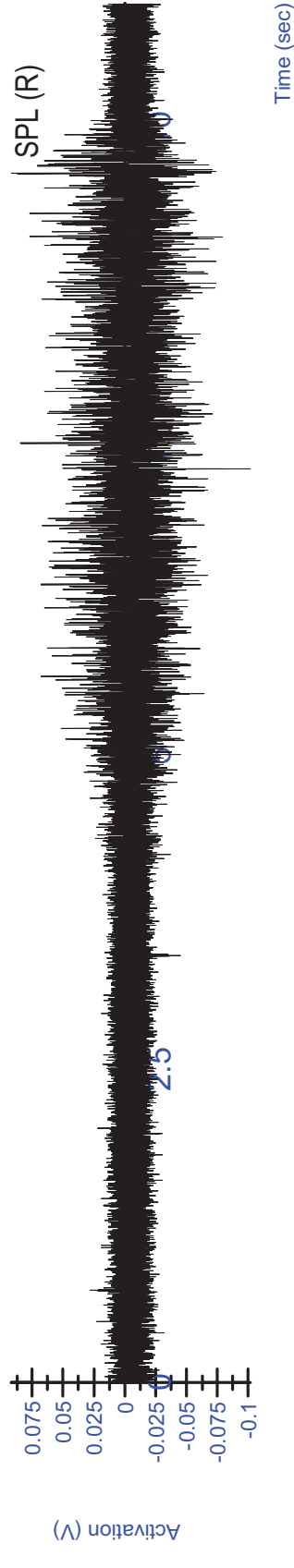
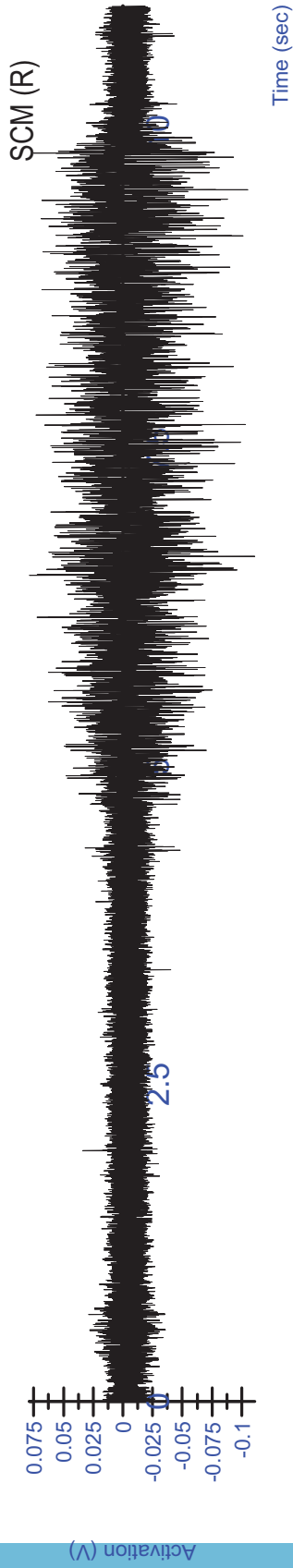
S14 MVC - Lateral (R) Trial 1 - Rectified/Filtered

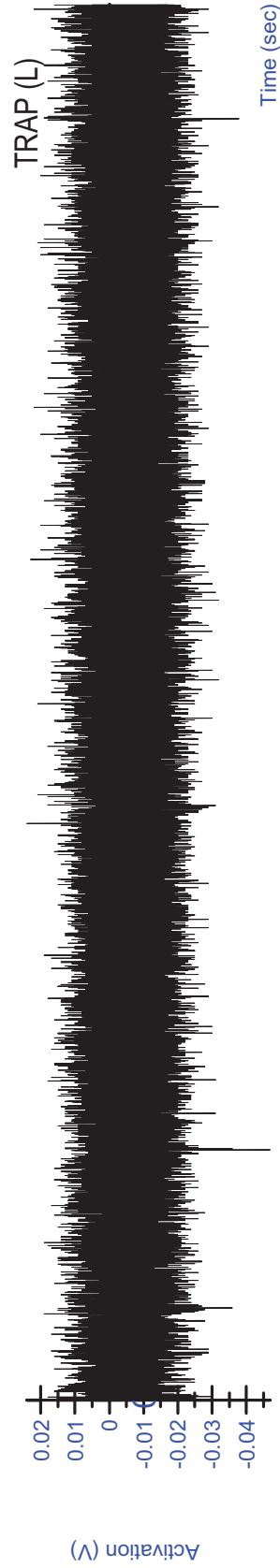
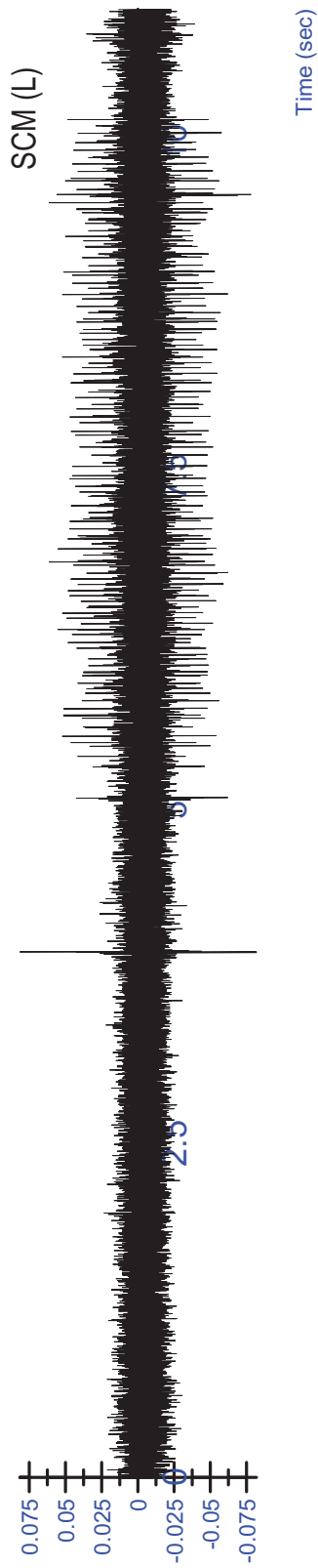
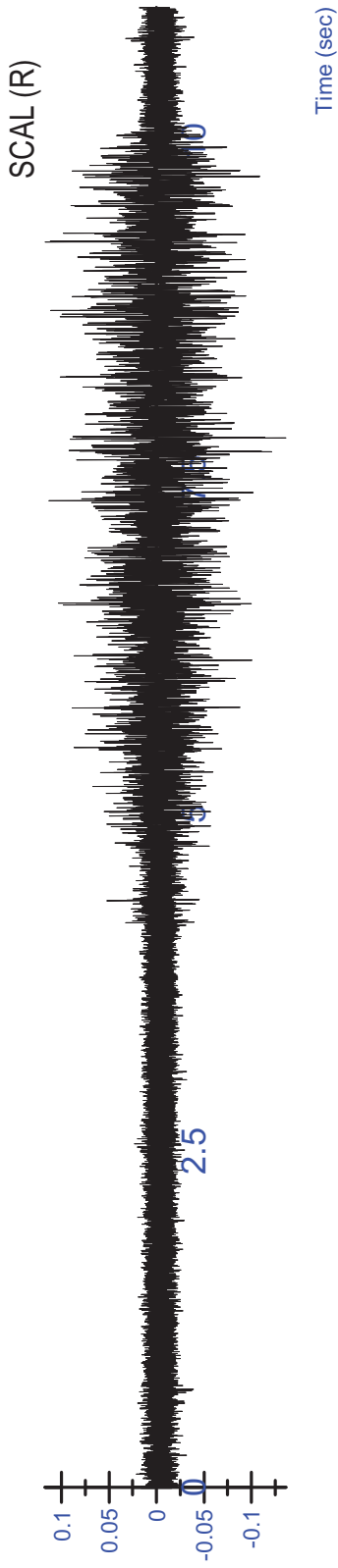


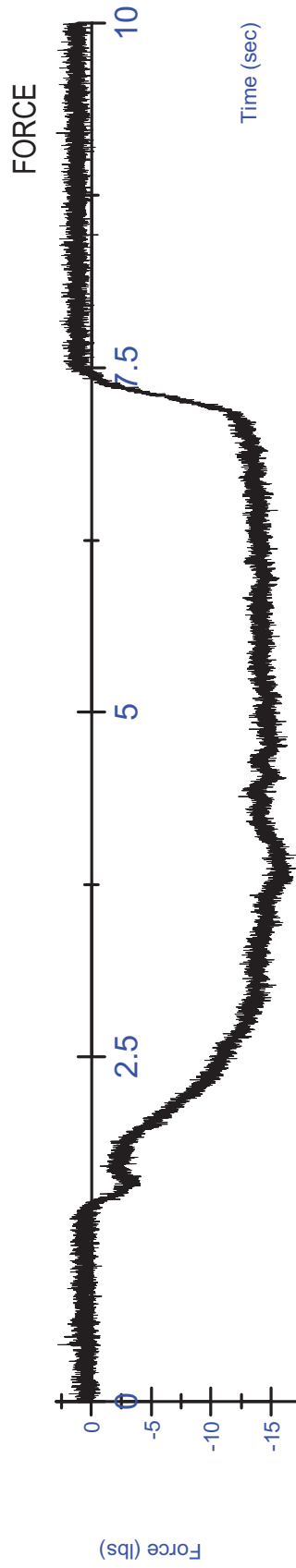
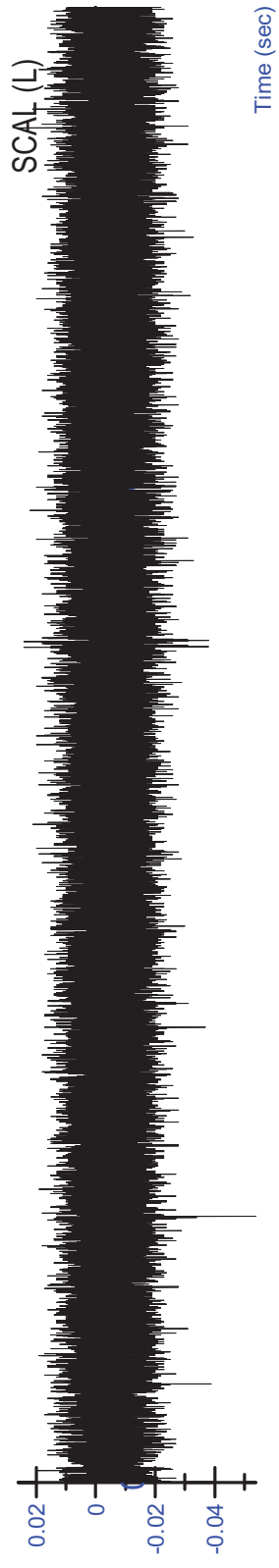
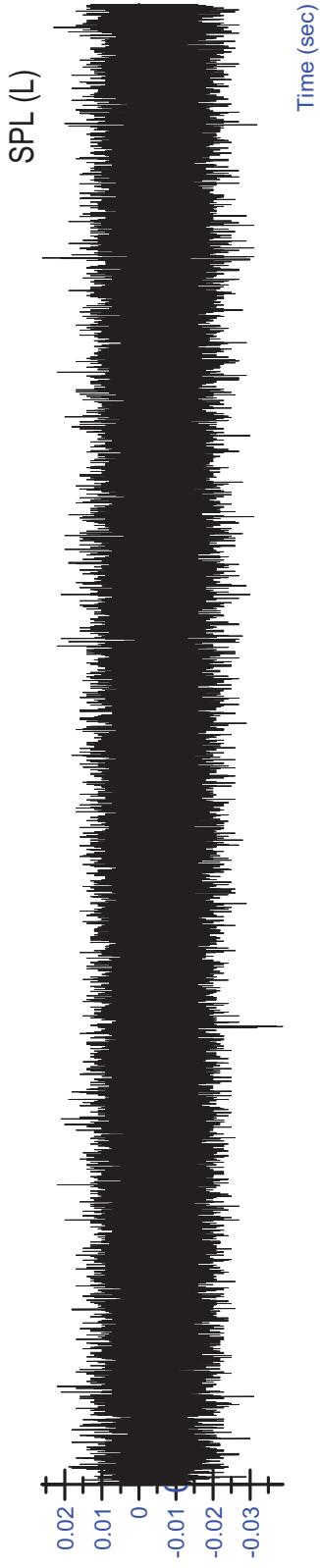


S14 MVC - Lateral (R) Trial 1 - Rectified/Filtered

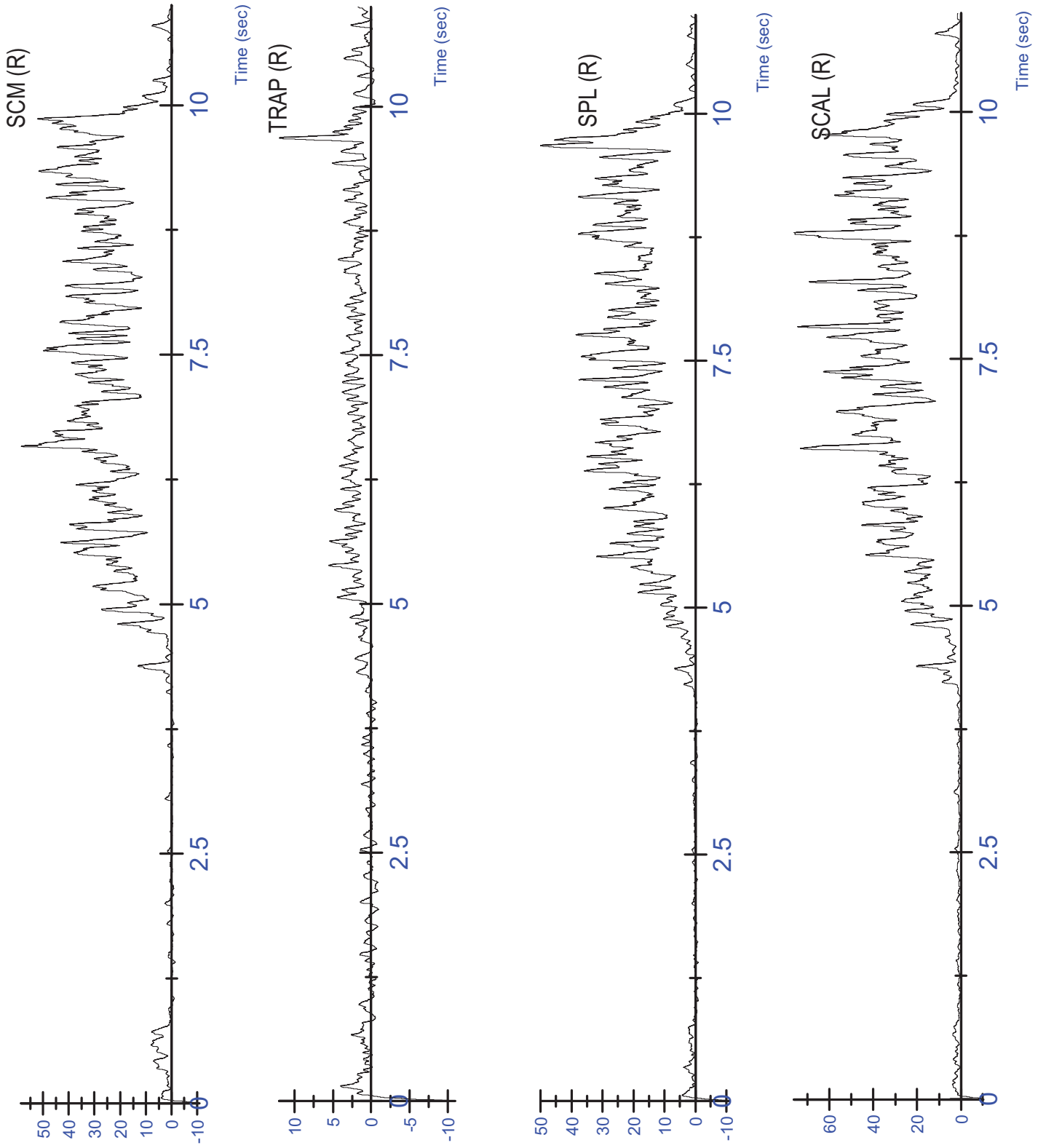
S14 MVC - Lateral (R) Trial 2 - Unfiltered



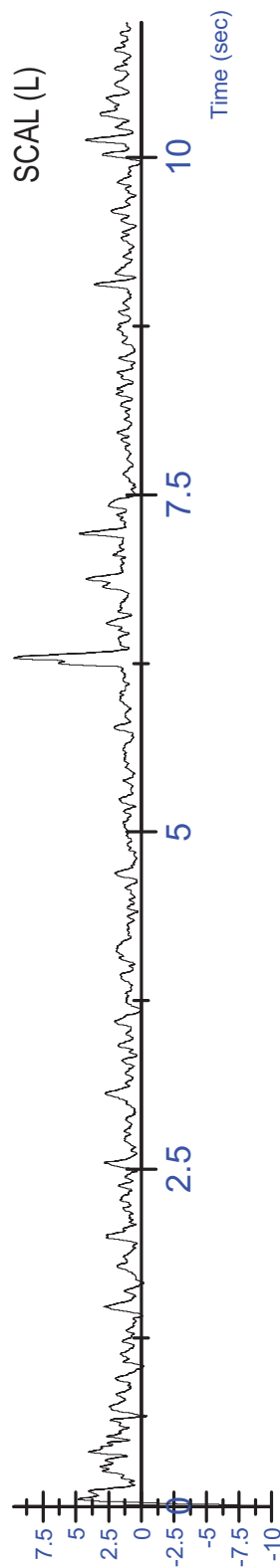
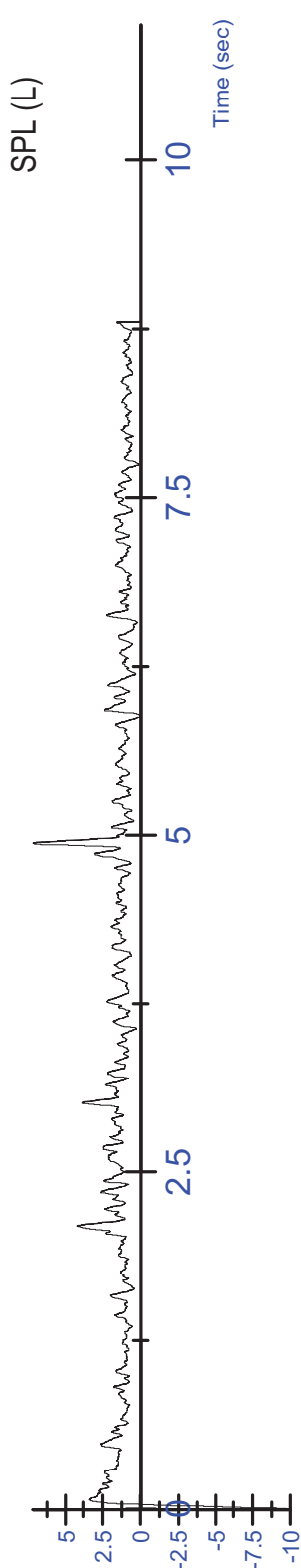
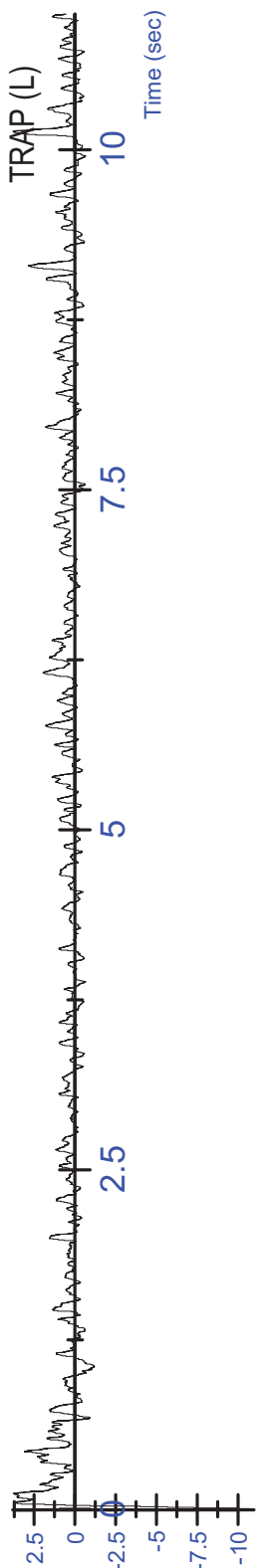
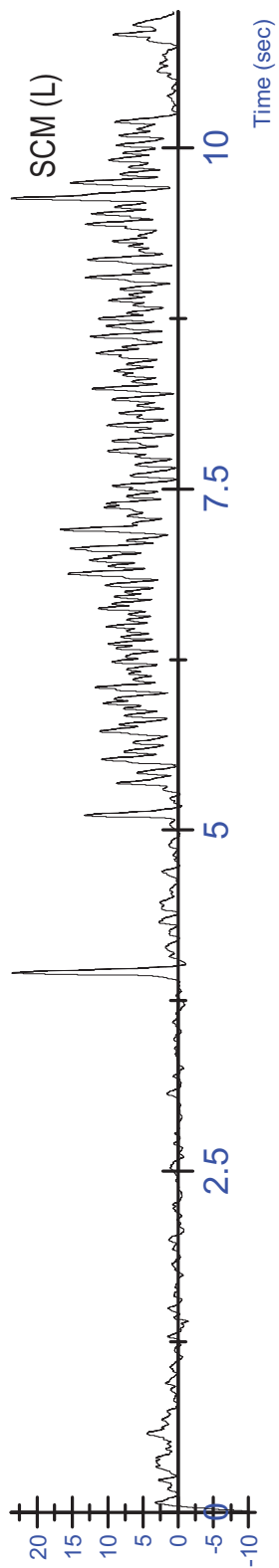


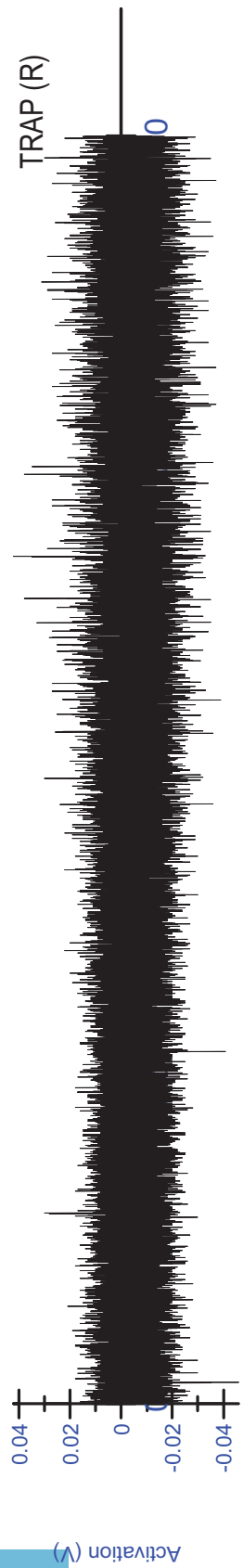
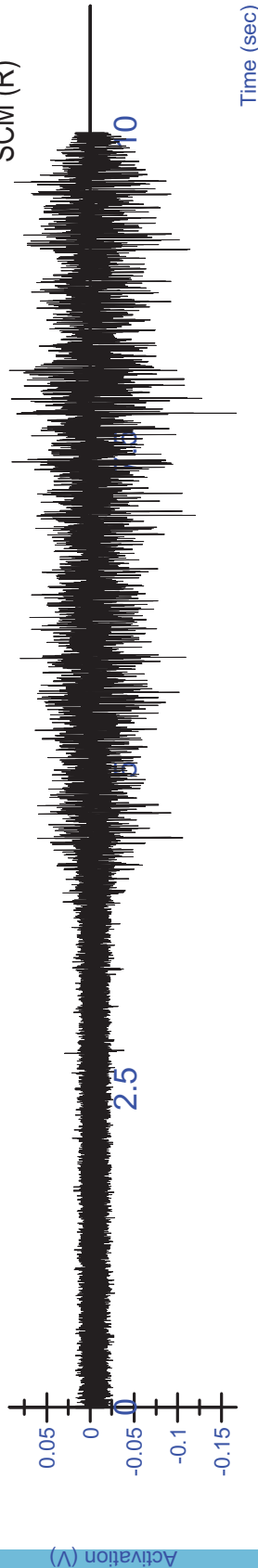


S14 MVC - Lateral (R) Trial 2 - Rectified/Filtered

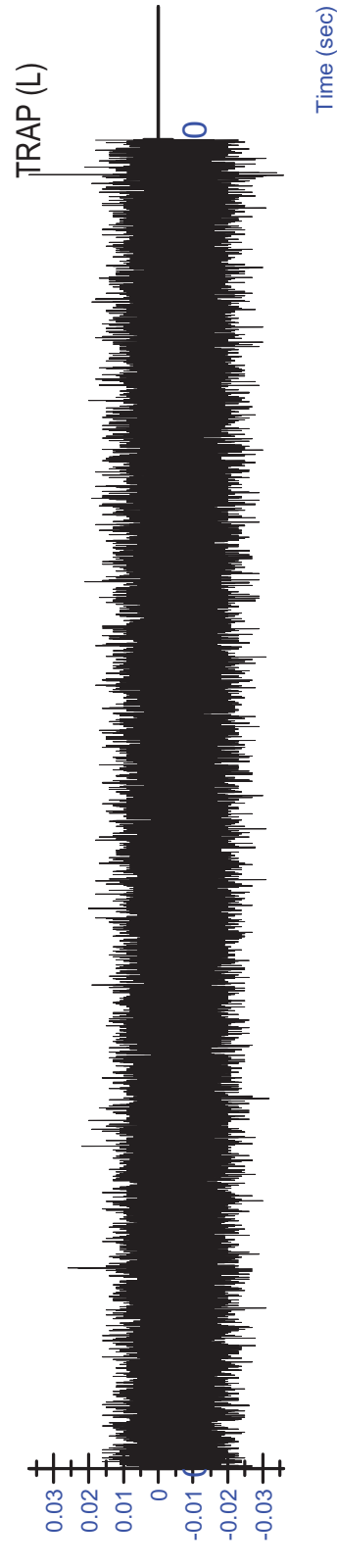
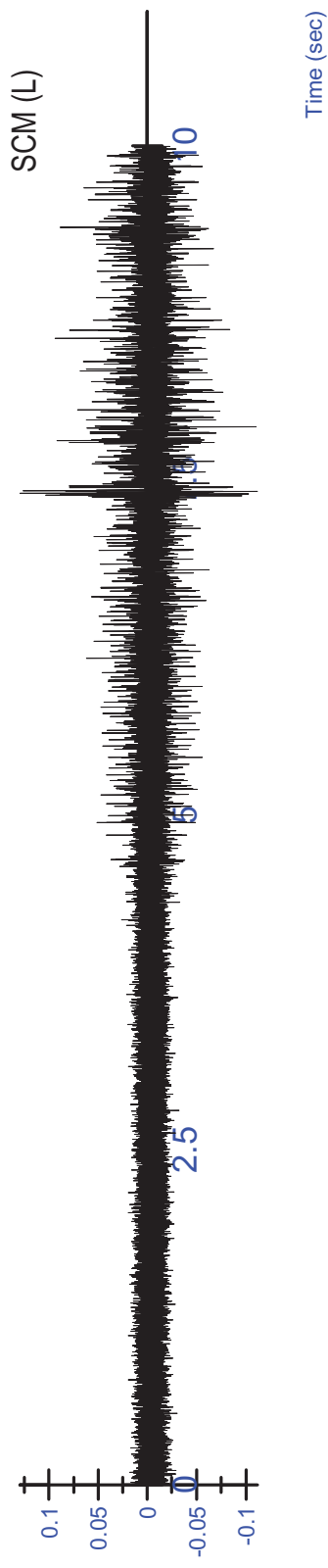
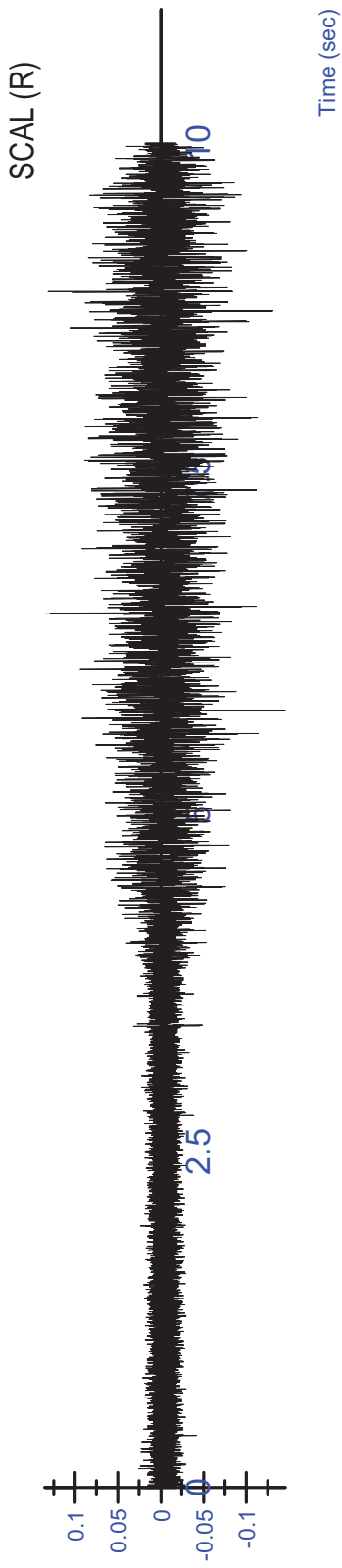


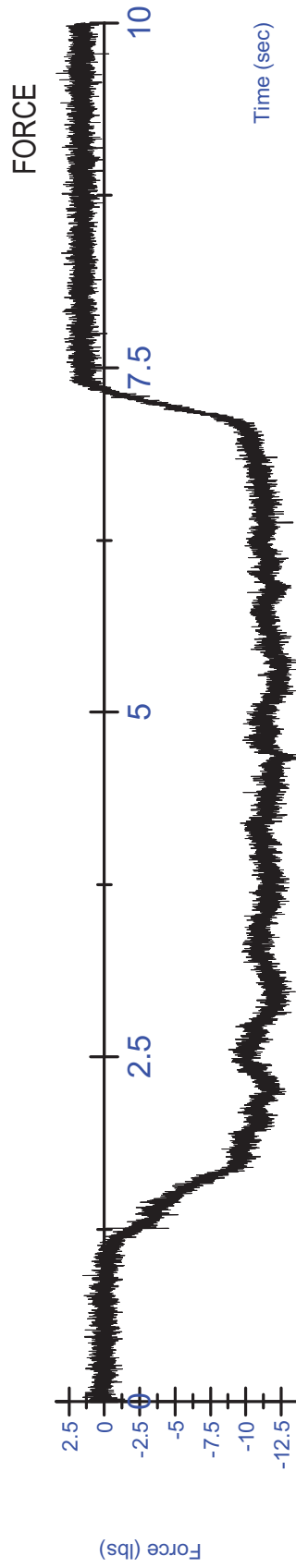
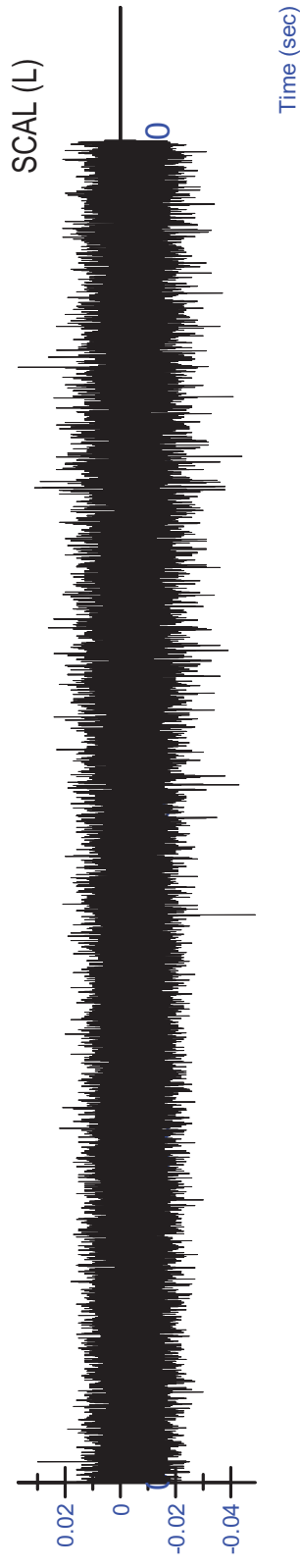
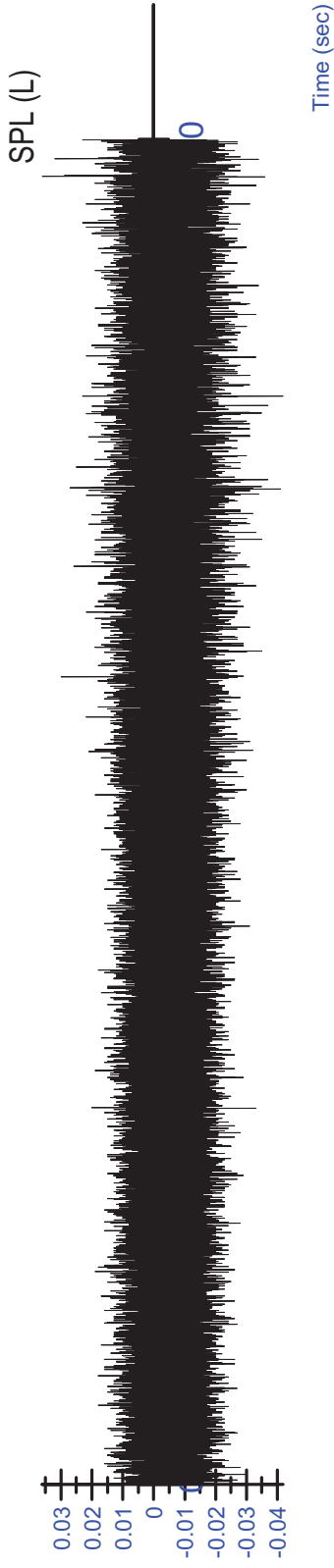
S14 MVC - Lateral (R) Trial 2 - Rectified/Filtered

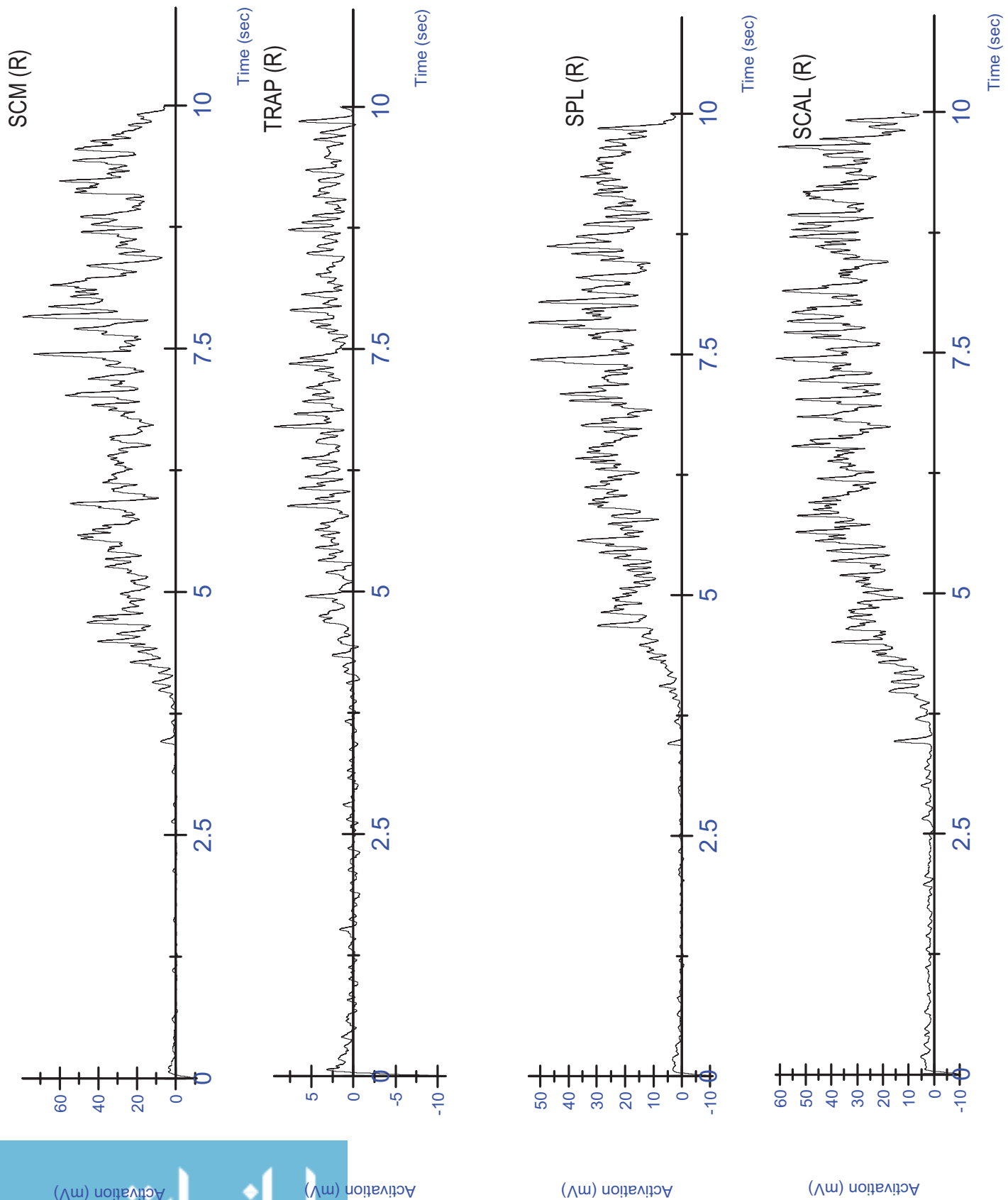




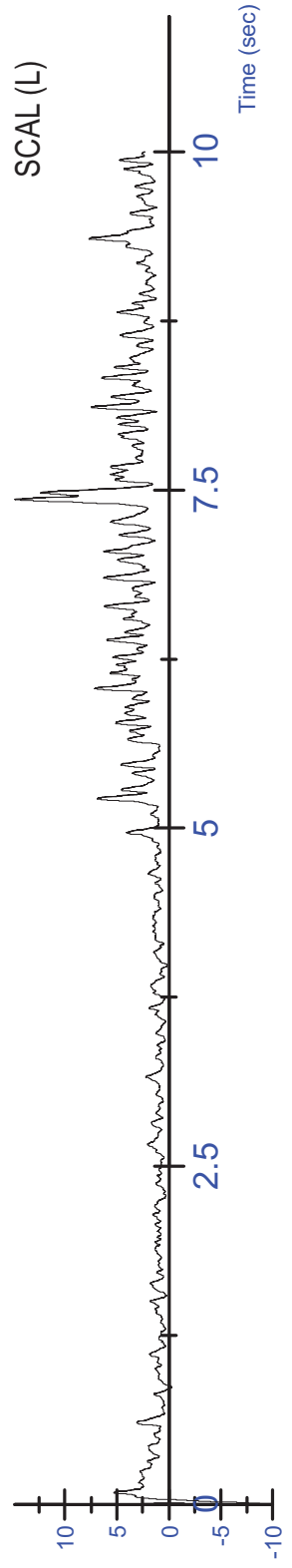
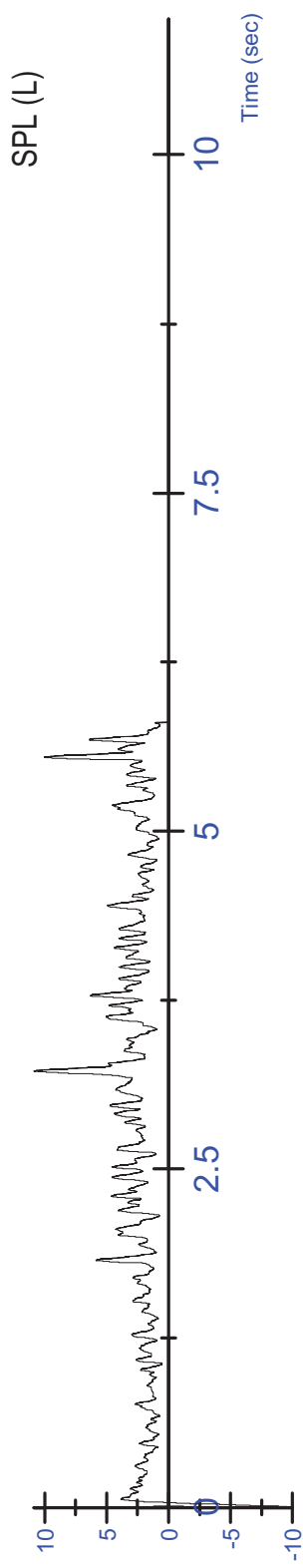
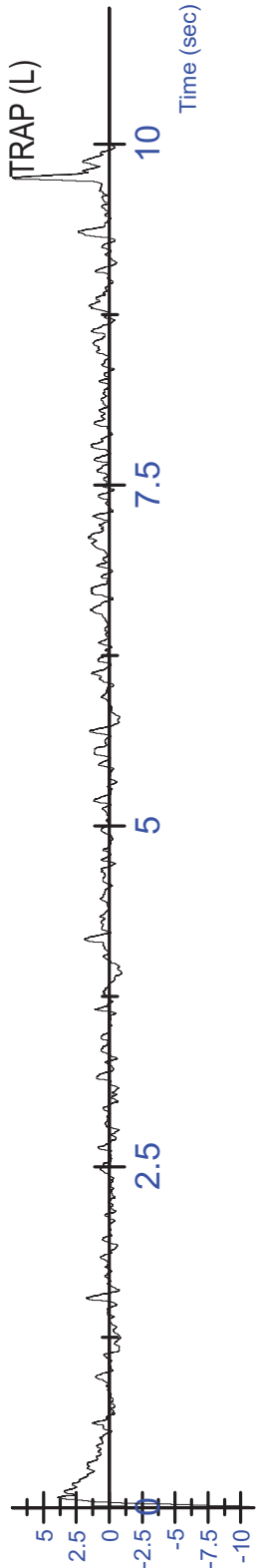
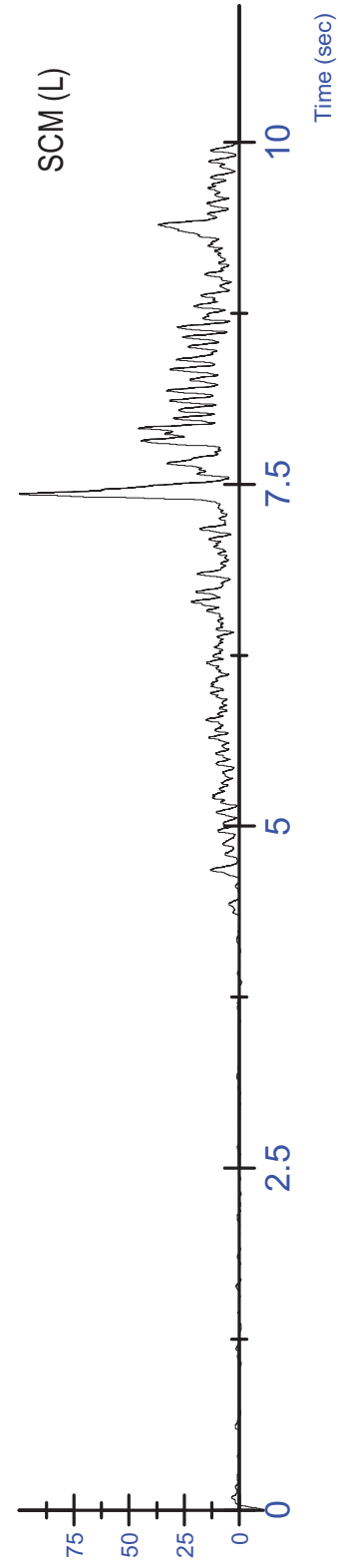
S14 MVC - Lateral (R) Trial 3 - Unfiltered







S14 MVC - Lateral (R) Trial 3 - Rectified/Filtered



S14 MVC - Lateral (R) Trial 3 - Rectified/Filtered

APPENDIX C

Tables and figures for Chapter 6: The Neck Muscle Responses of 50th
Percentile Adult Males and 10 Year Old Boys In Low Speed Frontal Impacts

Subject	Peak MVC EMG	Tensed - Peak EMG										
		Trial 1		Time(s)		(%MVC)		Trial 2		Time(s)		(%MVC)
K01	SCM (R) μ V	162.668	203.555	2.165	1.251	129.793	2.187	0.798				
	SCM (L) μ V	205.310	362.215	2.153	1.764	325.494	2.199	1.585				
	TRAP (R) μ V	38.101	55.44	2.124	1.455	60.085	2.136	1.577				
	TRAP (L) μ V	43.837	116.718	2.124	2.663	134.583	2.123	3.070				
	SPL (R) μ V	73.764	134.406	2.118	1.822	175.512	2.793	2.379				
	SPL (L) μ V	67.080	248.952	2.121	3.711	125.595	2.133	1.872				
	SCAL (R) μ V	81.114	113.381	2.604	1.398	134.264	2.794	1.655				
	SCAL (L) μ V	51.809	154.789	2.121	2.988	88.096	2.137	1.700				
	Accel g		2.627	2.533		2.627	2.4887					
K03	SCM (R) μ V	156.775	275.027	2.449	1.754	186.074	2.17	1.187				
	SCM (L) μ V	236.143	99.403	2.204	0.421	77.821	2.187	0.330				
	TRAP (R) μ V	62.549	60.253	2.573	0.963	45.43	2.633	0.726				
	TRAP (L) μ V	71.288	63.394	2.616	0.889	79.529	2.613	1.116				
	SPL (R) μ V	186.656	99.607	2.623	0.534	68.976	2.111	0.370				
	SPL (L) μ V	191.956	71.366	2.629	0.372	168.754	2.108	0.879				
	SCAL (R) μ V	153.581	114.26	2.596	0.744	107.804	2.585	0.702				
	SCAL (L) μ V	104.943	42.29	2.629	0.403	110.294	2.107	1.051				
	Accel g		2.753	2.5337		2.806	2.5321					
K04	SCM (R) μ V	233.162	350.33	2.221	1.503	443.664	2.233	1.903				
	SCM (L) μ V	218.142	304.264	2.205	1.395	359.024	2.24	1.646				
	TRAP (R) μ V	100.717	114.154	2.597	1.133	109.328	2.649	1.086				
	TRAP (L) μ V	54.039	148.534	2.644	2.749	190.587	2.622	3.527				
	SPL (R) μ V	240.259	283.215	2.211	1.179	281.284	3.027	1.171				
	SPL (L) μ V	162.409	169.295	2.665	1.042	276.471	2.61	1.702				
	SCAL (R) μ V	107.343	98.801	2.218	0.920	151.425	2.58	1.411				
	SCAL (L) μ V	115.831	150.887	2.573	1.303	189.635	2.603	1.637				
	Accel g		2.643	2.492		2.66	2.4898					
K05	SCM (R) μ V	270.211	227.273	2.152	0.841	237.382	2.191	0.879				
	SCM (L) μ V	374.353	373.852	2.154	0.999	311.452	2.189	0.832				
	TRAP (R) μ V	66.869	81.779	2.165	1.223	92.023	2.651	1.376				
	TRAP (L) μ V	110.478	83.819	2.658	0.759	85.616	2.61	0.775				
	SPL (R) μ V	251.116	209.615	2.657	0.835	173.718	2.647	0.692				
	SPL (L) μ V	177.441	147.212	2.138	0.830	149.44	2.656	0.842				
	SCAL (R) μ V	71.602	148.634	2.546	2.076	191.276	2.601	2.671				
	SCAL (L) μ V	110.083	121.081	2.609	1.100	163.482	2.654	1.485				
	Accel g		2.892	2.4929		2.753	2.5815					
K06	SCM (R) μ V	220.372	111.33	2.646	0.505	69.59	2.145	0.316				
	SCM (L) μ V	151.332	84.322	2.158	0.557	75.486	2.115	0.499				
	TRAP (R) μ V	139.934	78.142	2.538	0.558	433.428	2.607	3.097				
	TRAP (L) μ V	98.797	70.6	2.613	0.715	64.544	2.106	0.653				
	SPL (R) μ V	176.971	101.211	2.148	0.572	54.075	2.142	0.306				
	SPL (L) μ V	123.192	120.336	2.32	0.977	65.91	2.614	0.535				
	SCAL (R) μ V	144.618	101.646	2.6	0.703	276.29	2.609	1.910				
	SCAL (L) μ V	120.000	203.019	2.138	1.692	168.288	2.553	1.402				
	Accel g		2.709	2.5343		2.506	2.4879					

Table C-1: Dynamic Peak EMG values, time of Peak EMG and %MVC for tensed muscle impact for 10 year old boys

Subject	Peak MVC EMG	Tensed - Peak EMG						
		Trial 1			Trial 2			
			(%MVC)		(%MVC)		(%MVC)	
K07	SCM (R) μV	181.666				150.476	2.143	0.828
	SCM (L) μV	179.784				199.181	2.607	1.108
	TRAP (R) μV	110.6665				118.398	2.527	1.070
	TRAP (L) μV	44.923				76.175	2.61	1.696
	SPL (R) μV	159.7215				371.878	2.543	2.328
	SPL (L) μV	175.865				152.13	2.549	0.865
	SCAL (R) μV	146.076				158.373	2.534	1.084
	SCAL (L) μV	11.4595				4.462	2.416	0.389
	Accel g					2.319	2.4661	
K09	SCM (R) μV	97.316	89.08	2.536	0.915	180.809	2.151	1.858
	SCM (L) μV	124.244	185.729	2.531	1.495	182.026	2.163	1.465
	TRAP (R) μV	42.412	57.669	3.001	1.360	63.531	2.656	1.498
	TRAP (L) μV	103.436	104.021	2.513	1.006	128.33	2.128	1.241
	SPL (R) μV	99.585	99.101	3.068	0.995	109.837	2.66	1.103
	SPL (L) μV	85.084	134.775	3.014	1.584	101.76	2.133	1.196
	SCAL (R) μV	105.858	159.768	2.52	1.509	88.259	2.073	0.834
	SCAL (L) μV	102.362	115.844	3.014	1.132	79.013	2.134	0.772
	Accel g		2.999	2.9351		2.75	2.531	
K10	SCM (R) μV	155.268	201.706	2.161	1.299	220.358	2.483	1.419
	SCM (L) μV	44.182	180.236	2.508	4.079	173.048	2.547	3.917
	TRAP (R) μV	123.223	140.566	2.649	1.141			
	TRAP (L) μV	89.824	93.628	2.709	1.042	108.918	2.569	1.213
	SPL (R) μV	187.484	170.743	2.446	0.911	165.796	2.535	0.884
	SPL (L) μV	64.013	126.212	2.54	1.972	200.361	2.502	3.130
	SCAL (R) μV	87.871	169.826	2.664	1.933	99.131	2.523	1.128
	SCAL (L) μV	52.448	116.132	2.534	2.214	113.937	2.56	2.172
	Accel g		2.926	2.5536		2.071	2.5037	
K11	SCM (R) μV	175.378	165.885	2.144	0.946	151.132	2.585	0.862
	SCM (L) μV	109.7275	224.304	2.157	2.044	165.06	2.121	1.504
	TRAP (R) μV	77.338	76.358	2.641	0.987	108.883	2.604	1.408
	TRAP (L) μV	84.9755	69.738	2.135	0.821	93.589	2.415	1.101
	SPL (R) μV	176.879	108.522	2.584	0.614	152.4	2.597	0.862
	SPL (L) μV	240.984	229.804	2.616	0.954	167.363	2.206	0.694
	SCAL (R) μV	233.289	117.396	2.135	0.503	149.442	2.416	0.641
	SCAL (L) μV	246.891	159.793	2.435	0.647	143.605	2.117	0.582
	Accel g		2.546	2.5174		2.591	2.4928	

Table C-1: Dynamic Peak EMG values, time of Peak EMG and %MVC for tensed muscle impact for 10 year old boys

Subject	Age			Peak MVC EMG	Tensed - Peak EMG					
					Trial 3	Time(s)	(%MVC)	Mean	Time(s)	(%MVC)
K01	10.000	SCM (R)	μV	162.668				166.674	2.176	1.025
		SCM (L)	μV	205.310				343.855	2.295	1.675
		TRAP (R)	μV	38.101				39.338	2.264	1.516
		TRAP (L)	μV	43.837				125.651	2.261	2.866
		SPL (R)	μV	73.764				154.959	2.456	2.101
		SPL (L)	μV	67.080				187.274	2.127	2.792
		SCAL (R)	μV	81.114				123.823	2.699	1.527
		SCAL (L)	μV	51.809				121.443	2.129	2.344
		Accel	g						2.627	
K03	10.000	SCM (R)	μV	156.775	142.831	2.586	0.911	201.311	2.402	1.284
		SCM (L)	μV	236.143	133.716	2.477	0.566	103.647	2.289	0.439
		TRAP (R)	μV	62.549	39.373	2.507	0.629	48.352	2.571	0.773
		TRAP (L)	μV	71.288	39.046	2.112	0.548	60.656	2.447	0.851
		SPL (R)	μV	186.656	65.884	2.11	0.353	78.156	2.281	0.419
		SPL (L)	μV	191.956	116.067	2.106	0.605	118.729	2.281	0.619
		SCAL (R)	μV	153.581	58.169	2.431	0.379	93.411	2.537	0.608
		SCAL (L)	μV	104.943	85.626	2.269	0.816	79.403	2.335	0.757
		Accel	g		2.498	2.535		2.686		
K04	10.000	SCM (R)	μV	233.162				396.997	2.227	1.703
		SCM (L)	μV	218.142				331.644	2.223	1.520
		TRAP (R)	μV	100.717				111.741	2.579	1.109
		TRAP (L)	μV	54.039				169.561	2.585	3.138
		SPL (R)	μV	240.259				282.250	2.577	1.175
		SPL (L)	μV	162.409				222.883	2.619	1.372
		SCAL (R)	μV	107.343				125.113	2.399	1.166
		SCAL (L)	μV	115.831				170.261	2.588	1.470
		Accel	g					2.652		
K05	11.000	SCM (R)	μV	270.211				232.328	2.172	0.860
		SCM (L)	μV	374.353				342.652	2.172	0.915
		TRAP (R)	μV	66.869				86.901	2.408	1.300
		TRAP (L)	μV	110.478				84.718	2.634	0.767
		SPL (R)	μV	251.116				191.667	2.652	0.763
		SPL (L)	μV	177.441				148.326	2.397	0.836
		SCAL (R)	μV	71.602				169.955	2.574	2.374
		SCAL (L)	μV	110.083				142.282	2.632	1.292
		Accel	g					2.823		
K06	11.000	SCM (R)	μV	220.372				90.460	2.396	0.410
		SCM (L)	μV	151.332				79.904	2.269	0.528
		TRAP (R)	μV	139.934				255.785	2.544	1.828
		TRAP (L)	μV	98.797				67.572	2.395	0.684
		SPL (R)	μV	176.971				77.643	2.263	0.439
		SPL (L)	μV	123.192				93.123	2.467	0.756
		SCAL (R)	μV	144.618				188.968	2.605	1.307
		SCAL (L)	μV	120.000				185.654	2.346	1.547
		Accel	g					2.608		

Table C-1: Dynamic Peak EMG values, time of Peak EMG and %MVC for tensed muscle impact for 10 year old boys

Subject	Age			Peak MVC EMG	Tensed - Peak EMG					
					Trial 3		(%MVC)		Mean	
K07	10.000	SCM (R)	μV	181.666	173.534	2.148	0.965	162.005	2.146	0.897
		SCM (L)	μV	179.784	105.685	2.26	0.665	152.433	2.434	0.886
		TRAP (R)	μV	110.667	76.214	2.119	0.751	97.306	2.323	0.910
		TRAP (L)	μV	44.923	35.175	2.6	0.828	55.675	2.605	1.262
		SPL (R)	μV	159.722	1195.203	2.583	4.703	783.541	2.563	3.516
		SPL (L)	μV	175.865	88.315	2.533	0.589	120.223	2.541	0.727
		SCAL (R)	μV	146.076	131.523	2.116	0.922	144.948	2.325	1.003
		SCAL (L)	μV	11.460	4.879	2.532	0.518	4.671	2.474	0.454
		Accel	g			2.61	2.4996		2.465	
K09	9.500	SCM (R)	μV	97.316				134.945	2.344	1.387
		SCM (L)	μV	124.244				183.878	2.543	1.480
		TRAP (R)	μV	42.412				60.600	2.729	1.429
		TRAP (L)	μV	103.436				116.176	2.398	1.123
		SPL (R)	μV	99.585				104.469	2.744	1.049
		SPL (L)	μV	85.084				118.268	2.555	1.390
		SCAL (R)	μV	105.858				124.014	2.362	1.172
		SCAL (L)	μV	102.362				97.429	2.574	0.952
		Accel	g						2.875	
K10	10.000	SCM (R)	μV	155.268				211.032	2.322	1.359
		SCM (L)	μV	44.182				176.642	2.528	3.998
		TRAP (R)	μV	123.223				140.566	2.649	1.141
		TRAP (L)	μV	89.824				101.273	2.639	1.127
		SPL (R)	μV	187.484				168.270	2.491	0.898
		SPL (L)	μV	64.013				163.287	2.521	2.551
		SCAL (R)	μV	87.871				134.479	2.594	1.530
		SCAL (L)	μV	52.448				115.035	2.547	2.193
		Accel	g						2.499	
K11	10.000	SCM (R)	μV	175.378				158.509	2.365	0.904
		SCM (L)	μV	109.728				194.682	2.139	1.774
		TRAP (R)	μV	77.338				92.621	2.623	1.198
		TRAP (L)	μV	84.976				81.664	2.275	0.961
		SPL (R)	μV	176.879				130.461	2.591	0.738
		SPL (L)	μV	240.984				198.584	2.411	0.824
		SCAL (R)	μV	233.289				133.419	2.276	0.572
		SCAL (L)	μV	246.891				151.699	2.276	0.614
		Accel	g						2.569	

Table C-1: Dynamic Peak EMG values, time of Peak EMG and %MVC for tensed muscle impact for 10 year old boys

Subject			Peak MVC EMG	Untensed - Peak EMG									
				Trial 1		Time(s)		(%MVC)		Trial 2		Time(s)	
K01	SCM (R)	μV	162.668	137.188	2.647	0.843	201.637	2.154	1.240				
	SCM (L)	μV	205.310	437.313	2.168	2.130	360.057	2.17	1.754				
	TRAP (R)	μV	38.101	86.967	2.576	2.283	63.042	2.636	1.655				
	TRAP (L)	μV	43.837	58.6	2.197	1.337	72.921	2.636	1.663				
	SPL (R)	μV	73.764	156.516	2.7	2.122	163.22	2.125	2.213				
	SPL (L)	μV	67.080	95.852	2.574	1.429	99.558	2.239	1.484				
	SCAL (R)	μV	81.114	130.7	2.701	1.611	129.764	2.552	1.600				
	SCAL (L)	μV	51.809	62.627	2.583	1.209	120.859	2.246	2.333				
	Accel	g		2.568	2.4889		2.565	2.4889					
K03	SCM (R)	μV	156.775	100.429	2.218	0.641	134.047	2.142	0.855				
	SCM (L)	μV	236.143	122.798	2.169	0.520	166.444	2.17	0.705				
	TRAP (R)	μV	62.549	49.947	2.556	0.799	49.232	2.561	0.787				
	TRAP (L)	μV	71.288	67.564	2.611	0.948	38.11	2.127	0.535				
	SPL (R)	μV	186.656	67.301	2.553	0.361	106.515	2.564	0.571				
	SPL (L)	μV	191.956	142.177	2.616	0.741	105.998	2.178	0.552				
	SCAL (R)	μV	153.581	48.31	2.546	0.315	62.006	2.555	0.404				
	SCAL (L)	μV	104.943	77.973	2.539	0.743	67.576	2.13	0.644				
	Accel	g		2.508	2.5301		2.652	2.535					
K04	SCM (R)	μV	233.162	399.696	2.167	1.714	457.118	2.222	1.961				
	SCM (L)	μV	218.142	368.036	2.241	1.687	430.092	2.153	1.972				
	TRAP (R)	μV	100.717	187.569	2.674	1.862	174.923	2.578	1.737				
	TRAP (L)	μV	54.039	209.859	2.248	3.883	154.355	2.232	2.856				
	SPL (R)	μV	240.259	280.166	2.154	1.166	237.664	2.227	0.989				
	SPL (L)	μV	162.409	148.354	2.198	0.913	158.989	2.188	0.979				
	SCAL (R)	μV	107.343	99.107	2.164	0.923	113.08	2.197	1.053				
	SCAL (L)	μV	115.831	166.18	2.219	1.435	223.752	2.218	1.932				
	Accel	g		2.593	2.4892		2.505	2.4859					
K05	SCM (R)	μV	270.211	197.363	2.135	0.730							
	SCM (L)	μV	374.353	422.958	2.136	1.130							
	TRAP (R)	μV	66.869	80.584	2.575	1.205							
	TRAP (L)	μV	110.478	81.003	2.161	0.733							
	SPL (R)	μV	251.116	169.846	2.561	0.676							
	SPL (L)	μV	177.441	139.094	2.117	0.784							
	SCAL (R)	μV	71.602	128.292	2.548	1.792							
	SCAL (L)	μV	110.083	122.224	2.136	1.110							
	Accel	g		2.724	2.491								
K06	SCM (R)	μV	220.372	109.393	2.156	0.496	192.094	2.162	0.872				
	SCM (L)	μV	151.332	175.743	2.148	1.161	106.05	2.167	0.701				
	TRAP (R)	μV	139.934	65.576	2.342	0.469	83.457	2.596	0.596				
	TRAP (L)	μV	98.797	54.355	2.633	0.550	65.503	2.607	0.663				
	SPL (R)	μV	176.971	98.016	2.161	0.554	154.574	2.165	0.873				
	SPL (L)	μV	123.192	111.376	2.352	0.904	59.403	2.64	0.482				
	SCAL (R)	μV	144.618	70.84	2.169	0.490	92.323	2.163	0.638				
	SCAL (L)	μV	120.000	124.819	2.353	1.040	179.291	2.621	1.494				
	Accel	g		2.633	2.4954		2.517	2.5519					

Table C-2: Dynamic Peak EMG values, time of Peak EMG and %MVC for untensed muscle impact for 10 year old boys

Subject			Peak MVC EMG	Untensed - Peak EMG						
				Trial 1			Trial 2			
				(%MVC)			(%MVC)			
K07	SCM (R)	μV	181.666							
	SCM (L)	μV	179.784							
	TRAP (R)	μV	110.6665							
	TRAP (L)	μV	44.923							
	SPL (R)	μV	159.7215							
	SPL (L)	μV	175.865							
	SCAL (R)	μV	146.076							
	SCAL (L)	μV	11.4595							
	Accel	g								
K09	SCM (R)	μV	97.316	139.299	2.213	1.318	179.236	2.142	1.842	
	SCM (L)	μV	124.244	131.771	2.231	1.046	92.614	2.138	0.745	
	TRAP (R)	μV	42.412	50.148	2.726	1.138	48.054	2.621	1.133	
	TRAP (L)	μV	103.436	395.772	2.695	2.807	116.638	2.618	1.128	
	SPL (R)	μV	99.585	84.132	2.232	0.878	78.846	2.53	0.792	
	SPL (L)	μV	85.084	114.398	2.227	1.256	94.727	2.165	1.113	
	SCAL (R)	μV	105.858	66.391	2.142	0.698	162.262	2.61	1.533	
	SCAL (L)	μV	102.362	58.629	2.728	0.651	101.684	2.607	0.993	
	Accel	g		2.881	2.6206		3.033	2.5208		
K10	SCM (R)	μV	155.268	173.821	2.162	1.091	168.607	2.166	1.086	
	SCM (L)	μV	44.182	215.118	2.174	3.379	199.037	2.167	4.505	
	TRAP (R)	μV	123.223	103.219	2.536	0.873	66.064	2.448	0.536	
	TRAP (L)	μV	89.824	109.024	2.59	1.161	78.524	2.48	0.874	
	SPL (R)	μV	187.484	121.199	2.584	0.715	141.384	2.599	0.754	
	SPL (L)	μV	64.013	156.872	2.58	1.993	144.015	2.483	2.250	
	SCAL (R)	μV	87.871	105.862	2.173	1.154	138.326	2.444	1.574	
	SCAL (L)	μV	52.448	109.794	2.519	1.765	93.831	2.483	1.789	
	Accel	g		2.547	2.5012		2.514	2.4982		
K11	SCM (R)	μV	175.378	174.185	2.583	0.995	246.027	2.175	1.403	
	SCM (L)	μV	109.7275	229.169	2.153	1.762	238.296	2.173	2.172	
	TRAP (R)	μV	77.338	64.122	2.225	0.866	112.139	2.592	1.450	
	TRAP (L)	μV	84.9755	81.688	2.119	0.970	75.908	2.634	0.893	
	SPL (R)	μV	176.879	112.569	2.628	0.706	133.155	2.568	0.753	
	SPL (L)	μV	240.984	176.818	2.122	0.788	197.697	2.189	0.820	
	SCAL (R)	μV	233.289	174.767	2.217	0.801	209.903	2.578	0.900	
	SCAL (L)	μV	246.891	195.073	2.608	0.834	192.153	2.564	0.778	
	Accel	g		2.729	2.4927		2.617	2.4938		

Table C-2: Dynamic Peak EMG values, time of Peak EMG and %MVC for untensed muscle impact for 10 year old boys

Subject			Peak MVC EMG	Untensed - Peak EMG					
				Trial 3	Time(s)	(%MVC)	Mean	Time(s)	(%MVC)
K01	SCM (R)	μV	162.668				169.413	2.401	1.041
	SCM (L)	μV	205.310				398.685	2.276	1.942
	TRAP (R)	μV	38.101				75.005	2.567	1.969
	TRAP (L)	μV	43.837				65.761	2.454	1.500
	SPL (R)	μV	73.764				159.868	2.453	2.167
	SPL (L)	μV	67.080				97.705	2.448	1.457
	SCAL (R)	μV	81.114				130.232	2.627	1.606
	SCAL (L)	μV	51.809				91.743	2.415	1.771
	Accel	g					2.567		
K03	SCM (R)	μV	156.775	113.198	2.116	0.722	115.891	2.159	0.739
	SCM (L)	μV	236.143	152.92	2.158	0.648	147.387	2.166	0.624
	TRAP (R)	μV	62.549	65.801	2.358	1.052	54.993	2.492	0.879
	TRAP (L)	μV	71.288	46.006	2.342	0.645	50.560	2.360	0.709
	SPL (R)	μV	186.656	122.865	2.36	0.658	98.894	2.492	0.530
	SPL (L)	μV	191.956	77.208	2.15	0.402	108.461	2.315	0.565
	SCAL (R)	μV	153.581	58.723	2.357	0.382	56.346	2.486	0.367
	SCAL (L)	μV	104.943	54.369	2.108	0.518	66.639	2.259	0.635
	Accel	g		2.683	2.5313		2.614		
K04	SCM (R)	μV	233.162				428.407	2.195	1.837
	SCM (L)	μV	218.142				399.064	2.197	1.829
	TRAP (R)	μV	100.717				181.246	2.580	1.800
	TRAP (L)	μV	54.039				182.107	2.322	3.370
	SPL (R)	μV	240.259				258.915	2.291	1.078
	SPL (L)	μV	162.409				153.672	2.193	0.946
	SCAL (R)	μV	107.343				106.094	2.181	0.988
	SCAL (L)	μV	115.831				194.966	2.219	1.683
	Accel	g					2.549		
K05	SCM (R)	μV	270.211				197.363	2.135	0.730
	SCM (L)	μV	374.353				422.958	2.136	1.130
	TRAP (R)	μV	66.869				80.584	2.575	1.205
	TRAP (L)	μV	110.478				81.003	2.161	0.733
	SPL (R)	μV	251.116				169.846	2.561	0.676
	SPL (L)	μV	177.441				139.094	2.117	0.784
	SCAL (R)	μV	71.602				128.292	2.548	1.792
	SCAL (L)	μV	110.083				122.224	2.136	1.110
	Accel	g					2.724		
K06	SCM (R)	μV	220.372				150.744	2.159	0.684
	SCM (L)	μV	151.332				140.897	2.270	0.931
	TRAP (R)	μV	139.934				74.517	2.497	0.533
	TRAP (L)	μV	98.797				59.929	2.620	0.607
	SPL (R)	μV	176.971				126.295	2.163	0.714
	SPL (L)	μV	123.192				85.390	2.496	0.693
	SCAL (R)	μV	144.618				81.582	2.166	0.564
	SCAL (L)	μV	120.000				152.055	2.487	1.267
	Accel	g					2.575		

Table C-2: Dynamic Peak EMG values, time of Peak EMG and %MVC for untensed muscle impact for 10 year old boys

Subject			Peak MVC EMG	Untensed - Peak EMG			
				Trial 3	(%MVC)	Mean	(%MVC)
K07	SCM (R)	μV	181.666				
	SCM (L)	μV	179.784				
	TRAP (R)	μV	110.6665				
	TRAP (L)	μV	44.923				
	SPL (R)	μV	159.7215				
	SPL (L)	μV	175.865				
	SCAL (R)	μV	146.076				
	SCAL (L)	μV	11.4595				
	Accel	g					
K09	SCM (R)	μV	97.316		159.268	2.178	1.580
	SCM (L)	μV	124.244		112.193	2.185	0.896
	TRAP (R)	μV	42.412		49.101	2.623	1.135
	TRAP (L)	μV	103.436		256.205	2.605	1.967
	SPL (R)	μV	99.585		81.489	2.420	0.835
	SPL (L)	μV	85.084		104.563	2.295	1.185
	SCAL (R)	μV	105.858		114.327	2.415	1.116
	SCAL (L)	μV	102.362		80.157	2.668	0.822
	Accel	g			2.957		
K10	SCM (R)	μV	155.268		171.214	2.164	1.088
	SCM (L)	μV	44.182		207.078	2.171	3.942
	TRAP (R)	μV	123.223		84.642	2.492	0.704
	TRAP (L)	μV	89.824		93.774	2.535	1.017
	SPL (R)	μV	187.484		131.292	2.592	0.735
	SPL (L)	μV	64.013		150.444	2.532	2.121
	SCAL (R)	μV	87.871		122.094	2.309	1.364
	SCAL (L)	μV	52.448		101.813	2.501	1.777
	Accel	g			2.531		
K11	SCM (R)	μV	175.378		210.106	2.379	1.199
	SCM (L)	μV	109.7275		233.733	2.163	1.967
	TRAP (R)	μV	77.338		88.131	2.409	1.158
	TRAP (L)	μV	84.9755		78.798	2.377	0.932
	SPL (R)	μV	176.879		122.862	2.598	0.730
	SPL (L)	μV	240.984		187.258	2.156	0.804
	SCAL (R)	μV	233.289		192.335	2.398	0.850
	SCAL (L)	μV	246.891		193.613	2.586	0.806
	Accel	g			2.673		

Table C-2: Dynamic Peak EMG values, time of Peak EMG and %MVC for untensed muscle impact for 10 year old boys

Subject	Peak MVC EMG	Tensed - Peak EMG						
		Trial 1		(%MVC)		Trial 2		(%MVC)
S13	SCM (R) μV	353.196	498.293	2.177	1.411	275.411	2.178	0.780
	SCM (L) μV	242.609	343.566	2.179	1.416	171.177	2.175	0.706
	TRAP (R) μV	116.345	101.503	2.647	0.872	91.437	2.478	0.786
	TRAP (L) μV	43.238	58.6	2.367	1.355	53.975	2.59	1.248
	SPL (R) μV	339.628	240.762	2.644	0.709	300.029	2.169	0.883
	SPL (L) μV	169.878	185.394	2.675	1.091	203.054	2.645	1.195
	SCAL (R) μV	263.067	260.572	2.175	0.991	260.163	2.637	0.989
	SCAL (L) μV	118.384	193.998	2.662	1.639	143.322	2.312	1.211
	Accel g		3.51			3.302		
S14	SCM (R) μV	136.430	210.303	2.11	1.541	94.177	2.218	0.690
	SCM (L) μV	146.744	179.116	2.111	1.221	119.661	2.216	0.815
	TRAP (R) μV	25.420	14.448	2.646	0.568	38.449	2.774	1.513
	TRAP (L) μV	12.514	20.353	2.736	1.626	49.109	2.974	3.924
	SPL (R) μV	51.495	26.556	2.123	0.516	17.667	2.738	0.343
	SPL (L) μV	49.215	41.021	2.115	0.834	43.48	2.211	0.883
	SCAL (R) μV	70.186	241.758	2.624	3.445	112.125	2.706	1.598
	SCAL (L) μV	57.425	44.691	2.127	0.778	38.823	2.208	0.676
	Accel g		3.192	2.509		3.095	2.594	
S15	SCM (R) μV	198.700	114.406	2.131	0.576			
	SCM (L) μV	174.949	400.759	2.64	2.291			
	TRAP (R) μV	36.171	146.01	2.622	4.037			
	TRAP (L) μV	27.516	35.622	2.563	1.295			
	SPL (R) μV	143.169	126.627	2.582	0.884			
	SPL (L) μV	91.699	103.771	2.625	1.132			
	SCAL (R) μV	333.043	175.563	2.649	0.527			
	SCAL (L) μV	54.177	45.355	2.158	0.837			
	Accel g		2.933	2.501				
S16	SCM (R) μV	98.101	210.822	2.413	2.149	207.382	2.167	2.114
	SCM (L) μV	96.506	217.371	2.167	2.252	205.281	2.16	2.127
	TRAP (R) μV	16.462	45.339	2.387	2.754	37.486	2.331	2.277
	TRAP (L) μV	14.991	47.935	2.7	3.198	25.06	2.63788	1.672
	SPL (R) μV	81.444	34.158	2.638	0.419	32.58	2.172	0.400
	SPL (L) μV	54.533	60.614	2.617	1.112	86.82	2.599	1.592
	SCAL (R) μV	76.754	25.572	2.6259	0.333	73.653	2.161	0.960
	SCAL (L) μV	84.550	81.97	2.17	0.969	64.738	2.177	0.766
	Accel g		3.125	2.483		3.24	2.51	

Table C-3: Dynamic Peak EMG values, time of Peak EMG and %MVC for tensed muscle impact for 50th percentile adult males

Subject			Peak MVC EMG	Tensed - Peak EMG					
				Trial 1		(%MVC)		Trial 2	
S17	SCM (R)	μV	83.940	191.02	2.184	2.276	164.325	2.173	1.958
	SCM (L)	μV	38.389				98.08	2.208	2.555
	TRAP (R)	μV	6.858	26.175	2.621	3.817	23.564	2.626	3.436
	TRAP (L)	μV	22.495	18.739	2.574	0.833	27.932	2.615	1.242
	SPL (R)	μV	98.737	108.388	2.685	1.098	186.419	2.177	1.888
	SPL (L)	μV	37.055	59.077	2.661	1.594	58.374	2.204	1.575
	SCAL (R)	μV	58.640	71.777	2.167	1.224	124.829	2.164	2.129
	SCAL (L)	μV	47.249	57.628	2.232	1.220	80.484	2.203	1.703
	Accel	g		2.992	2.511		3.26	2.508	
S20	SCM (R)	μV	133.741				205.79	2.145	1.539
	SCM (L)	μV	110.957	173.584	2.343	1.564	169.061	2.434	1.524
	TRAP (R)	μV	30.965	53.43	2.263	1.726	50.145	2.364	1.619
	TRAP (L)	μV	23.951	91.794	2.284	3.833	64.202	2.514	2.681
	SPL (R)	μV	31.304	58.951	2.773	1.883	77.301	2.346	2.469
	SPL (L)	μV	74.106	125.579	2.256	1.695	115.045	2.281	1.552
	SCAL (R)	μV	24.196	120.852	2.647	4.995	131.355	2.29	5.429
	SCAL (L)	μV	79.383	128.879	2.257	1.624	141.3	2.277	1.780
	Accel	g		3.29	2.533		3.13	2.511	

Table C-3: Dynamic Peak EMG values, time of Peak EMG and %MVC for tensed muscle impact for 50th percentile adult males

Subject	Age			Peak MVC EMG	Tensed - Peak EMG					
					Trial 3	(%MVC)		Mean	(%MVC)	
S13	29.000	SCM (R)	μV	353.196	373.695	2.172	1.058	382.466	2.176	1.083
		SCM (L)	μV	242.609	271.368	2.166	1.119	262.037	2.173	1.080
		TRAP (R)	μV	116.345	65.007	2.3	0.559	85.982	2.475	0.739
		TRAP (L)	μV	43.238	85.969	2.702	1.988	66.181	2.553	1.531
		SPL (R)	μV	339.628	162.211	2.165	0.478	234.334	2.326	0.690
		SPL (L)	μV	169.878	182.599	2.705	1.075	190.349	2.675	1.121
		SCAL (R)	μV	263.067	160.575	2.658	0.610	227.103	2.490	0.863
		SCAL (L)	μV	118.384	186.896	2.669	1.579	174.739	2.548	1.476
		Accel	g			3.354			3.389	
S14	26.000	SCM (R)	μV	136.430	170.048	2.675	1.246	158.176	2.334	1.159
		SCM (L)	μV	146.744	240.387	2.67	1.638	179.721	2.332	1.225
		TRAP (R)	μV	25.420	27.704	2.856	1.090	26.867	2.759	1.057
		TRAP (L)	μV	12.514	19.64	3.154	1.569	29.701	2.955	2.373
		SPL (R)	μV	51.495	27.023	2.669	0.525	23.749	2.510	0.461
		SPL (L)	μV	49.215	32.861	2.682	0.668	39.121	2.336	0.795
		SCAL (R)	μV	70.186	73.668	3.129	1.050	142.517	2.820	2.031
		SCAL (L)	μV	57.425	55.221	2.675	0.962	46.245	2.337	0.805
		Accel	g			3.257	3.073		3.181	
S15	40.000	SCM (R)	μV	198.700	101.855	2.111	0.513	108.131	2.121	0.544
		SCM (L)	μV	174.949	102.171	2.11	0.584	251.465	2.375	1.437
		TRAP (R)	μV	36.171	254.584	2.623	7.038	200.297	2.623	5.537
		TRAP (L)	μV	27.516	46.255	2.613	1.681	40.939	2.588	1.488
		SPL (R)	μV	143.169	212.027	2.641	1.481	169.327	2.612	1.183
		SPL (L)	μV	91.699	114.233	2.132	1.246	109.002	2.379	1.189
		SCAL (R)	μV	333.043	98.438	2.119	0.296	137.001	2.384	0.411
		SCAL (L)	μV	54.177	31.54	2.121	0.582	38.448	2.140	0.710
		Accel	g			3.309	2.519		3.121	
S16	47.000	SCM (R)	μV	98.101	246.831	2.462	2.516	153.273	2.330	2.260
		SCM (L)	μV	96.506	194.935	2.22	2.020	138.155	2.171	2.133
		TRAP (R)	μV	16.462	29.95	2.397	1.819	25.873	2.354	2.284
		TRAP (L)	μV	14.991	42.746	2.758	2.851	31.106	2.377	2.574
		SPL (R)	μV	81.444	44.027	2.559	0.541	26.786	1.866	0.453
		SPL (L)	μV	54.533	121.895	2.661	2.235	61.703	2.290	1.646
		SCAL (R)	μV	76.754	49.676	2.477	0.647	25.803	2.021	0.647
		SCAL (L)	μV	84.550	72.211	2.477	0.854	52.119	1.804	0.863
		Accel	g			3.131	2.549		3.165	

Table C-3: Dynamic Peak EMG values, time of Peak EMG and %MVC for tensed muscle impact for 50th percentile adult males

Subject	Age			Peak MVC	Tensed - Peak EMG					
				EMG	Trial 3		(%MVC)		Mean	
S17	54.000	SCM (R)	μV	83.940	134.355	2.955	1.601	163.233	2.437	1.945
		SCM (L)	μV	38.389	117.257	3.012	3.054	107.669	2.610	2.805
		TRAP (R)	μV	6.858	24.889	3.453	3.629	24.876	2.900	3.627
		TRAP (L)	μV	22.495	22.188	3.386	0.986	22.953	2.858	1.020
		SPL (R)	μV	98.737	121.827	3.02	1.234	138.878	2.627	1.407
		SPL (L)	μV	37.055	59.505	3.514	1.606	58.985	2.793	1.592
		SCAL (R)	μV	58.640	90.8	3.014	1.548	95.802	2.448	1.634
		SCAL (L)	μV	47.249	52.684	2.98	1.115	63.599	2.472	1.346
		Accel	g			3.373	3.128		3.208	
S20	42.000	SCM (R)	μV	133.741	96.735	2.654	0.723	151.263	2.400	1.131
		SCM (L)	μV	110.957	115.448	2.138	1.040	152.698	2.305	1.376
		TRAP (R)	μV	30.965	27.005	2.69	0.872	43.527	2.439	1.406
		TRAP (L)	μV	23.951	40.592	2.573	1.695	65.529	2.457	2.736
		SPL (R)	μV	31.304	40.832	2.683	1.304	59.028	2.601	1.886
		SPL (L)	μV	74.106	58.948	2.672	0.795	99.857	2.403	1.347
		SCAL (R)	μV	24.196	96.591	2.659	3.992	116.266	2.532	4.805
		SCAL (L)	μV	79.383	33.401	2.671	0.421	101.193	2.402	1.275
		Accel	g			3.179	2.531		3.200	

Table C-3: Dynamic Peak EMG values, time of Peak EMG and %MVC for tensed muscle impact for 50th percentile adult males

Subject			Peak MVC EMG	Untensed - Peak EMG					
				Trial 1		(%MVC)		Trial 2	
S13	SCM (R)	μV	353.196	371.373	2.199	1.051	346.373	2.176	0.981
	SCM (L)	μV	242.609	296.489	2.19	1.222	363.889	2.187	1.500
	TRAP (R)	μV	116.345	67.025	2.667	0.576	53.451	2.649	0.459
	TRAP (L)	μV	43.238	54.536	2.225	1.261	51.805	2.238	1.198
	SPL (R)	μV	339.628	273.318	2.19	0.805	232.871	2.17	0.686
	SPL (L)	μV	169.878	84.272	2.185	0.496	120.534	2.163	0.710
	SCAL (R)	μV	263.067	194.388	2.183	0.739	235.015	2.174	0.893
	SCAL (L)	μV	118.384	67.729	2.196	0.572	118.642	2.175	1.002
	Accel	g		3.137			3.167		
S14	SCM (R)	μV	136.430	203.455	2.14	1.491	155.862	2.107	1.142
	SCM (L)	μV	146.744	253.839	2.141	1.730	261.49	2.112	1.782
	TRAP (R)	μV	25.420	54.36	2.557	2.139	92.811	2.318	3.651
	TRAP (L)	μV	12.514	12.604	2.63	1.007	13.541	2.649	1.082
	SPL (R)	μV	51.495	33.552	2.441	0.652	54.634	2.182	1.061
	SPL (L)	μV	49.215	37.089	2.215	0.754	36.95	2.131	0.751
	SCAL (R)	μV	70.186	54.275	2.572	0.773	57.171	2.581	0.815
	SCAL (L)	μV	57.425	54.648	2.212	0.952	84.035	2.618	1.463
	Accel	g		3.345	2.526		3.313	2.527	
S15	SCM (R)	μV	198.700	199.525	2.161	1.004	58.884	2.17	0.296
	SCM (L)	μV	174.949	103.927	2.569	0.594	143.102	2.64	0.818
	TRAP (R)	μV	36.171	113.612	2.657	3.141	214.775	2.624	5.938
	TRAP (L)	μV	27.516	86.227	2.646	3.134	19.68	2.639	0.715
	SPL (R)	μV	143.169	122.12	2.634	0.853	245.4	2.619	1.714
	SPL (L)	μV	91.699	94.182	2.592	1.027	47.202	2.61	0.515
	SCAL (R)	μV	333.043	162.114	2.158	0.487	140.192	2.166	0.421
	SCAL (L)	μV	54.177	58.169	2.523	1.074	48.602	2.613	0.897
	Accel	g		3.347	2.521		3.327	2.508	
S16	SCM (R)	μV	98.101	166.325	2.182	1.695	137.702	2.19	1.404
	SCM (L)	μV	96.506	144.659	2.169	1.499	178.255	2.176	1.847
	TRAP (R)	μV	16.462	17.509	2.587	1.064	18.855	2.58334	1.145
	TRAP (L)	μV	14.991	26.213	2.6259	1.749	33.012	2.63788	2.202
	SPL (R)	μV	81.444	25.564	2.191	0.314	21.616	2.623	0.265
	SPL (L)	μV	54.533	35.765	2.66	0.656	100.217	2.592	1.838
	SCAL (R)	μV	76.754	72.373	2.174	0.943	59.339	2.187	0.773
	SCAL (L)	μV	84.550	75.858	2.174	0.897	61.078	2.602	0.722
	Accel	g		3.492	2.509		3.071	2.485	

Table C-4: Dynamic Peak EMG values, time of Peak EMG and %MVC for untensed muscle impact for 50th percentile adult males

Subject			Peak MVC EMG	Untensed - Peak EMG					
				Trial 1		(%MVC)		Trial 2	
S17	SCM (R)	μV	83.940	186.928	2.202	2.227	185.532	2.196	2.210
	SCM (L)	μV	38.389	132.004	2.193	3.439	148.32	2.173	3.864
	TRAP (R)	μV	6.858	25.682	2.641	3.745	15.595	2.693	2.274
	TRAP (L)	μV	22.495	44.906	2.256	1.996	12.693	2.628	0.564
	SPL (R)	μV	98.737	125.246	2.182	1.268	133.104	2.174	1.348
	SPL (L)	μV	37.055	55.375	2.643	1.494	74.573	2.899	2.012
	SCAL (R)	μV	58.640	52.254	2.207	0.891	51.349	2.211	0.876
	SCAL (L)	μV	47.249	67.649	2.632	1.432	72.335	2.194	1.531
	Accel	g		2.94	2.512		2.902	2.509	
S20	SCM (R)	μV	133.741	173.841	2.153	1.300	142.891	2.157	1.068
	SCM (L)	μV	110.957	284.019	2.149	2.560	159.782	2.155	1.440
	TRAP (R)	μV	30.965	21.277	2.683	0.687	76.325	2.738	2.465
	TRAP (L)	μV	23.951	44.398	2.566	1.854	68.22	2.717	2.848
	SPL (R)	μV	31.304	13.489	2.698	0.431	10.422	2.8952	0.333
	SPL (L)	μV	74.106	14.018	2.593	0.189	18.825	2.15328	0.254
	SCAL (R)	μV	24.196	89.942	2.632	3.717	53.983	2.606	2.231
	SCAL (L)	μV	79.383	14.436	2.161	0.182	16.506	2.17762	0.208
	Accel	g		3.048	2.526		3.289	2.539	

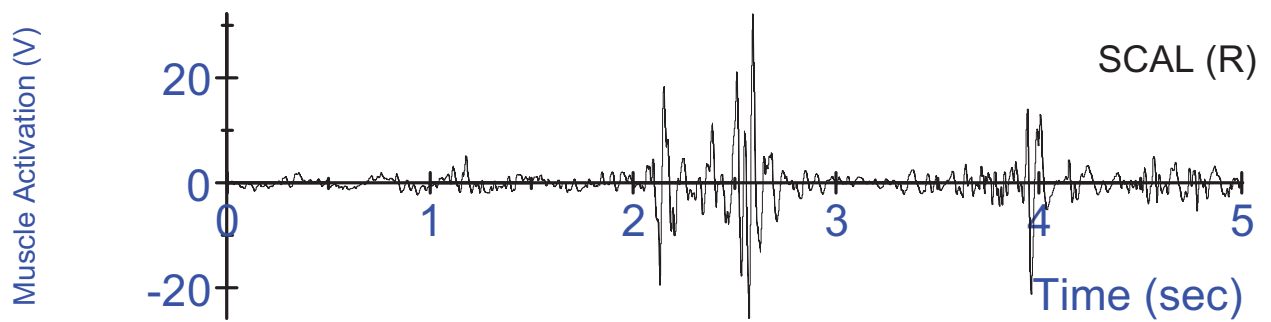
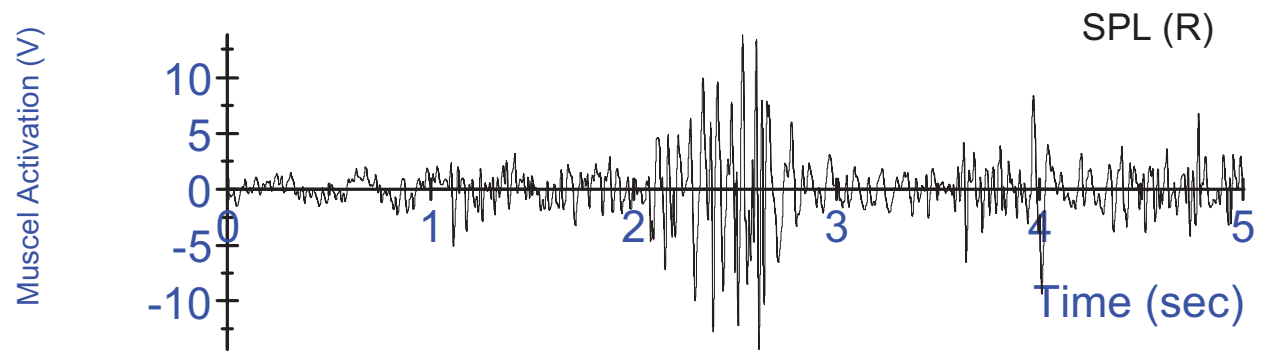
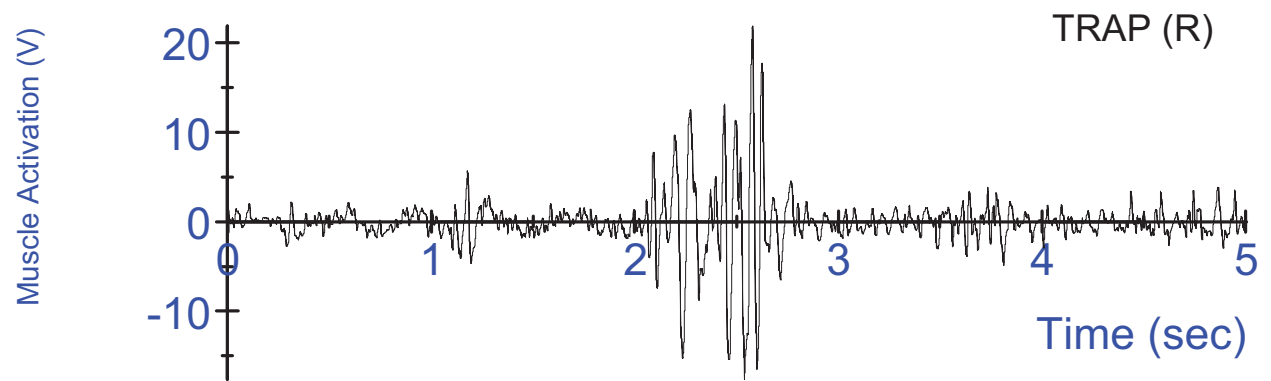
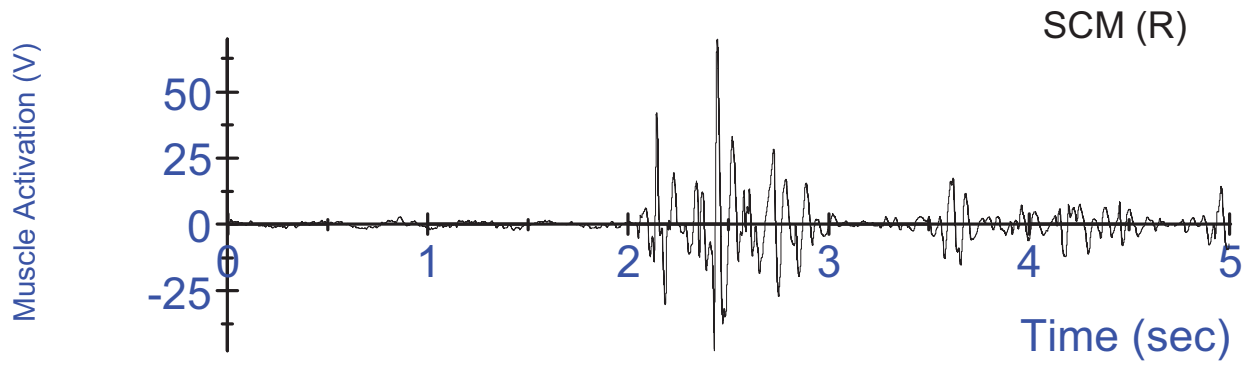
Table C-4: Dynamic Peak EMG values, time of Peak EMG and %MVC for untensed muscle impact for 50th percentile adult males

Subject	EMG	Untensed - Peak EMG							
		Trial 3	(%MVC)		Mean	(%MVC)			
S13	SCM (R) μV	353.196	401.132	2.176	1.136	372.959	2.184	1.056	
	SCM (L) μV	242.609	422.673	2.17	1.742	361.017	2.182	1.488	
	TRAP (R) μV	116.345	40.154	2.585	0.345	53.543	2.634	0.460	
	TRAP (L) μV	43.238	29.748	2.887	0.688	45.363	2.450	1.049	
	SPL (R) μV	339.628	193.176	2.169	0.569	233.122	2.176	0.686	
	SPL (L) μV	169.878	76.915	2.169	0.453	93.907	2.172	0.553	
	SCAL (R) μV	263.067	179.345	2.169	0.682	202.916	2.175	0.771	
	SCAL (L) μV	118.384	78.944	2.166	0.667	88.438	2.179	0.747	
	Accel g		3.167			3.157			
S14	SCM (R) μV	136.430	267.275	2.116	1.959	208.864	2.121	1.531	
	SCM (L) μV	146.744	192.008	2.127	1.308	235.779	2.127	1.607	
	TRAP (R) μV	25.420	55.865	2.336	2.198	67.679	2.404	2.662	
	TRAP (L) μV	12.514	13.852	2.599	1.107	13.332	2.626	1.065	
	SPL (R) μV	51.495	60.817	2.584	1.181	49.668	2.402	0.965	
	SPL (L) μV	49.215	25.65	2.62	0.521	33.230	2.322	0.675	
	SCAL (R) μV	70.186	112.527	2.587	1.603	74.658	2.580	1.064	
	SCAL (L) μV	57.425	111.391	2.611	1.940	83.358	2.480	1.452	
	Accel g		3.383	2.533		3.347			
S15	SCM (R) μV	198.700	41.418	2.814	0.208	99.942	2.382	0.503	
	SCM (L) μV	174.949	78.182	2.630	0.447	108.404	2.613	0.620	
	TRAP (R) μV	36.171	78.182	2.63	2.161	135.523	2.637	3.747	
	TRAP (L) μV	27.516	32.264	2.627	1.173	46.057	2.637	1.674	
	SPL (R) μV	143.169	88.95	2.638	0.621	152.157	2.630	1.063	
	SPL (L) μV	91.699	86.171	2.638	0.940	75.852	2.613	0.827	
	SCAL (R) μV	333.043	44.025	2.611	0.132	115.444	2.312	0.347	
	SCAL (L) μV	54.177	47.899	2.614	0.884	51.557	2.583	0.952	
	Accel g		3.338	2.517		3.337			
S16	SCM (R) μV	98.101	134.021	2.175	1.366	146.016	2.182	1.488	
	SCM (L) μV	96.506	176.212	2.182	1.826	166.375	2.176	1.724	
	TRAP (R) μV	16.462	38.001	2.574	2.308	24.788	2.581	1.506	
	TRAP (L) μV	14.991	40.952	2.207	2.732	33.392	2.490	2.227	
	SPL (R) μV	81.444	15.583	2.181	0.191	20.921	2.332	0.257	
	SPL (L) μV	54.533	63.167	2.609	1.158	66.383	2.620	1.217	
	SCAL (R) μV	76.754	35.428	2.193	0.462	55.713	2.185	0.726	
	SCAL (L) μV	84.550	87.772	2.631	1.038	74.903	2.469	0.886	
	Accel g		3.609	2.511		3.391			

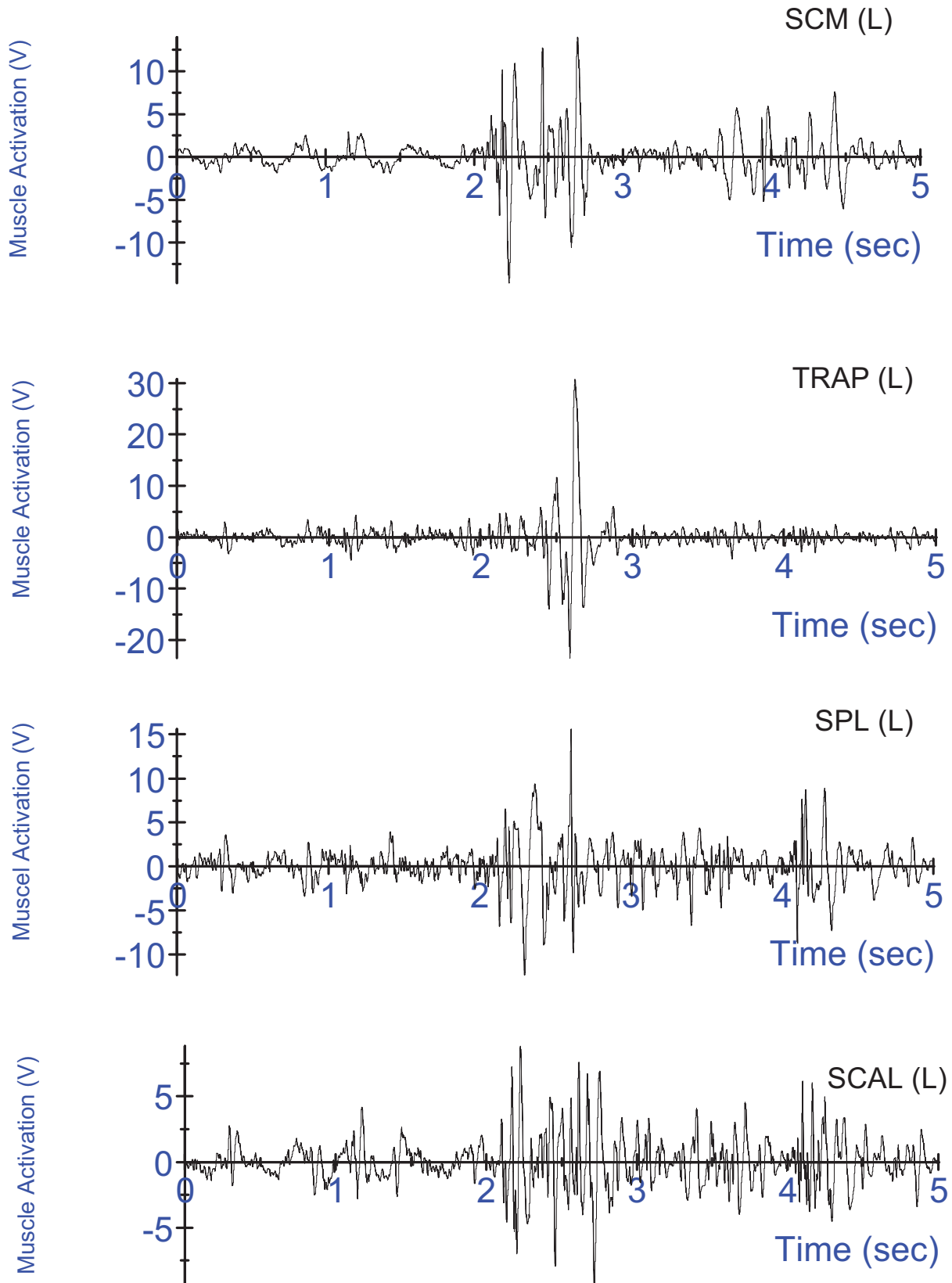
Table C-4: Dynamic Peak EMG values, time of Peak EMG and %MVC for untensed muscle impact for 50th percentile adult males

Subject	EMG	Untensed - Peak EMG							
		Trial 3		(%MVC)		Mean		(%MVC)	
S17	SCM (R)	μV	83.940	157.837	2.196	1.880	176.766	2.198	2.106
	SCM (L)	μV	38.389	164.663	2.208	4.289	148.329	2.191	3.864
	TRAP (R)	μV	6.858	21.983	2.659	3.206	21.087	2.664	3.075
	TRAP (L)	μV	22.495	25.758	2.681	1.145	27.786	2.522	1.235
	SPL (R)	μV	98.737	185.95	2.169	1.883	148.100	2.175	1.500
	SPL (L)	μV	37.055	81.673	2.633	2.204	70.540	2.725	1.904
	SCAL (R)	μV	58.640	110.659	2.183	1.887	71.421	2.200	1.218
	SCAL (L)	μV	47.249	92.302	2.648	1.954	77.429	2.491	1.639
	Accel	g		3.154	2.5186		2.999		
S20	SCM (R)	μV	133.741				158.366	2.155	1.184
	SCM (L)	μV	110.957				221.901	2.152	2.000
	TRAP (R)	μV	30.965				48.801	2.711	1.576
	TRAP (L)	μV	23.951				56.309	2.642	2.351
	SPL (R)	μV	31.304				11.956	2.797	0.382
	SPL (L)	μV	74.106				16.422	2.373	0.222
	SCAL (R)	μV	24.196				71.963	2.619	2.974
	SCAL (L)	μV	79.383				15.471	2.169	0.195
	Accel	g					3.169		

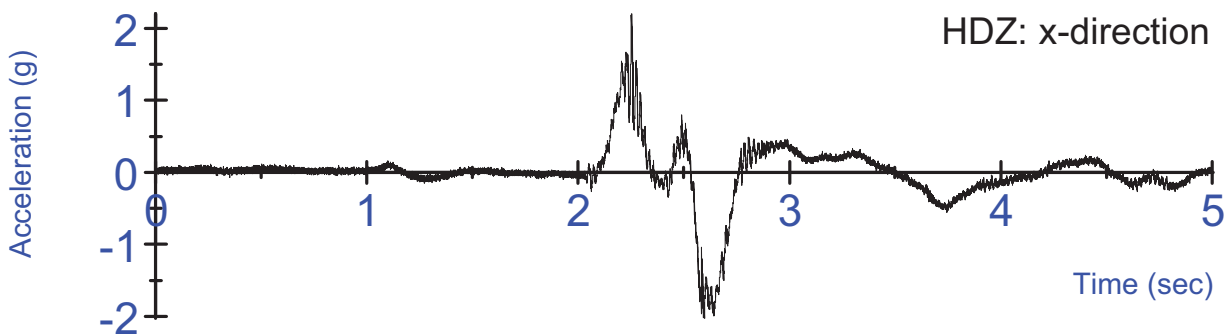
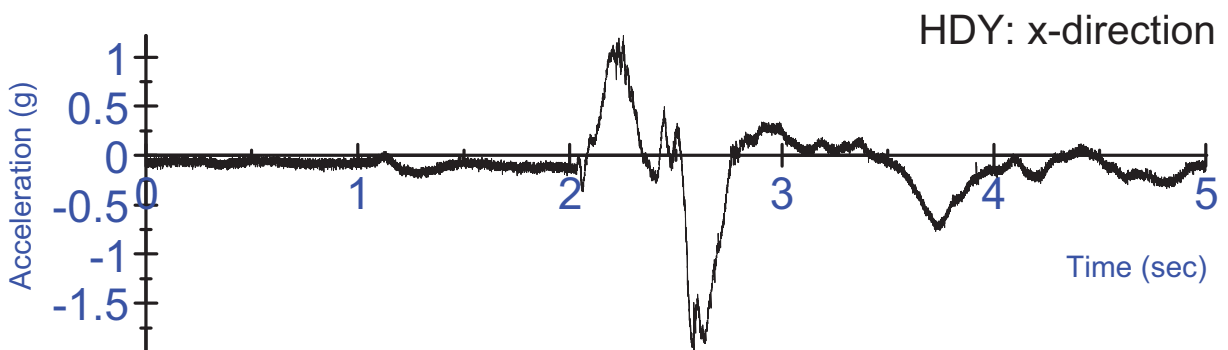
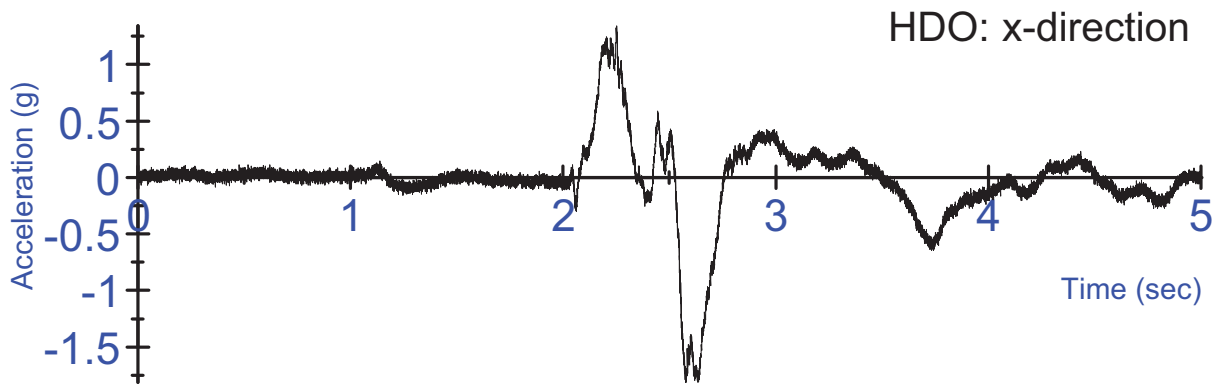
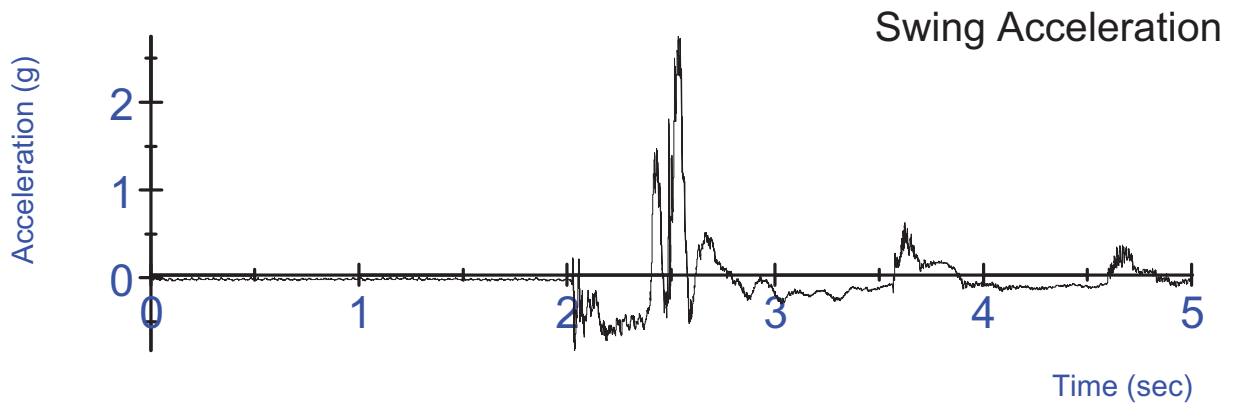
Table C-4: Dynamic Peak EMG values, time of Peak EMG and %MVC for untensed muscle impact for 50th percentile adult males



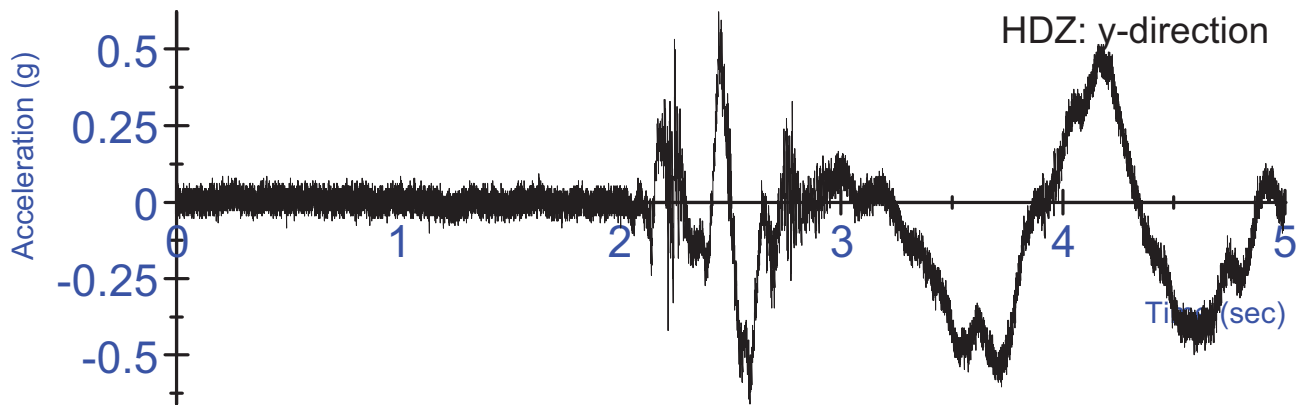
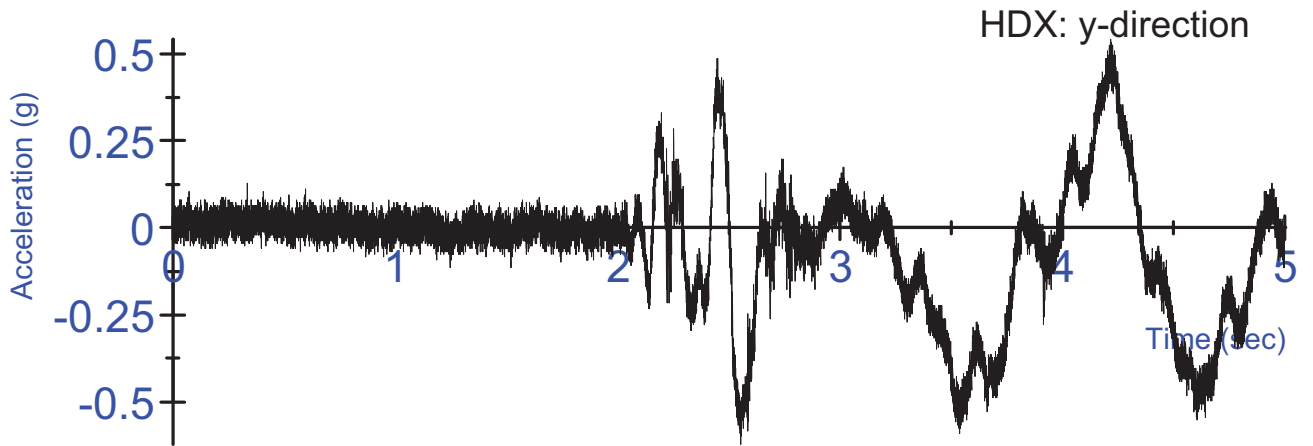
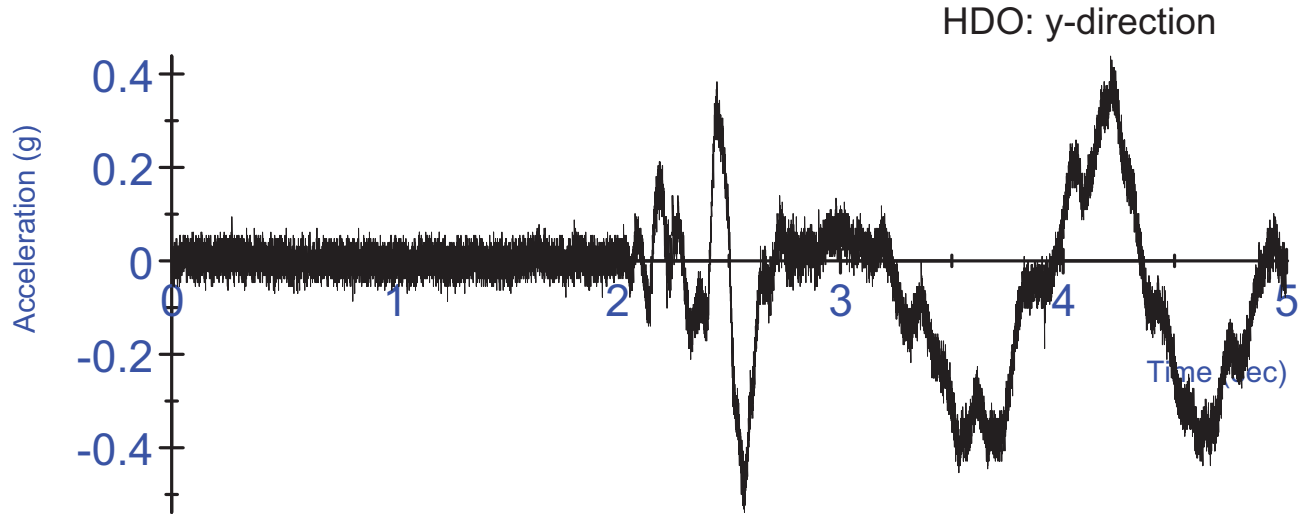
K03 Tensed Test #1 - Right Side EMG activation voltage
Un-rectified, Filtered at 10Hz



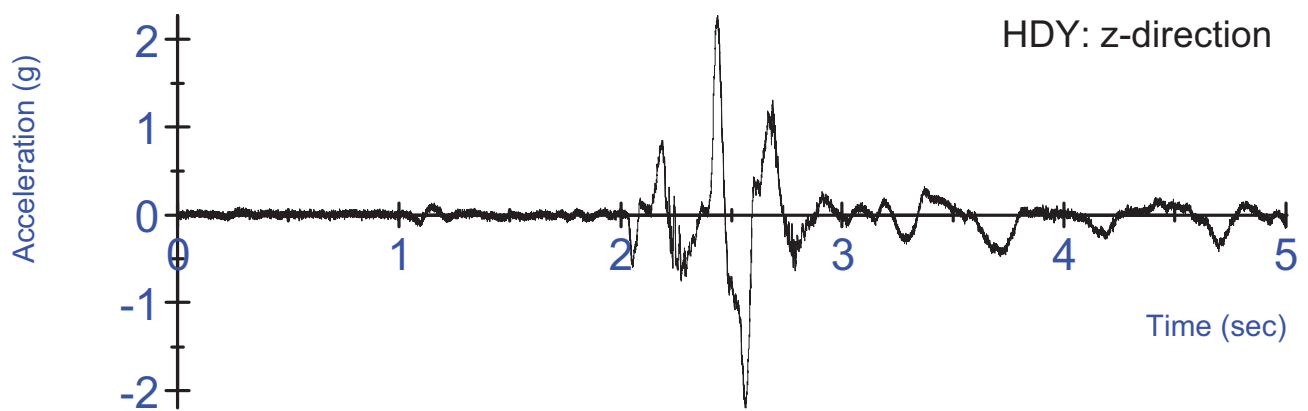
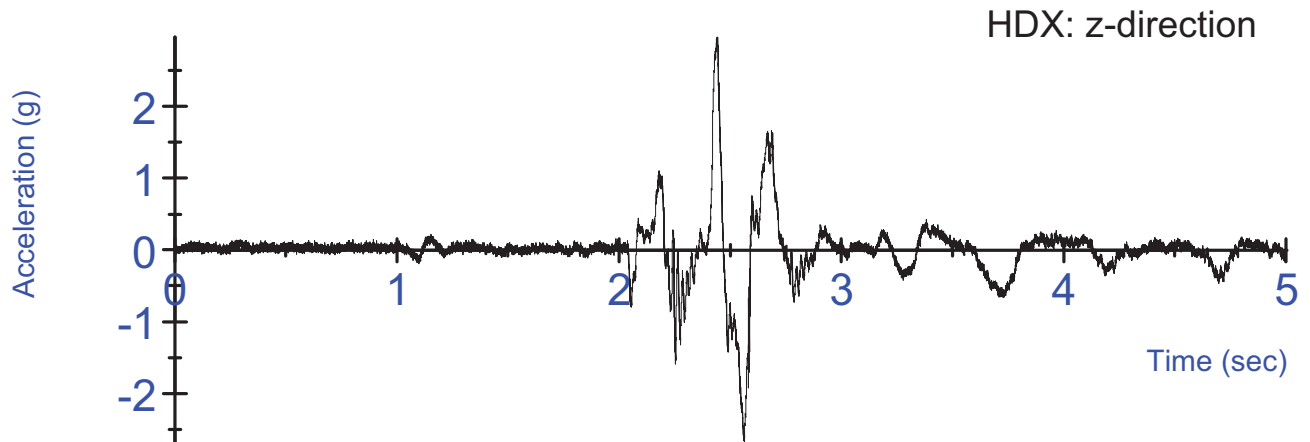
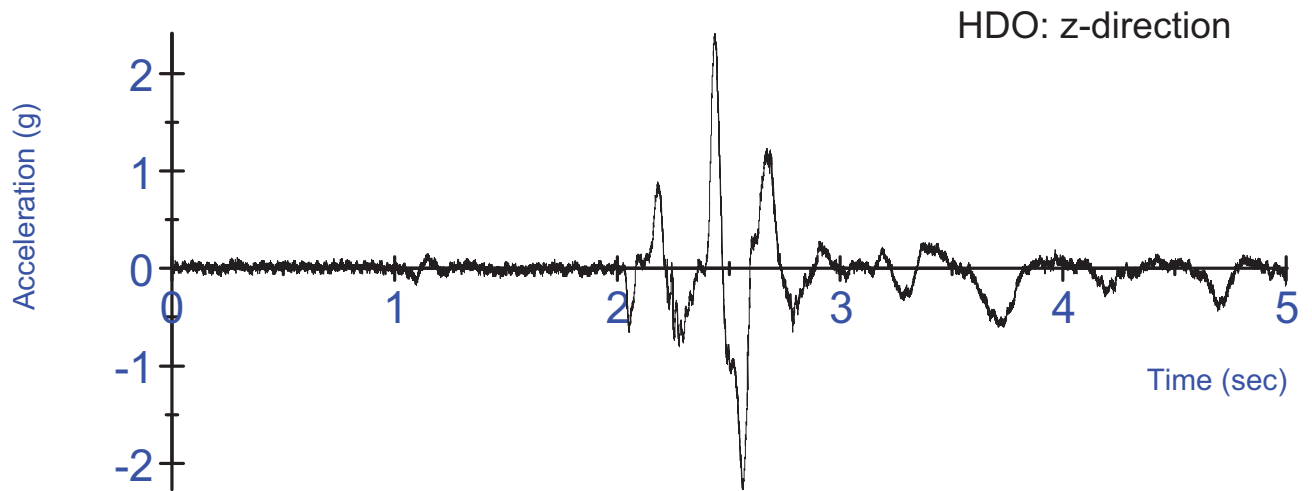
K03 Tensed Test #1- Left Side EMG activation voltage
Un-rectified, Filtered at 10Hz



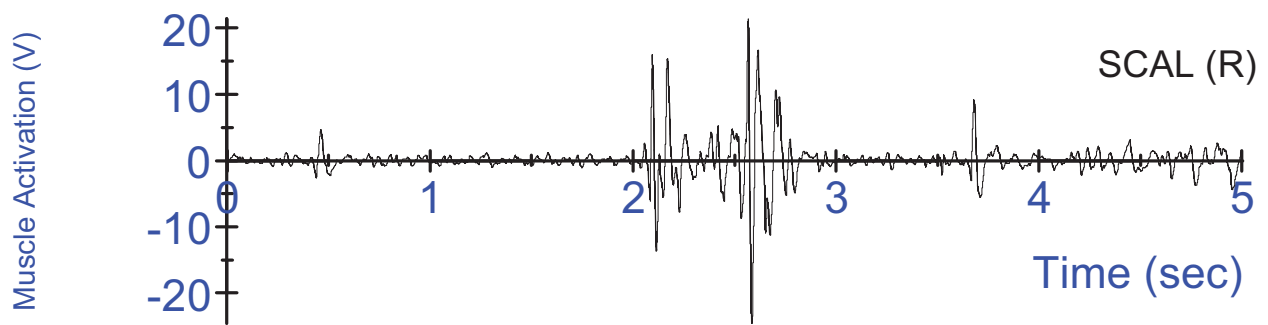
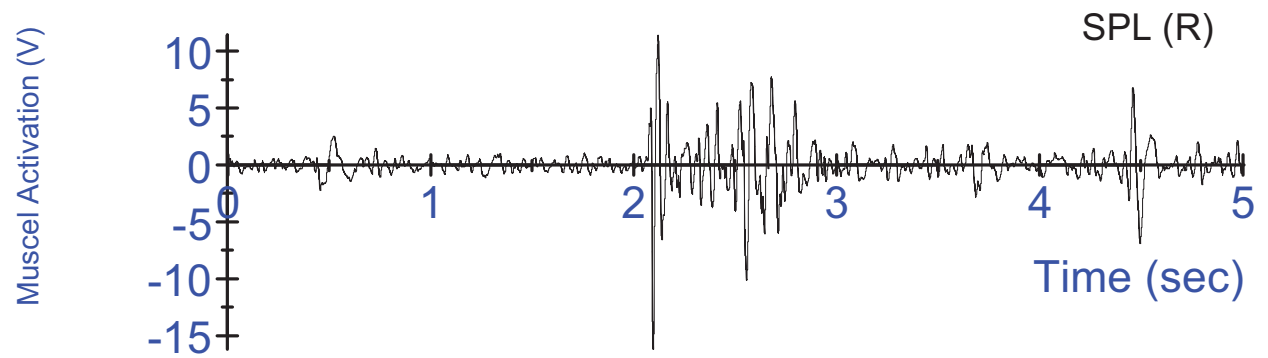
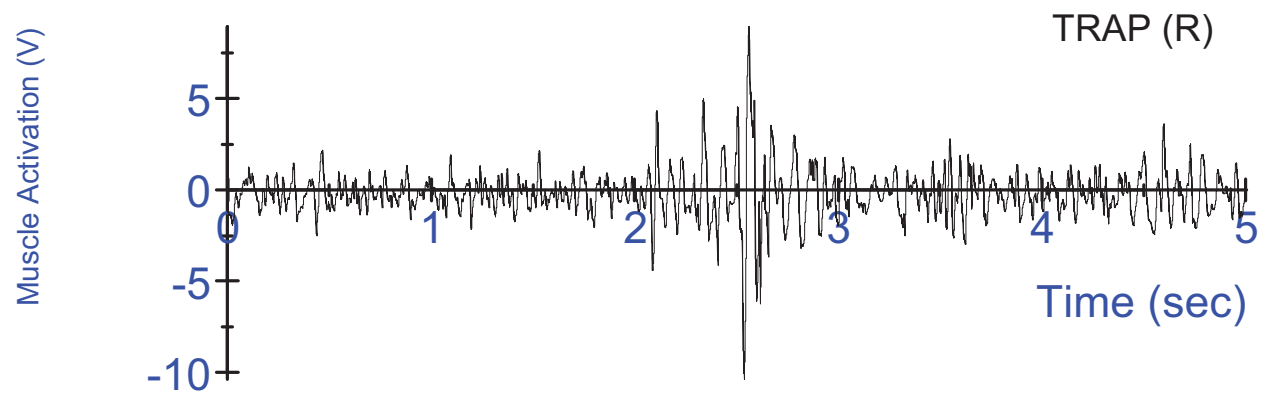
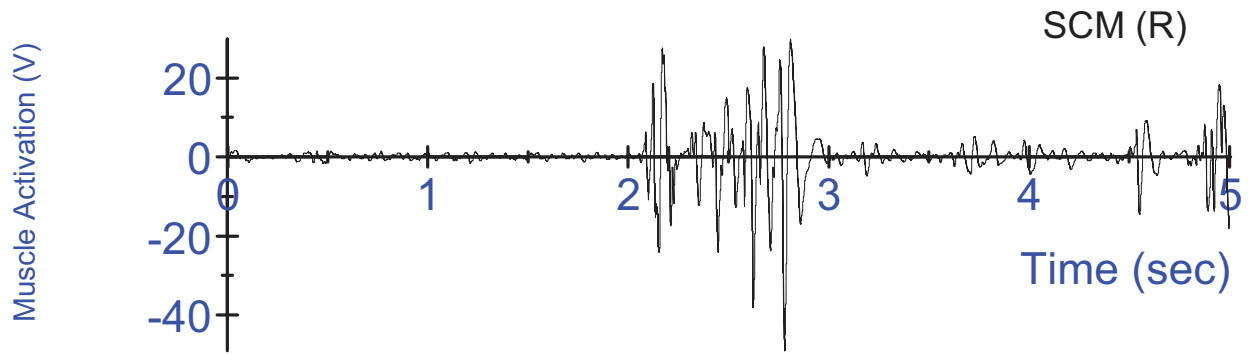
K03 Tensed Test #2 - Swing acceleration, filtered at 180Hz;
3-2-2-2 head acceleration, unfiltered



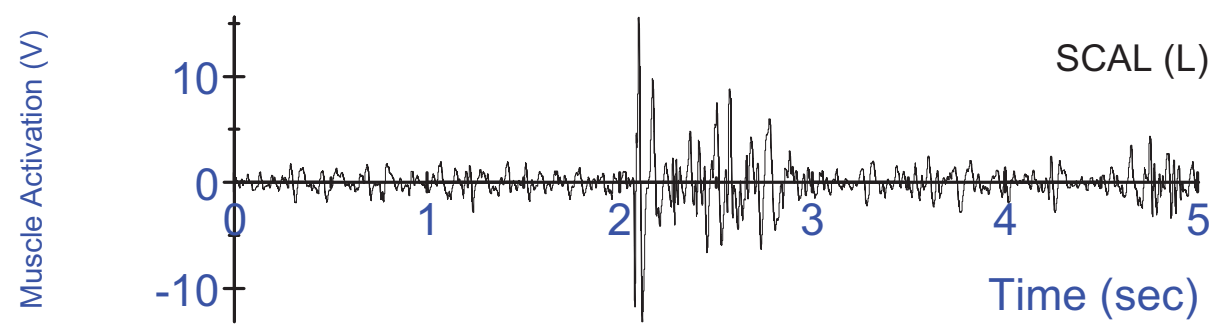
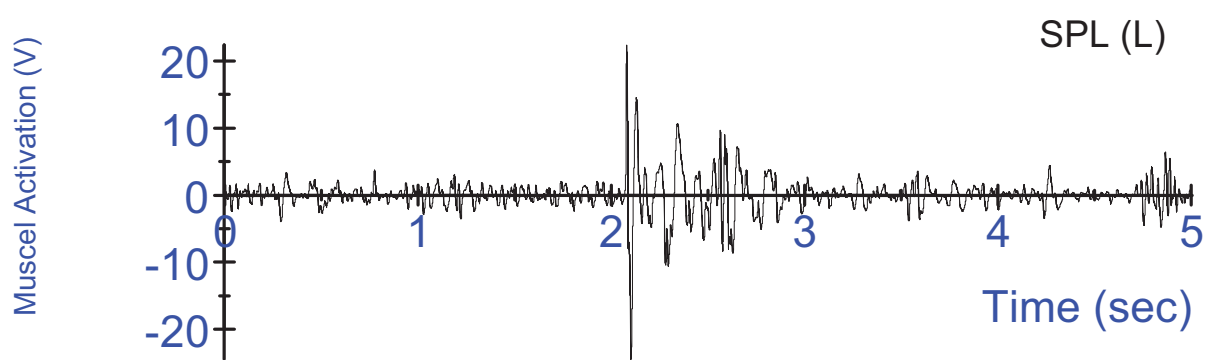
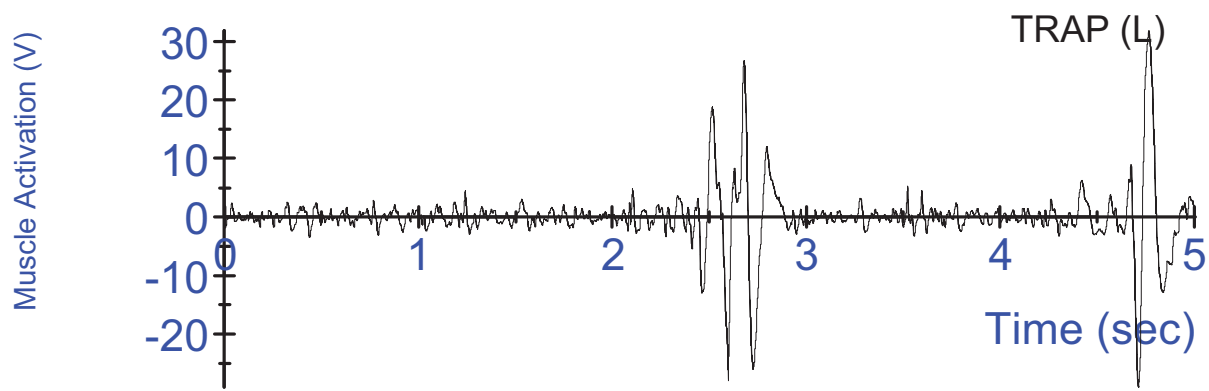
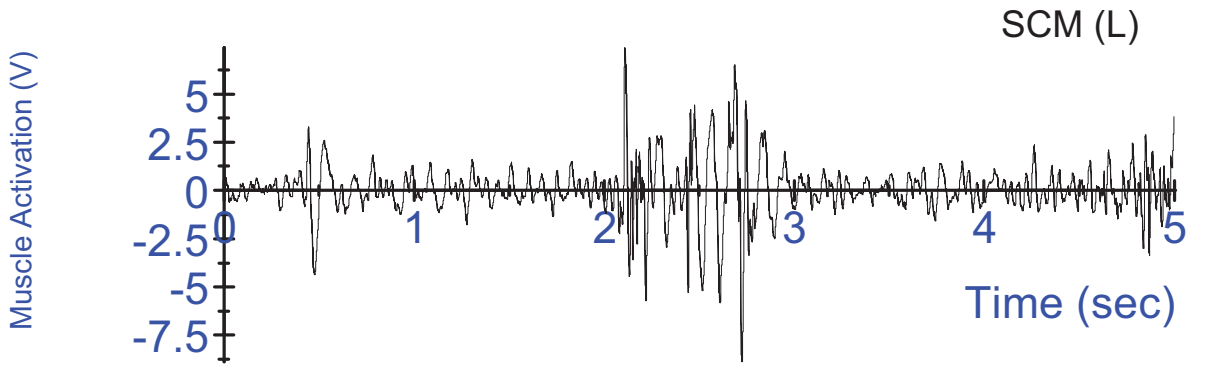
K03 Tensed Test #1 - Swing acceleration, filtered at 180Hz;
3-2-2-2 head acceleration, unfiltered



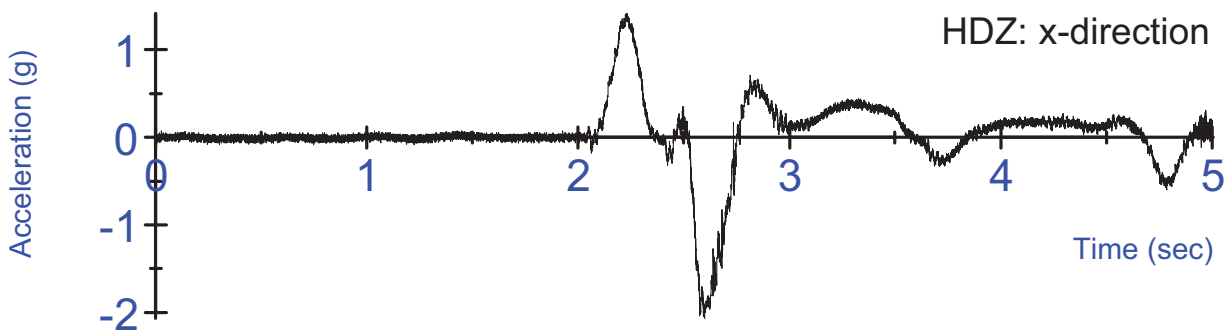
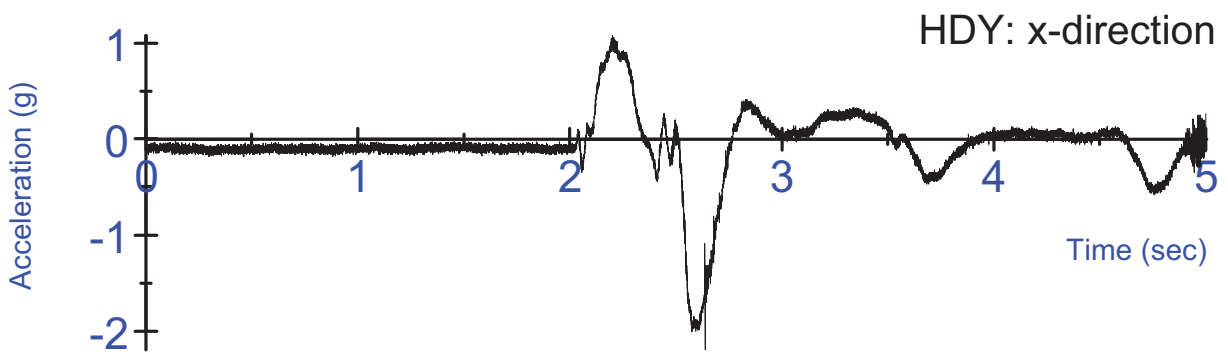
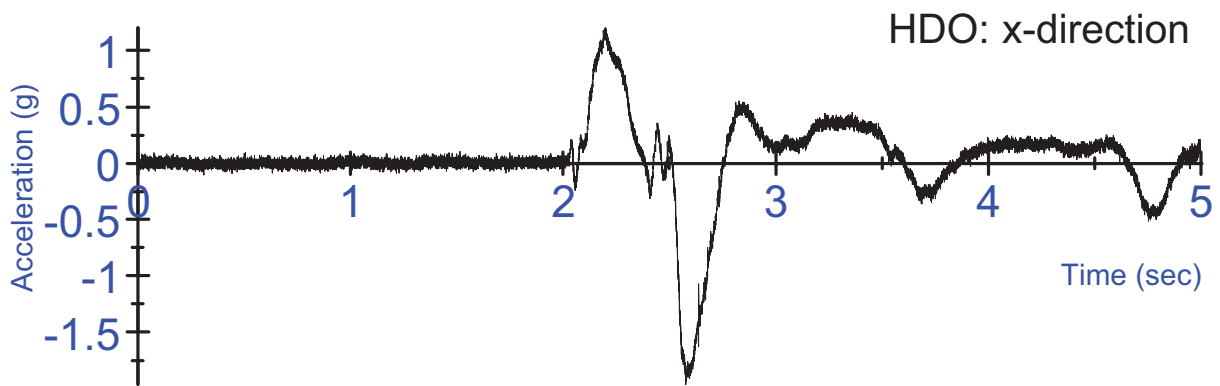
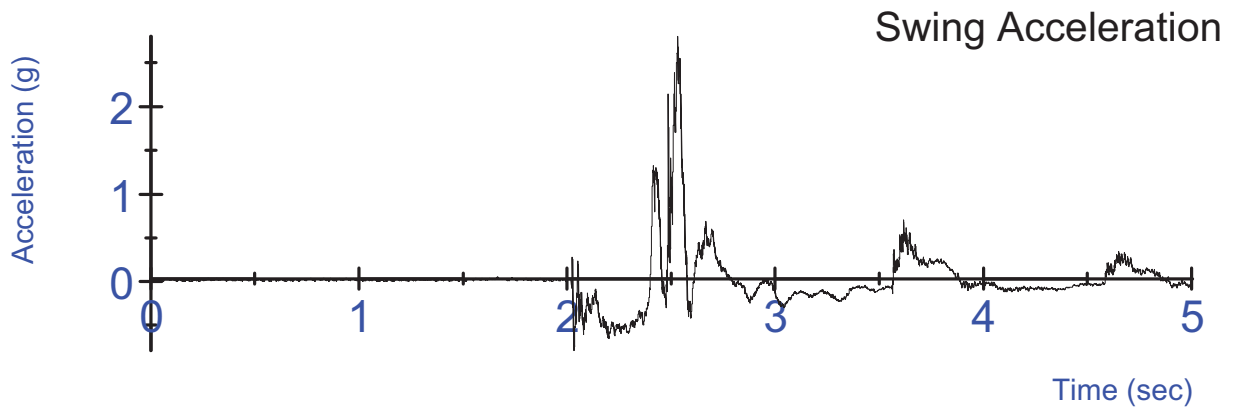
K03 Tensed Test #1 - Swing acceleration, filtered at 180Hz;
3-2-2-2 head acceleration, unfiltered



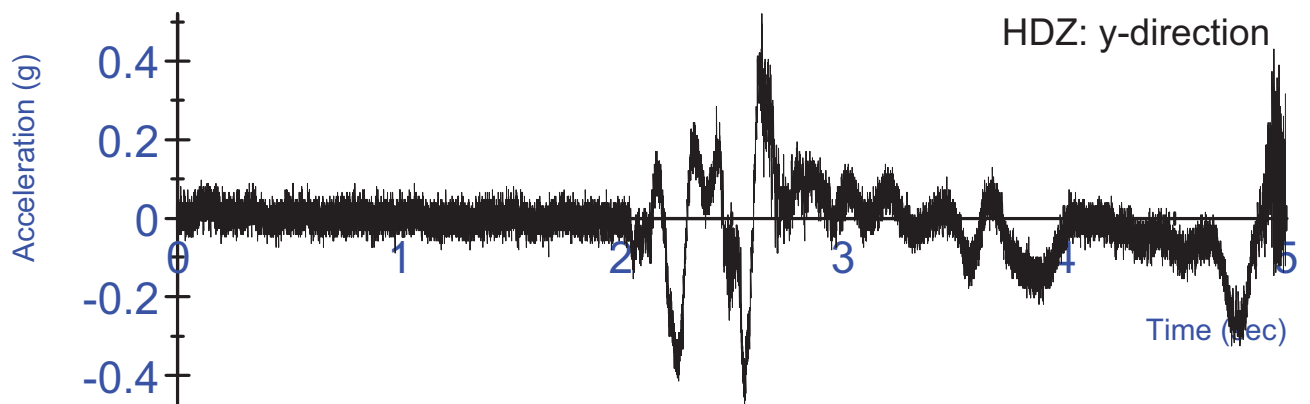
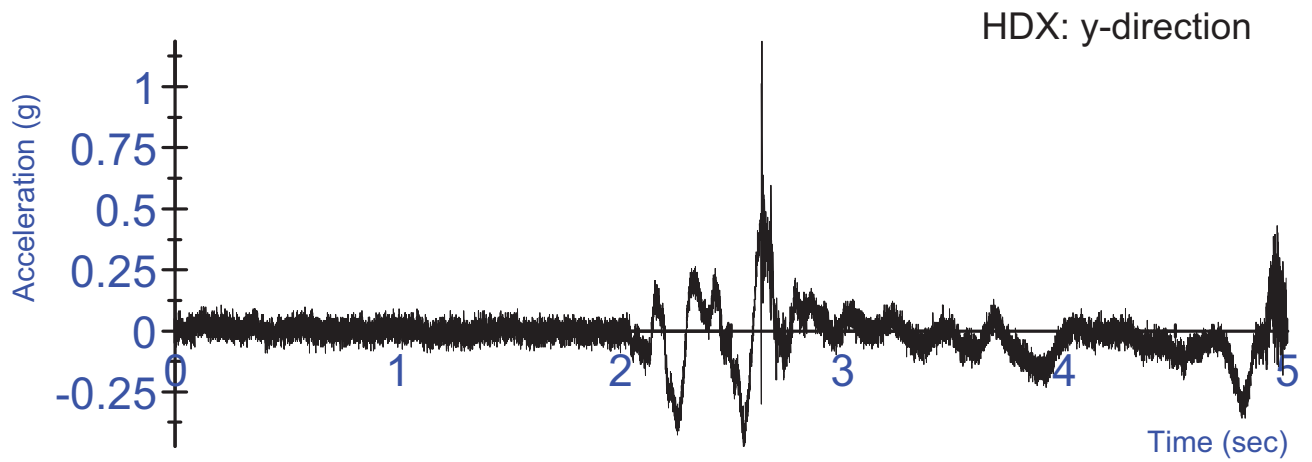
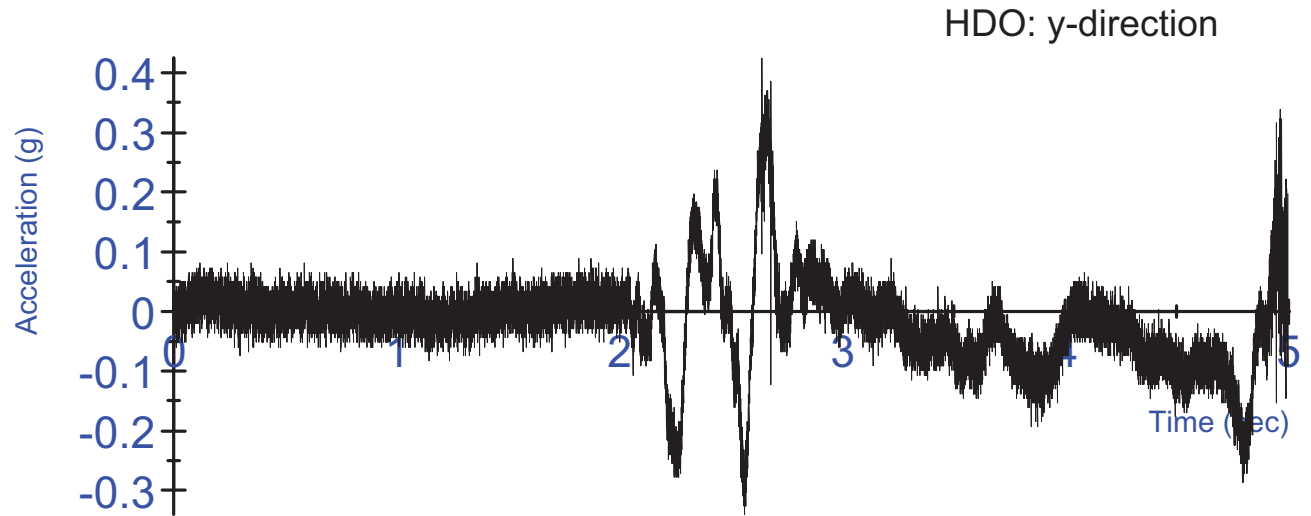
K03 Tensed Test #2 - Right Side EMG activation voltage
Un-rectified, Filtered at 10Hz



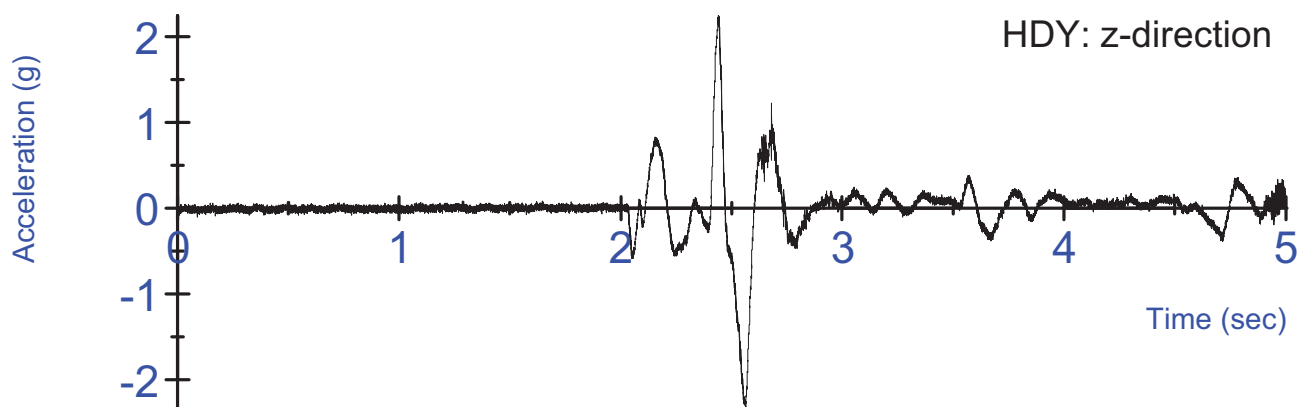
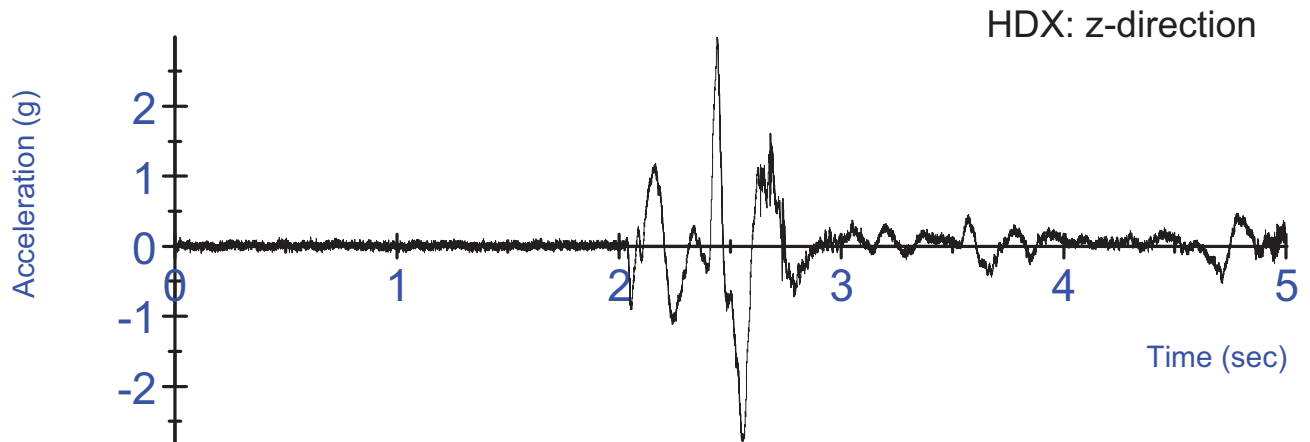
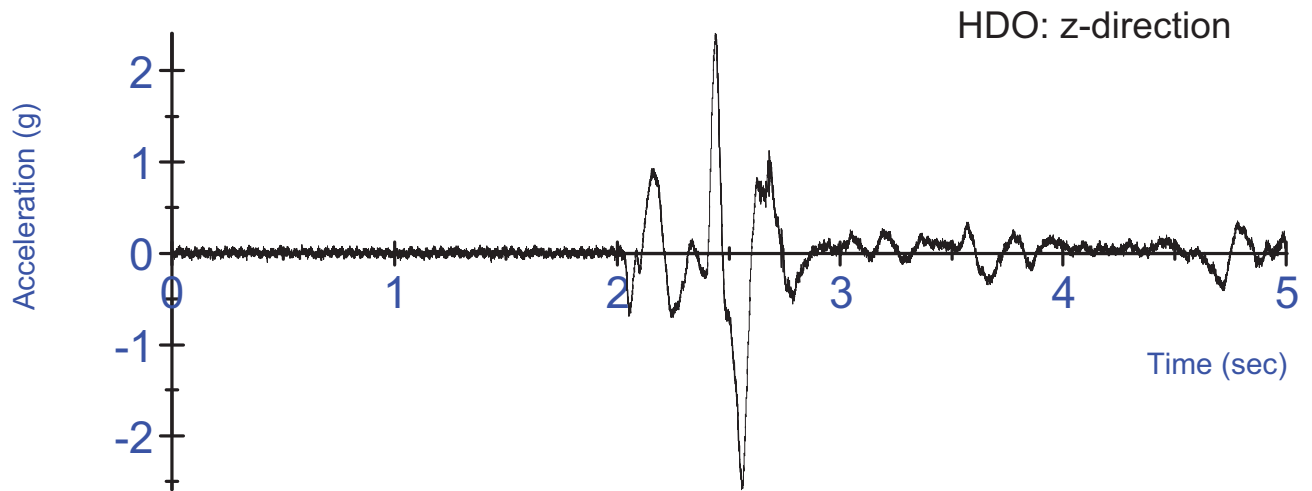
K03 Tensed Test #3- Left Side EMG activation voltage
Un-rectified, Filtered at 10Hz



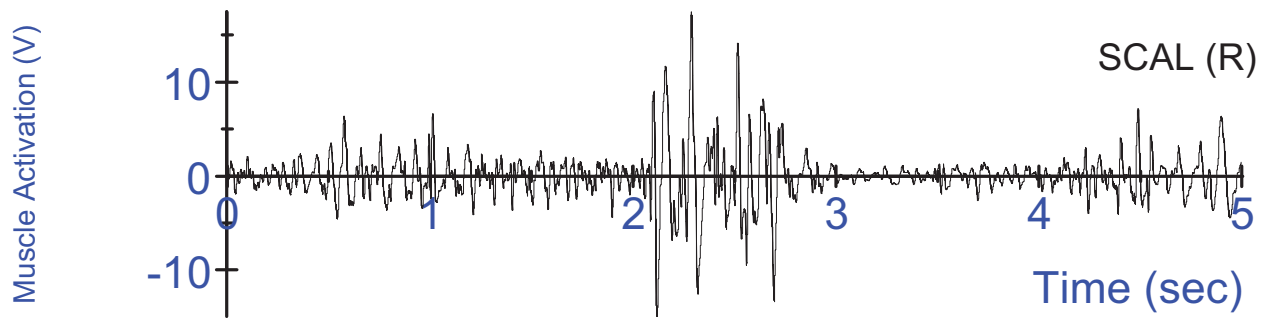
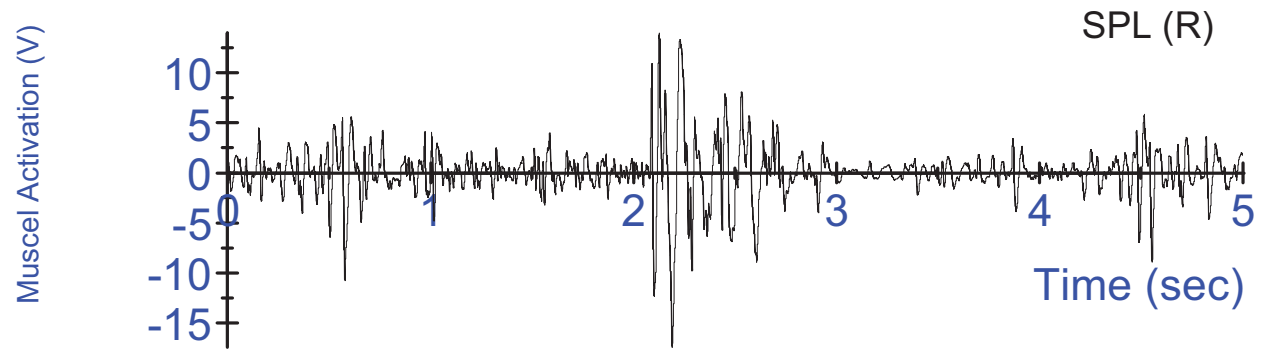
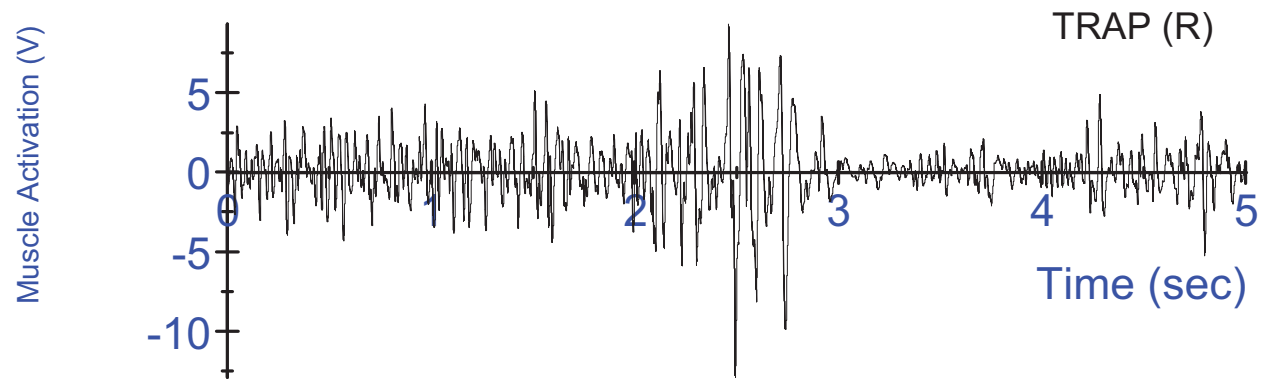
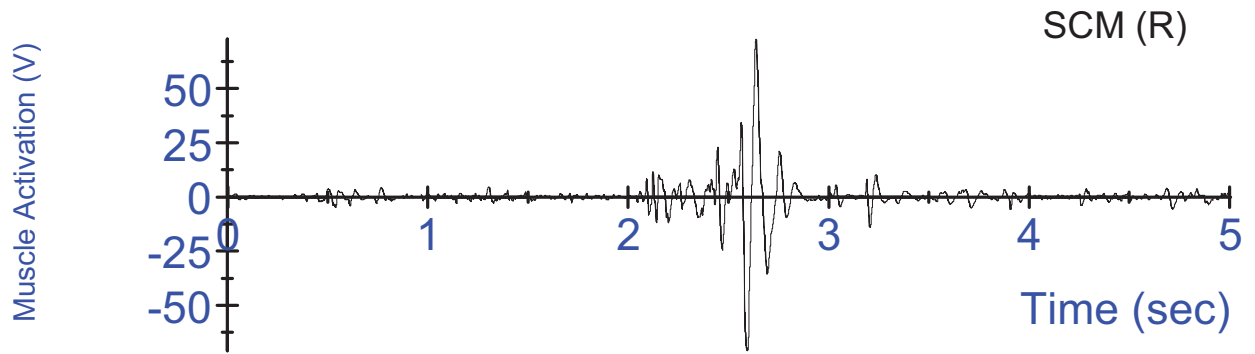
K03 Tensed Test #2 - Swing acceleration, filtered at 180Hz;
3-2-2-2 head acceleration, unfiltered



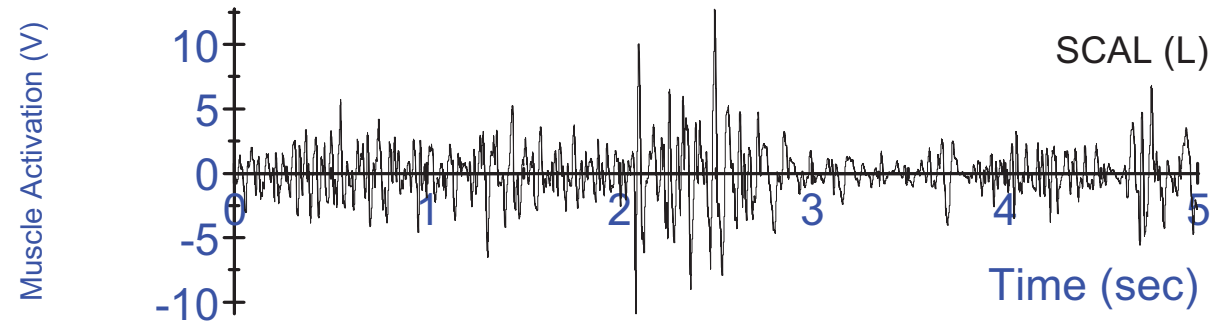
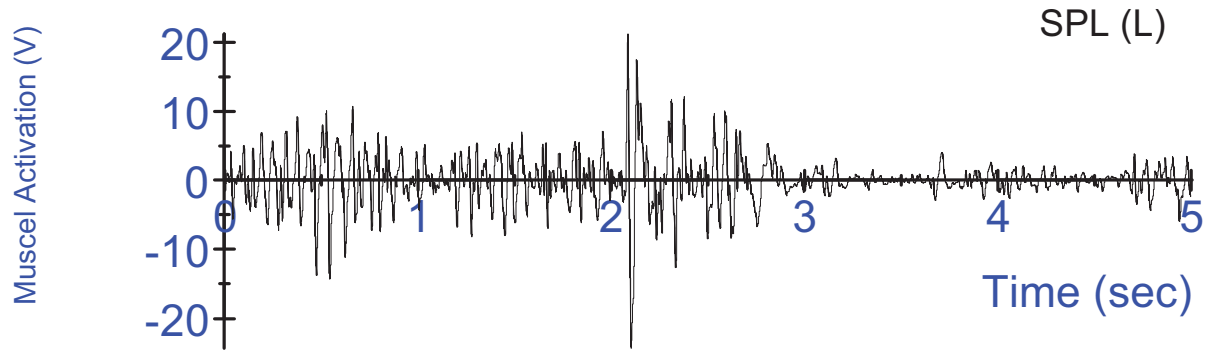
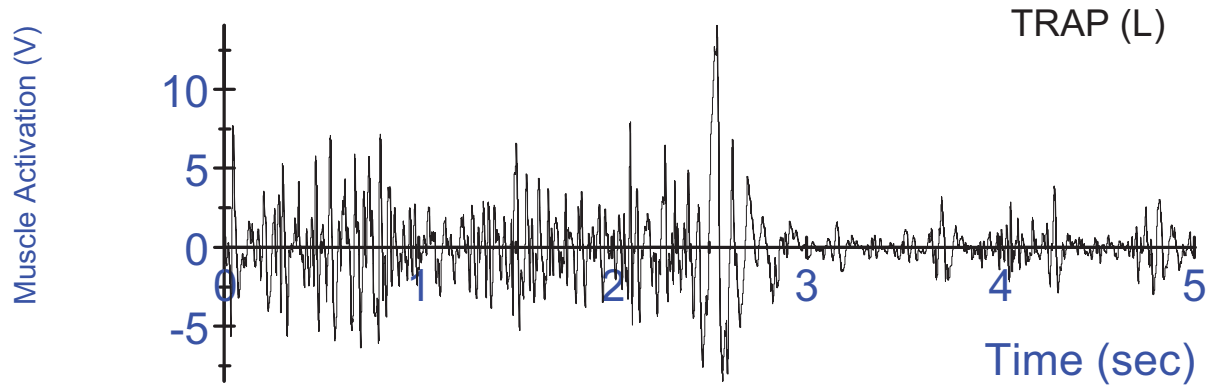
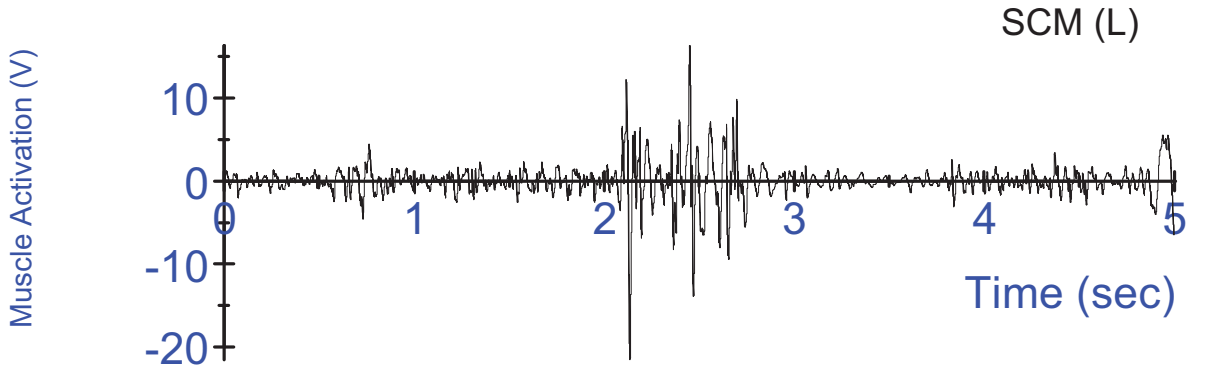
K03 Tensed Test #2 - Swing acceleration, filtered at 180Hz;
3-2-2-2 head acceleration, unfiltered



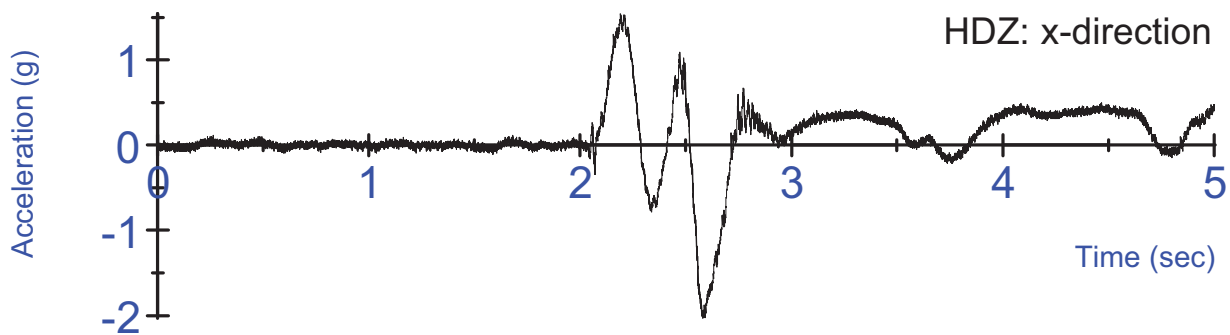
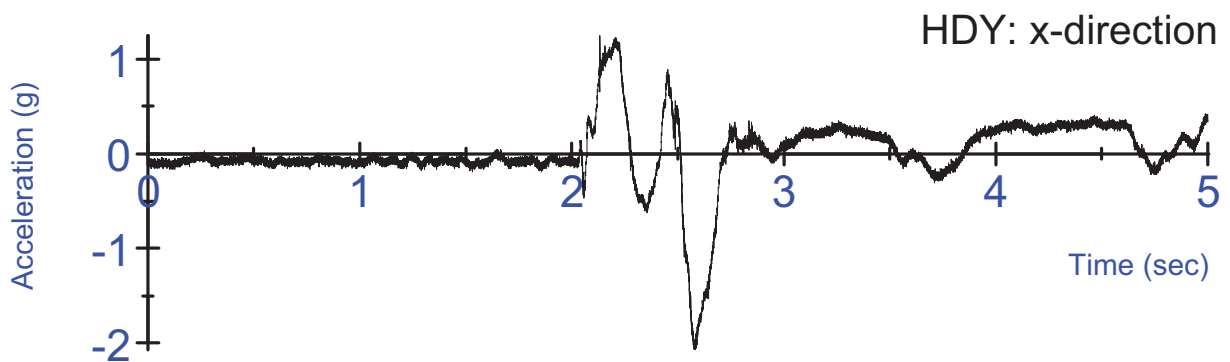
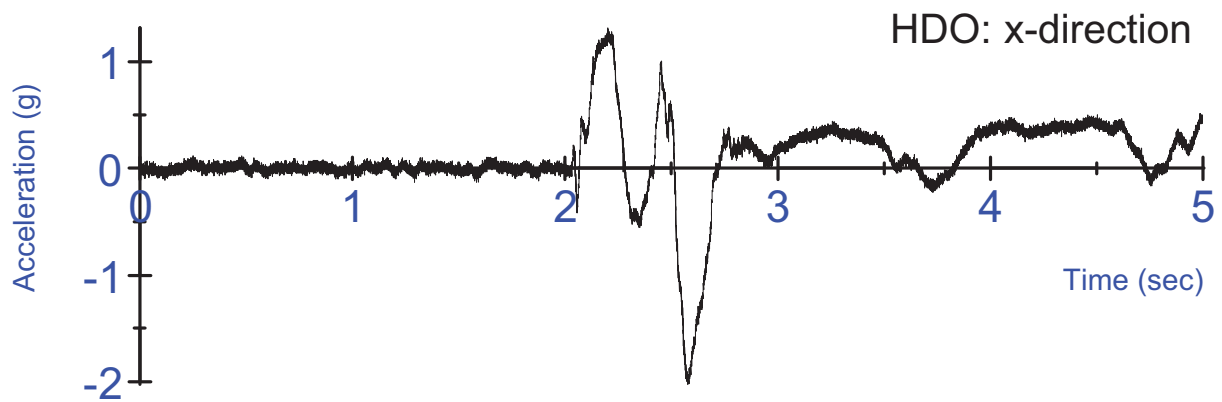
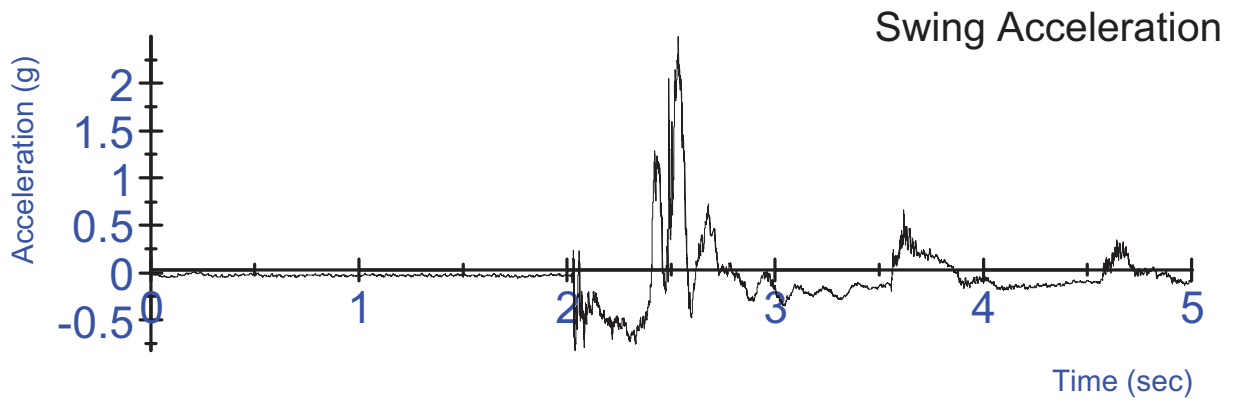
K03 Tensed Test #2 - Swing acceleration, filtered at 180Hz;
3-2-2-2 head acceleration, unfiltered



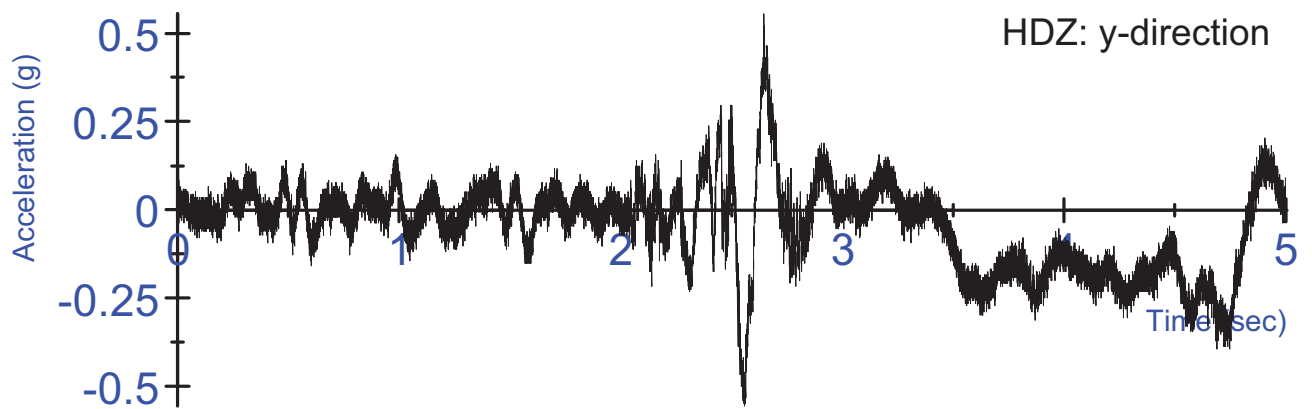
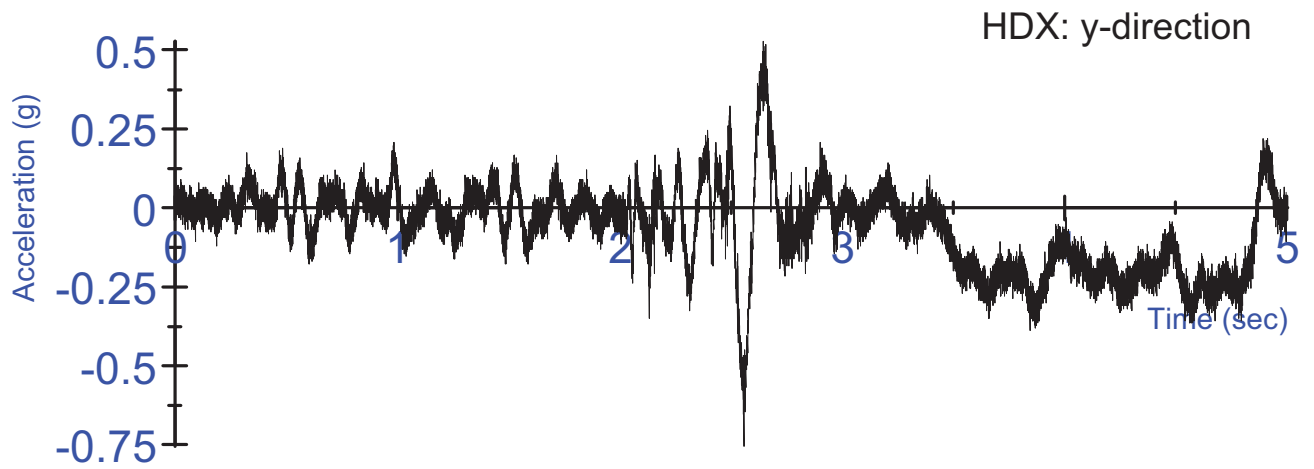
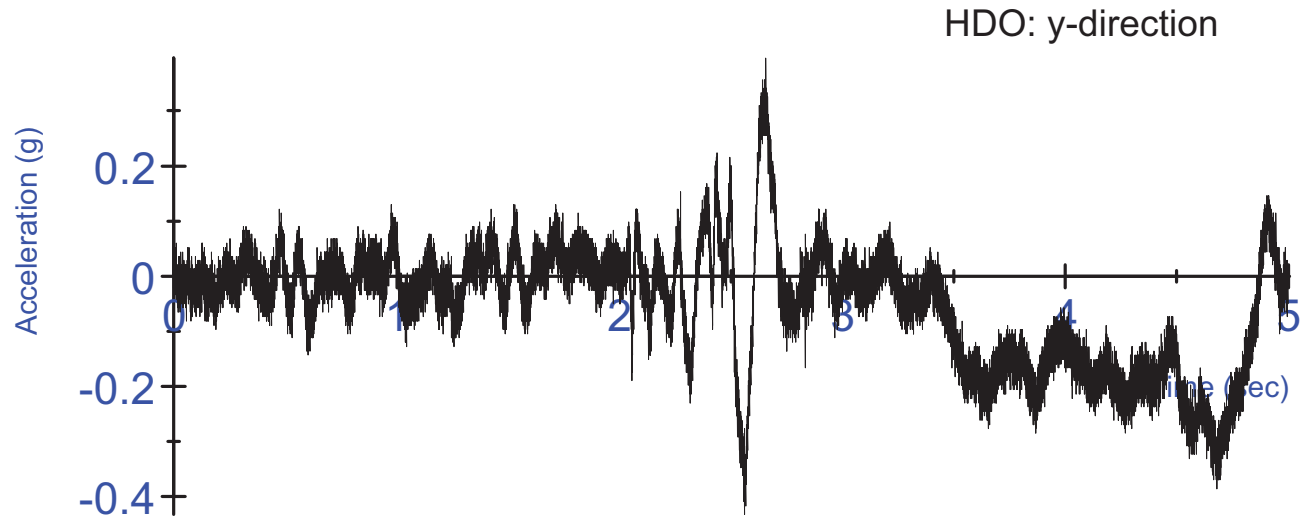
K03 Tensed Test #3 - Right Side EMG activation voltage
Un-rectified, Filtered at 10Hz



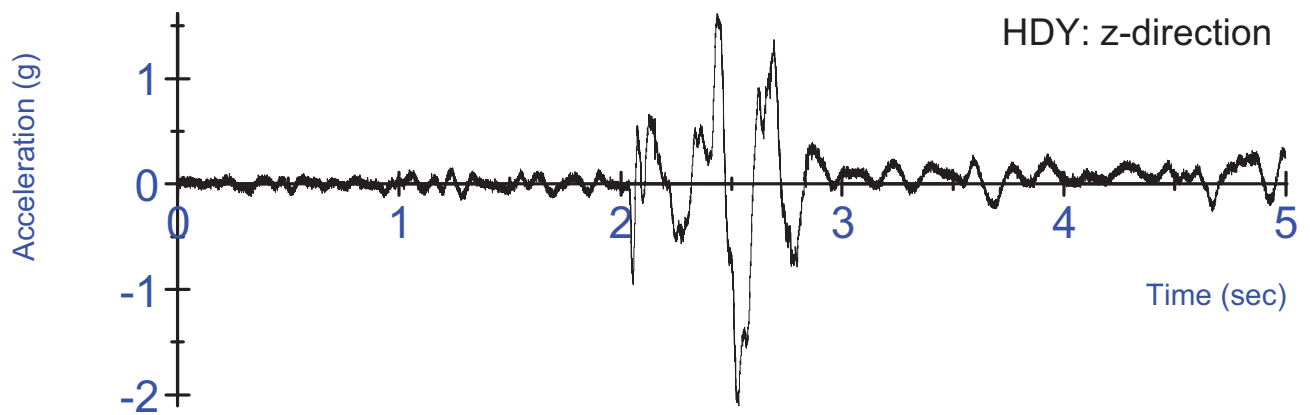
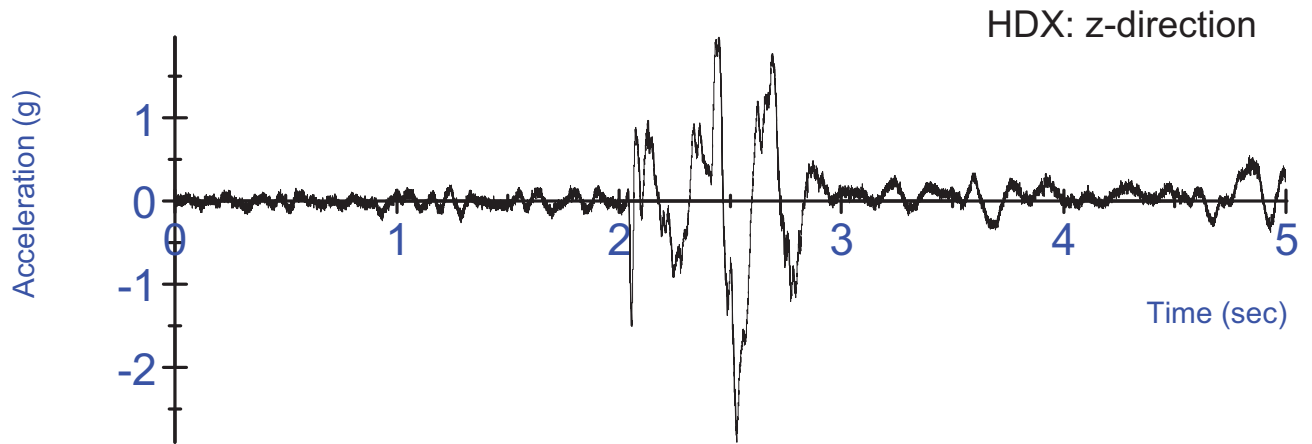
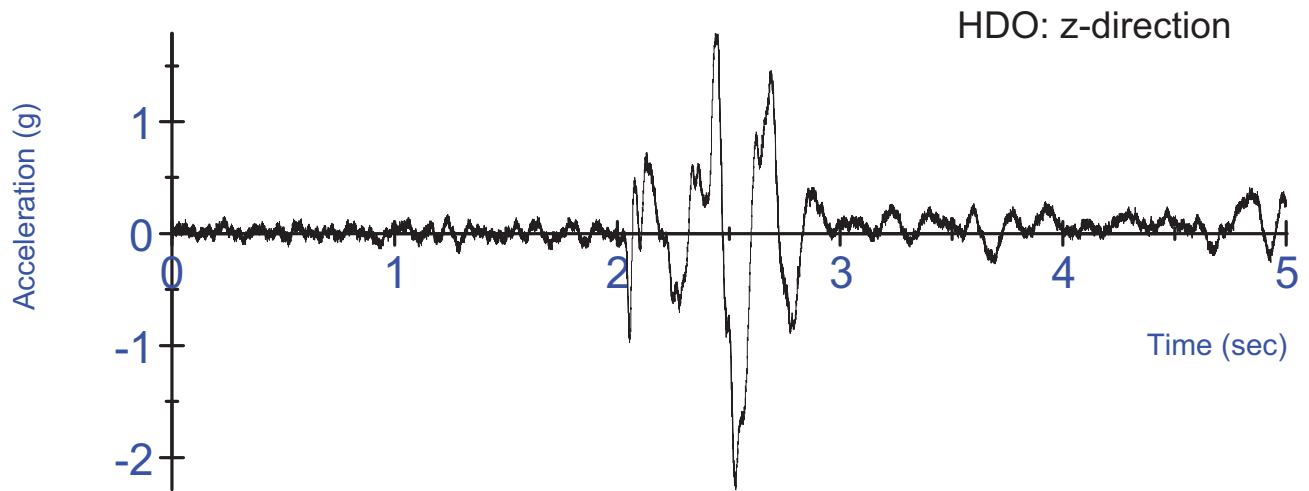
K03 Tensed Test #3- Left Side EMG activation voltage
Un-rectified, Filtered at 10Hz



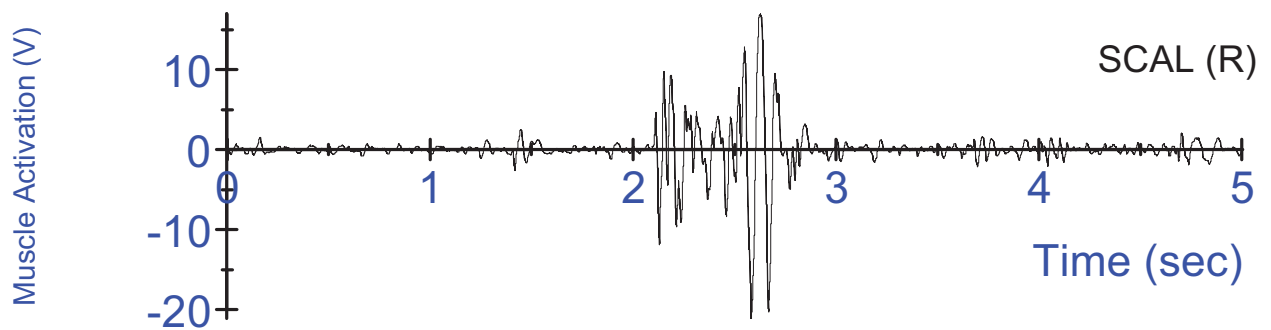
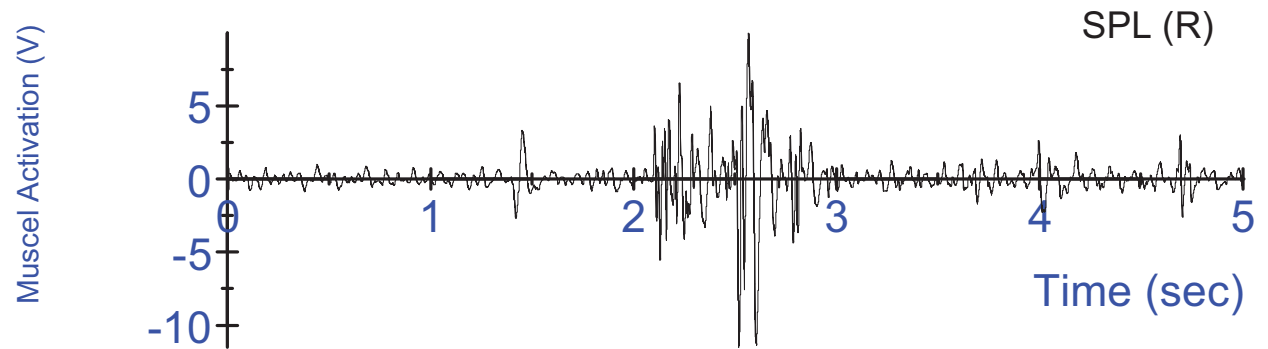
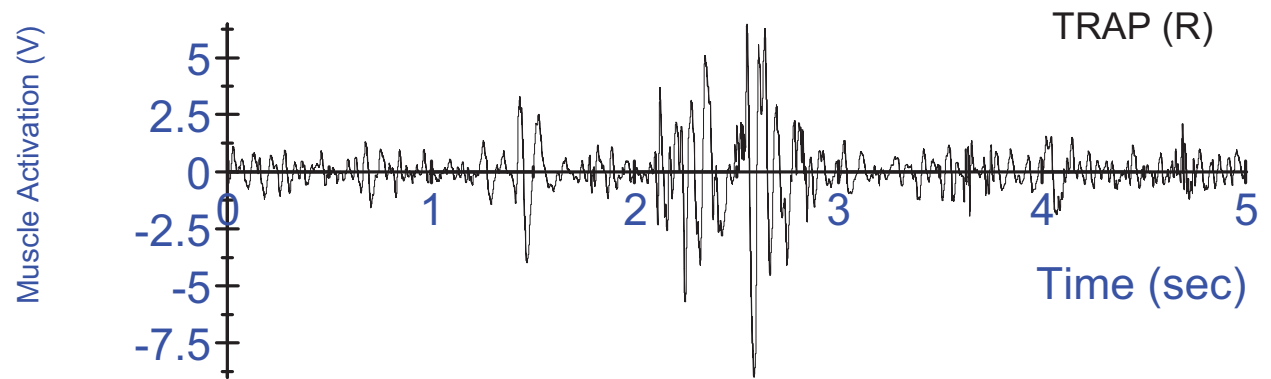
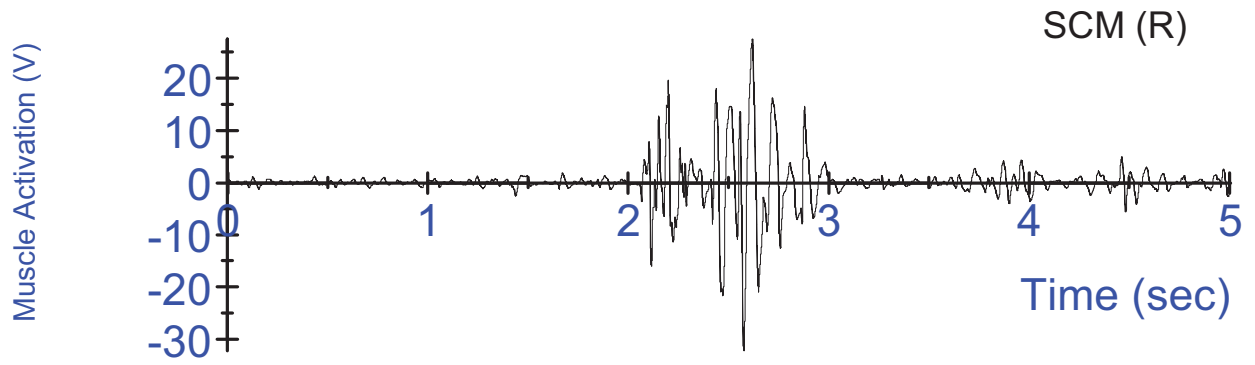
K03 Tensed Test #3 - Swing acceleration, filtered at 180Hz;
3-2-2-2 head acceleration, unfiltered



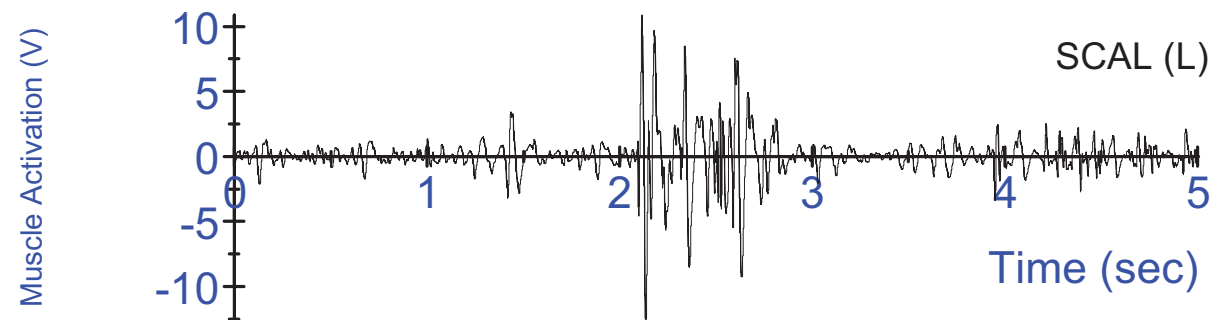
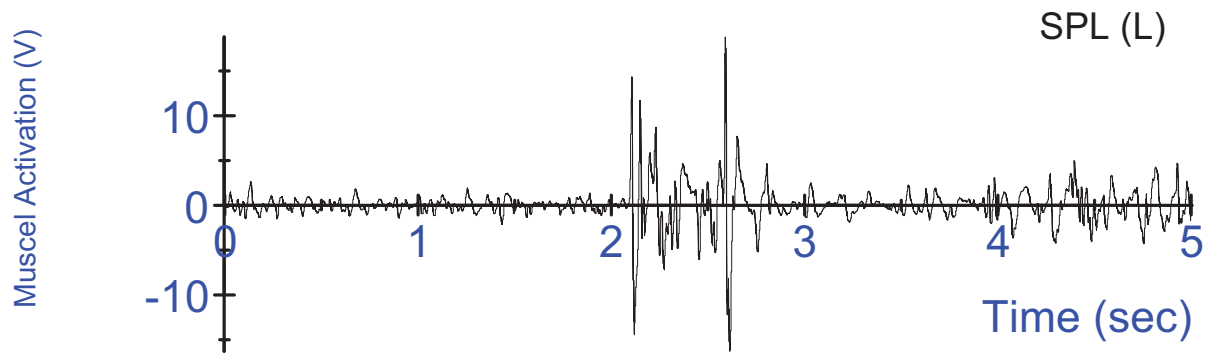
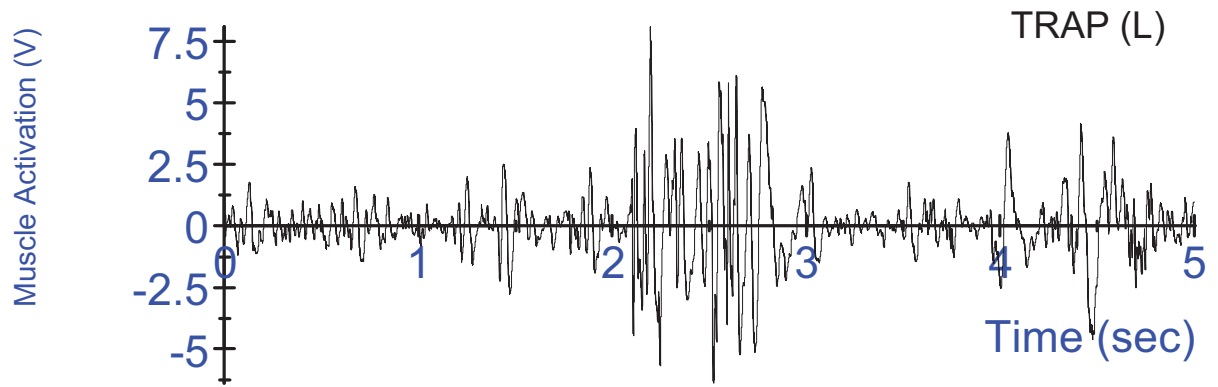
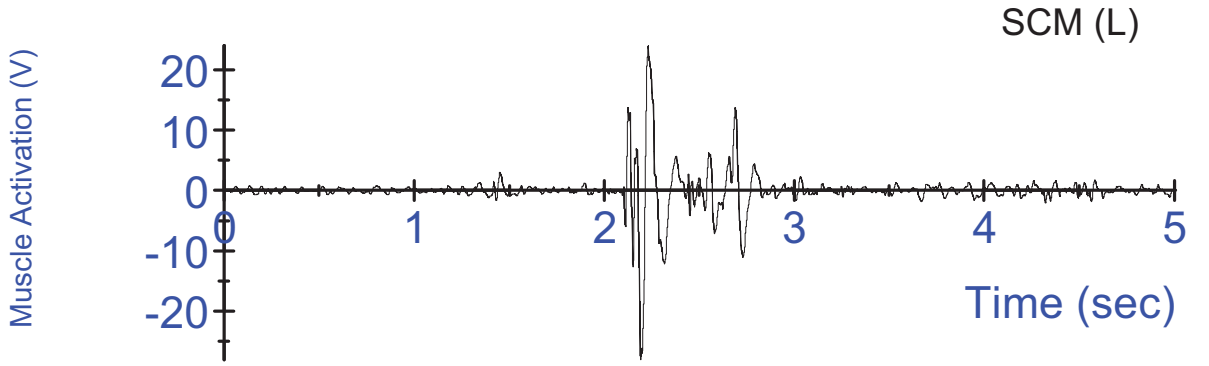
K03 Tensed Test #3 - Swing acceleration, filtered at 180Hz;
3-2-2-2 head acceleration, unfiltered



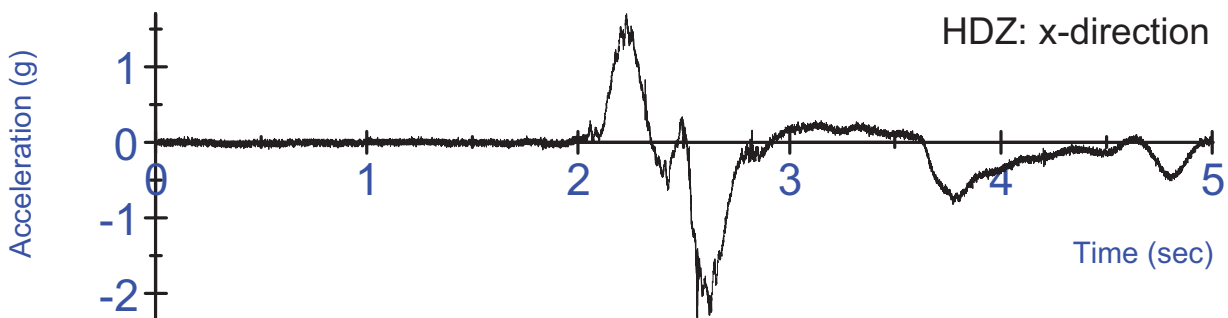
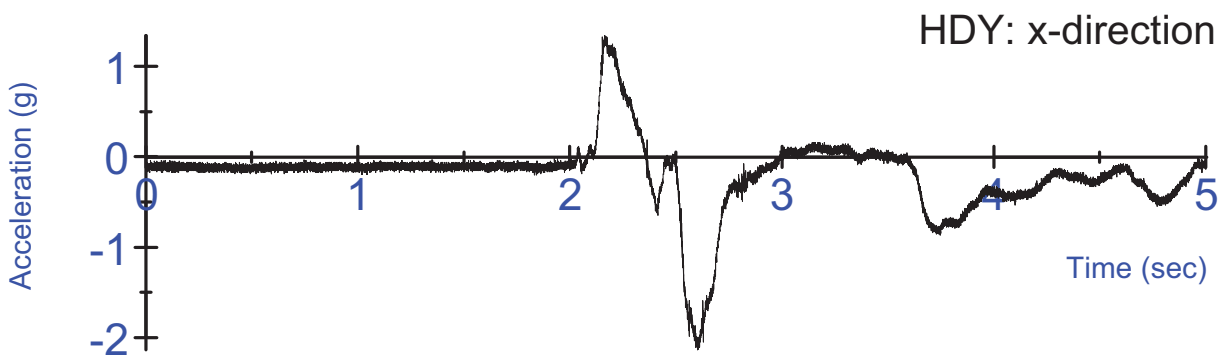
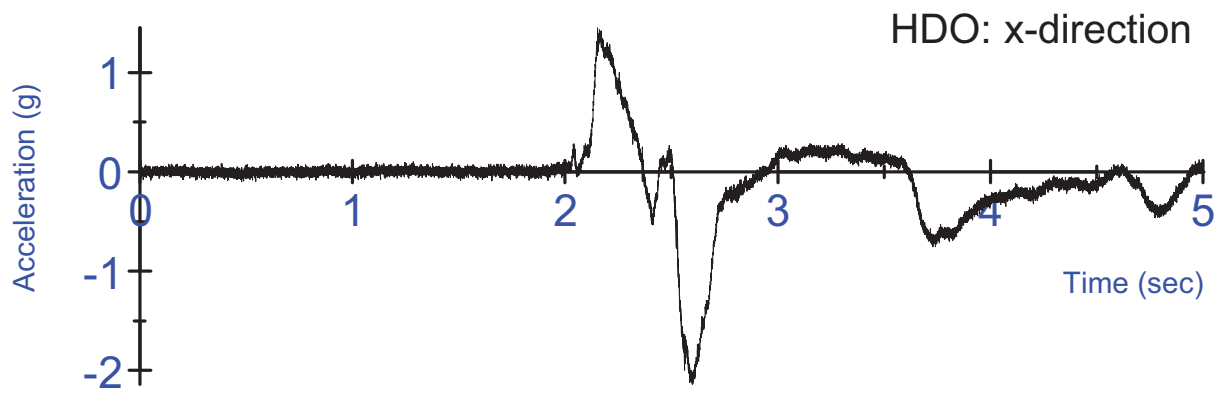
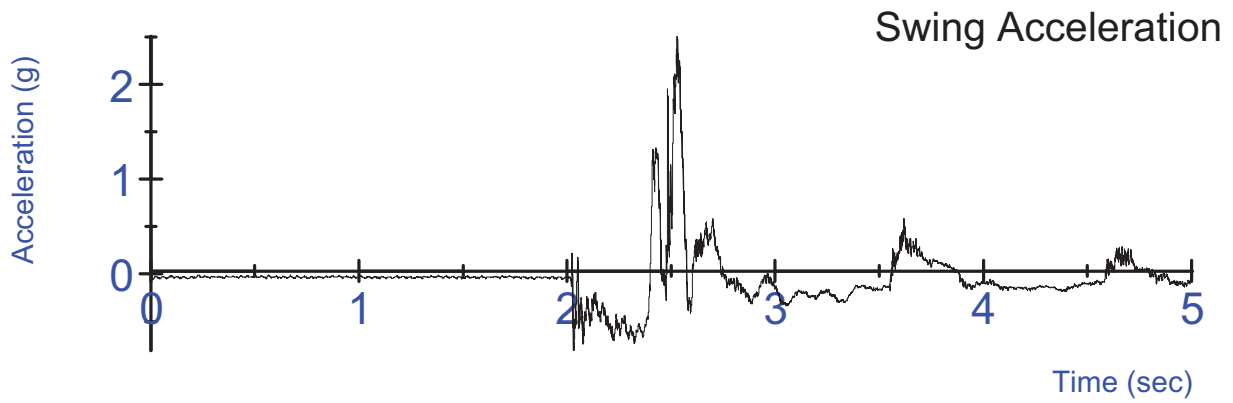
K03 Tensed Test #3 - Swing acceleration, filtered at 180Hz;
3-2-2-2 head acceleration, unfiltered



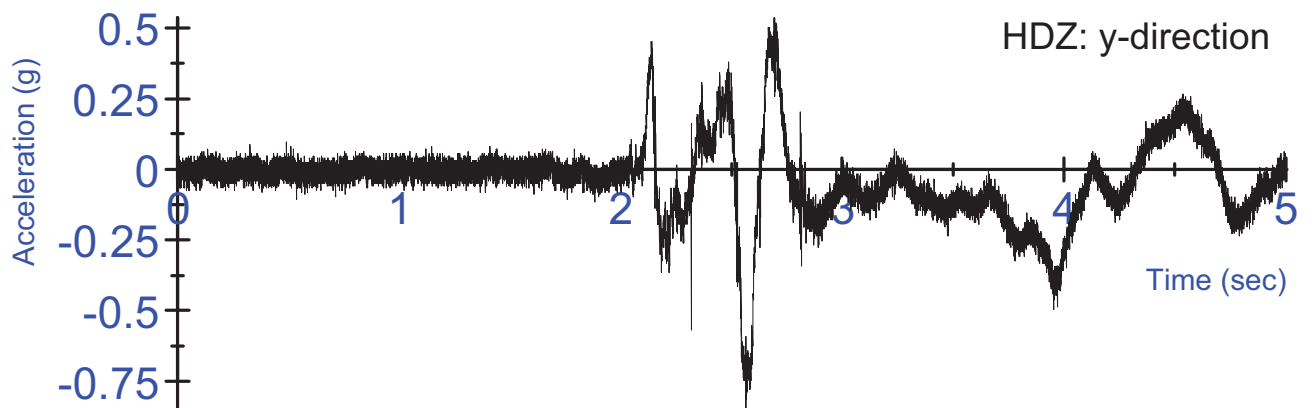
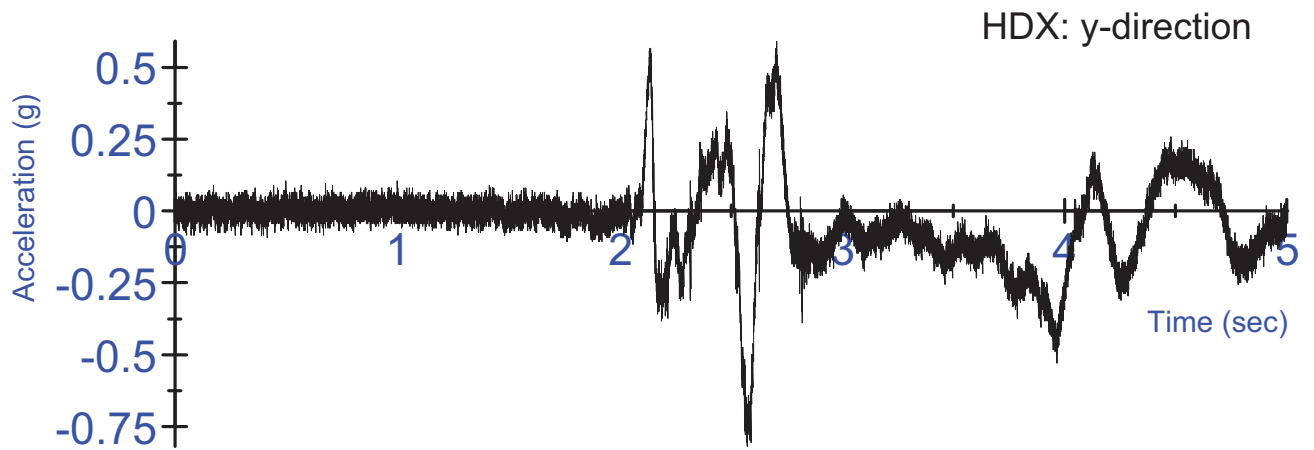
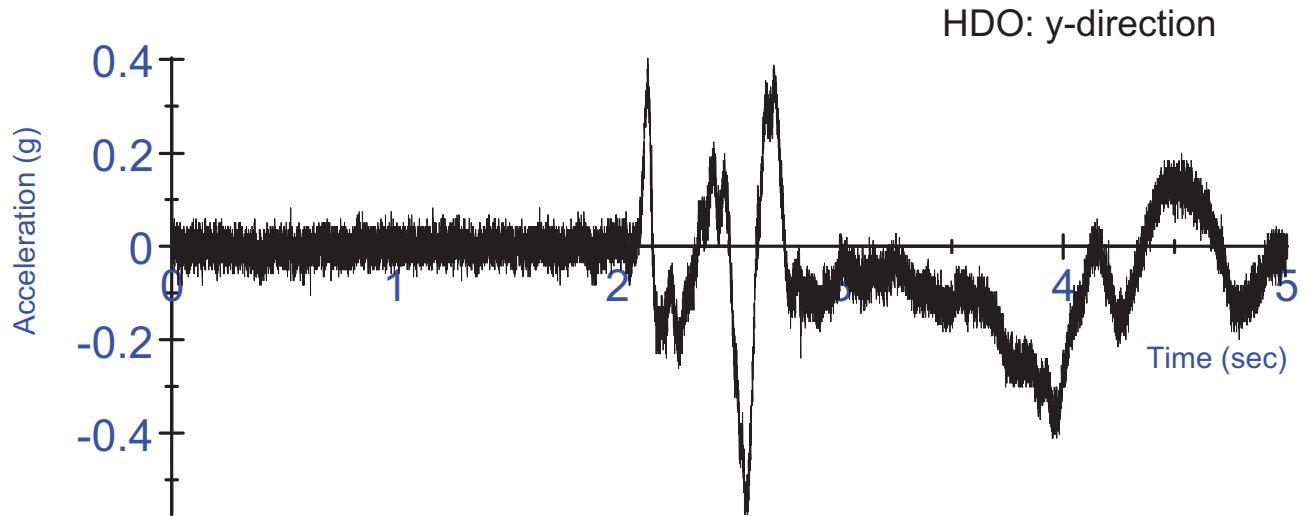
K03 Untensed Test #1 - Right Side EMG activation voltage
Un-rectified, Filtered at 10Hz



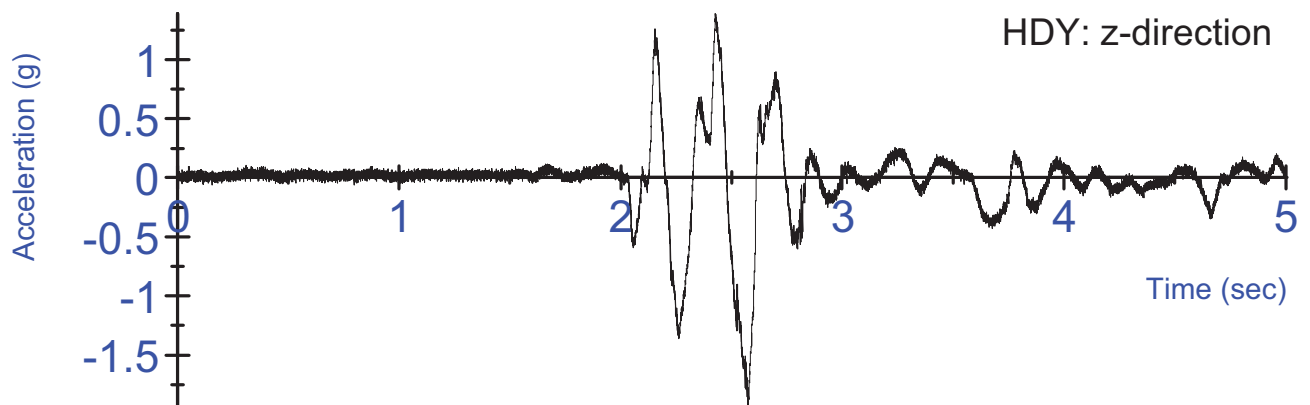
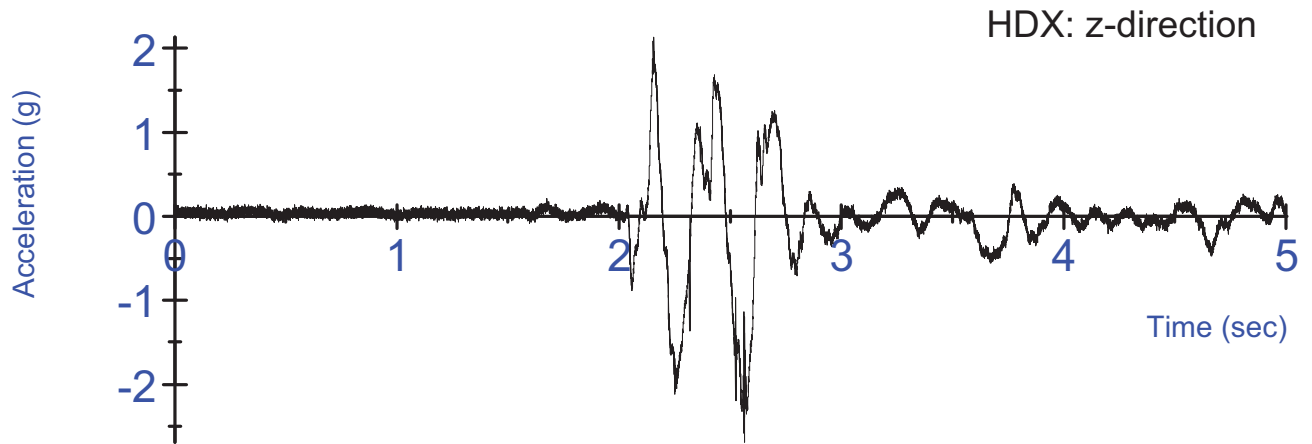
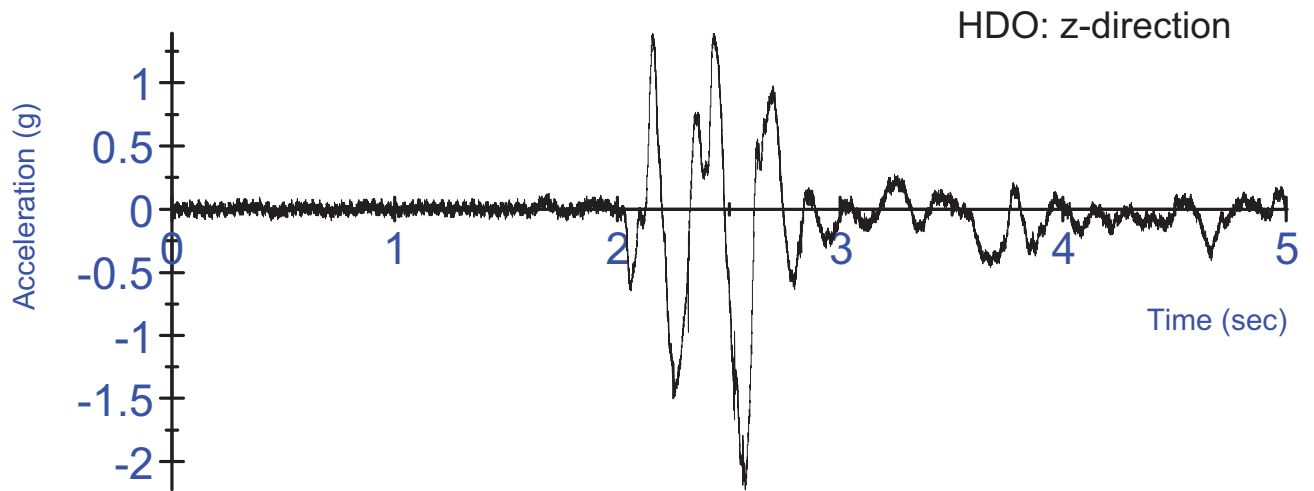
K03 Untensed Test #1- Left Side EMG activation voltage
Un-rectified, Filtered at 10Hz



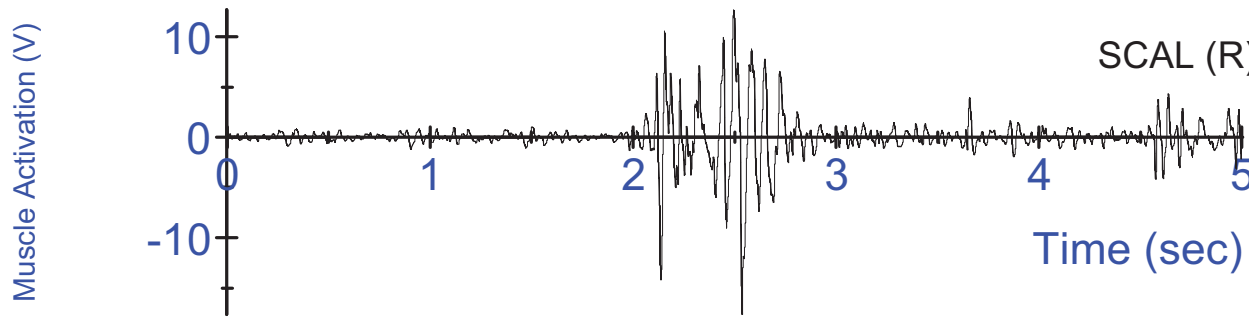
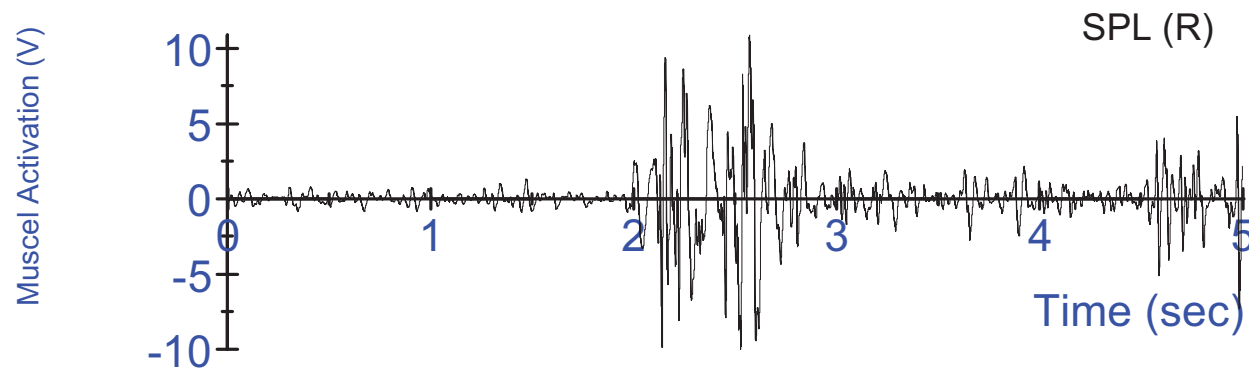
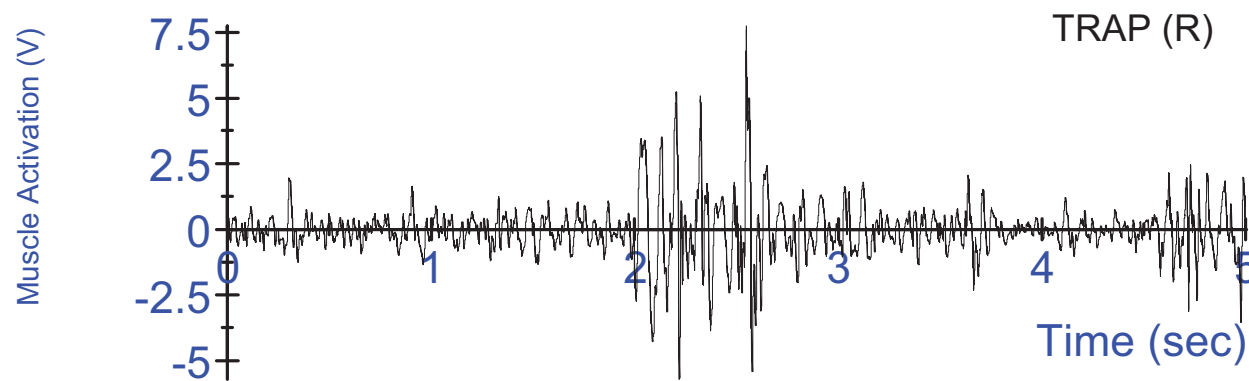
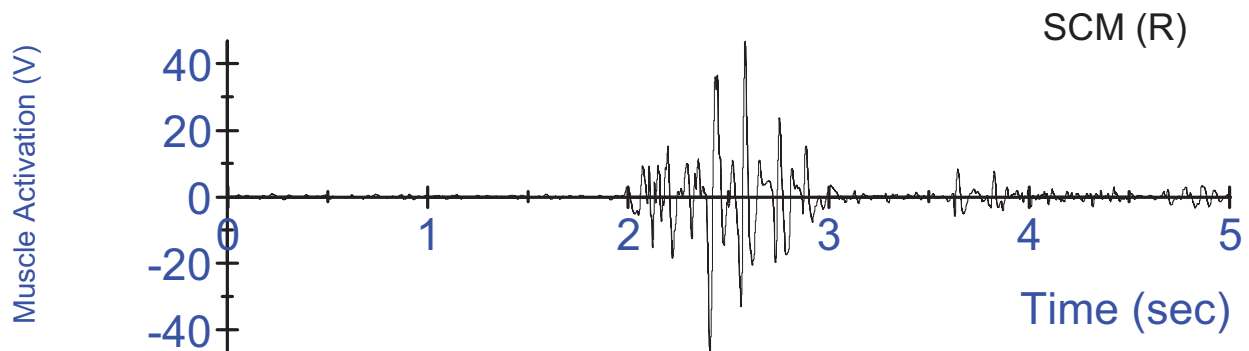
K03 Untensed Test #1 - Swing acceleration, filtered at 180Hz;
3-2-2-2 head acceleration, unfiltered



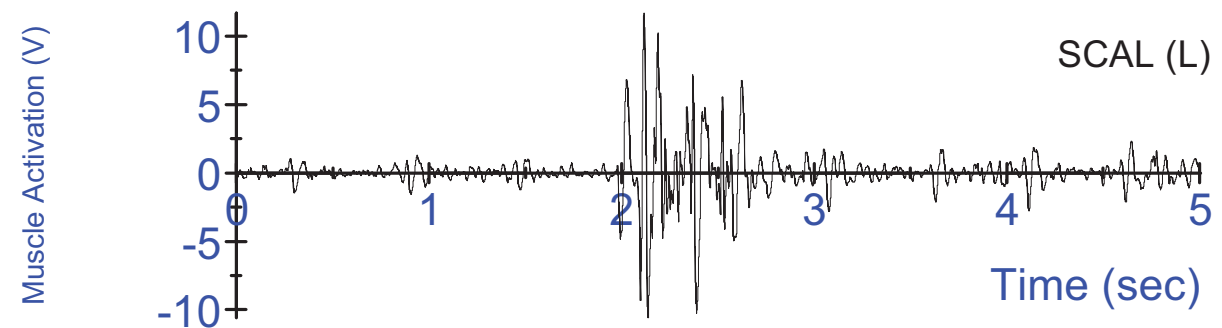
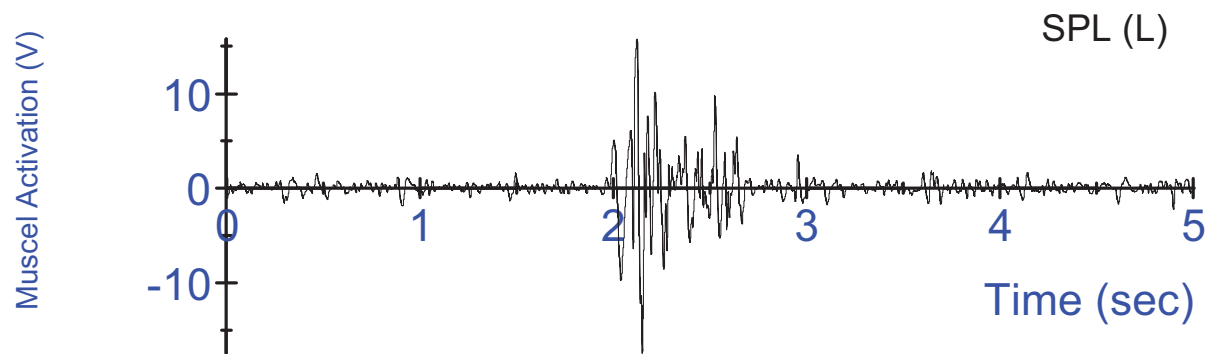
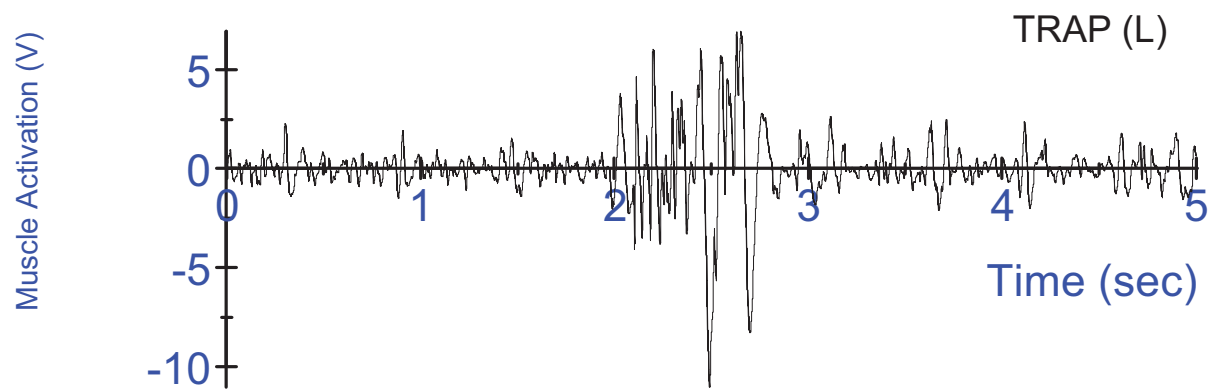
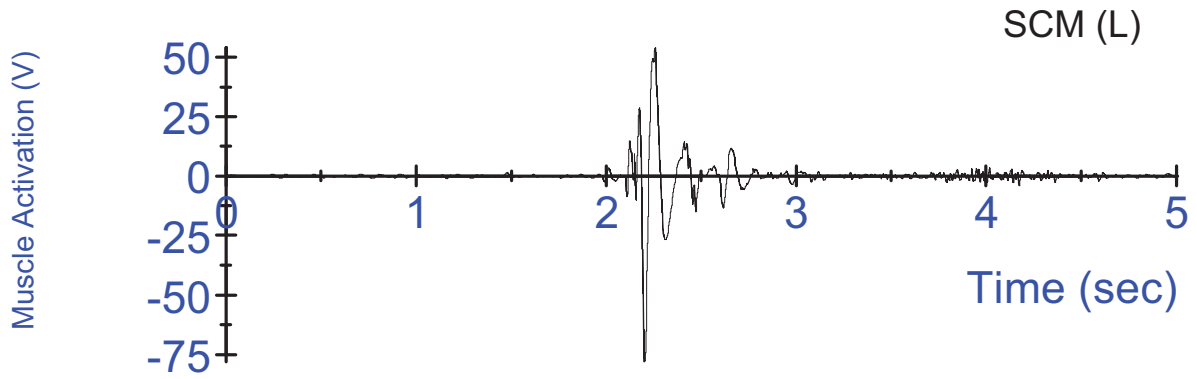
K03 Untensed Test #1 - Swing acceleration, filtered at 180Hz;
3-2-2-2 head acceleration, unfiltered



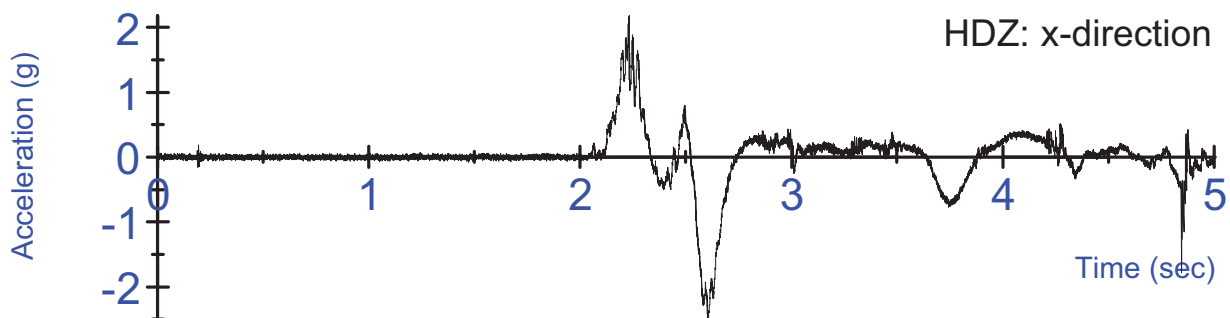
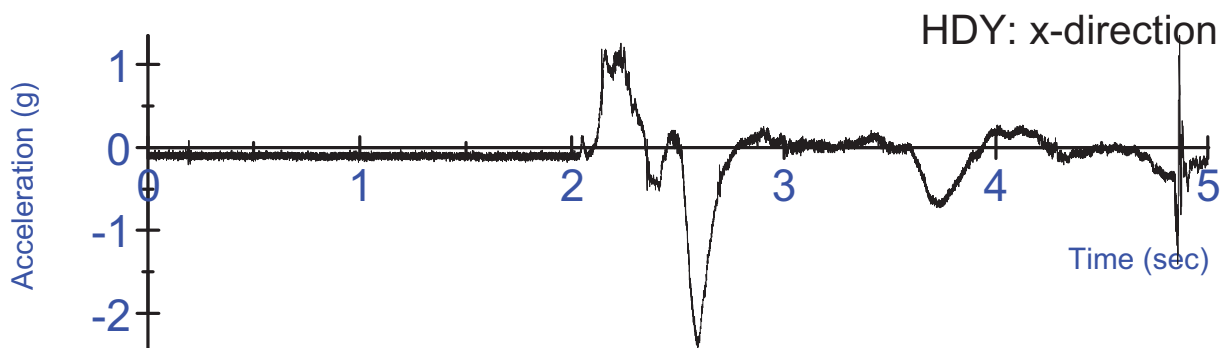
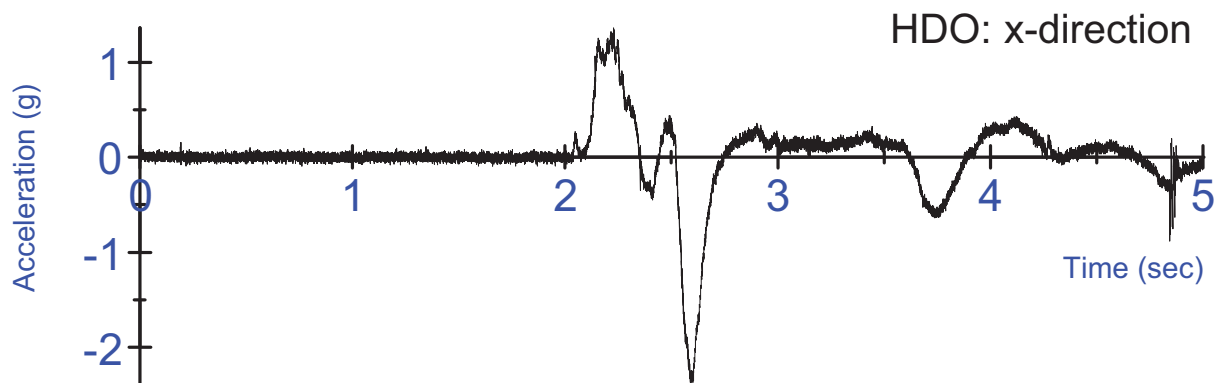
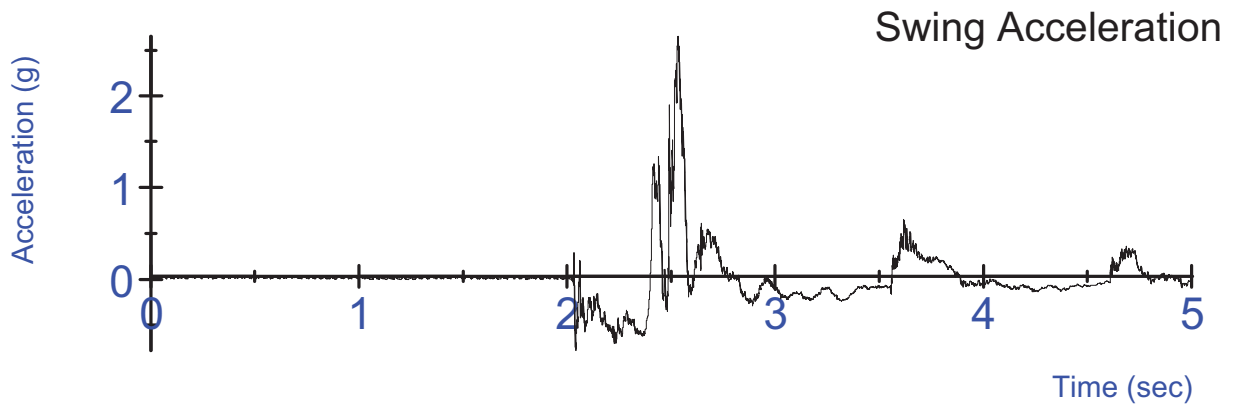
K03 Untensed Test #1 - Swing acceleration, filtered at 180Hz;
3-2-2-2 head acceleration, unfiltered



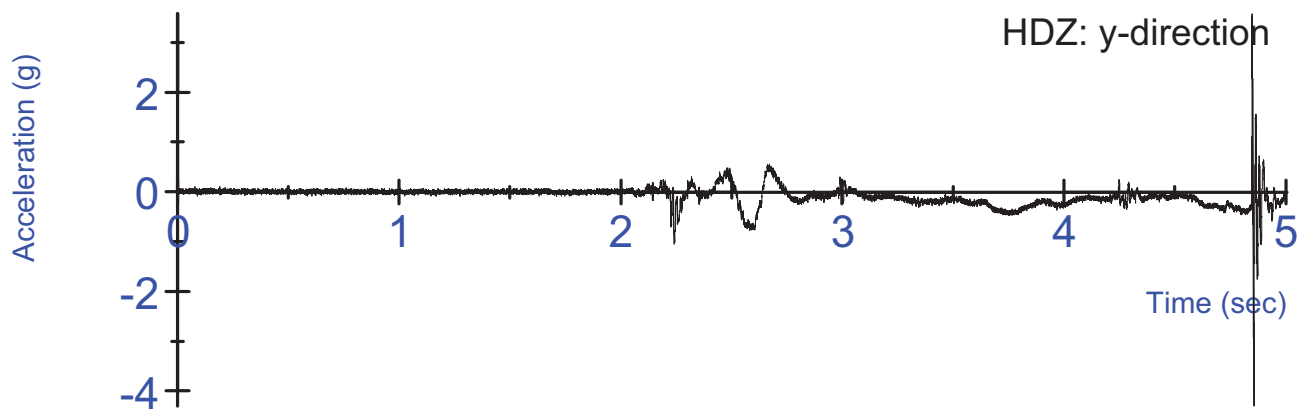
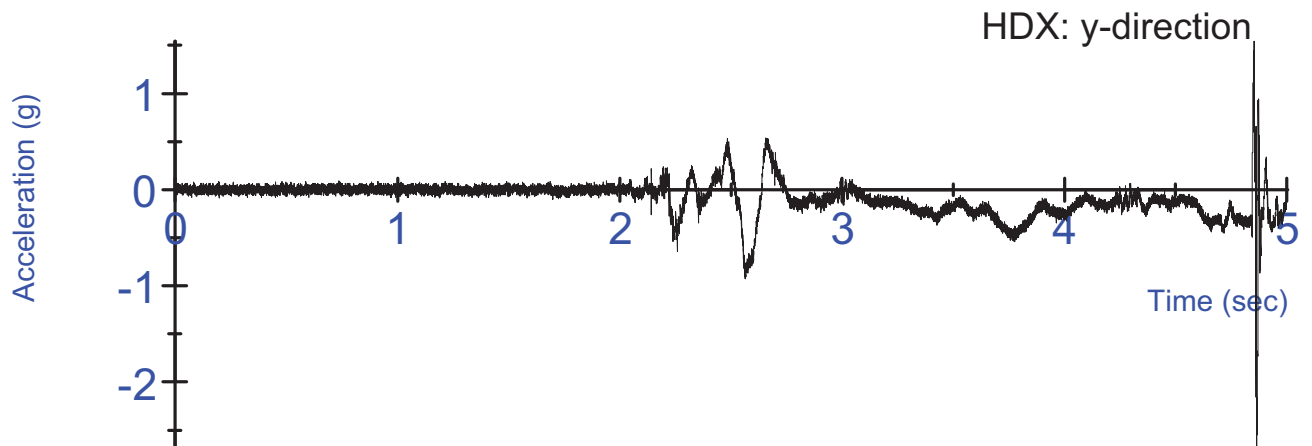
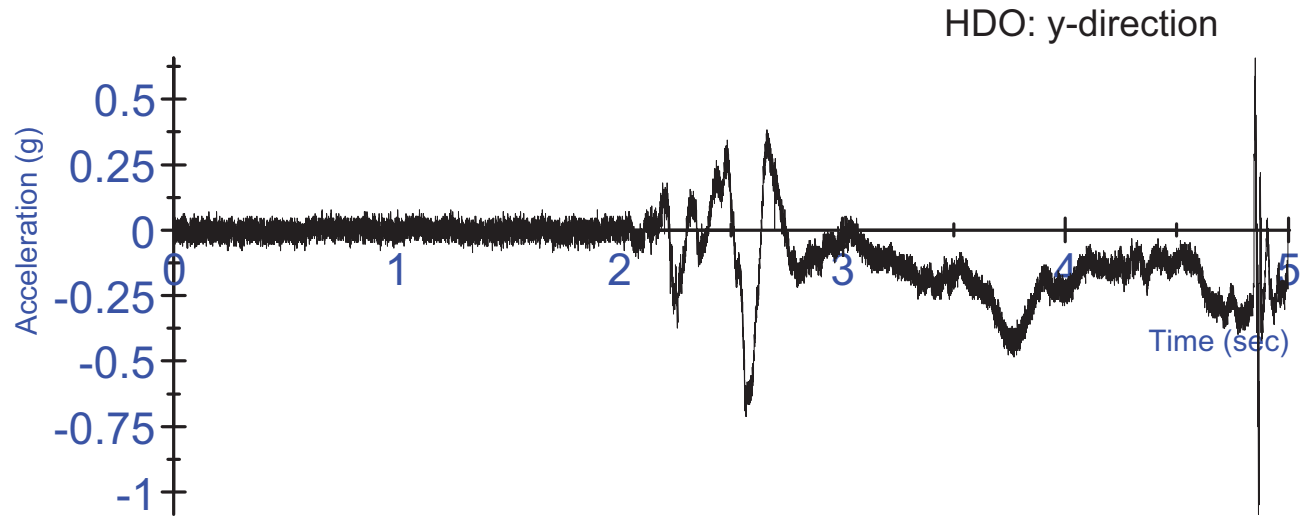
K03 Untensed Test #2 - Right Side EMG activation voltage
Un-rectified, Filtered at 10Hz



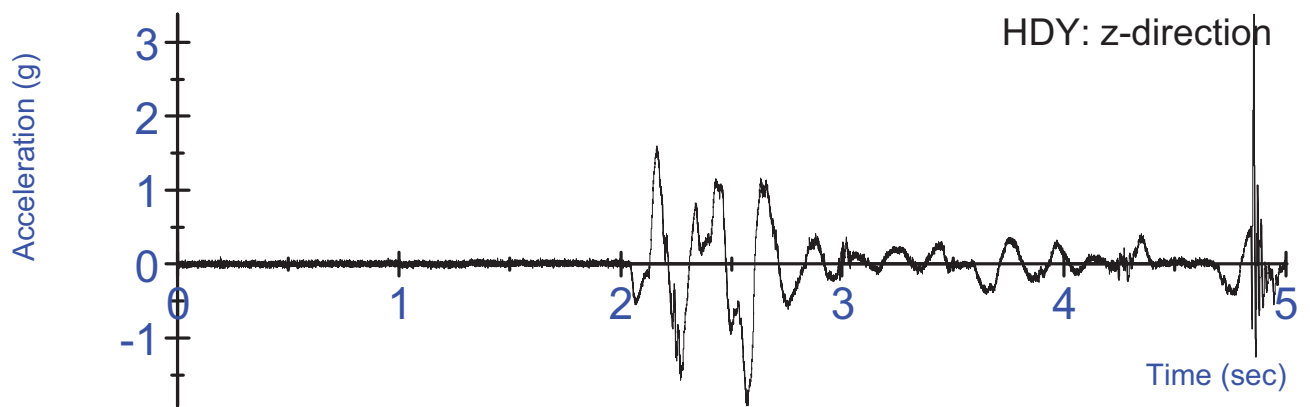
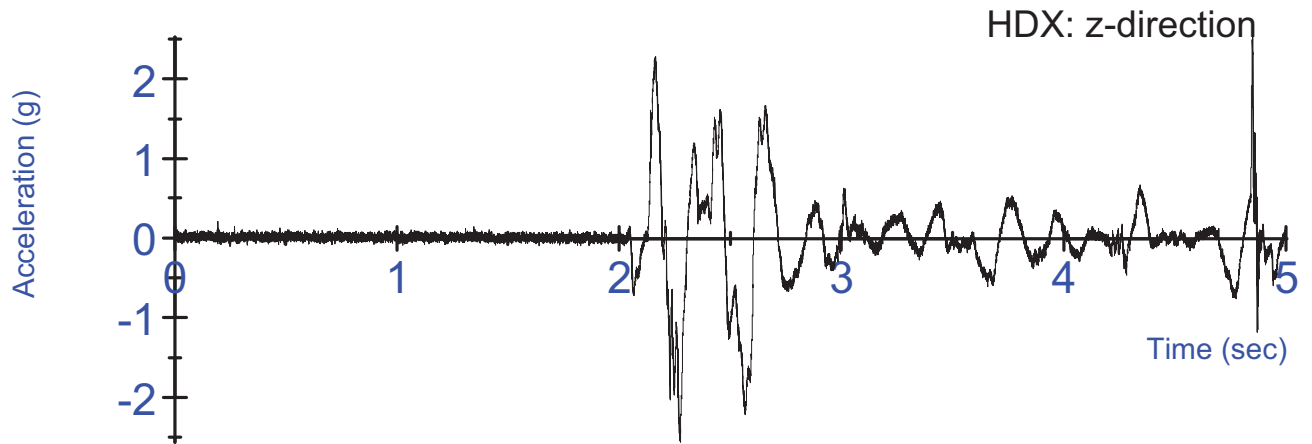
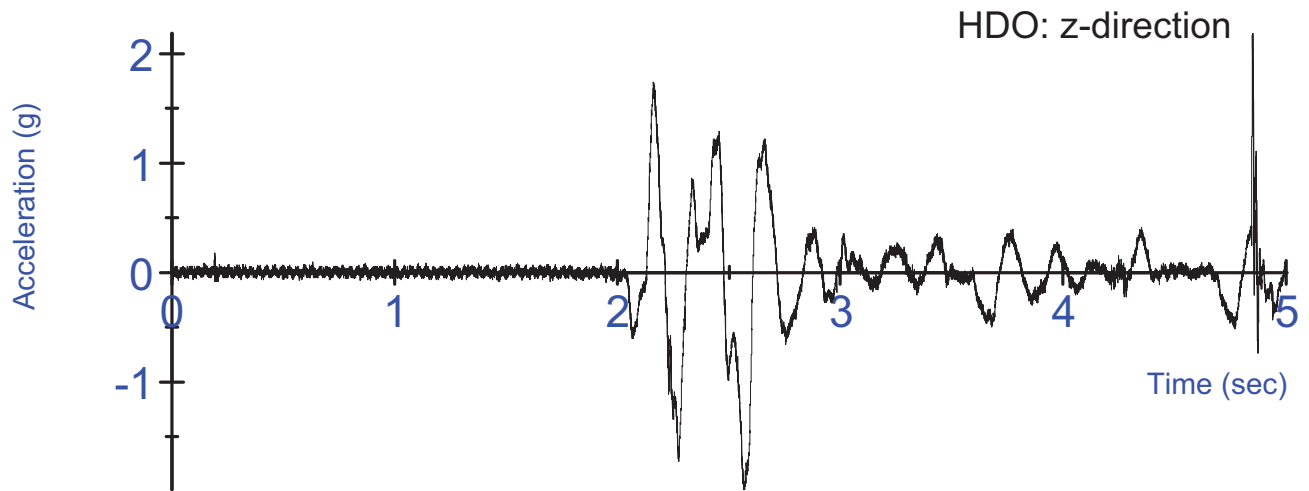
K03 Untensed Test #2- Left Side EMG activation voltage
Un-rectified, Filtered at 10Hz



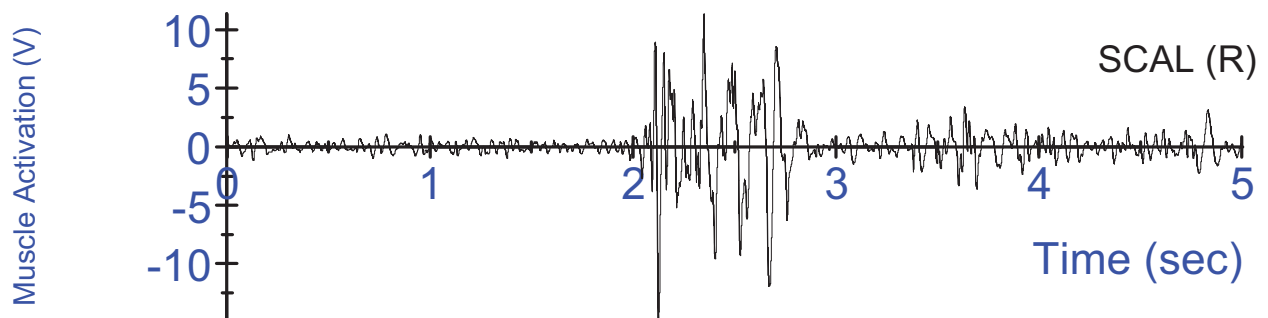
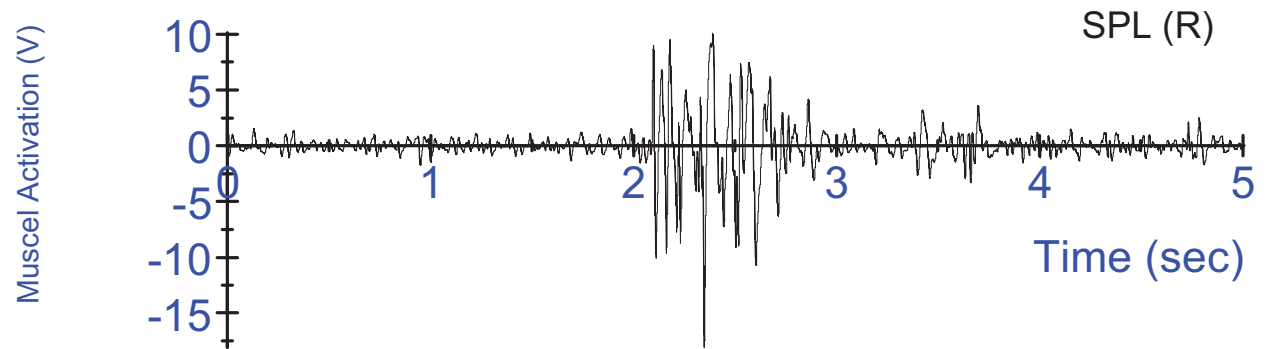
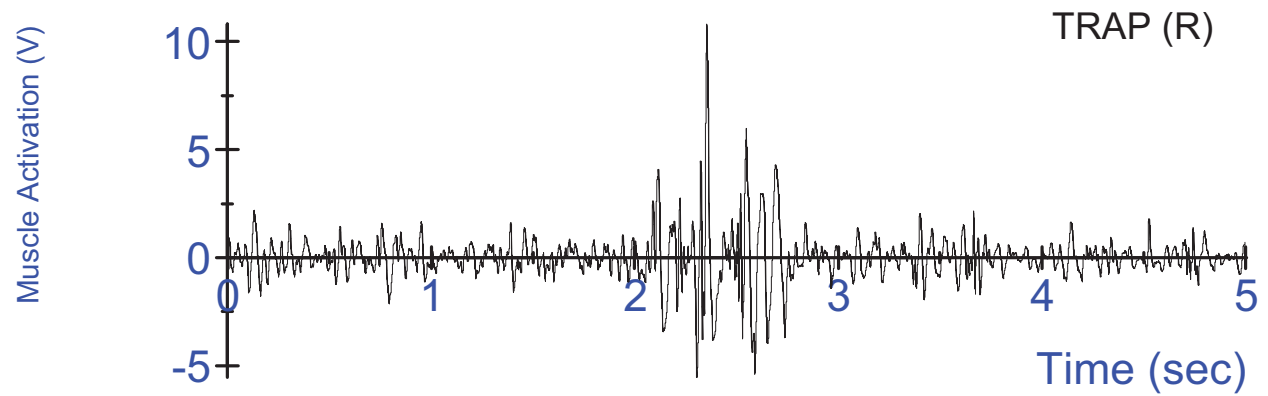
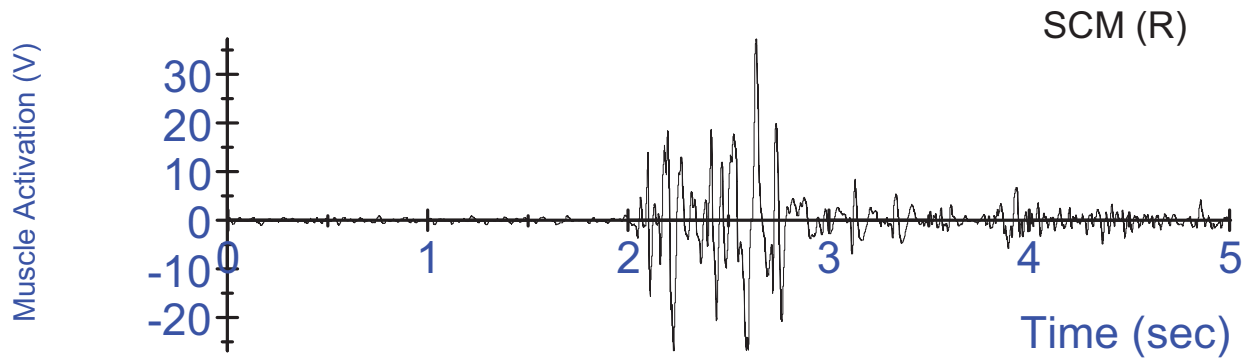
K03 Untensed Test #2 - Swing acceleration, filtered at 180Hz;
3-2-2-2 head acceleration, unfiltered



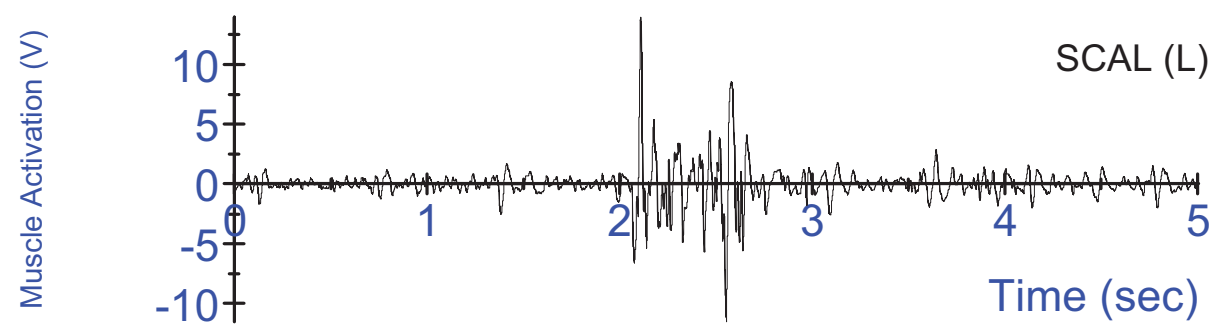
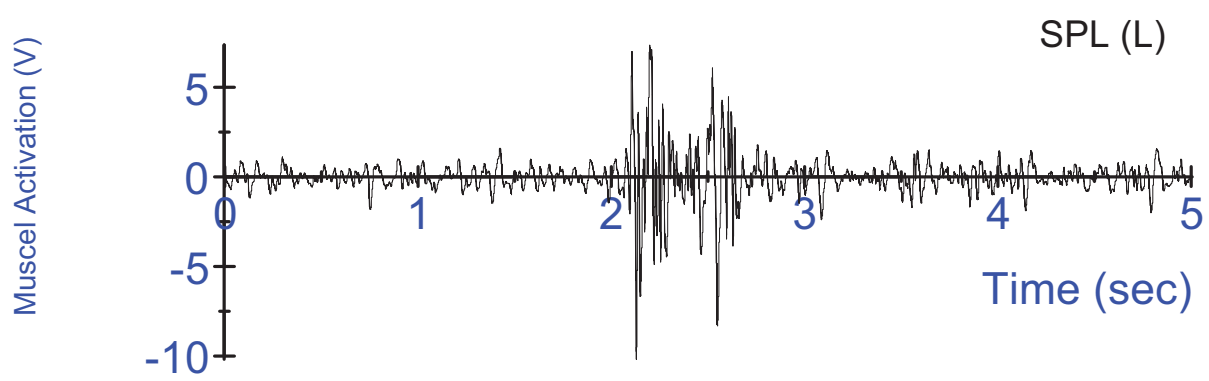
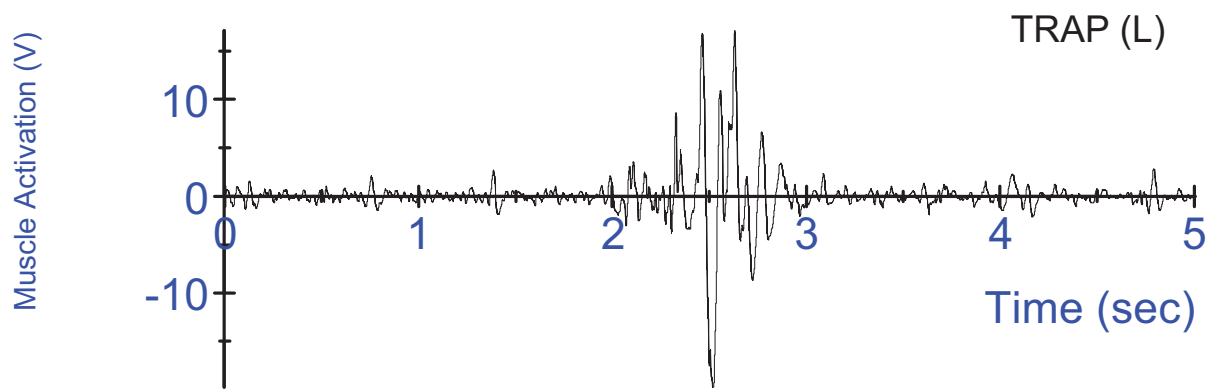
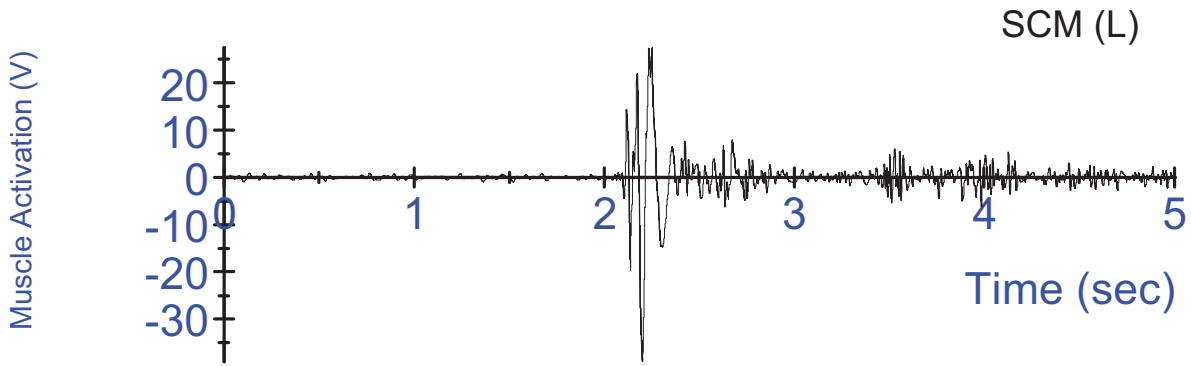
K03 Untensed Test #2 - Swing acceleration, filtered at 180Hz;
3-2-2-2 head acceleration, unfiltered



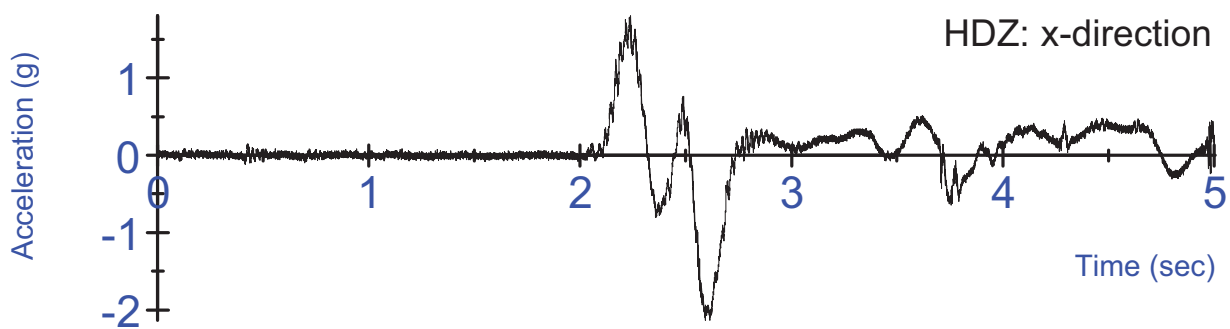
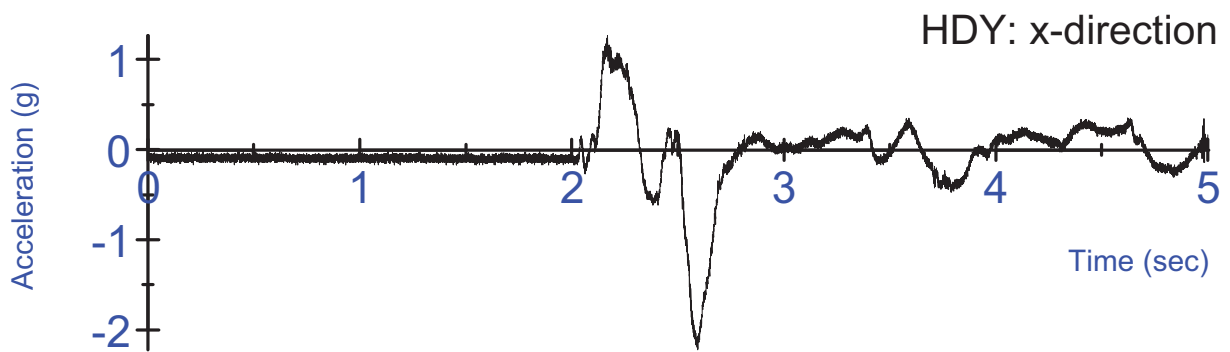
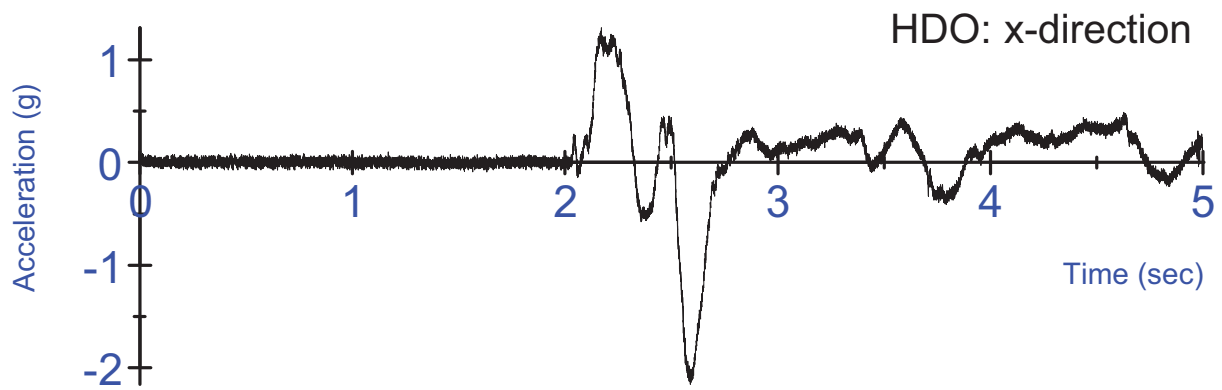
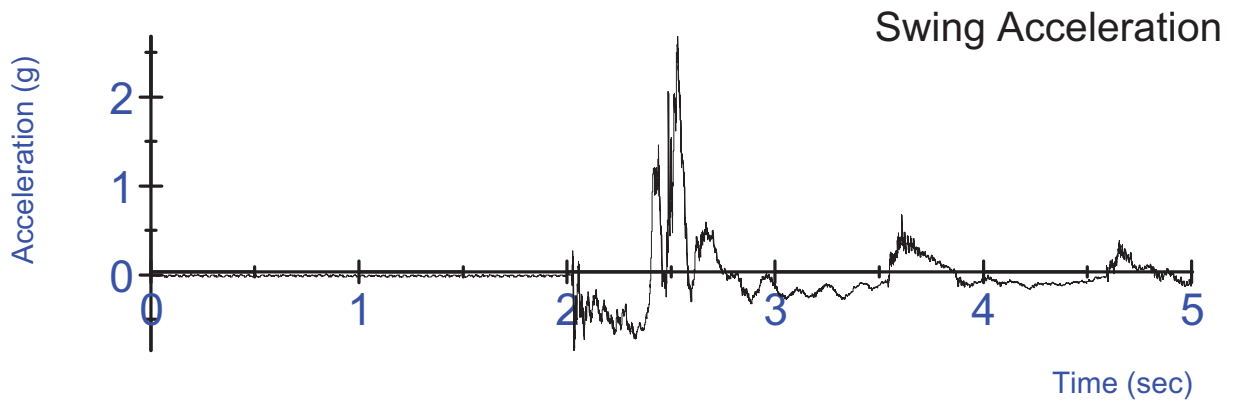
K03 Untensed Test #2 - Swing acceleration, filtered at 180Hz;
3-2-2-2 head acceleration, unfiltered



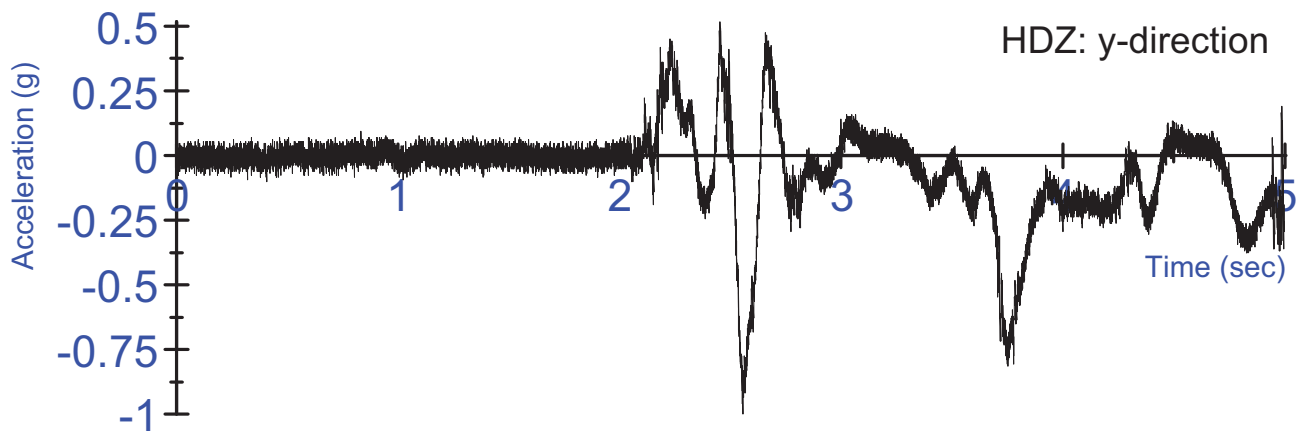
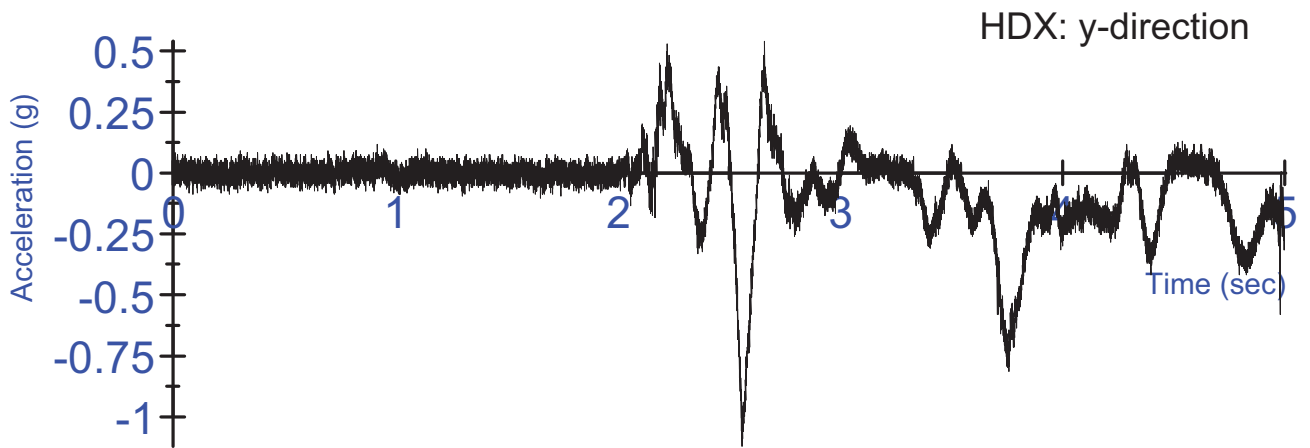
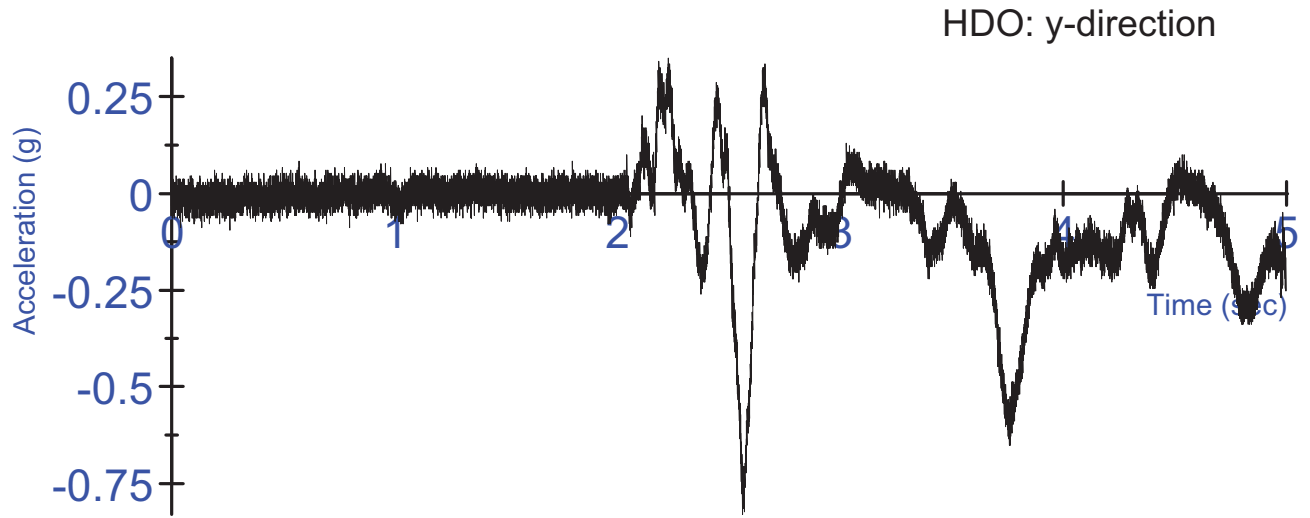
K03 Untensed Test #3 - Right Side EMG activation voltage
Un-rectified, Filtered at 10Hz



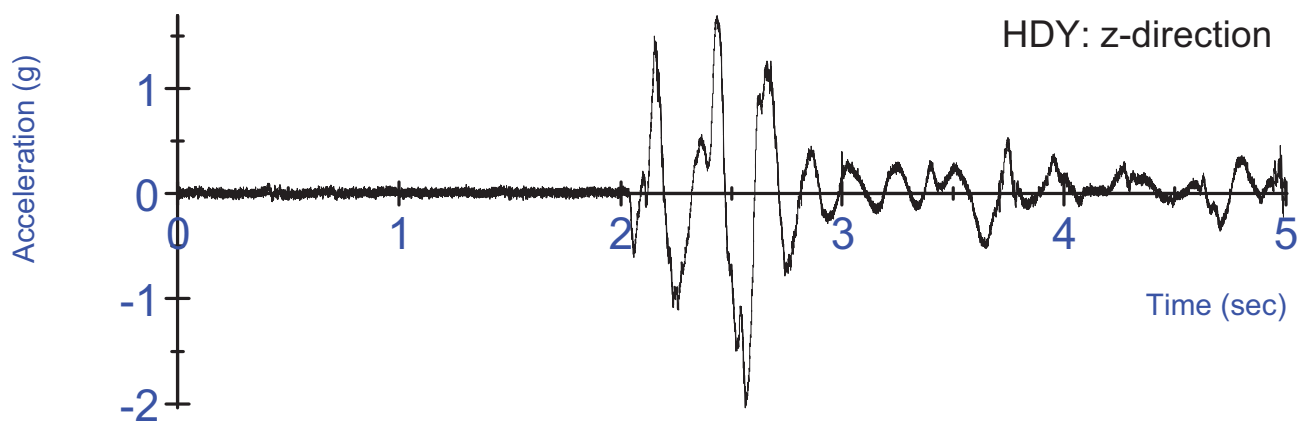
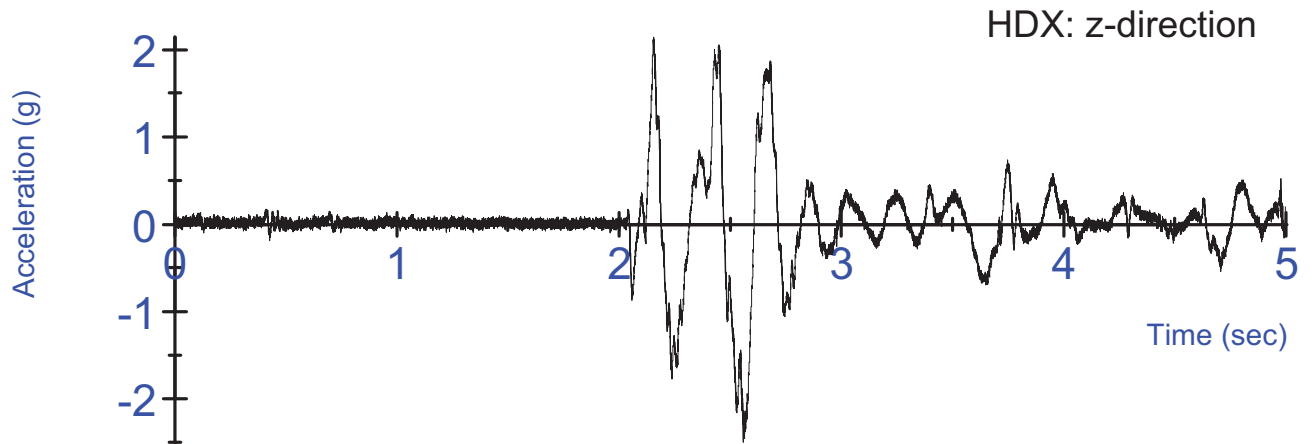
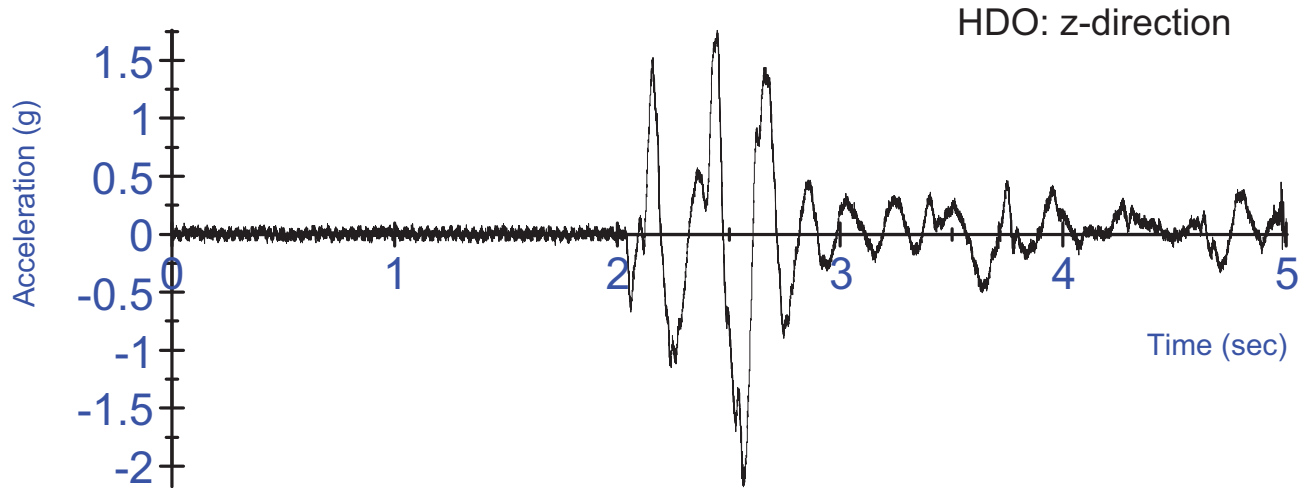
K03 Untensed Test #3- Left Side EMG activation voltage
Un-rectified, Filtered at 10Hz



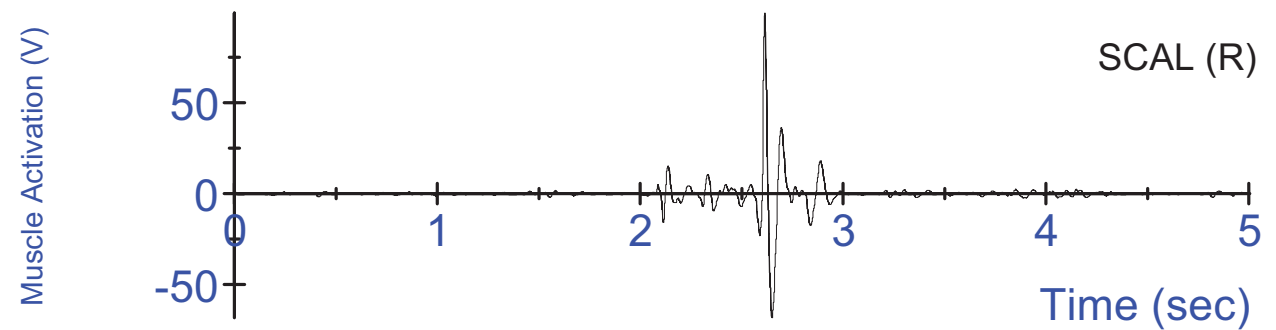
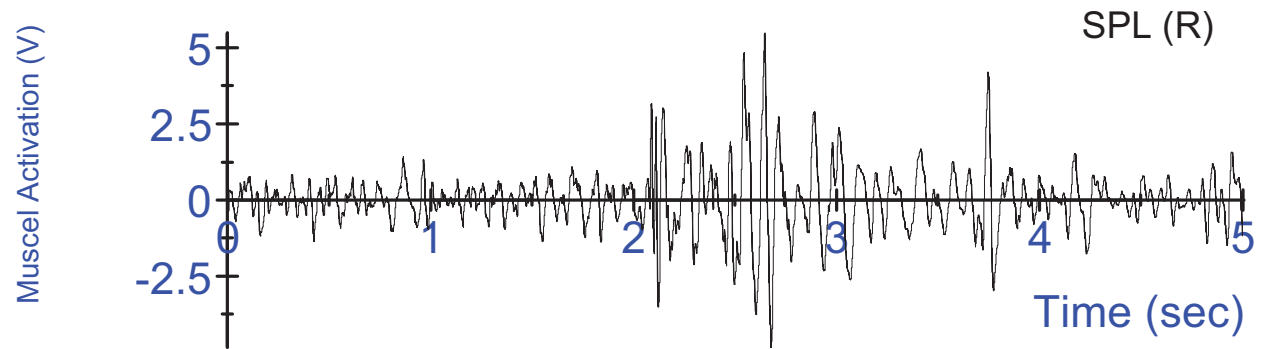
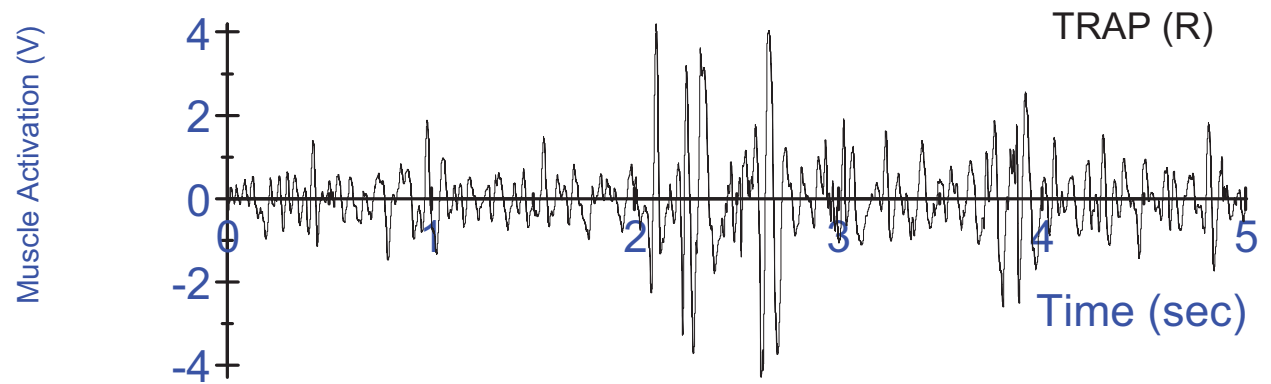
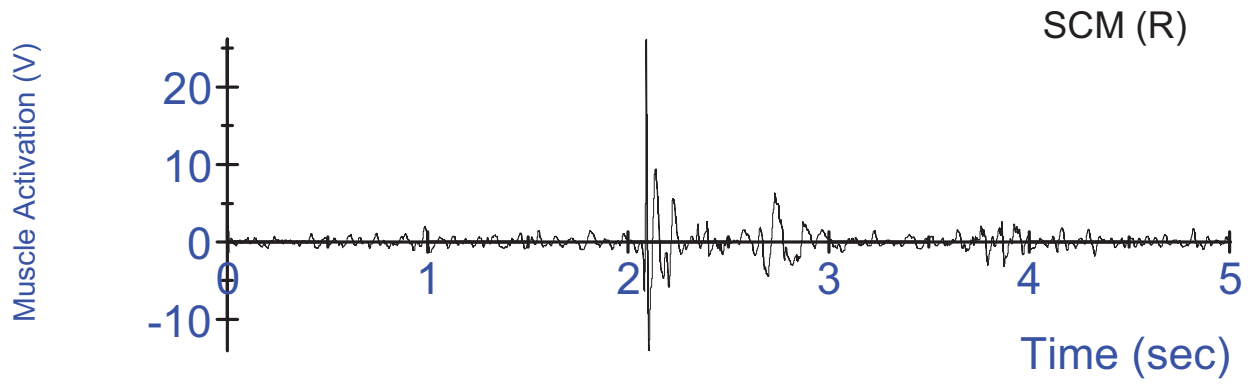
K03 Untensed Test #3 - Swing acceleration, filtered at 180Hz;
3-2-2-2 head acceleration, unfiltered



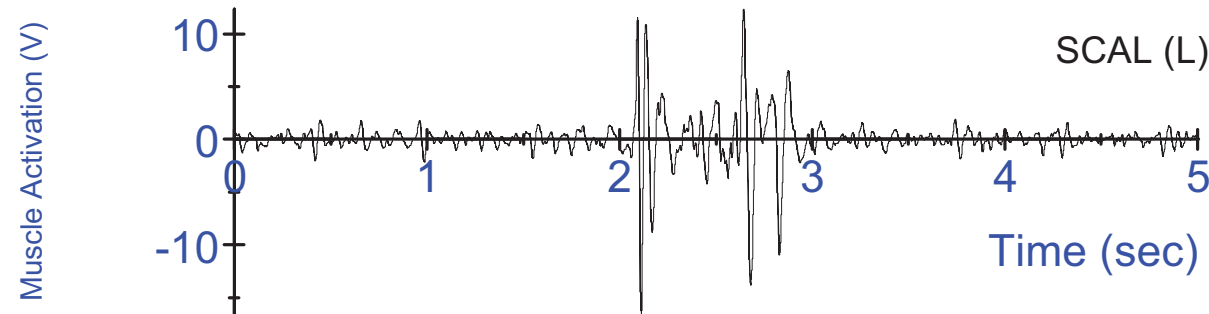
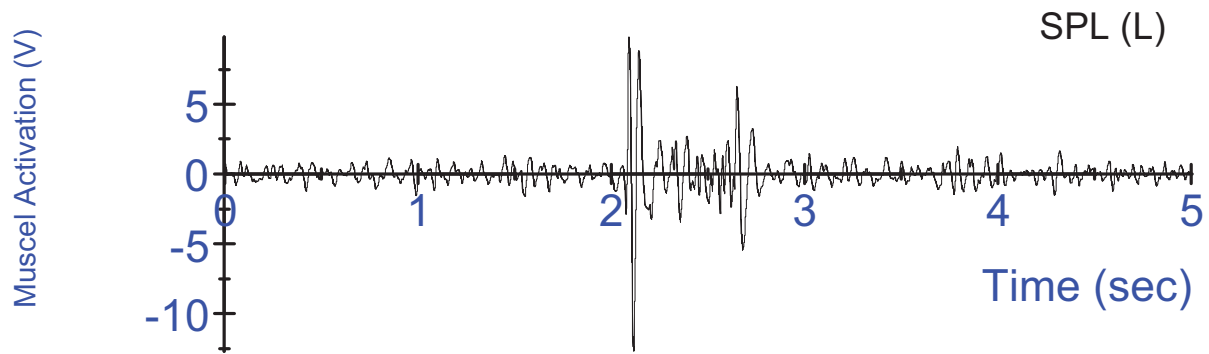
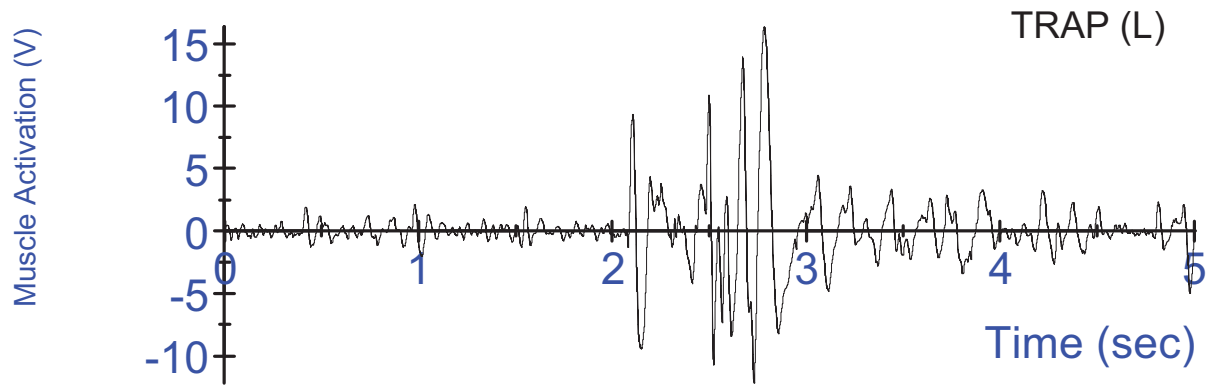
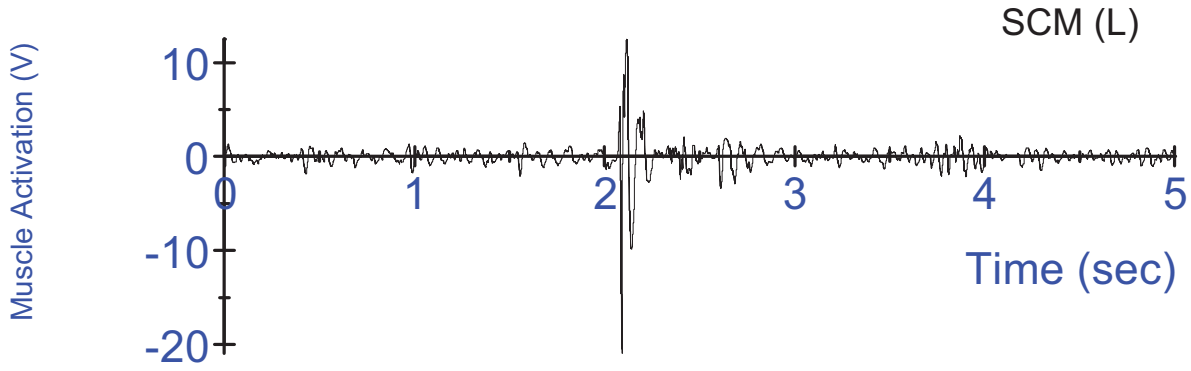
K03 Untensed Test #3 - Swing acceleration, filtered at 180Hz;
3-2-2-2 head acceleration, unfiltered



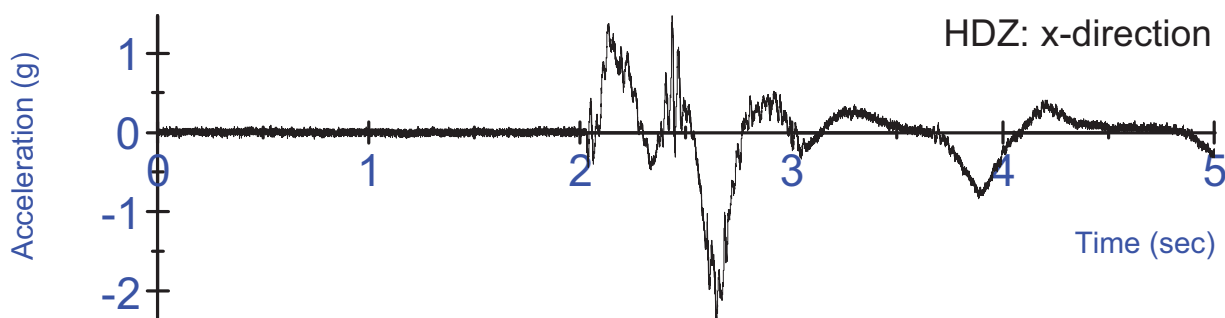
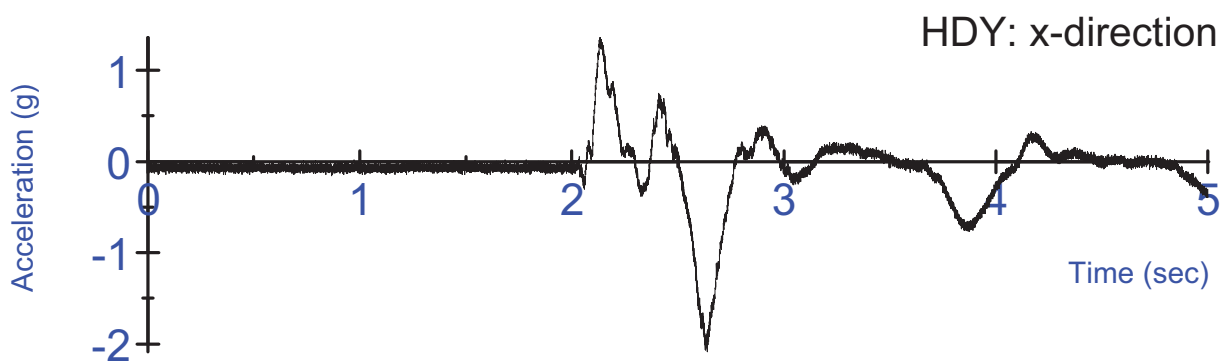
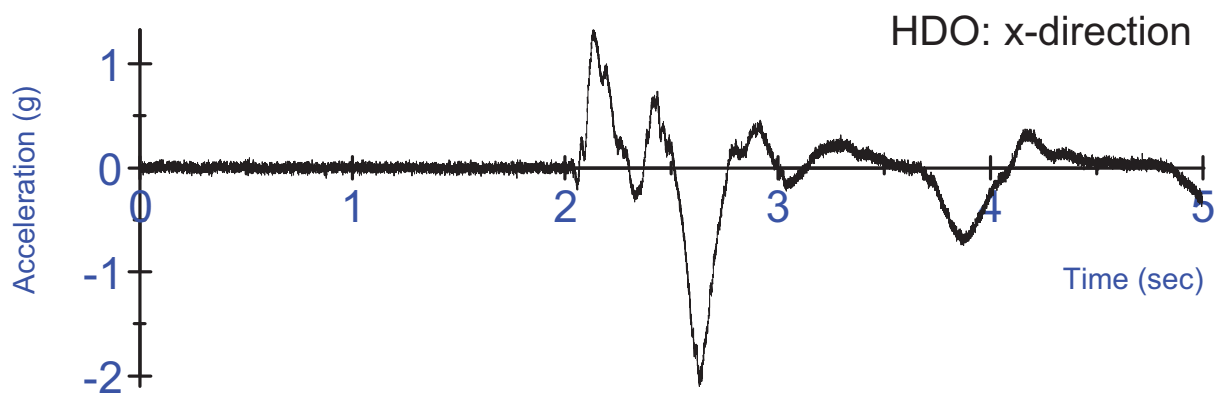
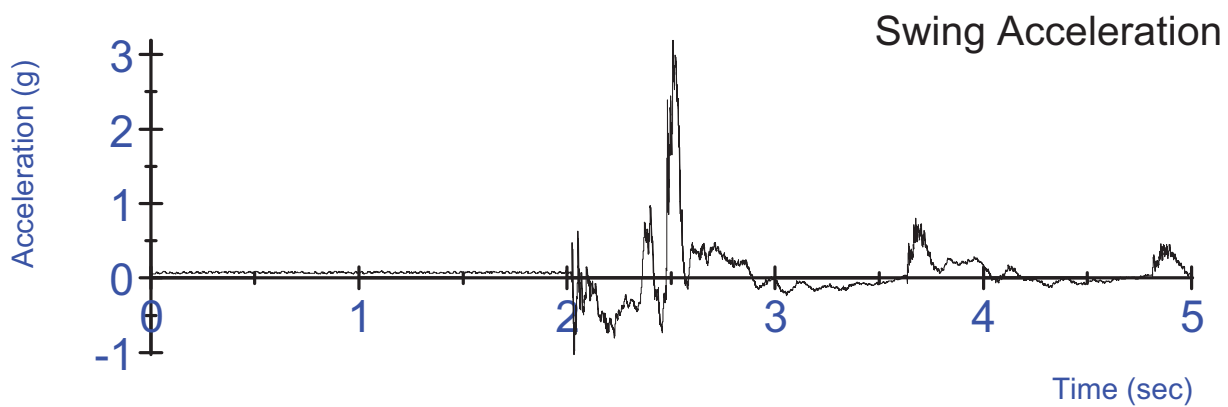
K03 Untensed Test #3 - Swing acceleration, filtered at 180Hz;
3-2-2-2 head acceleration, unfiltered



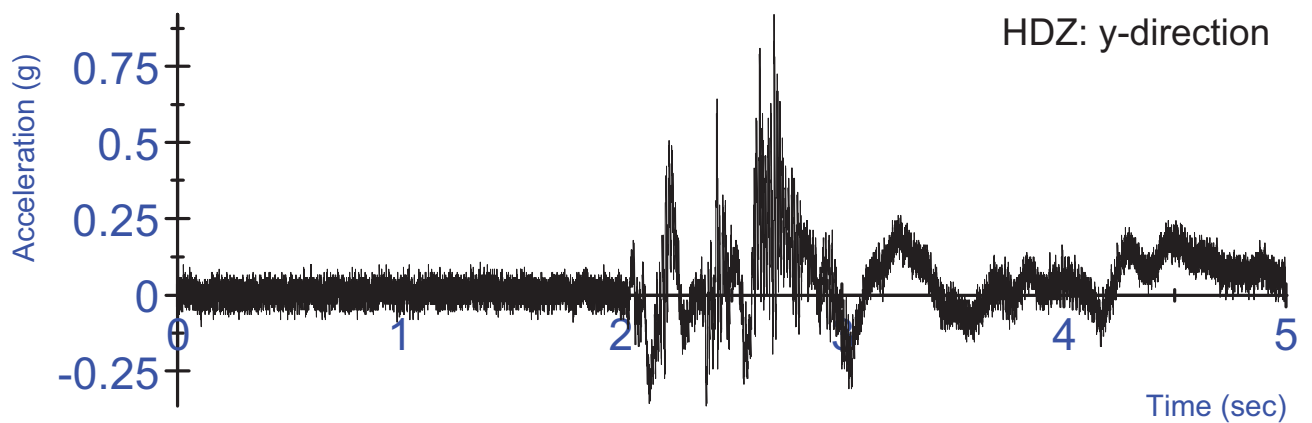
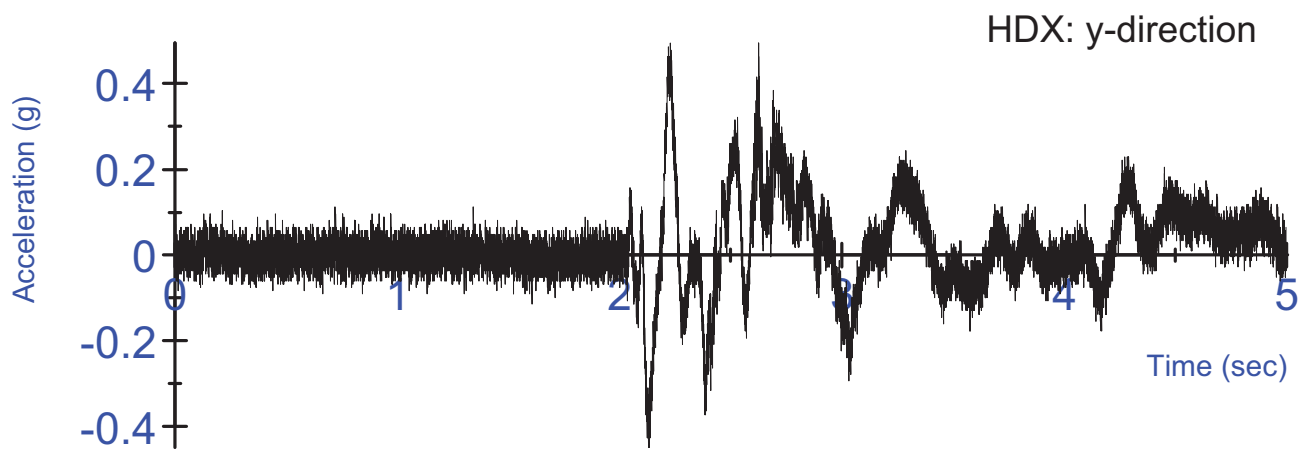
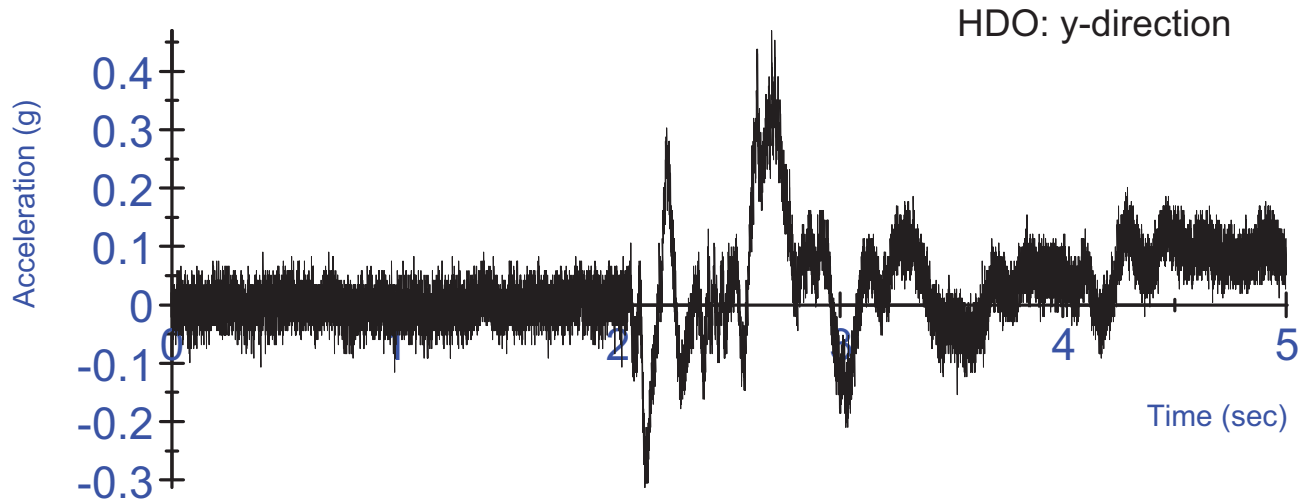
S14 Tensed Test #1 - Right Side EMG activation voltage
Un-rectified, Filtered at 6Hz



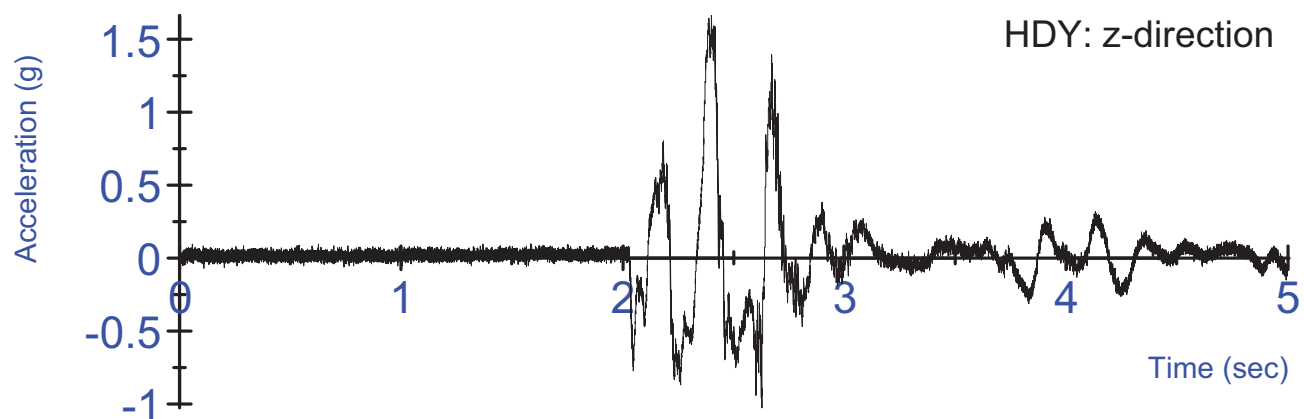
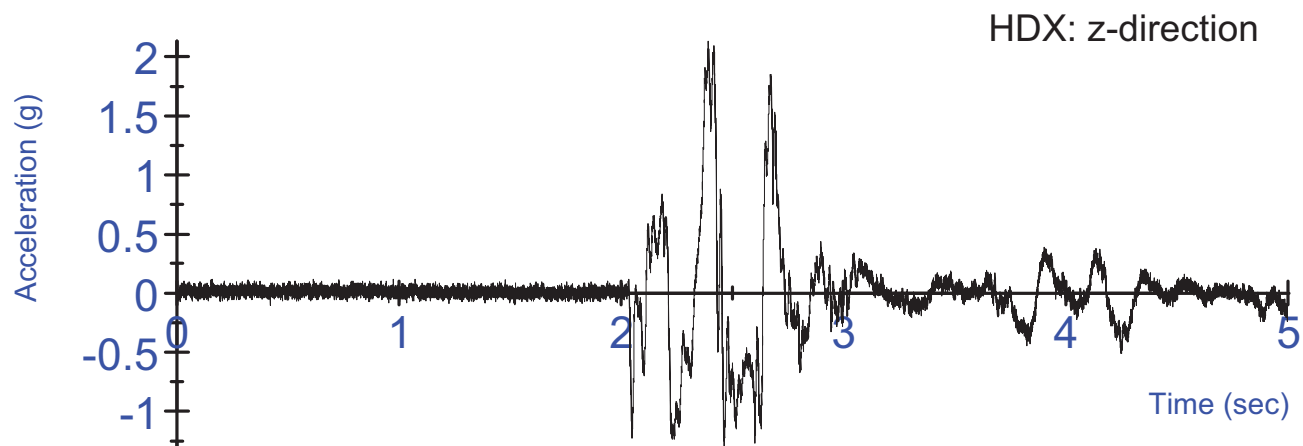
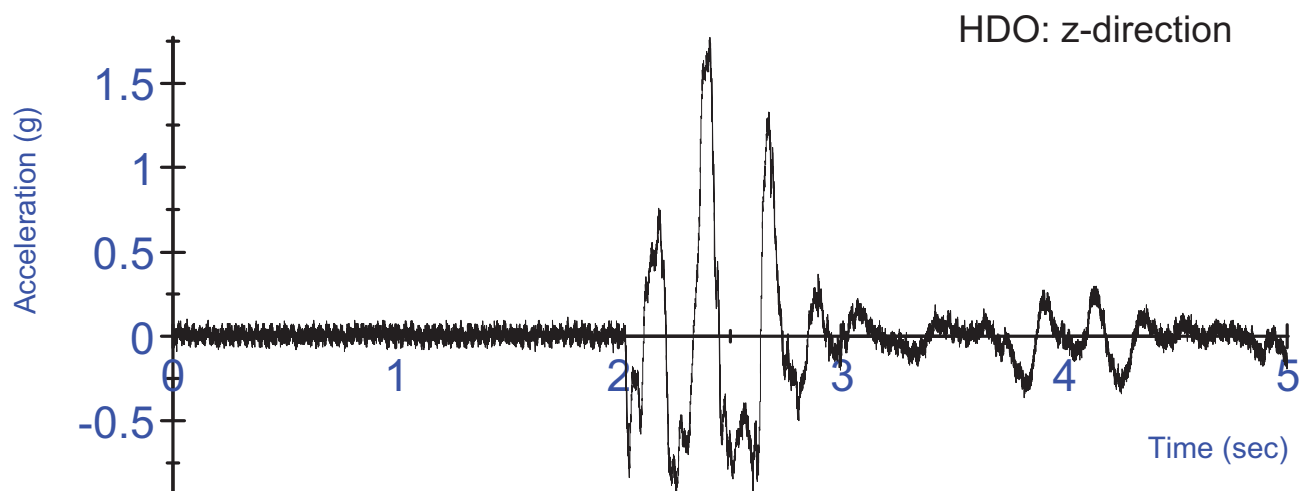
S14 Tensed Test #1 - Left Side EMG activation voltage
Un-rectified, Filtered at 6Hz



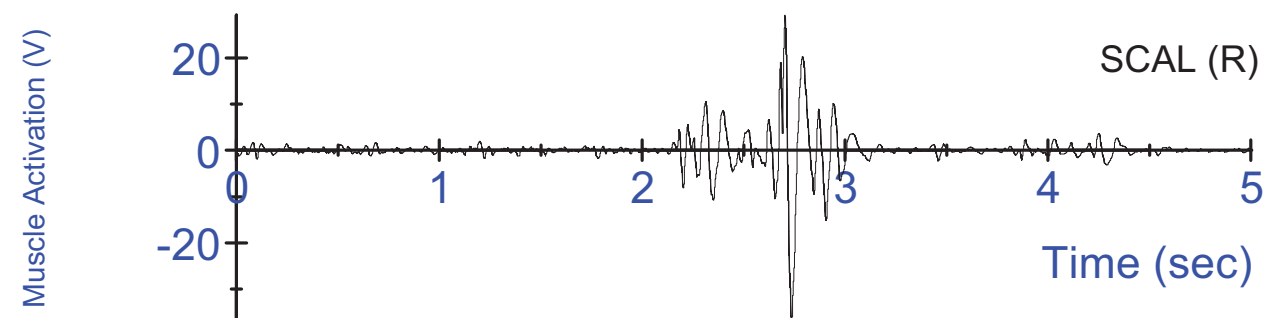
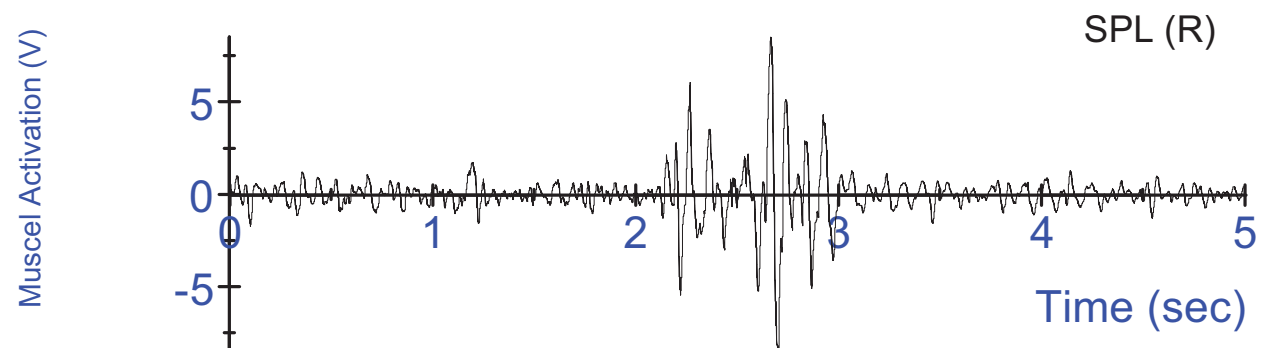
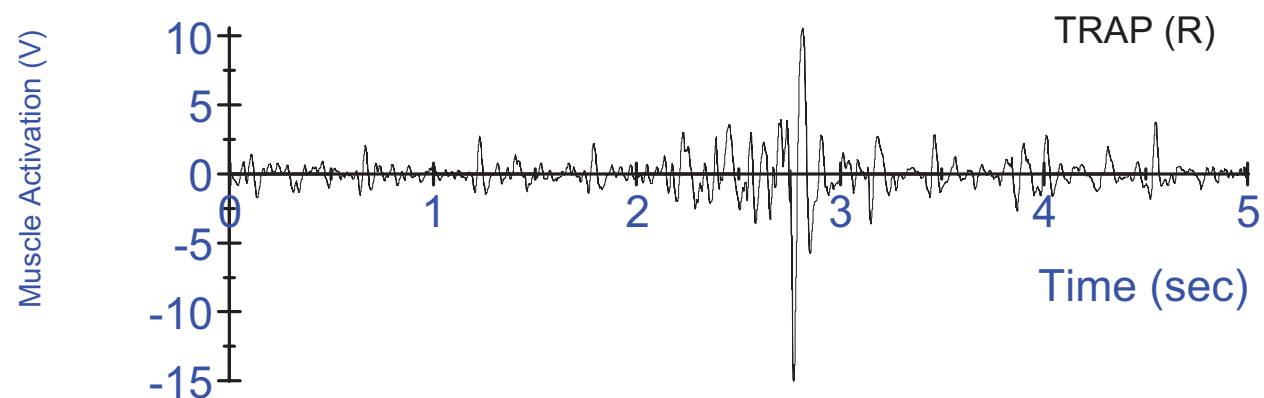
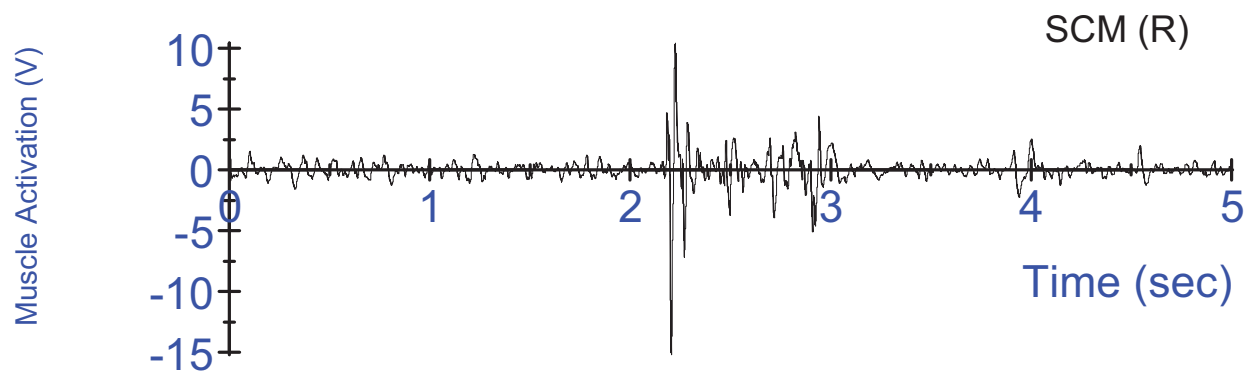
S14 Tensed Test #1 - Swing acceleration, filtered at 180Hz;
3-2-2-2 head acceleration, unfiltered



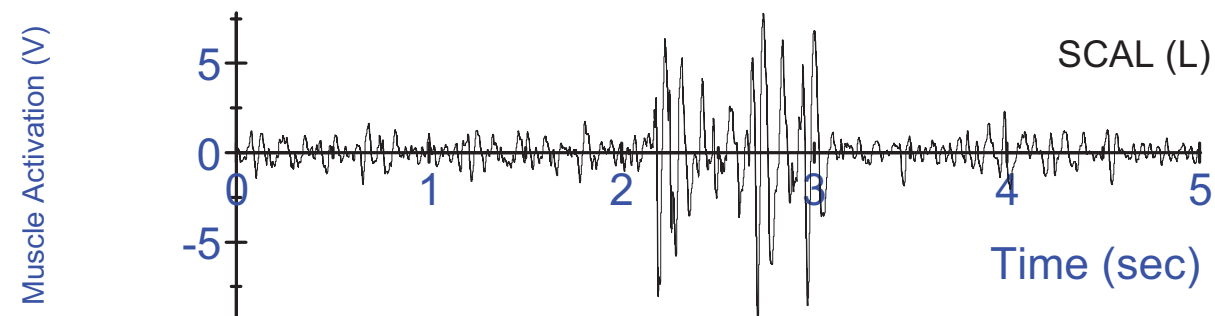
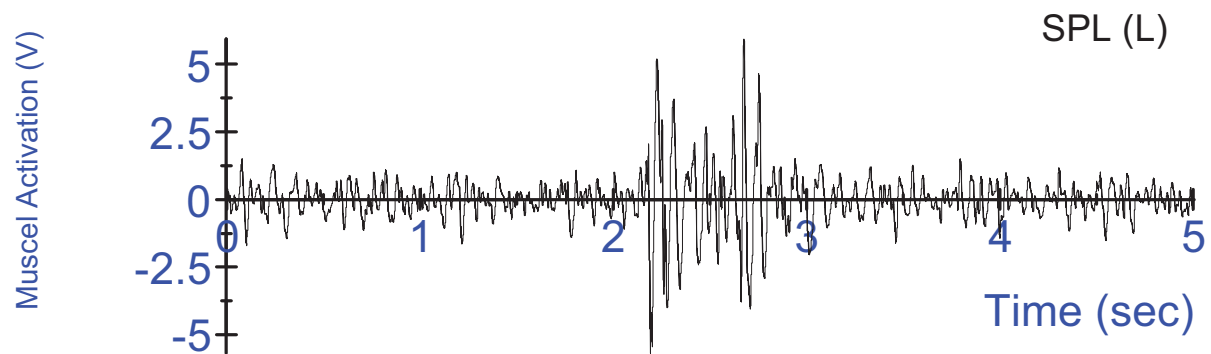
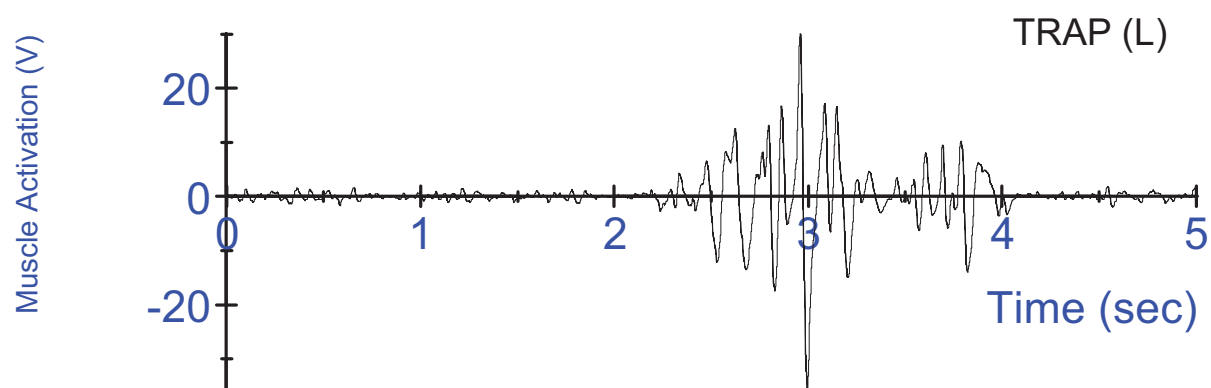
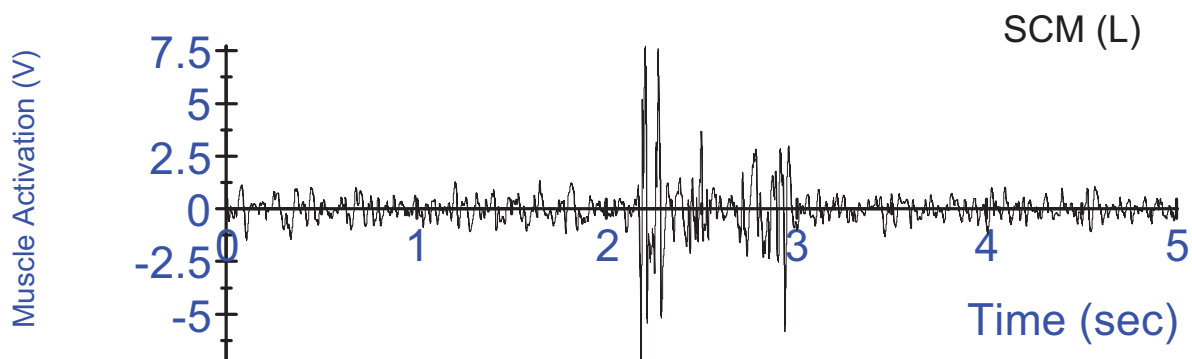
S14 Tensed Test #1 - Swing acceleration, filtered at 180Hz;
3-2-2-2 head acceleration, unfiltered



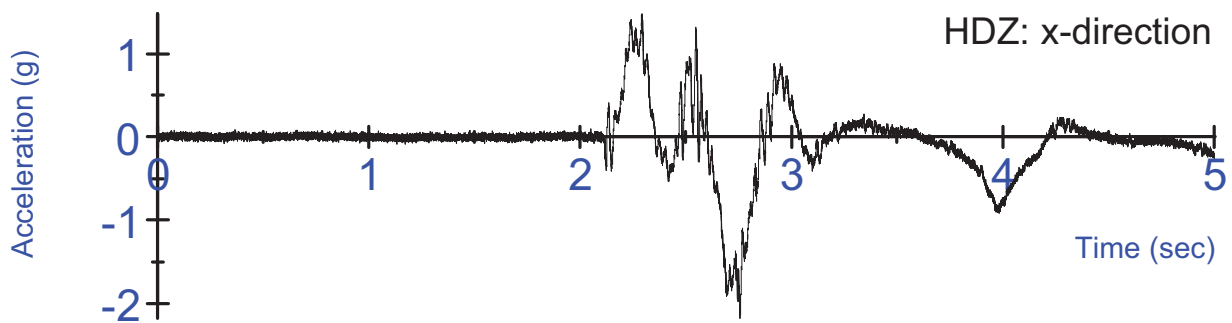
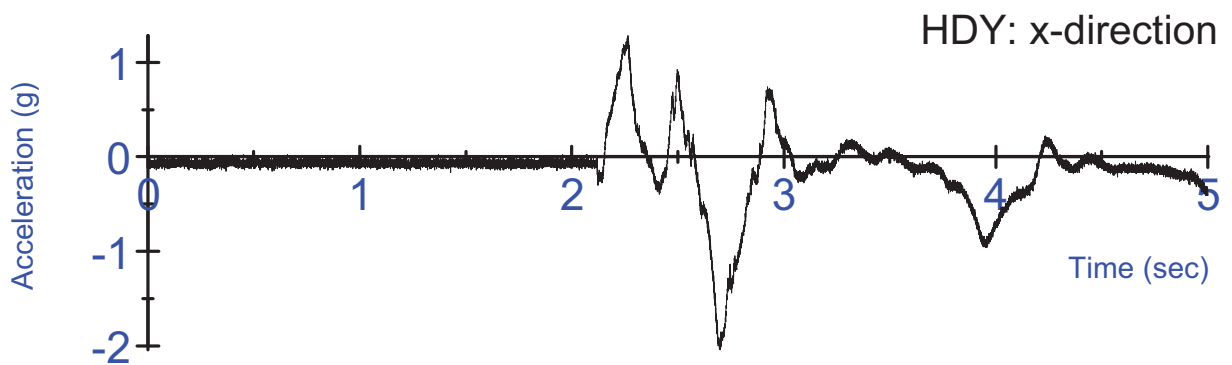
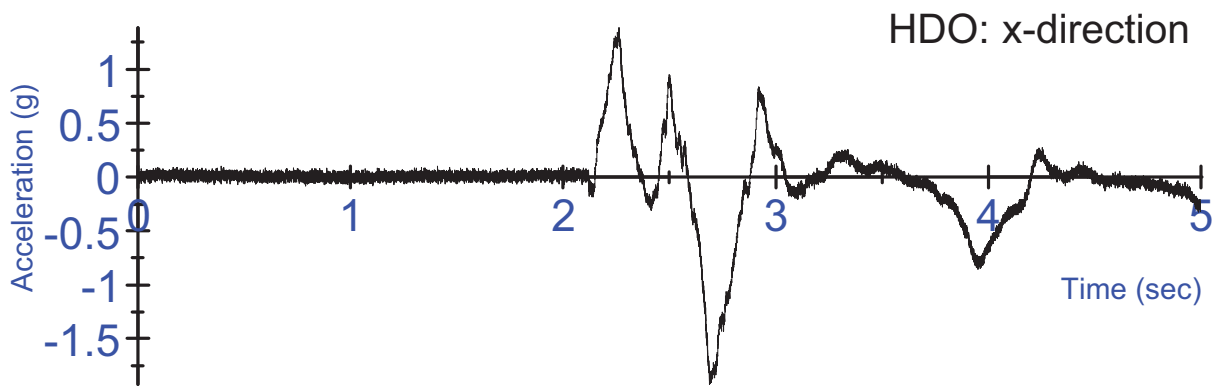
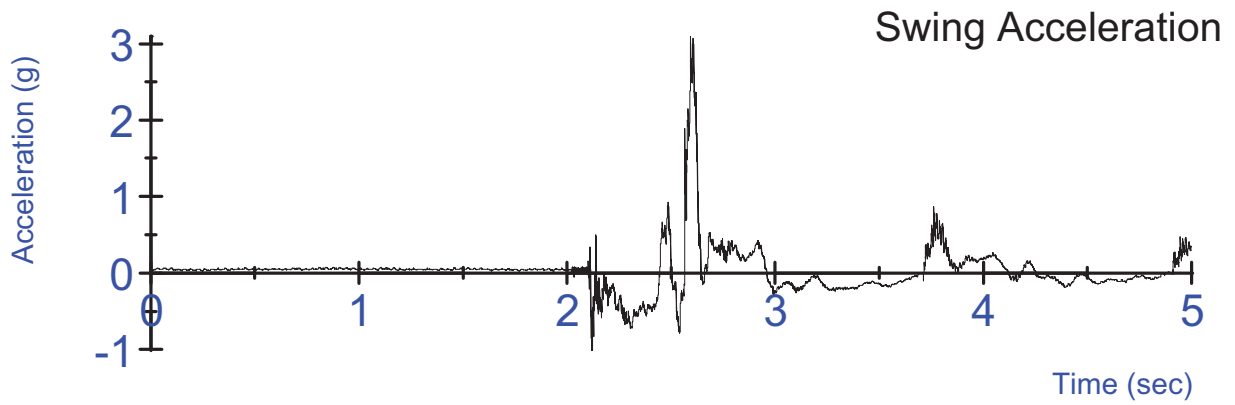
S14 Tensed Test #1 - Swing acceleration, filtered at 180Hz;
3-2-2-2 head acceleration, unfiltered



S13 Tensed Test #2 - Right Side EMG activation voltage
Un-rectified, Filtered at 6Hz

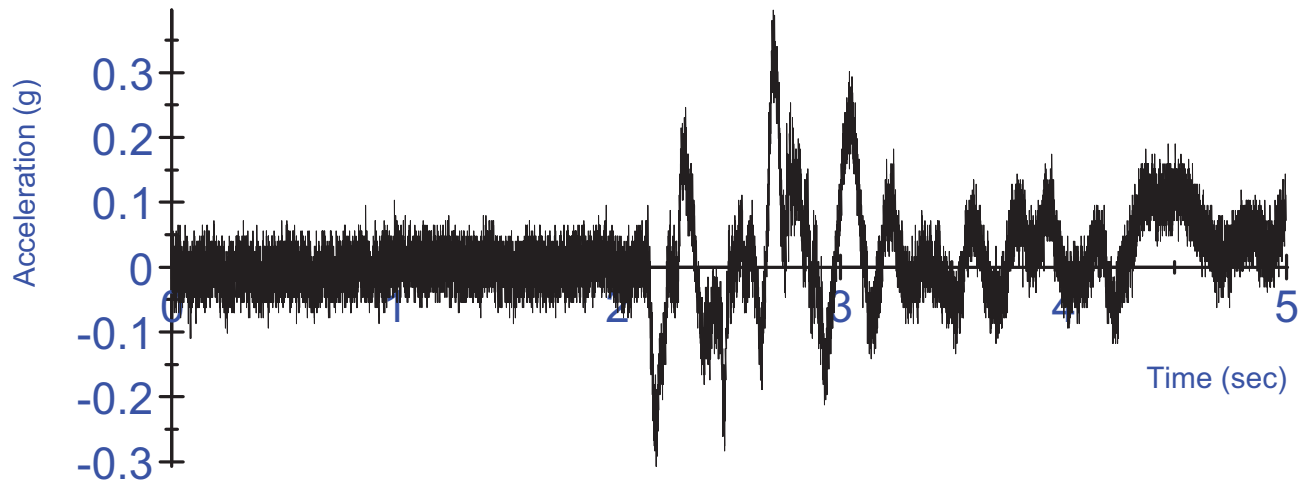


S14 Tensed Test #2 - Left Side EMG activation voltage
Un-rectified, Filtered at 6Hz

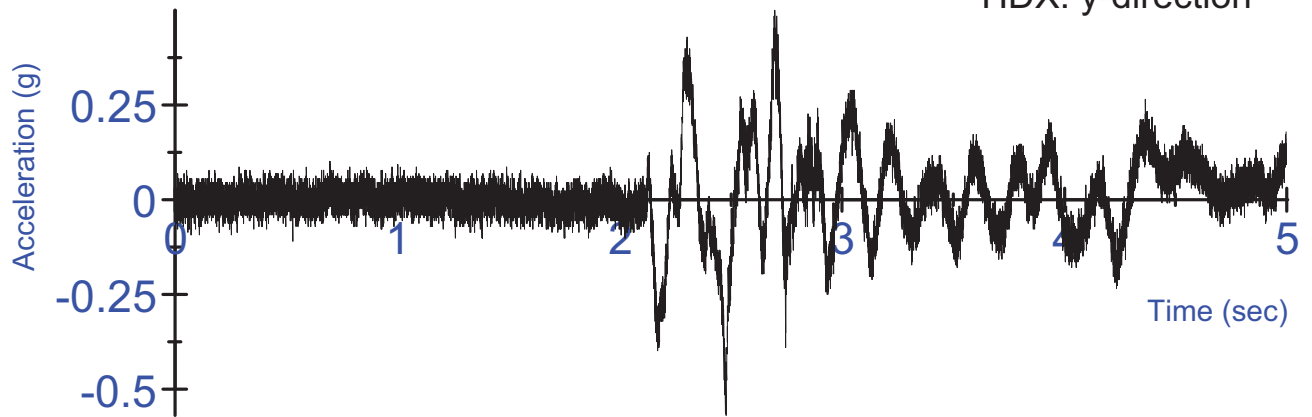


S14 Tensed Test #2 - Swing acceleration, filtered at 180Hz;
3-2-2-2 head acceleration, unfiltered

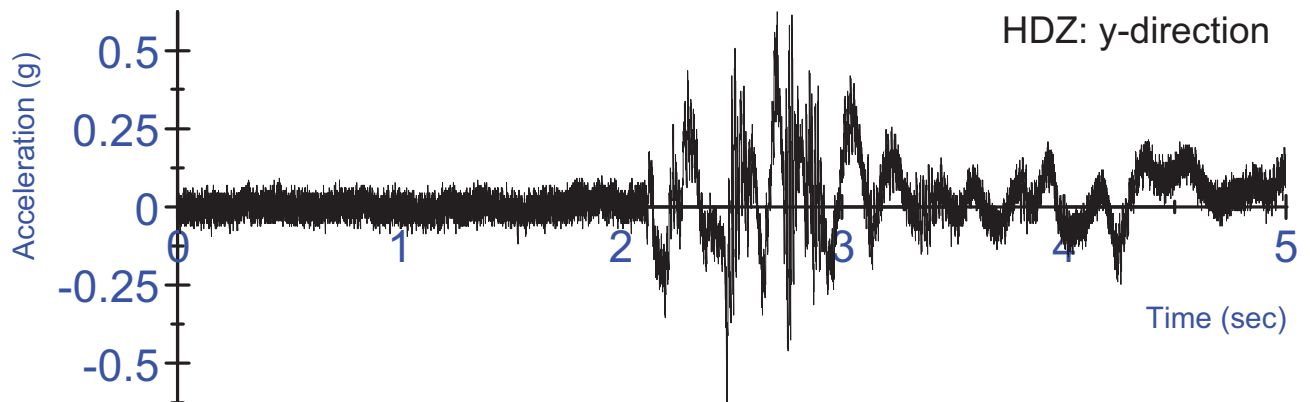
HDO: y-direction



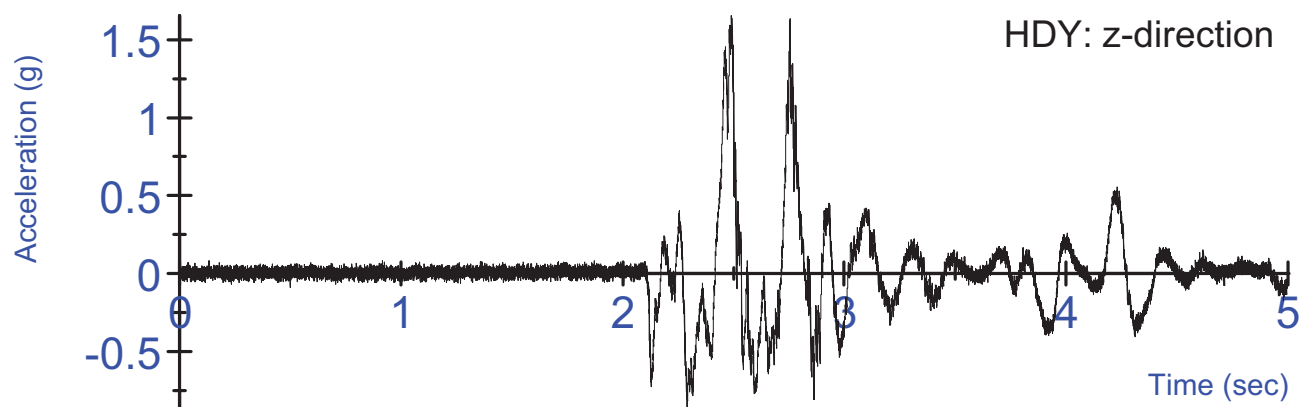
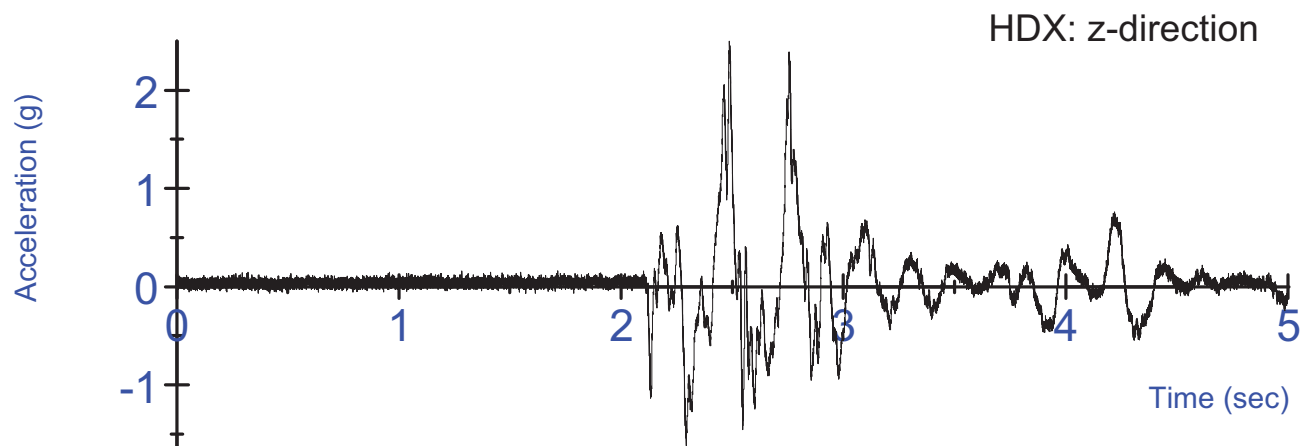
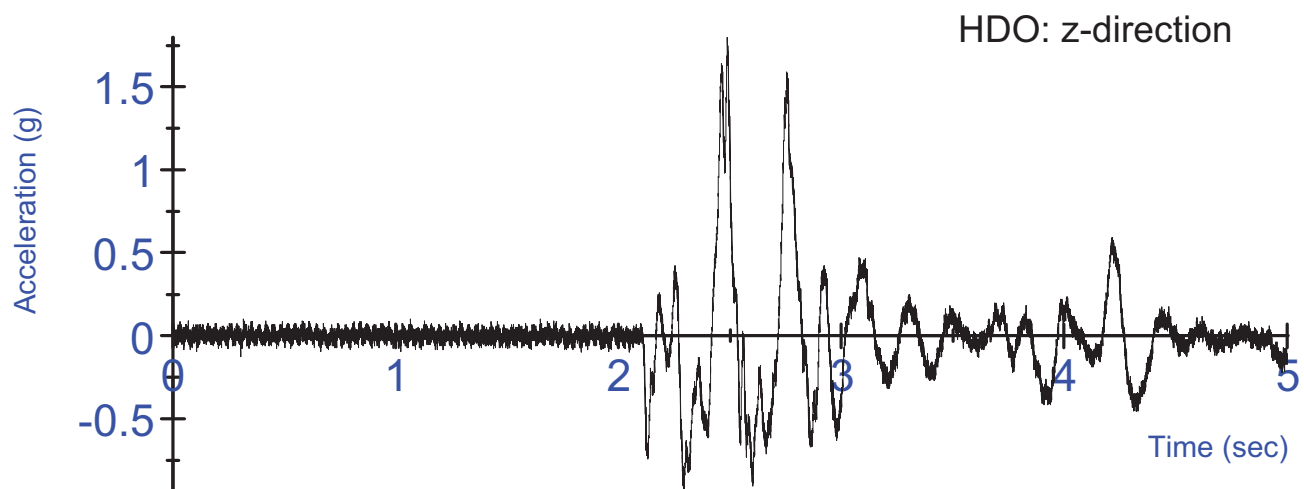
HDX: y-direction



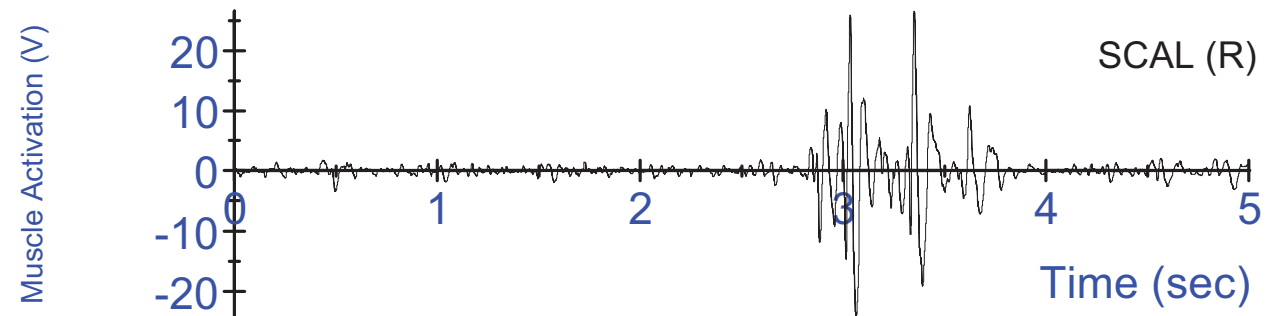
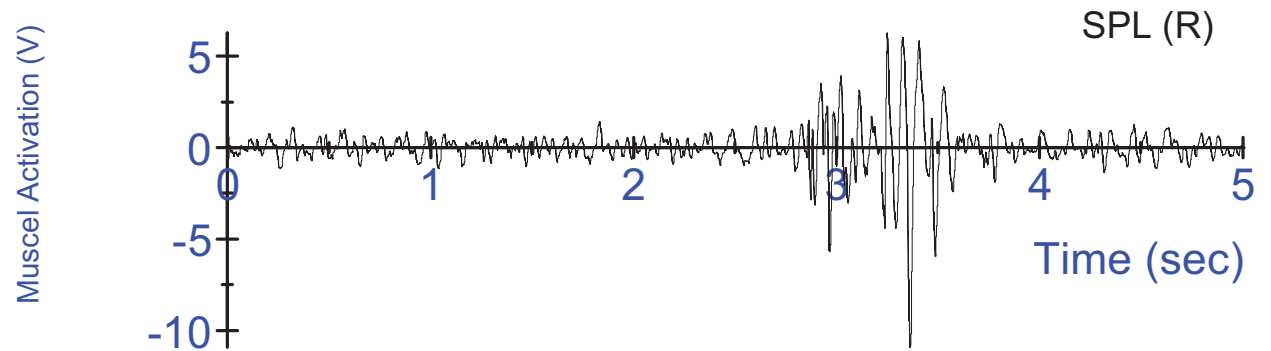
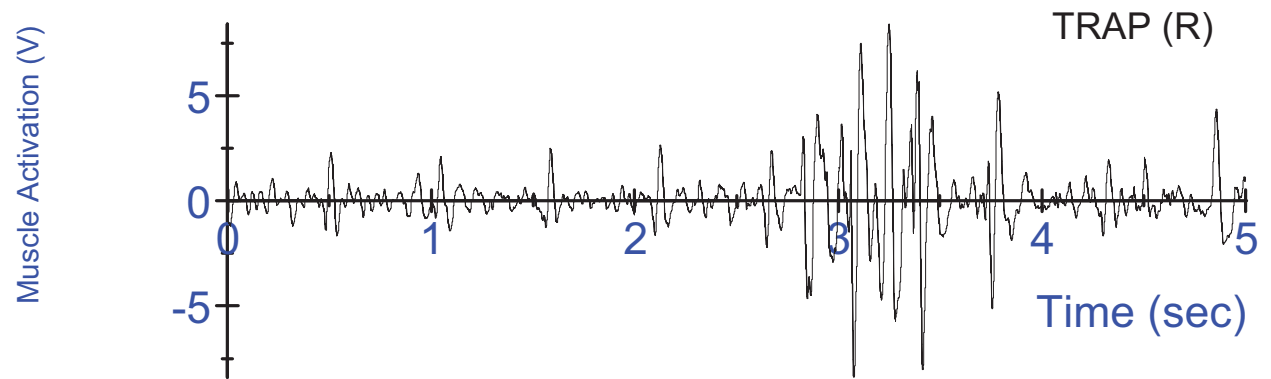
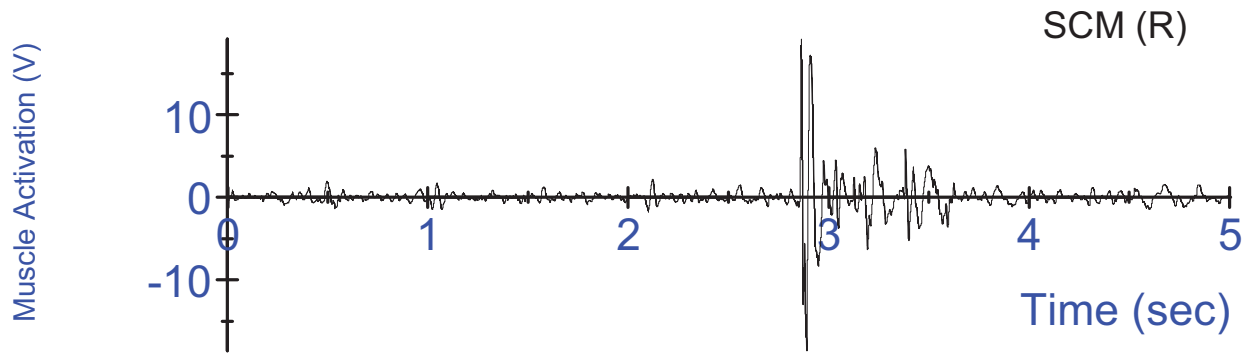
HDZ: y-direction



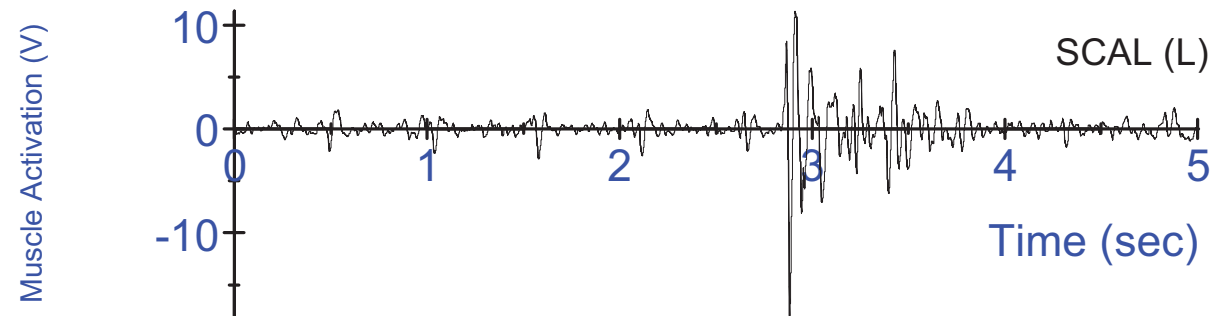
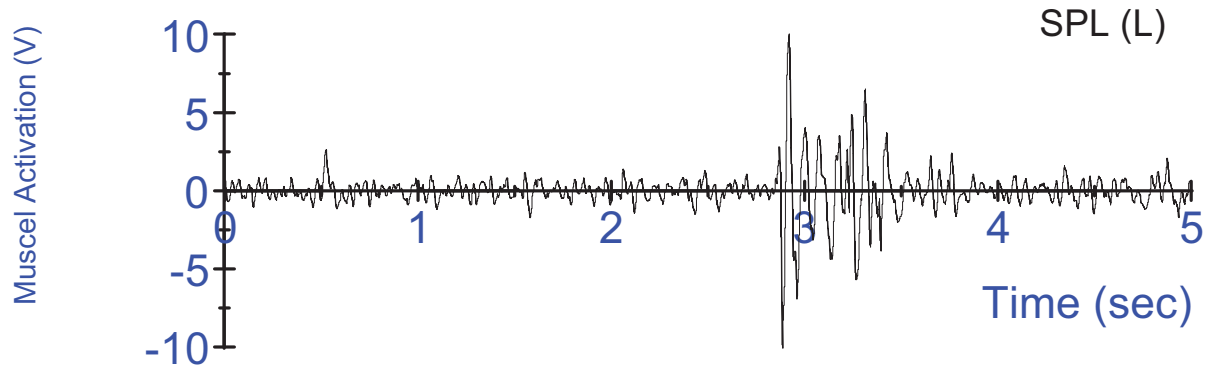
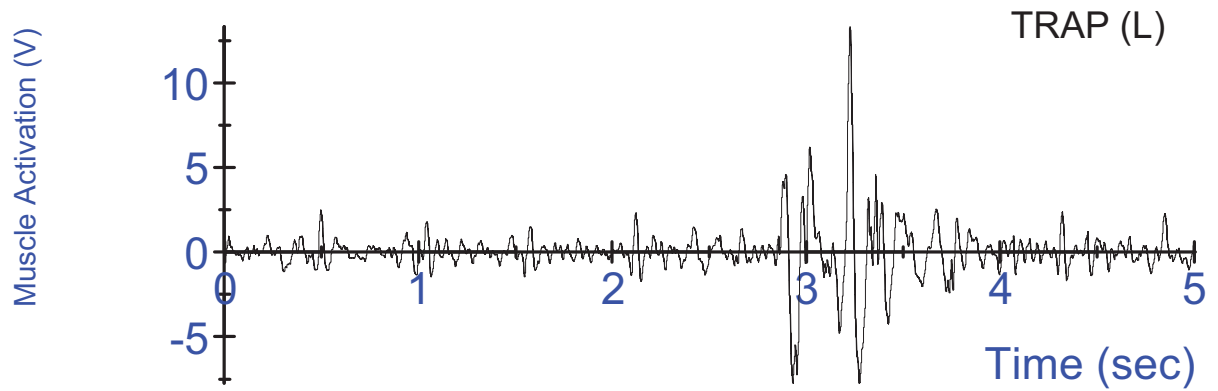
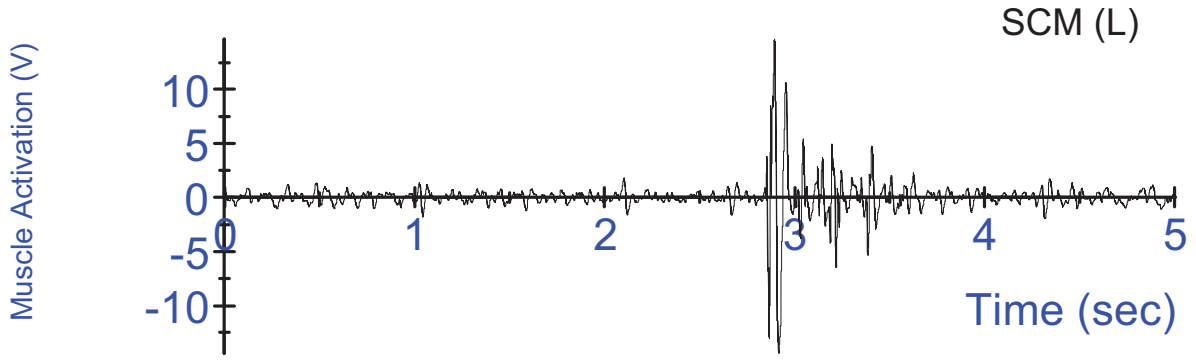
S14 Tensed Test #2 - Swing acceleration, filtered at 180Hz;
3-2-2-2 head acceleration, unfiltered



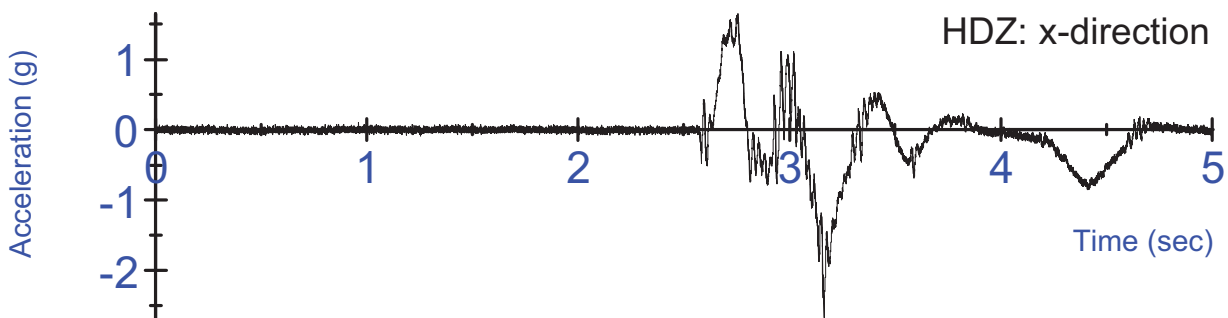
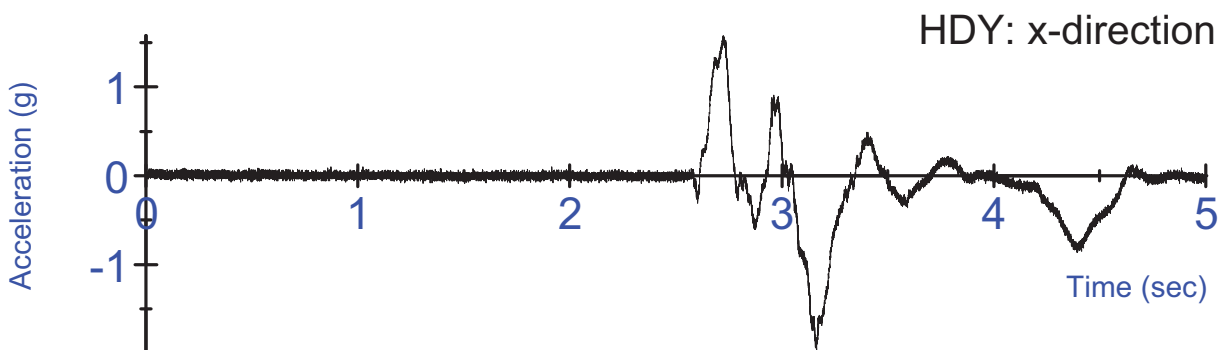
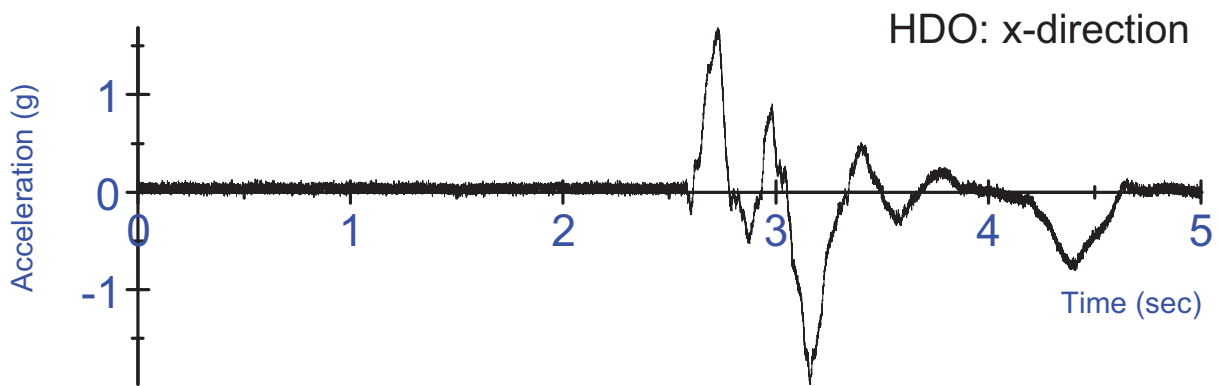
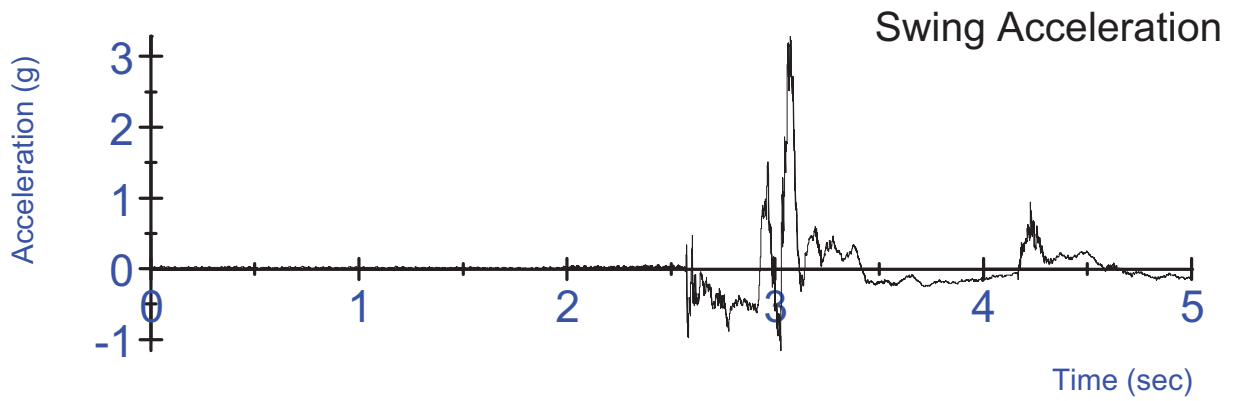
S14 Tensed Test #2 - Swing acceleration, filtered at 180Hz;
3-2-2-2 head acceleration, unfiltered



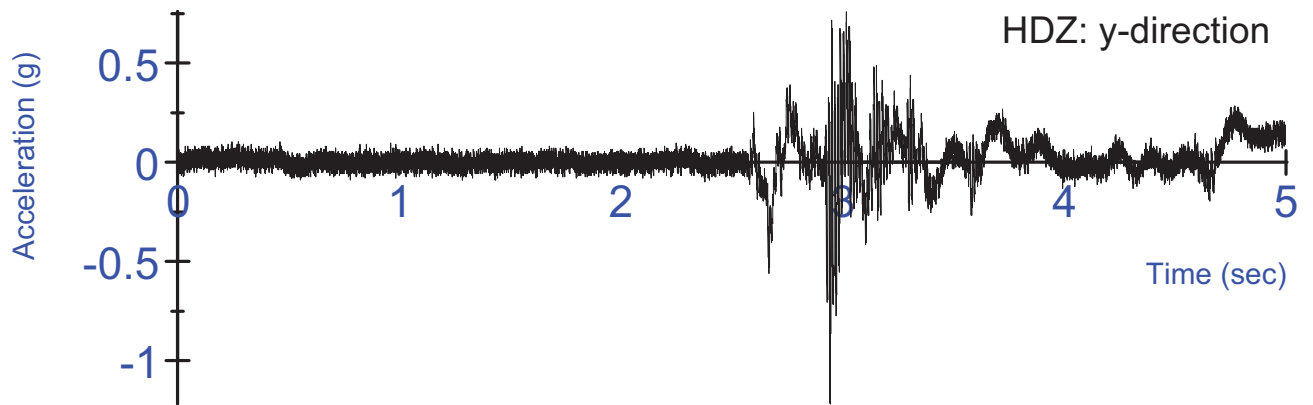
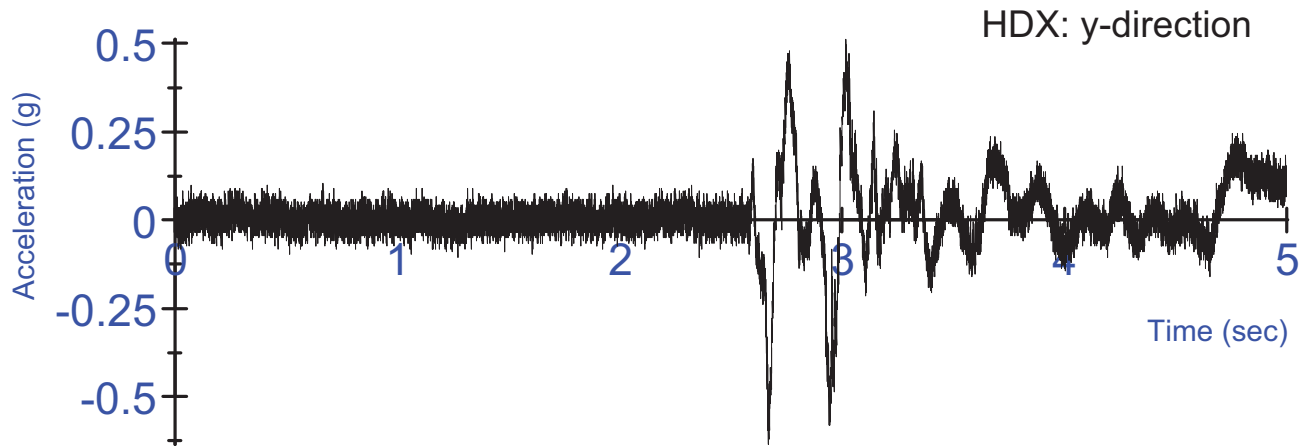
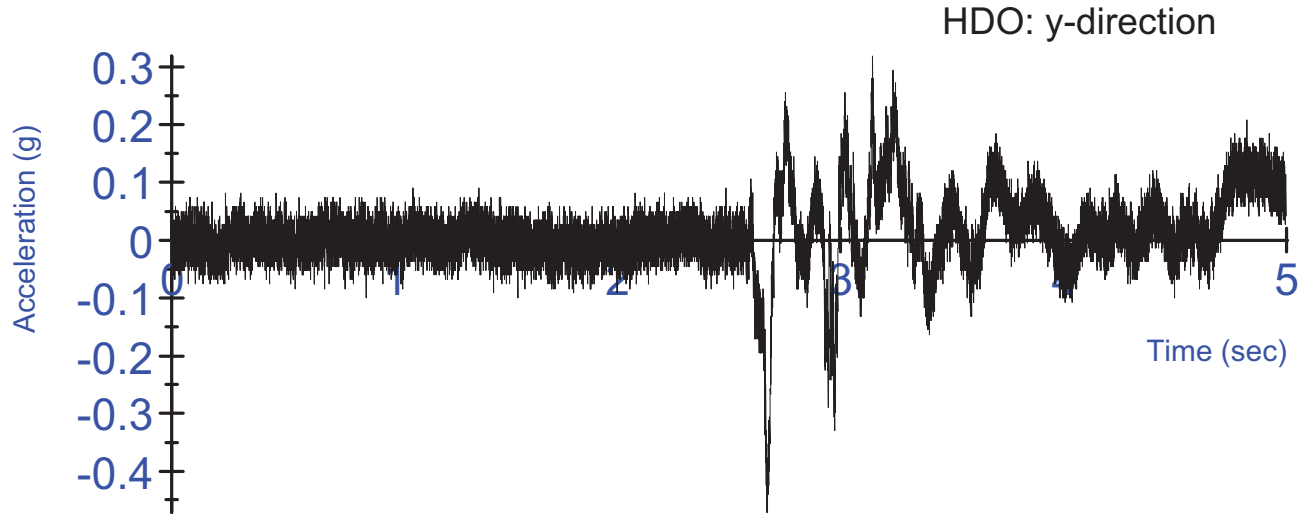
S14 Tensed Test #3 - Right Side EMG activation voltage
Un-rectified, Filtered at 6Hz



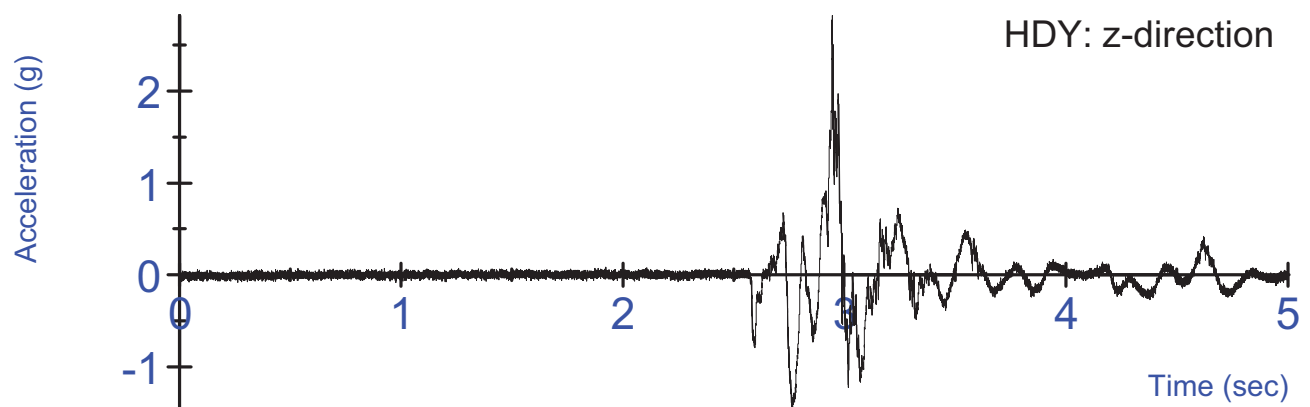
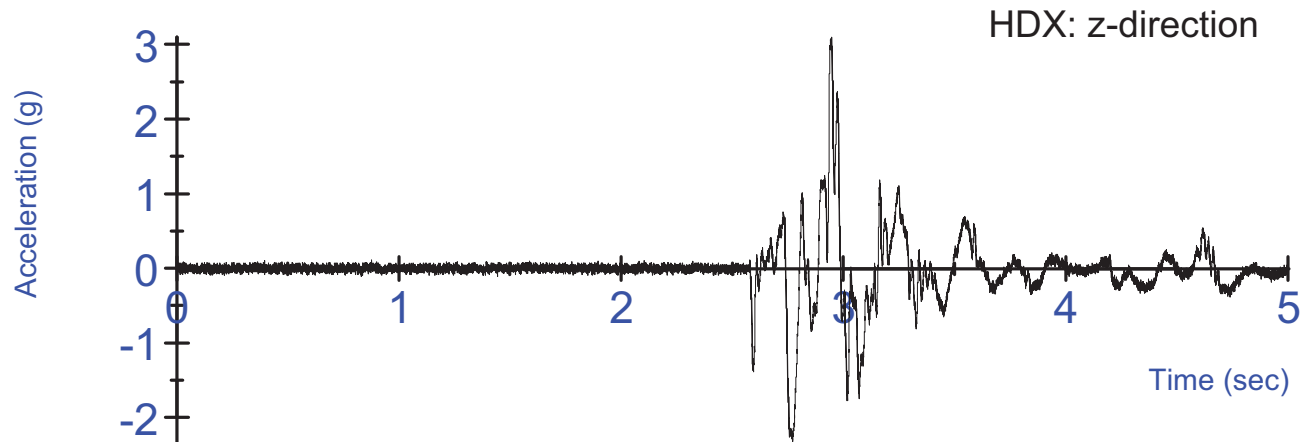
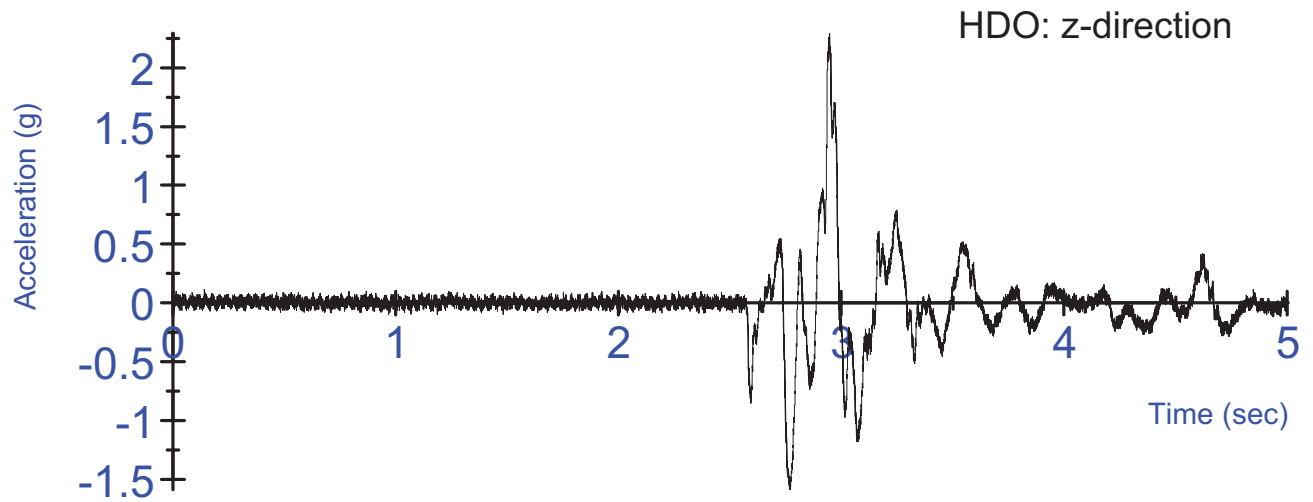
S14 Tensed Test #3 - Left Side EMG activation voltage
Un-rectified, Filtered at 6Hz



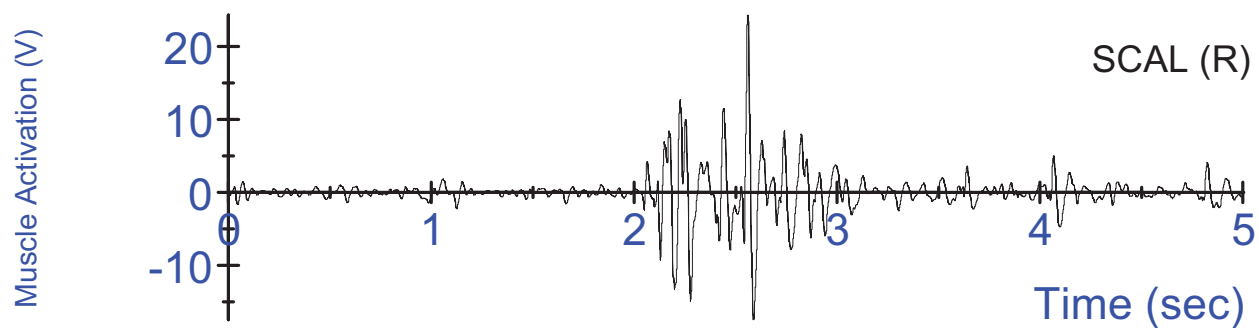
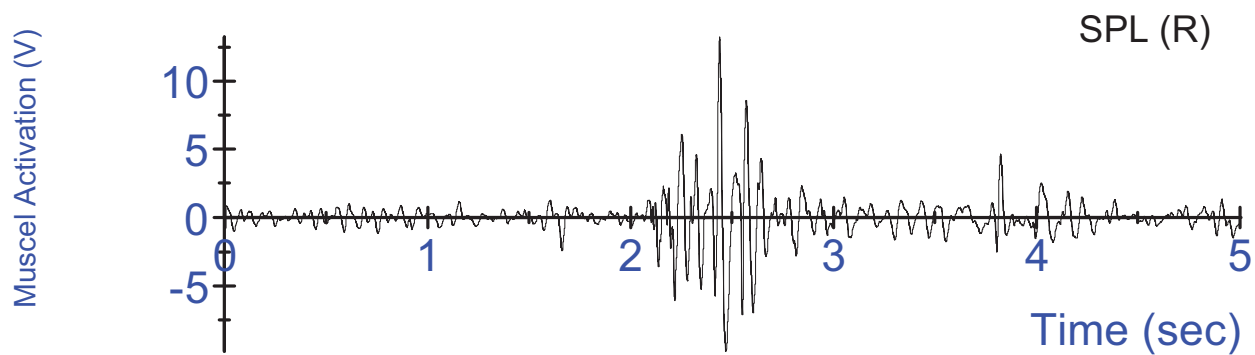
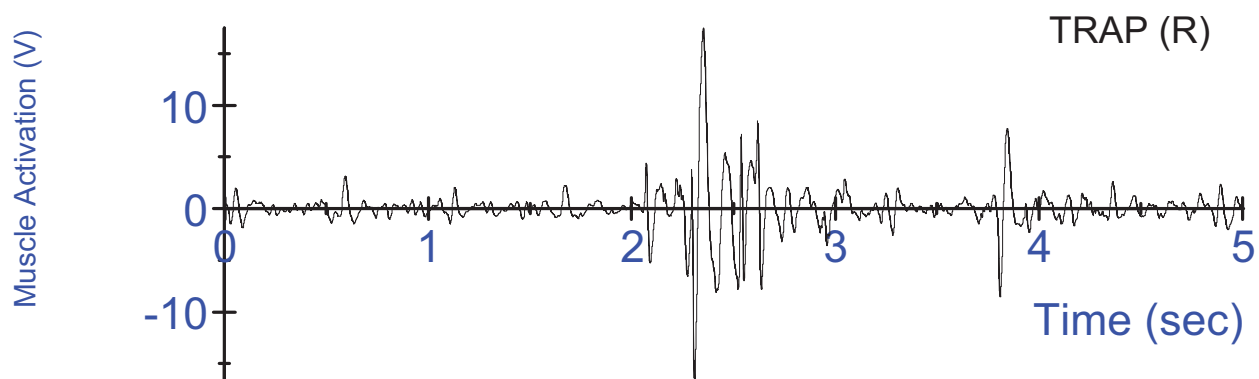
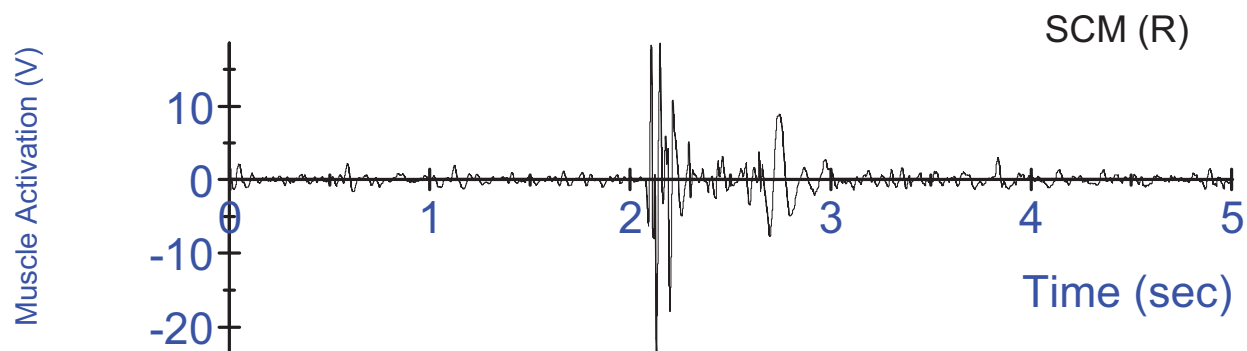
S14 Tensed Test #3 - Swing acceleration, filtered at 180Hz;
3-2-2-2 head acceleration, unfiltered



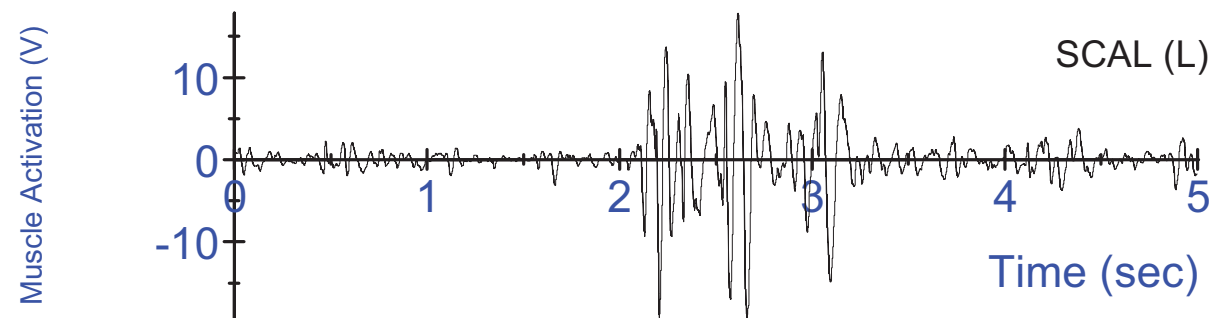
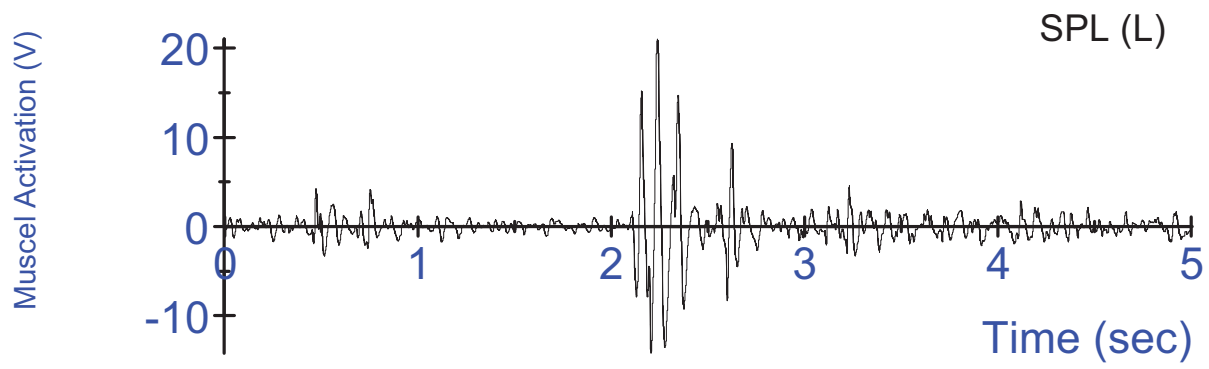
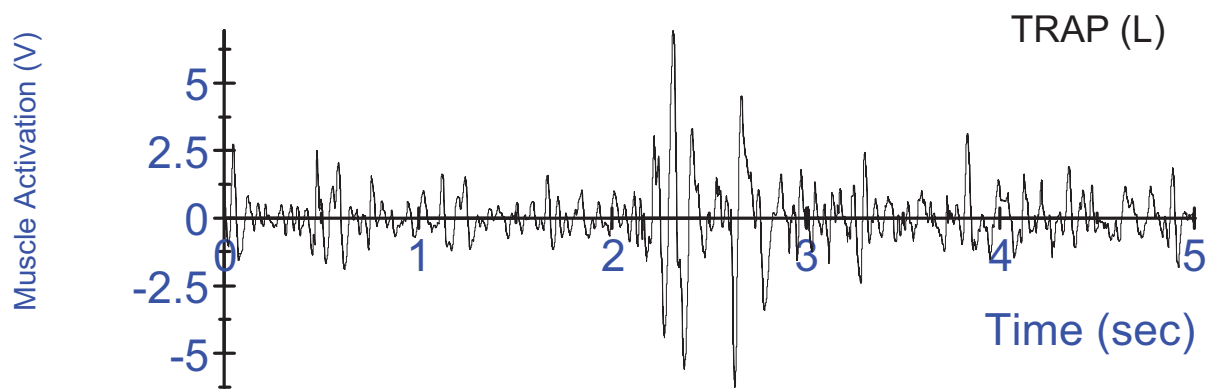
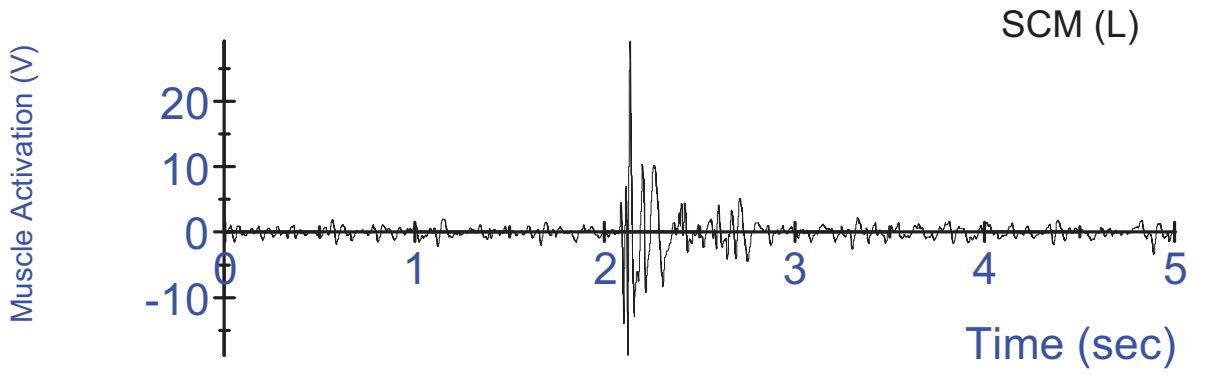
S14 Tensed Test #3 - Swing acceleration, filtered at 180Hz;
3-2-2-2 head acceleration, unfiltered



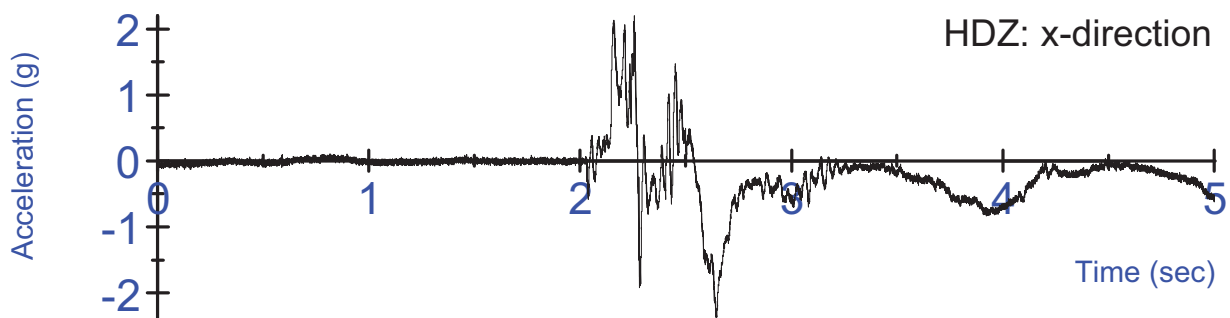
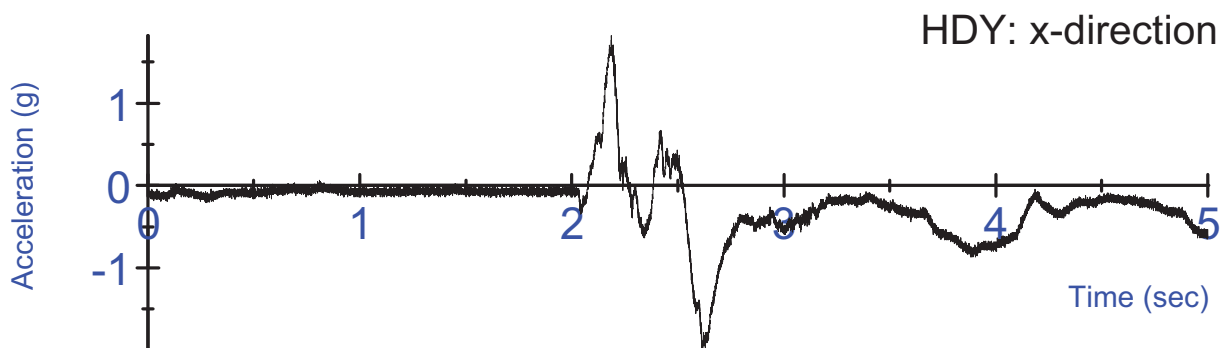
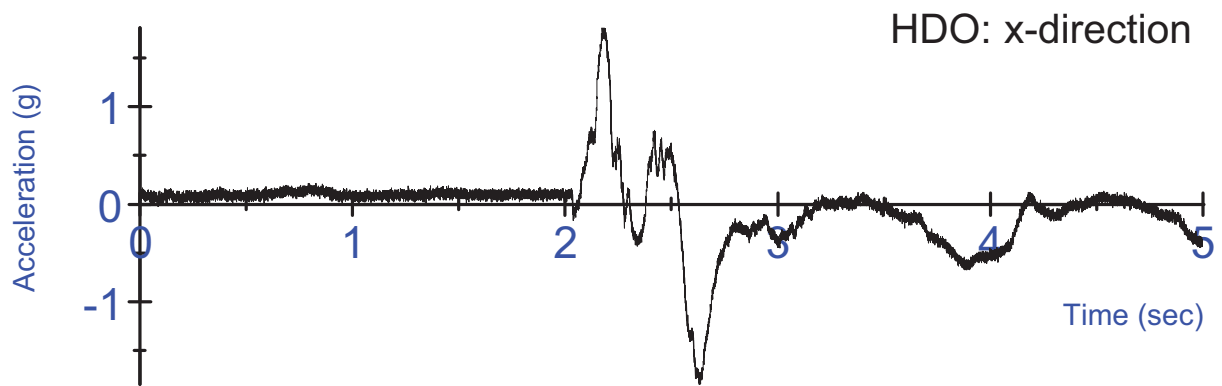
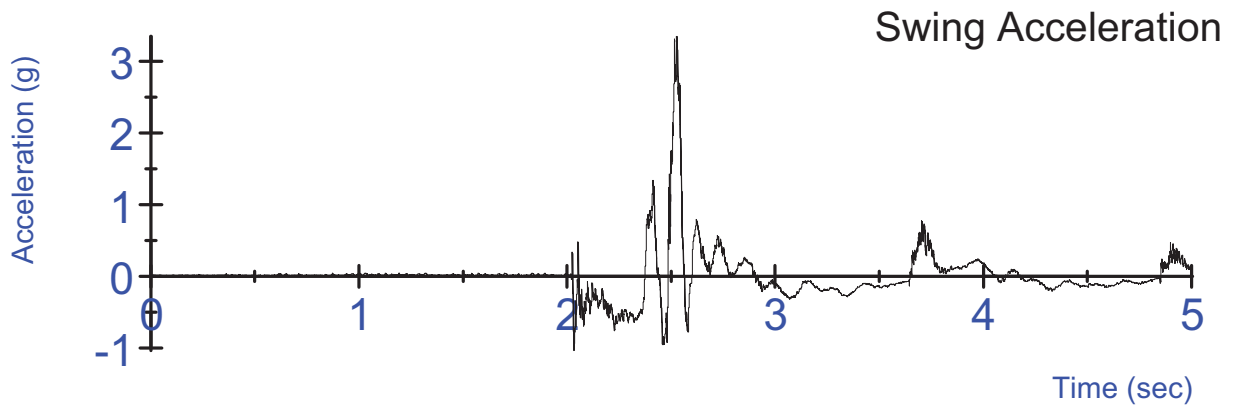
S14 Tensed Test #3 - Swing acceleration, filtered at 180Hz;
3-2-2-2 head acceleration, unfiltered



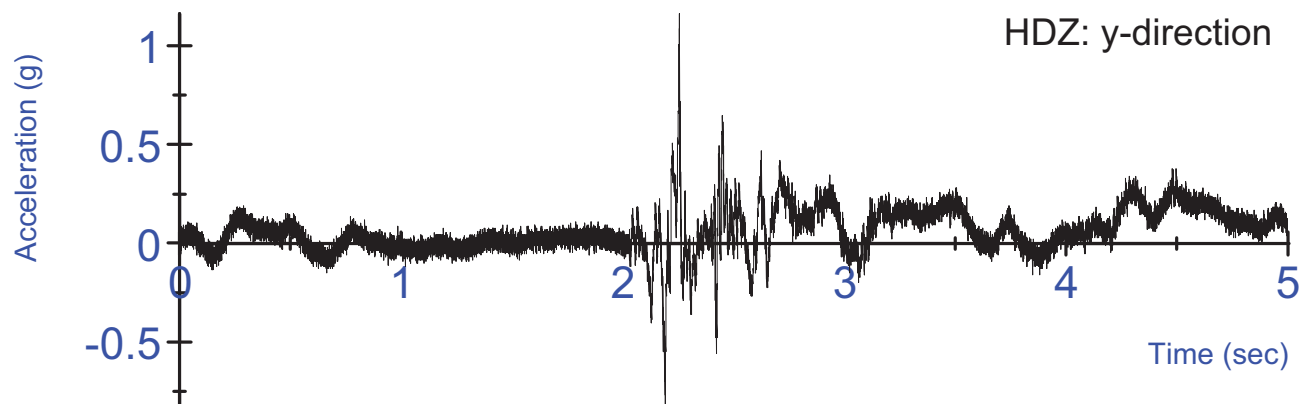
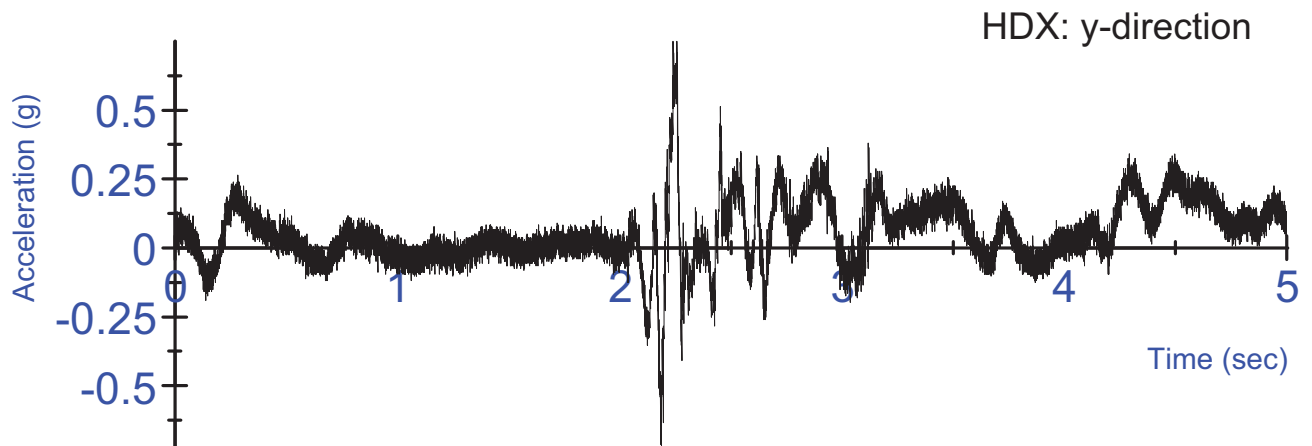
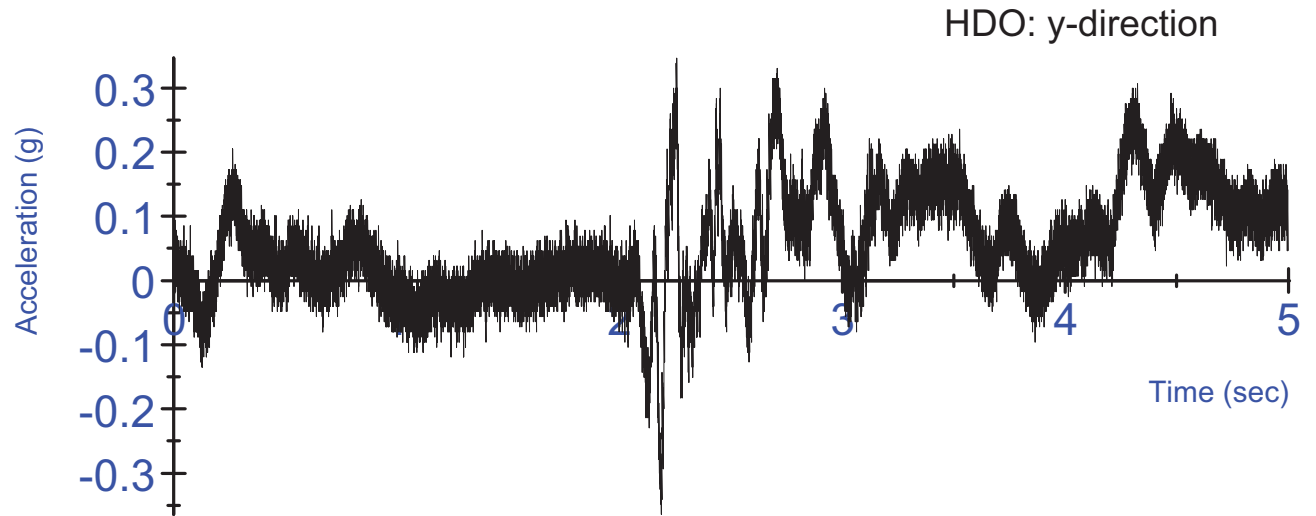
S14 Untensed Test #1 - Right Side EMG activation voltage
Un-rectified, Filtered at 6Hz



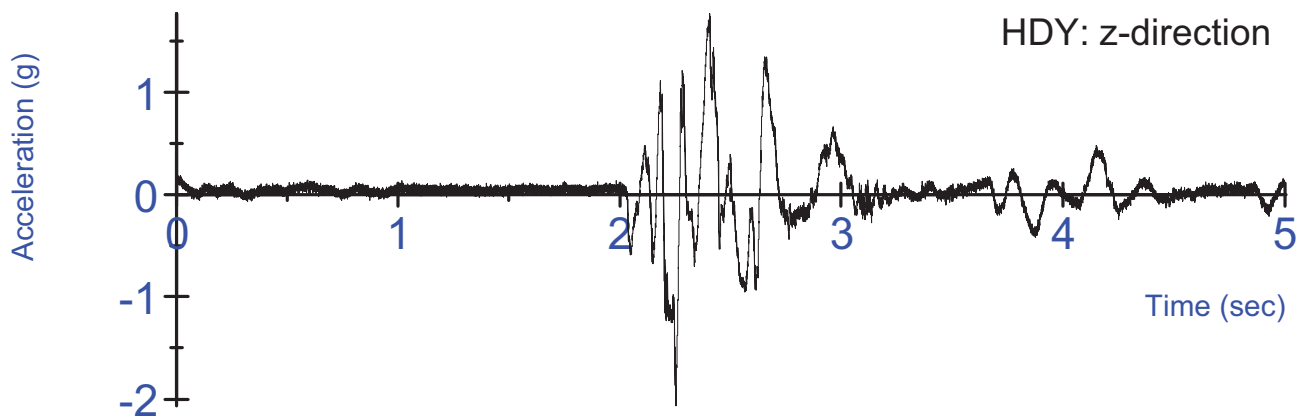
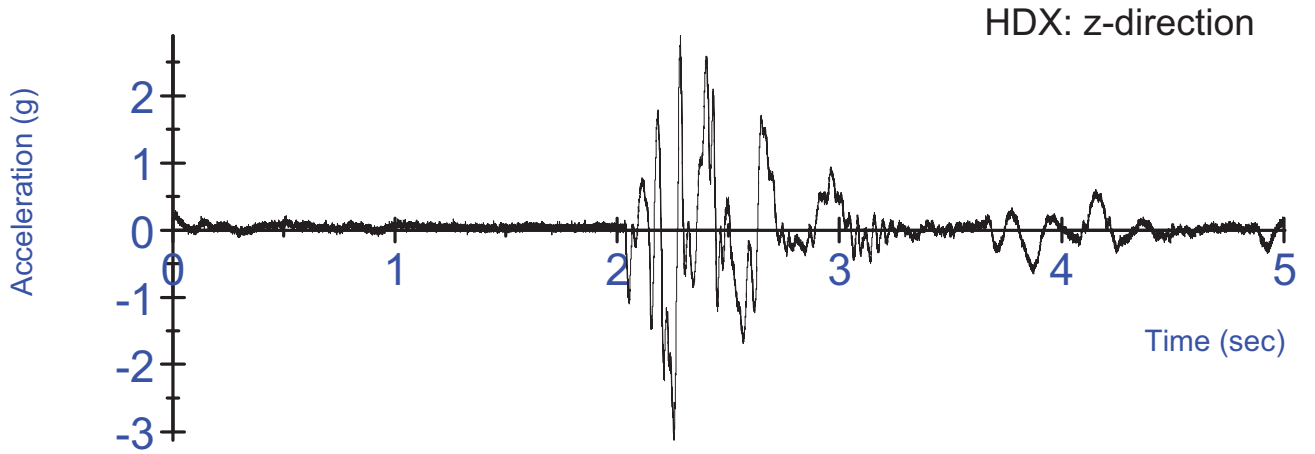
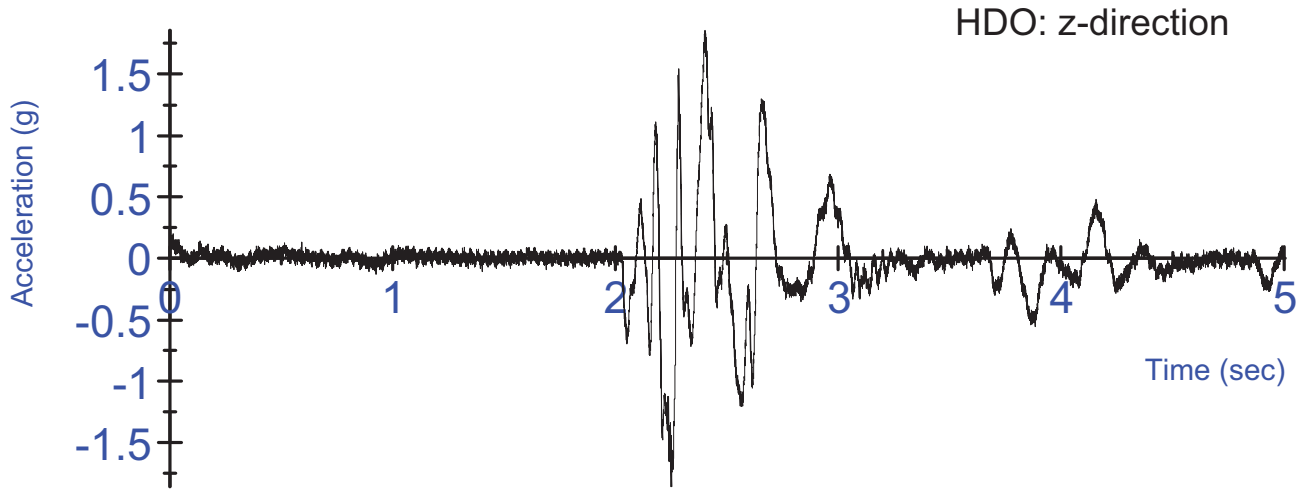
S14 Untensed Test #1 - Left Side EMG activation voltage
Un-rectified, Filtered at 6Hz



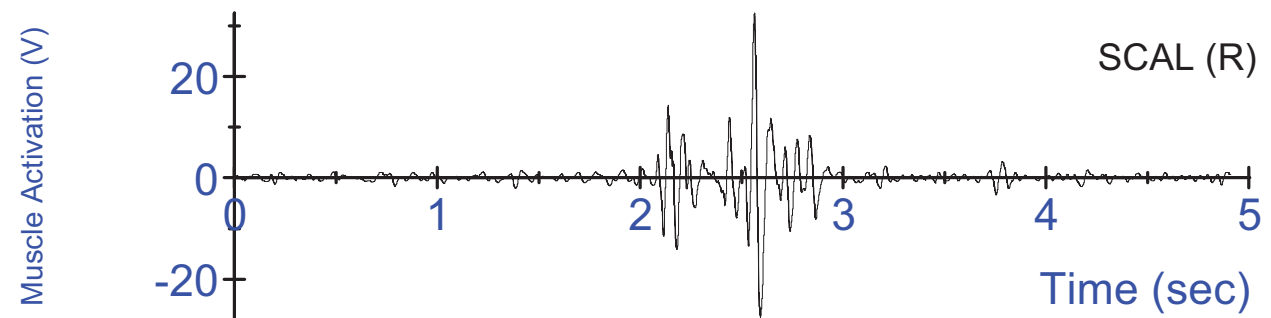
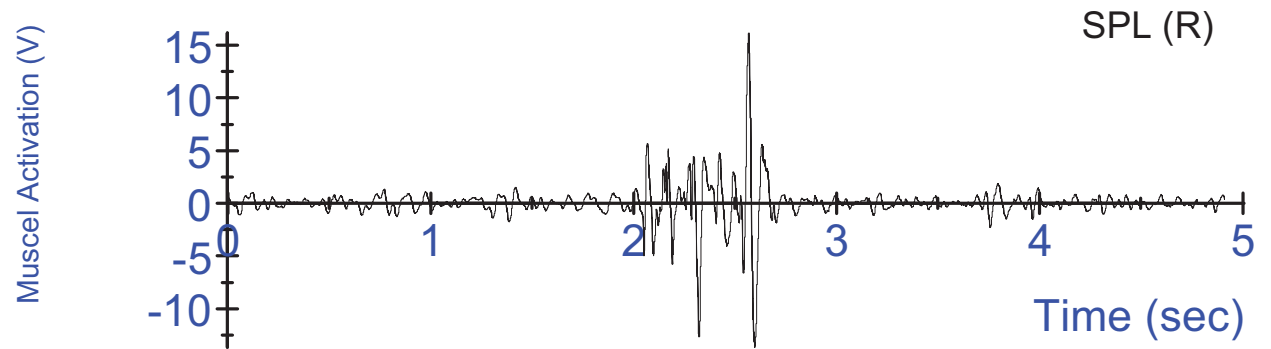
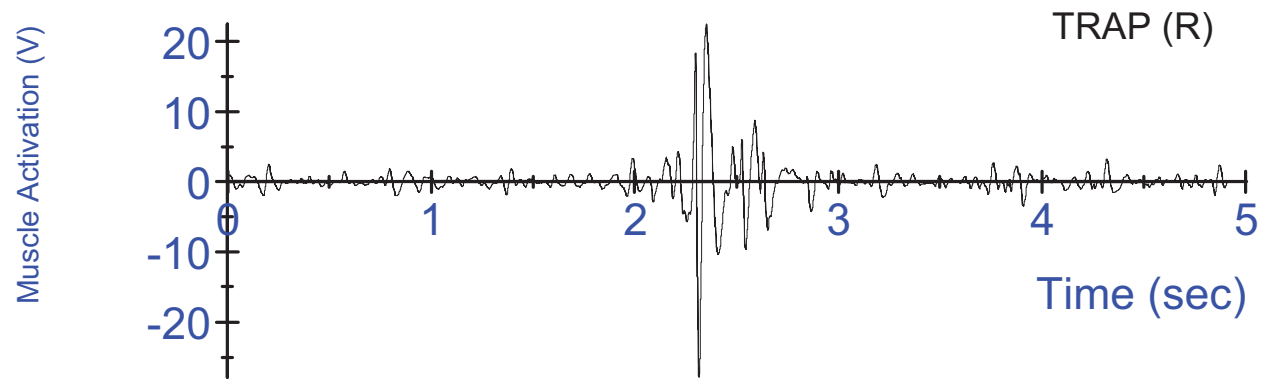
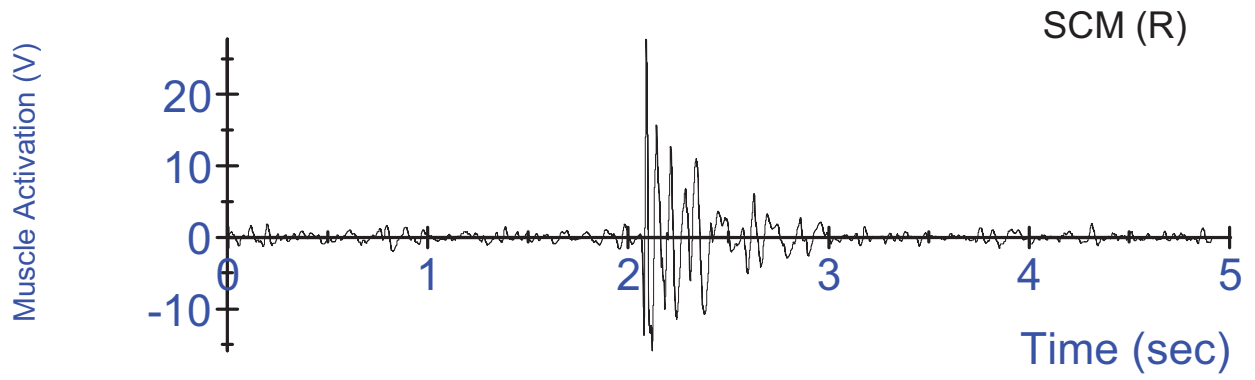
S14 Untensed Test #1 - Swing acceleration, filtered at 180Hz;
3-2-2-2 head acceleration, unfiltered



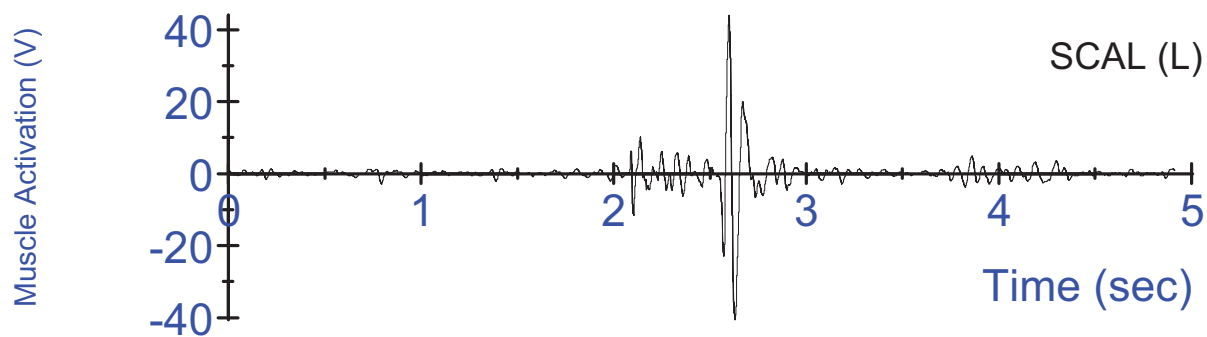
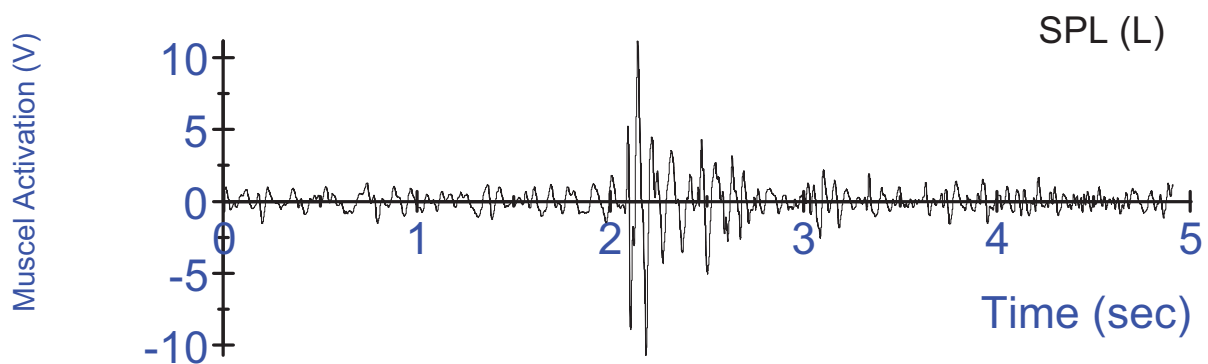
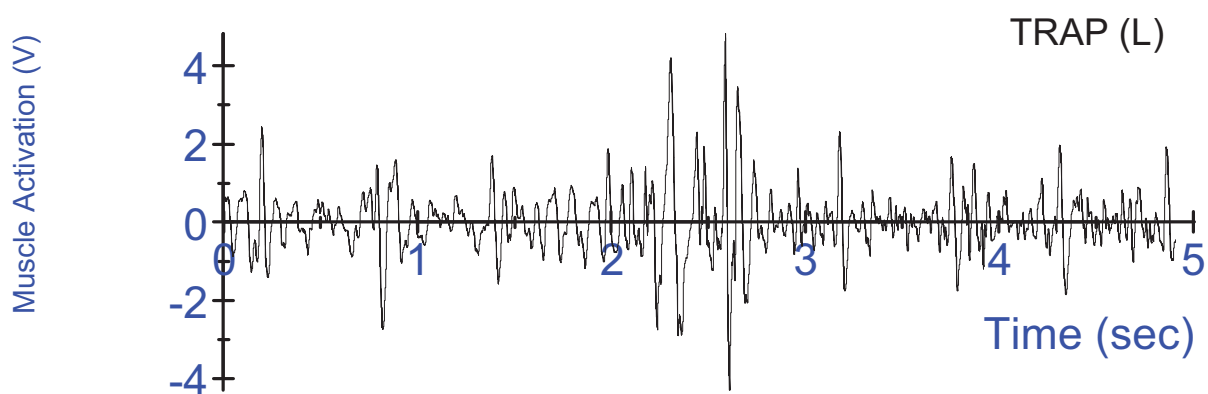
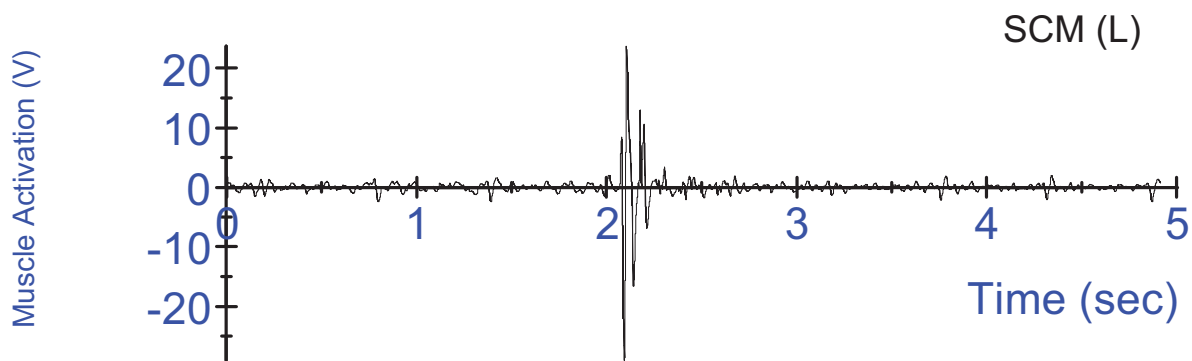
S14 Untensed Test #1 - Swing acceleration, filtered at 180Hz;
3-2-2-2 head acceleration, unfiltered



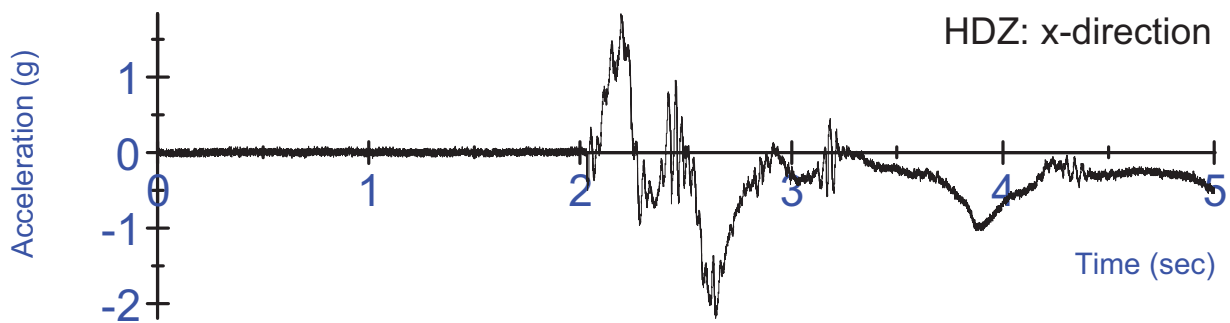
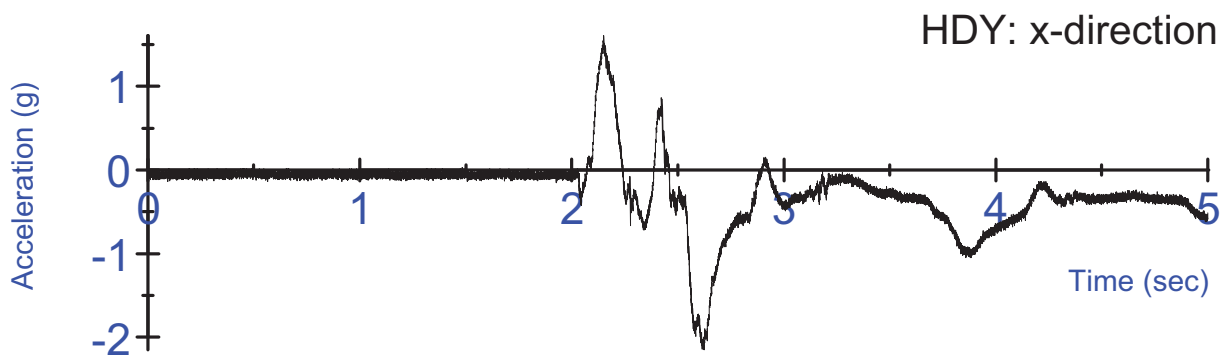
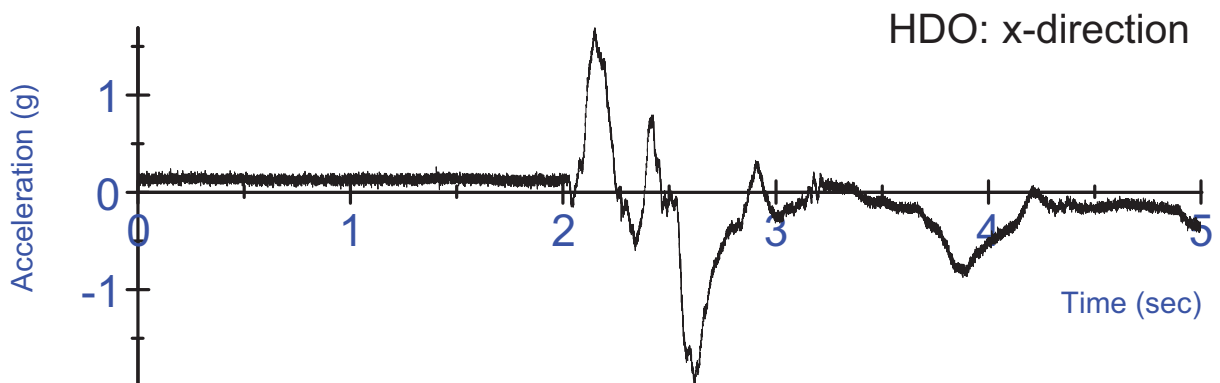
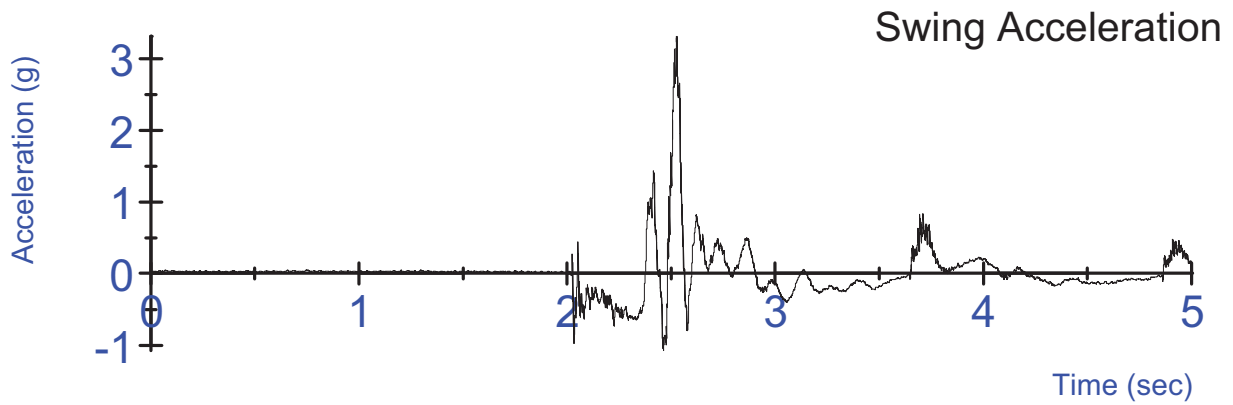
S14 Untensed Test #1 - Swing acceleration, filtered at 180Hz;
3-2-2-2 head acceleration, unfiltered



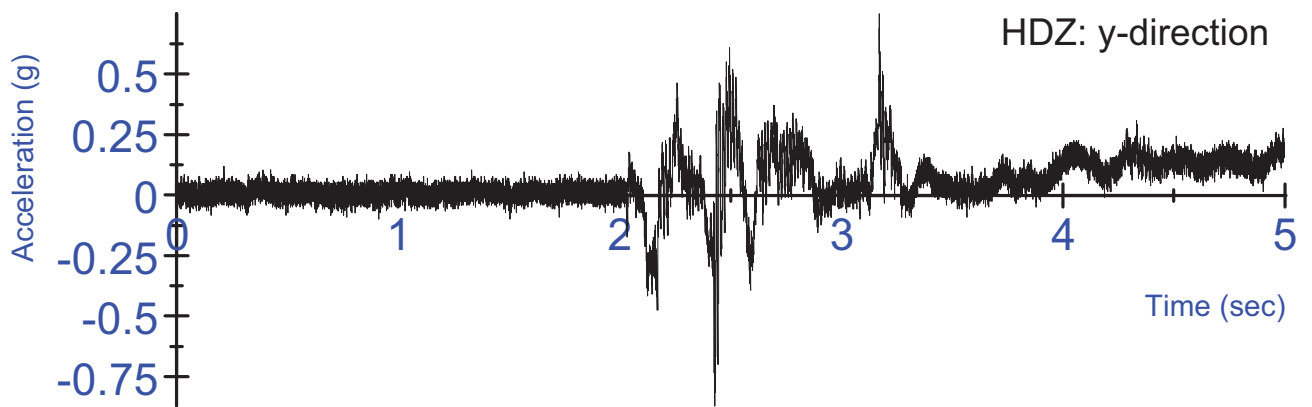
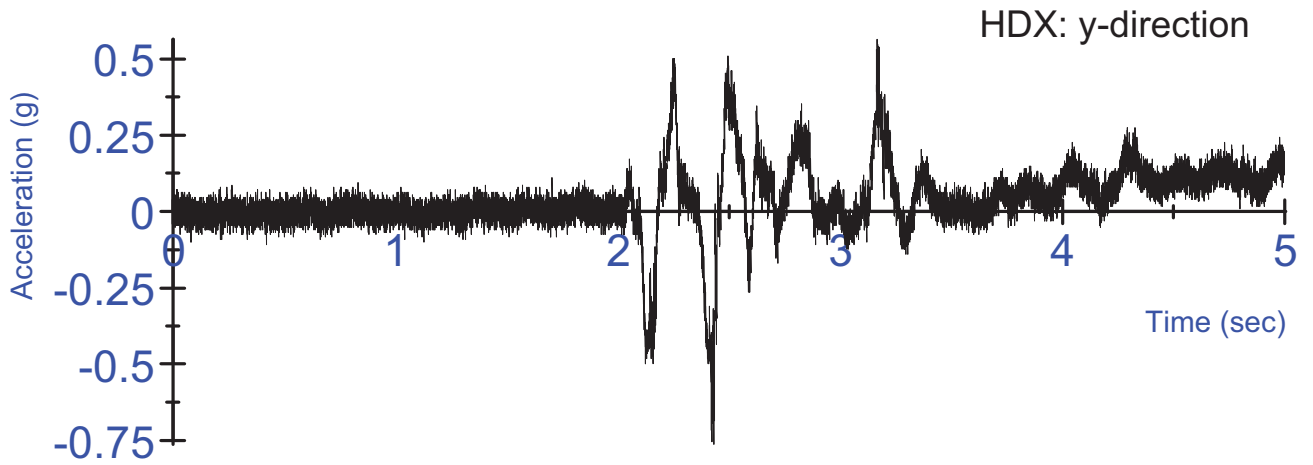
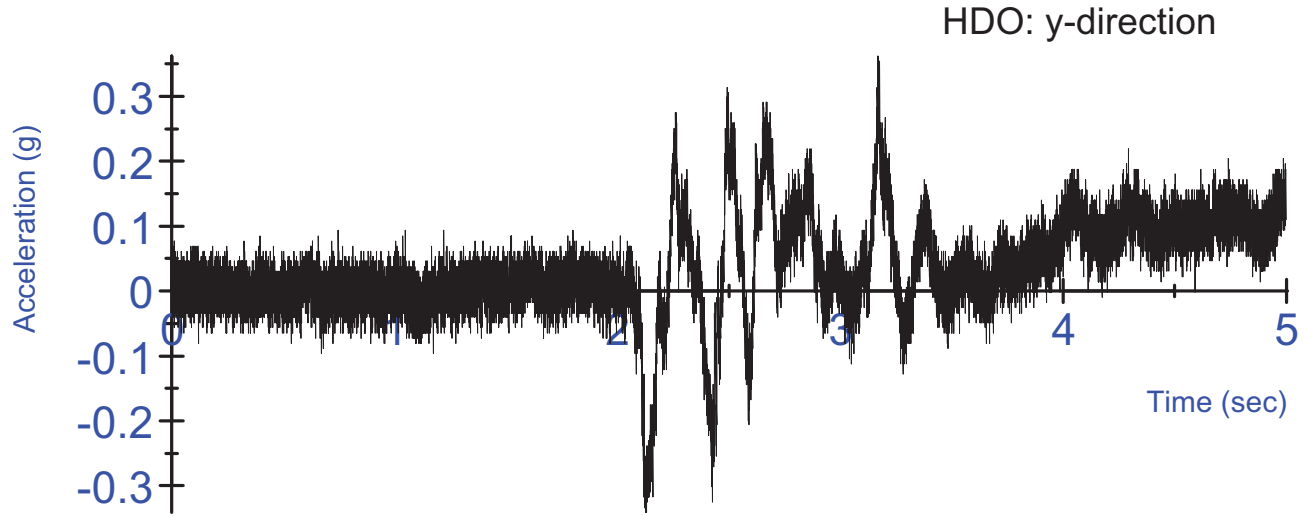
S14 Untensed Test #2 - Right Side EMG activation voltage
Un-rectified, Filtered at 6Hz



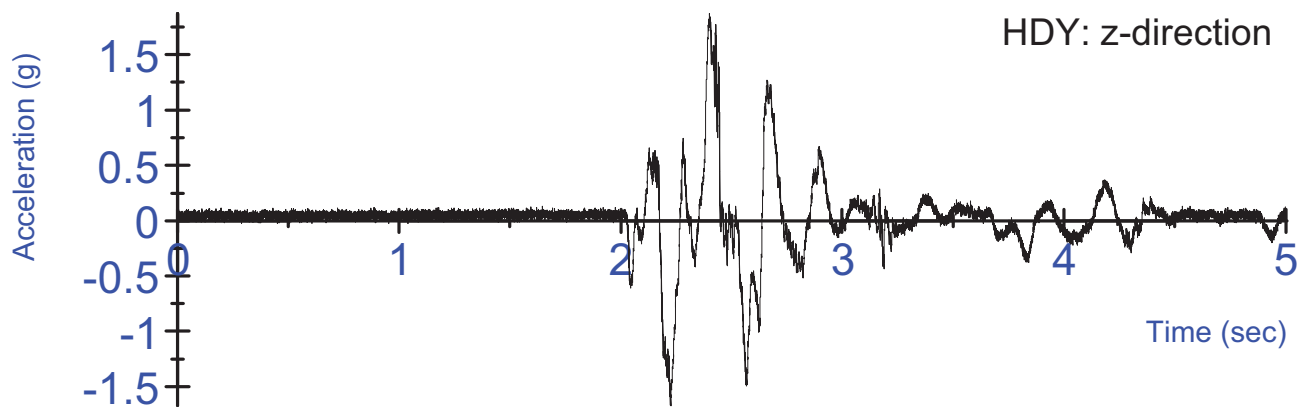
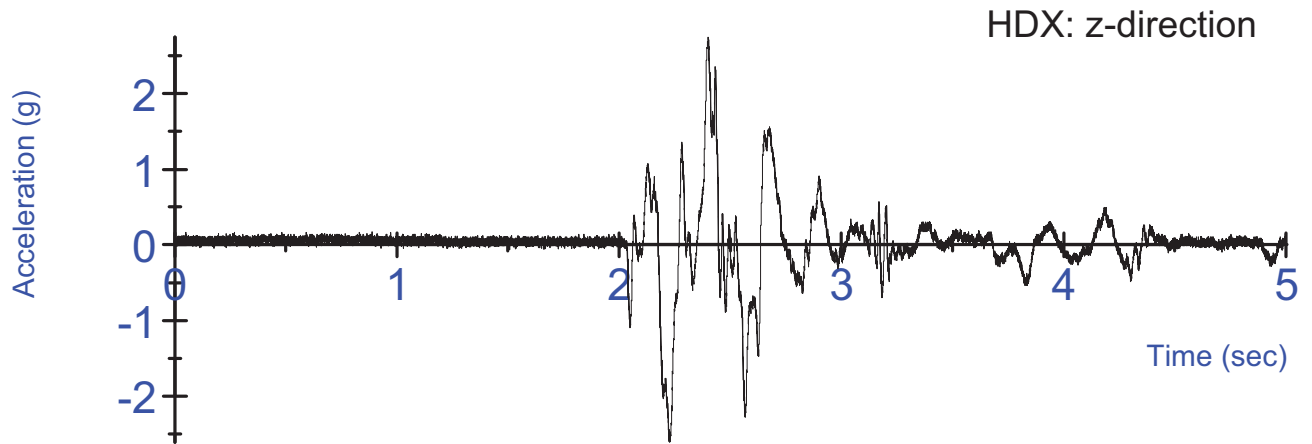
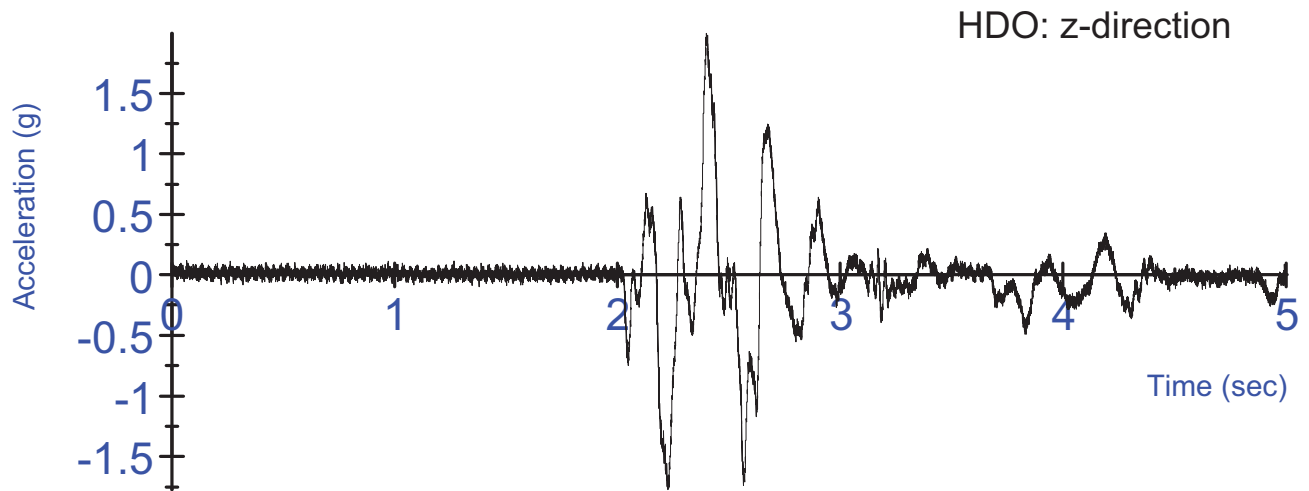
S14 Untensed Test #2 - Left Side EMG activation voltage
Un-rectified, Filtered at 6Hz



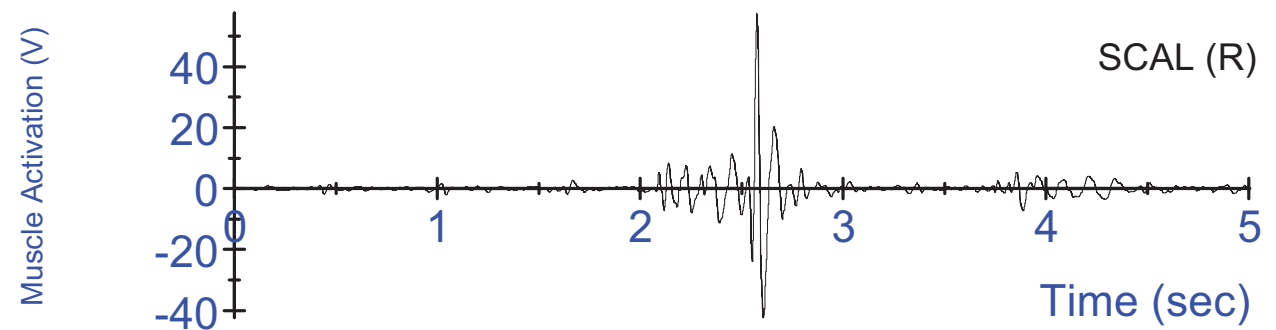
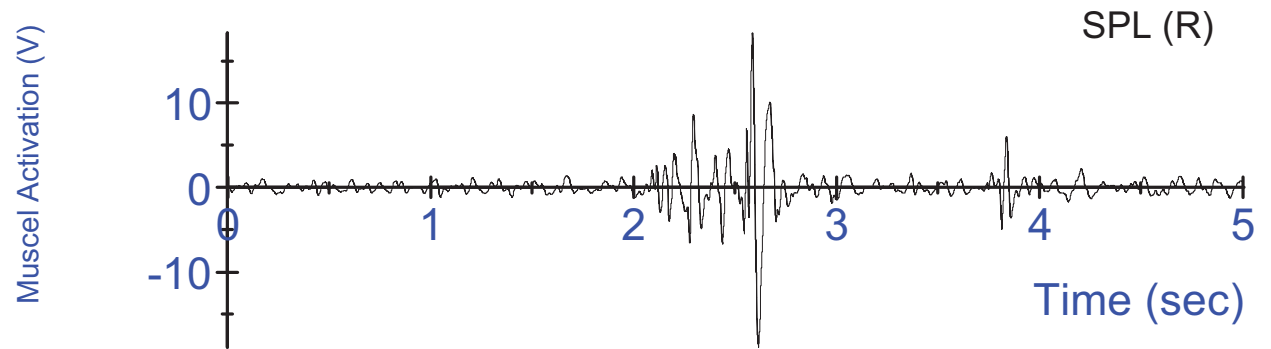
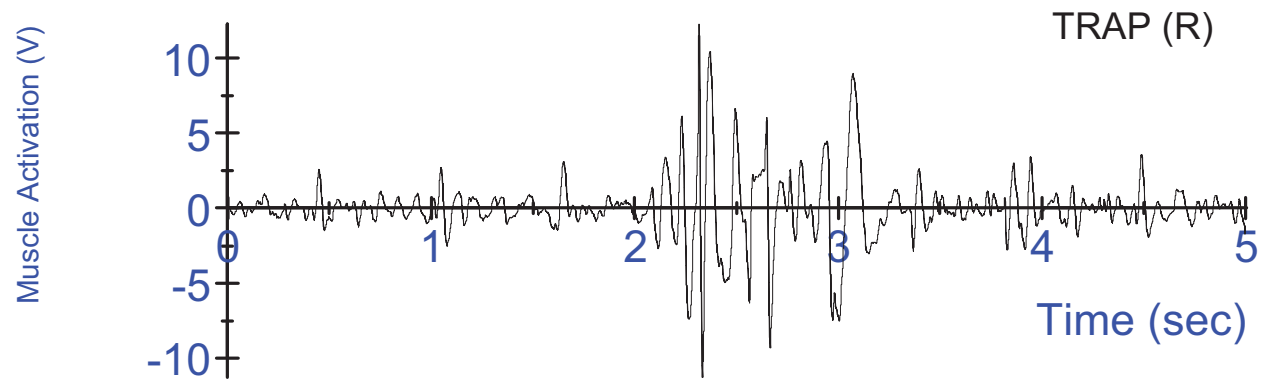
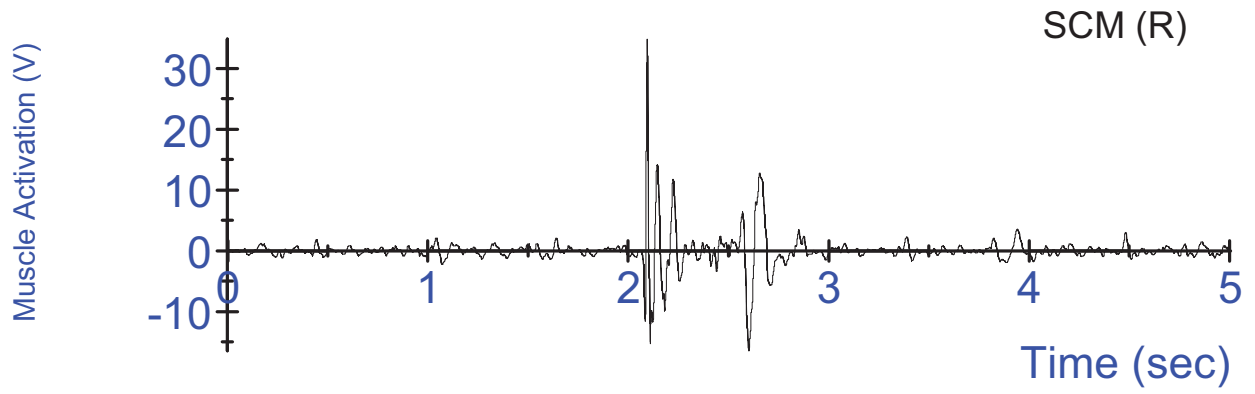
S14 Untensed Test #2 - Swing acceleration, filtered at 180Hz;
3-2-2-2 head acceleration, unfiltered



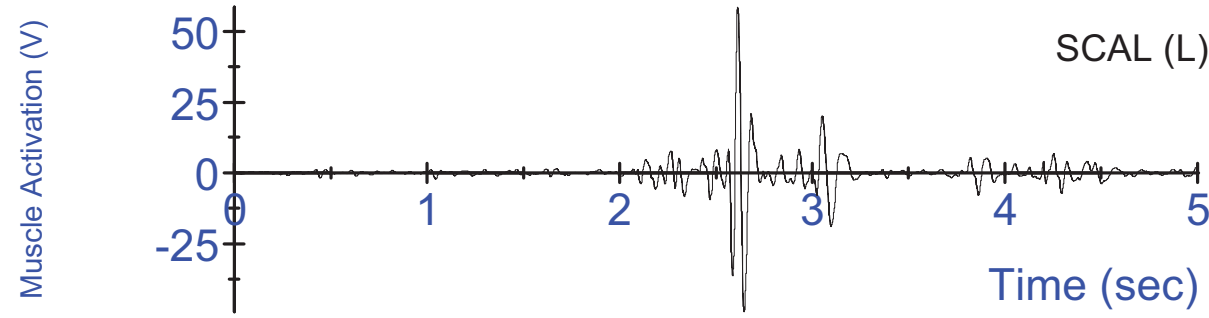
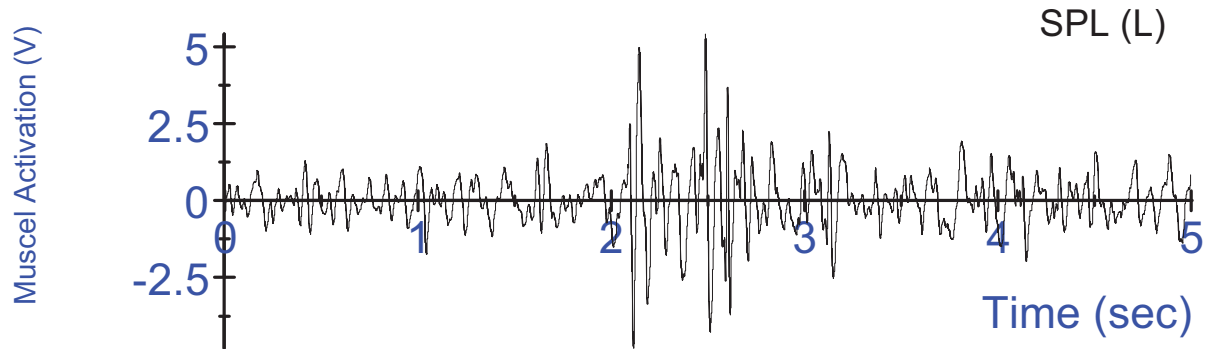
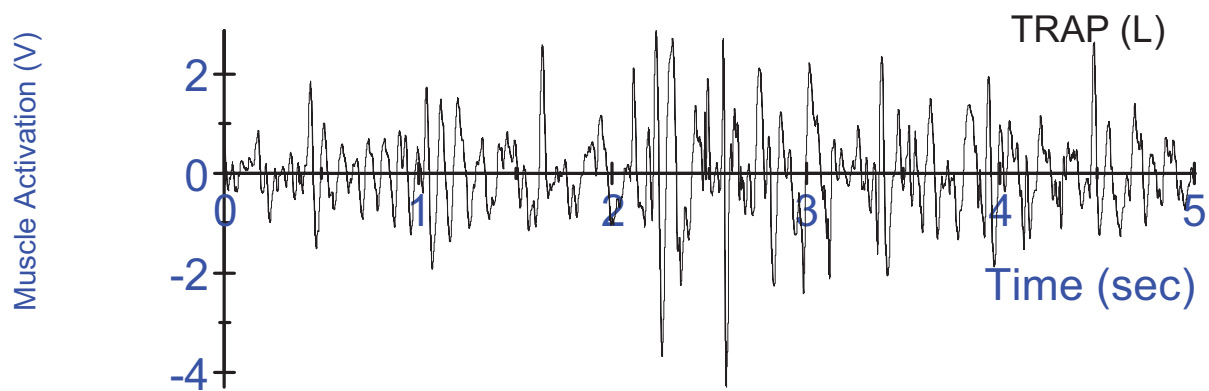
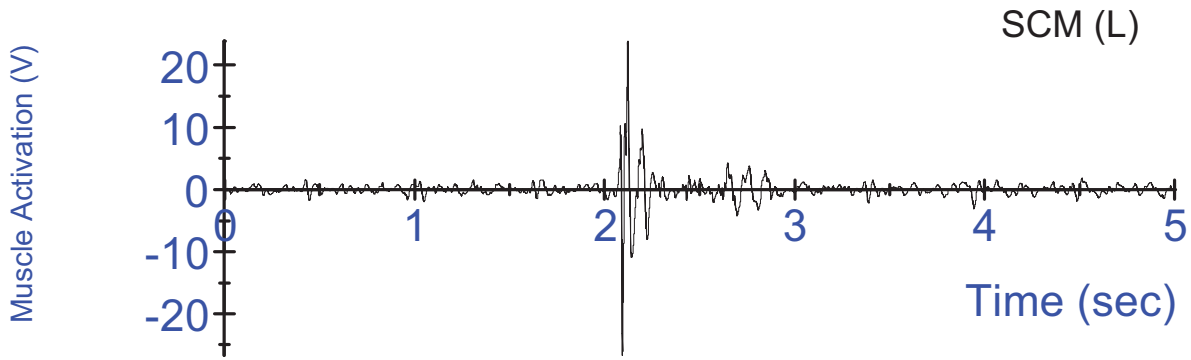
S14 Untensed Test #2 - Swing acceleration, filtered at 180Hz;
3-2-2-2 head acceleration, unfiltered



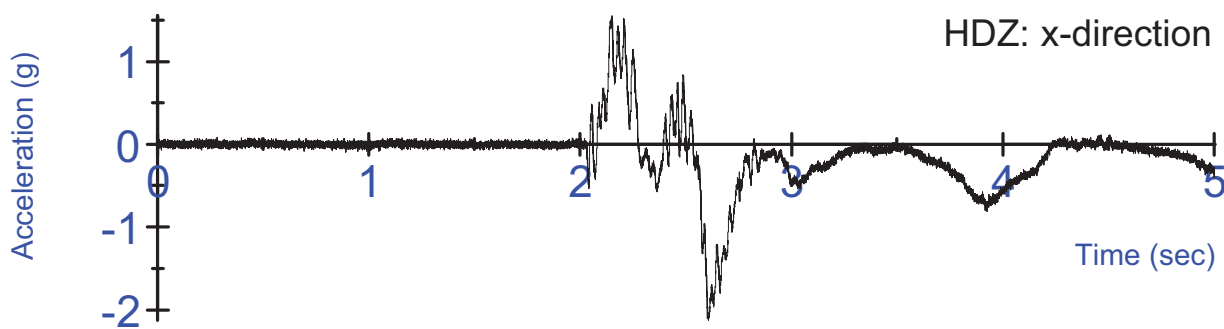
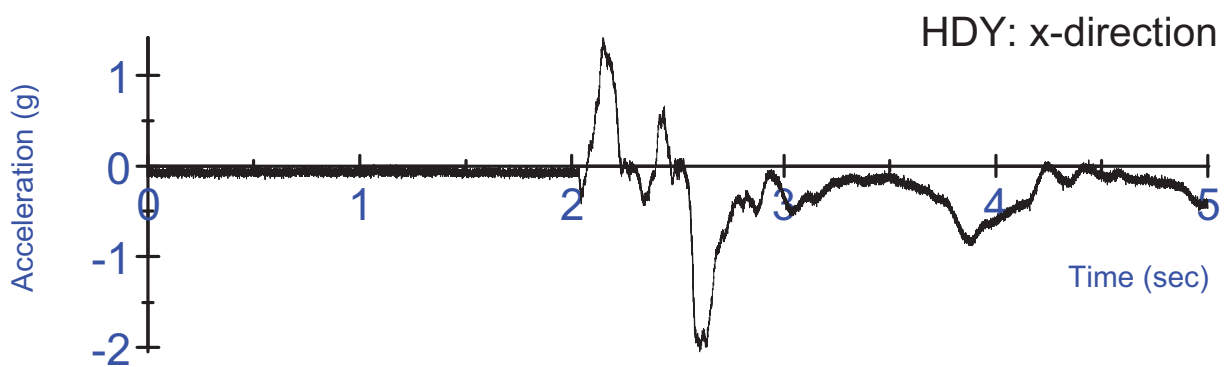
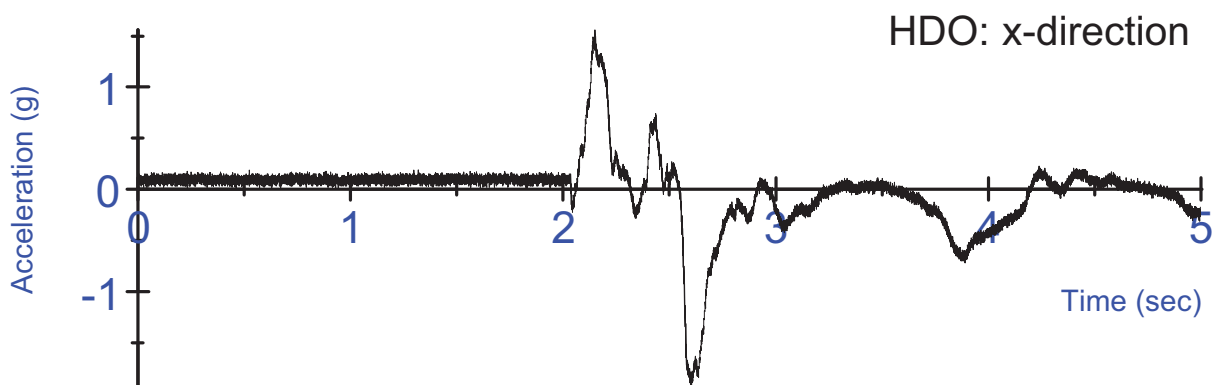
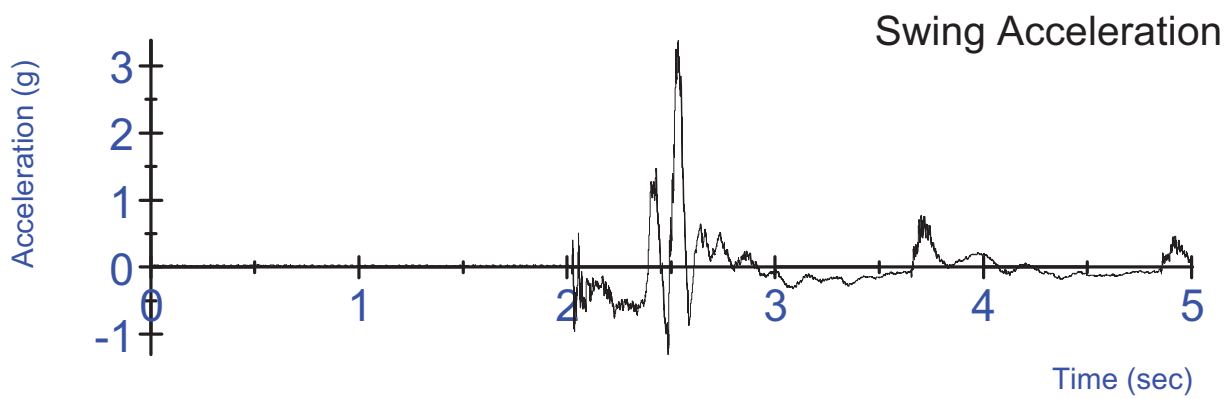
S14 Untensed Test #2 - Swing acceleration, filtered at 180Hz;
3-2-2-2 head acceleration, unfiltered



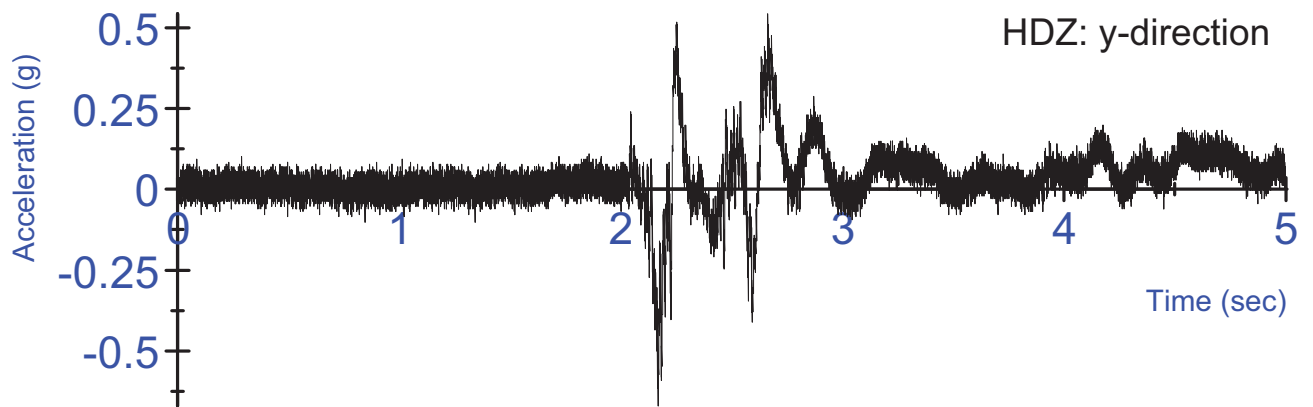
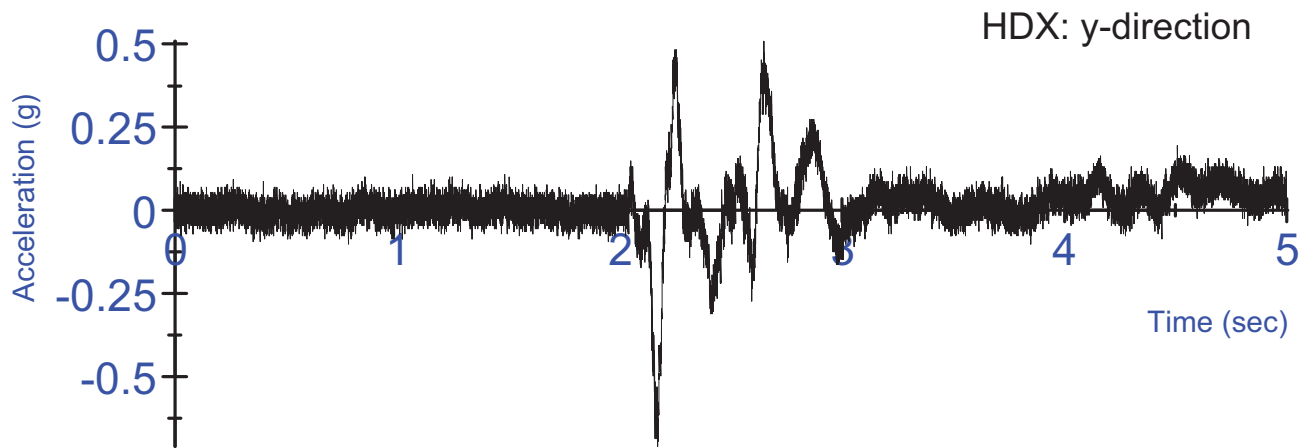
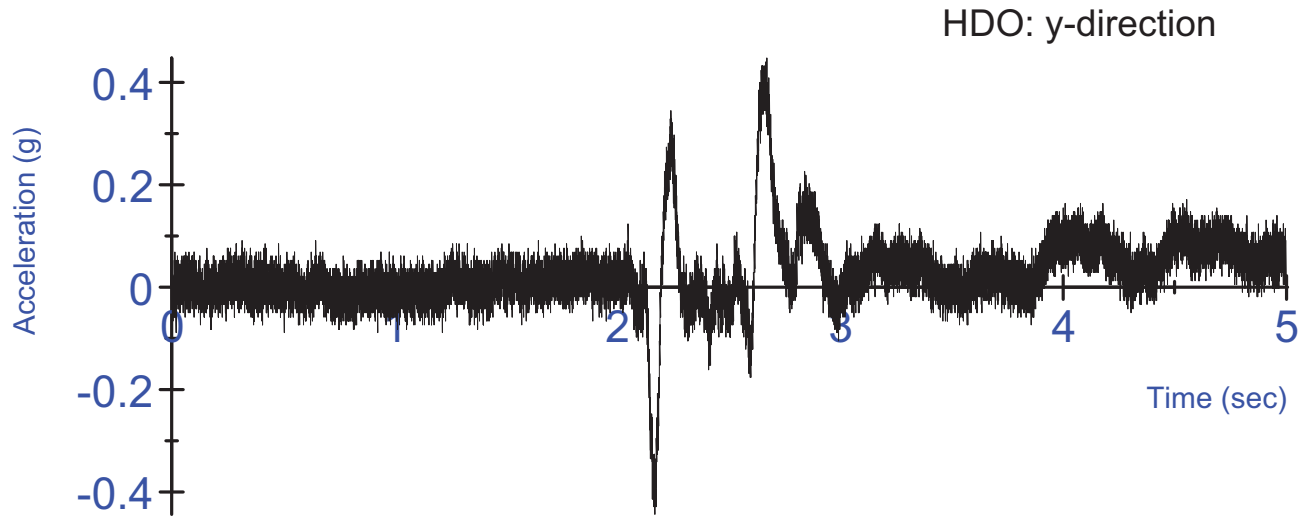
S14 Untensed Test #3 - Right Side EMG activation voltage
Un-rectified, Filtered at 6Hz



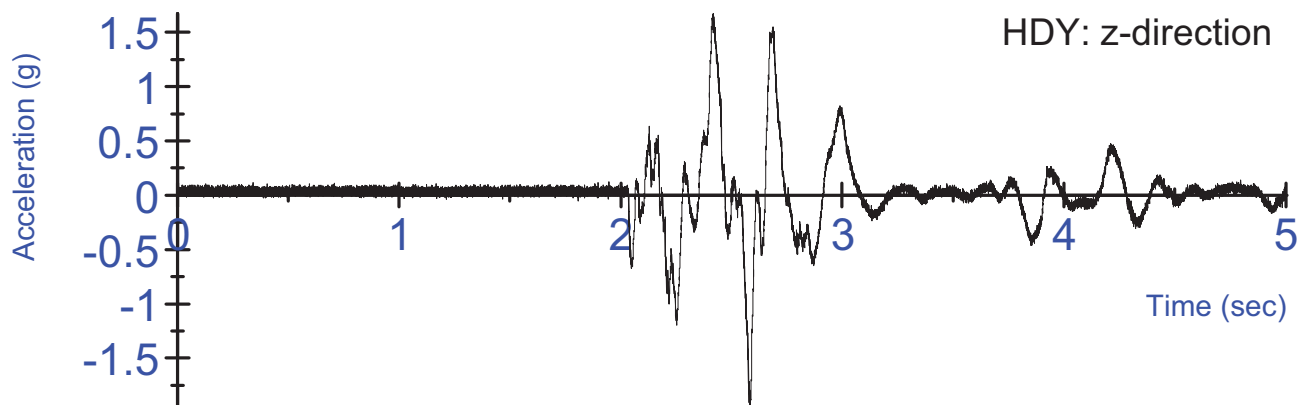
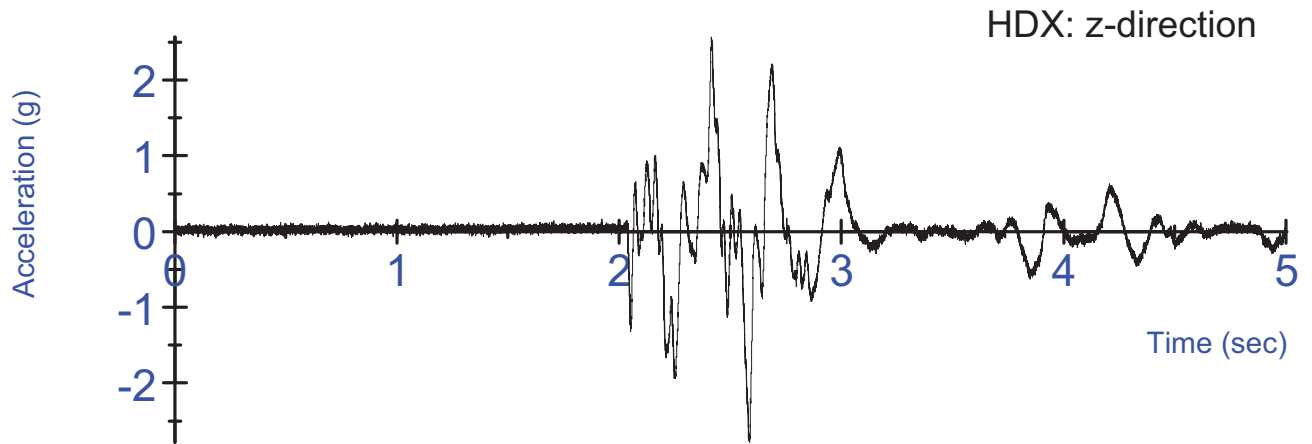
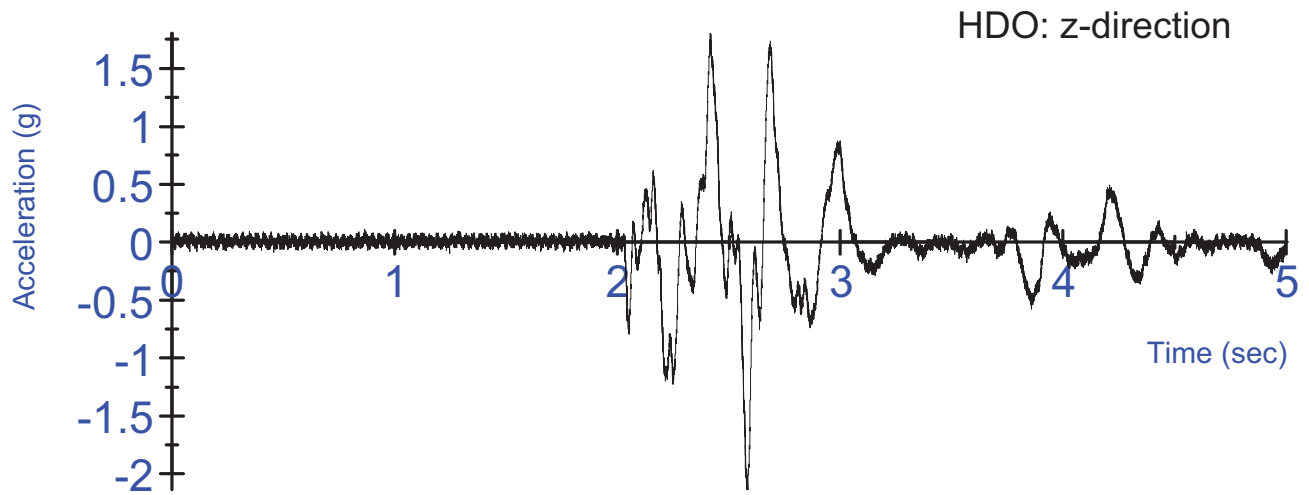
S14 Untensed Test #3 - Left Side EMG activation voltage
Un-rectified, Filtered at 6Hz



S14 Untensed Test #3 - Swing acceleration, filtered at 180Hz;
3-2-2-2 head acceleration, unfiltered



S14 Untensed Test #3 - Swing acceleration, filtered at 180Hz;
3-2-2-2 head acceleration, unfiltered



S14 Untensed Test #3 - Swing acceleration, filtered at 180Hz;
3-2-2-2 head acceleration, unfiltered

APPENDIX D

Figures D-1 through D-5: Drawings of the various components of the swing fixtures design, including a full dimensional schematic of the swing fixture, and the swing fixture's turntable floor. Specifications for the swing's four shock absorbers are also included.

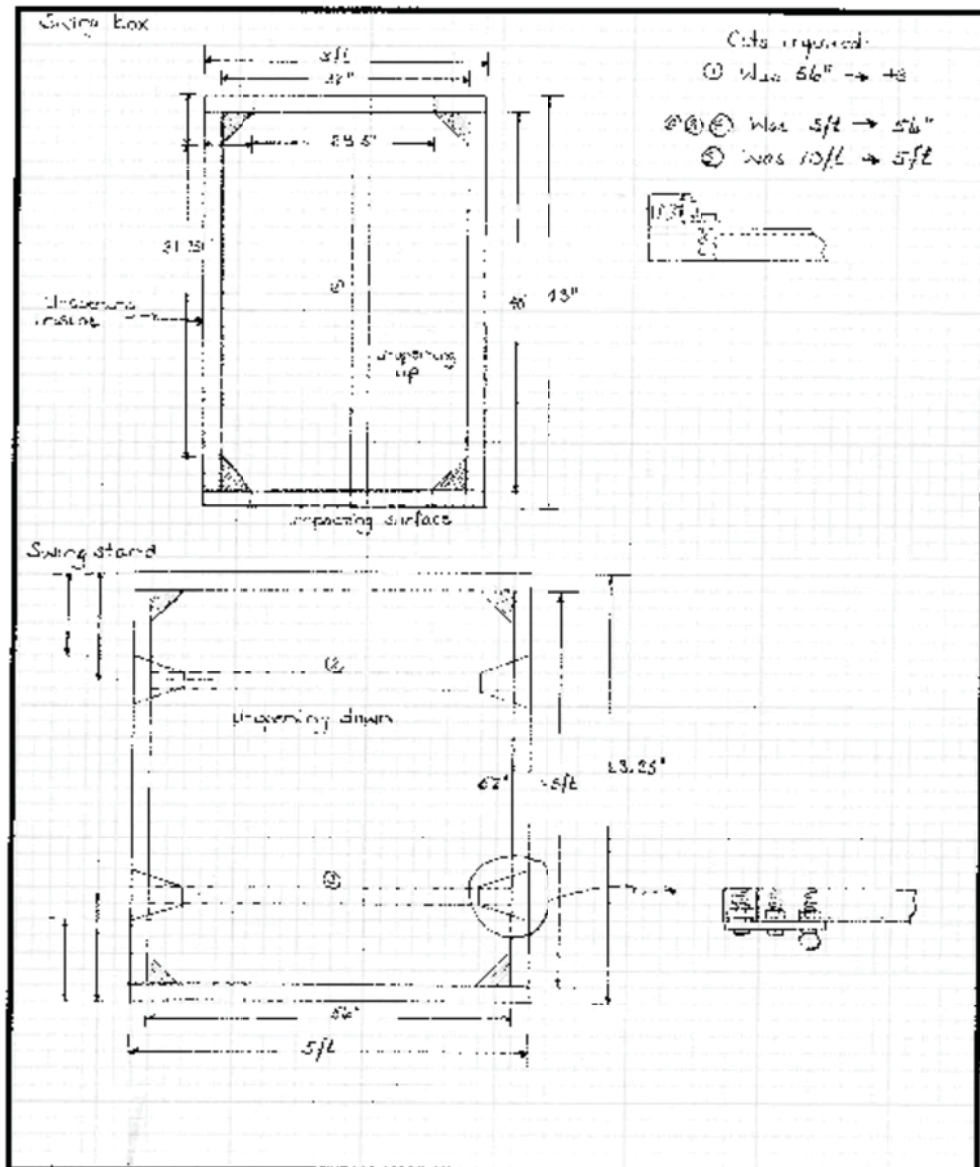


FIGURE D-1: Dimensional schematic of the swing fixture

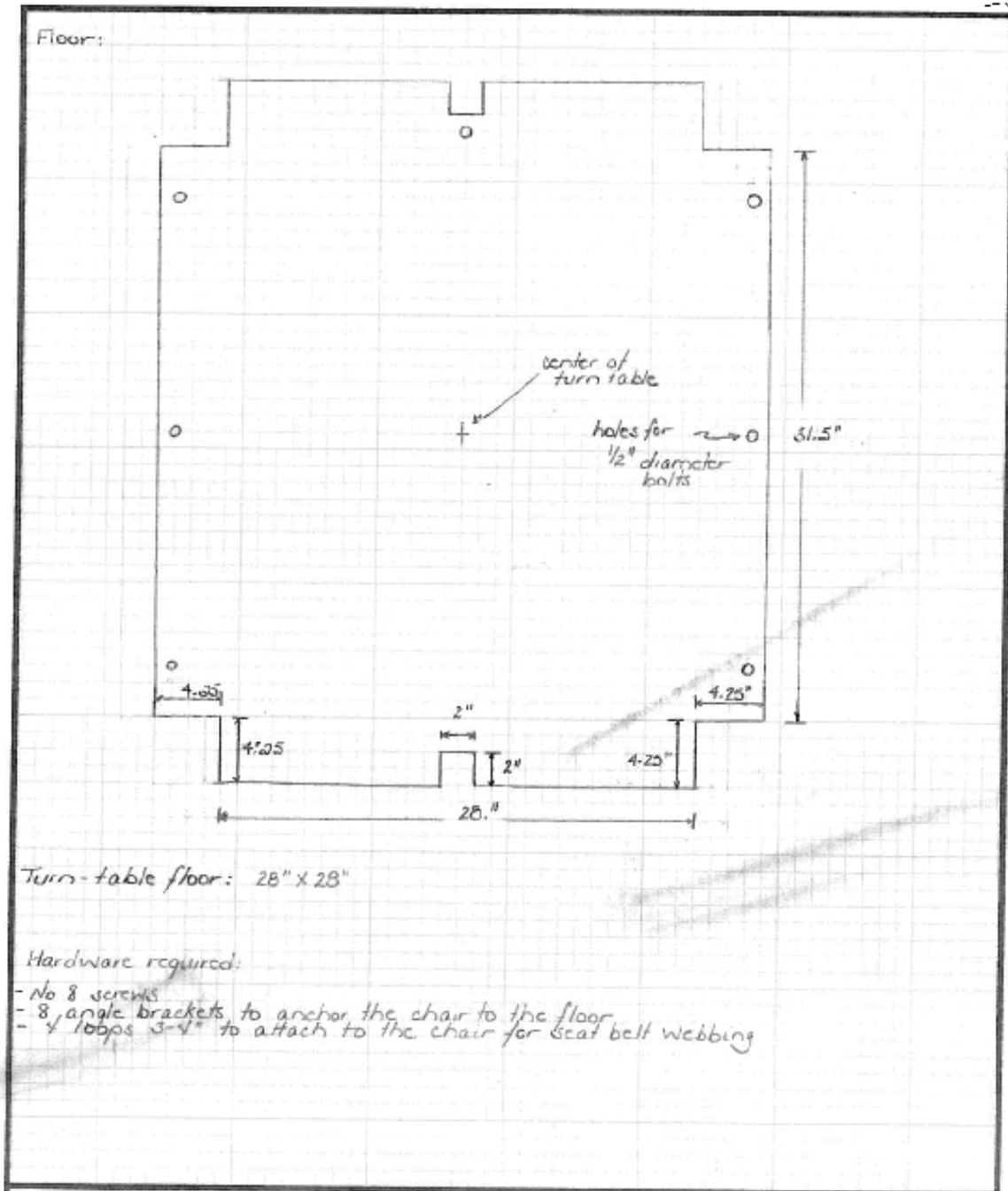


FIGURE D-2: Dimensions and construction schematic for the occupant compartment of the swing fixture

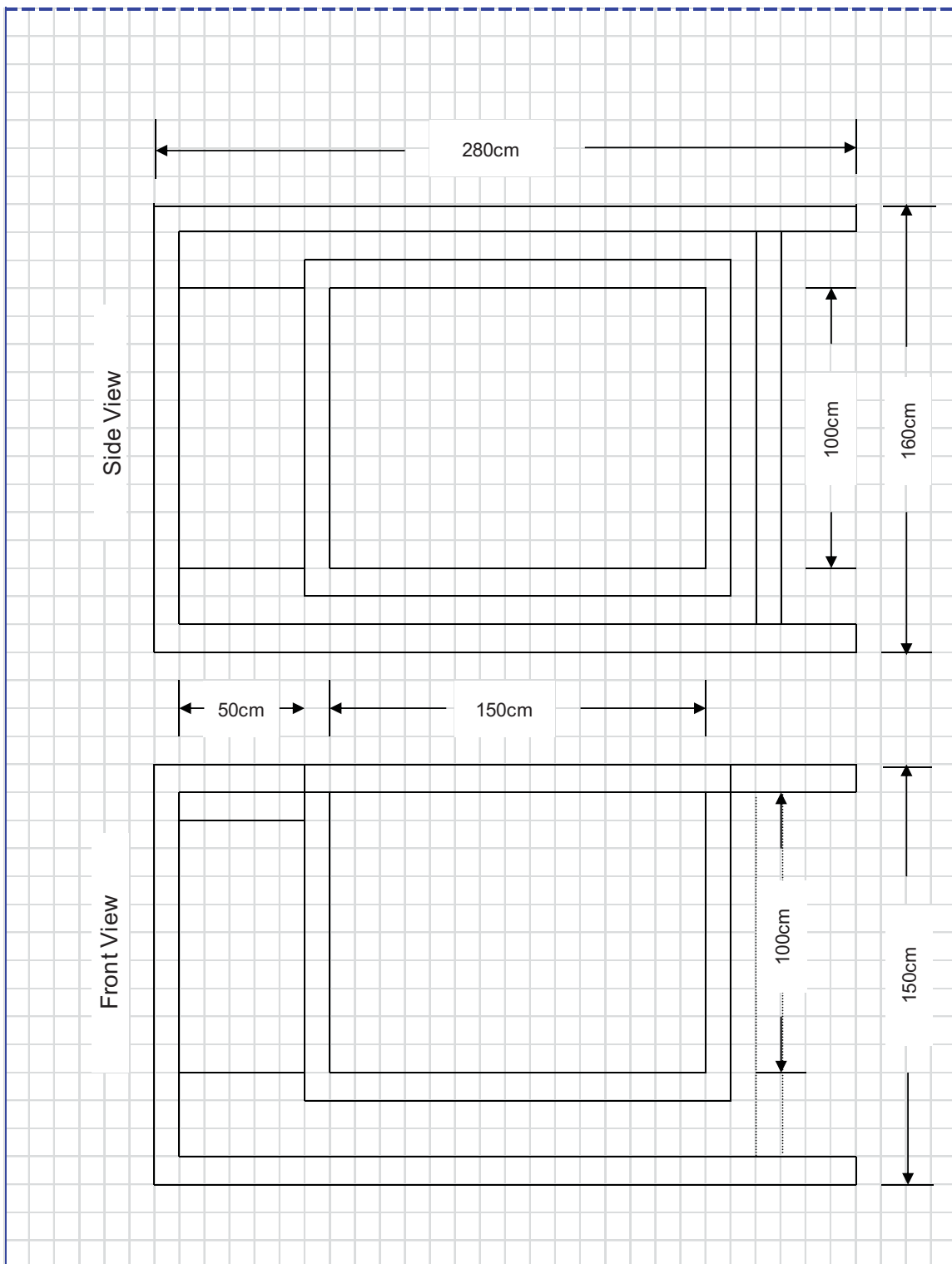


Figure D-3: Dimensional drawing of the occupant compartment floor

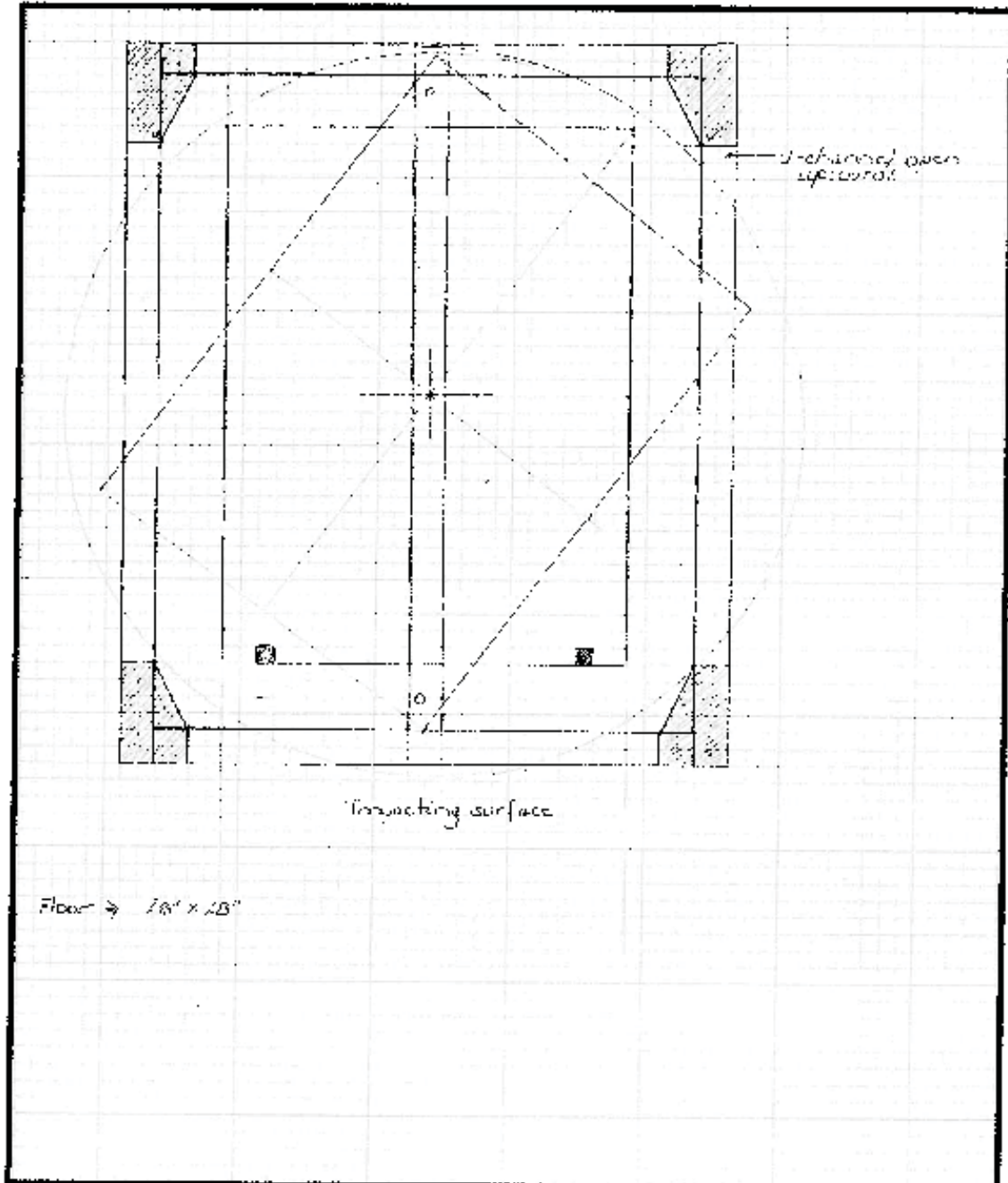


FIGURE D-4: Dimensional drawing of the turntable assembly of the occupant compartment floor

Miniature Shock Absorbers

MC 9 to MC 75



Self-Compensating

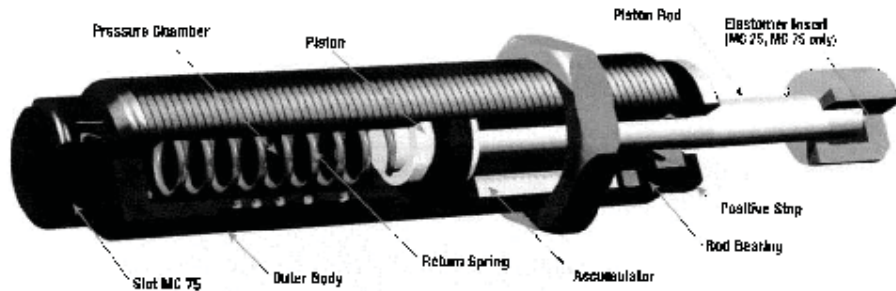
ACE Miniature Shock Absorbers are self-contained hydraulic units. The MC 9 to MC 75 model range has a very short overall length and low return force. Its small size allows for high energy absorption in confined spaces, while the wide effective weight ranges accommodate a variety of load conditions. With threaded outer bodies and multiple accessories, MC models can be mounted in numerous configurations.

Applications include: small linear slides, material handling and packaging equipment, small robotics, office and medical equipment, as well as instrumentation.

Miniature Shock Absorbers MC 9 to MC 75

Self-Compensating

22



Ordering Information

MC 75 - 1

MC Series	Model Number	Effective Weight	Button Options
	9	MC 7M	MC 2M & 4M
	10	1 Light	Extended My Button
	25	2 Medium	-B Detrain Button
	30	MC 10	MC 25 & 75
	35	L Light Range	Striked x 3 Button
		H Heavy Duty	-M3 No Button, Short Head
	40	MC 50	-B0 No Button, Striked Flat
	M 48 x 1 Metric	L Light Range	BP Steel Pullout/Retractive Cap Assembly
	L 48 x 0.75 Metric	H Heavy Range	MC 50 & MC 200-2
	MC 75	MC 50-5 MC 200-2	1 Light
	M 75 x 1 Metric	2 Medium	2 Medium
	Standard (UNF)	3 Heavy	3 Heavy
	M 75 x 1 Metric	MC 75	MC 75
	Standard (UNF)	1 Light	1 Light
	M 75 x 1 Metric	2 Medium	2 Medium
	MC 75	3 Heavy	3 Heavy
	Standard (UNF)	MC 75	MC 75
	M 75 x 1 Metric	1 Light	1 Light
	Standard (UNF)	2 Medium	2 Medium
	M 75 x 1 Metric	3 Heavy	3 Heavy



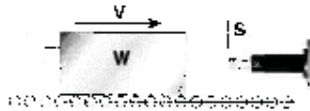
ACE Controls Inc. 800-521-3591 • (248) 478-4293 • Fax (248) 475-2470 • www.acecontrols.com • email: shop@acecontrols.com

FIGURE D-5: Technical specifications of the swing's shock absorbers

Horizontal Sizing Examples

W = Moving Weight (lbs)	Hp = Motor Power (horsepower)	E _k = Kinetic Energy (ft-lbs)
V = Initial Velocity (ft/sec)	Mu = Coefficient of Friction	E _p = Propelling Force Energy (ft-lbs)
Ta = Known Propelling Force (lbs)	C = Cycles per Hour	E _c = Energy per Cycle (ft-lbs)
D = Propelling Cylinder Bore (inches)	S = Stroke Length of Shock Absorber (inches)	E _t = Energy per Hour (ft-lbs/hour)
P = Propelling Cylinder Rod (inches)	S = Propelling Force of Shock Absorber (lbs)	W _{eq} = Effective Weight (lbs)
P = Air Pressure (psi)		

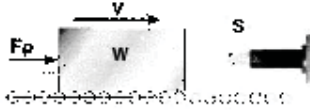
H1 Weight with No Propelling Force Examples: Crash Testers, Emergency Stops



FORMULA	EXAMPLE
$E_k = 0.186 \cdot W \cdot V^2$	W = 500 lbs
$F = F \cdot W$	V = 2 ft/sec
$E_c = E_k \cdot C$	C = 1
$E_t = F \cdot V \cdot C$	
$W_{eq} = E_t / 38.7$	

H1 - Select from Model Rating Chart: MC 3325-3 or MA 3325

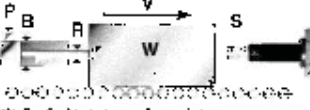
H2 Weight with Propelling Force Transfer Devices, Safety Doors, Cutting Shears



$F = F_p$	W = 140 lbs	C = 30	S = 31 in
$E_k = 0.186 \cdot W \cdot V^2$	V = 22 ft/sec	$E_c = 0.186 \cdot 140 \cdot 22^2 = 12,816$	
$F = F_p$	Fp = 30 lbs	C = 100 cph	
$E_c = F \cdot V \cdot C$	C = 100 cph	$E_t = 12,816 \cdot 100 = 1,281,600$	
$L = L \cdot C$	L = 0.4 inches	$W_{eq} = 1,281,600 / 38.7 = 33,116$	
$W_{eq} = E_t / 38.7$			

H2 - Select from Model Rating Chart: MC 75-3

H3 Weight with Propelling Cylinder Pick-and-Place Units, Linear Slides, Robotics

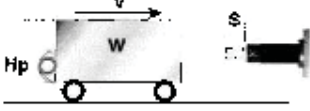


Note: B = Cylindrical or ball cylinder with spring or air pressure.

$E_k = 0.186 \cdot W \cdot V^2$	W = 20 lbs	F = 0.7854 \cdot D^2 \cdot P \cdot L	
$E_c = 0.186 \cdot W \cdot V^2$	V = 2 ft/sec	L = 0.31416 \cdot D \cdot L	
$F = F \cdot W$	D = 5/16 inches	E = 152 \cdot 0.75	
$E_c = E_k \cdot C$	C = 100 cph	E = 114	
$E_t = F \cdot V \cdot C$	P = 60 psi	$E_t = 114 \cdot 2 \cdot 100 = 22,800$	
$W_{eq} = E_t / 38.7$	C = 60 cph	$W_{eq} = 22,800 / 38.7 = 589$	
	S = 0.5 inches		

H3 - Select from Model Rating Chart: MA 225 or SC 300-4

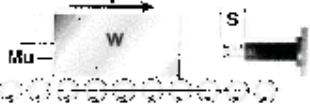
H4 Weight with Motor Drive Lift Trucks, Stacker Units, Overhead Cranes



$F = 33000 \cdot Hp$	W = 11 lbs	L = 0.31416 \cdot D^2 \cdot L	
$E_k = 0.186 \cdot W \cdot V^2$	V = 100 ft/sec	E = 152 \cdot 0.75	
$F = F \cdot W$	Hc = 2 ft	E = 114	
$E_c = E_k \cdot C$	C = 20 cph	$E_t = 114 \cdot 100 \cdot 20 = 228,000$	
$E_t = F \cdot V \cdot C$	S = 20 cph	$W_{eq} = 228,000 / 38.7 = 5891$	
$W_{eq} = E_t / 38.7$			

H4 - Select from Model Rating Chart: ML 6450 or MC 6450-4

H5 Weight on Power Rollers/Conveyor Pallet Line, Precision Conveyor Roll, Steel Tube Transfer



$F = W \cdot Mu$	W = 200 lbs	F = 250 \cdot 0.2	
$E_k = 0.186 \cdot W \cdot V^2$	V = 25 ft/sec	C = 3000 \cdot 0.2 \cdot 10	
$F = F \cdot W$	Mu = 0.2	E = 1200	
$E_c = E_k \cdot C$	C = 100 cph	$E_t = 1200 \cdot 10 = 12,000$	
$E_t = F \cdot V \cdot C$	S = 100 cph	$W_{eq} = 12,000 / 38.7 = 310$	
$W_{eq} = E_t / 38.7$			

H5 - Select from Model Rating Chart: MA 600 or SC 650-3

ACE Controls, Inc. 800-621-3320 (24hr) 476-0213 Fax: 476-4770 www.acecontrols.com email: info@acecontrols.com

FIGURE D-6: Application guide for the swing's shock absorbers

APPENDIX E

Approvals from Human Investigations Committee

**WAYNE STATE
UNIVERSITY**

HUMAN INVESTIGATION COMMITTEE
101 East Alexandrine Building
Detroit Michigan 48201
Phone: (313) 577-1628
FAX: (313) 993-7122
<http://hic.wayne.edu>

NOTICE OF FULL BOARD APPROVAL

To: Renee Dawson
Biomedical Engineering
519 Talthorpe Place

From: Virginia Delaney-Black, M.D., MPH
Chairperson, Medical/Pediatric Institutional Review Board (MP4)

Date: April 03, 2007

RE: HIC #: 026307MP4F
Protocol Title: Pediatric Cervical Muscle Response to Static and Dynamic Loading
Sponsor:
Coeus#: 0702004670

Expiration Date: April 02, 2008

Risk Level/Category: Greater than minimal risk but potential for direct benefit for participant.45 CFR 46.405

The above-referenced protocol and items listed below (if applicable) were **APPROVED** following *Full Board Review* by the Wayne State University Institutional Review Board (MP4) for the period of 04/03/2007 through 04/02/2008. This approval does not replace any departmental or other approvals that may be required.

- Protocol and Revised Protocol Summary Form (received in the HIC office 4/2/07)
- Parental Consent Form (revision date 4/3/07)
- Assent Form (revision date 4/3/07)
- Flyer

-
- Federal regulations require that all research be reviewed at least annually. You may receive a "Continuation Renewal Reminder" approximately two months prior to the expiration date; however, it is the Principal Investigator's responsibility to obtain review and continued approval **before** the expiration date. Data collected during a period of lapsed approval is unapproved research and can never be reported or published as research data.
 - All changes or amendments to the above-referenced protocol require review and approval by the HIC **BEFORE** implementation.
 - Adverse Reactions/Unexpected Events (AR/UE) must be submitted on the appropriate form within the timeframe specified in the HIC Policy (<http://www.hic.wayne.edu/hicpol.html>).

NOTE:

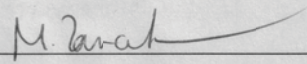
1. Upon notification of an impending regulatory site visit, hold notification, and/or external audit the HIC office must be contacted immediately.
2. Forms should be downloaded from the HIC website at each use.

**WAYNE STATE
UNIVERSITY**

HUMAN INVESTIGATION COMMITTEE
101 East Alexandrine Building
Detroit Michigan 48201
Phone: (313) 577-1628
FAX: (313) 993-7122
<http://hic.wayne.edu>

NOTICE OF FULL BOARD CONTINUATION APPROVAL

To: Fenee Dawson
Biomechanics Center
519 Talthorpe Place

From: Manuel Tancer, M.D. 
Chairperson, Medical Institutional Review Board (M1)

Date: December 06, 2006

RE: HIC #: 121204M1F
Protocol Title: Cervical Muscle Response to Static and Dynamic Lateral Loading
Sponsor: FORD MOTOR COMPANY FUND
Coeus #: 0504001778

Expiration Date: December 07, 2007

Continuation for the above-referenced protocol and items listed below (if applicable) were **APPROVED** following Full Board review by the Wayne State University Institutional Review Board (M1) for the period of 12/06/2006 through 12/07/2007. This approval does not replace any departmental or other approvals that may be required.

- Consent Form (revised 11/20/05) and Advertisement
- NOTE TO PI: Data for this protocol collected between November 30, 2006 through December 6, 2006 is unapproved research, cannot be included with data collected during an approved period, and can never be reported or published as research data.

- Federal regulations require that all research be reviewed at least annually. You may receive a "Continuation Renewal Reminder" approximately two months prior to the expiration date; however, it is the Principal Investigator's responsibility to obtain review and continued approval **before** the expiration date. Data collected during a period of lapse of approval is unapproved research and can never be reported or published as research data.
- All changes or amendments to the above-referenced protocol require review and approval by the HIC **BEFORE** implementation.
- Adverse Reactions/Unexpected Events (AR/UE) must be submitted on the appropriate form within the timeframe specified in the HIC Policy (<http://www.hic.wayne.edu/hicpol.html>).

NOTE:

1. Upon notification of an impending regulatory site visit, hold notification, and/or external audit the HIC office must be contacted immediately.
2. Forms should be downloaded from the HIC website at **each** use.

REFERENCES

- Alway SE, Stray-Gundersen J, Grumbt WH, Gonyea WJ, 1990, *Muscle cross-sectional area and torque in resistance-trained subjects*, European Journal of Applied Physiology, v60: 86-90.
- Amarantini D, Martin L, 2004, *A method to combine numerical optimization and EMG data for the estimation of joint moments under dynamic conditions*, Journal of Biomechanics 37 1393–1404
- Arbogast KB, Balasubramanian S, Seacrist T, Maltese MR, García-España JF, Hopely T, Constans E, Lopez-Valdes FL, Kent RW, Tanji H, Higuchi K , 2009, *Comparison of Kinematic Responses of the Head and Spine for Children and Adults in Low-Speed Frontal Sled Tests* Stapp Car Crash Journal, Vol. 53:329-372
- Arnold AS, Salinas S, Asakawa DJ, Delp SL, 2000, *Accuracy of muscle moment arms estimated from MRI-based musculoskeletal models of the lower extremity*, Computer Aided Surgery, v5: 108-119
- Baker SK, 2009, *Characterization of a novel C8 phasic muscle stretch reflex*, Muscle Nerve 40: 529–534
- Beier, G., Schuller, E., Schuck, M., Ewing, C. L., Becker, E. D., Thomas, D. J. 1980, *Center of Gravity and Moment of inertia of human heads* .International IRCOBI on the Biomechanics of Impacts 218-28.
- Begeman PC, King AI, Levine RS, 1980, *Biodynamic response of the musculoskeletal system to acceleration*, Society of Automotive Engineers (SAE #801312)

- Ben-Noun L, Laor A, 2006, *Relationship between changes in neck circumference and cardiovascular risk factors* Experimental Clinical Cardiology, v.11(1):14-20.
- Blimkie CJ, Ebbesen B, MacDougall D, Bar-Or O, Sale D.,1989, *Voluntary and electrically evoked strength characteristics of obese and nonobese preadolescent boys*, Human Biology. Aug;61(4):515-32
- Bluestone CD, 2003, Pediatric Otolaryngology v.2, Elsevier Science, Philadelphia, p.1369.
- Bogey RA, Perry J, Gitter AJ, 2005, *An EMG-to-Force Processing Approach for Determining Ankle Muscle Forces During Normal Human Gait*, IEEE Transactions on Neural Systems and Rehabilitation Engineering, v 13,(3) pp:302-310
- Brown RL., Brunn MA., Garcia VF , 2001, *Cervical Spine injuries in children: A review of 103 patients treated consecutively at a level 1 Pediatric Trauma Center* Journal of Pediatric Surgery v.36(8): 1107-1114
- Cassan, BF, Page M, Pincemaille Y, Kallieris D, Tarrière C, 1993, *Comparative Study of Restrained Child Dummies and Cadavers in Experimental Crashes*, Society of Automotive Engineers (SAE #933105)
- Cholewicki J, McGill SM., 1994, *EMG assisted optimization: a hybrid approach for estimating muscle forces in an indeterminate biomechanical model*, Journal of Biomechanics,.v.27(10):1287-9
- Cirak B, Ziegfeld S, Knight VM, Chang D, Avellino AM, Paidas CN., 2004, *Spinal Injuries in Children* Journal of Pediatric Surgery v.39(4): 607-612

- Cesari D., et al., 2001, *WorldSID Prototype Dummy Biomechanical Responses*, Proceedings of the 45th Stapp Car Crash Conference (SAE # 2001-22-0013)
- Choi H., Vanderby R., 2000, *Muscle forces and spinal loads at C4/5 level during isometric voluntary efforts*, *Medicine in Science, Sports and Exercise*, v.32:830-838
- Clark MA., Lucett SC., Corn RJ., editors, 2008, NASM Essentials of Personal Fitness Training, Lippincott Williams and Wilkins, p.145
- Crownshield RD, 1978, *Use of Optimization techniques to predict muscle forces*, *Journal of Biomechanical Engineering*, v.100:88-92
- Cuson ML.,2004, *An Investigation of Acceleration Measurement Techniques in Volunteers*, Master Thesis submitted to Wayne State University
- Deighan M., Armstrong N, De Ste Croix MBA, 2002, *Peak torque per MRI-determined cross-sectional area of knee extensors and flexors in children, teenagers and adults* [abstract] 3rd Commonwealth Sports Conference, British Association of Sports and Exercise.
- De Loose V., Van den Oord M., Keser I., Burnotte F., Van Tiggelen D., Dumary A., Cagnie B., Witvrouw E., Danneels L., 2009, *MRI Study of the Morphometry of the Cervical Musculature in F-16 Pilots*, *Aviation, Space and Environmental Medicine*, v.80, pp:727-731
- De Ste Croix MBA., Deighan MA., Armstrong N., 2003, *Assessment and Interpretation of Isokinetic muscle strength during growth and maturation*, *Sports Med* v.33(10):727-743

Docket No. 02-12151, 2002 – National Highway Traffic Safety Administration
(NHTSA) Department of Transportation

Engstrom CM, Loeb GE, Reid JG, Forrest WJ, Avruch L., 1991, *Morphometry of the human thigh muscles. A comparison between anatomical sections and computer tomographic and magnetic resonance images*, Journal of Anatomy, v.173:139-156

Rolf Eppinger, 2001, *Occupant Restraint Systems*, in Accidental Injury: Biomechanics and Prevention. 2nd Ed. Edited by Alan M Nahum and John W Melvin, Springer-Verlag

Erdemir A, McLean S, Herzog W, van den Bogert AJ, 2007, *Model-based estimation of muscle forces exerted during movements*, Clinical Biomechanics v.22 pp: 131–154

Forsberg H, Hirschfeld, 1997, *Postural adjustments in sitting humans following external perturbations: muscle activity and kinematics*, Experimental Brain Research v.97:515-527

Foust DR, Chaffin DB, Snyder RG, Baum JK, 1973, *Cervical Range of Motion and Dynamic Response and strength of cervical muscles*, Society of Automotive Engineers (SAE #730975)

Fredriks AM, van Buuren S, van Heel WJM, Dijkman-Neerincx RHM, Verloove-Vanhorick SP, Wit JM, 2005, *Nationwide age references for sitting height, leg length, and sitting height/height ratio, and their diagnostic value for disproportionate growth disorders*, Archives of Disease in Childhood v.90 pp:807–812

- Fukunaga T, Roy RR, Shellock FG, Hodgson JA, Day MK, Lee PL, Kwong-Fu H, Edgerton VR., 1992, *Physiological cross-sectional area of human leg muscles based on magnetic resonance imaging*, Journal of Orthopedic Research, v.10: 928-934.
- Gagnon D, Larivière C, Loisel P, 2001, *Comparative ability of EMG, optimization and hybrid modeling approaches to predict trunk muscle forces and lumbar spine loading during dynamic saggital plane lifting*, Clinical Biomechanics, v16: 359-372
- Garcés Gl., Medina D., Milutinovic L., Garavote P., Guerado E., 2002, *Normative database of isometric cervical strength in a healthy population*, Medicine in Science,. Sports and Exercise, v. 33(3): 464-470
- Gerdle B, Karlsson S, Crenshaw AG, Elert J, Fridén J., 2000, *The influences of muscle fibre proportions and areas upon EMG during maximal dynamic knee extensions*, European Journal of Applied Physiology. v.81(1-2):2-10
- Givens TG., Polley KA., Smith CF., Hardin WD Jr., 1996, *Pediatric Cervical Spine Injury: A three year experience*, The Journal of Trauma, Injury, Infection and Critical Care v. 41(2): 310-314,
- Gray H, 1918, Gray's Anatomy 15th edition, Barnes and Nobles Books, NY
- Grosset JF, Mora I, Lambertz D, Pérot C.,2008 *Voluntary activation of the triceps surae in prepubertal children*, Journal of Electromyography and Kinesiology v.18(3):455-65

- Gzik M., Wolanski, W., Tejszerska D.,2008, *Experimental determination of cervical spine mechanical properties*, Acta of Bioengineering and Biomechanics, v10:49-54.
- Hain TC, 2009, Postural, Vestibulospinal and Vestibulocollic Reflexes, Dizziness-and-Balance.com,
- Halin R., Germain P., Bercier S., Kapitaniak B., Butelli O., 2003, *Neuromuscular response of young boys versus men during sustained maximal contraction*, Medicine in Science, Sports and Exercise, v.35(6):1042-1048
- Hatipoglu N, Mazicioglu MM, Kurtoglu S, Kendirci M., 2010, *Neck circumference: an additional tool of screening overweight and obesity in childhood*, European Journal of Pediatrics, v169(6):733-9
- Heintz, S, Gutierrez-Farewik EM, 2006, *Static optimization of muscle forces during gait in comparison to EMG-to-force processing approach*, Gait & Posture 26:279–288
- Hooper, Scott L,(1999–2010), ["Central Pattern Generators"](#). *Encyclopedia of Life Sciences*. John Wiley & Sons.
- Horak FB., Shupert CL, Dietz V, Horstmannet G, 1994, *Vestibular and somatosensory contributions to responses to head and body displacements in stance*, Experimental Brain Research, 100:93–106
- Ichinose, Y., Kanehisa, H., Ito, M., Kawakami, Y., Fukunaga, T., 1998, *Morphological and functional differences in the elbow extensor muscle between highly trained male and female athletes*, European Journal of Applied Physiology and Occupational Physiology, v.78: 109-14.

- Ito Y, Corna S, von Brevern M, Bronstein A, Gresty M, 1997, *The functional effectiveness of neck muscle reflexes for head-righting in response to sudden fall*, Experimental Brain Research v.117:266-272
- Jorgensen MJ, Marras WS, Granata KP, Wiand JW.,2001, *MRI-derived moment-arms of the female and male spine loading muscles*, Clinical Biomechanics, v.16: 182-193.
- Bjarne Laursen B, Jensen RB, Németh G, Sjøgaard G, 1998, *A model predicting individual shoulder muscle forces based on relationship between electromyographic and 3D external forces in static position*, Journal of Biomechanics, v.31: 731-739
- Lee SH, Terzopoulos D, 2006, *Heads up! Biomechanical modeling and neuromuscular control of the neck*, ACM Transactions on Graphics, v.25(3):1188-1198
- Lu WW, Bishop PJ., 1996, *Electromyographic activity of the cervical musculature during dynamic lateral bending*, Spine (Phila Pa 1976). v.21 (21):2443-2449
- Kamibayashi LK., Richmond FJR., 1998, *Morphometry of Human Neck Muscles*, Spine, v.23: 1314-1323.
- Kanehisa, H., et al., 1994a, *Strength and Cross Sectional Area of Knee Extensor Muscles in Children*, European Journal of Applied Physiology
- Kanehisa HA., Ikegawa S., Fukunaga T, 1994b, *Comparison of muscle cross-sectional area and strength between untrained men and women*, European Journal of Applied Physiology v. 68: 148-154

- Kanehisa H., Yata H., Ikegawa S., Fukunaga T., 1995, *A cross-sectional study of size and strength of the lower leg muscles during growth* European Journal of Applied Physiology, v.72:150-156
- Kokoska ER, Keller MS, Rallo MC, Weber TR 2001, *Characteristics of pediatric cervical spine injuries*, Journal of Pediatric Surgery, v.36(1): 100-105
- Kumar S., Narayan Y., Amell T., 2000 *Role of Awareness in head-neck acceleration in low velocity rear-end impacts*, Accident Analysis and Prevention, v. 32:233-241
- Kumar S., Narayan Y., Amell T., 2001, *Cervical Strength of Young Adults in Sagittal, Coronal and Intermediate Planes*, Clinical Biomechanics v.16:380-388
- Kumar S., Narayan Y., Amell T.,2002, *Electromyography of Superficial Cervical Muscles with Exertion in the Sagittal, Coronal and Oblique Planes*, European Spine Journal v.11:27-37
- Kumar S., Narayan Y., Amell T.,2003, *Analysis of Low Velocity Frontal Impacts*, Clinical Biomechanics v.18:694-703
- Kuramochi R, Kimura T, Nakazawa K, Akai M, Torii S, Suzuki S, 2004, *Anticipatory modulation of neck muscle reflex responses induced by mechanical perturbations of the human forehead*, Neuroscience Letters v.366:206–210
- Lambertz D, Mora I, Grosset JF, Pérot, C, 2003, *Evaluation of musculotendinous stiffness in prepubertal children and adults, taking into account muscle activity*, Journal of Applied Physiology, v.95: 64–72

- Loeb GE, Gans C, 1986, Electromyography for Experimentalists, The University of Chicago Press, ISBN 0-226-49014-9, Chicago
- Loyd AM, Nightingale R, Bass CR, Mertz HJ, Frush D, Daniel C, Lee C, Marcus JR, Mukundan S, Myers BS, 2010, *Pediatric Head Contours and Inertial Properties for ATD Design*, *Stapp Car Crash Journal*, v.54:167-196
- Lustin ES., Karkas SP., Ortiz AO., Cinnamon J., Castillo M., Vaheesan K., Brown JH., Diamond AS., Black K., Singh S., 2003, *Pediatric Cervical Spine: Normal Anatomy, Variants and Trauma*, *Radiographics*, v.23:539-560
- Maganaris CN., Baltzopoulos V., Ball D., Sargeant J., 2001, *In Vivo Specific Tension of Human Skeletal Muscle*, *Journal of Applied Physiology* v.90: 865-872
- Mathews EA., Seacrist T., Maltese MR., Higuchi K., Tanji H., St. Lawrence S., Arbogast KB., Balasubramanian S., 2011, *Electromyography responses of pediatric and adult volunteers in low speed frontal impacts*, *2011 Ohio State University Injury Biomechanics Symposium*
- Mayoux-Benhamou MA, Wybier M, Revel M, 1989, *Strength and cross-sectional area of the dorsal neck muscles*, *Ergonomics*, v.32(5):513-8.
- Mazicioglu MM, Kurtoglu S, Ozturk A, Hatipoglu N, Cicek B, Ustunbas HB., 2010, *Percentiles and mean values for neck circumference in Turkish children aged 6-18 years*, *Acta Paediatrica*, 99(12):1847-53
- McCall T., Fassett D., Brockmeyer D., 2006, *Cervical Spine Trauma in Children: A Review*, *Neurosurgery Focus*, v. 20

- McDowell MA, Fryar CD, Ogden CL, Flegal KM, 2008, *Anthropometric Reference Data for Children and Adults: United States, 2003–2006*. National Health and Statistics Report, US Department of Health and Human Services, No 10.
- Merriam-Webster's Medical Desk Dictionary, 2002, Merriam-Webster, Inc., Springfield, MA
- Mertz, H.J. and L.M. Patrick, 1967, *Investigation of the Kinematics and Kinetics of Whiplash*", SAE 670919
- Mertz, H.J. and L.M. Patrick, 1971, *Strength and Response of the Human Neck*", Society of Automotive Engineers (SAE#710855)
- Miller AE, MacDougall JD, Tarnopolsky MA, Sale DG, 1993, *Gender differences in strength and muscle fiber characteristics* European Journal of Applied Physiology v.66: 254-262, 1993
- Moore KL., Daley AF, 1999, *Clinically Oriented Anatomy*, 4th Edition, Lippincott Williams & Wilkins, Philadelphia
- Moroney SP, Schultz AB, Miller JA, 1988, *Analysis and measurement of neck loads*, Journal of Orthopedic Research, v.6(5):713-20
- Morningstar MW, Pettibon BR, Schlappi H, Schlappi M, Ireland TV, 2005, *Reflex control of the spine and posture: a review of the literature from a chiropractic perspective*, *Chiropractic & Osteopathy* , v.13:16
- Nafiu OO, Burke C, Lee J, Voepel-Lewis T, Malviya S, Tremper KK, 2010, *Neck Circumference as a Screening Measure for Identifying Children With High Body Mass Index*, Pediatrics, v.126:e306-e310

- Narici MV, Roi GS, Landoni L., 1988, *Force of knee extensor and flexor muscles and cross-sectional area determined by nuclear magnetic resonance imaging*, European Journal of Applied Physiology and Occupational Physiology, v.57(1):39-44
- Newman JA., Dalmatos D. 1993, *Atlanto-Occipital Fracture Dislocation in Lap-belt Restrained Children*, Society of Automotive Engineers, SAE # 933099
- Normann RA., 1988, Principles of BioInstrumentation, John Wiley and Sons, Inc.
- Nuckley DJ, Hertsted SM, Eck MP, Ching RP, 2005, *Effect of displacement rate on the tensile mechanics of pediatriccervical functional spinal units*, Journal of Biomechanics, v.38:2266–2275
- Nuckley DJ, Ching RP.,2006, *Developmental biomechanics of the cervical spine: Tension and compression*, Journal of Biomechanics,v;39(16):3045-54
- Ono K., Kaneoka K., Wittek A., Kajzer, J., 1997, *Cervical Injury Mechanism Based on the Analysis of Human Cervical Vertebral Motion and Head-Neck-Torso Kinematics During Low Speed Rear Impacts*, Proceedings from the 41st Stapp Car Crash Conference, Society of Automotive Engineers (SAE# 973340).
- Oksanen A., Erkintalo M., Metsahonkala L., Anttila P., Laimi K., Hiekkanen H., Salminen J., Aromaa M., Sillanpää M., 2008, *Neck Muscle Cross-Sectional Area in Adolescents with and without Headache – MRI Study*, European Journal of Pain, v.12:952-959.
- Padgaonkar A., Krieger K., King A., 1975, *Measurement of Angular Acceleration of a Rigid Body using Linear Accelerometers*, Applied Mechanics, v.42(3)

- Patrick L.M., Chou C.C., 1976, *Response of the Human Neck in Flexion, Extension and Lateral Flexion*, Vehicle Research Institute Report VRI 7.3
- Prasad, VSSV., Schwartz A., Bhutani R., Sharkey PW., Schwartz ML., 1999, *Characteristics of injuries to the cervical spine and spinal cord in polytrauma patient population: experience from a regional trauma unit*, Spinal Cord, v.37:560-568.
- Preis SR, Massaro JM, Hoffmann U, D'Agostino RB Sr, Levy D, Robins SJ, Meigs JB, Vasan RS, O'Donnell CJ, Fox CS.,2010, *Neck circumference as a novel measure of cardiometabolic risk: the Framingham Heart study*, J Clinical Endocrinology and Metabolism, v.95(8):3701-10.
- Seacrist T, Balasubramanian S, García-España JF, Maltese MR, Arbogast KB, Lopez-Valdes FJ, Kent RW, Tanji H, Higuchi K, 2010, *Kinematic Comparison of Pediatric Human Volunteers and the Hybrid III 6-Year-Old Anthropomorphic Test Device*, Annals of Advances in Automotive Medicine, v.54:97-108
- Seeman MR, Lustick LS, Frisch GD, 1984, *Mechanism for control of head and neck dynamic response*, Society of Automotive Engineers, (SAE# 841669v001)
- Seng, K., Peter, VL., Lam P.,2002, *Neck Muscle Strength across the Sagittal and Coronal Planes: an Isometric Study*, Clinical Biomechanics v.17: 545-547
- Siegmund GP, Sanderson DJ, Myers BS, Inglis JT, 2003, *Awareness affects the response of human subjects exposed to a single whiplash-like perturbation*, Spine (Phila Pa 1976) v.28(7):671-679

- Siegmund GP, Sanderson DJ, Inglis JT., 2004, *Gradation of Neck Muscle Responses and Head/Neck Kinematics to Acceleration and Speed Change in Rear-end Collisions*, Stapp Car Crash Journal, v.48:419-30
- Siegmund GP, Blouin JS, Carpenter MG, Brault JR, Inglis JT, 2008, *Are cervical multifidus muscles active during whiplash and startle? An initial experimental study*, *BMC Musculoskeletal Disorders* v.9:80
- Staudenmann D, Potvin JR, Kingma I, Stegeman DF, van Dieën JH, 2007, *Effects of EMG processing on biomechanical models of muscle joint systems: sensitivity of trunk muscle moments, spinal forces, and stability*, *Journal of Biomechanics*, v.40(4): 900-909
- Staudenmann D, Kingma I, Stegeman DF, van Dieën JH. 2005, *Towards optimal multi-channel EMG electrode configurations in muscle force estimation: a high density EMG study*, *Journal of Electromyography and Kinesiology*. V.15(1):1-11
- Smeulders MJC., van den Berg S., Oudeman J. Nederveen AJ., Kreulen M., Maas M.,2010, *Reliability of in vivo determination of forearm muscle volume using 3.0T magnetic resonance imaging*, *Journal of Magnetic Resonance Imaging*, v.31:1252-1255.
- Stemper BD., Baidisen JL., Yognanadan N., Pintar FA., Pakoff GR., Shender BS., 2010, *Determination of Normative Neck Muscle Morphometry Using Upright MRI with Comparison to Supine Data*, *Aviation, Space and Environmental Medicine*, v81:878-882.

- Smith DH., Meaney DF., 2002, *Roller Coasters, G Forces, and Brain Trauma: On the Wrong Track?*, J. Neurotrauma, v.19 (10):1117-1120.
- Snyder, R., et al.,1977, *Anthropometry of Infants, Children, and Youths to Age 18 for Product Safety Design*, Society of Automotive Engineers
- Sunnegårdh J, Bratteby LE, Nordesjö LO, Nordgren B., 1988, *Isometric and Isokinetic Muscle Strength, Anthropometry and Physical Activity in 8 and 13 Year Old Swedish Children*, European Journal of Applied Physiology, v. 58(3):291-7.
- Squire LR, 2003, Fundamentals of Neuroscience 2nd edition, Elsevier Academic Press,
- Tarriere C., and Sapin C., 1969, *Biokinetic Study of the Head t Thorax Linkage* Society of Automotive Engineers (SAE#690815)
- Szabo TJ., Welcher JB.,1996, *Human Subject Kinematics and Electromyographic Activity During Low Speed Rear Impacts*, Proceedings from the 40th Stapp Car Crash Conference, Society of Automotive Engineers (SAE# 962432)
- Torg, JS., Pavlov H., O'Neill MJ., Nichols CE. III., Sennett B., 1991, *The axial load teardrop fracture: A biomechanical, clinical, and roentgenographic analysis*, The American Journal of Sports Medicine, v19:355-364.
- Van der Horst MJ., Thunnisse JGM., Happee R., van Haaster RMHP., Wismans JSHM., 1997, *The influence of Muscle Activity on Head-Neck response during impact*, Society of Automotive Engineers, (SAE #973346).

- Vander AJ, Sherman JH, Luciano DS, 1990, Human Physiology – The Mechanisms of Body Function 5th edition, McGraw Hill Publishing Company, New York,
- Van den Kroonenberg A, Philippens M, Cappon H, Wismans J, Hell W, Langwieder K, 1998, *Human Head-Neck Response During Low-Speed Rear End Impacts*, Proceedings from the 42nd Stapp Car Crash Conference, #983158
- Van Ee CA., Nightingale RW., Camacho DLA., Chancey VC., Knaub KE., Sun EA., Myers BS, 2000, *Tensile Properties of the human muscular and ligamentous cervical spine*, Proceedings from the 44th Stapp Car Crash Conference, 2000-01-SC07.
- Vasavada AN., Li S., Delp SL., 1998, *Influence of muscle morphometry and moment arms on the moment-generating capacity of human neck muscles*, Spine, v.23:412-422.
- Vasavada AN., Siping L., Delp SL., 2001, *Three dimensional isometric strength of neck muscles in humans*” Spine v. 26(17):1904-1909.
- Wismans J, Maltha J, 1979, *Child restraint evaluation by experimental and mathematical simulation*, Society of Automotive Engineers (SAE#791017)
- Wismans J., Spenny C.H., 1983, *Performance Requirements for Mechanical Necks in Lateral Flexion*, Society of Automotive Engineers (SAE # 831613)

Wittek A, Ono K, Kajzer J, Ortengren R, Inami S, 2001, *Analysis and comparison of reflex times and electromyograms of cervical muscles under impact loading using surface and fine wire electrodes*, IEEE Transactions on Biomedical Engineering, v.48(2):143-153.

Wolanin, M.J., and Mertz, H.J., 1982, *Description and Basis of a Three-Year-Old Child Dummy for Evaluation Passenger Inflatable Restraint Concepts*, Society of Automotive Engineers (SAE #826040)

Wysocki J., Kielska E., Orszulak P., Reymond, J., 2008, *Measurements of pre- and post pubertal human larynx: A cadaver study*, Surgical and Radiologic Anatomy, v30 (3):191-9

Yoganandan, N, Pintar FA , Zhang J, Baisden JL, 2009, *Physical properties of the human head: Mass, center of gravity and moment of inertia*, Journal of Biomechanics, v.42 1177–1192,

Zuckerbraun BS., Morrison K., Gaines B., Ford HR., Hackam DJ., 2004, *Effects of Age on cervical spine injuries in children after motor vehicle collisions: effectiveness of restraint devices”* Journal of Pediatric Surgery v.39(3): 483-486

(www.sirinet.net/~jgjohnso/amuscle.html)

[www.thefullwiki.org/Vestibular_system#Vestibulo-ocular_reflex .28VOR.29](http://www.thefullwiki.org/Vestibular_system#Vestibulo-ocular_reflex_.28VOR.29)

http://mac6.ma.psu.edu/lin_equations/index.html

ABSTRACT**COMPARISON OF ADULT AND PEDIATRIC NECK MUSCLE
STRENGTH AND RESPONSE**

by

RENEE M DAWSON

August 2012

Advisor: Dr. J.M. Cavanaugh
Major: Biomedical Engineering
Degree: Doctor of Philosophy

In 2000 and 2001 an estimated 150,000 children between the ages of 0 and 8 years old were injured or killed in a motor vehicle accident. Despite advances in child safety restraints and vehicle restraints, automobile accidents remain the primary cause of death for children in the 0-8 year old age group. In 1982, in an attempt to reduce the number of deaths and injuries of children, the first child crash test dummy was developed. The responses of this dummy were scaled from the adult response data based on the assumption that children were similar to adults both anatomically and physiologically, only children were smaller. It was also assumed that the soft tissue response, such as muscle force, was the same as for an adult.

Recent studies have shown that not only are children different from adults due to the development of their skeleton, but that their ability to develop muscle force for a given cross-sectional area of muscle is also different. This difference calls into question not only the relationship that was used to develop the child

crash test dummies but also the ability of these crash dummies to predict child injuries due to automobile impact.

METHODS

The aim of this study was to determine if the assumption of equivalent stress is appropriate. The muscle response of the neck muscles in 50th percentile adult male was compared to the neck muscle response of the 10-year-old boy under static and dynamic loading conditions. Magnetic resonance imaging was used to measure the muscle length, moment arm and cross-sectional area of the superficial flexor and extensor muscles of the neck.

Two EMG studies were used to analyze the muscle force generated in the neck in response to static and dynamic loads. In the static study, subjects were asked to generate a maximal voluntary contraction (MVC) in four bending directions – flexion, extension and lateral left and right bending. Using an EMG-assisted optimization model, the forces and stresses in the superficial flexor/extensor muscles was calculated. The second EMG study was conducted during a low speed frontal impact in two test conditions – aware and unaware of the up-coming impact. The dynamic moment and displacement of the head were calculated. Latency of muscle activation in response to the onset of swing acceleration and peak swing acceleration were also examined.

RESULTS

Results of the MRI study confirmed the relationship between age and muscle moment arm ($r=0.855$, $p=0.05$ for the SCM), and age and muscle cross-

sectional area ($r=0.741$, $p=0.05$ for the SCM) used in the Wolanin et al. scaling relationship.

Both EMG studies showed that adults were able to generate higher applied moments ($p<0.05$) and muscle forces and moments ($p<0.05$) than 10-year old children in the same testing conditions. There was no difference in the stress generated during static loading of the neck muscles. The results of the study did show, however that the neuromuscular efficiency [Grosset, 2008] was significantly higher in adults than in children, suggesting that due to an immature neuromuscular system, children are unable to fully recruit their muscles during a contraction. These results are further supported by the latency results which show that children, in spite of early muscle activation when aware of an impact are unable to generate sufficient muscle tension to reduce the moment of the head or its maximum displacement.

CONCLUSION

The results of this study are unable to contradict the scaling model put forth by Wolanin et al. [1982] since there was no difference found between the adult and child muscle stress under various loading conditions. The results do however suggest that scaling may be more accurate at low speeds if an additional factor were added to the model which takes into account the inefficiencies of the pediatric neuromuscular system.

AUTOBIOGRAPHICAL STATEMENT

RENEE M DAWSON

EDUCATION

- Ph.D. Biomedical Engineering, Wayne State University, Detroit, MI, 2011
M.S. Biomedical Engineering, Wayne State University, Detroit, MI, 2003
B.Eng Mechanical Engineering, Technical University of Nova Scotia,
Halifax, Nova Scotia, Canada, 1998
B.Sc Physics, Dalhousie University, Halifax, Nova Scotia, Canada, 1995

POSITIONS

- 1998-1999 Design Build Engineer, Honeywell Ltd., Windsor, ON, Canada
1999-2001 Release Engineer, Aerotek for Daimler Chrysler Corporation,
Auburn Hills, MI
2001-2003 Safety Systems Integrator, Takata, Auburn Hills, MI
2003-2006 Graduate Research Assistant, Bioengineering Center, Wayne State
University

HONORS AND AWARDS

- 2003-2004 Graduate Professional Scholarship, Wayne State University
2004-2005 Ford Fellowship, Wayne State University